Predicting the ecological effects of metals in marine sediments

Lower Restronguet Creek, Cornwall, England.

Solomon Chibuzo Udochi

A thesis submitted in fulfilment of the requirements for the degree of Doctor of Philosophy

School of Environmental Sciences
University of East Anglia

September 2020

ABSTRACT

Despite advances in the regulation of marine pollution, there remains considerable uncertainty about metal concentrations in sediments that can elicit adverse ecological effects. A key gap has been the work that relates metal contamination to *ecological* endpoints in *field-contaminated sites*. Consequently, the main aim of this thesis was to assess dose-response relationships of metals in marine sediments: to determine what chemical measures of contamination best predict ecological effects and the threshold concentrations at which these effects begin to occur. The study was conducted, primarily, in the Fal and Hayle estuaries, Cornwall, England, which are grossly contaminated by mine drainage. I assessed physicochemical characteristics of sediments and porewater at twelve study sites over a two-year period and in three different seasons. To quantify exposure to benthic fauna, I measured metal contamination using Diffusion Gradients in Thin Films (DGT), Equilibrium Partitioning (EqP) derivations, and traditional measures: total porewater (PW), organic carbon-normalised porewater (PW Cu/OC), acid-extractable (AEM), and total sediment (Sed) concentrations. I quantified ecological effects using the occurrence of pollution-tolerant nematode communities (PICT) and nematode community structure defined by univariate diversity indices and multivariate techniques. The EqP model downplays dietary toxicity. Therefore, I assessed the importance of dietary toxicity and the validity of the EqP in predicting (non-)toxicity of copper to a deposit-feeding snail, *Peringia ulvae*. Overall, the results reveal a combination of metal uptake routes that raises questions about regulatory guidelines based on single measures. Where dissolved metals were important predictors, DGT offered little above PW. Where sediment-bound metals were important, Sed proved more useful than widely considered. In both instances, the EqP performed poorly. This thesis also showed that medium to long-term redox changes in Fal and Hayle sediments can remobilise metals at potentially toxic concentrations. Recommendations for metal regulation in marine sediments are provided.

LIST OF CONTENTS

LIST OF TABLES

Chapter 2

Chapter 3

Chapter 4

Chapter 5

Chapter 6

Chapter 7

LIST OF FIGURES

Chapter 1

Chapter 2

Chapter 3

Chapter 4

Chapter 5

Chapter 6

Chapter 7

ABBREVIATIONS AND GLOSSARY OF TERMS

AEM	Acid-Extractable Metal. The fraction of metals in sediment that is extractable by 1 M HCl.
AIC	Akaike Information Criterion
ANOVA	Analysis of Variance
ANOSIM	Analysis of Similarity
ASW	Artificial seawater
AVS	Acid Volatile Sulphides. The fraction of sulphides in the sediment that is liberated after treatment with 1 M HCl.
Bioaccumulation	The enrichment of contaminants in an organism's tissue relative to the environment, which results from the balance between uptake and excretion processes (Borga, 2013).
Bioavailability	The fraction of metals in the environment that is available for uptake by an organism of interest (Simpson *et al.*, 2016).
BIOENV	A non-parametric method used to link biotic dissimilarities with environmental variables. This method was first described by Clarke and Ainsworth (1993) and is now included in the "BEST" methods that identify the (subset of) environmental variable(s) that best explain(s) biotic patterns.
BLM	Biotic Ligand Model
Body burden	The concentration of metals that is accumulated in an organism's tissues.
CBR	Critical Body Residue
C_{DGT}	The interfacial porewater metal concentration measured using the DGT device.
CoP	Coefficient of Pollution
DET	Diffusive Equilibrium in Thin Films
DGT	Diffusive Gradients in Thin Films
Dissolved metals	The fraction of metals in the environment <0.45 µm in size.
DMSO	Dimethyl sulphoxide

DO	Dissolved Oxygen
DOC	Dissolved Organic Carbon
$EC_{20\ or\ 50}$	Effective Concentration 20 or 50. The concentration of metal reducing a biological response to 20% or 50% of its value in the control population, respectively.
Ecological effects	The impairment of normal functioning in an organism, e.g. reduction in growth, reproduction, and survival, as a result of exposure to a contaminant. Effects are distinguished from indicators, such as body burdens or biomarker responses, reflective of exposure but not definitive harm.
EDTA	Ethylenediaminetetraacetic acid
Eh	Standard hydrogen potential
EqP	Equilibrium Partitioning (model)
FIAM	Free-Ion Activity Model
Field-contaminated sediment	That sediment contaminated by natural or anthropogenic activities in field sites. This sediment has typically been equilibrated with the contaminant for long periods under natural conditions in the field and is distinguished from spiked sediments wilfully contaminated in laboratories for the purpose of experimentation or toxicity testing.
Fz	Ferrozine
GFAAS	Graphite Furnace Atomic Absorption Spectroscopy
GLM	Generalised Linear Models
HDPE	High Density Poly Ethylene
ICP-MS	Inductively Coupled Plasma – Mass Spectrometry
ICP-OES	Inductively Coupled Plasma – Optical Emission Spectrometry
ISA	International Seabed Authority
J_{DGT}	The interfacial porewater metal flux into the DGT device.
LBC	Lethal Body Concentration

LC_{50}	Lethal Concentration 50. The concentration of metal lethal to 50% of test population.
LOI	Loss on Ignition. A highly-correlated measure of sediment TOC derived using weight loss from ashing dried sediment at 400 ^{o}C for 24 hrs.
LT_{50}	Lethal Time 50. The median lethal time for a test population exposed to a defined concentration of metal.
Marine	Saline waters. This is used in the thesis to include brackish, coastal and, especially, estuarine systems.
MBR	Methylene Blue Reagent. This denotes Cline's (1969) reagent, which turns blue upon reacting with sulphides.
MDS	Non-metric multidimensional scaling
Metal	This term is used interchangeably with "heavy metal" and "trace metal" in this thesis to incorporate potentially toxic metals and metalloids as reflected in the relevant literature.
Metal speciation	The partitioning of metals in the environment, either as free ions or in complexed, adsorbed, precipitated, or co-precipitated chemical forms (Landner & Reuther, 2004).
MRT	Multivariate Regression Trees
NPOC	Non-Purgeable Organic Carbon. The measure of DOC used in this thesis, which is derived after acidifying samples with 10% HCl and purging with purified air to remove inorganics.
NRC	National Research Council, Canada
OC	Organic Carbon
OLW	Overlying water
ORP	Oxidative-Redox Potential. This is mainly referred to as Redox Potential in this thesis.
PCA	Principal Components Analysis
PES	Polyethersulphone
PICT	Pollution-Induced Community Tolerance
PW	Porewater or interstitial water

Regulation	The setting and/or enforcement of regulatory provisions against metal contamination in order to protect biodiversity.
sBLM	Sediment Biotic Ligand Model
SED	Sediment Column
SEM	Simultaneously-Extracted Metals. This is the same measure as AEM in this thesis, but refers to the fraction of metals in the sediment liberated during the measurement of AVS.
SIMPER	Similarity Percentages
SQGs	Sediment Quality Guidelines. This is used to include other regulatory provisions for sediment quality, such as Criteria, Standards, or Environmental Benchmarks, with or without enforcement penalties.
SWI	Sediment-Water Interface
TOC	Total Organic Carbon in the sediment phase.
Toxicity	The tendency of a metal to cause harm, defined by established ecological endpoints, such as death and impairment of growth and reproduction. Metal toxicity begins when an organism's rate of uptake exceeds its combined rate of excretion and detoxification (Rainbow, 2002).
TRA	Tissue Residue Approach
Uptake	The introduction of metals into an organism's body, without regard to subsequent storage, metabolism, and/or excretion (Blowes *et al.*, 2003). This occurs through various routes, e.g. the body surface (i.e. metals present in the surrounding environment) or gut (i.e. metals present in the diet).
UPW	Ultrapure water
USEPA	United States Environmental Protection Agency
USGS	United States Geological Survey
WFD	Water Framework Directive (2015) legislation
XRF	X-ray Fluorescence

ACCOMPANYING MATERIAL

Accompanying this thesis are the following:

1. 3-D models of the DGT probes and gel cutters used in Chapter 3. The models are also available for download via the following link: tiny.cc/dgtmodels

2. Codes for a "global.best" function written in the R programming language to perform BIO-ENV analysis (Clarke & Ainsworth, 1993) and test its significance using the associated Global Best test (Clarke *et al.*, 2008). The function requires the following existing packages in R: vegan, ggplot2, svglite, MASS, grid, and ggthemes. It is available for download via the following link: tiny.cc/GlobalBestR

3. Codes for a "global.BVstep" function written in the R programming language to perform the BVStep (option of the BIOENV) analysis (Clarke & Warwick, 1998) and test its significance using the associated Global Best test (Clarke *et al.*, 2008). The function is robust, taking inputs for a fixed matrix (which can be species or environmental data), a variable matrix (which can also be species or environmental data), a fixed matrix distance method (any of the distance measures in the "vegan" R package), and a variable matrix distance method (again as in "vegan"). This means that BIO-BIO, ENV-BIO, BIO-ENV, and ENV-ENV analyses (see Clarke *et al.*, 2014) can be performed and their significance tested using the Global Best method. The function requires all the packages listed for the "global.best" function above and uses the "BVstep" source code for the "sinkr" package (Taylor, 2017). It is available for download via the following link: tiny.cc/GlobalBVstepR

DEDICATION

In memory of

Dear Mum
Ngozi Udochi
Nov 1965 – Jun 2019

Dear friend
Ngozi Ogbonnaya
Jan 1990 – May 2017

ACKNOWLEDGEMENTS

God has been extremely good to me, and my heart is filled with gratitude!

I thank my supervisors, Prof. Alastair Grant and Prof. Alex Baker, for their "open door" policy, invaluable guidance, and feedback on my work. I am especially grateful to Alastair, my primary supervisor, and consider myself privileged to have been under his tutelage. Also, I thank Dr Paul Somerfield and Dr Trevor Tolhurst for their excellent review and feedback.

I thank the technical team in ENV for their wonderful support. Amongst others, Mr. Simon Ellis was helpful in the several trips to Cornwall, Gt. Yarmouth, and the North Norfolk Coast. Mr. Graham Chilvers helped in the ICP-OES and ICP-MS analyses. And Mr Bertrand Leze helped in the XRF analysis. The DGT probes in Chapter 3 were designed and 3-D printed by Dr. Stephen Laycock of the School of Computing Sciences, UEA.

I am indebted to my parents, Mr & Mrs Sunday Udochi. It is for their incredible vision and hard work that I am educated up to this level, today. I also thank the rest of my family, relatives, and friends for their continuous support and encouragement.

I thank my Norwich families for their kindness, hospitality, and care. They made me a home away from home: Dr. Hussein Aldosari and his family, Pst. Chioma and Dr. Jonathan Onyeme, Mr. Augustine Edema and his family, Mr. Gabriel Okorie and his family, Mr. Gallab Alotaibi, and Mr. Hamdan Alzahrani. I also thank Dr Elizabeth Duxbury and Dr Agatha Nthenge, amongst other office colleagues, for the helpful discussions and advice.

I thank all tutors and lecturers who have been instrumental in my progress, so far. Especially, Prof. Solomon Umeham at Abia State University shaped my interest in the Environmental Sciences. Dr. Debapriya Mondal and Dr. Chiara Benvenuto supervised my MSc dissertation at the University of Salford. My interest in Marine Ecotoxicology is credit to their tutelage, dedication, and exciting field trips to the Mersey Estuary. Dr Habibat Chahul's Chemistry classes at F.G.C. Odogbolu were invaluable. Mr. Victor Esiekpe's lessons at Heroes were an important foundation. And Mr. Paul Nwokolo mentored me at the Bestway Academy.

Lastly, I thank the management of Abia State University for granting me study leave to complete this work. Late Prof. Kalu M. Kalu approved my leave, as H.O.D., and was an incredible pillar for me. May his memory remain evergreen!

Solomon C. Udochi was a Commonwealth Scholar, funded by the UK government.

Chapter 1.

Predicting metal bioavailability and toxicity in marine sediments: the journey thus far

1.1 Introduction

Detrimental ecological risks posed by the presence of heavy metals in elevated concentrations has led to their regulation in marine and estuarine sediments (Simpson & Batley, 2007; Burton, 2010; Chapman, 2018). So far, several regulations in the form of guideline values, criteria, or standards (but jointly referred to as sediment quality guidelines, SQGs, in this work) have been devised as threshold exposure concentrations to protect aquatic organisms (e.g. Burgess *et al.*, 2013; Long *et al*., 1995; MacDonald *et al.*, 1996; Simpson *et al.*, 2013; Water Framework Directive [WFD], 2015). The SQGs are developed from the predicted relationship between sediment contamination (as a measure of organism exposure) and toxic response. They often inform the official designation of contaminated sediments as well as remediation and/or removal of the same (Burton, 2002; Birch, 2018).

Despite advances in the development of SQGs, there is still considerable uncertainty in the scientific literature about metal concentrations that can result in ecological effects. Many of the currently available SQGs are based on the total concentration of metals in the sediment (Burton, 2002, 2010; Simpson & Batley, 2007). However, it has been shown that due to a combination of several factors – including the occurrence of metal speciation, the temporal and spatial variability in sediment physicochemical properties, as well as the variability in organism physiology and feeding behaviour – only a fraction of metals present in sediments is available to interact with and elicit toxicity to biota (Chapman *et al.*, 1998; Simpson & Batley, 2007; Burton, 2010). Consequently, the total concentration of metals in the sediment may not be reflective of their bioavailability to inhabiting organisms, and SQGs based on this measure are at considerable risk of false-positives.

In view of the foregoing, SQGs would ideally be based on the bioavailable metal fraction in the sediments. However, exactly what fraction or measure of metal concentration is best predictive of ecological effects in the field is yet unknown and has been an enduring subject of research (Tessier & Campbell, 1987; Luoma, 1989; Ankley *et al.*, 1996; Simpson & Batley, 2007; Vaananen *et al*., 2018). The current thesis explores this research gap,

motivated by the need to develop SQGs that are more reliable. The literature review in this chapter addresses metal speciation, bioavailability, and approaches to the prediction of bioavailability and toxicity in marine systems, with emphasis on sediments. For clarity, the term "marine" is used in this thesis to include brackish, coastal, and especially estuarine systems, where the majority of research on this topic has focussed. In addition, the term "metal" is used interchangeably with "heavy metal" and "trace metal" to incorporate potentially toxic metals and metalloids as reflected in the relevant literature. Focus throughout the thesis is on the five common divalent metals, Cd, Ni, Pb, Zn, and especially Cu, which have been identified as priority contaminants in several existing regulations.

1.2 Metal partitioning and speciation in aquatic systems

Research in field-contaminated aquatic systems has long demonstrated that metals do not only exist as free ions, but also in various combined chemical forms or species (Allen *et al.*, 1980; Luoma & Bryan, 1981; Morel, 1983; Luoma, 1985). Upon discharge from a source, the metal is first partitioned between the solid and dissolved phases (Luoma & Rainbow, 2008). Partitioning of dissolved metals to the solid phase may be by direct binding to suspended particles or non-living organic matter, which eventually settle to the sediments as metal sources therein. Partitioning may also be by uptake and metabolism by pelagic organisms, which upon their death also settle to the sediments. Ultimately, the sediments act as a sink for metals, accumulating relatively high metal concentrations that may be later re-suspended with particles to the overlying water (e.g. by bioturbation or tidal currents), dissolved in the interstitial (henceforth, pore) water, or remain bound in exchangeable or mineral solid phases (Salomons *et al.*, 1987; Cooper & Morse, 1998; Luoma & Rainbow, 2008; Tercier-Waeber & Taillefert, 2008).

Figure 1.01 below shows the potential sources of metals to aquatic systems and their subsequent partitioning and speciation. Within each phase – solid or dissolved – there is further speciation of metals between specific ligands. Speciation is determined by several factors, including concentration of the ligands, strength of each metal-ligand association, and physicochemical characteristics of the medium, such as temperature, pH and redox potential (Luoma, 1985; Luoma & Rainbow, 2008; Zhao *et al.*, 2016). Metals can exist in the dissolved phase as hydrated free ions or become associated in complexes with negatively-charged inorganic (e.g. chloride, hydroxyl, or carbonate) or organic (e.g. humic acids, fulvic acids, and natural organic matter) ligands (Luoma & Rainbow, 2008; Zhao *et al.*, 2016). The

metal ions may be present in different oxidation states with different reactivity – for example, Fe(II) and Fe(III), Cu(I) and Cu(II), and Mn(II) and Mn(IV) (Landner & Reuther, 2004; Luoma & Rainbow, 2008). In the analysis of water samples, "dissolved" metal is usually operationally defined as that which passes through a 0.45 µm membrane filter (Landner & Reuther, 2004). However, some of this metal will be bound into colloidal complexes, particle sizes between 1 nm and 0.45 µm (Tercier-Waeber & Taillefert, 2008; Aiken *et al*., 2011), rather than being "dissolved" in a physicochemical sense.

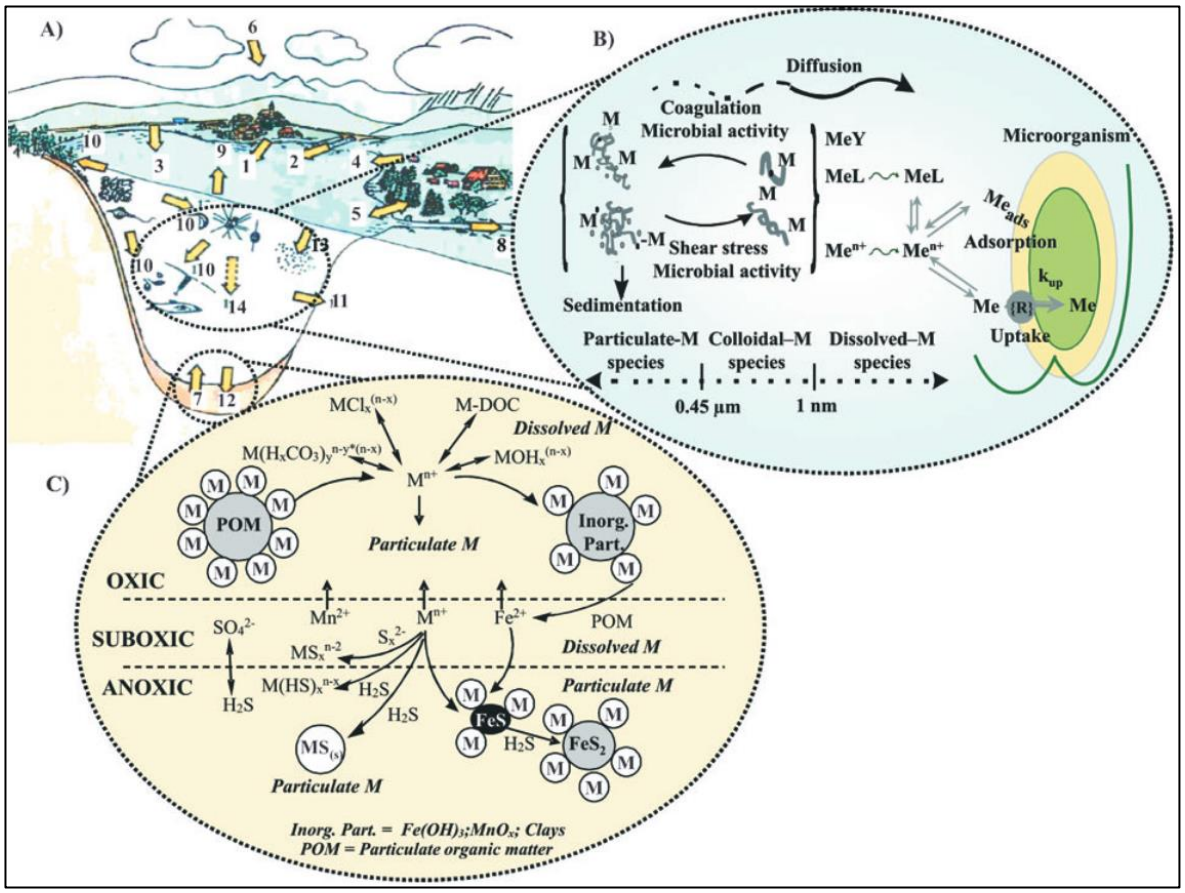

Fig. 1.01: Schematic representation of metal flux to aquatic ecosystems (A) and speciation in the water column (B) and sediments (C). 1 – 8 represent metal influx from (1) water treatment, (2) tributaries, (3) roads, (4) soils, (5) groundwater, (6) atmospheric deposition, (7) sediments, and (8) effluent discharge. 9 – 14 represent metal efflux by (9) evaporation, (10) organism uptake, (11) infiltration into groundwater, (12) reaction in the upper sediment layers, (13) adsorption to suspended matter, and (14) sedimentation, respectively (Republished with permission of the Royal Society of Chemistry, from Tercier-Waeber & Taillefert, 2008)

In the sediments, metals exist as complexes with organic matter, complexes with Fe and Mn (oxy)hydroxides and sulphides, depending on the redox stratification, as well as in exchangeable fractions or bound in the crystal structure of the sediment particles (Tessier *et al.*, 1979; Luoma & Rainbow, 2008; Tercier-Waeber & Taillefert, 2008). Sequential and/or other chemical extraction procedures have been used to operationally define these different metal forms. The sequential extraction procedure was first described by Tessier *et al.* (1979). Using different extractants, Tessier and co-workers were able to separate sediment metals into five fractions: (i) exchangeable metals – are adsorbed onto particulates and easily accessible to organisms, (ii) metals bound to carbonates – can be precipitated at acidic pH, (iii) metals bound to Fe- and Mn-oxides – are sensitive to redox changes in the sediments, (iv) metals bound to organic matter – are only available to organisms after oxidation of the organic matter, and (v) the residual metals – are embedded in the crystal lattice of sediments and permanently inaccessible to organisms. The sequential extraction procedures have since undergone several modifications to improve phase selectivity and reproducibility (see review by Bacon & Davidson, 2008), albeit with limited success.

1.3 Metal bioavailability

1.3.1 The concept of bioavailability

It is well acknowledged in the scientific literature that the total concentration of metals in aquatic systems is not a good predictor of toxicity (Tessier & Campbell, 1987; Di Toro *et al.*, 2005; Simpson & Batley, 2007; Burton, 2010; Zhang & Davison, 2015). This is because only a fraction of the total concentration of metals is readily available to interact with and be taken up by organisms. That exact fraction will depend on several geochemical and biological factors including the speciation of the metals in the medium, the physicochemical properties of the medium, and the behaviour of the organism (Section 1.3.2). Even when taken up by biota, metals, depending on their metabolic role, may be available for body metabolism and/or cause toxicity, may be bound in an insoluble, and therefore detoxified, form, or may be excreted by the organism (Rainbow, 2002, 2007). Figure 1.02 below is a representation of this metal partitioning in the body of a typical decapod crustacean. Toxicity would therefore reflect the availability of a metal in an environmental medium and the potential organism-specific uptake, metabolism, and detoxification or excretion.

"Bioavailability" (or biological availability) denotes the proportion of metals which is available to cause harm. As toxicity results from a complex interplay of various chemical

and biological factors, the term is challenging to define and to measure. The term may include the physicochemical availability of metals in the environment, the actual demand by biological organisms, and/or the toxicological behaviour of accumulated metals in the organisms (Landner & Reuther, 2004; Luoma & Rainbow, 2008).

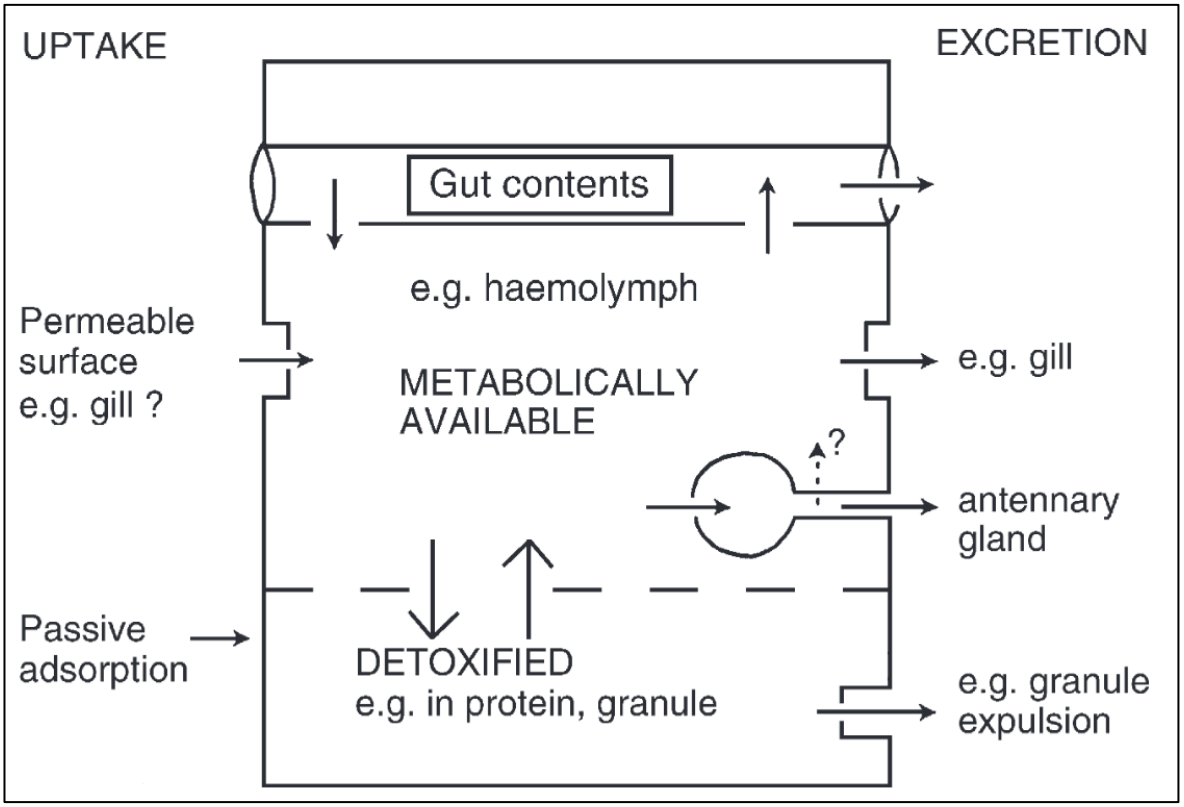

Fig. 1.02: Schematic representation of metal accumulation in a decapod crustacean (Republished with permission of Elsevier Science & Technology Journals, from Rainbow, 2007)

1.3.2 Factors affecting metal bioavailability and toxicity

1.3.2.1 Organism behaviour and physiology

Benthic organisms are exposed to metals in the dissolved and particulate phases. Exposure to dissolved metals is primarily through the epithelial uptake of metals in the porewater, burrow water, and/or overlying water, whereas exposure to the sediment phase is primarily through the ingestion of food or sediment (Wang & Fisher, 1999; Lee *et al.*, 2000a; Campana *et al.*, 2012; Wang, 2013a). Metal accumulation, thus toxicity, would be influenced by

uptake from either route (DeForest & Meyer, 2015) as well as the partitioning of accumulated metal into metabolically-available or detoxified forms (Rainbow, 2002, 2007).

An organism's feeding and burrowing behaviour has been shown to influence the proportional uptake from either of the metal phases. For example, sediment ingesters (also called deposit feeders) such as the clam *Macoma balthica* appear to accumulate metals primarily from sediment-bound forms, rather than the dissolved phase (Lee *et al.*, 2000a; Griscom & Fisher, 2004). However, depending on the degree of contact with the sediments, suspension feeders such as mussels and copepods may be exposed to an equal measure of, or more, metals from the dissolved than the sediment phases (Bervoets *et al.*, 2005; DeForest & Meyer, 2015; Kadiene *et al.*, 2019).

Other biological factors influencing metal toxicity may include the life stage, exposure history, and type and availability of metal transport process as well as the metabolism of accumulated metals by the organism (Luoma, 1989; Rainbow, 2007). As earlier highlighted, metal metabolism is an important consideration. Benthic invertebrates vary in their metal tolerance thresholds, depending on their ability to regulate body concentrations of certain metals or store other metals in detoxified forms (Rainbow, 2002, 2007).

1.3.2.2 Metal partitioning in the sediment

Aquatic sediments serve as a sink for heavy metals and a source of exposure to benthic organisms (Salomons *et al.*, 1987; Luoma & Rainbow, 2008). As metals partition between phases in the sediments, benthic organisms are exposed to metals in a variety of forms. The bioavailability of sediment-bound metals is linked to their partitioning into the different sediment phases (Luoma & Bryan, 1981; Tessier *et al.*, 1984; Burton, 2010).

Despite substantial research linking metal speciation with bioavailability, it remains unclear exactly what metal species are bioavailable. The Free Ion Activity Model (discussed in more detail in Section 1.4.2) relates metal uptake and toxicity in the dissolved phase with the activity of free metal ions (Morel, 1983). However, this does not imply that only the free ions are taken up by biota. For example, where the uptake flux of an organism is greater than the supply of free ions by diffusion, weakly-bound (also known as "labile") metals, such as those bound to chlorides, may dissociate from their complexes to contribute to this flux (Fortin & Campbell, 2000; Zhao *et al.*, 2016), and hence become bioavailable. Also, metal ions in low molecular weight organic complexes have previously been observed to

contribute to toxicity to aquatic biota (see review by Luoma, 1983). On the contrary, metals in sulphide, (oxy)hydroxide, and/or larger organic complexes are believed to be too tightly-bound to contribute to organism uptake flux and/or too large to permeate membrane surfaces or bind with receptors (Di Toro *et al.*, 2005; Amiard *et al.*, 2007; Zhao *et al.*, 2016). Consequently, these complexes are not considered bioavailable. Complexation would, overall, be expected to reduce the bioavailability of metals.

Sediment ingesters, by the action of digestive juices in their guts, are additionally exposed to otherwise tightly-bound sediment metals (Griscom & Fisher, 2004). Although gut extraction is challenging to replicate, several studies have attempted to extract sediment with digestive juices and body fluids (e.g. Chen & Mayer, 1999; Yan & Wang, 2002; Peng *et al.*, 2004). These studies reveal that the availability of metals in ingested sediment would depend on the strength of the digestive fluid and the sediment gut retention time, which may differ significantly between species.

1.3.2.3 Sediment grain size

The sediment grain size may be an important influence on the bioavailability of metals. Finer grain sediments such as silt and clay have higher affinity for metals and particulate organic carbon due to their higher surface area/volume ratio and increased surface charge (Ackermann, 1980; Birch, 2003). Therefore, for a particular volume of ingested sediment, deposit feeders inhabiting fine-grain sediments would be expected to have higher dietary exposure to metals than the organisms in coarse sediments, typically of lower metal concentrations. However, for suspension feeders or epibenthic invertebrates, the low metal binding capacity of coarse sediments may lead to higher porewater concentrations in contaminated systems, thus increasing the likelihood of metal toxicity (Strom *et al.*, 2011).

1.3.2.4 Other sediment physicochemical properties

Oxidation-reduction potential (ORP, henceforth redox potential), pH, salinity, organic matter content, and temperature have been recognised as critical physicochemical factors influencing the partitioning and, ultimately, bioavailability of metals in sediments, especially in the dissolved phase (see Luoma, 1983; Elder, 1988; Chapman & Wang, 2001; Zhang *et al.*, 2014 and citations therein for details).

In summary, ORP reflects the presence of oxygen in the sediments and controls the availability of some ligands for metal complexation. An increase in sediment ORP would

increase the rate of oxidation of sulphides and organic compounds and prompt the release of complexed metal ions, which would be expected to enhance metal bioavailability (also see Ankley *et al.*, 1996). In oxic sediments, however, Fe and Mn (oxy)hydroxides are present, potentially increasing metal complexation and ultimately reducing bioavailability (also see Di Toro *et al.*, 2005; Section 1.4.3.3). An increase in pH enhances the precipitation and complexation of metal ions, resulting in a decrease in metal bioavailability. Increased salinity and (dissolved or particulate) organic matter content would increase the availability of reactive ligands such as chloride ions and humic acids, potentially increasing metal complexation and decreasing metal bioavailability to biota (Bryan & Hummerstone, 1971). The effect of temperature may vary with the chemistry of the sediment and the nature of organisms present. Temperature changes might influence the rates of sensitive chemical reactions in the dissolved phase or indirectly influence sediment pH or ORP. Furthermore, an increase in temperature within a species-specific tolerable range may result in an increase in key biological processes such as metal uptake and efflux rates in aquatic organisms, thereby influencing accumulation and toxicity in such species (e.g. Mclusky *et al.*, 1986).

1.4 Approaches to predicting metal bioavailability and toxicity in sediments

1.4.1 Chemical extraction techniques

The partitioning of metals in sediments will influence their bioavailability. Whilst models have been more recently developed to estimate this partitioning (e.g. Tessier & Campbell, 1987; Wood *et al.*, 1995), chemical extraction remains widely used for this purpose – and to a greater extent in the assessment of metal bioavailability (Luoma & Bryan, 1981; Chapman & Wang, 2001; Bacon & Davidson, 2008). Tessier *et al.*'s (1979) sequential extraction procedure using magnesium chloride, sodium acetate, sodium dithionite, nitric acid, and a hydrofluoric–perchloric acid mixture, and subsequent modifications, has been mentioned earlier in this chapter. Extractions involving concentrated or dilute forms of strong and weak acids (such as hydrochloric acid and acetic acid) as well as other compounds, including ammonium acetate and sodium hydroxide, have also been previously reported in the literature (Luoma & Bryan, 1981; Chao & Zhou, 1983).

Earlier research on the bioavailability of sediment-bound metals involved treating sediments with the various chemical extractants and then relating measured concentrations with metal bioaccumulation in sediment biota (see Tessier & Campbell, 1987; Luoma, 1989; Bryan & Langston, 1992; Luoma & Rainbow, 2008 for reviews). Although mainly comparing grossly

contaminated estuaries with less contaminated ones, these studies overall suggest that metal measurements in sediment extracts using dilute or weak extractants, especially 1 M HCl, better predict metal bioaccumulation in benthic invertebrates than the total metal concentration in the field. Metal concentrations in 1 M HCl extracts have also shown good correlations with bioaccumulation by benthic fauna in spiked sediments (e.g. Amato *et al.*, 2015; Belzunce-Segarra *et al.*, 2015). Other recent studies (e.g. Amiard *et al.*, 2007) have attempted to estimate "labile" sediment fractions by combining the percentage desorption of metals in a weak acid with the total metal concentrations measured in strong acid extracts.

The suitability of chemical extraction techniques in predicting metal bioavailability will depend on several factors including the physiology and feeding behaviour of the organism as well as the geochemistry of the sediment. Deposit feeders, for example, differ from filter feeders with respect to their major uptake route, the latter being mainly exposed to metal in porewater (see Section 1.3.2.1). Furthermore, strong acids can potentially extract less-labile sediment phases such as metal sulphides, where present (Allen *et al.*, 1993; Cooper & Morse, 1998; also see Section 1.4.3.2). There are also criticisms surrounding the lack of reproducibility of some extraction procedures (Martin *et al.*, 1987; Nirel & Morel, 1990; Bacon & Davidson, 2008), especially amongst geochemically dissimilar samples (Luoma, 1989; Whalley & Grant, 1994).

1.4.2 The Free-Ion Activity Model (FIAM)

The Free-ion Activity Model (FIAM) applies mainly to bioavailability in the water column, but it is now widely considered to apply also to the dissolved phase in sediments and soils (Chapman *et al.*, 1998; Zhao *et al.*, 2016). The model was described by Morel in 1983 based on the results of earlier experiments (Anderson & Morel, 1978; Anderson *et al.*, 1978) comparing dose-response curves for Cu and Zn toxicity using total metals and metal ion activity in the presence of organic chelators such as EDTA. The model hypothesises that rather than total concentrations, the free ion activity of a metal in the dissolved phase would determine its biological effects. The key assumption is that the occurrence of physiological effects is a reflection of metal binding to specific receptor sites on an organism and is determined by the activity of the metal, which is in turn determined by its free ion activity in the bulk water (Morel, 1983).

The FIAM has since formed the consensus for the assessment of bioavailability based on the speciation of dissolved metals in aquatic systems. However, a number of exceptions have

been observed where free metal ions do not solely influence metal uptake or toxicity (see Brown & Markich, 2000; Batley *et al.*, 2004; Zhao *et al.*, 2016 for detailed review). Briefly, metal complexes around an organism may dissociate and contribute to the uptake flux where the rate of uptake by an organism is rapid compared to the rate of supply of metal ions by diffusion from the bulk solution. In addition, metal complexes may directly bind to receptor sites or be taken-up by passive, rather than active, diffusion.

1.4.3 Equilibrium partitioning approaches

1.4.3.1 The use of porewater metal concentrations

The Equilibrium Partitioning (EqP) approach stemmed from early observations of strong correlations between contaminant concentrations in the porewater and observed biological effects. Adams *et al.* (1985) first made these observations using kepone, a non-ionic organic pesticide, where observed effects were consistent across sediments with varying properties when toxicity was related to porewater concentrations. This was then followed by similar observations with heavy metals, involving Cd toxicity to the marine amphipod, *Rhepoxynius abronius* (Swartz *et al.*, 1985; Kemp & Swartz, 1988).

The observed correlations between porewater metal concentrations and toxicity to biota were rationalised in what became known as the EqP – that contaminants partition in equilibrium between the porewater, different sediment phases, and organisms, and that biological effects are a result of the chemical activity of the single phase or the equilibrated system (Di Toro *et al.*, 1991). The assumptions of this model are detailed in Chapter 5 of this thesis. SQGs were consequently developed and proposed based on the normalisation of sediment concentrations (the SEM - AVS approach - discussed in more detail in Section 1.4.3.2) or on the measurement of porewater concentrations (Ankley *et al.*, 1996).

1.4.3.2 The SEM - AVS approach

For cationic metals (specifically Cu, Cd, Ni, Pb and Zn), acid volatile sulphide (AVS, mainly FeS) was identified as a key partitioning phase influencing toxicity in anoxic sediments (Di Toro *et al.*, 1990, 1992). AVS binds the metal ions on a molar basis to produce insoluble sulphides with minimal biological availability, and it is operationally defined as the sulphide released from the treatment of wet sediment with 1 M HCl (Allen *et al.*, 1993; Ankley *et al.*, 1996). Di Toro and co-workers (1990, 1992) were able to show that when molar AVS concentration is in excess of the sediment metal concentrations expressed in molar terms as

Simultaneously Extracted Metals (SEM), toxicity to biota would not occur. This finding (also referred to as the SEM - AVS approach) was later confirmed for a wide range of test organisms and extended to include metal mixtures by summing the SEM concentrations (see Hansen *et al.*, 1996 for review). The EqP model forms the basis for some of the most advanced sediment regulatory guidelines currently available (e.g. Burgess *et al.*, 2013).

One limitation of the SEM - AVS approach relates to its applicability in oxic or sub-oxic conditions. By allowing the inflow of oxygen-rich overlying water, many benthic invertebrates create sub-oxic or entirely oxic conditions in their burrows within sulphidic sediments (Forster, 1996; Gallon *et al.*, 2008). Under these conditions, AVS tends to be oxidised, releasing previously bound metals (Simpson *et al.*, 2012a; Remaili *et al.*, 2018), and hence are no longer key metal-binding phases as assumed by the model. Fe and Mn (oxy)hydroxides as well as organic carbon are believed to more actively bind metals in oxic sediments (Chapman *et al.*, 1998; Di Toro *et al.*, 2005).

Another important limitation of the SEM - AVS approach is in its ability to predict only non-toxicity. When molar concentrations of AVS is greater than (the sum of) SEM, the metals are all predicted to be bound in insoluble sulphides, therefore are not expected to elicit toxicity. However, in the reverse situation where molar SEM concentration is greater, toxicity does not always ensue (Ankley *et al.*, 1996). This is linked to the presence of other important metal-binding phases such as organic carbon, Fe and Mn (oxy) hydroxides not accounted for by the approach. The application of relevant sediment normalisations for organic carbon has been proposed (Di Toro *et al.*, 2005; also see Section 1.4.3.3), albeit with limited success in its application (Simpson & Batley, 2007; Burton, 2010). Hence, SQGs based on the SEM/AVS approach are thresholds that at best can screen-out sediments not likely to elicit acute toxicity, but above which more site-specific risk assessments are required to establish safe levels. The application of the EqP to deposit feeders is investigated in Chapter 5 of this thesis.

1.4.3.3 The Biotic Ligand Model (BLM) and Sediment Biotic Ligand Model (sBLM)

The most recent modification of the SEM - AVS EqP approach is the Sediment Biotic Ligand Model (sBLM) (Di Toro *et al.*, 2005). The sBLM seeks to address some of the limitations of the SEM - AVS approach by incorporating it with an already existing Biotic Ligand Model (BLM) for aquatic organisms.

On its own, the BLM (Di Toro *et al.*, 2001) relates to the uptake and ultimate toxicity of dissolved metals in the overlying water. It is an extension of the FIAM. In addition to the binding of potentially toxic metal ions to receptors (the biotic ligand) on the body surface of an organism, the BLM considers competition between the toxic metal ion and other metal ions as well as competition between the biotic ligand and other aqueous ligands present in the surrounding water. The model assumes that metal ions, metal-ligand complexes in the water, and metal-biotic ligand complexes are in chemical equilibrium. It predicts that toxicity would occur as free metal ions bind to the biotic ligand, reaching a threshold metal ion-biotic ligand concentration. This threshold metal-biotic ligand concentration, the model predicts, can be estimated from biotic ligand site densities, metal-ligand stability constants, and the aqueous LC_{50} metal concentrations.

The sBLM uses the BLM to estimate the porewater LC_{50} that results in a metal concentration at the biotic ligand that can cause 50% mortality to a particular species. It then uses the EqP approach to calculate the sediment metal concentration equivalent to this porewater concentration (Di Toro *et al.*, 2005). In estimating this sediment metal concentration, the sBLM further extends the SEM - AVS approach to include partitioning to organic carbon and gives provisions for the partitioning to other major sediment phases, if practicable (Di Toro *et al.*, 2005). The various complexes and considerations of the sBLM are represented in Figure 1.03. By accounting for partitioning to other sediment phases in addition to the effect of AVS, and further considering binding to biotic ligands in the organism, the sBLM can theoretically predict direct effects in metal-contaminated sediments rather than lack of toxicity as in the original SEM - AVS approach.

Despite their success in predicting acute toxicity, the BLM and sBLM have several limitations (see Slaveykova & Wilkinson, 2005; Campbell *et al.*, 2006; Simpson & Batley, 2007 for detailed reviews). Amongst others, the models have a limited scope, as biotic ligands and other key partitioning coefficients are organism-specific and have only been estimated for a small number of species. The models are also based on data compiled mainly from laboratory toxicity studies using spiked sediments or water, which may not be representative of field conditions. Inadequately-equilibrated spiked sediments bias metal partitioning, resulting in higher porewater metal concentrations than obtainable in field-contaminated sediments (Lee *et al.*, 2000a, b; Hill *et al.*, 2011). Moreover, environmental risk assessment is now more focused on chronic, rather than acute, toxicity which is manifested at environmentally-realistic exposures (Vangheluwe *et al.*, 2013; Wang, 2013a).

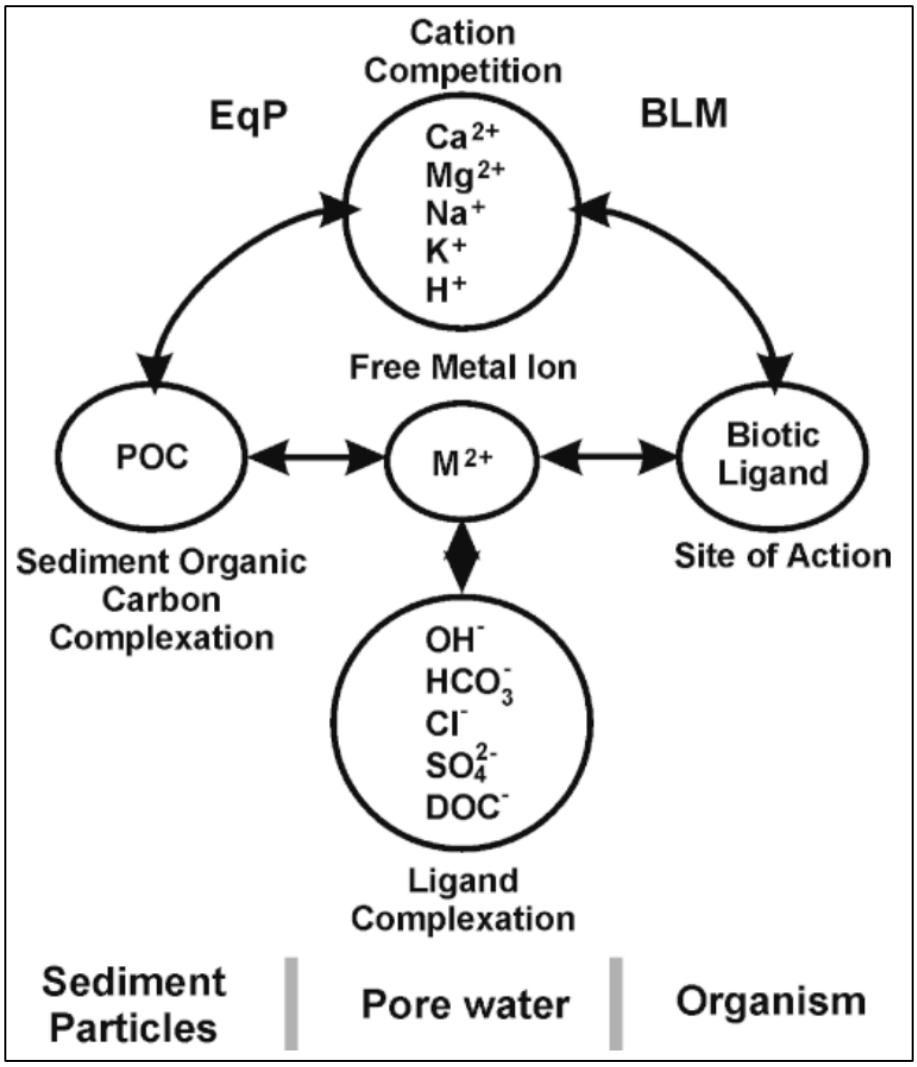

Fig. 1.03: Schematic representation of the Sediment Biotic Ligand Model (sBLM), combining the existing Equilibrium Partitioning (EqP) model for sediment toxicity and the BLM for dissolved metal toxicity. POC = particulate organic carbon; DOC = dissolved organic carbon; HCO_3^- = bicarbonate; OH^- = hydroxide; Cl^- = chloride; SO_4^{2-} = sulphate (Republished with permission of John Wiley & Sons - Books, from Di Toro *et al.*, 2005)

1.4.4 Metal bioaccumulation and the Tissue Residue Approach (TRA)

Metal bioaccumulation in invertebrates has long been used as an indication of exposure and bioavailability in the sediments. Studies relating chemical concentrations of metals in sediments to their bioavailability in sediment biota have earlier been alluded to (see Section 1.4.1). These studies measured accumulated concentrations in certain tissues or in the whole body of several invertebrates and related them with chemical measurements in the sediments. Strong correlations were observed between sediment and body metal concentrations, albeit

stronger for certain "sentinel" species, which were consequently projected as useful biomonitoring tools. At present, models have been developed to estimate metal bioaccumulation in aquatic organisms (e.g. biodynamic model by Luoma & Rainbow, 2005). The use of biomarkers (i.e. substances produced in response to contaminant exposure) such as metallothionein has also been proposed as an approach to monitoring the effects of metal pollution (see reviews by Monserrat *et al.*, 2007; Burton, 2010). The measurement of metals in body fluids (e.g. Tan *et al.*, 2013) has been further proposed.

Following observed correlations between body and sediment metal concentrations, it was conceived that body concentrations were reflective of metal exposures in organisms and could be used in the prediction of toxicity, potentially circumventing the challenge of speciation in sediments. This approach became known as the Tissue Residue Approach (TRA) (Adams *et al.*, 2011), or more commonly, the Critical Body Residue (CBR) and the Lethal Body Concentration (LBC) (Borgmann, 2000, 2003; Borgmann *et al.*, 2001). The key assumption was that the accumulated concentration of metals was indicative of dose to the organism, and that toxicity occurs when a threshold – the "critical" – body concentration is exceeded. Borgmann and co-workers (see above citations) were able to apply the TRA in predicting toxicity to the amphipod *Hyalella azteca*, amongst other organisms in lake sediments, as well as in developing sediment quality guidelines.

Despite the seeming success of the TRA and similar approaches, several limitations exist. One limitation is the possible influence of organism sex, size, and gut sediment contents, amongst others, on body concentrations of some benthic invertebrates (Bryan & Hummerstone, 1971; Chapman, 1985; Tessier & Campbell, 1987; Gillis *et al.*, 2005; Beltrame *et al.*, 2010). Therefore, a group of individuals of the same species may be exposed to the same level of metals in the sediments, but differ markedly in accumulated concentrations as a result of factors which may be unrelated to bioavailability.

Another important limitation of the TRA approach is the difference in metal accumulation strategies in aquatic invertebrates within and between taxonomic groups (Bryan & Hummerstone, 1971; Rainbow 2002, 2007). Earlier alluded to, certain organisms are able to regulate their body concentrations of essential metals by excretion, such that increasing metal exposure does not reflect in whole-body burdens until a threshold is exceeded. Some organisms are also able to store certain metals in detoxified forms, which contribute to the overall body concentration but not to toxicity. Taken together, these observations suggest

that body concentrations may not accurately reflect metal exposure, bioavailability or toxicity in some species. These limitations complicate the applicability of the TRA and similar approaches. And in several instances where applied (e.g. Casado-Martinez *et al.*, 2010 and articles cited therein), the approach has been deemed unsuccessful.

1.4.5 The use of passive sampling techniques

Passive samplers are relatively new techniques in the assessment of metal bioavailability and toxicity in aquatic systems. They range from devices measuring total metal concentrations in the dissolved phase to those based on the exclusive extraction of one or more labile metal forms, including free metal ions (Greenwood *et al.*, 2007; Peijnenburg *et al.*, 2014). As the lability of the metal species influences their bioavailability to aquatic biota (Section 1.3.2.2), some passive sampling techniques measuring labile forms have expectedly shown some success in the assessment of metal bioavailability. This section presents a summary of the passive samplers currently used in sediments and an assessment of their promise in predicting metal bioavailability and toxicity.

1.4.5.1 Porewater peepers

Peepers (also called dialysis cells) were first described by Hesslein (1976), but have undergone subsequent modifications (e.g., Doig & Liber, 2000). The device consists of several small wells filled with deionised water and covered with a semipermeable membrane, through which ions can diffuse from the surrounding porewater until equilibrium is attained. In typical peepers, metal concentrations in a fully-equilibrated device are the same as total concentrations dissolved in the interfacial porewater; however, membrane pore size can be varied to selectively exclude certain complexes based on size fractionation (Teasdale *et al.*, 1995). The equilibration duration, usually one or two weeks, depends on the diffusion coefficient of the metal; the porosity, temperature, and tortuosity (i.e. pore space convolution) of the sediment; the degree of metal sorption to the solid phase; and the design factor of the device – ratio of well volume to the surface area of the exposed membrane (Doig & Liber, 2000; Peijnenburg *et al.*, 2014).

The advantage of peepers is in their ability to sample porewater in a relatively undisturbed state in comparison with the traditional centrifugation techniques (Chapman *et al.*, 2002; Peijnenburg *et al.*, 2014). Peeper-measured porewater concentrations have also been predictive of metal toxicity (e.g. Liber *et al.*, 2011). However, as dissolved metal

concentrations tend to be low, the prior requirement of a pre-concentration phase (Teasdale *et al.*, 1995; Doig & Liber, 2000) makes the use of peepers more challenging in metal analysis. For the devices with relatively large membrane pore sizes, peepers also incorporate large metal complexes, which may not be readily bioavailable. They are therefore considered to be of little use in the direct assessment of metal bioavailability.

1.4.5.2 Diffusive Equilibration in Thin Films (DET)

The Diffusive Equilibration in Thin Films (DET) was first described by Davison and co-workers in 1991 as an upgrade to peepers in the measurement of solute concentrations in waters and sediments. Like peepers, the DET establishes diffusive equilibrium with porewater solutes once deployed in the sediments, albeit with shorter equilibration period, often within few hours. This relatively rapid equilibration is made possible by replacing the peeper cells with a thin film of polyacrylamide gel as the equilibration medium (Davison *et al.*, 1991; Harper *et al.*, 1997).

The use of a thin diffusive film makes DET more portable and, in addition to a purpose-built plastic holder, readily deployable, causing minimal disturbance in sediments. Depending on the pore size of the hydrogel, simple inorganic and smaller organic complexes are able to diffuse through and equilibrate in the gel, leaving out larger organic complexes greater than 10 nm in diameter (Davison & Zhang, 1994; Zhang & Davison, 1999). However, DET equilibrates with the porewater – again usually of low metal concentrations in natural waters – and the accurate determination of this concentration in the gels can be challenging (Peijnenburg *et al.*, 2014) and/or involve complex procedures (Zhang & Davison, 1999). With the subsequent development of the DGT technique (Section 1.4.5.3), there has been limited use of DET in the direct assessment of metal bioavailability. Notably, Gillan *et al.* (2012) found significant positive correlations between DET-measured As, Co, Fe, and Mn concentrations and bacterial biomass in the North Sea. They also found significant positive correlations with bacterial diversity for Co.

1.4.5.3 Diffusive Gradient in Thin Films (DGT)

The Diffusive Gradient in Thin Films (DGT) was first described by Davison and Zhang in 1994 and can be used to measure a wide range of metals in waters, soils, and sediments. Like DET, DGT is based on the diffusion of metals in a polyacrylamide hydrogel. An important distinguishing feature, however, is the presence of a resin gel layer, typically a

polyacrylamide gel impregnated with chelex® beads, which binds and concentrates metal species that diffuse through the diffusive gel. A membrane layer, typically made of polyethersulfone, is placed to screen out particles in the sediments and, together with the diffusive gel, forms the diffusive layer. The arrangement of these layers in an assembled sediment probe is shown in Figure 1.04.

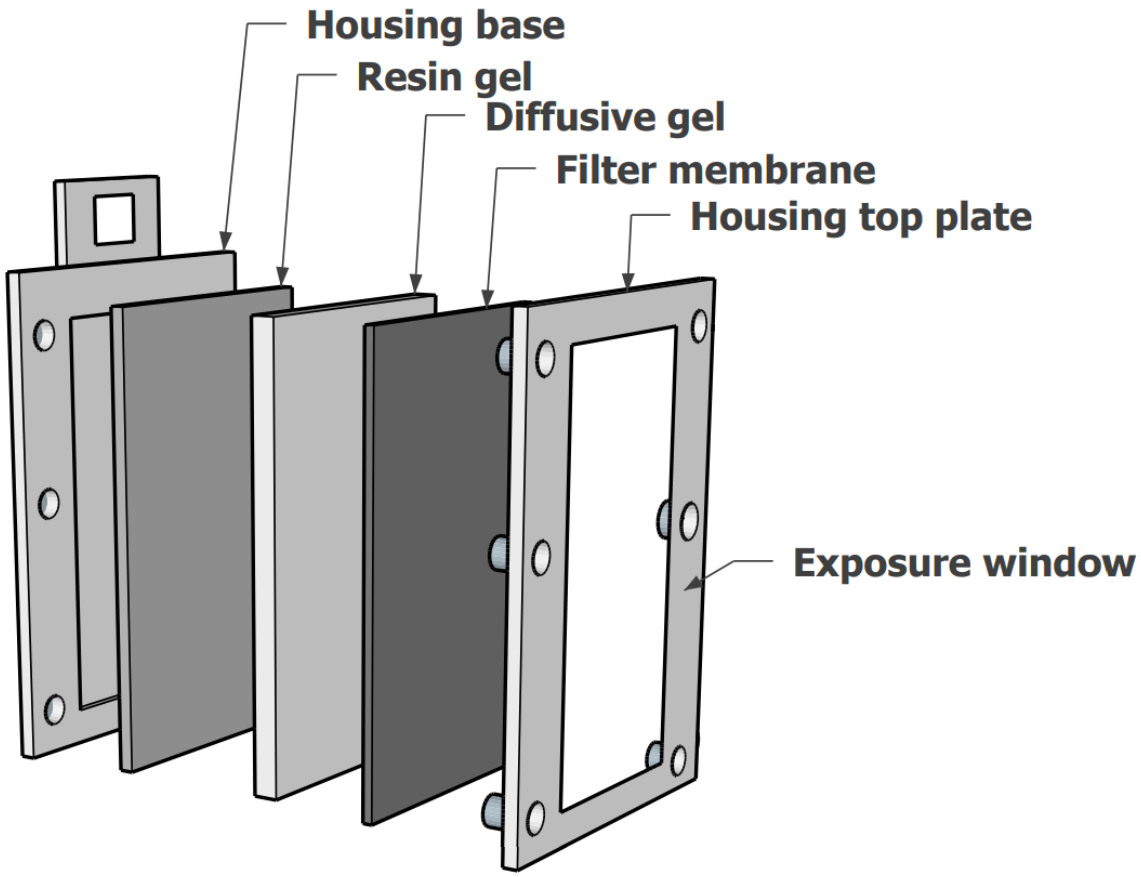

Fig. 1.04: Schematic diagram of a DGT piston assembly. Dimension of the exposure window in the typical probe is 15 cm x 1.8 cm.

DGT is designated as a dynamic technique (Zhang & Davison, 2015). This is because the resin gel rapidly binds free metal ions and actively induces a diffusive flux through the diffusive layer upon deployment in sediments. Diffusion is therefore not passive as in DET and porewater peepers. The rapid removal of metals by the resin ultimately depletes free metal ions at the device interface, extending the diffusion layer for a few millimetres in the sediment. In response, labile species in the adjacent sediment buffer this high demand through desorption from the solid phase and dissociation from complexes in the dissolved phase (Zhang *et al.*, 2002; Lehto, 2016), ultimately contributing to the flux.

An assembled DGT device is portable and typically requires a deployment period of 24 hours (Jolley *et al.*, 2016). The mass of metals accumulated in the resin is proportional to the deployment time and the thickness of the diffusive layer. This mass can be determined by elution in an acid solution and used to extrapolate the time-averaged flux to the device (J) or interfacial porewater concentration (C_{DGT}), using Fick's first law of diffusion (Davison *et al.*, 2012). Equations for the calculation of J and C_{DGT}, as well as an assessment of their predictive capacity of effects in field sediments, are provided in Chapter 3 of this thesis.

The lability of metal complexes to the DGT device would depend on the pore size and thickness of the diffusive layer. The metal complex must be small enough to penetrate the pores of the diffusive gel and to dissociate in the short passage period within the diffusive layer (Zhang & Davison, 1999; Davison *et al.*, 2012; c.f. Puy *et al.*, 2012). There is limited information on the exact pore sizes of the gels used in DGT. However, the typical gel (termed "APA" – made up of polyacrylamide crosslinked with a patented agarose derivative) is believed to allow the diffusion of free metal ions as well as simple inorganic and organic (bound to humic and fulvic substances) complexes of at most 5 – 10 nm in diameter, but restrict larger organic molecules and colloids (Scally *et al.*, 2006; Zhang & Davison, 1999, 2000, 2015). Similarly, a smaller-pored gel ("Restricted Gel" – polyacrylamide crosslinked with bis-acrylamide; pore size ~ 2 nm) has been described to limit the diffusion of most humic and fulvic complexes (Scally *et al.*, 2006; Zhang & Davison, 1999, 2000, 2015). Ultimately, DGT is able to selectively accumulate free metal ions and simple, (DGT-) labile complexes, which may be relevant to aquatic biota.

For its selective measurement of labile metals, the DGT technique has been projected as a useful tool to predict metal bioavailability and toxicity in aquatic systems (Simpson *et al.*, 2012b; Zhang & Davison, 2015). The technique has shown to be successful for some benthic invertebrates in several laboratory experiments or field deployments based on spiked sediments (see Zhang & Davison, 2015; Degryse & Smolders, 2016; Eismann *et al.*, 2020 for reviews). However, more evidence is needed to form any conclusions on the promise of DGT. Only few of these studies have compared the predictive capability of DGT with traditional and/or EqP-based measures of metal concentrations. It is also unclear whether DGT metal uptake is predictive of bioavailability across various organism feeding behaviours. Importantly, most of the studies evaluating DGT have either dosed invertebrates using spiked-sediments, and/or measured metal bioaccumulation as an end-point, and/or assessed acute toxicity in laboratory and/or transplanted assays. While these are useful

surrogates that have been employed in ecotoxicology, their relevance to field conditions has been questioned (Luoma & Rainbow, 2008; Burton 2010; Johnson & Sumpter, 2016; also see Section 1.4.3.3). In particular, limitations surrounding the applicability of (i) heavily-spiked sediments to conditions in field-contaminated sites (Lee *et al.*, 2000a,b; Hutchins *et al*., 2008; Hill *et al*., 2011) and (ii) bioaccumulation as an indication of metal toxicity (Luoma & Rainbow, 2008; DeForest & Meyer, 2015) have been discussed in the literature. There is therefore the need for studies that evaluate the predictive capability of DGT using actual ecological effects in field-contaminated sites.

1.5 Aims of this project

The preceding sections of this chapter reviewed chemical measurements and approaches to the prediction of the bioavailability and toxicity of metals in marine sediments. Amongst the most common measures in the literature are total metal concentrations, 1 M HCl extracts, the EqP model, and, more recently, DGT, some of which have been successfully applied in previous studies. Although several regulations are still based on total metal concentrations, the EqP is increasingly adopted and forms a key component in addressing bioavailability in some of the most advanced SQGs currently available. There are also recent proposals for the adoption of DGT in this regard. While these represent considerable progress, thus far, a key limitation identified across the literature is the reliance on acute toxicity and/or laboratory bioassays and/or spiked sediments and/or metal bioaccumulation as an endpoint in establishing the several benchmarks. The danger of these surrogates is that they may not represent the realities of actual ecological effects in field-contaminated sites. In addition, the complicated influence of organism feeding behaviour and physiology on metal toxicity has been largely overlooked in the development of SQGs, thus far.

The main aim of this thesis is to define dose-response relationships in marine sediments – the relationship between actual ecological effects and chemical measurements of metal concentration and availability – in order to determine what measures of contamination are the best predictors of effects and to identify the threshold concentrations at which these effects begin to occur. I do not describe new tools or chemical measures for use in SQGs. Rather, I rigorously test the existing and proposed (for DGT) measures, given the realities in field-contaminated sites. Estuaries that are grossly contaminated with metals as a result of mining activities are ideal systems in this regard. They provide gradients of metal concentrations that are stable over time, as the metals equilibrate with the sediments. The

majority of this thesis is therefore set in the Fal and Hayle estuaries, Cornwall, England, which are grossly contaminated by mine drainage and share the aforementioned characteristics (Rainbow, 2020).

In the course of the investigation, a strong relationship between the concentration of Fe and potentially toxic metals (Cu and Zn) was observed in the surface sediments of the study sites. These metals could potentially be remobilised in the several redox-altering physical processes that occur in intertidal sediments, having even more devastating effects on the benthic fauna than previously considered. A similar release from anoxic sediments may also affect burrowing invertebrates in their oxic/sub-oxic microhabitats. Consequently, a second aim of this thesis was to assess the potential remobilisation of Cu and Zn from surface and deeper sediments in redox transitions across study sites in the Fal and Hayle estuaries.

1.6 Thesis outline and contributions to literature

This thesis is arranged into seven chapters. Chapter 1 (the current, introductory chapter) has reviewed the progress made, thus far, in predicting metal bioavailability and toxicity in marine sediments. The aims of this thesis have also been defined.

In Chapter 2, I report physicochemical characteristics, including metal concentrations, across the contamination gradient in the Fal and Hayle estuaries, Cornwall, England. These estuaries have been well studied in the literature. I therefore provide an update of their contamination status over a two-year sampling period. Repeated sampling of sediments from the same sites also enabled the investigation of temporal variations in characteristics, which can be useful in the interpretation of long-term ecological effects. I compare metal concentrations with a reference, uncontaminated site, Breydon Water, in Norfolk, England.

In Chapters 3 and 4, I compare the capability of DGT in predicting ecological effects across the Fal and Hayle estuaries with other traditional measures of metal contamination, including EqP-based normalisations. These represent two of the first few evaluations of the DGT technique using actual ecological effects in field-contaminated sites. I discuss the strengths and limitations of the technique in adoption for the development of SQGs. I also define dose-response relationships and effect thresholds across the different chemical measures of metal contamination, using site data. In Chapter 3, I quantify ecological effects of Cu using the occurrence of pollution-tolerant nematode communities in the field. And in Chapter 4, I use nematode community structure in both univariate and multivariate assessments. An

additional highlight of Chapter 4 is the response of nematode community structure to metal contamination, despite the wide variation in physicochemical characteristics across our study sites. I show for the first time that multivariate analysis (non-metric multidimensional scaling, MDS) of nematode communities in the Fal and Hayle is robust to the variation in site characteristics, suggesting that the "nuisance" effect of site variations become more pronounced in low-resolution, larger-scale studies comparing whole creeks or estuaries.

The development and adoption of the EqP model has proceeded with limited consideration of dietary toxicity, especially to deposit-feeding invertebrates. Several concerns have been raised in this regard, with studies demonstrating the overwhelming bioaccumulation of sedimentary metals at very low or negligible dissolved concentrations. The contribution of dietary, solid-phase[1] intake to overall toxicity has also been shown in pelagic and benthic organisms. However, proponents of the EqP argue that the model is not designed to predict bioaccumulation, which is not necessarily a measure of toxicity (Di Toro *et al.*, 2005), and that water-only thresholds are protective of diet-borne exposures (DeForest & Meyer, 2015). In Chapter 5, I demonstrate overwhelming dietary toxicity to a deposit feeder. Using feeding depression in the marine mudsnail, *Peringia ulvae*, I show that (i) sediment-bound metals are primarily responsible for Cu toxicity in this species and, for the first time, that (ii) Cu sulphides, in the presence of excess AVS, may also be toxic, contrary to expectations. I then present a critical assessment of the EqP and its current use in sediment metal regulation.

In Chapter 6, I address the second aim of this thesis. Using a batch experimental design, I show that medium to long-term redox changes in intertidal sediments of the Fal and Hayle estuaries can, indeed, remobilise Cu and Zn at potentially toxic concentrations. The magnitude of metal release was greater in anoxic sediments than at the surface. I discuss these results in the light of potential ecological effects, whilst highlighting possible ongoing geochemical processes. There are only few remobilisation studies in the published literature on marine field sites with such elevated concentrations of toxic metals.

I summarise findings from the overall thesis in Chapter 7 and provide recommendations for the development SQGs that are more reliable as well as for future work.

[1] Kadiene *et al.* (2019) showed that the bioaccumulation of metals by two calanoid copepods, *Pseudodiaptomus annandalei* and *Eurytemora affinis*, is primarily through the oral intake of water – and not solid-phase diet.

Chapter 2.

Physicochemical characteristics of sediment and porewater in tributaries of the Fal and Hayle estuaries, Cornwall, England

2.1 Introduction

The legacy of mining in Cornwall, Southwest England is well documented (Barton, 1968,1971; Dines, 1969; Bryan & Gibbs, 1983; Rollinson *et al*., 2007; Rainbow, 2020). At the edges of granite intrusions in this area, there is an abundance of mineral lodes, containing several ores that include arsenopyrite (FeAsS), cassiterite (SnO_2), chalcopyrite ($CuFeS_2$), galena (PbS), pyrite (FeS_2), and sphalerite (ZnS) (Johnson, 1986; Rollinson *et al*., 2007; Rainbow, 2020). Mining and processing of these metalliferous ores peaked over the 18th to 19th century, but continued until closure of the last Sn mine in 1998, leaving behind old mine adits and spoil heaps which continue to drain to this day. Mining activities around the Carnon River catchment has led to mineral drainage into the Fal estuary, beginning at the Restronguet Creek where metal-laden freshwater inputs mix with seawater. A similar legacy in the Hayle Estuary catchment also grossly contaminates the two branches of the estuary (Rollinson *et al*., 2007). Together, the Fal and Hayle estuaries present a stable gradient of sediment metal contamination, with total concentrations higher in areas closest to mine water inflows. Metal concentrations at the most contaminated areas far exceed those reported in other United Kingdom estuaries (Bryan & Langston, 1992; Rainbow, 2020). Given the dearth of other interfering pollutants, the Fal and Hayle are ideal sites for investigating the effects of metal contamination on *in situ* benthic communities (Rainbow, 2020).

As discussed in Chapter 1, the complex interactions between the chemical partitioning of metals and the different organism uptake routes pose challenges in predicting metal bioavailability and ecological effects to biota. Simpson and Batley (2016) recently documented physicochemical properties important in linking metal contamination to ecological effects in marine sediments. Characteristics such as salinity, pH, and dissolved organic carbon (DOC) may affect dissolved metal speciation, and they have been earlier highlighted (also see Chapman & Wang, 2001; Chapter 1). Sediment grain size, total organic carbon (TOC) and redox potential (ORP) are important in the partitioning of metals and the activity of the marine benthos (also see Di Toro *et al*., 2005; Burton, 2010; Strom *et al*., 2011). A number of different chemical measurements of metal concentrations in sediment

have also been used. In addition to total metal concentration, strong acid extracts, especially 1 M hydrochloric acid (HCl), are common surrogates of bioavailability in marine sediments (Bryan & Langston, 1992; Burton 2010). Furthermore, the equilibrium partitioning model (EqP) underscores the importance of measuring metal concentrations in porewater, simultaneously-extracted metals (SEM) in sediments, and concentrations of acid volatile sulphides (AVS). The hypothesis argues that if the combined SEM concentration of five common and toxic divalent metals and Ag (ΣSEM = SEM Ag + SEM Cu + SEM Pb + SEM Cd + SEM Zn + SEM Ni) is less than AVS concentration, then sediment toxicity is not expected (Ankley *et al*., 1996; Berry *et al*., 1999; Burgess *et al*., 2013).

This chapter documents results from three field surveys undertaken between October 2017 and July 2019 in the Fal and Hayle estuaries. By combining rigorous chemical measurements of metal contamination with the assessment of important physicochemical properties across both estuaries, the aim is to update understanding of their contamination status and reveal current conditions in which inhabiting benthic invertebrates are exposed. Importantly, this chapter sets the scene for the rest of the thesis. Methods used throughout the thesis are detailed and discussed. The results also form the basis for further biological and chemical investigations in Chapters 3, 4, and 6.

2.2 Methodology

2.2.1 Study design

Eleven sites were chosen to cover the entire metal contamination gradient across the Fal and Hayle estuaries in Cornwall, Southwest England (Figure 2.01), as documented in previous studies (Bryan & Gibbs, 1983; Millward & Grant, 2000; Rollinson *et al*., 2007; Grant, 2010). Within the Fal, the Helford River was initially chosen as a control site, having relatively low metal concentrations but environmental conditions similar to those across the other sites (Millward, 1995). This site was, however, found to be more contaminated than Percuil River – the true control site (Section 2.3.5). An uncontaminated site, Breydon Water, in Norforlk, England was additionally sampled as a reference (Greenwood, 2001). All study sites were in the mid shore, inundated in high spring or neap tides but exposed in low tides.

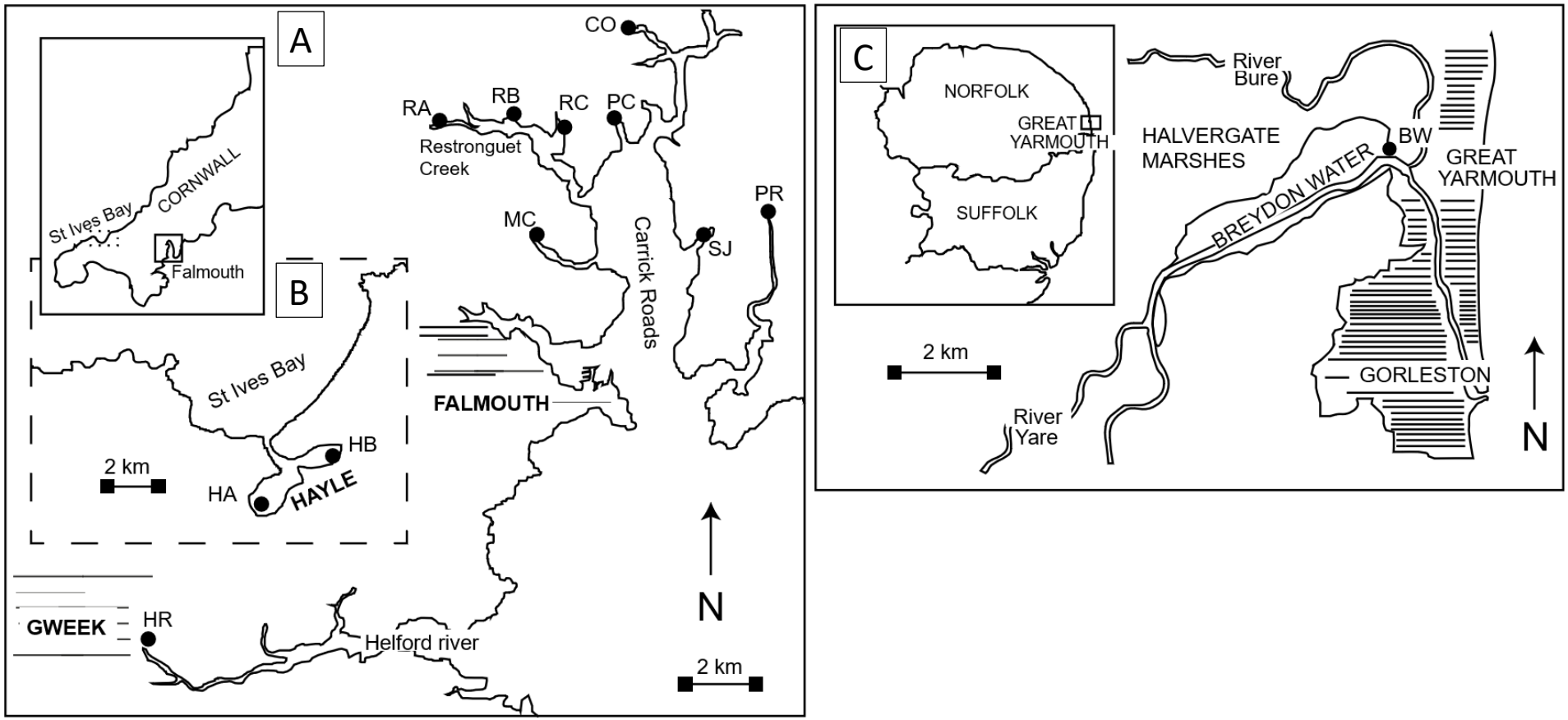

Fig. 2.01: Mid shore study sites in the Fal (A) and Hayle (B) estuaries as well as in Norfolk (C). British Grid Reference in parentheses. HB = Hayle B, Copperhouse Pool (SW 566379); HA = Hayle A, River Hayle (SW 546364); HR = Helford River (SW 707266); MC = Mylor Creek (SW 806359); RA = Restronguet Creek A, Kennall (SW 784388); RB = Restronguet Creek B, Tallack's (SW 802388); RC = Restronguet Creek C, Penpol (SW 812386); PC = Pill Creek (SW 826385); CO = Cowlands (SW 830408); SJ = St Just (SW 847358); PR = Percuil River (SW 861363); BW = Breydon Water (TG 516081)

Field surveys were undertaken in Autumn 2017 (September for Site BW; October for Cornwall sites), Winter 2019 (January), and Summer 2019 (July) to observe temporal variability in sediment physicochemical characteristics. Across all surveys, surface sediment (top 1 cm in summer, but top 2 cm at other times, henceforth referred to as "oxic") was sampled, which was the brown, oxidised layer in most sites[2]. In Summer 2019, deeper sediments (5 – 10 cm, henceforth referred to as "anoxic") were additionally sampled to characterise the anoxic layer.

2.2.2 Laboratory wares and chemicals

All laboratory wares used throughout this thesis, except otherwise stated, were washed using detergent and distilled water, soaked in 10% (v/v) HNO_3 for at least 24 hrs, and afterwards rinsed for at least three times (until neutral pH) with ultrapure water (UPW; Elga Purelab Ultra, 18.2 MΩ cm). Only plastic materials were used in contact with sediment or porewater samples. However, glassware was used in the preparation and storage of reagents. All washed wares were allowed to dry under a laminar flow cabinet and afterwards enclosed in plastic containers until use.

Chemicals used throughout this thesis were, at least, of analytical reagent grade, purchased from Fisher Scientific, UK, unless otherwise stated. Procedures requiring clean conditions were completed under a laminar flow cabinet to limit external metal contamination.

2.2.3 Sediment sampling and preservation

Sediments were sampled at low tide, using one scoop per site, and stored in sealable sampling bags. Bottom, anoxic sediments were double-bagged using ~20 L bags, with a layer of anoxic sediment in-between to limit oxidation. Due to a high proportion of gravel observed in Autumn 2017, surface sediments from the Hayle Copperhouse Pool (HB) were sieved *in situ* to <2 mm, using a stainless steel sieve, in subsequent surveys.

All samples from Cornwall were collected on the same day. However, due to the logistics of sampling in Cornwall, time taken between the first sample being collected and laboratory

[2] Sampling was done by depth to collect (relatively) oxidised surficial sediments. However, Sites HB, HR, MC, PC, and SJ were black-coloured at the surface all through the sampling surveys, indicating reduced conditions. RC was black-coloured in the Summer 2019 survey. The term "oxic" throughout this thesis therefore refers to the sampled sediment layer and not necessarily the redox state of the sediment.

storage was at most 36 hrs. In Autumn 2017 and Summer 2019, samples were stored and transported in ice. Sediments from Breydon Water were transported to the laboratory within 1 hr of collection. Upon reaching the laboratory, sediment samples were homogenised and subsampled for (i) AVS/SEM analysis – stored in 15 mL centrifuge tubes and frozen at -15 ^{o}C until use, (ii) TOC and percentage moisture – frozen in 50 mL centrifuge tubes until processed, and (iii) total metal concentration – oven dried at 105 ^{o}C to constant weight and afterwards stored in a desiccator until use. The remaining portion was frozen and later subsampled (50 g wet weight) for grain size analysis. A separate sample bag for porewater extraction was refrigerated at 4 ^{o}C in the dark until processed.

2.2.4 Porewater extraction

Porewater was extracted within 48 hrs of arrival in the laboratory. This was done by centrifuging homogenised sediments at 3500 rpm for 10 mins (Simpson *et al*., 2000). Three[3] pseudo-replicates were processed per site. Unfiltered composite samples were collected for salinity and pH measurements, as required (see Section 2.2.6).

Extracted porewater samples were filtered under N_2 gas atmosphere in a glove bag (Sigma-Aldrich AtmosBag), using Fisherbrand polyethersulphone (PES) syringe filters. Prior to filtration, syringes and syringe filters were flushed, in sequence, with 5 - 10 mL of 10% HNO_3, 20 mL of UPW, and 3 - 5 mL of sample. In Autumn 2017, porewater was filtered to <0.45 µm and <0.2 µm. However, in subsequent surveys, only 0.45 µm filters were used. Filtered porewater was subsampled for (i) DOC – (acidified to 0.025% H_3PO_4 for Breydon Water samples in 2017 and) stored frozen in 50 mL centrifuge tubes (Tupas *et al*., 1994) and (ii) trace metal analysis – acidified to 2% HNO_3 in 2017, but 1% HNO_3 subsequently, and refrigerated at 4 ^{o}C until use.

2.2.5 Measurement of sediment temperature and redox potential

Sediment temperature and redox potential (ORP) were measured *in situ*. Temperature was measured using a digital soil thermometer (VWR International) inserted to a depth of around 2 cm. ORP was measured using a platinum combination sensor (VWR 3.5 M KCl/ Ag/AgCl reference) fitted into the HANNA HI 9025 microcomputer pH meter. The ORP probe was inserted into the top 1 cm of the sediment until a stable reading was observed. The reading

[3] Due to an analytical mistake leading to considerable loss of sample, not all replicates were available for porewater metal analysis.

was then recorded to the nearest 10 mV and, afterwards, converted to the Standard Hydrogen Potential (Eh) using manufacturer-supplied half-cell potential and temperature coefficient. Accuracy of the electrode was checked using ZoBell's solution.

2.2.6 Measurement of porewater pH and salinity

Porewater salinity and pH were determined only in Autumn 2017 and Summer 2019. In 2017, pH was measured in the laboratory from composite porewater samples using a pH meter (Mettler Toledo SevenEasy S20). However in 2019, pH was measured *in situ* using electrodes connected to the HANNA HI 9025 microcomputer pH meter. Both instruments were calibrated at pH 4 and 7 using certified standards (NIST – National Institute of Standards and Technology). Salinity was measured in the laboratory using a WTW LF 340 salinity meter calibrated with 0.01 M KCl, according to manufacturer's instruction.

2.2.7 Assessment of sediment grain size distribution

Sediment grain size was assessed using 50 g of homogenised, composite wet samples. 250 mL of deionised water and 10 mL of 6.2 g/L sodium hexametaphosphate was added to the weighed sediment in a beaker (Kenny & Sotheran, 2013). The sediment suspension was stirred at 1000 rpm for 15 mins to disperse clay particles and, afterwards, washed through a nested sieve set at 4 mm, 2 mm, and, in Autumn 2017, 1 mm. Fractions retained on the respective sieves were dried and weighed. And the fraction that passed through the sieves was analysed, in triplicates, by laser diffraction using the Malvern Mastersizer 2000.

Results from both the sieve and laser diffraction analyses were combined to calculate the median grain size (50^{th} percentile), percentage fines (particles less than 63 µm), and percentage gravel (particles greater than 2 mm). Due to considerable gravel content in some sites, grain size characteristics are additionally reported for the fraction less than 2 mm, which is considerably more relevant for benthic meiofauna.

The Folk and Ward's (1957) inclusive graphic standard deviation (σ_1) was additionally estimated. This measure of dispersion is more able to handle departures from a normal grain size distribution. The method was used to categorize the degree of sorting of the sediment in a verbal scale (Folk & Ward, 1957) as follows:

$\sigma_1 < 0.35$	Very well sorted (VWS)
$0.35 \leq \sigma_1 < 0.50$	Well sorted (WS)

$0.50 \leq \sigma_1 < 1.00$ Moderately sorted (MS)

$1.00 \leq \sigma_1 < 2.00$ Poorly sorted (PS)

$2.00 \leq \sigma_1 \leq 4.00$ Very poorly sorted (VPS)

$\sigma_1 > 4.00$ Extremely poorly sorted (EPS)

2.2.8 Determination of percentage moisture and total organic carbon in sediments

Subsamples for TOC analysis were freeze-dried to constant weight, with the weight difference used to calculate percentage moisture for sediment particle size analysis (Section 2.2.7). For AVS and SEM analyses (Sections 2.2.11 & 2.2.12), moisture content was determined after oven-drying at 105 ^{o}C to constant weight. Percentage moisture was calculated as follows:

$$\% \text{ Moisture} = \frac{\text{Mw} - \text{Md}}{\text{Mw}} * 100$$

Where:

Mw = Mass of wet sediment
Md = Mass of dry sediment

TOC content was assessed using two methods. In Autumn 2017 and Winter 2019, TOC was analysed by loss on ignition (LOI) method as well as using an elemental analyser (Exeter Analytical CE440). This provided comparable results for the two methods. In Summer 2019, TOC was assessed only by loss on ignition.

Elemental analysis was done on replicate samples by modifying the method of Verardo *et al*. (1990). To remove inorganic carbon, excess 6% sulphurous acid (H_2SO_3) was added to 2 g of freeze-dried samples in plastic containers under a fume cupboard. Acidified samples were freeze-dried after 12 hrs and ball-milled to yield finer particle sizes. Approximately 15 mg of fine sediment was then weighed into tin capsules, in triplicates, for analysis. The machine was calibrated for every six samples using acetanilide standards. Empty capsules were run as analytical blanks, with benzoic acid serving as an additional organic standard. Marine sediment reference materials PACS-1 (NRC – National Research Council Canada) and Goole Harbour (QUASIMEME laboratory performance studies) were used to assess precision of the analysis. And the 1941b certified reference (NIST) was used to assess

accuracy. TOC is reported as a dry weight percentage after applying correction factors for weight loss during drying and H_2SO_3 acidification.

Loss on ignition was completed by heating freeze-dried sediment at 400 ^oC for 24 hrs (Shipp & Grant, 2006). The precision of this method was assessed by triplicate analysis of sediment sampled from Breydon Water in September 2017. Percentage loss of weight on ignition was calculated as follows:

$$\text{LOI (\%)} = \frac{\text{Md} - \text{Ma}}{\text{Md}} * \ 100$$

Where:

Md = Mass of dry sediment

Ma = Mass of ashed sediment

2.2.9 Measurement of dissolved organic carbon in porewater

DOC was measured in Autumn 2017 and Winter 2019, only, as non-purgeable organic carbon (NPOC) after acidification of replicate samples with 10% HCl (Skalar Formacs^{HT} TOC/TN, CA15). The procedure was completed in the same laboratory and using similar methods described by Chaichana *et al*. (2019). In order to limit sample degradation, frozen samples were thawed by refrigerating at 4 ^oC a day before the analysis.

NPOC analysis was calibrated using standards (n = 5) prepared from potassium hydrogen phthalate (KHP) in UPW matrix. UPW blanks were run approximately after every five samples to prevent clogging of tubes. The documented instrumental blank for this machine is low relative to analysed concentrations (~ 0.36 mg/L, Chaichana *et al*., 2019). In the current study, instrumental blank was accounted for by calibrating the instrument using peak areas of the five-point calibration standards, without the UPW blank. This provided a more stable correction of the instrumental blank – as the y-axis intercept – than traditional UPW measurements (e.g. Benner & Strom, 1993), which varied considerably during the analysis, possibly as a result of salinity differences between samples (6.6 – 39.5 S, Section 2.3.1). Due to the lack of saline reference materials in a relevant concentration range, accuracy and precision of analysis was assessed using independently-prepared[4] 25 mg C/L and 30 mg C/L solutions in UPW and 30 S artificial seawater (ASW, Tropic Marin® PRO-REEF) matrices.

[4] Calibration standards were prepared by a technician. But the reference solutions were prepared by the author in a different laboratory using a different KHP stock.

Accuracy of the calibration was determined in Autumn 2017 by analysing the CRANBERRY-05 lake water certified reference material (Environment Canada).

2.2.10 Determination of total sediment metal concentrations

Dry sediment samples were pulverised in a vibratory disc mill (Retsch RS 200) for metal analysis. Total metal concentration was then determined by X-ray Fluorescence Spectrometry (XRF, Brucker-AXS S4 Pioneer) according to Middleton and Grant (1990). Nineteen trace elements – including As, Cu, Ni, Pb, and Zn – were measured in pressed pellets, using 10 g of pulverised sediments held together by a binder (Mahlhife, Polysius Polab). Also, ten major element oxides – including Al_2O_3, CaO, Fe_2O_3, and MnO – were measured in fused beads prepared using 0.4 g of sediment and 7.6 g of Lithium Tetraborate.

The XRF machine was calibrated using the manufacturer-supplied "GEO-QUANT" solutions (Bruker, 2020). Accuracy of the analysis was checked using certified sediment reference materials across the assessed range of concentrations[5]: SDO-1 (Berkovits & Lukashin, 1984), SRM 2702 (NIST), STSD-2 (NRCan – Natural Resources Canada), PACS-1 (NRC), and MESS-2 (NRC). For Cu, in which previously-reported concentrations (> 2000 µg/g) exceeded the GEO-QUANT calibration range (1000 µg/g) and available sediment reference materials, U.S. Geological Survey (USGS) reference materials – GXR-1 (jasperoid) and GXR-4 (soil) – were used to assess recovery up to 6000 µg/g. These USGS standards have no certified values; however, recommended values derived using NIST guidelines have been reported (Gladney & Roelandts, 1990). Concentrations of As, Cu, Ni, Pb, and Zn were normalised to the fraction of fine particles (<63 µm) to account for temporal and spatial grain size differences[6], which may cause significant bias (Ackerman, 1980; Grant & Middleton, 1998).

2.2.11 Determination of acid volatile sulphides in sediments

AVS was determined using the rapid method (Simpson, 2001, 2016). This method involves exposing small quantities of wet sediment to Cline's (1969) reagent (henceforth, Methylene

[5] In Autumn 2017, reference materials were analysed before drying; therefore, results were adjusted for moisture content (0.2 – 1.7%).

[6] Whole sediment samples were pulverised and analysed. Accordingly, fine grain fraction of the total sediment composition was used in metal normalisations.

Blue Reagent, MBR), followed by the colourimetric measurement of extracted sulphides. Although the rapid method may underestimate sediment AVS concentrations by up to 30% relative to the traditional purge-and-trap method (Simpson, 2001)[7], the relatively high sample throughput and similar precision has led to its increased adoption (Campana *et al*., 2015; Amato *et al*., 2018, Remaili *et al*., 2018; Richards *et al*., 2018). Results are, however, to be interpreted with caution, especially in comparison with SEM concentrations for EqP assessments.

Briefly, about 100 mg (dry weight equivalent) of homogenised sediment was weighed, in triplicates, onto a small piece of Parafilm™. This process was completed quickly to limit AVS oxidation. Weighed sediment was transferred into a 50 mL centrifuge tube, to which 50 mL of UPW and 5 mL of MBR were gently added. In Autumn 2017, due to minimal AVS concentration in the oxidised sediments, 10 mL of UPW and 1 mL of MBR were added in 15 mL centrifuge tubes, originally, in order to lower the method detection limit. However, this increased sediment:volume ratio was later discovered to underestimate AVS concentration by up to a factor of four, mainly due to increased MBR adsorption to sediment particles (Simpson, 2001). AVS analysis for Autumn 2017 was therefore repeated using samples that had been re-frozen after the initial analysis. Filled tubes were gently agitated and, after few minutes, centrifuged at 2500 rpm for 2 mins. The tubes were then left for 2 hrs in darkness to develop colour. Method blanks were processed using only Parafilm™.

Colourimetry was completed by measuring absorbance at 670 nm using 10 mm PerkinElmer quartz SUPRASIL cuvettes (UV/VIS Spectrophotometer: Unicam 8625 in Autumn 2017; PerkinElmer Lambda 25 controlled by a Windows PC in 2019). The analysis was calibrated using sulphide standards prepared each day from sodium sulphide nonahydrate ($Na_2S.9H_2O$) and standardised by iodometry (Simpson, 2016). Where absorbance was higher than the UV/VIS linear range, coloured MBR-sulphide solution was diluted, as appropriate, using 1 M H_2SO_4. This dilution yielded similar results as dilution of the original sulphide solution with 1 M NaOH before MBR reaction. Sulphide standards and working solutions were prepared in a nitrogen-filled glove bag. But the MBR reaction was done in a fume cupboard.

[7] Correction factor of 1.3 (Simpson, 2001) was not applied throughout this thesis because methodological over- or under-estimation varies with assessed concentrations.

2.2.12 Determination of acid-extractable metal concentrations

Acid-extractable metal concentrations were determined using subsamples of the same homogenised sediment used for AVS determination (Simpson *et al*., 2002). Approximately 100 mg (dry weight equivalent) of wet sediment was extracted for 30 mins in 10 mL of 1 M HCl, in order to match sediment:volume ratios initially used in the AVS analysis[8]. Method blanks were processed by extracting only Parafilm™. Because this extraction is analogous to simultaneously-extracted metals (Simpson, 2001, 2016), concentrations derived for Cd, Cu, Ni, Pb, and Zn were expressed in µmol/g to reflect this measure.

Sediment extracts were analysed for metals either by Inductively Coupled Plasma – Optical Emission Spectrometry (ICP-OES; Varian Vista-Pro) or Triple Quadrupole Inductively Coupled Plasma – Mass Spectrometry (ICP – MS- QQQ; Thermo Icap-TQ). Single-element calibration standards (PlasmaCAL) were prepared in a similar acid matrix. A multi-element standard solution (CLMS2A, SPEX CertiPrep) was prepared in a similar matrix to assess precision of the analysis. And accuracy was assessed using certified lake water references, TM-27.3 and TMDA-64.2, both from Environment Canada.

2.2.13 Determination of metal concentrations in porewater

Due to their saline matrix and often low concentrations, direct measurement of metals in seawater can pose a considerable challenge using conventional methods. In this study, metals were recovered from porewater by batch equilibration with Chelex® resins (Figura & McDuffie, 1980), following sample digestion. Metals were then extracted from resins using strong acid for analysis by ICP techniques. The final method is summarised in Figure 2.02.

[8] Although sediment:volume ratio was later changed in the AVS analysis (Section 2.2.11), ratios for sediment metal extraction was kept consistent to facilitate comparison between surveys. SEM Cu and Zn concentrations of surface sediments in this study are similar to those reported by Greenwood (2001) using the traditional purge-and-trap method.

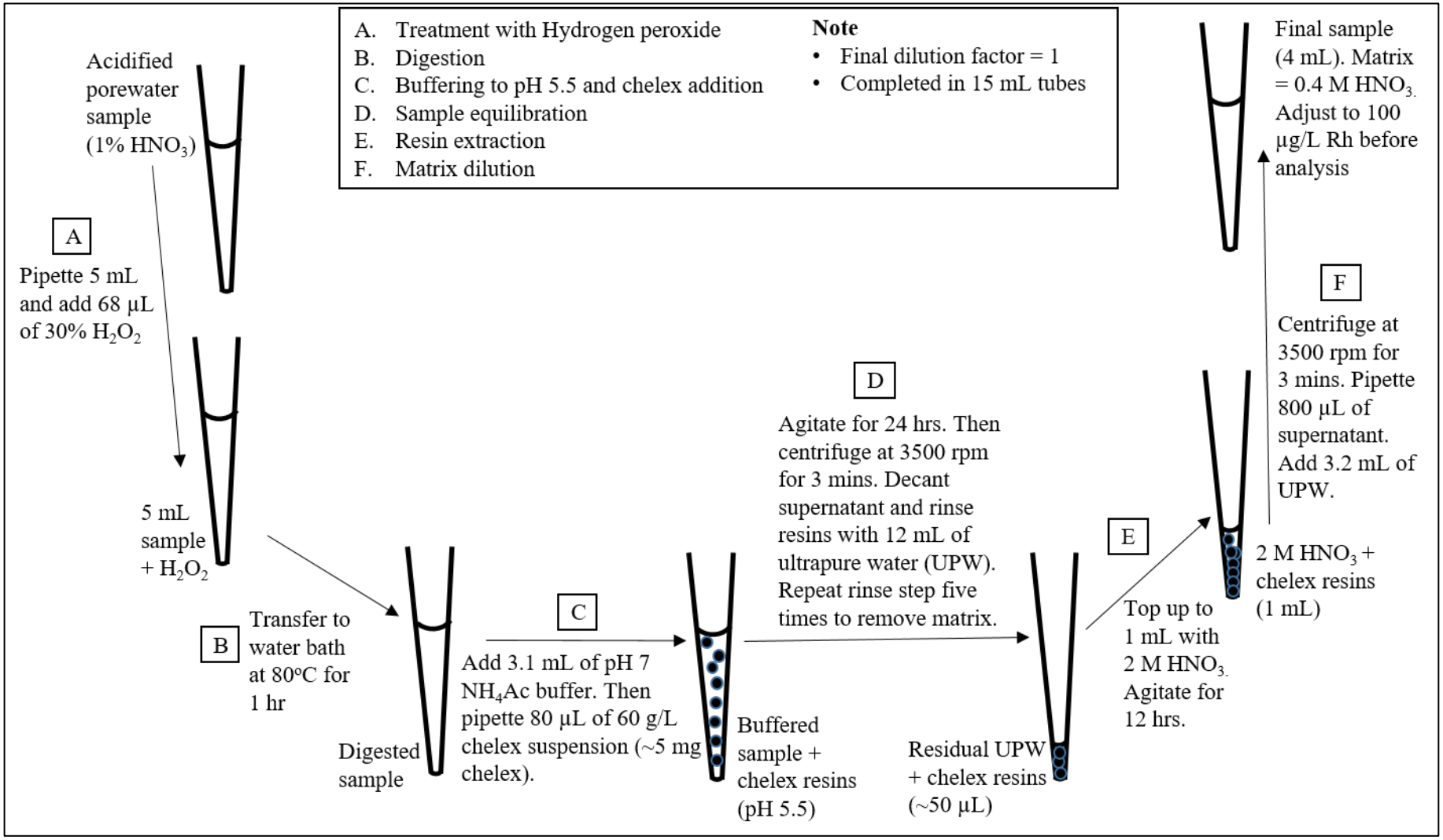

Fig. 2.02: Schematic diagram for saline sample chelation

Na-form Chelex-100 resins (3.5 g wet weight) were cleaned by agitating for 15 mins in 50 mL centrifuge tubes containing 2 M HNO_3, followed by centrifuging at 3500 rpm for 3 mins to remove solution. This process converts the Na-form chelex to hydrogen-form, and it was repeated twice, with a third repetition agitated for 12 hrs before centrifugation. To remove excess acid, resins were rinsed with UPW, centrifuged, and supernatant was decanted (henceforth referred to as the wash cycle). Acid-washed resins were washed in three wash cycles using clean[9] pH 7.0 ammonium acetate (NH_4Ac) buffer solution in order to convert from the hydrogen-form to ammonium-form (Sondergaard *et al.*, 2015). This conversion was necessary to maintain resin stability and ion-exchange capability (Biorad, n.d.). Ammonium-form resins were stored in 50 mL of clean pH 5.5 NH_4Ac until use, assuming a nominal resin concentration of 60 mg/mL given losses during decantation.

Prior to resin equilibration, filtered porewater samples were digested, according to Nicolai *et al*. (1999), in order to liberate metals from organic matter and colloids. Sample treatment was achieved by, first, adding 68 µL of 30% hydrogen peroxide to 5 mL of sample in 15 mL centrifuge tubes. Peroxide-treated samples were then heated in a water bath at 80^{o}C for 1 hr. After cooling to laboratory temperature, digested samples were buffered to pH 5.5 by adding appropriate amounts of clean pH 7 NH4Ac solution: 3.1 mL and 6.1 mL for 1% and 2% acidified solutions, respectively. Equilibration at this pH is quantitative for Cu, Fe, and Zn measurements, but poor for Mn determination (Pai *et al*., 1988)[10]. Approximately 5 mg of clean resin (as 80 µL of the 60 mg/mL suspension) was then added to the buffered porewater samples, followed by agitation at 120 rpm for 24 hrs to recover metals.

Equilibrated samples were rinsed in five wash cycles using UPW, in order to remove the saline matrix. pH of original supernatant was measured, at random, to confirm sample buffering at 5.5. Metals were then extracted from resins by topping up to 1 mL with 2 M HNO_3 and agitating for 12 hrs at 120 rpm. Following extraction, resins were centrifuged at

[9] Buffer solutions were prepared using appropriate volumes of glacial acetic acid and ammonium hydroxide. The buffers were cleaned by equilibrating with excess acid-washed Chelex resins for 12 hrs, followed by vacuum filtration using a 0.45 µm PES membrane. The PES filters were cleaned prior to use by soaking for 12 hrs in 10% HNO_3 and rinsing to neutral pH with UPW.

[10] Metal extraction with Chelex is, amongst other things, pH dependent. The recovery of Cu and Zn is quantitative at pH 5 – 6, Fe at pH < 6, and Mn at pH > 7 (Smith 1974; Pai *et al.*, 1988). Here, a pH of 5.5 was chosen to maximise recovery of Cu, Fe, and Zn.

3500 rpm for 3 mins. 800 µL of clear acid solution was pipetted into a second centrifuge tube and topped up to 4 mL with UPW to achieve an overall dilution factor of one.

Metals in porewater extracts were analysed using two methods. In Autumn 2017 and Winter 2019, samples were initially analysed by ICP – MS – QQQ, using 10 µg/L Rh as internal standard. This analysis was calibrated using seawater from the North Sea[11] (henceforth, saline calibration standard), which was filtered to <0.45 µm, cleaned using chelex, spiked, and processed in the same manner as the samples. Due to a lack of saline reference materials with appropriate metal concentrations, recovery of the method was assessed by spiking the GEOTRACES GS seawater reference material. Precision of the method was similarly assessed using filtered and spiked seawater collected from Breydon Water in Autumn 2017.

Analysis of porewater extracts was repeated using samples from all surveys. For Autumn 2017, where 0.45 µm-filtered samples were insufficient, 0.2 µm-filtered samples were used instead. This latter analysis was done by ICP-OES and calibrated using conventional, non-saline standards and 100 µg/L Rh as internal standard. Recovery and precision of the chelation method was assessed using North Sea seawater, which was filtered, cleaned, and spiked to 100 µg/L metal. Accuracy and precision of the analytical calibration was assessed using the TM-27.3 and TMDA-64.2 certified lake water reference materials, with the CLMS2A multi-element standard serving as a further precision check. Because this latter analysis was tied to certified reference materials and represent actual calibration standards, the results obtained are of higher confidence and therefore used in this study.

Preliminary experiments were completed to determine optimal equilibration and extraction duration as well as the need for ammonium acetate pre-extraction (Kingston *et al.*, 1978) and sample digestion. These experiments were completed using filtered and spiked – but not cleaned[12] – seawater samples from Breydon Water. Extracts here were analysed by ICP-MS-QQQ calibrated using non-saline standards.

[11] North Sea seawater was sampled off the coast of Lowestoft, England and provided by the Centre for Environment, Fisheries and Aquaculture Science (CEFAS).

[12] This sample, unlike the North Sea seawater used for accuracy assessment, was not cleaned with chelex prior to spiking. Accuracy here was therefore determined by spike recovery, taking into account metal concentrations in unspiked samples.

2.2.14 Calculation of limit of detection, accuracy, and precision

Throughout this thesis, limit of detection is calculated as three times the standard deviation ($n \geq 3$) of a blank solution, unless otherwise stated. Analytical accuracy and precision are reported as percentage recoveries and relative standard deviations, respectively, as follows:

$$\text{Accuracy (\%)} = \frac{\text{Mean of n replicates measured}}{\text{Mean certified value}} * 100$$

$$\text{Precision (\%)} = \frac{\text{Standard deviation of n replicates measured}}{\text{Mean of n replicates measured}} * 100$$

Where n = number of replicates

2.3 Results and discussion

Throughout this thesis, references are made to figures and tables within the main body of the work, which are conventionally numbered. References are also made to figures and tables in the appendices. This latter group is prefixed with the letter "A" – for example A2.01 referring to Appendix 2.01 for Chapter 2.

Furthermore, within each figure and table, results are arranged in order of increasing metal contamination across the sites (see Section 2.3.5 for actual data). This order was derived by averaging the total sediment concentrations of the five key metals (As, Cu, Ni, Pb, and Zn) across all surveys and collapsing these using Component 1 of a correlation-based Principal Components Analysis (PCA), accounting for 75% of the total variation. The PCA was prepared using the "princomp" function in R (R Core Team, 2020), and the biplot is displayed in Figure 2.03.

2.3.1 Porewater pH, salinity, and redox potential across the study sites

pH, salinity and redox potential measured across the surveys are reported in Table 2.01. pH values ranged between 7.00 and 8.11, which are similar to values earlier reported in the Fal (Greenwood, 2001; Ogilvie & Grant, 2008) and those expected in seawater. Salinity also ranged from brackish (6.6 S), as expected at the head of the Restronguet Creek (RA), to fully marine ($\geq$ 35 S) away from incoming rivers and in Breydon Water. In Summer 2019, salinity across the sites were higher than expected. This is likely to be because of evaporation due to high temperatures at low tide when sediments were sampled.

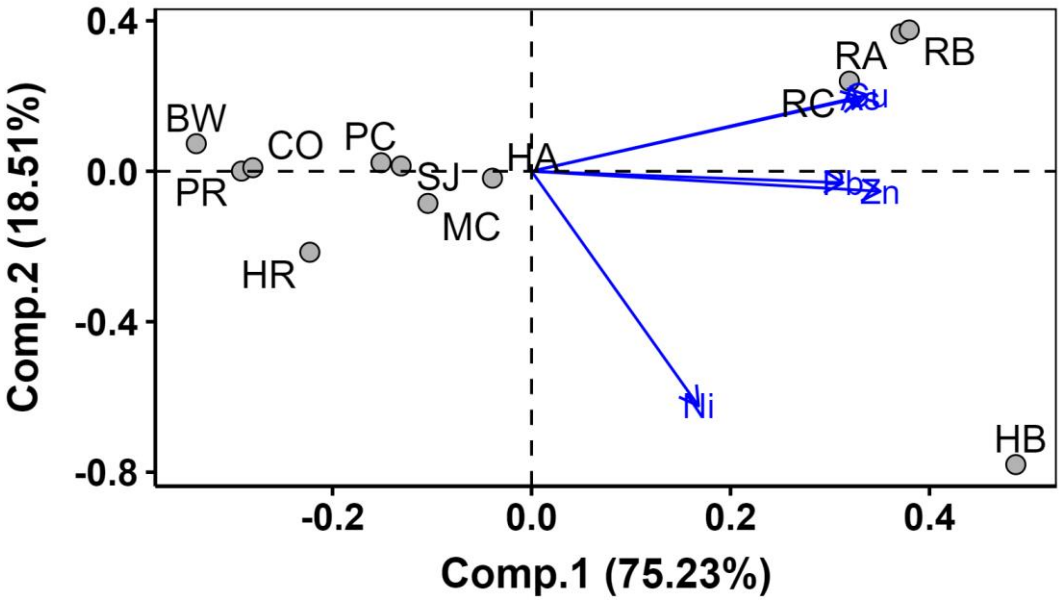

Fig. 2.03: PCA ordination of standardised total sediment metal concentrations averaged across the sampling surveys. Arrangement from left to right in the Comp. 1 axis is used to represent increasing metal contamination across the study sites

Table 2.01: Salinity (Sal), pH and redox potential (Eh) in surface sediments across the study sites

Site	2017 Autumn			2019 Winter	2019 Summer		
	Salinity (S)	Eh (mv)	pH	Eh (mv)	Salinity (S)	Eh (mv)	pH
BW	36.6	56	7.76	371	32.4	219	8.04
PR	19.8	296	7.65	198	29.9	224	NA
CO	35	163	7.58	266	35.2	240	7.20
HR	21	161	7.67	169	33.2	77	7.42
PC	35.9	72	8.11	66	34.8	28	7.20
SJ	39.5	151	7.76	78	35.8	120	7.14
MC	31.2	148	7.76	206	43.2	146	7.42
HA	21.3	437	7.69	417	38	277	7.00
RC	32	83	7.64	66	38.1	148	7.16
RA	6.6	405	7.78	208	25.2	177	7.26
RB	31.3	171	7.70	212	38.9	256	7.30
HB	26.8	85	7.69	267	36	218	7.15

NA = Not Available

Redox potential varied widely (28 – 437 mv) in surface sediments across the sites. The lowest values were consistently observed in the black-coloured Pill Creek, a colouration indicative of reduced sediments (Hutchings *et al.*, 2019). On the other hand, the highest Eh

was recorded in the sandy sediments of River Hayle (HA), where the oxidised sediment depth was observed to be in excess of 5 cm in autumn and winter. Given the high solubility of oxygen at low sediment temperatures (de Klein *et al*., 2017) and higher aerobic microbial activity in warmer conditions (Biddanda & Cotner, 2002), Eh values were generally highest in winter. Vershinn and Rozanov (1982) classify redox conditions based on Eh values: oxidation (400 – 550 mv), weak oxidation (200 – 400 mv), weak reduction (0 – 200 mv), and reduction (0 – -200 mv). Considering their winter Eh values, surface sediments across the study sites can be grouped into oxidised (HA), weakly-oxidised (BW, HB, CO, MC, RB, and RA), and weakly-reduced (PR, HR, SJ, RC, and PC).

2.3.2 Sediment grain size characteristics of study sites

Sediment grain size characteristics across the surveys are presented in Tables 2.02 – 2.05. Sediments were mainly poorly sorted or very poorly sorted. However, anoxic sediments of HR and MC in Summer 2019 were extremely poorly sorted, indicating a large spread in grain size composition (Kenny & Sotheran, 2013). In Autumn 2017, surface sediments of the Hayle Copperhouse Pool (HB) consisted of nearly 60% gravel, interspersed in fine sediments. A similarly high gravel content (30 and 42%, respectively) was observed in anoxic sediments of MC and HR in Summer 2019. This high gravel content tended to result in unreasonably high median particle size (e.g. 3.2 mm in HB), which might not be relevant to benthic meiofauna inhabiting finer sediment particles.

For comparability, relevant grain size characteristics were further determined in the fraction < 2mm. Based on this fraction, surface sediments were mainly fine-grained (< 63 µm), at least 50% across the sites. Except in Summer 2019, median grain size was, as expected, highest in the sandy Hayle (HA), corroborating previous surveys (Greenwood, 2001; Shipp, 2006). Larger grain sizes were generally observed in summer, compared to sampling in winter and autumn. Coarser grains have been reported in San Francisco Bay (Thomson-Becker & Luoma, 1985) and the Yangtze River Estuary (Zhang *et al*., 2020) in summer relative to colder seasons, both attributed to stronger tidal currents, higher wind velocity, and/or lower precipitation, which facilitate the deposition of heavier particles and/or the reduction of finer inputs. Especially in HB, the fraction of fine particles (29 and 50% in oxic and anoxic sediments, respectively) were, therefore, lower in Summer 2019.

Table 2.02: Sediment grain size distribution in Autumn 2017, including characteristics for the fraction <2mm

Site	Total sediment composition					Fraction <2 mm		
	<63 µm (%)	**>2 mm (%)**	**Mean (ϕ)**	**Median (µm)**	**Sorting**	**<63 µm (%)**	**Mean (ϕ)**	**Median (µm)**
BW	84.3	0.0	6.1	13.1	PS	84.3	6.1	13.1
PR	68.0	5.5	5.0	31.4	VPS	72.9	5.2	27.7
CO	63.4	12.2	4.2	32.0	VPS	73.4	5.3	23.2
HR	81.5	3.3	5.5	21.3	VPS	84.8	5.6	20.2
PC	77.0	0.6	5.3	22.9	VPS	77.9	5.4	22.5
SJ	78.1	2.3	5.4	22.8	PS	80.8	5.5	21.7
MC	72.9	1.8	5.1	27.8	PS	74.7	5.2	26.7
HA	56.8	0.0	4.6	53.8	PS	57.0	4.6	53.6
RC	84.9	0.0	5.5	23.1	PS	84.9	5.5	23.1
RA	74.8	2.9	5.2	25.5	VPS	77.4	5.3	24.1
RB	82.4	0.0	5.4	24.2	PS	82.8	5.4	24.1
HB	23.4	59.2	0.3	3194.2	VPS	69.5	5.1	30.0

<63 µm (%) = Percentage fines >2 mm (%) = Percentage gravel content
PS = Poorly Sorted VPS = Very poorly sorted

Table 2.03: Sediment grain size distribution in Winter 2019

Site	**<63 µm (%)**	**>2 mm (%)**	**Mean (ϕ)**	**Median (µm)**	**Sorting**
BW	73.5	0.0	5.4	29.8	PS
PR	75.1	3.5	5.2	26.3	VPS
CO	78.0	0.1	5.5	21.0	PS
HR	84.5	0.5	5.6	21.0	PS
PC	79.6	0.4	5.5	21.8	PS
SJ	84.1	0.0	5.6	20.2	PS
MC	69.0	1.3	5.0	32.6	PS
HA	63.8	0.0	4.7	44.5	PS
RC	82.2	0.4	5.5	22.6	PS
RA	75.9	0.0	5.3	25.5	PS
RB	85.4	0.1	5.5	22.8	PS
HB	66.1	0.7	4.8	37.7	VPS

<63 µm (%) = Percentage fines >2 mm (%) = Percentage gravel content
PS = Poorly Sorted VPS = Very poorly sorted

Table 2.04: Sediment grain size distribution for oxic sediments in Summer 2019

Site	<63 µm (%)	>2 mm (%)	Mean (ϕ)	Median (µm)	Sorting
BW	71.1	0.0	5.2	27.6	VPS
PR	69.6	0.0	5.0	27.7	PS
CO	61.4	0.0	4.7	37.6	VPS
HR	81.8	0.0	5.4	23.0	PS
PC	55.1	0.0	4.1	50.1	VPS
SJ	72.6	0.0	5.1	27.3	PS
MC	71.9	0.0	5.0	29.1	PS
HA	53.3	0.0	4.3	58.0	PS
RC	74.8	0.0	5.0	31.8	PS
RA	67.6	0.0	4.9	33.9	PS
RB	76.4	0.0	5.1	29.8	PS
HB	29.1	0.0	3.1	152.1	VPS

<63 µm (%) = Percentage fines >2 mm (%) = Percentage gravel content
PS = Poorly Sorted VPS = Very Poorly Sorted

Table 2.05: Sediment grain size distribution for anoxic sediments in Summer 2019, including characteristics for the fraction <2mm

Site	Total sediment composition					Fraction <2 mm		
	<63 µm (%)	>2 mm (%)	Mean (ϕ)	Median (µm)	Sorting	<63 µm (%)	Mean (ϕ)	Median (µm)
BW	78.1	0.0	5.5	21.9	PS	78.1	5.5	21.9
PR	66.4	0.0	5.0	32.7	PS	66.4	4.8	32.7
CO	65.2	0.5	4.8	31.9	VPS	65.5	4.9	31.5
HR	44.2	41.8	0.0	105.7	EPS	75.9	5.1	26.6
PC	51.1	9.7	5.8	59.4	VPS	56.6	4.3	46.7
SJ	66.2	8.3	6.3	32.2	PS	72.1	5.0	27.8
MC	47.4	29.9	1.5	73.2	EPS	67.6	4.9	31.9
HA	50.7	0.0	4.2	61.8	PS	50.7	4.2	61.8
RC	75.2	0.0	5.2	30.3	PS	75.2	5.1	30.3
RA	64.3	0.0	4.9	37.8	PS	64.3	4.7	37.8
RB	72.6	1.7	5.7	30.9	PS	73.8	5.1	30.1
HB	49.7	3.6	4.0	63.5	VPS	51.6	4.1	59.4

<63 µm (%) = Percentage fines >2 mm (%) = Percentage gravel content
PS = Poorly Sorted VPS = Very poorly sorted

2.3.3 Total organic carbon in sediment

TOC was determined by direct elemental analysis as well as by loss on ignition (LOI) as a proxy. Elemental analysis was done only in Autumn 2017 and Winter 2019. Although organic carbon content was overestimated (almost doubled) using LOI, results from both

methods are well correlated (Figure 2.04, $R^2 = 0.96$, $p < 0.001$), facilitating comparison in organic carbon content between sampling surveys (Figure 2.05). The overestimation of TOC based on LOI is attributable to a potential loss of carbonates upon ashing (Heiri *et al*., 2001), especially from the limestone-rich sediments from Hayle (Selwood *et al*., 1998; Rollison *et al*., 2007). Earlier trials at 550 ºC for 4 h (Heiri *et al*., 2001; data not shown) yielded similar higher, but correlated, values. Data on LOI and TOC across the sites, including analytical accuracy and precision, are reported in Tables A2.01 and A2.02.

TOC ranged between 1.4 and 10%, lowest in BW and the Hayle sites but highest in Percuil River, especially in autumn. Across the Fal estuary, TOC content remained around 5%. Temporal variations in organic carbon were observed across the sites, with higher contents in summer, as has been reported in other estuaries (e.g. Kubo & Kanda, 2017). Observed TOC content in this study agree with those reported in the Fal using similar methods (Greenwood, 2001; Ogilvie & Grant, 2008). The relatively high carbon content at Site PR in Autumn 2017 is likely an artefact of allochthonous plant material decomposition: the narrow creek is bound by trees in close proximity, and Greenwood (2001) noted the presence of leaf litter in the sediments.

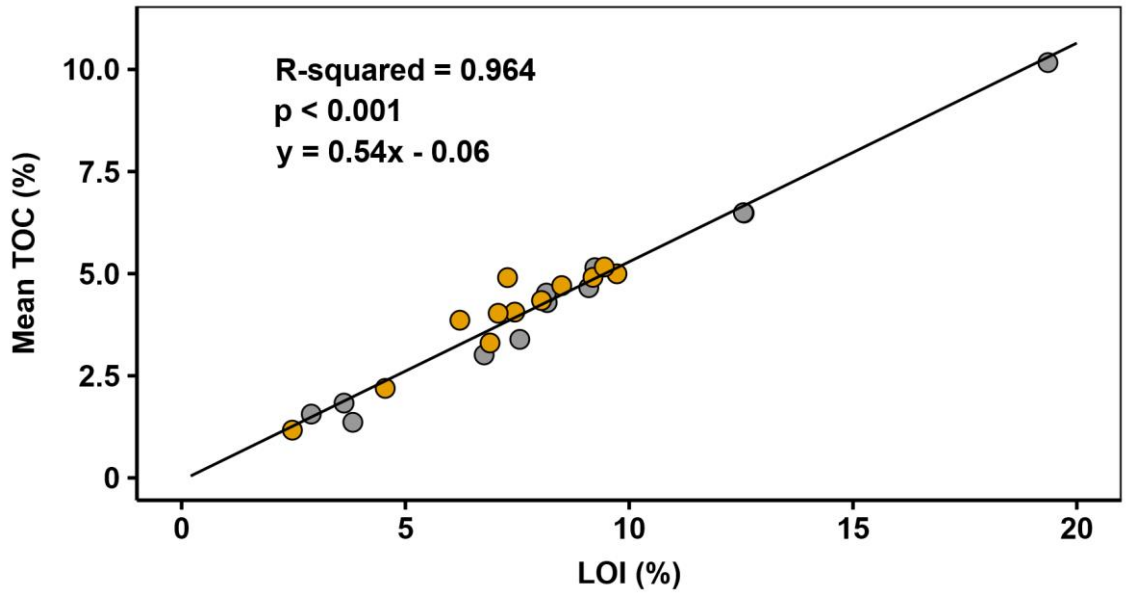

Fig. 2.04: Percentage Loss on Ignition (LOI; at 400 ºC) as a predictor of percentage Total Organic Carbon (TOC) content across the study sites. Data (n = 24) represent samples collected in Autumn 2017 (grey circles) and Winter 2019 (yellow circles)

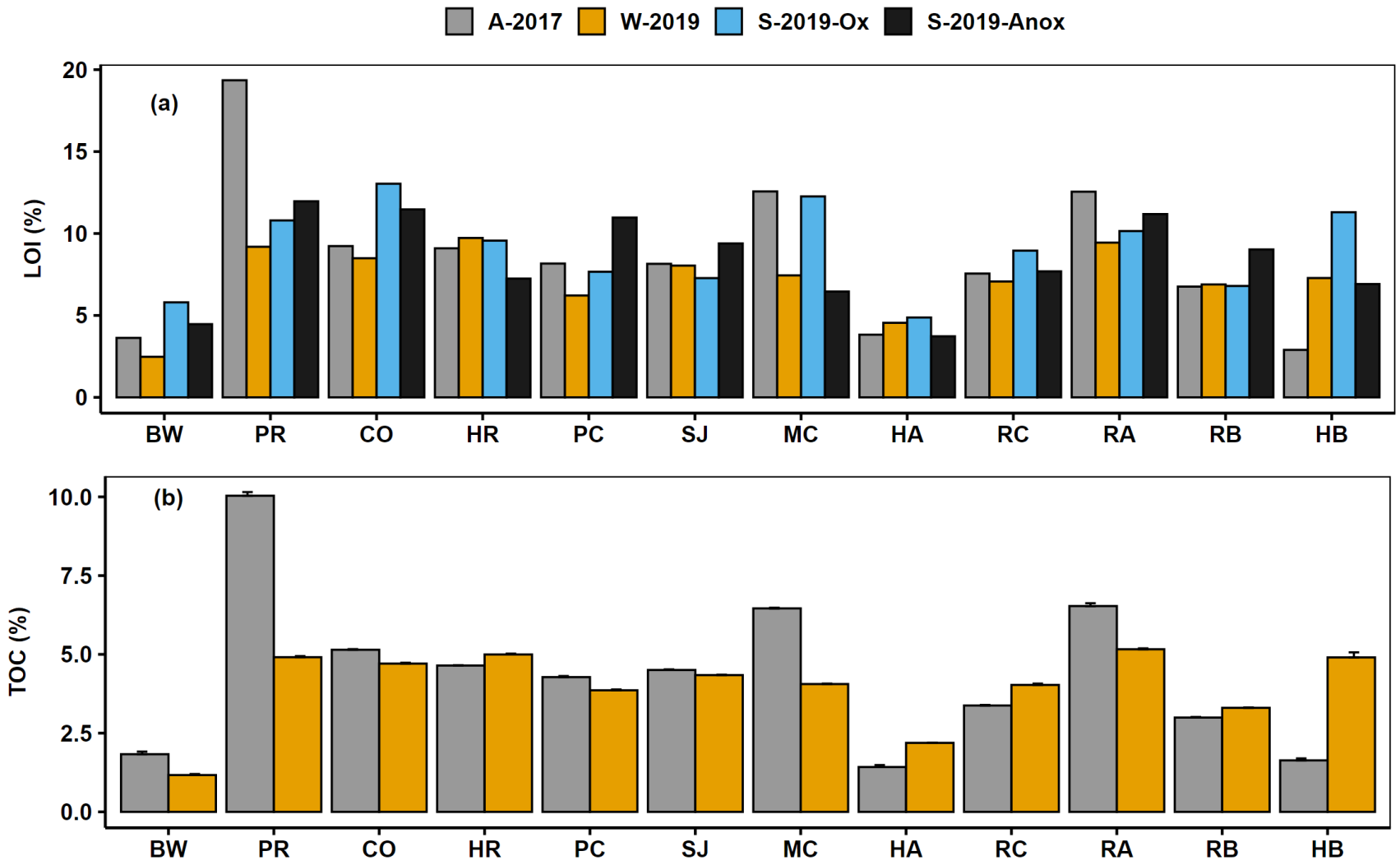

Fig. 2.05: Percentage Loss on Ignition (LOI %, A) and Total Organic Carbon (TOC %, B, Mean ± SD) across the study sites. A-2017 = Autumn 2017, W-2019 = Winter 2019, S-2019-Ox and -Anox = Summer 2019 Oxic and Anoxic sediment.

2.3.4 Dissolved organic carbon in porewater

DOC concentrations as well as the analytical accuracy and precision are reported in Tables A2.03 and A2.04. Variations across the sampling surveys are shown in Figure 2.06. Concentrations ranged between 5 and 47 mg/L and did not seem to be influenced by size fractionation (0.2 or 0.45 µm). As expected, dissolved concentrations were highest in River Hayle (HA), where the coarse grains might be limiting the sorption and/or retention of organic matter (Bergamaschi et al., 1997; Burdige, 2007; Kaiser & Guggenberger, 2007). This explanation agrees with the correspondingly low TOC values at HA (Section 2.3.3). DOC values were also higher in winter, possibly associated with the reduction in heterotrophic biological activity due to colder temperatures (Biddanda & Cotner, 2002).

2.3.5 Total metal concentrations in sediments

Data for all analysed elements, including analytical accuracy and precision, across the surveys are reported in Tables A2.05 – A2.12. Recovery of Cu from the GXR-4 reference material (6520 µg/g) was within 3% of the reference value (Table A2.11), even though the nominal maximum for the calibration is 1000 µg/g. This high recovery indicates that concentrations herein reported are accurate beyond the highest calibration point. Metal concentrations are reported alongside average shale levels (Turekian & Wedepohl, 1961), which have been used as an indicator of pre-industrial, uncontaminated conditions for marine muds (Middleton & Grant, 1990). For key metals (As, Cu, Ni, Pb, and Zn), site comparisons are shown in Figure 2.07. In summary, the results corroborate documented reports that As, Cu, and Zn (in increasing order) are enriched in the Fal and Hayle sediments (Bryan & Gibbs, 1983; Rollinson *et al.*, 2007; Rainbow, 2020). Grain size-normalised metal concentrations are around two orders of magnitude higher than average shale values (13 µg As/g, 45 µg Cu/g, and 95 µg Zn/g) in the most contaminated reaches of the Restronguet Creek and Hayle. Conversely, metal concentrations at the reference Breydon Water site are less than those in average shale, confirming that this site is uncontaminated.

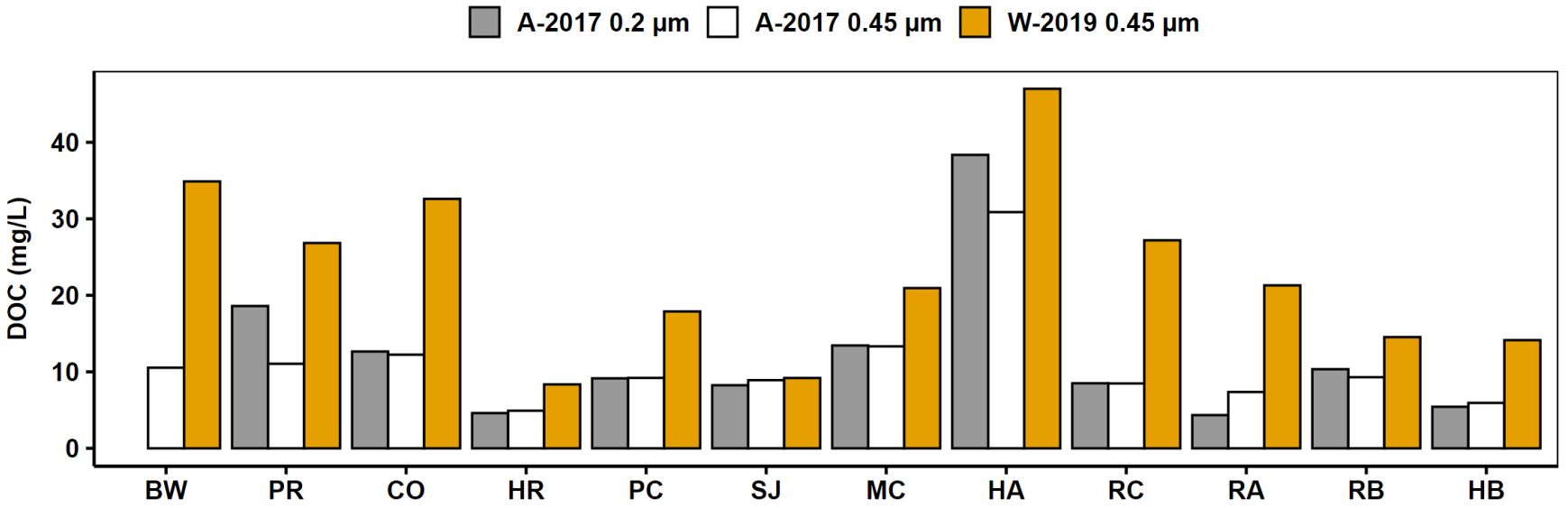

Fig. 2.06: Dissolved Organic Carbon (DOC) concentration in porewater across the study sites in samples filtered to less than 0.2 µm and 0.45 µm. A-2017 = Autumn 2017, W-2019 = Winter 2019, S-2019-Ox and -Anox = Summer 2019 Oxic and Anoxic sediment. No data available for Site BW filtered at 0.2 µm in Autumn 2017

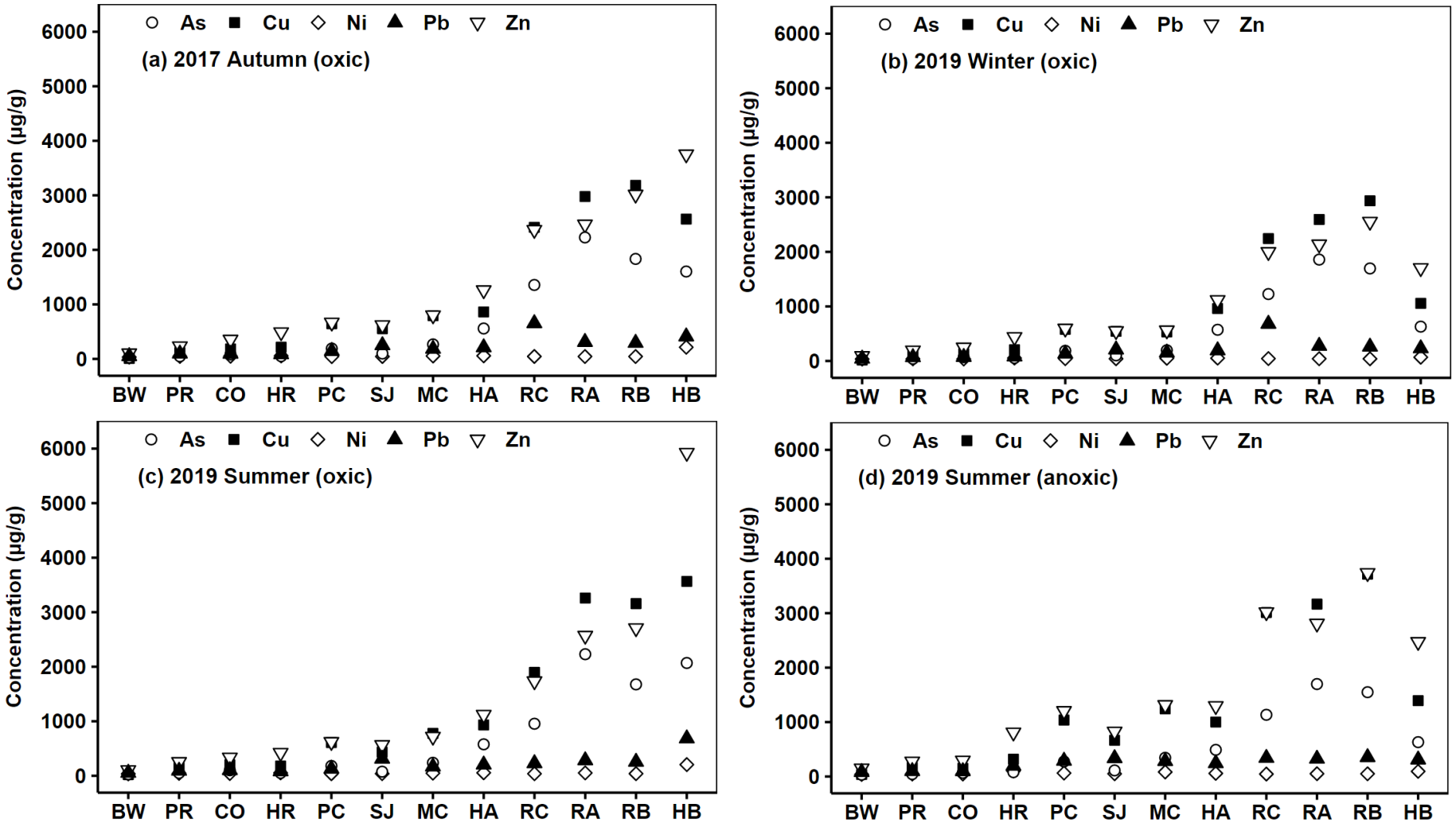

Fig. 2.07: Total metal concentrations (grain size-normalised) in sediments across the study sites. Actual figures are provided in Appendices 2.05 – 2.10

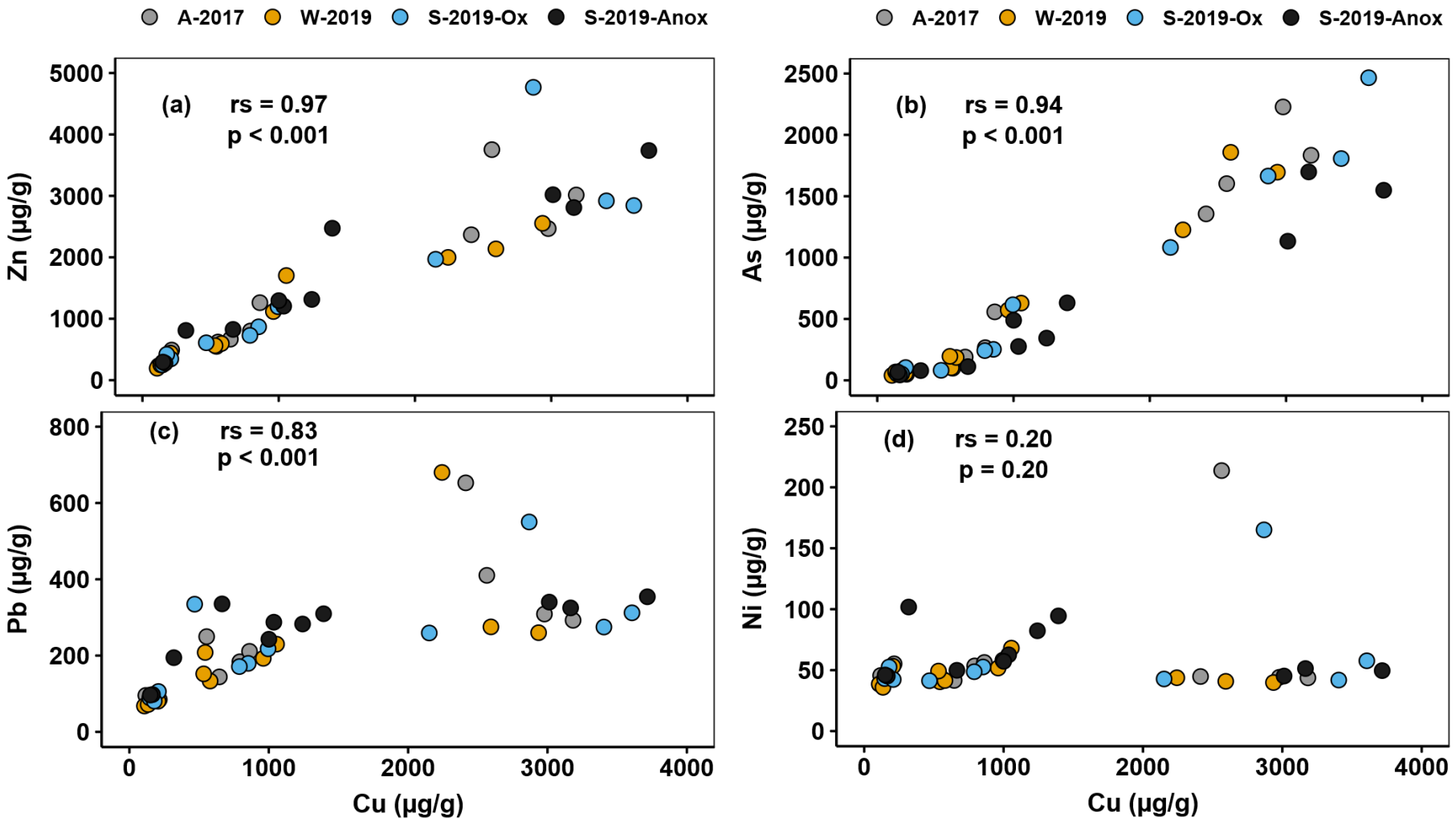

Fig. 2.08: Relationships between sediment Cu and Zn, As, Pb, and Ni concentrations (grain size-normalised, A - D), plus Spearman correlations, across the sites in Cornwall. A-2017 = Autumn 2017; W-2019 = Winter 2019; S-2019-Ox and -Anox = Summer 2019 Oxic and Anoxic sediment

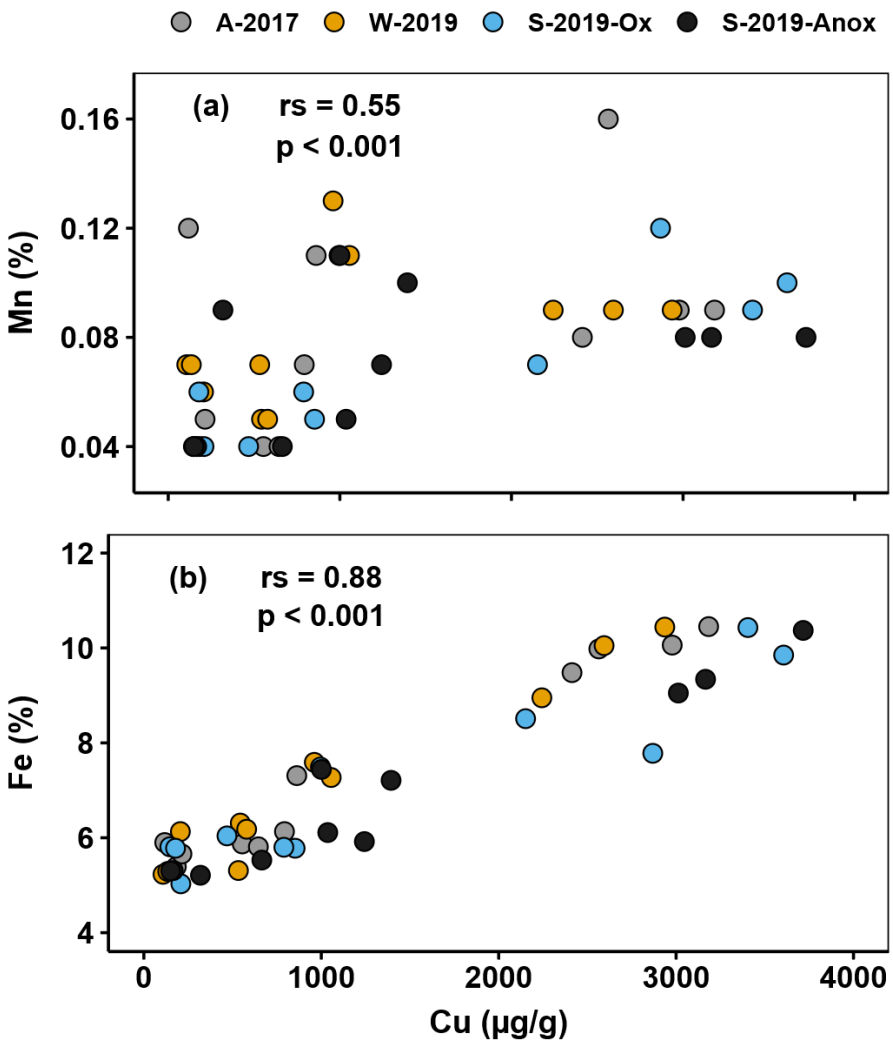

Fig. 2.09: Relationships between sediment Cu (grain size-normalised) and Fe (a) and Mn (b) concentrations, plus Spearman correlations, across the sites in Cornwall. A-2017 = Autumn 2017; W-2019 = Winter 2019; S-2019-Ox and -Anox = Summer 2019 Oxic and Anoxic sediment

Ag, Cd, and Sn were not quantifiable by XRF. Previous studies show that concentrations of Ag and Cd in the Restronguet Creek and Hayle are very low (maximum of 6.2 and 8.0 µg As/g as well as 1.8 and 0.47 µg Cd/g, in both sites respectively; Rainbow, 2020). For Sn, reported concentrations are in excess of 3000 µg/g in the Restronguet Creek, 5000 µg/g in River Hayle, and 10000 µg/g in the Copperhouse Pool (Greenwood, 2001; Rollinson *et al.*, 2007; Rainbow, 2020). Elevated concentrations of Sn in both estuaries is expected, given largescale mining operations in their respective catchments, until recently (Rollinson *et al.*, 2007). It is, however, noteworthy that Sn in these sediments is extremely tightly bound in the mineral cassiterite and is not released by standard extraction agents, including

concentrated nitric acid (Rainbow, 2020). Therefore, despite these high levels, Sn is likely to be of limited bioavailability[13] to benthic organisms in the Fal and Hayle estuaries.

Within the Fal estuary, concentrations of As, Cu, and Zn, as expected, increased with distance upstream. The mixture of freshwater inputs with seawater in the upper Restronguet Creek results in the co-precipitation and/or adsorption of metals in iron (oxy)hydroxides, leading to their rapid removal from solution and subsequent deposition in the sediments (Bryan & Gibbs, 1983; Johnson, 1986; Bryan & Langston, 1992; Somerfield *et al.*, 1994a). This phenomenon is demonstrated in the current study by strong correlations between concentrations of Fe and enriched metals, using Cu as a proxy (Figures 2.08 and 2.09; $p < 0.001$; $rs > 0.80$). However, the oxidation of As (as arsenate) and its association with Fe (oxy)hydroxides in surface sediments may result in a limited bioavailability to benthic fauna (Bryan & Langston, 1992), similar to Sn. Cu and Zn concentrations measured in the Restronguet Creek are in excess of 2000 µg/g across the surveys, exceeding 3000 µg/g in Tallack's (RB) in Summer 2019. In Percuil River, the least contaminated tributary, metals drop to around twice the average shale values. Tolerance of nematode communities to Cu in this site is comparable to those in BW (Millward & Grant, 2000; Grant, 2010; Chapter 3), suggesting that the ecological effects of Cu is limited in Percuil River.

Metal concentrations in the Hayle estuary are also elevated. Similar to findings by Greenwood (2001), concentrations of Cu and Zn are higher in the Copperhouse Pool (HB, >2000 µg/g) relative to the sandy River Hayle (HA, ~800 – 1000 µg/g) sediments. In Summer 2019, the highest concentrations throughout this study (3565 µg Cu/g and 5924 µg Zn/g) were recorded in the fine fraction of surface sediments at HB, higher than previous reports in the estuary (Greenwood, 2001; Rollinson *et al.*, 2007; Grant, 2010). Zn concentration (3753 µg/g) was also higher in HB than the Restronguet Creek in Autumn 2017, unlike Cu and As.

Given that concentrations across the contamination gradients have remained stable in the Fal and Hayle estuaries for several decades (Bryan & Gibbs, 1983; Somerfield *et al.*, 1994a; Greenwood, 2001; Rollinson *et al.*, 2007; Rainbow *et al.*, 2011; Rainbow, 2020), wide temporal variations in sediment metal concentrations were not expected in the current study. Concentrations observed here are comparable with earlier reports in the both estuaries,

[13] Bryan and Langston (1992) report that Sn accumulation by the clam, *Scrobicularia plana*, in the Fal estuary reflects concentrations of tributyltin, which is more readily bioavailable.

except for the high Cu and Zn concentrations at HB in Summer 2019. At HB, metal concentrations may have been overestimated upon grain size normalisation, given the relatively low fine sediment fraction[14]. Applying a PCA to total As, Cu, Ni, Pb, and Zn concentrations averaged across the sampling surveys, study sites can be ranked in order of increasing contamination as follows: BW < PR < CO < HR < PC < SJ < MC < HA < RC < RA < RB < HB (Figure 2.3; See preamble to Section 2.3).

2.3.6 Acid-extractable metal, SEM, and AVS concentrations in sediments

For the five common divalent metals which bind with AVS (Cd, Cu, Ni, Pb, and Zn), extractable concentrations are reported as molar SEM concentrations to facilitate comparison (Figure 2.10; Tables A2.13 – A2.15). Ag was not measured in the current study due to analytical constraints. However, total Ag concentrations previously reported in the Fal and Hayle are less than 5 µg/g (Rainbow, 2020). Greenwood (2001) has also shown that Ag constitutes less than 1% of ΣSEM across the sites, with concentrations ranging between ~ 0.01 and 0.03 µmol/g in summer and winter. Concentrations of As, Fe, and Mn, where analysed in the current study, are reported in µg/g. Analytical accuracy and precision of acid extractions are reported in Table A2.16. AVS concentrations are presented in Table A2.17.

Concentrations of SEM Cu (0.14 – 27.72 µmol/g; 8 – 1760 µg/g) and SEM Zn (0.59 – 25.87 µmol/g; 39 – 1692 µg/g) follow similar trends as total sediment concentrations across the sites (Figure 2.10), indicating that both metals are not only enriched, but may be bioavailable to the benthos. In the Fal and Hayle sediments, Cu and Zn jointly constitute 90 – 98% of ΣSEM for the divalent metals measured in Autumn 2017 and Winter 2019, hence the decision to measure only these metals in Summer 2019. Cd was not detectable in Winter 2019. As earlier highlighted, Cd concentrations are historically low in both estuaries sampled. In Breydon Water, where metal concentrations are very low, the percentage ΣSEM composition of Cu, Zn, Cd, Ni, and Pb are 13%, 56 – 65%, <0.001%, 7 – 13%, and 15 – 18%, respectively, using data from Autumn 2017 and Winter 2019. Considering the overall composition across the study sites and sampling seasons, SEM composition can be ranked as follows: Cd < Ni < Pb < Cu < Zn. These trends corroborate observations by Greenwood (2001). She reports a maximum ΣSEM concentration of 62.61 µmol/g in surface sediments

[14] Non-normalised Cu and Zn concentrations in surface sediments of HB in Summer 2019 are 834 µg Cu/g and 1386 µg Zn/g, in comparison with 3565 µg Cu/g and 5924 µg Zn/g in the fine sediment fraction.

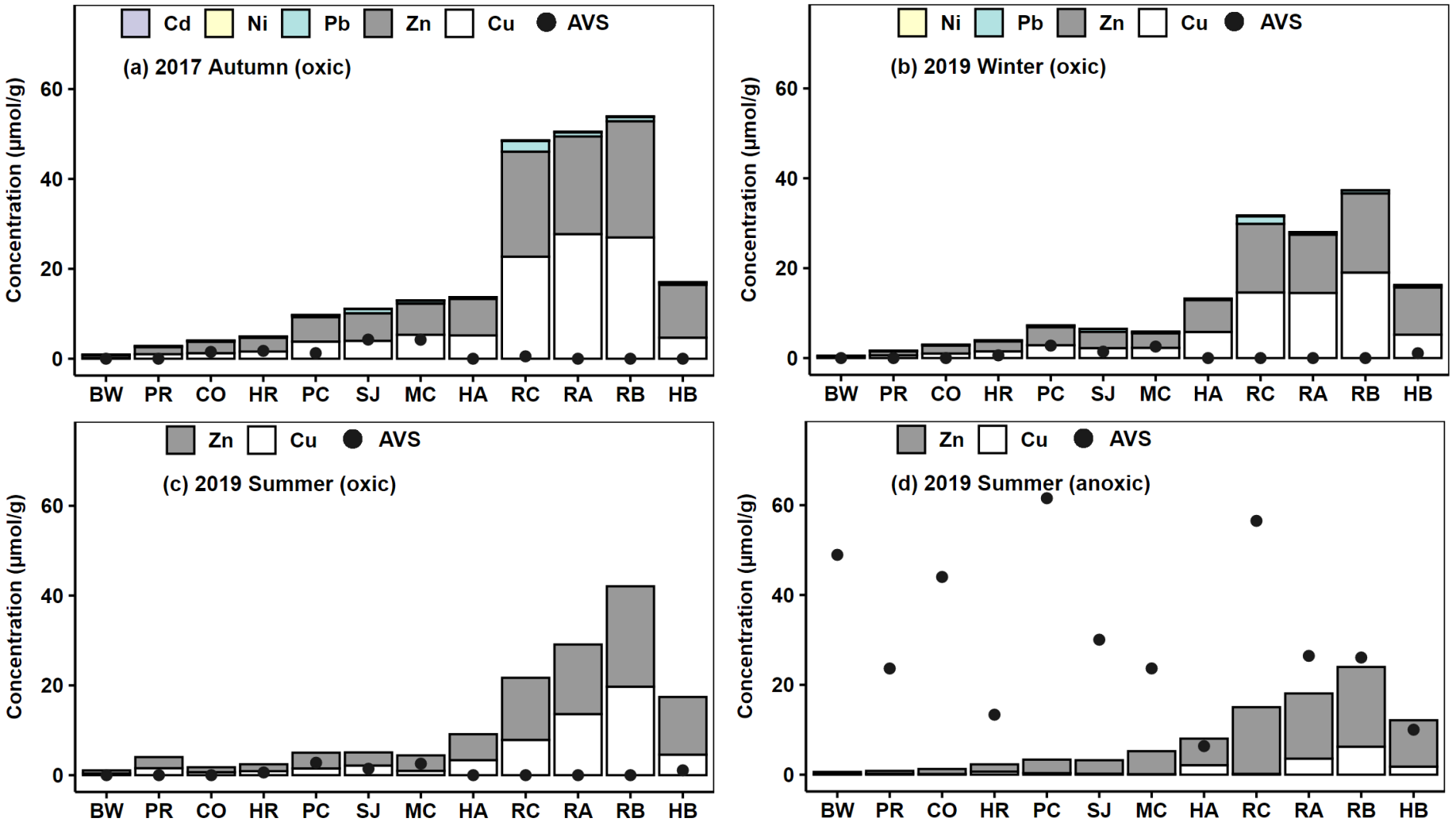

Fig. 2.10: Sediment AVS and molar [SEM] concentrations of key divalent metals across the study sites

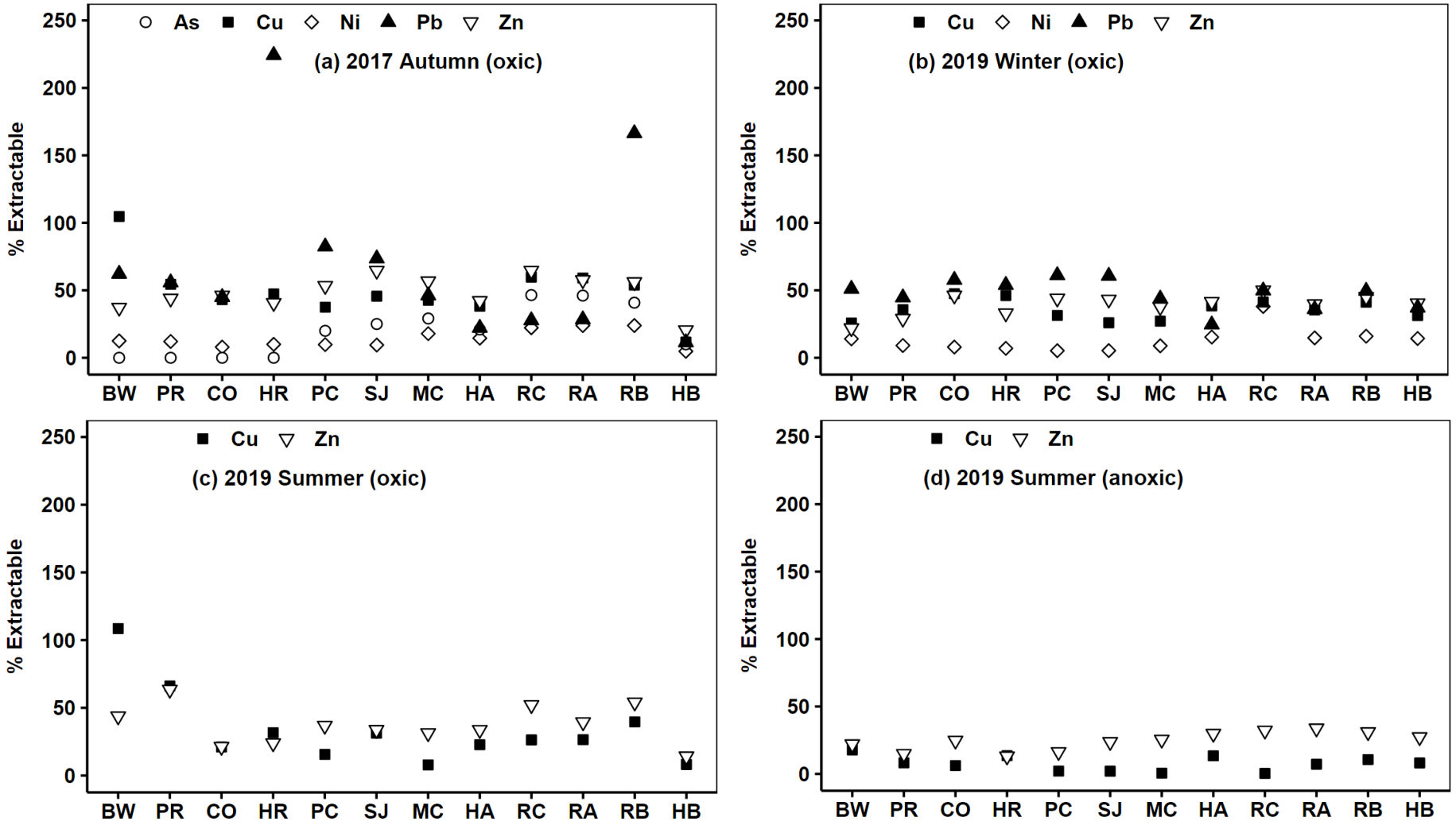

Fig. 2.11: Percentage of total sediment metal concentrations (grain size-normalised) extractable in 1M HCl across the study sites. Values exceed 100% for low-concentration sites and metals where differences in methodology (i.e. XRF vs strong acid extraction) are amplified

of the Restronguet Creek, which is similar to 53.92 µmol/g recorded here in Autumn 2017. Both studies report SEM Cd, Ni, and Pb less than 1 µmol/g across the sites, except for Site RC in this study (SEM Pb = 2.35 and 1.63 µmol/g, respectively, in Autumn 2017 and Winter 2019). These relatively high concentrations of "bioavailable" Cu and Zn support ecological effects linked to both metals in the estuaries (Rainbow, 2020).

Measured SEM Cu concentrations are diminished in Summer 2019, corresponding with an increase in AVS concentrations across the sites (Figure 2.10; Table A2.17). This observation is consistent with the formation of metal sulphides in reduced sediments. Unlike other divalent metals, Cu and Ni sulphides formed from reaction with AVS are poorly soluble in 1 M HCl (Cooper & Morse, 1998; Simpson, 2001). AVS concentrations in the anoxic sediments are in excess of ΣSEM, except in both Hayle sites, ranging from 6.4 µmol/g to 61.5 µmol/g at Pill Creek. AVS concentrations in surface sediments are also high in Summer 2019 (< 0.5 – 23.8 µmol/g) in comparison with concentrations less than 5 µmol/g in the most anoxic sites in autumn and winter. The relatively high summer AVS concentrations are expected. As earlier highlighted, solubility of oxygen reduces (de Klein *et al*., 2017) and biological activity increases (Biddanda & Cotner, 2002) with increasing sediment temperature. The resulting oxygen depletion in marine sediments accelerates the dissimilatory reduction of available electron acceptors, including sulphates (see review by Thamdrup & Canfield, 2000; Chapter 6), as well as the direct bacterial reduction of sulphates (see review by Jorgensen *et al*, 2019), both of which result in the accumulation of sulphides. The highest surface AVS concentrations were measured in the black-coloured sediments of PC, MC, and SJ, consistent with Greenwood's (2001) study. According to EqP predictions (AVS > ΣSEM), anoxic sediments in the Fal are not expected to elicit metal toxicity. This hypothesis is explored further in Chapter 5 of this thesis.

The percentage of total metal concentrations extractable in 1 M HCl across the sites is shown in Figure 2.11. The proportion of metals extractable often exceeded 100% for sites or metals with low contamination, reflecting the minimal differences in the extraction method versus XRF analysis. As observed by Greenwood (2001), there was a wide variation between metals, between sites, and between sampling seasons. Using surface sediments of the Restronguet Creek as an example, extractable Cu (>22.7 µmol/g; 1441 µg/g), Zn (>21.73 µmol/g; 1421 µg/g), As (>630 µg/g) and Fe (>18563 µg/g) measured represent ~59, 58, 46, and 20% of total concentrations, respectively. In Winter 2019, recovery of total Cu, Zn and Fe concentrations in the same creek dropped to ~35, 40, and 12%, respectively. However,

extractable Cu, Zn and Fe concentrations in Summer 2019 in RC were ~26, 52, and 10% of total concentrations, respectively. Extractability of metals appears to reduce proportionately in the Copperhouse Pool, highlighting site-specific differences. There are several possible explanations for this variation, including the relative concentrations of different metal binding phases in the sediments. For Cu, the importance of AVS is already described in the preceding paragraph. Overall, binding of metals to carbonates, crystalline Fe oxides, and/or organic matter (Chao & Zhou, 1983; Whalley & Grant, 1994; Bacon & Davidson, 2008) may affect sediment extraction. Notwithstanding, the concentrations reported in the current study are within the range previously observed in the Fal estuary (Millward, 1995; Greenwood, 2001; Shipp, 2006).

2.3.7 Recovery of metals from saline samples

The high salt content of seawater poses several challenges for the direct analysis of trace metals. Key difficulties include (i) the exacerbation of spectral and non-spectral interferences due to the complex matrix, (ii) the potential loss in accuracy due to low analyte concentrations, and (iii) the potential damage of machinery due to excessive deposition of salt (Field *et al*., 2007; Jackson *et al*., 2018). Consequently, several methods of sample pre-treatment, including solvent extraction, co-precipitation, and solid-phase extraction with resins, have been described to separate analytes of interest from the saline matrix (Jackson *et al*, 2018; Wuttig *et al*., 2019).

Throughout this thesis, saline samples were processed by chelex resin extraction, prior to metal analysis. The procedure was designed to maximise extractable concentrations, maximise precision, and minimise external contamination – all done using simple, low-cost laboratory materials and equipment. It was necessary to remove colloids and organic ligands, through sample digestion, to enable measurement of total dissolved concentrations (Nicolai *et al*., 1999). Because metal binding with chelex is kinetically driven (Figura & McDuffie, 1980; Herrin *et al*., 2001; Quattrini *et al*., 2017), preliminary experiments were completed, using spiked seawater samples, to determine optimal equilibration times. Further experiments were conducted to determine optimal resin extraction times as well as the effectiveness of ammonium acetate pre-extraction, which is often necessary to selectively remove alkali and alkaline-earth metals (Kingston *et al*., 1978). This is because excess resins and/or long equilibration times during batch extraction may result in the chelation of "nuisance" alkali and alkali-earth metals (e.g. Na, K, Mg, and Ca), which could influence

analytical accuracy. Kingston and coworkers (1978) showed that these metals can be selectively removed by pre-extraction with 1 M NH4Ac at pH 5.5

The preliminary experiments revealed that (i) a duration of 72 hrs is optimal for both equilibration and acid extraction in undigested samples (Figure A2.18, corroborating Figura & McDuffie, 1980), (ii) ammonium acetate pre-extraction may also remove transition metals of interest (Figure A2.19), and (iii) sample digestion is important for the removal of colloids, with acid-extraction duration of 12 hrs optimal for treated samples (Figure A2.20). The ammonium acetate pre-extraction step was consequently removed. In order to increase sample throughput, an equilibration duration of 24 hrs was selected. Recovery of Cu, Zn and Fe was $\gtrsim$ 80% in the final, non-saline calibration method (Tables A2.21 and A2.22). However, recovery of Mn further dropped to ~2.5%. Precision of the method is relatively high: <3.8% for Cu, <9.3% for Zn, <3.7% for Fe, and ~10.2% for Mn (Tables A2.21 and A2.22). Amongst others, the reliance on tube graduation during acid extraction (Step E, Figure 2.02) may affect method accuracy and precision. It is therefore important to use (preferably new) 15 mL centrifuge tubes purchased from the same manufacturer.

2.3.8 Porewater metal concentrations across the study sites

Porewater metal concentrations were determined using two methods – saline versus non-saline calibration standards – in Autumn 2017 and Winter 2019 (Tables A2.23 and A2.24). Except for Sites RA and RB, metal concentrations derived from both methods were similar. For Site RA in Autumn 2017, Cu and Fe concentrations derived using non-saline calibration were nearly halved versus using saline calibration standards. However, in Winter 2019, differences in Cu, Zn and Fe were nearly an order of magnitude. A similar difference in Fe was noted for Site RB in Winter 2019. The reason for such disparity is unclear. It might be related to high Fe concentrations, especially in Winter 2019, resulting in poor solubility of metals in extracted porewater (Simpson & Batley, 2003), despite acidification to 1% nitric acid. Or, especially in Autumn 2017, perhaps due to the presence of colloidal Fe(III) present in the 0.45 µm filterate, but removed by filteration at 0.2 µm.

Recovery of Cu, Zn, and Fe were within 5% and 20% of spiked seawater concentrations, respectively, for the saline and non-saline calibration method (Tables A2.21 & A2.22). For the non-saline calibration, which was linked to certified reference materials, analytical accuracy was within 20% of certified values (Table A2.22). Given the superior confidence in calibration associated with the use of certified references, results from the non-saline

calibration are preferred. Metal concentrations measured in Summer 2019, calibrated using non-saline standards, are presented in Table A2.24. The results are reported alongside relevant Water Framework Directive (2015, henceforth, WFD) thresholds, below which surface water bodies are legally designated as being of "good" chemical status. Variations in Cu and Zn concentrations across the surveys are shown in Figure 2.12.

Unlike the sediment, porewater Cu concentrations in River Hayle (HA) were higher than or comparable to the maximum levels measured in the Restronguet Creek (223.9 vs 130.3 µg/L at RA in Autumn 2017; 112.7 vs 128.6 µg/L at RB in Winter 2019; and 12.5 vs 34.8 µg/L at RA in Summer 2019). These concentrations, except in summer, are higher than the 25.1 µg Cu/L WFD threshold[15]. In sandy sediments of HA, metals are notably more bioavailable than elsewhere across the Fal and Hayle (Grant, 2010). Partitioning of metals to the porewater is likely facilitated by the relatively low sediment TOC content (Di Toro *et al*., 2005) and coarser grain size (Simpson *et al*., 2011), among other factors. Within the Restronguet Creek, porewater Cu tended to be higher in the Kennal River (RA) than at Tallack's (RB), contrary to sediment concentrations (Figure 2.12; Tables A2.23 – A2.25), highlighting a possible effect of salinity in metal partitioning (Chapman & Wang, 2001; Bryan & Hummerstone, 1971; Chapter 1). The lowest concentrations were measured at BW (<5 µg/L across the surveys), followed by Percuil River in the Fal. The relatively low concentrations in summer coincides with the variation in redox potential and AVS content, consistent with the formation of insoluble metal sulphides (Burgess *et al*., 2013; Section 2.3.6). Cu levels drop below 6 µg/L in the anoxic sediments, except at Cowlands, where AVS was lowest among the sites analysed.

Porewater Zn concentrations across the sites followed similar trends as described for Cu. The highest concentrations were measured in the Copperhouse Pool (HB) in Autumn 2017 (913.6 µg/L vs 7.9 µg Zn/L WFD threshold), coinciding with high values for total sediment Zn during the same survey. Otherwise, Zn concentrations ranged between 20.0 – 270.0 µg/L in Autumn 2017, 5.8 – 219.1 µg/L in Winter 2019, 5.2 – 138.3 µg/L in surface sediments in Summer 2019, and 6.2 – 30.1 µg/L in anoxic 2019 sediments. Except in SJ in Winter 2019, concentrations across the Fal and Hayle estuaries were higher than the WFD threshold, suggesting a possibility of toxic effects to benthic organisms.

[15] Cu limit derived using average DOC (<0.45 µm) across the sites in 2017 and 2019 (17.0 mg/L), as recommended.

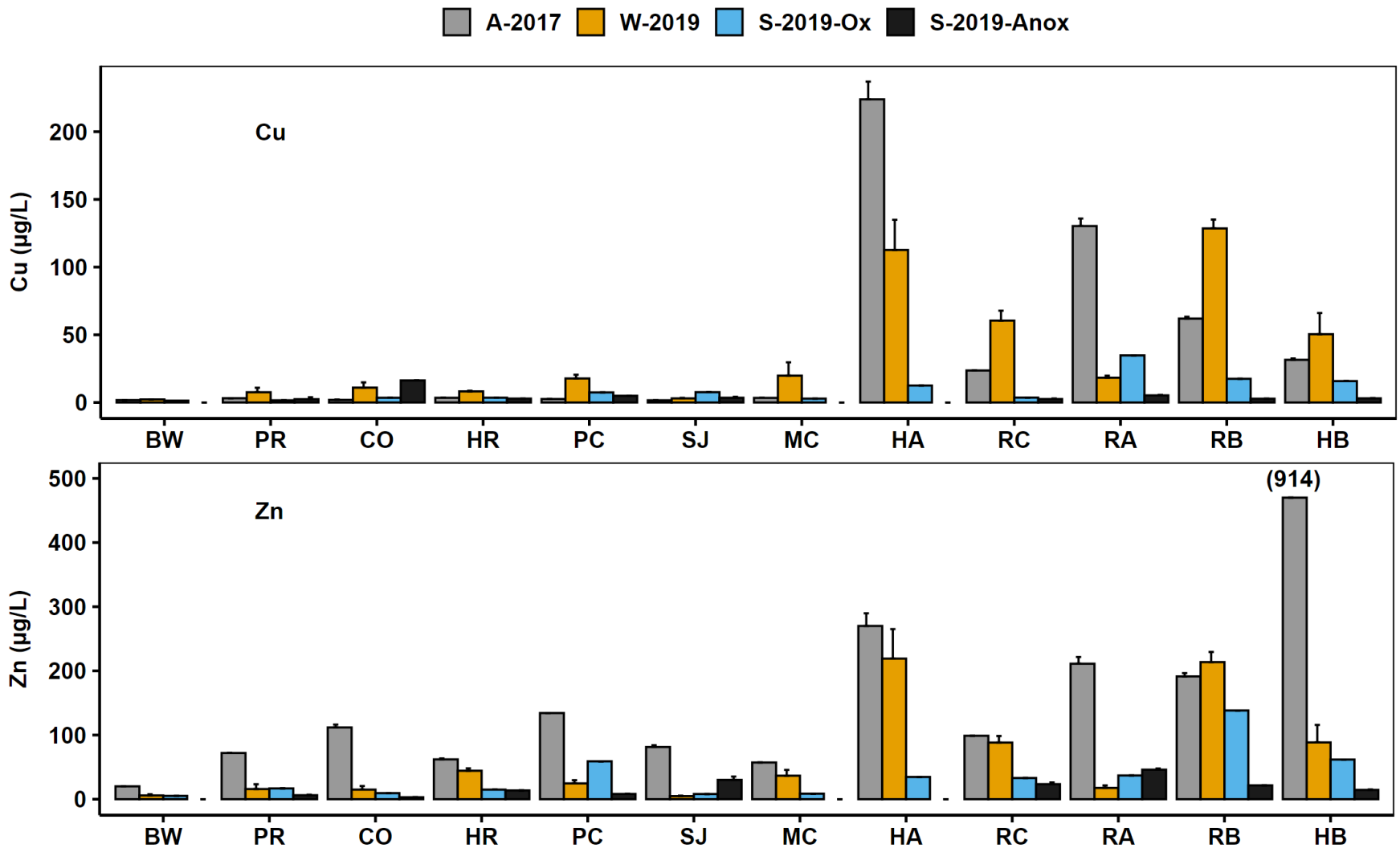

Fig. 2.12: Porewater Cu and Zn concentrations across the study sites. A-2017 = Autumn 2017, W-2019 = Winter 2019, S-2019-Ox and -Anox = Summer 2019 Oxic and Anoxic sediment. Error bars = SD. No data for BW, MC, and HA in S-2019-Anox sediment.

Fe and Mn are redox sensitive metals. Dissolved concentrations often reflect, amongst other processes, the formation or reduction of (oxy)hydroxides in surface sediments as well the formation of sulphides or pyrite (FeS_2) in anoxic sediments (see review by Raiswell & Canfield, 2012). Accordingly, dissolved Fe and Mn concentrations varied widely between sampling sites and seasons. The highest Fe concentrations in surface sediments were recorded in Summer 2019, 22352.5 µg/L at Pill Creek, but concentrations were greater than the WFD threshold (1000 µg Fe/L) in all sites, except BW, HR, HB, and RB. Surface porewater Mn concentrations (43.9 - 245 µg/L)[16] were also highest in Summer 2019. The relatively low concentrations in Winter 2019 surface sediments and Summer 2019 anoxic sediments are likely as a result of metal precipitation as (oxy)hydroxides and sulphides, respectively, as earlier highlighted. In the Fal and Hayle estuaries, the particular importance of Fe in controlling trace metal concentrations has been earlier described (Section 2.3.5). This phenomenon is explored further in Chapter 6.

In contrast with the wealth of data on sediment concentrations, relatively few studies have reported metal concentrations in porewater in the Fal and Hayle estuaries. Using voltammetric techniques, Greenwood (2001) reported total concentrations up to 495.7 µg Cu/L and 405.3 µg Zn/L in River Hayle as well as 68.2 µg Cu/L and 413.8 µg Zn/L in the Restronguet Creek. In a later survey in which metals were measured using Graphite furnace atomic absorption spectroscopy (GFAAS), she reports concentrations up to 3378.2 µg Cu/L and 247.8 µg Zn/L in River Hayle, 769.64 µg Cu/L and 200 µg Zn/L in the Copperhouse Pool, as well as 62.20 µg Cu/L and 362 µg Zn/L in Restronguet Creek. Measured by direct ICP-OES analysis, Ogilvie and Grant (2008) recorded concentrations up to 783 µg Cu/L and 413.8 µg Zn/L in River Hayle, 463 µg Cu/L and 163 µg Zn/L in the Copperhouse Pool, as well as 27.65 µg Cu/L and 25.92 µg Zn/L in Restronguet Creek. However, Bryan and Gibbs (1983) report porewater concentrations up to 83 µg Cu/L and 396 µg Zn/L in surface sediments of Restronguet Creek. The trend across these studies shows increased porewater concentrations in the Hayle, relative to the Fal, as shown in the current study. Differences in actual concentrations reported may reflect differences in analytical methodologies or temporal variation, as observed in the current study.

[16] Note that Mn concentrations reported in this study represent 2 – 2.5% of actual values (Table A2.22).

2.4 Chapter summary

Summarising the content of this Chapter, the Fal and Hayle estuaries are grossly contaminated with As, Cu, Sn, and Zn as a result of historical mineral mining activities in their catchment. In both estuaries, sediment metal concentrations have been stable through several decades of measurement, establishing a contamination gradient across the study sites from Percuil River to the Restronguet Creek. In the upper reaches of the Restronguet Creek, which is closest to mine drainage inputs, metal concentrations in sediments are two orders of magnitude higher than pre-industrial values, determined from average shale, and nearly three orders of magnitude higher than in an uncontaminated site, Breydon Water, in Norfolk. In the Hayle Copperhouse Pool, metal concentrations are slightly higher than in Restronguet Creek, but these might have been overestimated upon grain size normalisation, given the relatively low fraction of fine sediment there. Despite their high concentrations, the chemical forms of As and Sn in these sediments greatly limit their bioavailability, meaning that toxicity of these sediments to organisms is more likely due to Cu and Zn.

Sediment physicochemical characteristics vary markedly across the contamination gradient, resulting in wide differences in metal bioavailability. Porewater Cu and Zn concentrations tend to be highest in the relatively oxidised and sandy sediments of River Hayle. However, porewater concentrations in the relatively reduced Pill Creek, despite high sediment levels, are similar to those in Percuil River, the least contaminated tributary of the Fal. These varying physicochemical attributes as well as the absence of other interfering pollutants make the Fal and Hayle ideal sites for investigating the effects of metal contamination on *in situ* benthic communities. Considering sediment concentrations of As, Cu, Ni, Pb, and Zn (the five key divalent metals – see Chapter 1) across the surveys, the study sites are ranked using a PCA in order of increasing contamination as follows: BW < PR < CO < HR < PC < SJ < MC < HA < RC < RA < RB < HB, which is the same order in which results have been reported throughout this thesis.

Chapter 3.

Are Diffusive Gradients in Thin Films (DGTs) useful predictors of the ecological effects of Cu in field sediments?

3.1 Introduction

It is widely agreed that the ecological effects of metals in marine sediments reflect their bioavailability, and not necessarily the total concentrations (Chapman *et al.*, 1998; Simpson & Batley, 2007; Burton, 2010). However, the varying influence of sediment geochemical properties as well as organism-specific uptake behaviour and physiology makes it challenging to assess bioavailability in the field (Simpson & Batley, 2007; Birch, 2018). The literature on metal speciation in sediments and current approaches to the prediction of bioavailability and toxicity have been reviewed in Chapter 1.

So far, no one method has proved universally applicable for predicting metal bioavailability to the sediment biota. The tissue residue approach (TRA) is confounded by physiological and physicochemical factors affecting metal bioaccumulation in organisms (Rainbow 2002, 2007). Equilibrium-partitioning (EqP) approaches based on the measurement of acid-volatile sulphides (AVS) and simultaneously-extracted metals (SEM) have been useful in predicting the lack – but not presence – of toxicity (Ankley *et al.*, 1996; Di Toro *et al.*, 2005) and may not apply to oxic or sub-oxic conditions that exist in the burrows of benthic invertebrates (Simpson *et al.*, 2012a; Remaili *et al.*, 2016). Furthermore, in oxidised, surface sediments where AVS is negligible or exhausted, normalisation using organic carbon (OC) content under the current EqP framework overlooks the importance of metal binding to Fe (oxides), amongst other sediment phases (Di Toro *et al.*, 2005). Chemical extraction, especially using 1 M HCl, has shown strong correlations with accumulation in laboratory experiments (Amato *et al.*, 2015; Belzunce-Segarra *et al.*, 2015) and in the field (see review by Bryan & Langston, 1992). However, extractants such as HCl are capable of extracting metals in non-labile complexes (e.g. AVS, Ankley *et al.*, 1996), thus potentially exaggerating metal bioavailability in the sediments.

In the search for simple, yet effective, tools for predicting metal bioavailability in sediments, diffusive gradients in thin films (DGTs) have shown good promise. DGT is a kinetic technique for quantifying labile species in aqueous systems (Davison & Zhang, 1994; Davison *et al.*, 2012; Chapter 1). The technique has been used successfully for predicting

nutrient response as well as metal uptake and toxicity in plants (see review by Zhang & Davison, 2015). For benthic invertebrates, DGT-measured concentrations correlated strongly with metal accumulation and acute toxicity in some laboratory and transplantation experiments involving spiked sediments (e.g. Simpson *et al.*, 2012b; Amato *et al.*, 2015, 2016, 2018), prompting conclusions that DGT is a useful tool for assessing sediment metal bioavailability (Eismann *et al.*, 2020). However, spiking sediments at high concentrations, as carried out in these studies, may bias partitioning of metals to the porewater in comparison with actual field conditions (Lee *et al.*, 2000a,b). Also, bioaccumulation is not an ecological effect and has limited use in the derivation of sediment quality criteria (Di Toro *et al.*, 2005; Burton, 2013). In order to form any conclusions about the usefulness of DGT in assessing metal bioavailability in marine sediments, there is, therefore, the need for studies that relate DGT-labile concentrations with actual ecological effects in field-contaminated sites.

In this study, the capability of DGT to predict ecological effects of Cu along a contamination gradient in the Fal and Hayle estuaries is assessed against traditional measures – total sediment metal concentration, total porewater concentration, OC–normalised porewater concentration (Water Framework Directive, 2015, henceforth WFD)[17], and the EqP OC-normalised sediment measurement. Ecological effects are assessed using the pollution-induced tolerance of nematode communities (henceforth, PICT; Millward & Grant, 1995, 2000), which is based on the occurrence of heritable tolerance as a result of the selective pressure of Cu in the sites as well as the switch of the community composition towards more tolerant species (Grant, 2002). The objective is to determine which measure of metal concentration best predicts the effects of Cu across the study sites as well as the threshold concentrations at which these effects begin to occur.

3.2 Methodology

3.2.1 Experimental design

This study was designed to compare the capability of DGT-measured concentrations, total sediment concentration, acid-extractable concentration, total porewater concentration, OC–normalised porewater concentration, and the EqP OC-normalised sediment measurement in predicting the ecological effects of Cu in field-contaminated sites. DGT probes were

[17] The WFD (2015) standard for Cu includes an adjustment based on DOC concentration on the basis that DOC limits Cu bioavailability. This has been confirmed in recent toxicity studies (e.g. Strivens *et al.*, 2019), hence the OC-normalised porewater measure.

deployed *in situ* across the contamination gradient in the Fal and Hayle estuaries as well as in the uncontaminated Breydon Water site, spanning nearly three orders of magnitude in total sediment Cu concentrations (Chapter 2). Sediments were concurrently analysed for traditional measures of Cu contamination. The ecological effects of Cu were assessed using the occurrence of tolerance (measured as median time to death) in established nematode communities at the study sites (Millward & Grant, 1995, 2000). Although several metals occur in potentially-toxic concentrations in the Fal and Hayle estuaries (Chapter 2; Rainbow, 2020), pollution tolerance is a powerful tool that can isolate effects resulting from a single toxicant in exposed species (Grant *et al.*, 1989; Blanck, 2002; Grant, 2002).

3.2.2 DGT probes: design, assembly, and performance testing

DGT probes were assembled according to standard procedures in a Class II laminar flow cabinet (Jolley *et al.*, 2016; Chapter 1; Figure 3.01). Chelex® binding gel strips (0.4 mm thick) and APA diffusive gel sheets (0.8 mm thick) were purchased from DGT Research LTD, Lancaster. Polyethersulphone (PES) filter membrane sheets (0.45 μm pore size, 0.14 mm thickness) were purchased from GVS filter Technology, UK, LTD. Thickness of the materials was confirmed using a digital micrometer screw gauge. The gels were cut to size on a glass plate using bespoke gel cutters and gently placed, in sequence, in the probe housing base. The diffusive gel was then covered with a layer of PES membrane, before enclosing with the probe top. Gels and assembled devices were handled using acid-washed, plastic forceps and spatulas to limit contamination. All gels as well as the glass plate were moistened using manufacturer-supplied conditioning solution to prevent desiccation.

Sediment probe housings were 3-D printed to be of similar dimensions with the standard DGT probe, albeit with a shorter length (4 cm versus 15 cm exposure window) to reflect the burrowing behaviour of marine nematodes (top 2 cm, Schratzberger & Warwick, 1999). Gel cutters of appropriate dimensions were also printed. In studies, such as this, where metal concentrations measured in surface sediments are more relevant, bespoke sediment probes are advantageous as they utilise less resources, limit sediment redox disturbance during deployment, and can be designed to include site details and to mark the sediment-water interface (SWI). 3-D models of sediment probes and gel cutters used in this study are provided in the compact disk drive attached to this thesis. Details of the "plastic" printing material used are provided in Appendix 3.01 (Stratasys, 2015). All 3-D printed probes and cutters were soaked in 1 M NaOH for 2 hrs to remove support residue (Stratasys, 2013).

They were then washed, as described in Chapter 2 for other laboratory wares, using detergent, 10% v/v HNO_3 and ultrapure water (UPW), prior to assembly. PES membranes were washed in acid and UPW as previously described (Chapter 2). The assembled DGT probes were conditioned for at least 24 hrs in 0.5 M NaCl prior to testing and field deployment, in order to match the average salinity (30 S) across the sites (Jolley *et al.*, 2016).

A performance test was conducted to assess the recovery of DGT from known solutions. The test was done using three conditioned probes deployed for 25 hrs in 50 µg Cu/L (nominal concentration; Figure 3.01). The test solution was prepared in 0.5 M NaCl matrix using anhydrous $CuSO_4$ (BDH, Poole, England), and actual Cu concentration was determined using Inductively Coupled Plasma – Optical Emission Spectrometry (ICP-OES) after batch extraction with chelex (see Chapter 2 for details). A fourth probe, deployed in an unspiked 0.5 M NaCl solution for the same duration, was analysed as the method blank. The test was conducted at 15^{o}C (average sediment temperature across the sites) in an environmental cabinet under well-stirred conditions (Davison & Zhang, 1994). Undeployed resin gels (n = 3) were further analysed as chelex blanks (Jolley *et al.*, 2016).

3.2.3 Fieldwork

Fieldwork for this study coincided with the Autumn 2017 survey already described in detail in Chapter 2. DGT probes were transported to field sites submerged in the 0.5 M NaCl conditioning solution. The probes were deployed at low tide, in triplicates, on the day before sediment sampling (henceforth, Day 1), with at least 30 cm distance between any two probes. The deployment was done taking care not to disturb the sediment. Sediment temperature was measured and the time of deployment was noted to the nearest minute.

DGT probes were retrieved at low tide on Day 2, after approximately 25 hours of deployment. Retrieved probes were rinsed with ultrapure water, bagged, and preserved in ice inside a cooling box. Time of probe retrieval was noted, in order to estimate deployment duration to the nearest minute. Sediment temperature was also measured. This temperature was averaged with the measurement on Day 1 for use in estimating diffusion coefficients (see Section 3.2.4). At Sites MC, RB, and PR, one DGT probe was washed away by the tide and at MC, additionally fouled by gulls. Upon arrival at the laboratory, all retrieved probes were double-bagged and refrigerated at 4 ^{o}C until analysis.

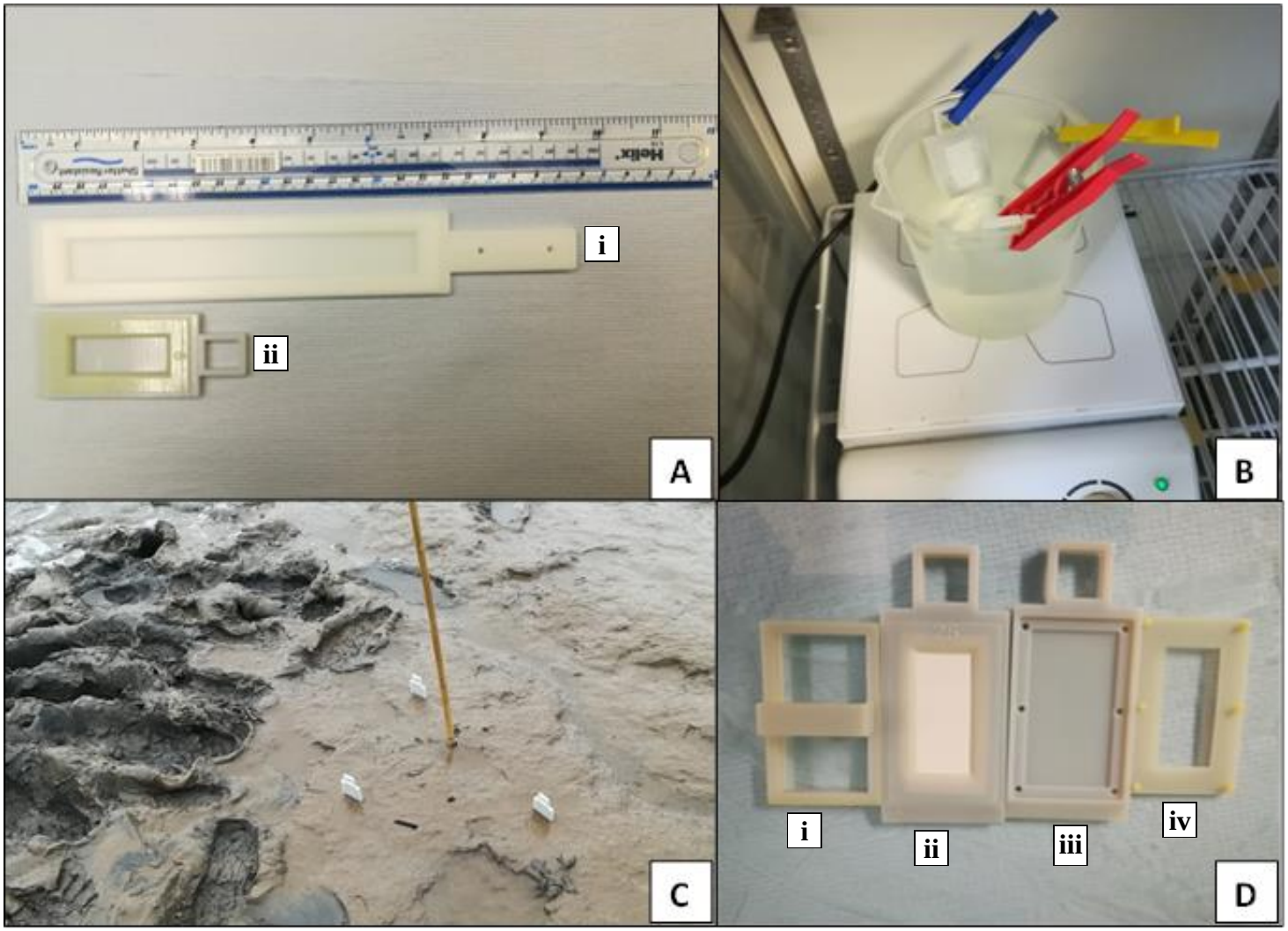

Fig. 3.01: Assembly (A & D), performance testing (B), and deployment (C) of DGT probes. Ai = Standard DGT probe. Aii = 3-D printed DGT probe. Di = 3-D printed gel cutter. Dii = Assembled DGT probe. Diii = DGT probe housing base. Div = DGT probe housing top

Surface (0 – 2 cm) sediments were also sampled on Day 2 using plastic scoops. The sediments for nematode PICT assay were collected in separate plastic bags[18]. Upon arrival in the laboratory, these samples were transferred into 1 L assay containers, topped-up with 30 S artificial seawater (Tropic Marin® PRO-REEF, henceforth, ASW), and aerated in an environmental chamber at 15 ºC and 18:6 day/night cycle until the assay was completed (Millward & Grant, 1995, 2000). The assessment of physicochemical characteristics has been described in detail in Chapter 2 of this thesis. The EqP measure was derived by dividing the molar excess of SEM Cu by the proportion of TOC content, i.e. [SEM Cu – AVS]/fOC. The WFD measure was derived by dividing porewater Cu concentrations by the DOC concentration, i.e. PW Cu/DOC, resulting in a unit of µg Cu/mg OC. For ease of reference, relevant sediment physicochemical data across the sampling sites are provided in Table A3.03.

3.2.4 DGT post-deployment processing and determination of measured concentrations

DGT probes were processed within one month of deployment. The device remains stable if refrigerated during this period (Jolley *et al.*, 2016). Resin gels were sliced through the exposure window, using a teflon-coated razor blade, in order to obtain a vertical profile as follows: a 2 cm slice at the SWI (-1.0 to +1.0 cm, DGT-SWI), and 1 cm slices above (+1.0 to +2.0 cm, overlying water layer, DGT-OLW) and below (-1.0 to -2.0 cm, sediment column, DGT-SED) the SWI (see Figure 3.02). Slicing the resin gels through the exposure window precludes the overestimation of DGT-labile concentrations due to the lateral diffusion of metals (Warnken *et al.*, 2006; Santner *et al.*, 2015). The vertical profiles generated enable metal measurement at higher spatial resolutions in the sediments (Zhang *et al.*, 1995; Santner & Williams, 2016).

Prior to elution, the sliced resin gels were rinsed, using UPW, to remove any sediment particle, blotted using a clean tissue paper, and weighed. The weight was used to calculate gel volume and area, given a specific gravity of 1 g/cm^3 (Zhang *et al.*, 1995) and a thickness of 0.04 cm. The gels were then transferred, individually, to 1.5 mL Eppendorf tubes and eluted using 1 mL of 1 M HNO_3 for 24 hrs (Jolley *et al.*, 2016; Zhang *et al.*, 1995). Eluents

[18] At Site BW, sediment for PICT was sampled within three weeks of DGT deployment (i.e. October 2017). However, median nematode survival at this site under the test conditions is stable (~24 hrs; Millward & Grant, 2000; Ogilvie, 2004). Sediment physicochemical characteristics also remained similar in the intervening period (Table A3.02)

were diluted 10-fold and analysed for metals by ICP-OES. Eluent blanks were determined by replicate (n = 3) analysis of the original 1 M HNO_3 solution. Analytical accuracy and precision, reported in Table A3.04, were assessed using replicate measurements of the TM 27.3 and TMDA 64.2 certified lake water reference materials (Environment Canada). Precision was further assessed using the CLMS2A multi-element standard solution (SPEX CertiPrep), prepared in similar acid matrix.

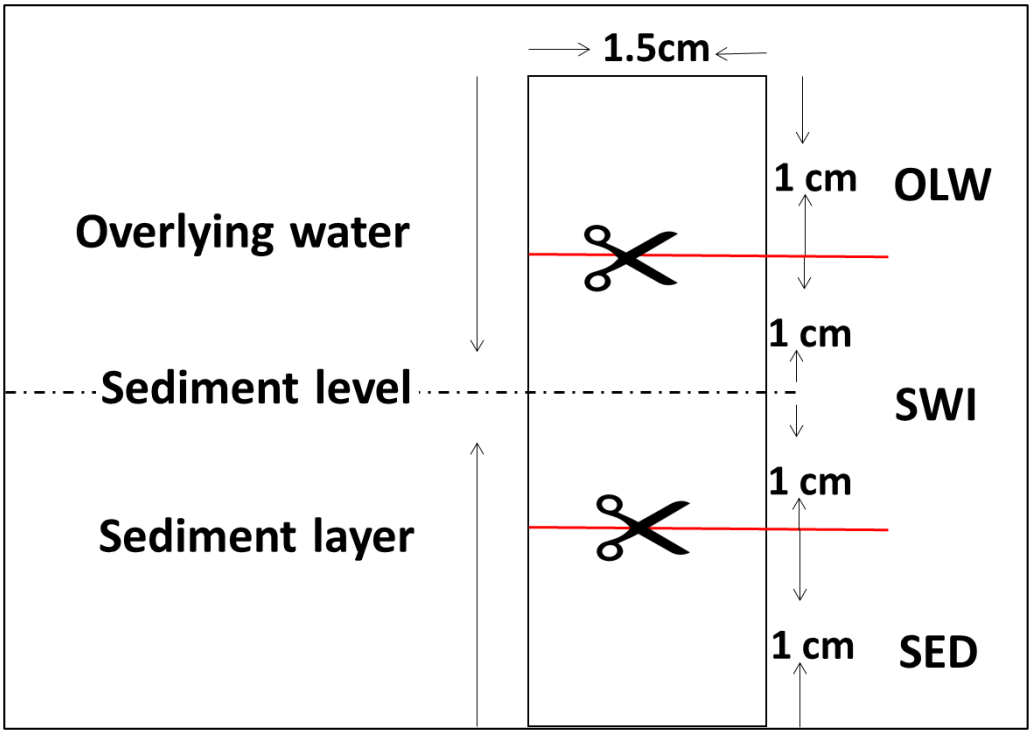

Fig. 3.02: Slicing the chelex resin gels of deployed DGT probes through the exposure window. OLW = overlying water; SWI = sediment-water interface; SED = sediment layer

The mass (M) of metal accumulated on the resin gel as well as the DGT-labile metal concentrations (C_{DGT}) in the sediment was determined according to the standard DGT equation (Jolley *et al.*, 2016; Equations i and ii), after corrections for the eluent and method blanks[19]. Diffusion coefficients (D) of metals in the APA diffusive gel, which are required for C_{DGT} calculations, are provided by Davison (2016). For Cu, Zn, Fe, and Mn, amongst

[19] Method blanks, chelex blanks, and field-deployed probes were eluted using different batches of the 1 M HNO_3 solution. Therefore, each measurement was corrected, first, by the appropriate elute blank, which was minimal.

others, diffusion coefficients are 85 per cent of the respective values in water, given the deployment conditions (Davison, 2016; Davison and Zhang, 2016a). The flux (J) of metals to the DGT device was similarly determined for field-deployed probes (Equation iii), in order to facilitate comparison with previous studies using this unit of measurement.

$$\mathrm{M} = \frac{\mathrm{Ce\ (Vbl + Ve)}}{f\mathrm{e}} \ldots\ldots\ldots\ldots\ldots\ldots\ldots\ldots\ldots\ldots\ldots \boldsymbol{eqn\ (i)}$$

Where:

M = Mass of metal accumulated (μg)

Ce = Metal concentration measured in eluent (μg/mL)

Vbl = Volume of the binding layer (mL)

Ve = Volume of eluent (1 mL)

fe = Elution factor = 0.8 (Zhang *et al.*, 1995)

$$C_{\mathrm{DGT}} = \frac{\mathrm{M}\ \Delta\mathrm{g}}{\mathrm{D\ Ap\ t}} * 1000 \ldots\ldots\ldots\ldots\ldots\ldots\ldots\ldots\ldots\ldots \boldsymbol{eqn\ (ii)}$$

$$\mathrm{J} = \frac{\mathrm{M}}{\mathrm{Ap\ t}} * 10000 * 3600 \ldots\ldots\ldots\ldots\ldots\ldots\ldots\ldots\ldots \boldsymbol{eqn\ (iii)}$$

Where:

J = DGT-metal flux (μg/h/m^2)

C_{DGT} = DGT-labile metal concentration (μg/L)

M = Mass of metal accumulated in the resin gel (μg)

Δg = Combined thickness of diffusive layer and PES membrane (0.094 cm)

D = Diffusion coefficient of metal through the diffusive gel and PES membrane (cm^2/s)

Ap = Exposure area of resin gel slice (cm^2)

t = Duration of deployment (s)

Note that the diffusion coefficients of metals through the APA diffusive gel and the PES membrane are equal (Davison & Zhang, 2016a)

Diffusion coefficients of metals in ionic solutions vary with temperature (Li & Gregory, 1974; Davison, 2016; Davidson & Zhang, 2016b). In the current study, temperature corrections of coefficients were made using equations provided by Davison (2016) for the

APA gel. The diffusion rates of cations in ionic solutions also vary with the ionic strength (i.e. salinity) of the medium, which results in viscosity differences (Simpson & Carr, 1958; Li & Gregory, 1974). This explains the variation in diffusion coefficients measured for the same metal, at the same temperature, but at different ionic strengths (see compilation by Davison & Zhang, 2016a). Given the wide range in salinity between the study sites (6.6 – 39.5 S, Table A3.03), this factor was important in the current study.

The relationship between temperature, viscosity, and the diffusion coefficient of ions in water is shown mathematically in Equation (iv) (Simpson & Carr, 1958). Having corrected for temperature (therefore assuming constant temperature), the relationship between the diffusion coefficient of ions in pure water (salinity = 0 S), the diffusion coefficient in seawater (salinity = sal S), and the respective viscosity is shown in Equation (v) (Li & Gregory, 1974; Brookes *et al.*, 2005). In the current study, temperature-corrected diffusion coefficients for metals were adjusted for the porewater salinity at each site using Equation (v), re-written as Equation (vi). The temperature-corrected viscosity of pure water (salinity 0 S) and seawater (salinity = site porewater salinity) were derived from the 'Seawater Density and Viscosity Calculator' provided by Bleninger *et al.* (2010).

$$\left(\frac{\mathrm{Do}\ \eta\mathrm{o}}{\mathrm{T}}\right)\mathrm{To} = \left(\frac{\mathrm{Do}\ \eta\mathrm{o}}{\mathrm{T}}\right)\mathrm{Tt} \quad \ldots\ldots\ldots\ldots\ldots\ldots\ldots\ldots\ldots\ldots\ldots\ldots\ldots\ldots\ldots\ldots\ldots\ldots \boldsymbol{eqn\ (iv)}$$

Where:

T = Absolute temperature between 0 - 100 ^{o}C (273.15 – 373.15 ^{o}K)

Do = Self-diffusion coefficient of water

ηo = Dynamic viscosity of water

$$\mathrm{Do}\ \eta\mathrm{o} = \mathrm{Dsal}\ \eta\mathrm{sal} \quad \ldots\ldots\ldots\ldots\ldots\ldots\ldots\ldots\ldots\ldots\ldots\ldots\ldots\ldots\ldots\ldots\ldots\ldots \mathbf{eqn\ (v)}$$

Where (at constant temperature):

Do = Diffusion coefficient of ion in water (salinity = 0 S)

ηo = Dynamic viscosity of water (salinity = 0 S)

Dsal = Diffusion coefficient of ion in water (salinity = sal S)

ηsal = Dynamic viscosity of water (salinity = sal S)

$$D_{gel.o}\ \eta_{gel.o} = D_{gel.sal}\ \eta_{gel.sal} \quad \textbf{eqn (vi)}$$

Where (at constant temperature):

Dgel.o = Diffusion coefficient of metal in APA gel (salinity = 0 S, temp = T)

ηo = Dynamic viscosity of water (salinity = 0 S, temp = T)

Dsal = Diffusion coefficient of metal in APA gel (salinity = sal S, temp = T)

ηsal = Dynamic viscosity of water (salinity = sal S, temp = T)

Note that the APA is a hydrogel consisting of 95% water (Davison & Zhang, 2016c)

3.2.5 Nematode extraction and pollution-induced community tolerance assay

Nematode PICT across the study sites was assessed as differences in survival times upon exposure to Cu-spiked seawater (Millward & Grant, 1995, 2000). Tests were initiated within two weeks of arrival in the laboratory. To extract the worms, sediment subsamples from the assay containers were sieved in 30 S ASW to <500 and <63 µm. Material remaining on the 63 µm sieve was washed into a 5 cm Petri dish, with live nematodes picked up, at random[20], using an entomological needle[21] under a binocular microscope.

Selected worms were transferred to a vented 3 cm Petri dish, 5 individuals per dish, containing 4.5 mL of freshly-prepared test solution – a 200 µg Cu/L (nominal concentration) solution prepared using anhydrous $CuSO_4$ (BDH, Poole, England) in 30 S ASW matrix. For each site, 25 individuals[22] were exposed to the test solution, whilst another group of 25, to a control solution of 30 S ASW, the average salinity across the sites. The exposed worms were transferred to an environmental chamber (conditions same as in Section 3.2.3), with dead[23] animals counted and removed every 24 hrs. Actual Cu concentration in test solutions was determined using ICP-OES after batch extraction with chelex (see Chapter 2 for details).

[20] This was ensured by picking all nematodes from successive sectors in a marked Petri dish.

[21] For larger-bodied and more active worms, scooping with bent staple pins was found to be helpful. It was important not to aspirate worms using micropipettes, because dilution of test solution by residual ASW – however minimal – was found to significantly affect results in preliminary experiments (data not shown).

[22] It was later observed that, both in treatment and control exposures, certain petri dishes contained more or less than 5 individuals, with a total of 26 – 30 worms across the sites.

[23] Death was assumed when nematodes did not respond to mechanical stimulus

Because nematode extraction is time-consuming, it was not possible to start all toxicity tests on the same day. Consequently, one replicate of five worms, including controls, was started from each site on each of five consecutive days, ensuring that the effect of storage time is orthogonal to the effect of site (Millward & Grant, 2000). The tests were terminated after 10 days (240 hrs) or earlier (at least 7 days) if control mortality increased significantly (Millward & Grant, 2000). For Site HA, where >50% of worms survived the original 10-day period, the toxicity test was terminated after 13 days (312 hrs).

At two sites (CO and HR, see Section 3.3.4), nematode tolerance was anomalously high, relative to measured metal concentrations and to observations in previous studies (Millward & Grant, 2000; Ogilvie, 2004). Millward and Grant (2000) had reported increased survival for nematodes stored for 2 or 3 weeks in the laboratory prior to toxicity testing, with survival time decreasing after 4 weeks of storage. Their explanation was the effect of stress during the storage period, leading to the possible death of more sensitive individuals within one week of storage, and of more tolerant species after 3 weeks. To investigate this possibility in the current study, the PICT assay was repeated after 4 weeks (i.e. on Week 5) of laboratory storage, using organisms from Sites BW and HA, the least and most tolerant communities, respectively (Section 3.3.4).

3.2.6 Data processing and analysis

Statistical analysis in this study was completed in R (R Core Team, 2020). Using the R package 'survival' (Therneau, 2020), nematode survival data was fitted and median survival times were determined with log-log confidence intervals. Survival curves based on Kaplan-Meier estimates were plotted using the R package 'survminer' (Kassambara *et al.*, 2020). The significance of differences in nematode survival between sites was determined using the Peto and Peto modification of the generalised Wilcoxon test (rho = 1) also in the 'survminer' package. The Peto and Peto modification provides the added advantage of being robust to censoring patterns, with comparisons between groups made on the overall survival experience (Hosmer *et al.*, 2008). Animals still alive at the end of the toxicity tests were treated as censored observations (Millward & Grant, 2000). To determine the best predictor of ecological effects, the relationship between median survival times and the different measures of metal concentrations was investigated using Pearson correlation following an observed linear relationship in scatter plots.

Table 3.1. Mass of metals (Mean ± SD) accumulated in DGT chelex and method blanks in this study compared to some previous studies

	Chelex blank (ng/cm^2)				Method blank (ng/cm^2)			
	Cu	**Zn**	**Fe**	**Mn**	**Cu**	**Zn**	**Fe**	**Mn**
This study	2.48 ± 0.43	12.09 ± 5.62	3.59 ± <0.01	0.42 ± 0.33	4.07 ± 2.46	21.16 ± 11.28	9.62 ± 3.77	0.96 ± 0.55
Pradit *et al.* (2013)	-	-	-	-	2.9 ± 0.1	3.9 ± 0.4	4.1 ± 0.7	0.55 ± 0.06
Wu *et al.* (2011)	-	-	-	-	-	-	60	90
Dunn *et al.*, 2007	-	-	-	-	0.57 ± 0.26	71.84 ± 7.2	-	-
***Gao *et al.* (2006)**	-	-	-	-	0.73 ± 0.29	16 ± 4	4.9 ± 3	0.35 ± 0.24
***Gao *et al.*, (2006)**	-	-	-	-	2.73 ± 0.46	12 ± 4	17 ± 8.6	1.30 ± 0.62
Leermakers *et al.* (2005)	-	-	-	-	0.73 ± 0.29	16 ± 4	4.9 ± 3	0.35 ± 0.24
Naylor *et al.* (2004)	-	-	-	-	-	8.7 ± 1.7	12 ± 7	1.3 ± 0.3
Dunn *et al.* (2003)	-	-	-	-	0.63 ± 0.29	72 ± 6.7	-	-

*Gao *et al.* (2006) report blank values for two different research groups; Method blank = chelex blank + potential contamination during processing; Dashes (-) indicate values not measured

3.3 Results

3.3.1 DGT: blanks, detection limits, and metal recovery from spiked solution

Masses of metals accumulated in DGT blanks in this study are reported in Table 3.1, in comparison with previous studies. The method blank includes the chelex blank and any potential contamination during DGT conditioning and processing. The mean mass of metals present in the resin gels ranged from 0.42 ng/cm^2 (for Mn) to 12.09 ng/cm^2 (for Zn) for the chelex blanks and from 0.96 ng/cm^2 (for Mn) and 21.16 ng/cm^2 (for Zn). The results suggest that much of the contamination was present in the chelex resin gels, as supplied. Assuming a 25-hr field deployment at 15^{o}C and salinity of 30 S, which are the average conditions across the study sites, equivalent water concentrations for the mean chelex blanks are 0.53 µg Cu/L, 2.64 µg Zn/L, 0.78 µg Fe/L, and 0.09 µg Mn/L. For the mean method blanks, equivalent water concentrations are 0.87 µg Cu/L, 4.62 µg Zn/L, 2.09 µg Fe/L, and 0.22 µg Mn/L. Method detection limits for this study, calculated as three times standard deviation of method blank (Jolley *et al.*, 2016), are 1.74 µg Cu/L, 8.21 µg Zn/L, 2.73 µg Fe/L, and 0.42 µg Mn/L. These detection limits were inflated by a relatively high value in one of the method blanks, increasing variability in the measurement. Final DGT concentrations (C_{DGT}) and fluxes (J) reported in this study have already had the method blank subtracted (see Section 3.2.4). All values, except Cu in the OLW and SWI layers for Site BW, are above the method detection limit (see asterisked values in Appendices A3.05 and A3.06).

In the performance test, the actual concentration of test solution measured by ICP-OES before and after the 25-hr deployment were 37.1 and 36.4 µg Cu/L, respectively, giving an average of 36.8 µg Cu/L. Relative to a C_{DGT} concentration of 36.2 ± 2.0 µg Cu/L (mean ± SD, n = 9) in the resin gel slices of deployed probes, the recovery and precision (as relative standard deviation) of DGT measurements in this study are 98.3% and 5.6%, respectively.

3.3.2 DGT-labile metal concentrations across the study sites

C_{DGT}-Cu concentrations across the study sites are shown in Figure 3.03, with fluxes and concentrations for all metals in Tables A3.05 – A3.07. The non-intact DGT probes yielded considerably different values and were, consequently, excluded. Although the arrangement of sites in the appendices of this chapter follows the conventional order throughout this thesis, site arrangements in-chapter figures are in increasing order of median tolerance (see Section 3.3.4; Figure 3.06a). This modification is made to facilitate data interpretation.

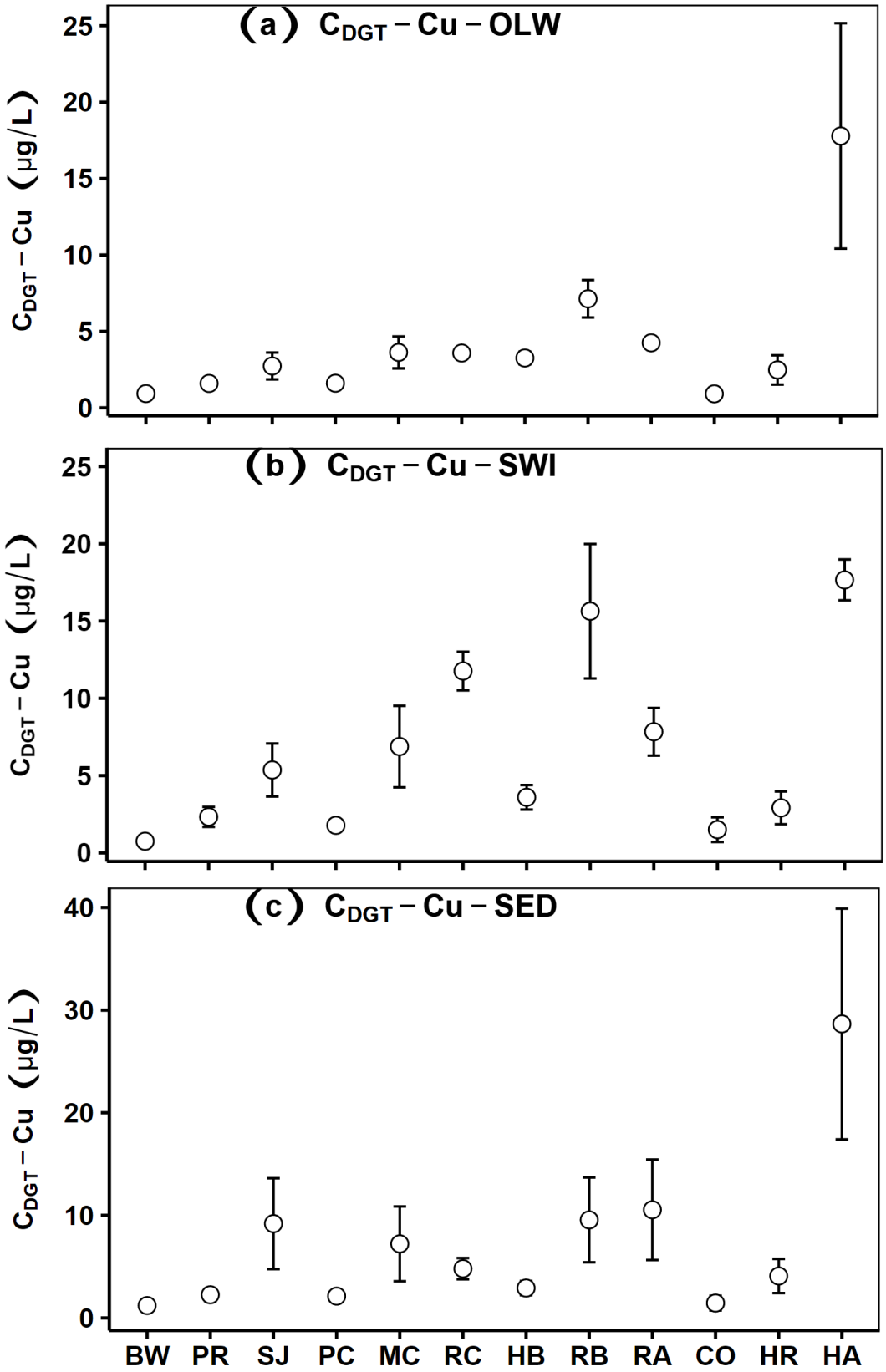

Fig. 3.03: C_{DGT}-Cu concentrations in the overlying water (OLW), sediment-water interface (SWI), and sediment column (SED) across the study sites. Error bars represent Standard Errors, n = 3, except PR, MC, and RB for which n = 2. Sites arranged in order of increasing nematode pollution-induced community tolerance

C_{DGT}-Cu in the OLW, SWI, and SED layers follow similar trends across the study sites (Figure 3.03; Tables A3.05 – A3.07; r for OLW vs SWI = 0.84, OLW vs SED = 0.96, SED vs SWI: = 0.80; all $p < 0.01$). In line with porewater concentrations (Table A3.03), C_{DGT}-Cu was, overall, highest in the sandy sediments of River Hayle (HA, 28.66 µg/L in SED) and lowest in the reference Breydon Water site (BW, 1.21 µg/L in SED). C_{DGT}-Cu concentrations within the Fal increased steadily from Percuil River (PR, 2.33 µg/L in SED) to the Restronguet Creek at Tallack's (RB, 15.64 µg/L in SED), reflecting the metal contamination gradient across these sites. However, the range in C_{DGT} (e.g. 1.21 – 28.66 µg Cu /L in SED) was about a tenth of the range in porewater concentrations (1.8 – 223.9 µg Cu/L).

For each of the three DGT layers, there was a significant correlation between Cu and Zn concentrations across the study sites ($R^2 = 0.59 – 0.95$; $p < 0.001$; Figure 3.04), similar to other measures of metal contamination (see Chapter 2). These correlations were, however, weakest in the SED layer, possibly reflecting differences in Cu and Zn lability to the DGT device. There was no significant correlation of Cu or Zn concentrations with Fe or Mn, or between Fe and Mn concentrations (data not shown). Furthermore, C_{DGT} metal concentrations were significantly correlated with DGT-labile fluxes (J) across the study sites ($R^2 \geq 0.995$; $p < 0.001$; Figure A3.08). This strong correlation between C_{DGT} and J is because, despite variations in salinity and temperature across the sites, there were only small differences in metal diffusion coefficients – a maximum of 14.4% difference due to temperature and 1% difference due to salinity (see Equations ii and iii).

DGT concentrations were highest in the sediment column (SED) and lowest in the overlying water (OLW) (Figure 3.03; Tables A3.05 – A3.07), mainly because porewater equilibrates much longer with intertidal sediments than the overlying water. However, the magnitude of this difference might have been over-estimated due to the deployment duration: the probes were deployed and retrieved at low tide, hence longer exposed in the sediment column. Although all sites sampled are in the mid shore, the exact time to high tide flooding were unknown, therefore C_{DGT}-OLW was derived using the full duration. The variation in C_{DGT}-Metal, within particular sites, was also highest in the sediment column, suggesting sediment heterogeneity even within the small spatial scale assessed. Metal concentrations measured in the SWI are higher than those in the OLW but less than those in the SED layer. The SWI incorporates (errors from) both OLW and SED measurements as well as the flux of metals between both of these layers. The relatively high concentrations in the SED layer suggests that DGT can potentially extract some metals from anoxic sediment phases.

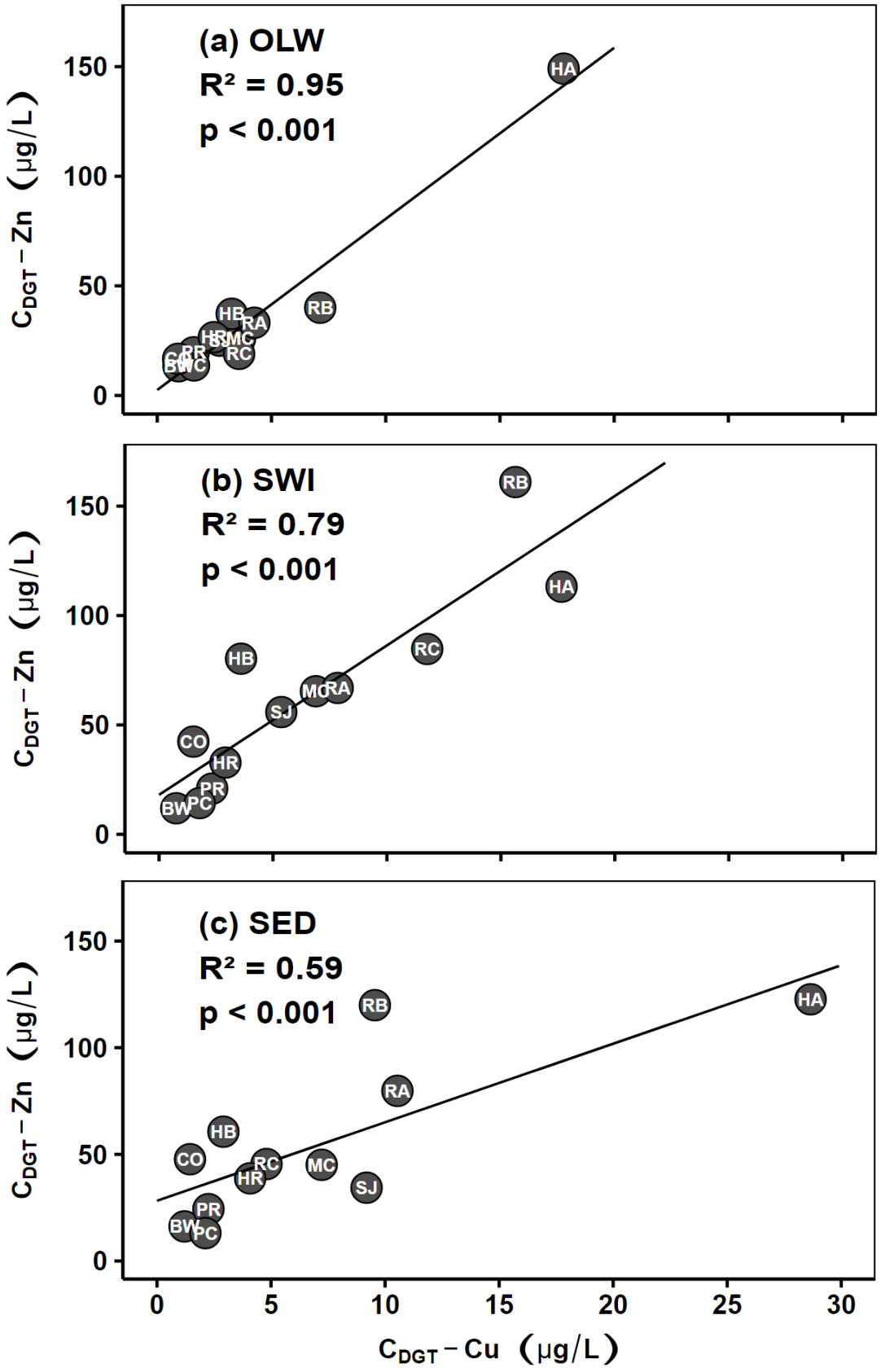

Fig. 3.04: Relationships between mean DGT-labile Cu (C_{DGT}-Cu) and Zn (C_{DGT}-Zn) concentrations at the overlying water (OLW), sediment-water interface (SWI), and sediment column (SED)

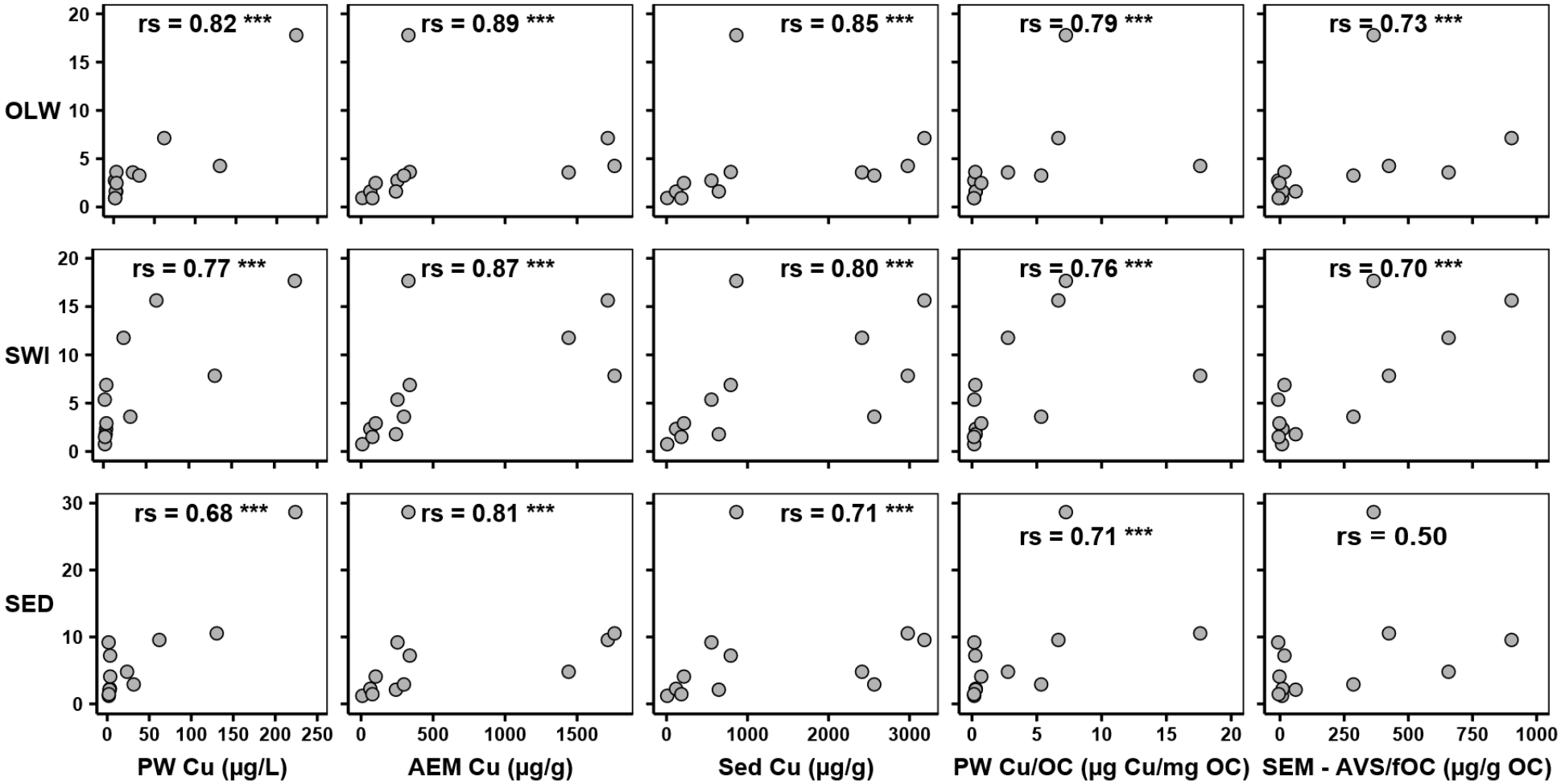

Fig. 3.05: Relationships, plus Spearman correlations, between mean values of traditional measures of Cu concentration and DGT-labile Cu (C_{DGT}-Cu) at the overlying water (OLW), sediment-water interface (SWI), and sediment column (SED). Significant correlations ($p < 0.05$) flagged by asterisks. PW = Porewater; AEM = Acid-extractable metal; Sed = Total sediment; PW Cu/OC = PW Cu/DOC; SEM – AVS/fOC = [SEM – AVS]/(TOC/100)

3.3.3 Relationship between DGT-labile and traditional metal concentrations

The relationships between C_{DGT}-Cu concentrations in the OLW, SWI, and SED layers with traditional measures of Cu are shown in Figure 3.05. All correlations assessed were strong and significant (r_s = 0.68 – 0.89, $p < 0.05$), except the organic carbon-normalised EqP measurement (SEM – AVS/*f*OC) in the SED layer (rs = 0.50; p = 0.09). The lowest correlations were observed with this EqP measurement (r_s = 0.50 – 0.73) across the three DGT layers. Expectations from the EqP are that metal bioavailability, hence DGT-labile concentrations, should be negligible when molar AVS concentration is in excess of SEM concentrations. However, contrary to this expectation, C_{DGT}-Cu and C_{DGT}-Zn concentrations were higher in the SED layer in Sites CO, HR, and SJ than at BW, despite the occurrence of AVS in excess of SEM concentrations at the surface (top 2 cm) of the former sites (Tables A3.03 and A3.07). The strongest correlations between C_{DGT} and traditional measures of Cu were observed with acid-extractable (AEM) Cu (r_s = 0.81 – 0.89), suggesting that weakly-bound sediment complexes can be DGT-labile. However, only porewater Cu (r_s = 0.68 – 0.82) was predictive of the high C_{DGT}-Cu concentrations in Site HA. Amongst the different DGT layers, the strongest correlations with C_{DGT}-Cu were observed in the OLW layer, possibly due to the more precise measurements therein (Section 3.3.2).

3.3.4 Nematode pollution-induced community tolerance to Cu across the study sites

Nematode PICT was used as a measure of ecological effects of Cu across the study sites. Median survival times (LT_{50}) of nematode communities and site pairwise comparisons are shown in Figures 3.06a,b. The Kaplan-Meier survival curves are shown in Appendix 3.09. Nematode LT_{50} ranged between 24 hrs for BW and 312 hrs – the entire 13-day exposure period – for the sandy River Hayle (HA). Community survival increased moderately from St Just (SJ), along the contamination gradient. However, a statistically significant difference ($p < 0.05$) in nematode survival from the BW reference was found in the Upper Restronguet Creek (Sites RB and RA), Cowlands (CO), Helford River (HR) and in HA. The widest confidence intervals in LT_{50} were found at CO and HR (>216 hrs), indicating the presence of less tolerant individuals or groups of species, despite the high community tolerance. Overall, the results reveal a trend in median survival related to dissolved Cu concentrations. The study sites can be broadly classified, based on pairwise comparisons, into those of "low" (BW – HB), "medium" (MC – RB), and "high" (HB – HA) ecological impacts, with intervening sites, especially HB, marking class transitions (Figures 3.06b).

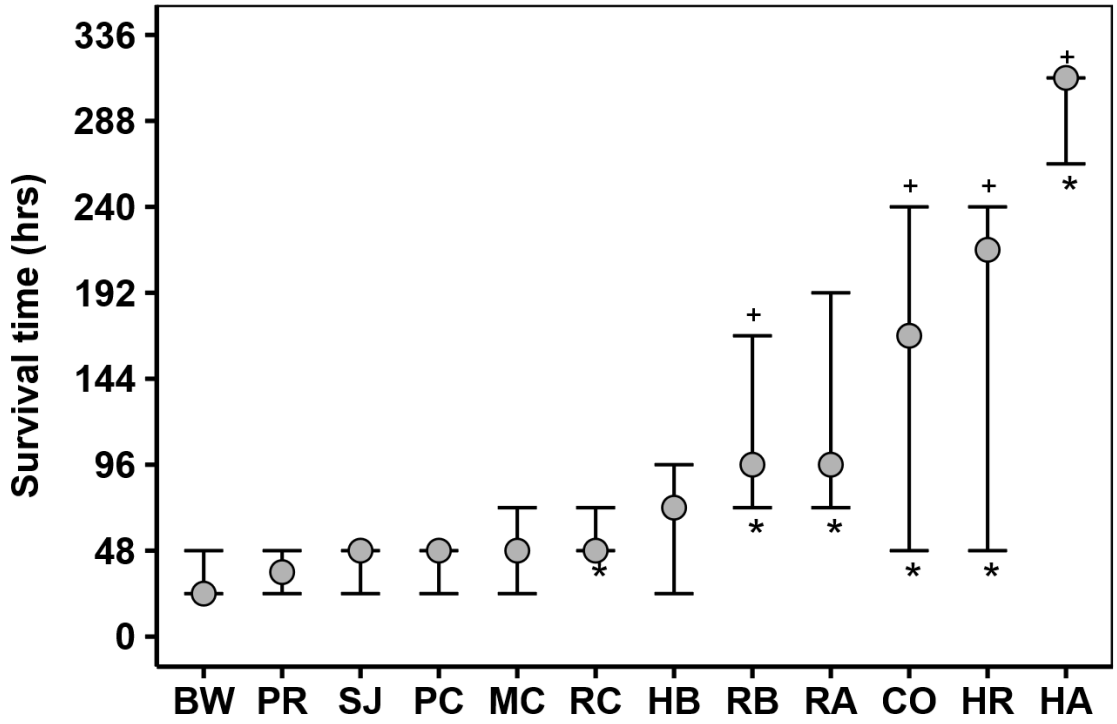

Fig. 3.06a: Median survival time (LT_{50} ± 95% CI) of nematode communities across the study sites. Asterisks (*) represent sites significantly different ($p < 0.05$) from BW. Crosses (+) represent Upper CL marked by the maximum duration of exposure

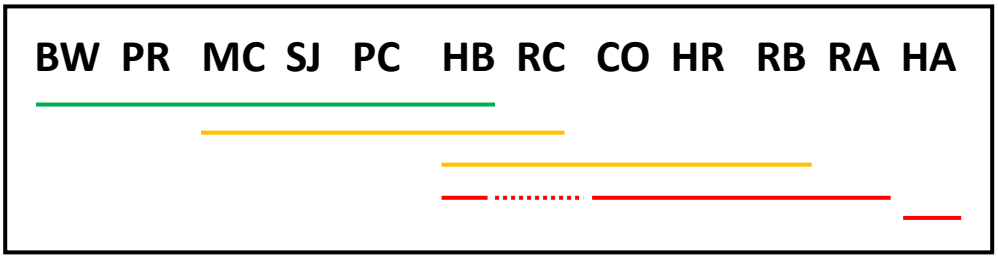

Fig. 3.06b: Pairwise comparison of nematode survival across the sites. Solid lines indicate groups of sites between which there are no significant differences in survival ($p > 0.05$). Colours differentiate sites of "low" (green), "medium" (yellow), and "high" (red) ecological impacts, given pairwise differentiations. Note that the site order is different from Fig. 3.06a, which follows median tolerance values and does not consider the lower 95% CL

For BW and HA, the survival of nematode communities was determined after 1 week (i.e. Week 2) and 4 Weeks (i.e. Week 5) of laboratory storage, in order to assess any bias due to storage time in the current study (Millward & Grant, 2000). No significant difference in survival was noted between nematode communities from Week 2 and Week 5 for either site ($p \geq 0.14$; Figure 3.07), suggesting that the influence of laboratory storage in this study was

negligible. Actual concentration of Cu in the test solutions was 123 ± 11 µg/L (mean ± SD; n = 4). The details of control/test mortality, duration of exposure, as well as actual survival times and confidence intervals across the sites are provided in Appendix 3.10. Control mortality was less than 20% for all sites, ranging between 0% at BW and HR to 19% at SJ and RA. This low control mortality suggests that experimental conditions were optimal.

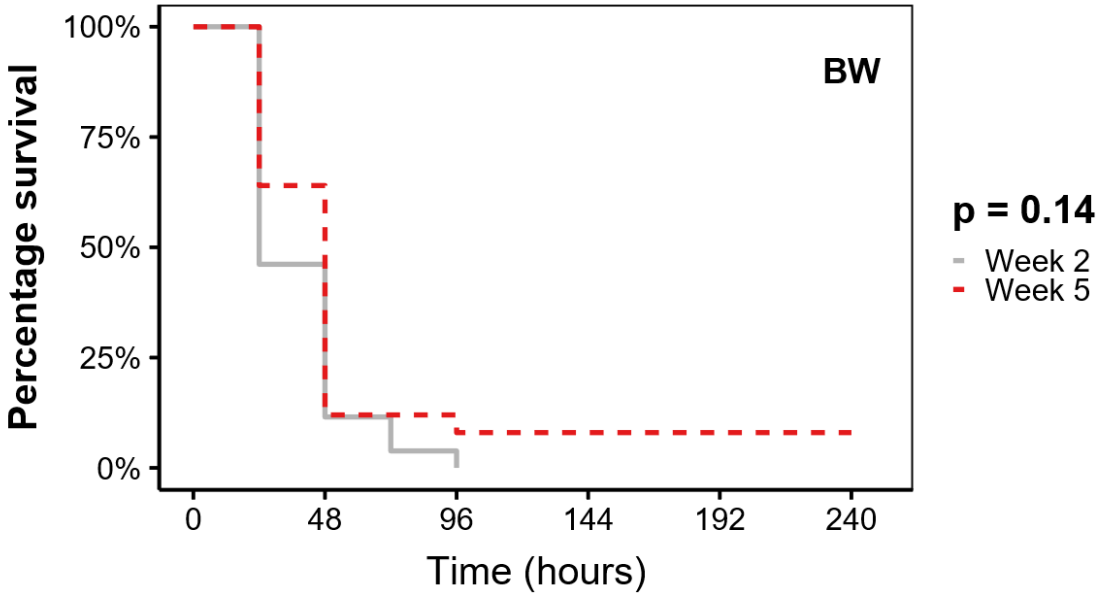

Fig. 3.07a: Survival of nematodes from Breydon Water (BW) within two (continuous line) and five (dotted line) weeks of laboratory storage

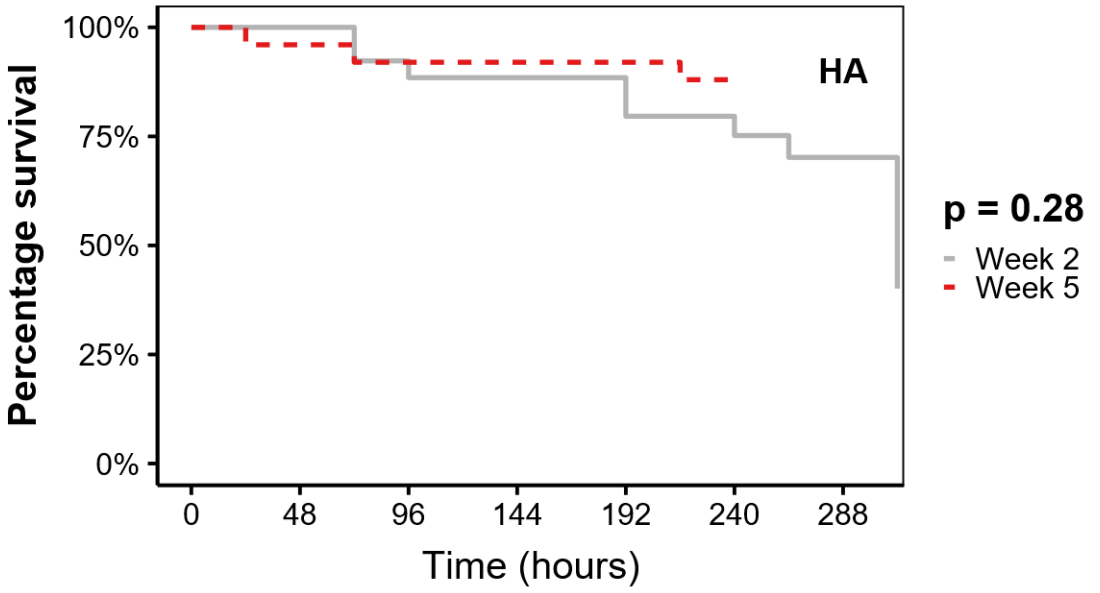

Fig. 3.07b: Survival of nematodes from River Hayle (HA) within two (continuous line) and five (dotted line) weeks of laboratory storage

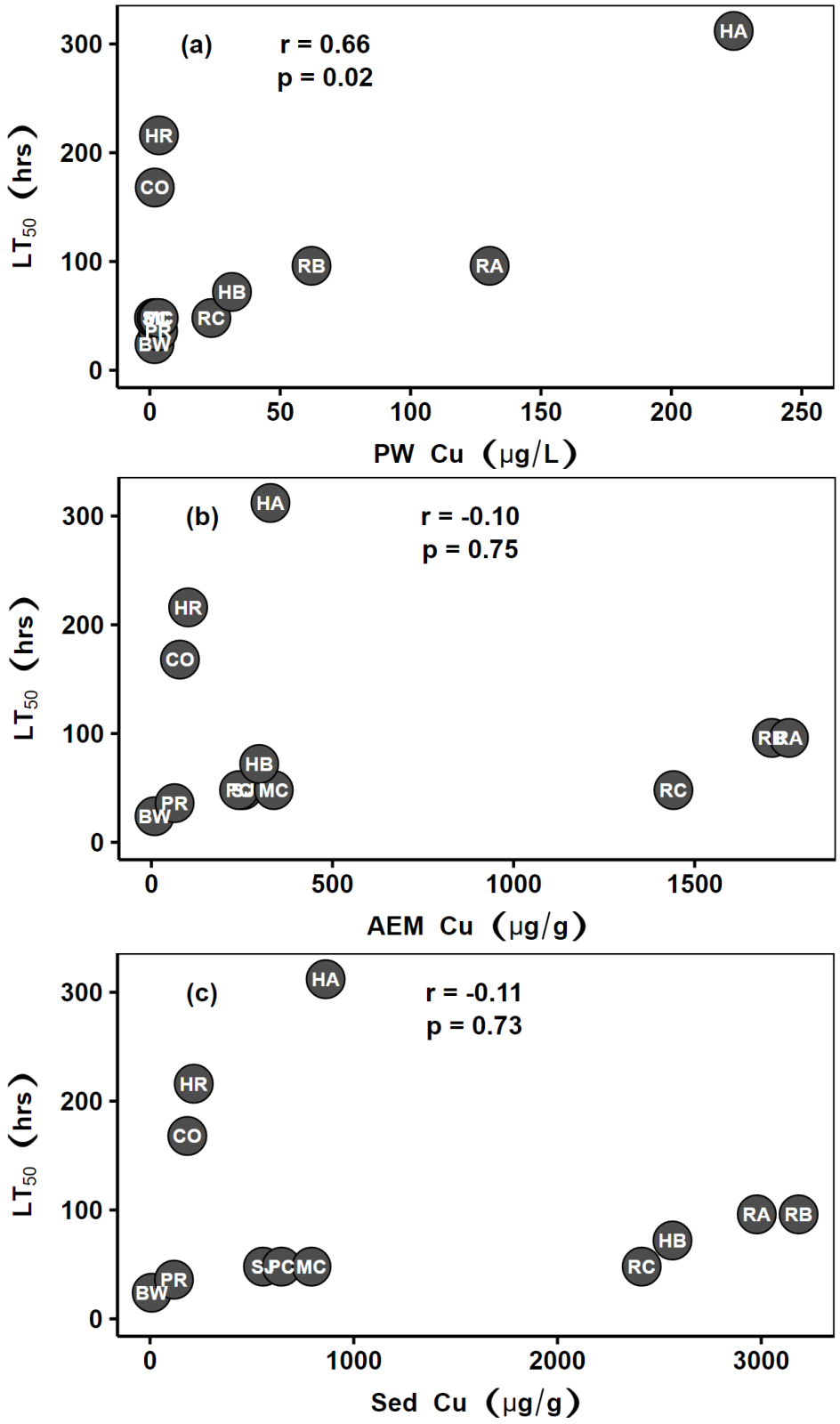

Fig. 3.08: Correlation between median nematode survival and porewater (PW), acid-extractable (AEM), and total sediment (Sed) Cu concentrations across the study sites. Error bars omitted for clarity (see Tables A3.03 and A3.10)

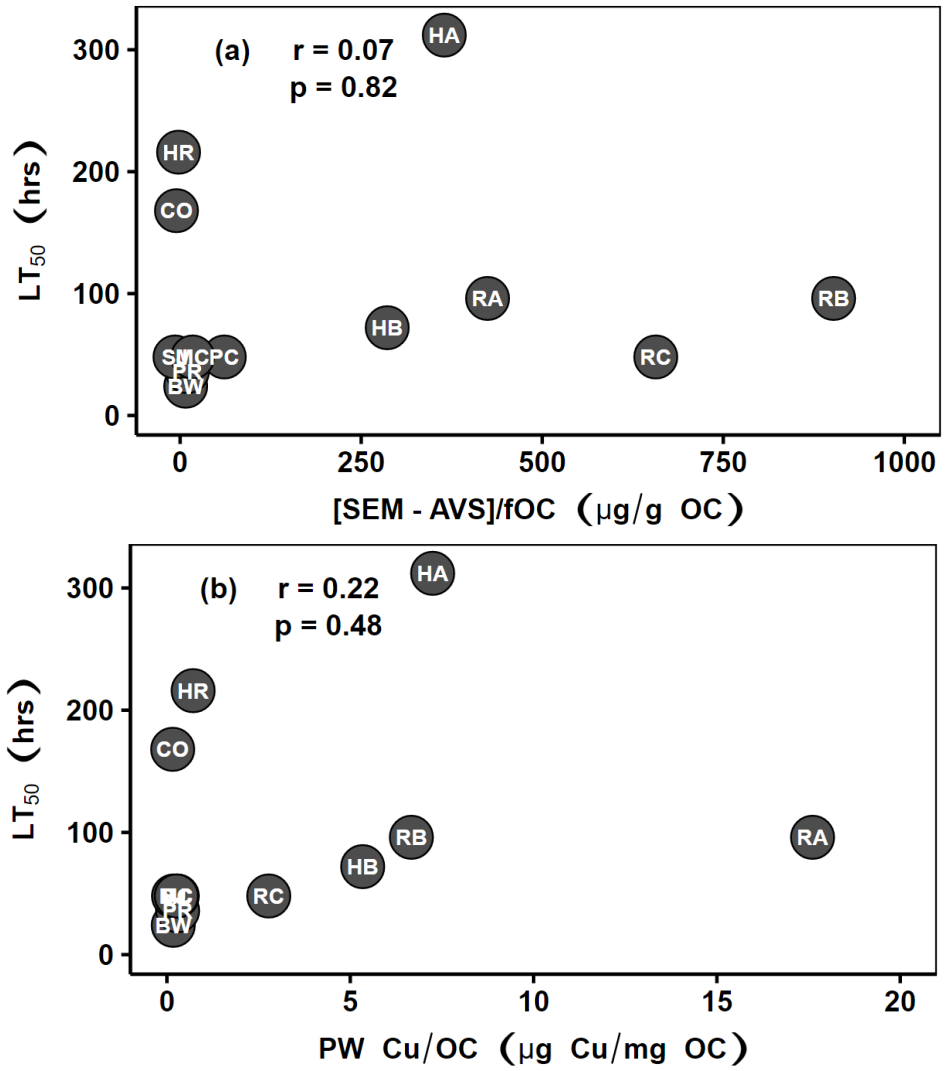

Fig. 3.09: Correlation between median nematode survival and organic carbon-normalised SEM (EqP) and porewater (WFD) metal concentrations across the study sites. Error bars omitted for clarity (see Tables A3.03)

3.3.5 Relationship between Cu concentrations and nematode pollution-induced community tolerance across the study sites

The capability of the different chemical measures of Cu concentration to predict ecological effects across the study sites was assessed using Pearson correlation (Figures 3.08 – 3.10). As was earlier highlighted, the survival of nematode communities from Sites CO and HR was high, relative to metal concentrations measured therein and to observations in previous studies. This anomalously high tolerance at CO and HR could not be explained by any of the measures of Cu concentration and is fully discussed in Section 3.4.

Of the measures of metal contamination assessed in this study, only porewater and DGT-labile Cu concentrations were significantly related to median nematode survival across the sites ($r = 0.66 – 0.71$; $p < 0.05$; Figures 3.08 – 3.10), suggesting the importance of dissolved Cu concentrations in measuring metal bioavailability in the Fal and Hayle estuaries. DGT Cu in the OLW ($r = 0.71$) followed by SED ($r = 0.68$) layers were the best predictors of effects. Correlation with C_{DGT}-SWI was not significant ($r = 0.43$; $p = 0.16$). Considering site pairwise comparisons with BW, threshold concentrations marked by the no observed adverse effect level (NOAEL) are 31.5 µg/L PW (at HB), 3.62 µg/L C_{DGT}-OLW (at MC), and 9.19 µg/L C_{DGT}-SED (at SJ). Total, extractable, and EqP sediment concentrations were poor predictors of nematode PICT (r within ±0.3; $P > 0.73$). The WFD OC-normalised porewater concentrations, apart from CO and HR, could also not account for the elevated tolerance at HA, despite the high dissolved organic carbon (DOC) concentration.

3.4 Discussion

DGT has been projected as a useful tool for measuring metal bioavailability in aquatic ecosystems. A search for the keywords "("DGT" AND "metal*" AND "*availab*")" on the Scopus database[24] yields 370 results, most of which relate DGT-labile concentrations or fluxes to metal uptake and/or toxicity from spiked soils, waters, and sediments. Extensive reviews of these studies have been completed, notably by Zhang and Davison (2015), Degryse and Smolders (2016), and Eismann *et al.* (2020), with the latter focussing on aquatic ecosystems. General conclusions from these reviews are that for organisms with rapid, kinetically-driven metal uptake, DGT-measured concentrations can be indicative of metal bioavailability. Within aquatic sediments, DGT creates a contaminant sink for free metal ions and labile complexes in the dissolved phase as well as for weakly-bound sediment phases that potentially dissociate in response to the device flux (Zhang & Davison, 2015; Lehto, 2016). The similarity between DGT-labile and bioavailable metal complexes is responsible for the strong correlations documented in previous biomonitoring and toxicity studies. For this reason, DGT has been recommended for use in metal biomonitoring, with several authors (e.g. Amato *et al.*, 2014; Strivens *et al.*, 2019; Marras *et al.*, 2020) favouring applications in deriving regulatory quality thresholds.

[24] Last assessed on the 10th August, 2020

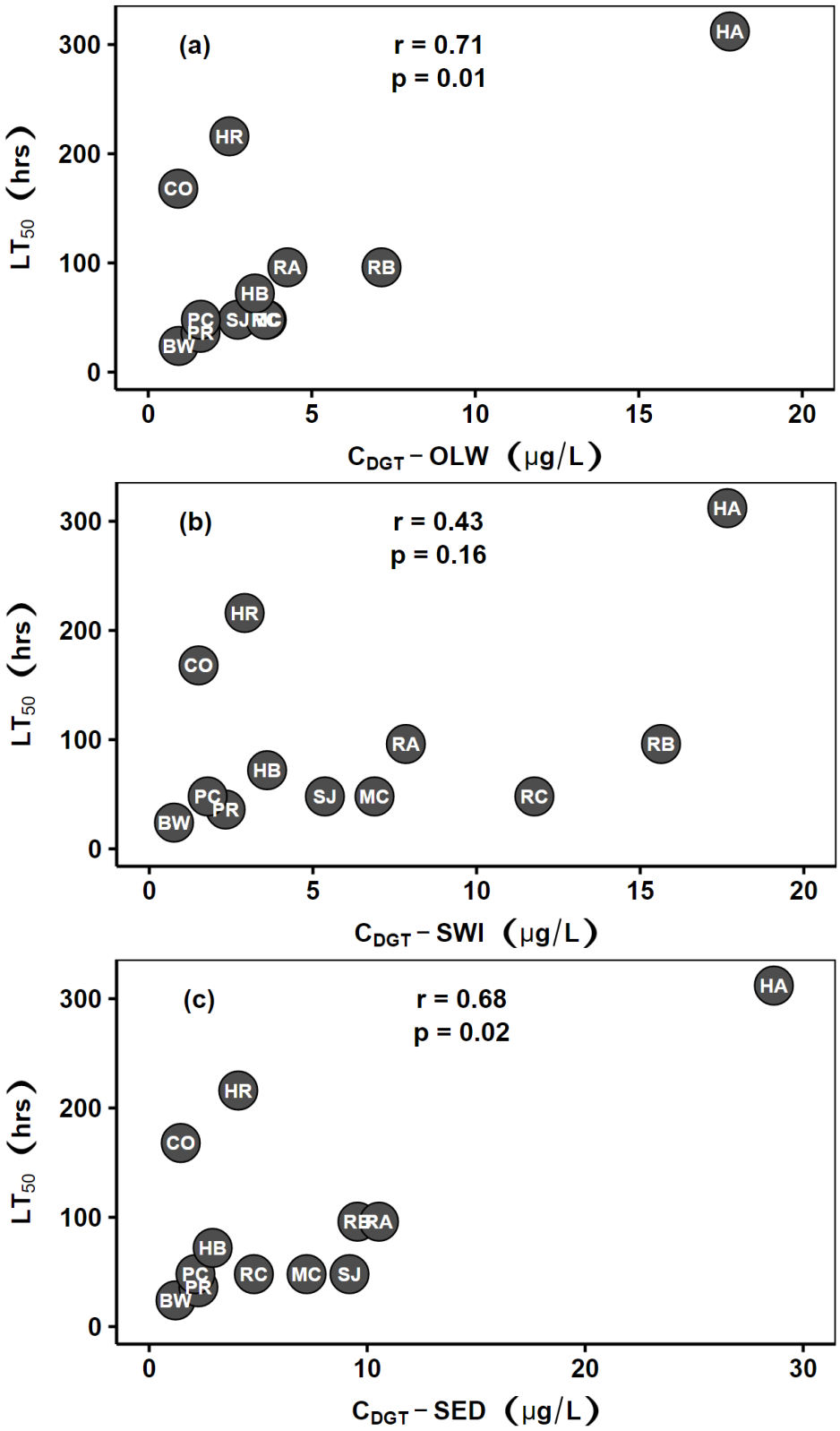

Fig. 3.10: Correlation between median nematode survival and DGT-labile metal concentrations across the study sites. Error bars omitted for clarity (see Tables A3.03 and A3.05 – A3.07)

In the current study, DGT-labile fluxes across the sites were strongly correlated with C_{DGT}. This correlation is expected, given only minimal differences in metal diffusion coefficients across the sites. Furthermore, C_{DGT} Cu across the sites was well correlated with other measures of metal contamination. The strongest correlation was with acid-extractable concentration, suggesting that metals weakly-bound in the sediment may be contributing to the diffusive flux. There was also a strong correlation with PW Cu, which was the only measure that explained the high C_{DGT} Cu in Site HA. These correlations corroborate other deployments in field (e.g. Costello *et al.*, 2012; Song *et al.*, 2018; Zhang *et al.*, 2019; Cindric *et al.*, 2020) and laboratory conditions (e.g. Amato *et al.*, 2014, 2015). However, the dynamic range of DGT was low, with C_{DGT}-SED Cu spanning between 1.21 – 28.66 µg/L relative to PW Cu of 1.6 – 223.9 µg/L.

There are several possible reasons for the relatively low C_{DGT}-Cu concentrations. In the current study, there was an almost complete recovery (98.3 ± 5.6%) of Cu from spiked seawater in laboratory deployments over the same 25-hr period, precluding the possibility of analytical errors. C_{DGT} concentrations also relate to the ability of the sediment to resupply metals in response to the device flux, with C_{DGT} shown to approximate porewater concentrations in conditions of high resupply (Harper *et al.*, 1998; Zhang *et al.*, 2002). Sediment resupply was not assessed in this study. However, in the highly contaminated sediments in the Restronguet and Hayle, where sediment resupply can be assumed to be high, C_{DGT} Cu was still ten times less than PW Cu. The lability of metal complexes to DGT has been well described in the literature. Free metal ions as well as weakly-bound metal complexes which can dissociate in the diffusive flux are labile to DGT (Davison *et al*., 2012; Puy *et al.*, 2012), therefore site-specific metal complexation may be playing an important role. For example, Paller *et al.* (2019) noted a strong influence of DOC on DGT metal uptake, with concentrations underestimated up to a factor of six in high DOC (5 mg C/L) relative to low DOC (< detection limit) solutions. A similar observation was made by Strivens *et al.* (2019). Also, Cindric *et al.* (2020) only observed conforming concentrations in estuarine waters after normalising dissolved concentrations for DOC. Although normalised PW Cu in this study was not linearly related with C_{DGT} Cu (Figure 3.05), DOC across the study sites ranged between 5.9 – 30.9 mg C/L, permitting this possibility.

Whilst previous studies in the application of DGT to benthic fauna are important, it was necessary to assess the technique using actual ecological effects in field-contaminated marine sediments. The drawbacks of sediment spiking (Lee *et al.*, 2000a,b) as well as the

use of bioaccumulation as an endpoint (Burton, 2013) are well documented, as both may misrepresent actual ecological effects in field sites. The current study addressed these gaps, using an established gradient of metal contamination in the Fal and Hayle estuaries (Rainbow, 2020; Chapter 2) and nematode PICT (Millward & Grant, 1995, 2000) as a measure of the ecological effects of Cu. Pollution-induced community tolerance is causal evidence of the impact of a particular toxicant (Blanck, 2002; Grant, 2002; Millward & Klerks, 2002). This heritable tolerance has been demonstrated across a wide range of marine communities and in the presence of different chemical stressors (Grant, 2002; Tlili *et al.*, 2016). Within the Restronguet Creek, tolerant individuals of the estuarine Polychaete, *Hediste* (formerly *Nereis*) *diversicolor*, have been successfully used to map the separate impacts of Cu and Zn (Grant *et al.*, 1989), indicating a high metal specificity in community tolerance, which is a more sensitive endpoint (Grant, 2002).

In the current study, nematode PICT increased along the gradient of metal contamination (Figure 3.06a), as observed in previous assessments (Millward & Grant, 1995, 2000; Ogilvie, 2004). The survival of nematode communities from Sites RB, RA, CO, HR, and HA was significantly different from those in Breydon Water (BW) (Figure 3.06a, b). Study sites were ordered, by pairwise comparisons, into that of "low", "medium", and "high" ecological impacts, with areas such as HB marking the transition between site groupings. Notably, there was a marked difference in tolerance between upper (RA and RB) and lower (RC) Restronguet Creek communities, despite similar sediment Cu concentrations. This observation corroborates previous findings (e.g. Bryan & Gibbs, 1983; Grant *et al.*, 1989; Millward & Grant, 2000; Ogilvie & Grant, 2008) of differing metal biovailabilities within the Restronguet, which is, for example, due to different sediment types (Austen *et al*., 1994) and salinity (Bryan & Gibbs, 1983). Exact comparison of survival times between the current study and previous studies (Millward & Grant, 2000; Ogilvie, 2004) is limited by differences in salinity (30 vs 26.25 S) and possible differences in the actual concentration of test solutions (123 ± 11 µg Cu/L vs unreported). However, apart from Sites CO and HR, the trend in nematode tolerance across the sites assessed in this study is comparable to those with 200 µg Cu/L nominal test solution in the aforementioned studies.

Are the nematode PICTs in CO and HR, indeed, anomalous? If so, what factors are responsible? Sites CO and HR were moderately contaminated, with extractable Cu of 79 and 102 µg/g respectively, versus 1760 µg/g in the Upper Restronguet Creek (RA) (Table A3.03). However, median tolerance of nematodes at the two sites were very high (CO = 168;

HR = 216 hours) – higher than that at RA (96 hours) and only slightly lower than the median tolerance in the most impacted site (HA = 312 hours). These results differ markedly from previous studies (Millward & Grant, 2000; Ogilvie, 2004). There was also a wide LT_{50} confidence interval (>216 hrs), spanning almost the entire duration of the 10-day toxicity test. The observations show that Sites CO and HR deviate from expectations.

There are several possible reasons for the deviations in Sites CO and HR. Among other explanations, the similarities in survival of Week 2 and Week 5 nematode communities (Figure 3.07a,b) overrule the influence of laboratory storage time on tolerance (Millward & Grant, 2000). PICT was also repeated in a separate study in Winter 2019. Although nematode tolerance observed in some sites differed markedly from those in the current study, tolerance across the sites was well correlated with porewater Cu concentrations ($r = 0.65$, $p = 0.02$; see Figure 3.11 below). This observation demonstrates consistency in the results and a high sensitivity of nematode PICT to temporal changes in metal bioavailability. PICT is marked by a shift in community composition from sensitive to more tolerant individuals and species (Millward, 1995; Blanck, 2002; Grant, 2002, 2010). However, in intermediate pollution, tolerant species may possibly cohabit with less tolerant counterparts, without significant ecological costs. For example, although median survival times of nematode communities at two sites along the Percuil River (PR in this study) were 66.3 and 45.5 hrs, Millward (1995) observed tolerant species with similar survival time as conspecifics in the Restronguet Creek. He also identified nematode species with individual survival times (132 - >288 hrs) greater than the median community survival in two Restronguet Creek sites (135.8 and 115.2 hrs). These species agree with those found by Somerfield *et al.* (1994b) in highly-contaminated sites within the Fal estuary. The wide confidence intervals for Sites CO and HR allude to this possibility in the current study. Nematode community composition across the study sites is the subject of Chapter 4 of this thesis. The tolerant species (according to both studies), *Hypodontolaimus balticus* and *Axonolaimus paraspinosus*[25], were observed in both CO and HR. *Tripyloides marinus*, *Leptolaimus limicolus*, and *Microlaimus marinus*, were further observed in Site CO. A fourth explanation is the possibility of co-tolerance, with nematodes reacting to other unmeasured contaminants at the sites (Blanck, 2002; Grant, 2002). And a fifth possibility is that nematode community tolerance to Cu at CO and HR are indeed high, with transient metal bioavailability not adequately captured by the "snapshots" of PW Cu

[25] Millward (1995) identified the congeneric *Axonolaimus spinosus* as tolerant.

and C_{DGT} Cu measured in this study. In Chapter 6 of this thesis, I show that redox fluctuations across the study sites, as is common in intertidal sediments, may lead to the remobilisation of metals in potentially toxic pulses. Both CO and HR had AVS in excess of SEM Cu at the surface, which could potentially be remobilised upon oxidation. These pulses of metals are not likely detectable in short-term chemical measurements.

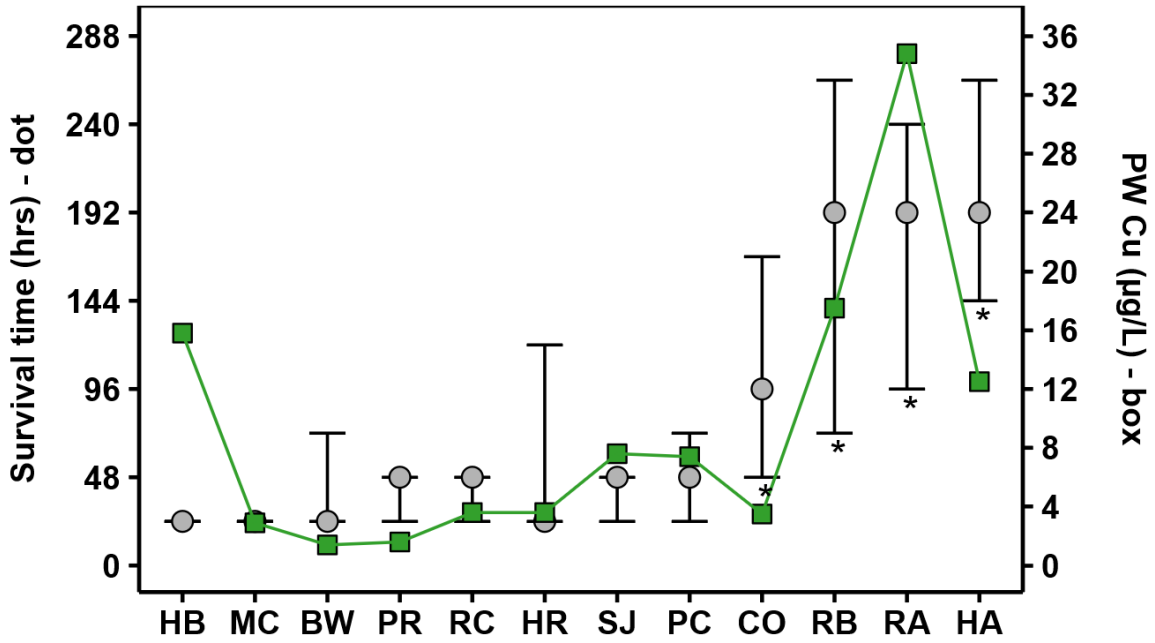

Fig. 3.11: Median survival time (LT_{50} ± 95% CI, grey dots) of nematode communities and porewater Cu concentrations (PW Cu, green boxes) assessed in Winter 2019. Asterisks (*) represent sites significantly different ($p < 0.05$) from BW. Actual concentration of test solutions = 139 ± 17 µg Cu/L (mean ± SD; n = 5). See Chapter 2 for further sediment physicochemical characteristics

Results from this study indicate that DGT is a good predictor of the effects of metals in marine sediments. Despite strong inter-correlations between the measures of metal contamination assessed, only DGT Cu and PW Cu concentrations were significantly correlated with nematode tolerance across the study sites (Figures 3.08 – 3.10). DGT Cu showed the strongest correlation with tolerance. The results corroborate previous findings using benthic fauna (see reviews by Zhang & Davison, 2015; Degryse & Smolders, 2016; Eismann *et al.*, 2020). Notably, Simpson *et al.* (2012) observed that both the overlying water Cu concentration and DGT-Cu flux at the SWI were predictive of toxicity to the bivalve,

Tellina deltoidalis, irrespective of the sediment grain size and OC content. Amato and colleagues (2014, 2015, 2016, 2018) also observed similarly strong correlations of bioaccumulation and/or toxicity with J_{DGT} - SWI for a range of invertebrate species. In the current study, C_{DGT} SWI was not significantly correlated with ecological effects, possibly because of the differing exposure times in the sediment and overlying water (see Section 3.3.2). The strongest correlation was observed in the DGT-OLW layer. Metal concentrations in the DGT-OLW layer has been attributed to the diffusive flux from porewater in surface sediments (Furrer & Wehrli, 1993; Tankere-Muller *et al.*, 2007). Furthermore, burrowing invertebrates may irrigate their burrows with water from this layer (Chapman *et al.*, 1998). Lower correlations with C_{DGT} SED in comparison with C_{DGT} OLW may be attributable to DGT uptake of non-bioavailable metal complexes.

Overall, strong correlations of ecological effects with DGT and PW Cu concentrations demonstrate the importance of dissolved metals to nematode toxicity across the sites. The lack of correlation with the EqP OC-normalised SEM fraction is remarkable, given that this model was designed to predict dissolved metal bioavailability (Di Toro *et al.*, 2005) and that it forms the basis for some of the most advanced sediment quality criteria available today (e.g. Burgess *et al.*, 2013). A further evaluation of the EqP model is undertaken in Chapter 5 of this thesis. Derived NOAELs are 31.5 µg/L PW, 3.62 µg/L C_{DGT}-OLW, and 9.19 µg/L C_{DGT}-SED, based concentrations from Sites HB, MC, and SJ, respectively. These C_{DGT} thresholds are significantly higher than the operational threshold, 0.152 µg/L, set by Marras *et al.* (2020). They are, however, within the EC_{50} range, 4.8 – 11.5 µg/L, determined at 0.896 – 8.36 mg/L DOC by Strivens *et al*. (2019) for embryos of the Mediterranean mussel, *Mytilus galloprovincialis*, possibly suggesting the influence of DOC on Cu bioavailability across the sites. The PW threshold is higher than the 3 µg Cu/L final chronic value proposed by Simpson *et al.* (2013) and the 3.76 µg/L nominal WFD (2015) standard, where DOC ≤ 1 mg/L, but closer to the 15.9 µg/L WFD threshold after adjustment for average DOC at Site HB (10 mg/L for Autumn 2017 and Winter 2019, see Chapter 2). The design of this study precludes the modelling of EC_{10} and EC_{20} values for Cu, which are more accurate thresholds, given the possible influence of exposure concentrations on NOAEL determination (Landis & Chapman, 2011; Jager, 2012). However, I recommend that DOC corrections be included in the derivation of dissolved SQGs for Cu.

Is DGT, therefore, a useful tool for benthic faunal monitoring? And can protective thresholds be defined based on DGT-labile concentrations, as advocated in the literature? DGT has

proven to be a good predictor of ecological effects in this study. However, several limitations hinder its practical use in sediment quality regulation:

I. First is the low dynamic range, earlier discussed. The Fal is one of the most contaminated estuaries in the United Kingdom (Bryan & Langston, 1992). However, mean C_{DGT}-Cu SED concentrations ranged between 1.45 at CO and 10.54 µg/L at RB, with around 8 µg/L difference between the relatively unimpacted Percuil River and the Upper Restronguet creek (RA). This low concentration range limits the comparison of sites with intermediate contamination where sediment may be toxic. Moreover, the technique offers little advantage over the traditional PW Cu measurement, having a similarly strong correlation with nematode tolerance (r C_{DGT}-SED = 0.68; r PW = 0.66).

II. DGT concentrations and fluxes can also be influenced by site-specific factors such as the rate of sediment resupply (for C_{DGT}-SED) or flow rate in the overlying water (for C_{DGT}-OLW; Davison & Zhang, 2016b; Zhang & Davison, 2015), which may not be relevant to faunal toxicity. This factor, including the challenge of defining "DGT-labile" complexes, further complicates comparison between sites or the setting of regulatory guideline values.

III. In intertidal sediments, varying tidal times within the standard 24-hr DGT deployment may confound the computation of the DGT-OLW and DGT-SWI concentrations, which become wholly exposed only during high tides. In the current study, the entire duration of deployment was used in DGT-metal computations, thus underestimating the actual DGT-OLW or DGT-SWI values.

IV. The DGT technique is labour intensive, requiring two visits to each site as well as multiple steps in device assembly and post-deployment processing. The technique is also expensive per sample, even after cutting down the size of gels needed relative to the standard sampler and gives numbers that are strongly correlated with porewater concentrations, but with a much lower dynamic range.

Therefore, although DGT can measure dissolved metal concentrations with little disturbance in aquatic sediments, I do not recommend the technique for use in marine sediment monitoring or in setting universal regulatory values.

Chapter 4.

Linking nematode community structure to metal concentrations in the Fal and Hayle estuaries

4.1 Introduction

There has been a recent drive for the inclusion of meiobenthic fauna as indicators of pollution in marine monitoring schemes (e.g. the European Water Framework Directive: Semprucci *et al.*, 2015, 2019; Schratzberger, 2012). For nematodes, advantages over traditional macro-invertebrates include their ubiquity, small size, high abundance, short life cycles, and limited mobility (Schratzberger *et al.*, 2000; International Seabed Authority [ISA], 2011). In fact, changes in nematode communities have been seen to reflect those of higher benthic taxa (Heip *et al.*, 1985; Schratzberger *et al.*, 2006), which are increasingly incorporated in similar ecological assessment frameworks (Borja *et al.*, 2017). It is argued that structural attributes such as abundance, diversity, and composition of nematode communities are sensitive to pollution (Coull & Chandler, 1992; Schratzberger *et al.*, 2006; Semprucci *et al.*, 2015).

Borja and Dauer (2008) detail several approaches to summarising benthic communities in ecological monitoring: univariate, multimetric, and multivariate methods. Univariate measures such as Shannon-Wiener diversity, taxonomic diversity, and taxonomic distinctness are used to explain relative abundances of individual species or taxa (Clarke & Warwick, 2001). Multimetric indices such as the Coefficient of Pollution (CoP) combine several responses into a single index. And multivariate techniques, including non-metric multi-dimensional scaling (MDS), have been developed as more sensitive measures of community composition (Clarke, 1993). Furthermore, Wieser (1953) divides nematodes into trophic groups based on feeding habit and mouthpart morphology: selective deposit feeders with tube-like buccal cavities for the ingestion of microorganisms (Group 1A), non-selective deposit feeders with wide, unarmed buccal cavities (Group 1B), epistrate feeders with lightly-armed buccal cavities (Group 2A), and predatory/omnivorous species with well-armed buccal cavities (Group 2B). These trophic groups have been used alongside traditional indices in nematode community assessments (Clarke *et al.*, 2014; Semprucci *et al.*, 2018).

Previous studies linking nematode community responses to metal contamination in marine field sites have focused on the Fal estuary, comparing communities in the Restronguet Creek and less-contaminated creeks (notably, Somerfield *et al.*, 1994a,b; Millward, 1995; Austen

& Somerfield, 1997). Incorporating careful sampling regimes, especially similar sediment particle sizes and salinity controls, these studies show that univariate diversity indices are less sensitive to but multivariate changes in nematode community structure between creeks are mainly reflective of metal contamination. However, favoured indicators of pollution for regulatory policies must distinguish the effects of contaminants from the "noise" due to other environmental variables (Grant, 2002, 2010). It has also been observed that metal availability in the Fal estuary could vary temporally and spatially, even along the same creek (Ogilvie, 2004; Ogilvie & Grant, 2008; Grant, 2010; Chapters 2 & 3 of this thesis). This creates a gap for gradient studies which assess the sensitivity of nematode communities to pollution in the presence of other varying physicochemical characteristics. And as discussed in Chapter 1 of this thesis, for incorporation into regulatory guidance, it is important to determine which measures of metal contamination best predict these ecological responses.

In this study, nematode community structure, assessed through a combination of univariate and multivariate methods, is used as an indicator of metal pollution across the contamination gradient in the Fal and also Breydon Water and Hayle estuaries. The sites vary disparately in several physicochemical conditions, but show a gradient of sediment Cu and Zn concentrations that span nearly three orders of magnitude (Chapter 2). I assess whether nematode communities are responding to the strong metal contamination gradient across the study sites, despite the widespread variation in other physicochemical characteristics. And if so, which measure(s) of metal contamination best explain nematode community structure, and by extension, metal bioavailability, across the sites.

4.2 Methodology

4.2.1 Sampling strategy

Sampling in this study was designed, as described in Chapter 3, to reflect the impact of metal contamination in surficial sediments (top 2 cm) along the concentration gradient in the Fal and Hayle estuaries. Whereas previous studies (e.g. Somerfield *et al.*, 1994a,1994b; Millward, 1995), at a spatial scale, focussed on differences between creeks of varying contamination, sampling in the current study was replicated within the specific sites (see Chapter 2), several of which might occur in a single creek (e.g. RA, RB, and RC all in Restronguet Creek) to account for differences in metal bioavailability therein. All sites were located mid shore, regularly flooded in high tides and exposed during low tides. Sampling of sediments was done in low tide.

4.2.2 Sample collection, storage and processing

Sampling for the current study coincided with the Autumn 2017 survey, already described in detail in Chapters 2 and 3. With the aid of a 50 mL centrifuge tube, about 10 mL of replicate sediment samples (n = 3) were collected to a depth of 2 cm. This sampling depth additionally reflects the thickness of the aerated, brown sediment layer across the sites[26], ensuring that most of the nematodes were included (Schratzberger & Warwick, 1999; Gao & Liu, 2018). Samples were preserved on site by topping-up to 50 mL with DESS, a solution of 20% dimethyl sulphoxide (DMSO) and 0.25 M disodium EDTA, saturated with NaCl (Yoder *et al.*, 2006). Preserved samples were refrigerated until processed.

Method for meiofauna sample processing was similar to that described by Warwick *et al.* (1998). Bulk-preserved sediment samples were stained with 500 µL of 1% Rose Bengal solution two weeks prior to processing. Using ultrapure water, the samples were washed thoroughly through 500 µm and 63 µm sieves to remove preservative, salt, macrofauna, and excessive silt. To extract nematodes, the fraction retained on the 63 µm sieve was washed into a 50 mL centrifuge tube using a 50% solution of Ludox® HS-40 (Sigma-Aldrich), and afterwards agitated and centrifuged at 1800 g for 10 minutes, according to Heip *et al.* (1985). The supernatant containing nematodes was decanted into a 63 µm sieve, and the residue was refilled with the 50% Ludox. This centrifugation and decantation step was repeated three times per replicate sample. Microscopic examination of the final residue for a sandy sediment (from River Hayle, HA) and a muddy sediment (from Restronguet Creek C, RC) sample confirmed that complete extraction of nematodes was achieved. The extracted worms were washed thoroughly using ultrapure water to remove any remaining Ludox and, afterwards, transferred into a glass block using a solution containing 5% glycerol, 5% pure ethanol and 90% ultrapure water. Nematodes in the glass block were left to slowly evaporate to anhydrous glycerol in a fume cupboard on top of a hot plate set at 40 ^{o}C.

To assess nematode community composition, a minimum of 100 worms[27] were subsampled at random from each replicate sample for identification, resulting in at least 300 worms per

[26] Depth of the brown, aerated sediment at the study sites in Autumn 2017: BW 2 cm, PR 1.5 cm, CO 1.5 cm, HR 2 cm, PC <1cm, SJ <1 cm, HB < 1 cm, HA 7 cm, MC < 1 cm, RC < 1 cm, RB 2 cm, and RA 1.5 cm.

[27] The occasional selection of more than the desired number of worms in some slides meant that more than 100 individuals were therein identified. Please refer to *Section 4.2.3* for data adjustments in calculating comparable site diversity scores.

site. Millward (1995) had shown that this subsample size was sufficient to discriminate between nematode communities in the Restronguet Creek and those in the relatively uncontaminated Helford and Percuil Rivers. In the third replicate of Restronguet Creek A (RA C), only 17 nematodes were found, all of which were identified. Furthermore, in River Hayle (HA), 79 worms sampled across the replicates were later identified as an annelid from the genus, *Dinophilus*. These annelids were removed from the analysis, resulting in a site total of 228 nematodes. Nematode subsamples were mounted in slides on a fresh drop of anhydrous glycerol, sealed and supported using nail polish. Under x1000 magnification, they were identified to species level, where possible, using pictorial keys by Platt and Warwick (1983, 1988) and Warwick *et al.* (1998). Nematode identification and nomenclature were additionally verified using the World Database of Nematodes (Bezerra *et al.*, 2020).

Having sampled on the same day, sediment physicochemical characteristics in the current study are the same as those reported in the Autumn 2017 survey (Chapters 2 & 3). Briefly, Diffusive Gradient in Thin films (DGT) probes, deployed for 25 hours at site, were retrieved on the day of sediment sampling. Redox potential (Eh) and temperature were measured at site. Salinity and pH were measured from an aliquot of extracted porewater. Sediment median particle size (ϕ50), percentage fines (less than 63 μm) in the absence of gravel (i.e. without fraction ≥2mm), sulphide, as well as dissolved (DOC) and total (TOC) organic carbon were determined in the laboratory. Metals (Cu and Zn) were measured as total (Sed) and extractable (AEM) concentrations in the sediment, in porewater (PW), as well as DGT-labile concentrations 2 cm above (-A), 2 cm below (-B), and within the sediment-water interface (-S). For Cu, the Equilibrium partitioning TOC-normalised measure (SEM – AVS/fOC, henceforth EqP) and the Water Framework Directive (2015, henceforth WFD) DOC-normalised porewater Cu (PW/OC) were also derived. These site characteristics constitute the "environmental variables" referred to in the current study.

4.2.3 Data processing and analysis

4.2.3.1 Univariate diversity indices

A number of univariate diversity indices were investigated for the replicate samples in this study. Number of species (SPN), average taxonomic distinctness (Δ^+, Tax dist), and the variation in taxonomic distinctness (Λ^+, VarTD) were determined using presence-absence data (Clarke & Warwick, 2001). Shannon-Wiener index using natural logarithms (H'), Simpson's index (1 - λ), Pielou's eveness (J'), and taxonomic diversity (Δ, Tax div) were

determined using the species abundance data expressed as a percentage of total nematodes identified for the given replicate sample[28], henceforth referred to as "species percentage" data. Taxonomic information was obtained from the World Database of Nematodes (Bezerra *et al*., 2020), categorised into eleven levels[29]. And Wieser's (1953) trophic groups were defined using mouthpart morphology or, where available, actual information on species feeding habits (Moens *et al.*, 1999; Danovaro & Gambi, 2002; Vafeiadou *et al.*, 2014).

All univariate indices were calculated using the "Vegan" package on the R statistical software (Oksanen *et al.*, 2020). Comparison of values between sites was done by Analysis of Variance (ANOVA) in R after confirming homogeneity of variances using Levene's Test in the "car" Package (Fox *et al.*, 2020). Pairwise post-hoc Tukey tests were completed using the "Agricolae" package (de Mendiburu, 2020) when there was an overall significant difference ($p < 0.05$) in mean values across the sites. The relationships between site means of all univariate indices and environmental variables were assessed using a correlation-based Principal Components Analysis (PCA), completed in SPSS after transformation[30] of environmental variables to homogenise variances (Clarke *et al.*, 2014). For variables showing strong (>0.5) correlations with components of the PCA, Spearman's bivariate correlations were then completed to assess significance of the highlighted relationships.

4.2.3.2 Multivariate analysis

Multivariate analysis of nematode community structure was also carried out using the "Vegan" package in R, except where otherwise stated. This was done on the "species percentage" data, after a further fourth-root transformation in order to moderate the contribution of dominant species (Somerfield *et al.*, 1994b). To investigate the structure of the nematode assemblage across the study sites, non-metric Multi-Dimensional Scaling (MDS) ordination was performed based on the Bray-Curtis dissimilarity index. The analysis was completed using the "metaMDS" function, which automatically detects the minimum stress solution within multiple iterations (n = 20). The ANOSIM test (Clarke, 1993) was

[28] This was to account for the varying number of individuals identified per replicate.

[29] Kingdom, Phylum, Class, Subclass, Order, Suborder, Superfamily, Family, Subfamily, Genus, and Species.

[30] All metal and organic carbon concentrations were ln-transformed. Sulphide was ln (0.1 + x) transformed due to the presence of zeros. And the EqP data was ln (6.1 + x) transformed due to the presence of negative values. Salinity, pH, ORP, median particle size, percentage fines were untransformed.

used to assess differences in nematode communities between site groups defined *a priori* based on metal contamination: grossly-contaminated sites (Hayle and Restronguet Creek) versus less-contaminated sites (all others) as well as the control sites (PR, HR, and BW) versus all the others (see Chapter 2). Where ANOSIM was significant, species contributing to dissimilarities between the site groups were investigated using the SIMPER procedure (Clarke, 1993), which identifies discriminating species using pairwise comparisons of Bray-Curtis dissimilarities.

Relationships between environmental variables and nematode community structure across the sites were investigated using the BIOENV procedure (Clarke & Ainsworth, 1993), which extracts the variable (or combinations thereof) that "best" explain(s) the biotic community dissimilarities. The environmental variables were transformed (as earlier described and standardised, by default, to zero mean and unit standard deviation in "vegan") for this analysis. To address collinearity, environmental variables with Pearson correlations ≥0.95 after transformation were removed (Clarke *et al.*, 2014), with Cu concentrations preferred due to previous causal links with ecological effects across the study sites (Grant, 2010). Euclidean distances were computed for the environmental matrix, and Bray-Curtis distances, for the "species percentage" data. The significance of the BIOENV relationships was assessed using the "global BEST" procedure[31], as described by Clarke *et al.* (2008). To achieve this, 999 random permutations of the environmental matrix were created using the "permatfull" function in the "Vegan" package, with fixed columns (i.e. environmental variables) and randomised rows (i.e. samples). The individual permuted matrices were then entered into the BIOENV procedure, and the "best" Spearman correlation coefficients were extracted. The upper limit of the p-value was calculated using Equation 1, below, where t of the T permuted "best" correlation coefficients were greater than or equal to the best correlation coefficient derived using the actual matrix (Clarke *et al.*, 2008; Legendre & Legendre, 2012).

[31] Both this "global BEST" BIOENV procedure and a "global BEST" test for the related, but stepwise, BVStep procedure (Clarke & Warwick, 1998; Clarke *et al*., 2014) have been automated in separate functions written in the R programming language and made available as accompanying materials to this thesis. The functions perform the underlying procedure (BIOENV or BVStep), perform the "global BEST" significance tests, and plot histograms of permuted coefficients showing the actual coefficient and permutation p-value. They were validated using the Clyde Macrofauna biomass and environmental datasets available in PRIMER, generating the same results as in the published studies (Clarke *et al*., 2008, 2014). The "global BVStep" function can fix or vary both biotic and environmental matrices.

$P_{upper} = (t+1) / (T+1)$ (Equation 1)

Where:

P_{upper} is the upper limit of the p-value,
t is the number of permuted "best correlation coefficients" ≥ actual best coefficient, and
T is the number of permutations (999).

Relationships between environmental variables and nematode community structure were further investigated by Multivariate Regression Trees (MRT) based on Bray-Curtis distances (De'ath, 2002) and bubble plots superimposed on the MDS ordination (Somerfield *et al.*, 1994b). MRT is a method of binary divisive clustering of samples, with divisions constrained according to the explanatory variable(s) with the best predictive power. The method is the precursor to the LINKTREE procedure (Clarke *et al.*, 2008), which uses the ANOSIM R statistic to optimise splits and the SIMPROF test to regulate subdivisions but is not yet available on open-source software. The MRT procedure was done using R Package "mvpart" (De'ath, 2014) by modifying Borcard *et al.*'s (2018) codes to apply Bray-Curtis distances to the "species percentage" data (see Appendix A4.1 for R codes), with 36 groups and 100 cross-validations. Raw environmental variables were used, as transformations do not alter results (Clarke *et al.*, 2008). The model with the lowest cross-validated error[32] was picked.

4.3 Results

4.3.1 Univariate diversity measures and trophic group proportions

Means and standard deviations of univariate diversity measures and trophic groups across the sites are presented in Tables 4.1 and 4.2. Although metal contamination differs markedly between the reference/control sites (BW, HR, and PR), the most contaminated areas in the Restronguet Creek and Hayle, and the sites in-between (Chapter 2), the univariate diversity measures did not adequately capture this difference. A downward trend in values (upward trend for VarTD) was visible with increasing metal contamination (movement down the table); however, the lowest scores tended to be found in the relatively anoxic sediments of PC and HB. For all other sites, there was no significant differences observed in mean diversity values versus the group of control sites (Table 4.1).

[32] The cross-validated error ("CV Error" in the plots) is a measure of the tree's predictive performance and is based on a repeated random sub-sampling of dataset (n = 100 here). CV Error varies from zero for a perfect predictor to ca. one for a poor predictor (De'ath, 2002).

Table 4.1. Mean and standard deviation of univariate diversity indices across the study sites. Different letters denote significant differences ($p < 0.05$) between site means following Tukey pairwise comparison. ANOVA results are provided as footnotes

Site	**SPN**	**H'**	**1 - λ**	**J'**	**Δ^+**	**Λ^+**	**Δ**
BW	21 ± 2 *ab*	2.5 ± 0.1 *ab*	0.89 ± 0.02 *a*	0.83 ± 0.04 *a*	77.3 ± 0.9 *a*	473 ± 28 *b*	68.5 ± 2.7 *ab*
PR	16 ± 2 *abcd*	2.3 ± 0.1 *abc*	0.86 ± 0.01 *a*	0.82 ± 0 *a*	80.7 ± 1.7 *a*	536 ± 37 *ab*	69.2 ± 2.6 *ab*
CO	24 ± 8 *ab*	2.5 ± 0.5 *ab*	0.87 ± 0.07 *a*	0.8 ± 0.09 *ab*	80.2 ± 1.6 *a*	417 ± 32 *b*	66.1 ± 9.7 *ab*
HR	18 ± 2 *abcd*	2.4 ± 0.2 *abc*	0.86 ± 0.05 *a*	0.82 ± 0.06 *a*	78 ± 3.1 *a*	459 ± 35 *b*	59.4 ± 4.7 *ab*
PC	9 ± 4 *d*	0.6 ± 0.2 e	0.24 ± 0.08 *c*	0.28 ± 0.06 *c*	65.6 ± 5.1 *bc*	477 ± 239 *b*	17.8 ± 6.6 *c*
SJ	26 ± 1 *a*	2.7 ± 0.1 *a*	0.91 ± 0.01 *a*	0.84 ± 0.02 *a*	77.7 ± 0.8 *a*	433 ± 63 *b*	72.3 ± 0.6 *a*
MC	20 ± 4 *abc*	2.6 ± 0.2 *ab*	0.9 ± 0.02 *a*	0.86 ± 0.02 *a*	79.5 ± 0.6 *a*	461 ± 43 *b*	69.5 ± 3 *a*
HA	11 ± 3 *cd*	1.6 ± 0.2 *bcd*	0.71 ± 0.08 *ab*	0.69 ± 0.03 *ab*	81.2 ± 2.4 *a*	612 ± 164 *ab*	58 ± 7.9 *ab*
RC	14 ± 1 *bcd*	1.7 ± 0.3 *bcd*	0.7 ± 0.11 *ab*	0.66 ± 0.1 *ab*	74 ± 2.3 *abc*	541 ± 41 *ab*	51 ± 7.9 *ab*
RA	11 ± 4 *cd*	1.5 ± 0.3 *cd*	0.64 ± 0.15 *ab*	0.66 ± 0.21 *ab*	82.1 ± 1.8 *a*	561 ± 37 *ab*	53.7 ± 14.6 *ab*
RB	18 ± 1 *abcd*	2.4 ± 0.2 *ab*	0.87 ± 0.04 *a*	0.84 ± 0.06 *a*	75.8 ± 3.4 *ab*	547 ± 95 *ab*	63.7 ± 2 *ab*
HB	10 ± 4 *cd*	1.3 ± 0.6 *de*	0.52 ± 0.25 *bc*	0.53 ± 0.19 *bc*	63.7 ± 11 *c*	784 ± 74 *a*	40 ± 26.1 *bc*

SPN ($F = 7.91$, $p < 0.001$): Number of species; H' ($F = 14.41$, $p < 0.001$): Shannon-Weiner diversity; $1 - \lambda$ ($F = 12.13$, $p < 0.001$): Simpson's diversity; J' ($F = 9.49$, $p < 0.001$): Pielou's evenness; Δ^+ (($F = 6.69$, $p < 0.001$): Average taxonomic distinctness; Λ^+ ($F = 3.22$, $p = 0.008$): Variation in taxonomic distinctness; Δ ($F = 7.26$, $p < 0.001$): Taxonomic diversity

Table 4.2. Mean and standard deviation of nematode trophic group (Wieser, 1953) proportions across the study sites. Different letters denote significant differences between site means following Tukey pairwise comparison. ANOVA results are provided as footnotes

Site	**1A**	**1B**	**2A**	**2B**
BW	0.01 ± 0.01 *b*	0.66 ± 0.06 *abc*	0.13 ± 0.04 *bc*	0.2 ± 0.04 *cd*
PR	0.01 ± 0.01 *b*	0.58 ± 0.12 *abc*	0.06 ± 0.02 *bc*	0.35 ± 0.11 *bcd*
CO	0.11 ± 0.08 *ab*	0.28 ± 0.08 *cd*	0.09 ± 0.1 *bc*	0.52 ± 0.22 *abc*
HR	0.02 ± 0.02 *b*	0.49 ± 0.03 *abc*	0.33 ± 0.02 *ab*	0.17 ± 0.04 *cd*
PC	0.05 ± 0.03 *ab*	0.04 ± 0.05 *d*	0.03 ± 0.03 *c*	0.88 ± 0.05 *a*
SJ	0.04 ± 0.02 *b*	0.56 ± 0.09 *abc*	0.07 ± 0.03 *bc*	0.33 ± 0.11 *bcd*
MC	0.16 ± 0.05 *a*	0.34 ± 0.05 *bcd*	0.18 ± 0.15 *bc*	0.32 ± 0.16 *bcd*
HA	0.02 ± 0.02 *b*	0.31 ± 0.14 *cd*	0.02 ± 0.02 *c*	0.65 ± 0.16 *ab*
RC	0.03 ± 0.01 *b*	0.41 ± 0.15 *abcd*	0.54 ± 0.17 *a*	0.01 ± 0.02 *d*
RA	0.08 ± 0.09 *ab*	0.77 ± 0.21 *a*	0.13 ± 0.09 *bc*	0.02 ± 0.03 *d*
RB	0.03 ± 0.01 *b*	0.74 ± 0.15 *ab*	0.22 ± 0.14 *bc*	0.01 ± 0.01 *d*
HB	0 *b*	0.67 ± 0.33 *abc*	0.2 ± 0.12 *bc*	0.13 ± 0.22 *d*

1A ($F = 4.24$, $p = 0.002$): Selective deposit feeders (or microvores) with no or narrow tubular buccal cavity
1B ($F = 6.75$, $p < 0.001$): Non-selective deposit feeders with large unarmed buccal cavity
2A ($F = 7.16$, $p < 0.001$): Epistrate feeders with lightly- or moderately-armed buccal cavity
2B ($F = 14.93$, $p < 0.001$): Predators/omnivores with well-armed buccal cavity

Trophic group proportions did not generally differ across the sites (Table 4.2). The most obvious trend was in the proportion of Group 2B nematodes (predators and omnivores), decreasing with metal contamination towards the upper reaches of the Restronguet Creek and in the Copperhouse Pool (HB). Except in Pill Creek (PC), Restronguet C (RC), and River Hayle (HA), non-selective deposit feeders (1B) tended to dominate nematode communities across the sites. The lowest proportions were with the microvores (1A), rising in abundance at Mylor Creek (MC). Nematode communities in PC and HA were dominated by predators and omnivores (Group 2B), mainly due to high relative abundances of *Chromadoropsis vivipara* and *Oncholaimus oxyuris*, respectively (see species listings in Appendix A4.2a – c). For RC, the proportion of epistrate feeders (2A) was highest mainly due to the nematode *Ptycholaimellus ponticus* occurring in relatively high numbers.

4.3.2 Relationship between univariate diversity scores and trophic proportions with environmental variables

Relationships between univariate diversity measures and Wieser trophic group proportions with environmental variables were investigated, firstly, using a correlation-based PCA of site means after Ln-transformation, where appropriate. Component plots for the first three components, jointly accounting for 72.8% of the variation, are provided in Figure 4.01. And details of the eigenvalues and component matrix are provided in Appendices A4.3 and A4.4. Indicatively strong relationships (≥ 0.5) were then assessed by Spearman's correlation.

The first component of the PCA (38.7% of the variation) was mainly an axis of increasing metal contamination, with strong positive correlations (≥ 0.7) for all metal concentrations assessed (Figure 4.01). This component was also strongly negatively correlated with salinity, as expected given the salinity gradient in the Fal, and positively with ORP and median grain size. The biotic variable, number of species (SPN), was also strongly negatively correlated with Component 1, suggesting a considerable decline with increasing metal contamination, grain size, and redox potential across the sites, but an increase with increase in salinity. In contrast, variation in taxonomic distinctness (VarTD) was positively correlated with Component 1, suggesting an increase with increasing metal contamination across the sites.

Along the Component 2 axis (20.6% of the variation), all univariate diversity indices, except VarTD, were shown to be more strongly correlated with pH (negative relationship) than metals (only DGT Zn concentration in the sediment layer, positive relationship). The third component (13.5% of the variation) revealed that the Wieser trophic groups 1A, 2A, and 2B are strongly correlated (in different directions) with ORP, DOC, and particle size. And along Component 4 (9.5% of the variation, A4.4), Groups 1A (positive) and 1B (negative) were strongly correlated with sulphide concentrations, which is reflective of sediment redox.

Overall, the PCA revealed that, other than SPN and VarTD, the univariate diversity indices and trophic groups were reflective of "nuisance" variables across the highly heterogeneous sediments rather than metal contamination. However, SPN and VarTD were related with metal contamination alongside few other environmental variables (salinity, ORP, and grain size). Significant bivariate correlations from these suggested relationships are plotted in Figures 4.02 – 4.04. VarTD and SPN were only significantly related with metals, mainly OC-normalised dissolved and EqP Cu concentrations, whereas Wieser Groups 1A and 2A were significantly correlated with sulphide and grainsize, respectively.

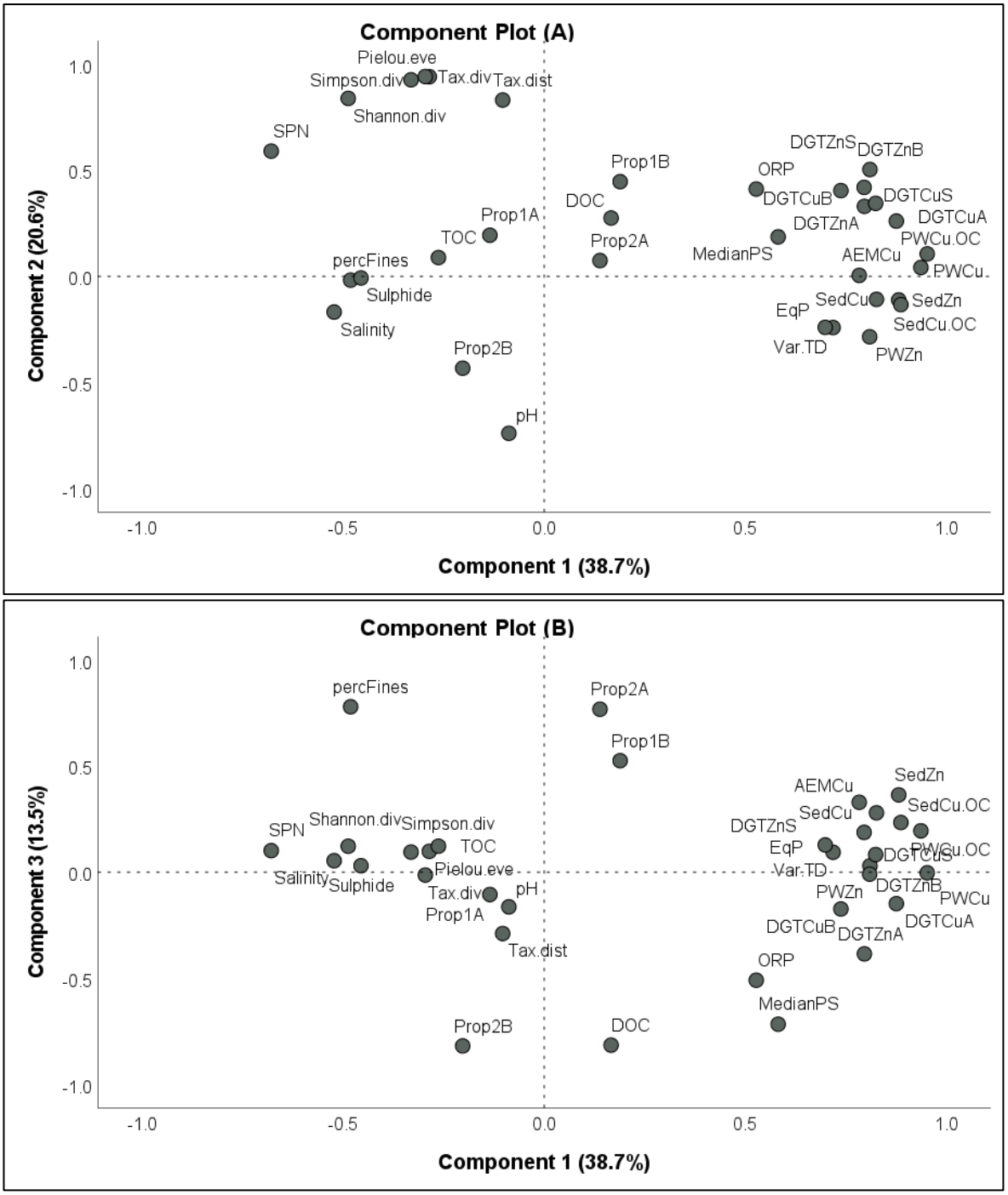

Figure 4.01: Component plots of the first three components of the correlation-based PCA using site means of univariate diversity indices and environmental variables ln-transformed as applicable (all except Salinity, percFines, ORP, and pH). DGT A, B, and S: DGT-labile concentrations measured above, below and at the sediment-water interface, respectively. AEM: 1M HCl extractable metal concentration; percFines: Percentage of particles <63µm in the fraction excluding gravel; Tax.div: Taxonomic diversity; Tax.Dist and Var.Tax.Dist: Average Taxonomic Distinctness and Variation in Taxonomic Distinctness, respectively.

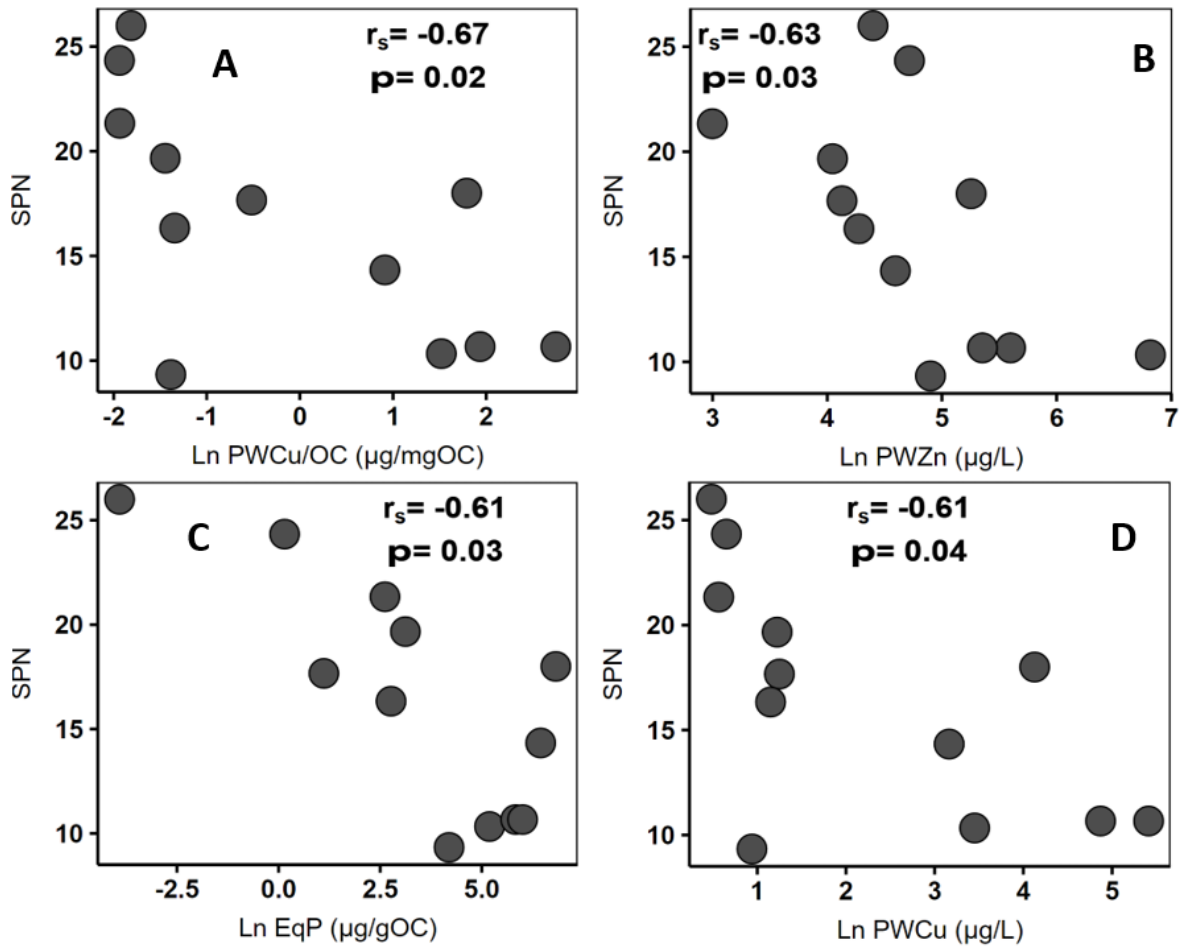

Figure 4.02: Significant Spearman correlations between mean number of species (SPN) and environmental variables across the sites. Figures arranged from A-D in decreasing correlation strength. Variables for bivariate correlation were chosen based on the strength of their correlation with Component 1 of the correlation-based PCA in Figure 4.01. Note that all variables have been Ln-transformed. Actual values and site SDs of environmental variables are provided in Chapter 2. SDs of SPN are provided in Table 4.1

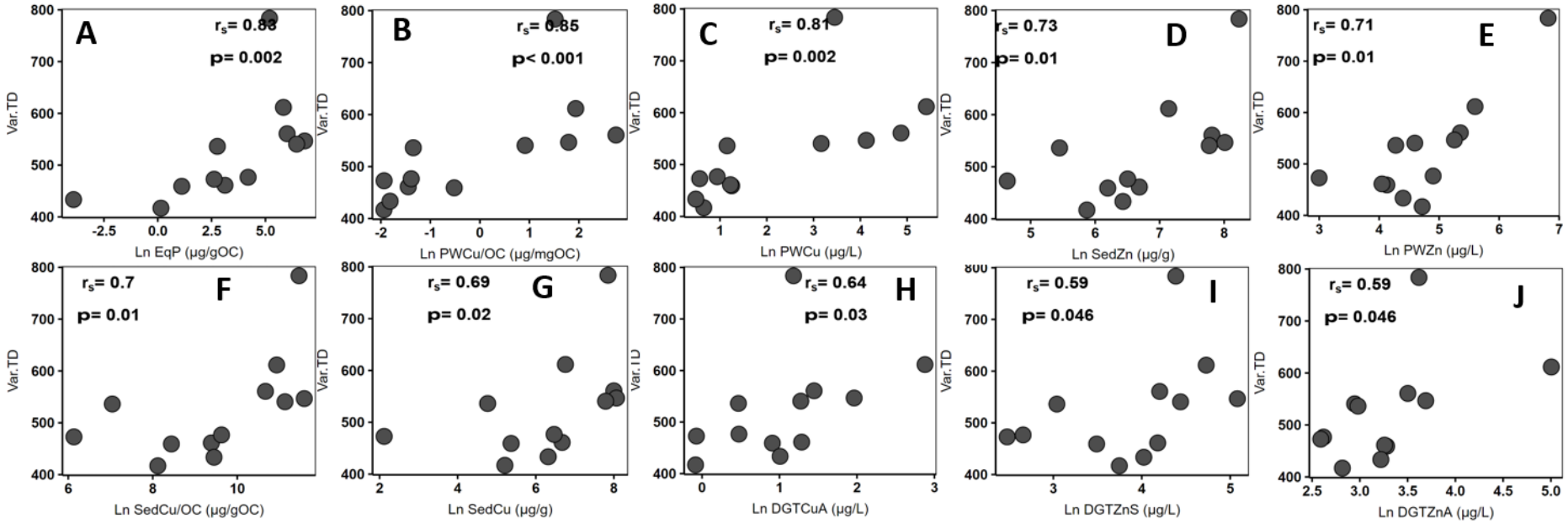

Figure 4.03: Significant Spearman correlations between mean number Variation in Taxonomic Distinctiveness (Var.TD) and environmental variables across the sites. Figures arranged from A-J in decreasing correlation strength. Variables for bivariate correlation were chosen based on the strength of their correlation with Component 1 of the correlation-based PCA in Figure 4.01. Note that all variables have been Ln-transformed. Actual values and site SDs of environmental variables are provided in Chapter 2. SDs of Var.TD are provided in Table 4.1

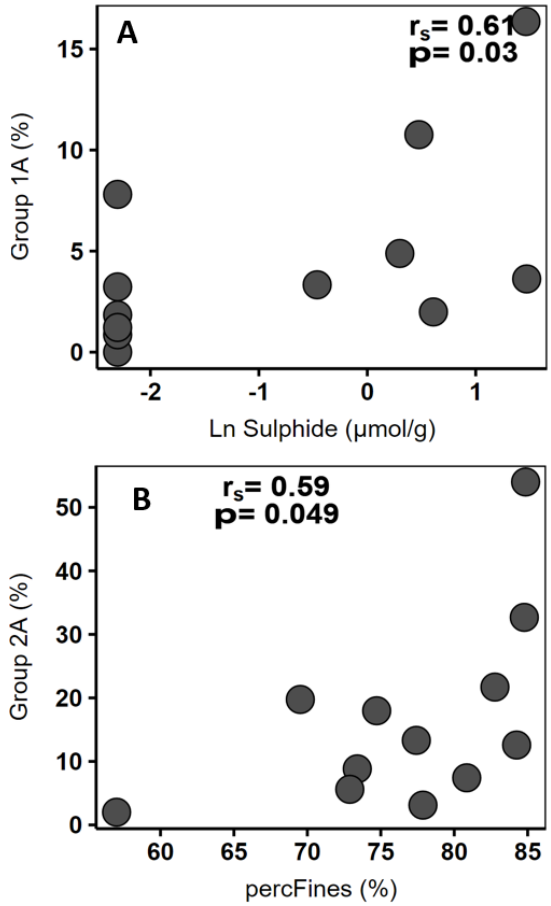

Figure 4.04: Significant Spearman correlations between mean of percentage of Wieser's trophic groups and environmental variables across the sites. Figures arranged in decreasing correlation strength. Variables for bivariate correlation were chosen based on the strength of their correlation with Components 3 and 4 of the correlation-based PCA in Figure 4.01. Note that Sulphide concentrations have been Ln-transformed. Actual values and site SDs are provided in Chapter 2. SDs of Wieser's groups (as proportions) are provided in Table 4.2

4.3.3 Multivariate analysis of community structure

MDS ordinations of fourth-root transformed percentage abundances of species are shown in Figures 4.05a and b, with and without the third replicate from Restronguet Creek A (RA-C) in which only 17 nematodes were found and identified. The corresponding Shepard diagrams are shown in Figure 4.06. Both ordinations resulted in a nearly identical pattern of nematode community structure, but removal of RA-C (and only RA-C in comparison with any other sample removed at random) reduced the "stress" from 0.2 to 0.18. In a separate plot where RA-C was included but species percentage abundances were treated by dispersion weighting (Clarke *et al.*, 2006, 2014) to moderate large variances prior to fourth root transformation, the same community pattern was retained and stress was reduced to 0.19 (Figure A4.5).

The stress of a 2-D MDS plot reflects the accuracy of its representation of site dissimilarities. Although this value tends to increase with number of samples, a nominal threshold has been defined such that stress <0.2 indicates a "potentially useful" representation, but values increasingly >0.2 represent considerable departures from the ranked dissimilarities (Clarke, 1993; Clarke *et al.*, 2014). Clearly, stress in the current study approaches 0.2 due to the inclusion of RA-C, albeit does not significantly alter the MDS plot. In the original representation (fourth-root transformed without dispersion weighting), a strong non-metric fit ($R^2 = 0.96$) is achieved (Figure 4.06a), as in others, therefore this representation is retained and analysed in the following paragraphs as useful for the dissimilarities across the sites.

Multivariate ordination separated the study sites into two distinct groups based on their level of metal contamination: the grossly-contaminated sites in Hayle and the Restronguet Creek to the bottom-left and the less-contaminated sites to the top-right (Figure 4.05a). Within each group, the sites appeared to be ordered diagonally in increasing metal contamination from top to bottom, consistent with distance from the Carnon River catchment in the Fal. On the top-left, starting at River Hayle (HA) to the mouth of the Restronguet Creek (RC). And on the right, beginning with the Pill Creek at the bottom, which is closest to Site RC, and then terminating at control sites in Percuil River (PR) and the Helford River (HR). This site groupings were corroborated by the MRT analysis (Figure 4.07, details in Section 4.3.4), indicating that initial grouping was based on Sed Cu concentrations and subdivisions based mainly on Sed Cu and PW Cu concentrations. As the original groups were defined *a priori*, ANOSIM was an ideal tool to statistically compare biotic communities and confirmed that nematode community composition in the grossly-contaminated sites (Hayle and Restronguet Creek) was significantly different from that in the other sites ($R = 0.47$, $p = 0.001$).

It is also noteworthy that nematode communities in Breydon Water (BW), an unimpacted site in East England, were ordinated together with the other control sites (PR and HR) within the Fal system, despite the variation in environmental characteristics. ANOSIM comparison of this control group with the rest of the study sites was, however, not significant ($R = 0.11$, $p = 0.11$) because of the related CO-A sample (Figure 4.05a), and any *a posteriori* inclusion of this sample invalidates test assumptions. Furthermore, replicate samples from the same site tended to cluster together (in both MRT and MDS). This close grouping suggests that the replicates were indicative of true community composition across the sites, with variance greater between – rather than within – sites (Global ANOSIM $R = 0.94$, $p = 0.001$). The only exception is the RA- C sample previously highlighted.

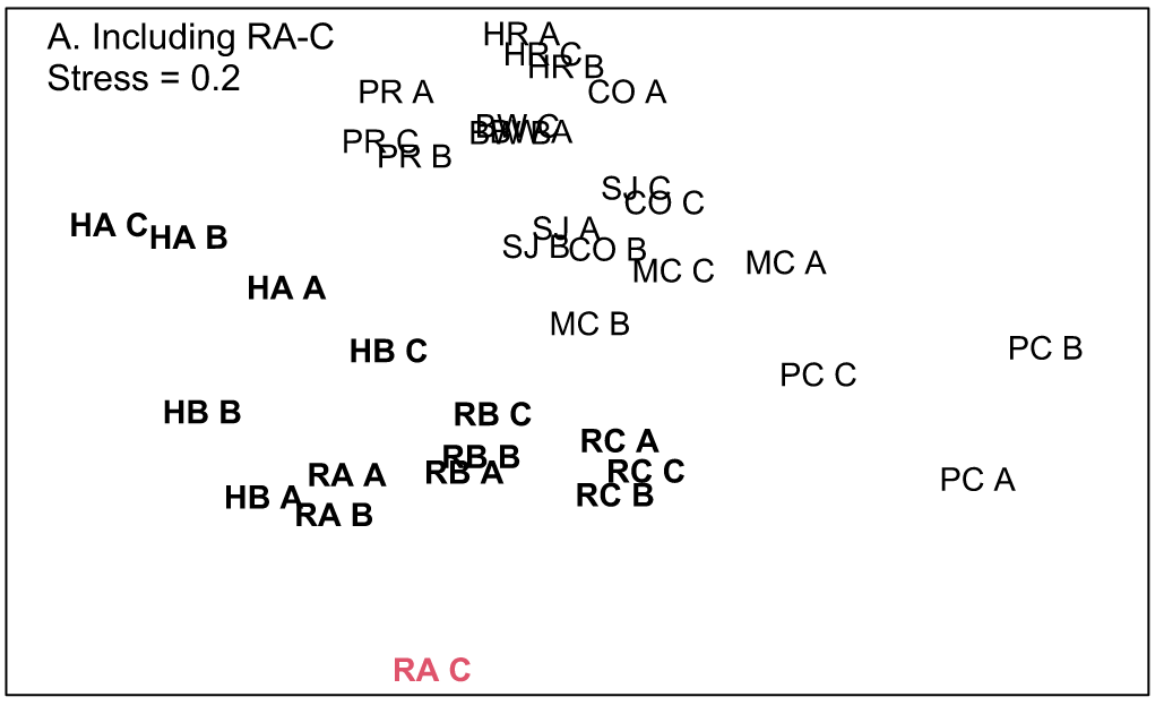

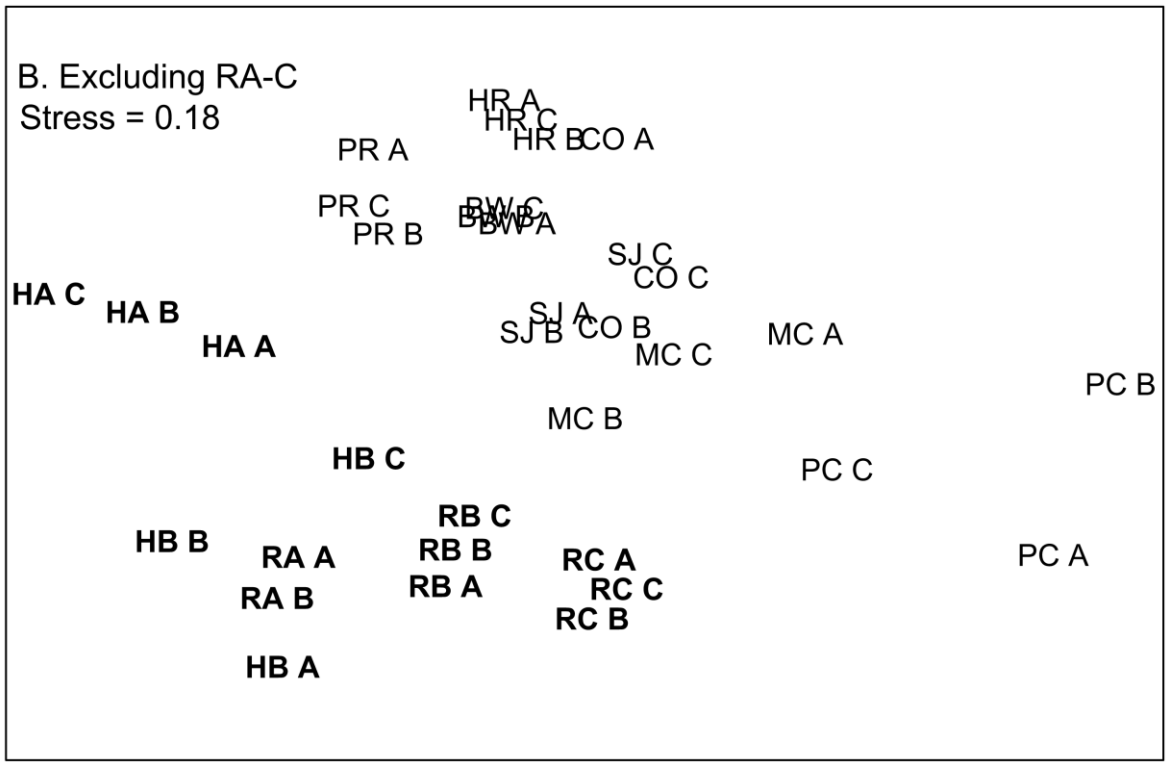

Fig. 4.05: MDS ordination of fourth-root transformed nematode percentage abundances across the study sites, generated with (A) and without (B) data for RA-C (red font), which is the replicate of Restronguet Creek A with only 17 individuals in the bulk sample. Bold font: grossly contaminated sites. Normal font: less contaminated sites

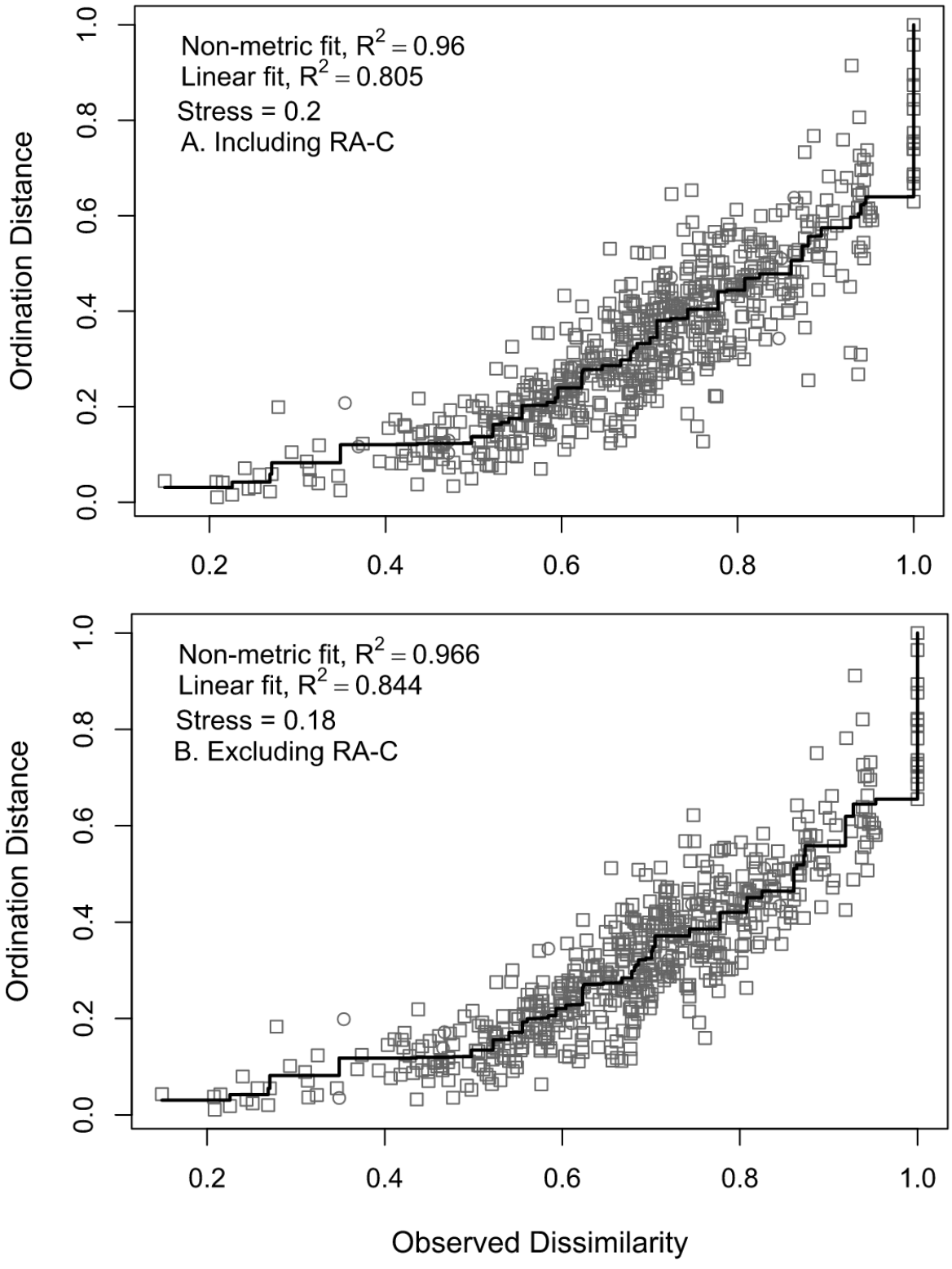

Fig. 4.06: Shepard diagrams showing Kruskal stress from MDS plots generated with (A) and without (B) species percentage data for RA-C, which is the replicate of Restronguet Creek A with only 17 individuals in the bulk sample

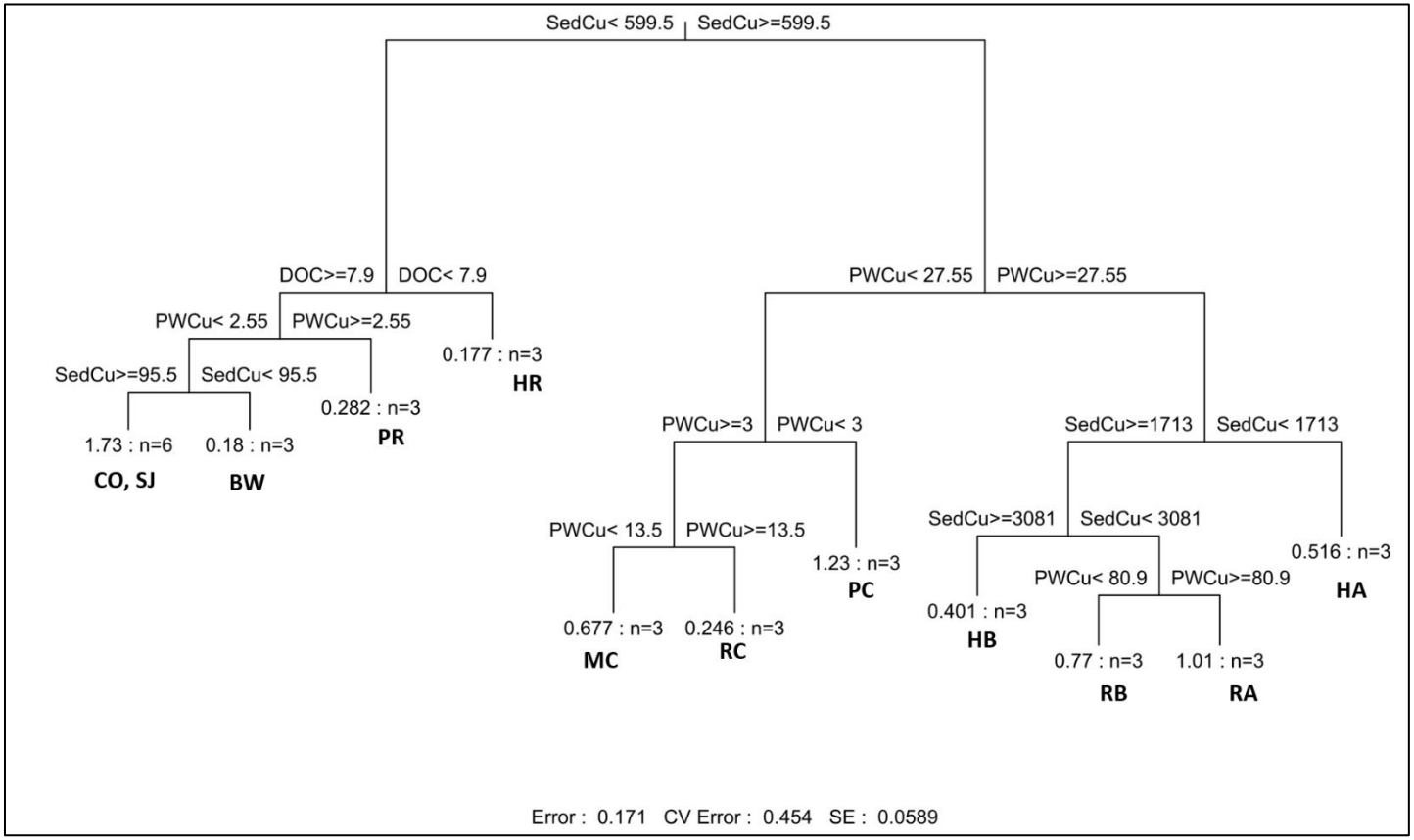

Figure 4.07: Multivariate Regression Tree (MRT) of nematode community Bray-Curtis dissimilarities constrained by explanatory environmental variables. The best three variables from the BIOENV procedure, PW Cu (porewater Cu), DOC (Dissolved Organic Carbon), and pH, were used in addition to grainsize-normalised sediment Cu (and Zn, SedCu & SedZn) following strong correlations in previous studies (e.g. Somerfield *et al.*, 1994b). For each leaf, the histograms show the relative abundances of species at each leaf, n is the number of sites, and the preceding value is the sum of squared errors. Error is the relative error of the tree, describing the overall fit (R-squared = 1 – Error). CV Error and SE represent the cross-validated error and its standard error (n = 100), respectively, which characterise predictive accuracy (CV Error 0 = strongest, 1 = weakest). Sites are provided in every leaf

Table 4.3: BIOENV spearman correlations between nematode community similarity and environmental variables across the study sites. Variables and their combinations are ranked in decreasing order of correlation with community similarity

Variables												r_s	Rank
PWCu												0.45	1
pH	PWCu											0.62	2
pH	PWCu	DOC										0.65	3
pH	PWCu	DOC	PWZn									0.66	4
pH	PWCu	DOC	PWZn	ORP								0.67	5
pH	PWCu	DOC	PWZn	Mn	ORP							0.66	6
Sal	pH	PWCu	DGTZnB	DOC	PWZn	Mn						0.65	7
Sal	%Fines	pH	PWCu	DGTZnB	DOC	PWZn	Mn					0.65	8
Sal	%Fines	pH	PWCu	DGTZnB	DOC	PWZn	Mn	ORP				0.63	9
Sal	%Fines	pH	PWCu	SedCu	DGTZnB	DOC	PWZn	Mn	ORP			0.62	10
Sal	%Fines	pH	PWCu	SedCu	DGTZnB	DOC	PWZn	Mn	ORP	EqP		0.61	11
Sal	%Fines	pH	PWCu	SedCu	DGTZnB	DOC	PWZn	Mn	ORP	EqP	Sul	0.58	12
Sal	%Fines	pH	PWCu	SedCu	DGTCuB	DGTZnB	DOC	PWZn	Mn	ORP	EqP	Sul	0.56	13

PW and Sed: Total metal concentration in the porewater and sediment, respectively. DGT A, B and S: DGT-labile concentrations measured above, below and at the sediment-water interface, respectively. Sal: Salinity. Sul: Sulphide. TOC: Sediment Total Organic Carbon. DOC: Dissolved Organic Carbon. ORP: Redox potential. %Fines: percentage grainsize <63µm after removing gravel content. Environmental variables were Ln-transformed (all except pH, Sal, ORP, and %Fines) and then standardised to zero mean and unit SD prior to BIOENV procedure. To address collinearity, variables with Pearson correlations ≥0.95 were removed, with preference for Cu concentrations where applicable. Bray-Curtis distances were used for the biotic matrix and Euclidean distances, for the environmental matrix.

4.3.4 Relationship between multivariate dissimilarity and environmental variables

BIOENV and MRT analyses were used to link multivariate dissimilarities to environmental variables. The BIOENV procedure was completed using transformed and standardised environmental variables, with Sed Zn, Sed Fe, AEM Zn, and DGT Cu and Zn concentrations above and at the sediment-water interface removed due to considerable collinearity ($R \geq 0.95$). The respective concentrations of Cu were preferred, where applicable. For PW and DGT concentrations in the sediment layer, both Cu and Zn values were included in the BIOENV analysis, allowing the comparison of "explanatory power" for both metals.

The BIOENV and its global BEST significance test confirmed that the variation in nematode community dissimilarities were mainly associated with the variation in metal contamination, measured as PW Cu, rather than "nuisance" environmental variables across the sites ($p < 0.001$, Table 4.3, Figures 4.07 and 4.08). The highest rank correlation for a single variable was with PW Cu ($r_s = 0.45$) and, afterwards, a combination of PW Cu concentration and pH ($r_s = 0.62$). Upon inclusion in the combination, other environmental variables either did not considerably improve – addition of DOC, PW Zn, and ORP in the best combination only improved r_s by 0.05 – or even degraded the Spearman's rank correlation.

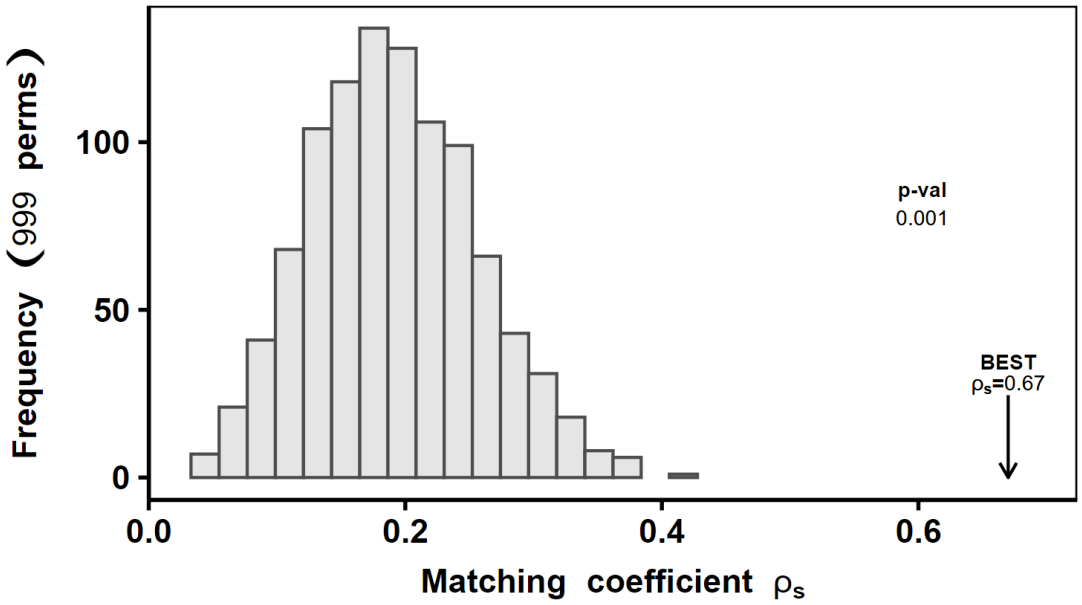

Fig. 4.08: Global Best (BIOENV) test for a significant relationship between nematode community similarity and environmental variables across the study sites. "P-val" represents the upper limit of the p value. "BEST" represents the Spearman correlation for the best BIOENV match using the actual environmental matrix. The histogram is the distribution of "best" correlations obtained using the 999 permuted matrices created to distort any apparent biota-environment relationship

The "best" three environmental variables which explain the variation in biotic dissimilarity, as selected in the BIOENV procedure, were used to generate the MRT. Sed Cu and Zn were further included, given the previous observations of strong correlations between nematode community dissimilarity and total sediment metal concentrations within the Fal (Somerfield *et al.*, 1994b). MRTs are robust to the collinearity of explanatory variables (De'ath, 2002).

The MRT confirmed BIOENV results, indicating that nematode community dissimilarities across the sites were strongly predicted by the gradient of metal contamination (Figure 4.07). The tree explained 82.6% of the variance in Bray-Curtis dissimilarities, with a CVRE of 0.45 indicative of a strong prediction (R^2 = 1 – Error). Of the explanatory variables used, site groupings were primarily defined by threshold concentrations of Sed Cu (and Zn[33]) and PW Cu, with the former accounting for the first split (and highest variance) but the latter explaining most of the variability across the tree. Taken together, the MRT and BIOENV results showed that nematode community composition across the sites was mainly driven by metal contamination, and that PW Cu followed by Sed Cu (and covarying variables, e.g. Zn) were the most significant predictors.

Superimposing MDS ordinations in bubble plots allowed easier visualisation of important explanatory variables (Figures 4.09 – 4.19). As seen in the BIOENV and MRT analyses, the clearest distinctions between the two major groups of site were observed in plots based on PW and Sed concentrations (Figures 4.09 – 4.13), particularly PW Cu (Figure 4.09a). The ordinations based on PW Cu/OC and EqP Cu were similar to porewater Cu, albeit less distinguishing of site groups (Figures 4.11 and 4.12). Ordering of the sites within individual groups was less clear, indicative of a decrease in PW Cu, but also an increase in Sed Cu, EqP Cu, Sed Zn, and PW Zn concentrations from top-left to bottom-right. EqP was negative for Sites CO, SJ, and HR – lower than at BW. And DGT concentrations were less indicative of community composition than PW and Sed, which is notable given its projection in the literature. Overall, sites were more readily distinguished based on their levels of Cu than Zn, suggesting that Cu might have a stronger effect on nematode communities across the sites.

[33] For every node characterised by a threshold in Sed Cu concentrations, Sed Zn explained the same fraction of variability. This was also the case with DOC, being equally explained by a threshold in PW Cu. In these situations where two or more explanatory variables yield the same results, the choice in the representation is only arbitrary and does not indicate superior predictive capability (Borcard *et al.*, 2018). Note that representations of DOC were equally explained by PW Cu, but not the reverse case (i.e. PW Cu by DOC).

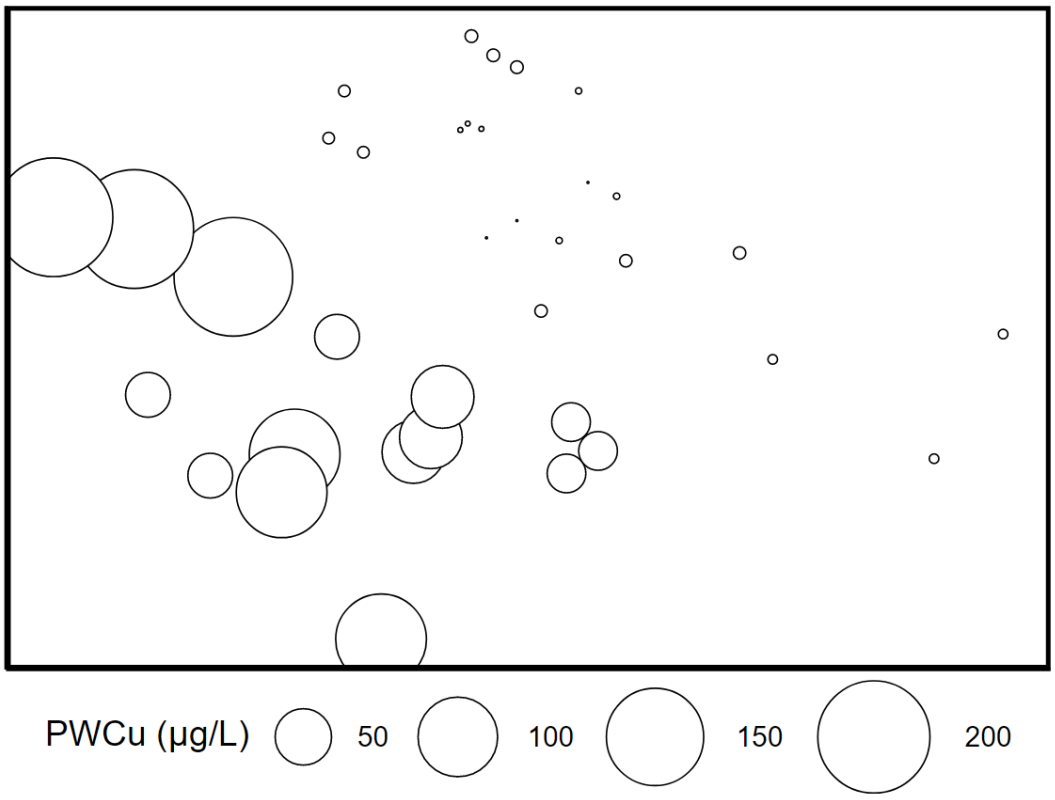

Fig. 4.09a: MDS ordination of fourth-root transformed nematode percentage abundances, with circles proportional in size to porewater Cu concentration

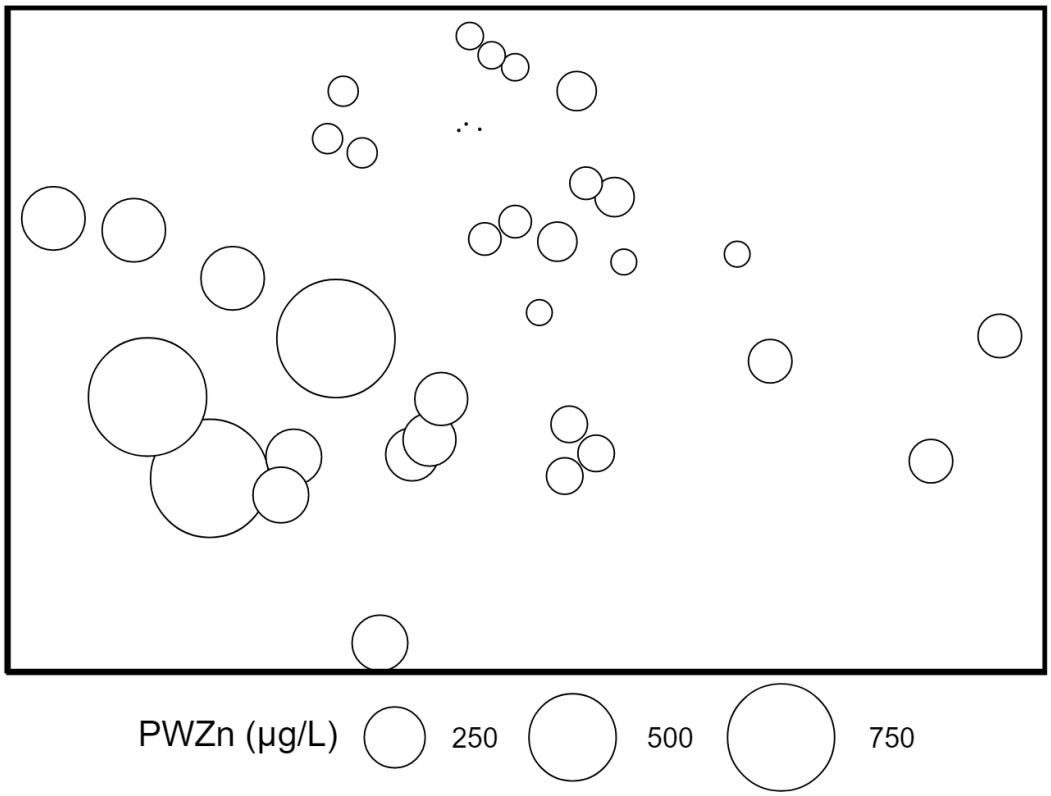

Fig. 4.09b: MDS ordination of fourth-root transformed nematode **percentage abundances**, with circles proportional in size to porewater Zn concentration

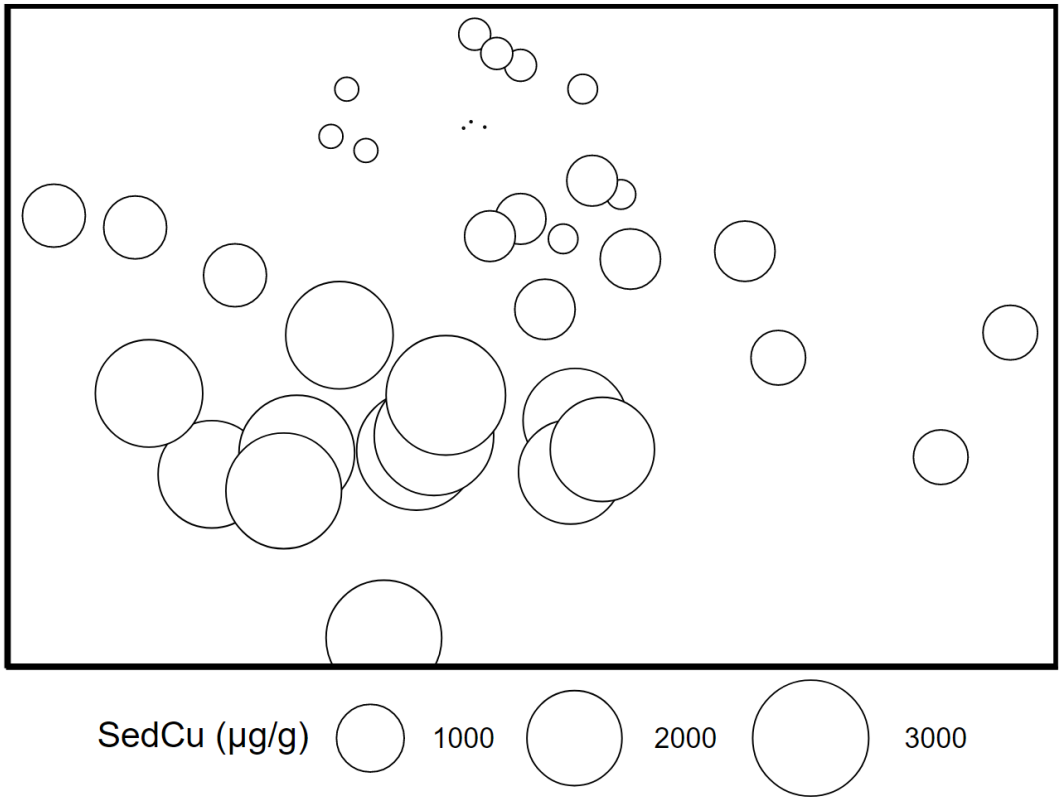

Fig. 4.10a: MDS ordination of fourth-root transformed nematode percentage abundances, with circles proportional in size to total sediment Cu concentration

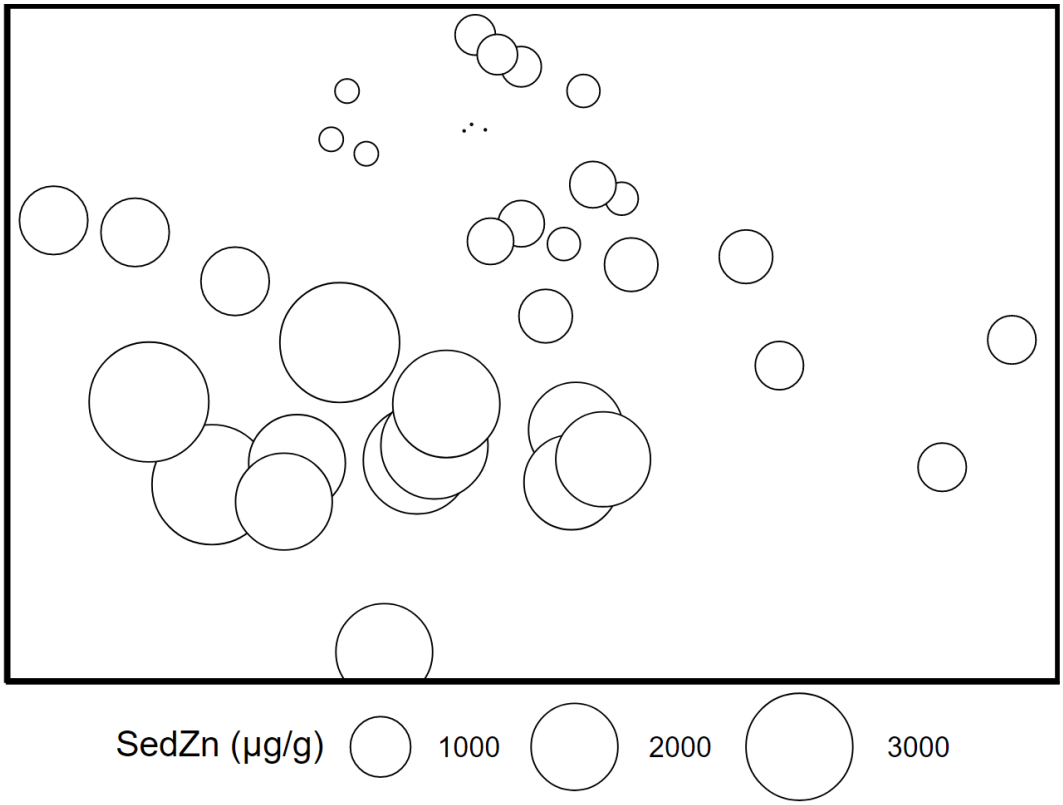

Fig. 4.10b: MDS ordination of fourth-root transformed nematode percentage abundances, with circles proportional in size to total sediment Zn concentration

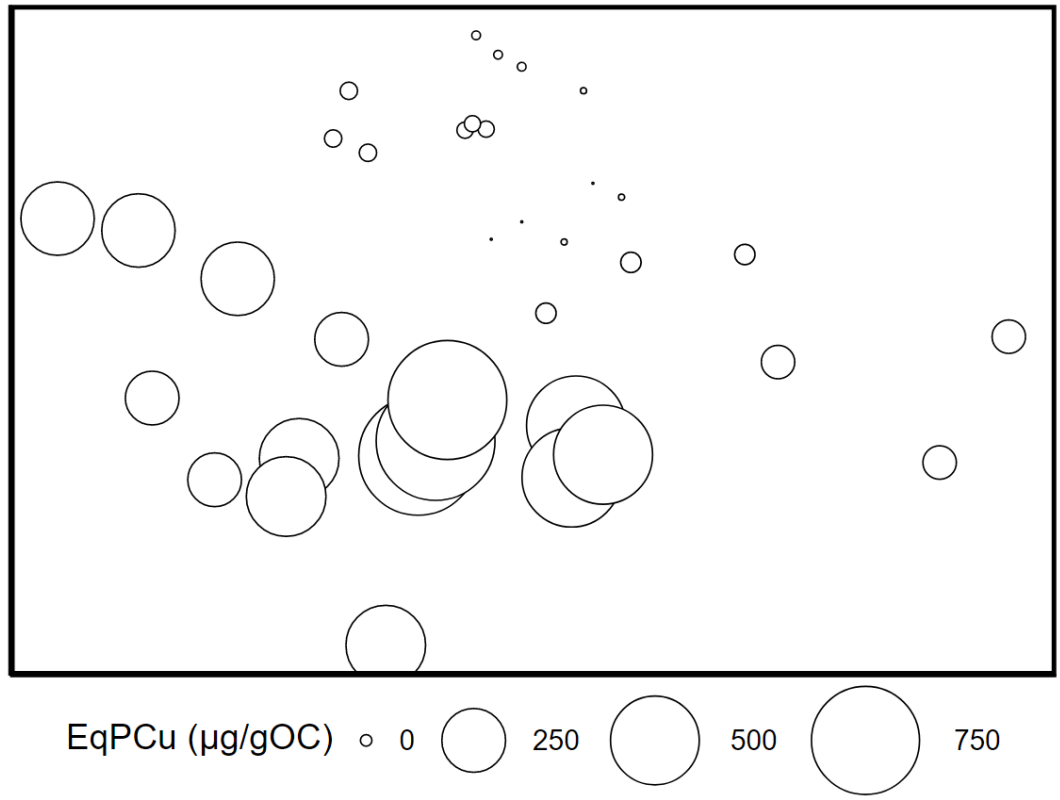

Fig. 4.11: MDS ordination of fourth-root transformed nematode percentage abundances, with circles proportional in size to EqP (SEM Cu – AVS/fOC) concentration

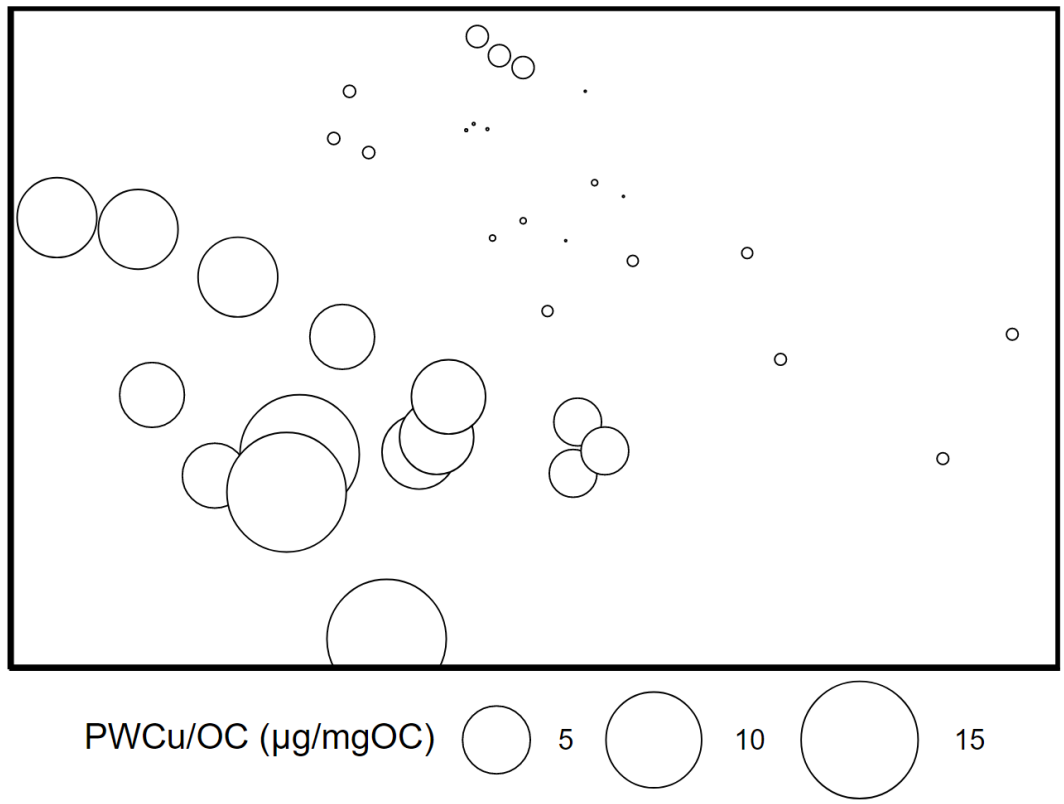

Fig. 4.12: MDS ordination of fourth-root transformed nematode percentage abundances, with circles proportional in size to WFD PW Cu/DOC concentration

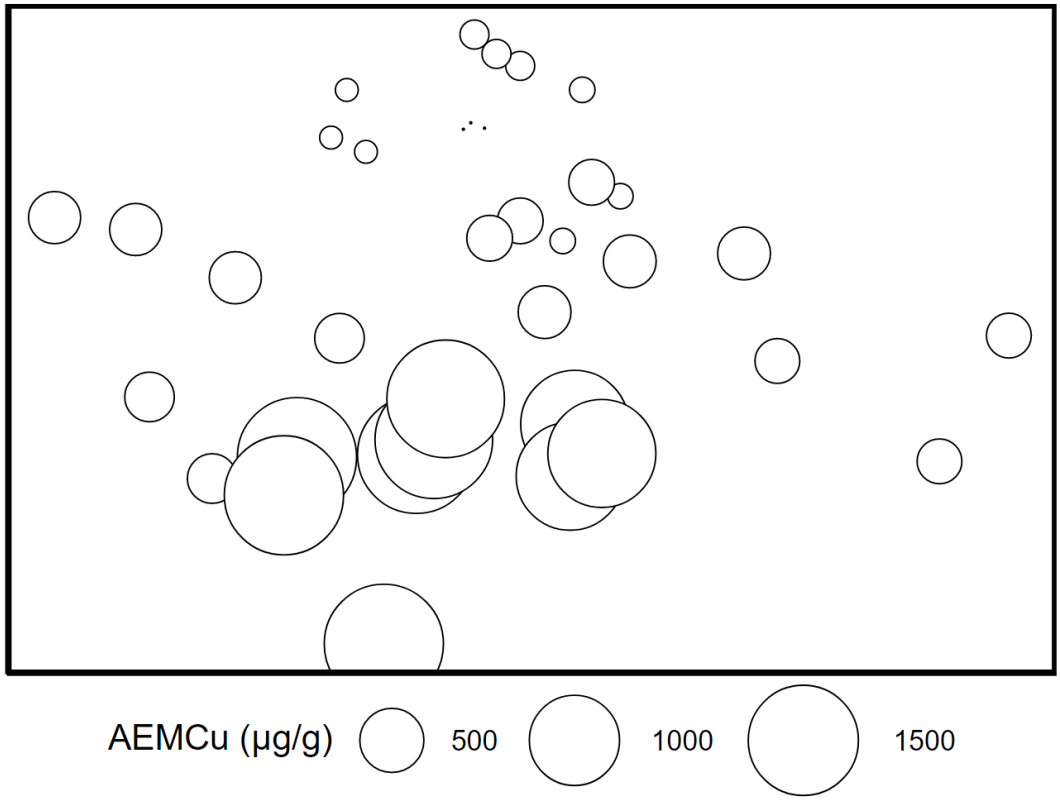

Fig. 4.13a: MDS ordination of fourth-root transformed nematode percentage abundances, with circles proportional in size to acid-extractable sediment Cu concentration

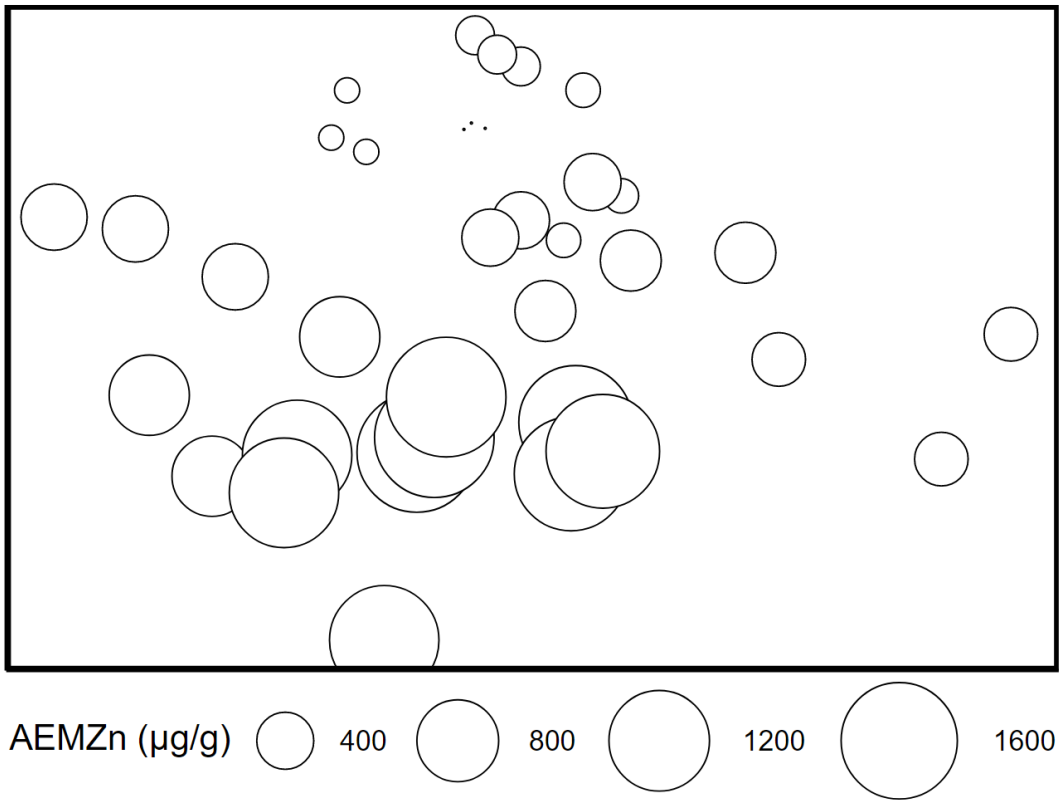

Fig. 4.13b: MDS ordination of fourth-root transformed nematode percentage abundances, with circles proportional in size to acid-extractable sediment Zn concentration

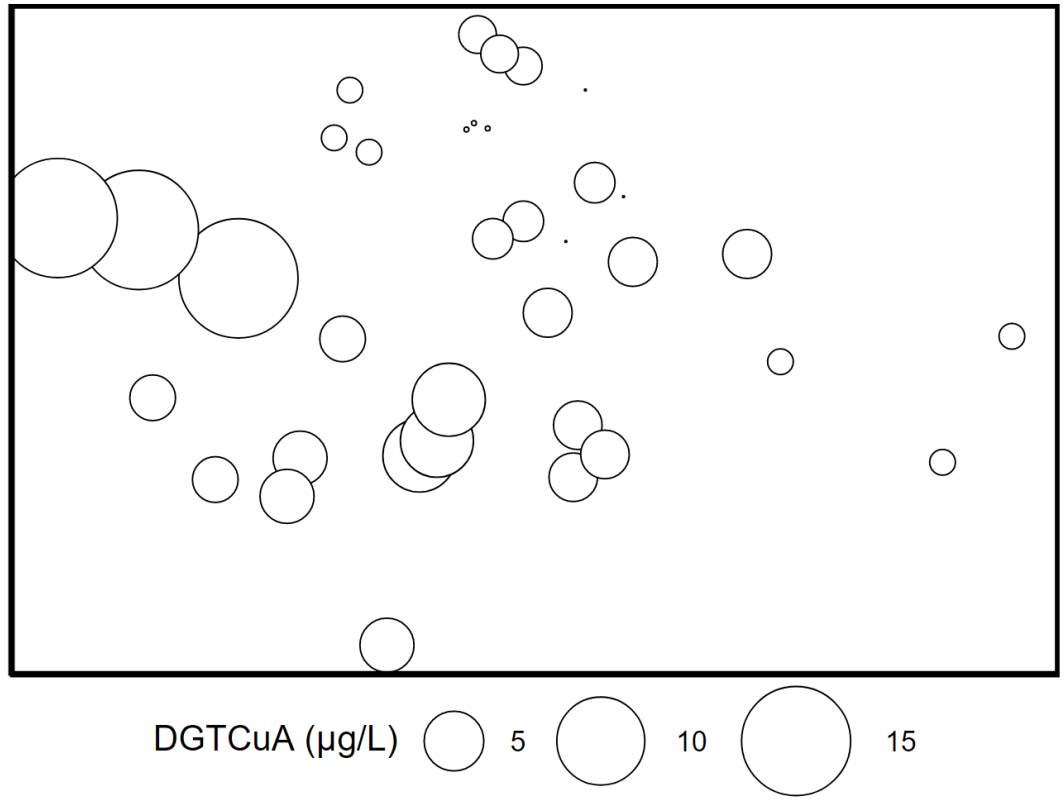

Fig. 4.14a: MDS ordination of fourth-root transformed nematode percentage abundances, with circles proportional in size to DGT Cu concentration above sediment-water interface

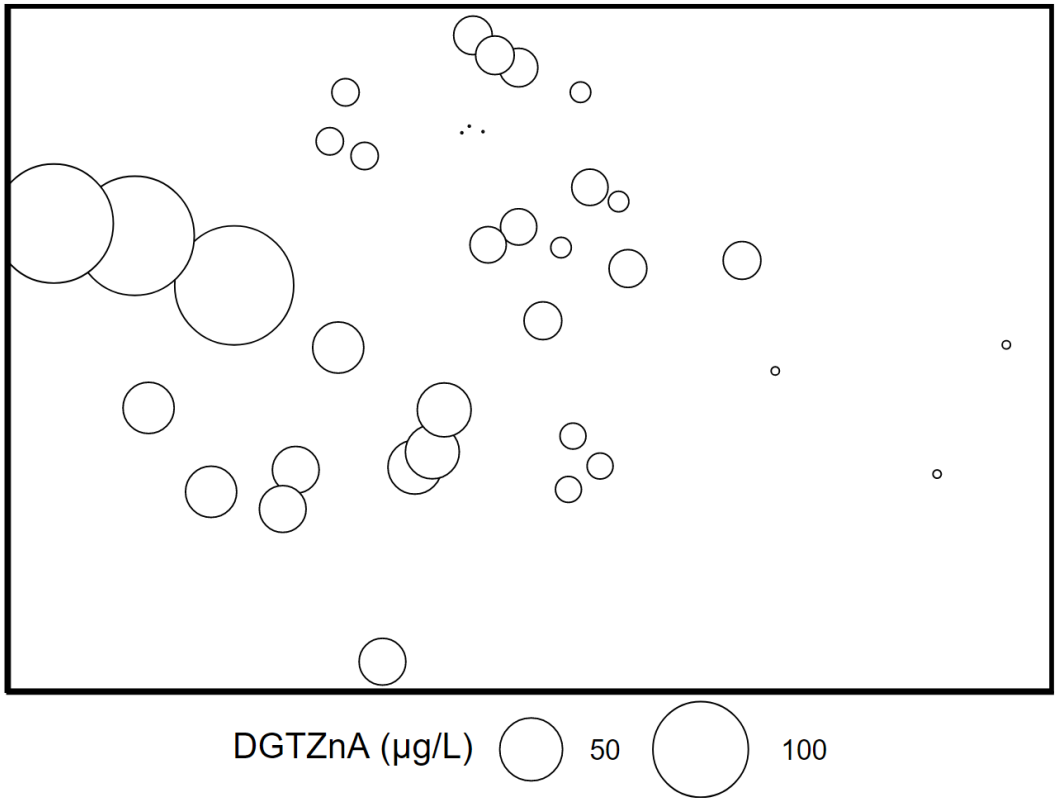

Fig. 4.14b: MDS ordination of fourth-root transformed nematode percentage abundances, with circles proportional in size to DGT Zn concentration above the sediment-water interface

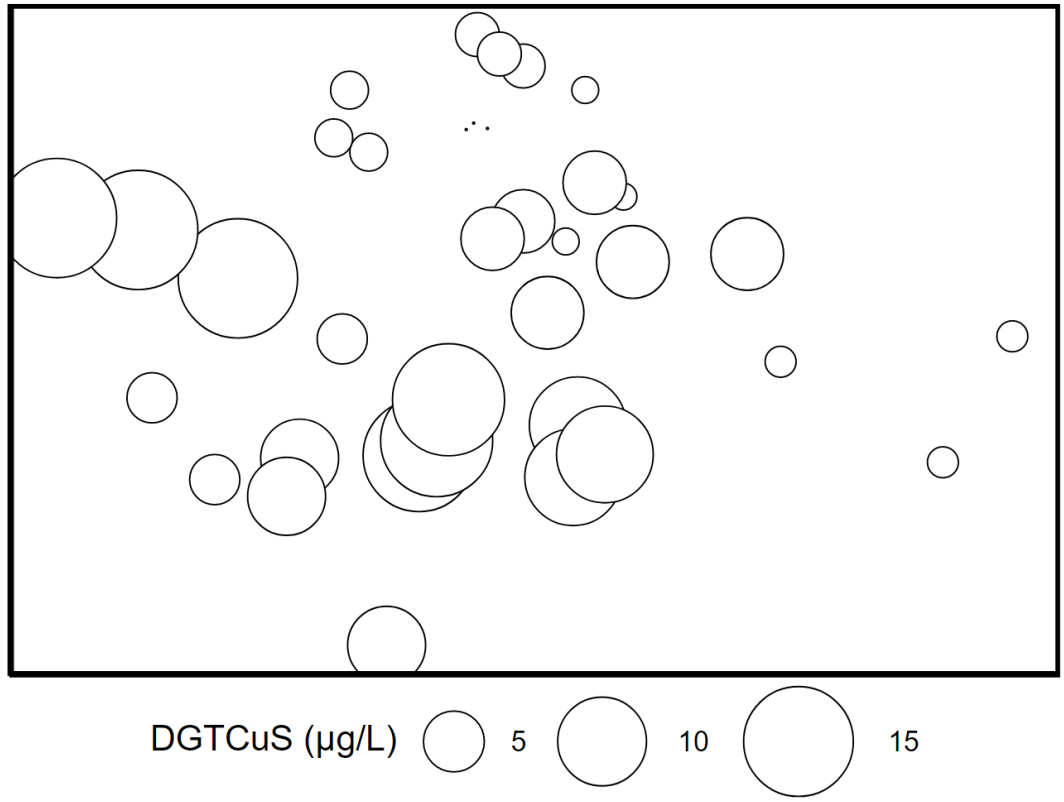

Fig. 4.15a: MDS ordination of fourth-root transformed nematode percentage abundances, with circles proportional in size to DGT Cu concentration at the sediment-water interface

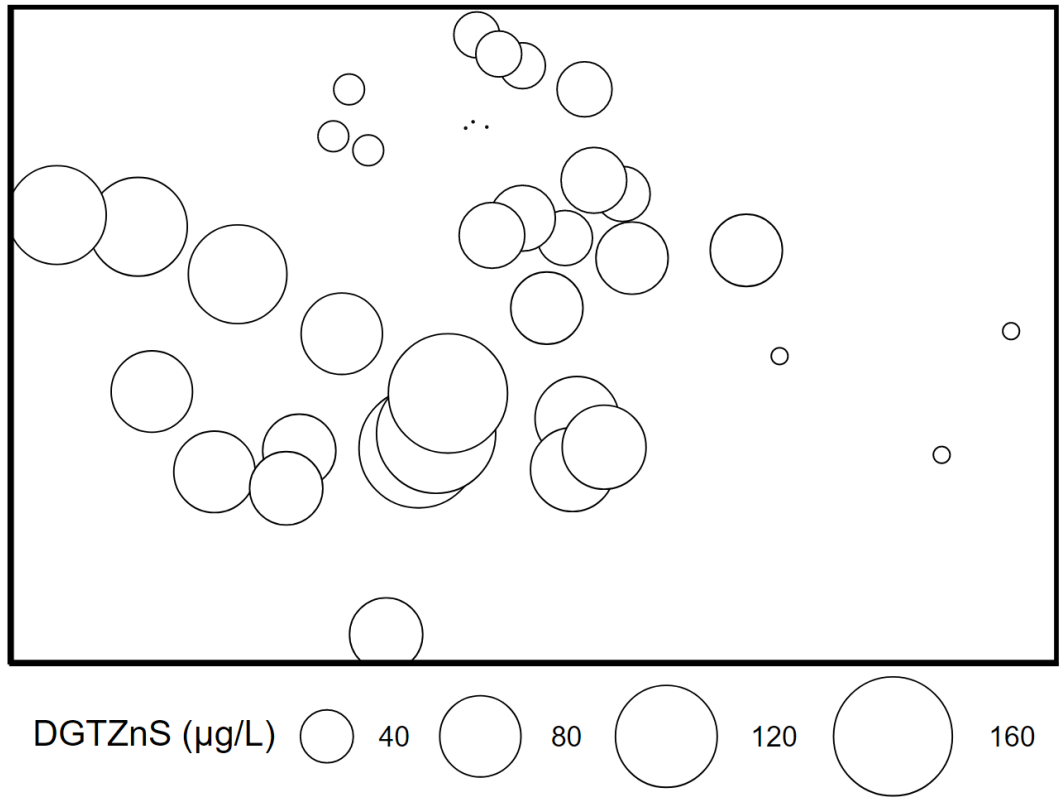

Fig. 4.15b: MDS ordination of fourth-root transformed nematode percentage abundances, with circles proportional in size to DGT Zn concentration at the sediment-water interface

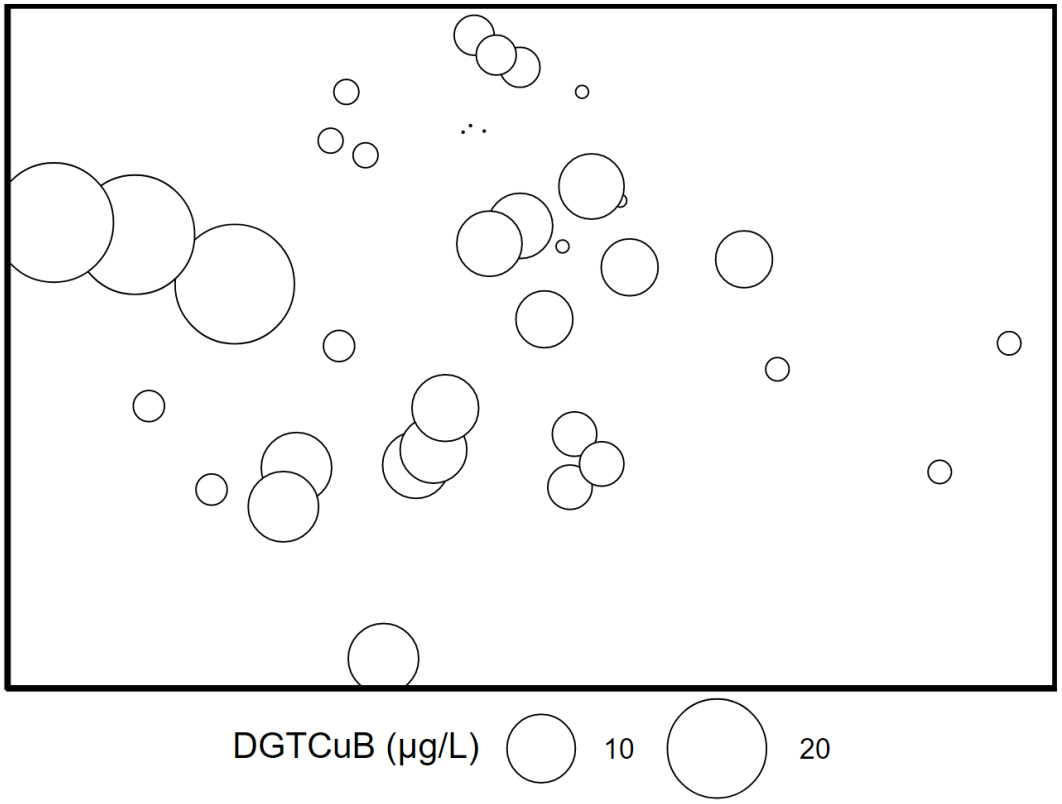

Fig. 4.16a: MDS ordination of fourth-root transformed nematode percentage abundances, with circles proportional in size to DGT Cu concentration below sediment-water interface

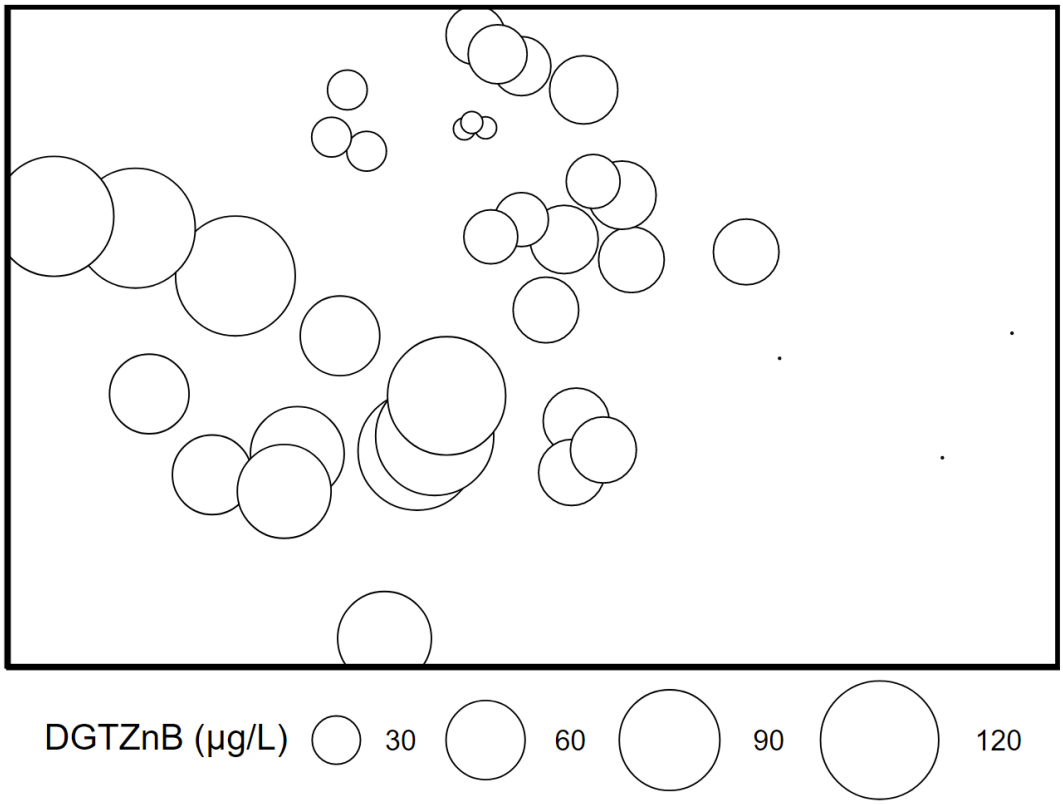

Fig. 4.16b: MDS ordination of fourth-root transformed nematode percentage abundances, with circles proportional in size to DGT Zn concentration below sediment-water interface

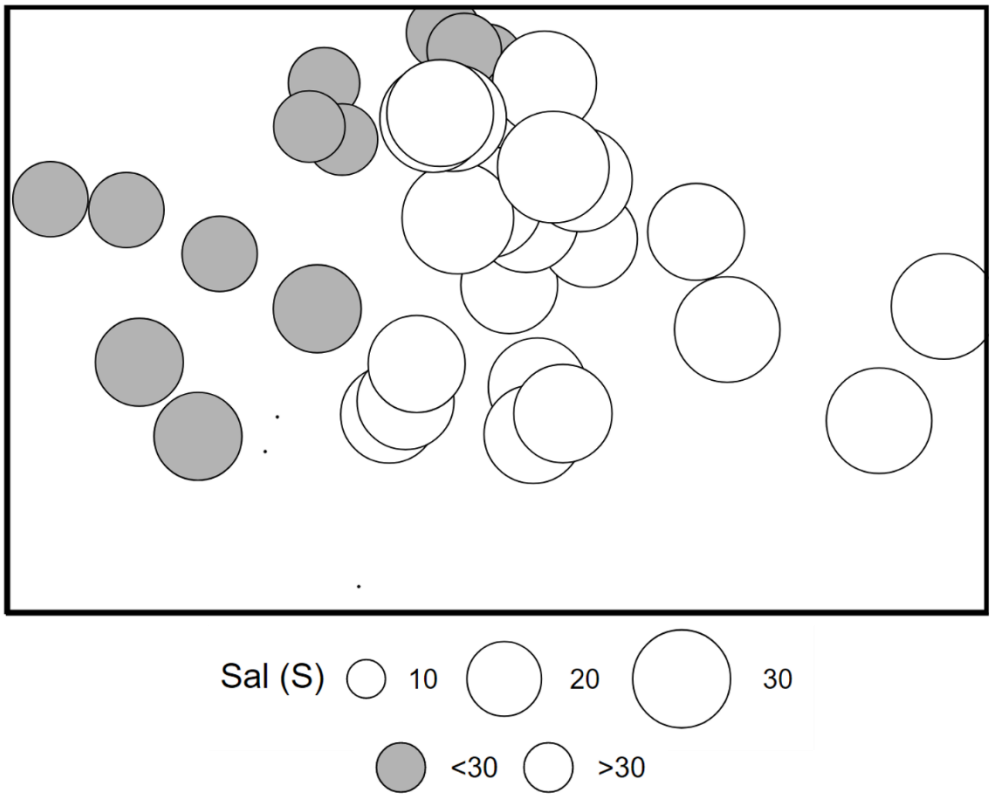

Fig. 4.17: MDS ordination of fourth-root transformed nematode percentage abundances, with circles proportional in size to salinity. Filled circles: salinity < 30 S

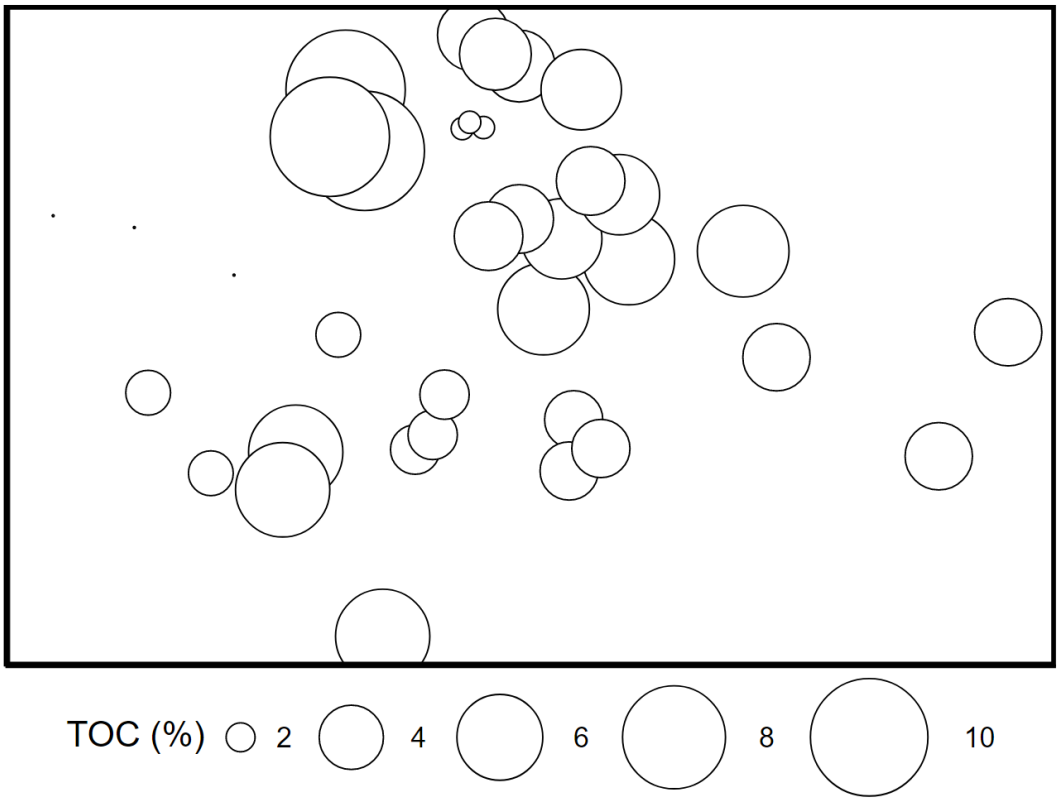

Fig. 4.18: MDS ordination of fourth-root transformed nematode percentage abundances, with circles proportional in size to sediment total organic carbon

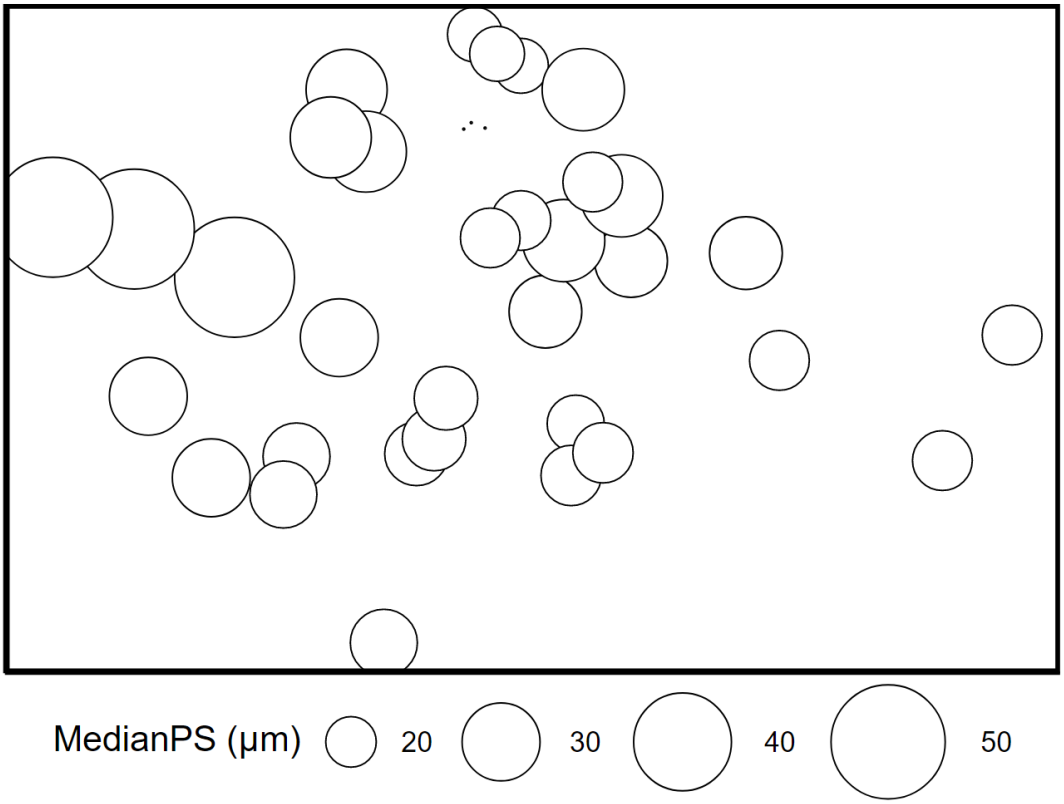

Fig. 4.19a: MDS ordination of fourth-root transformed nematode percentage abundances, with circles proportional in size to sediment median particle size

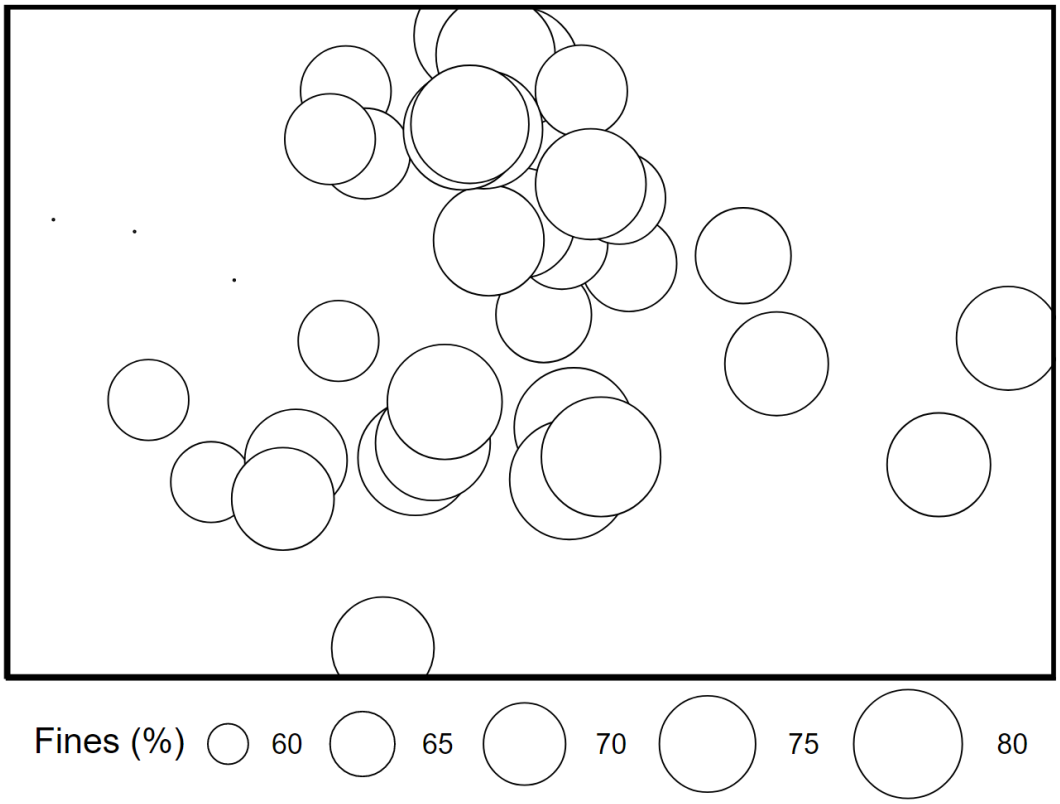

Fig. 4.19b: MDS ordination of fourth-root transformed nematode percentage abundances, with circles proportional in size to sediment percentage fines

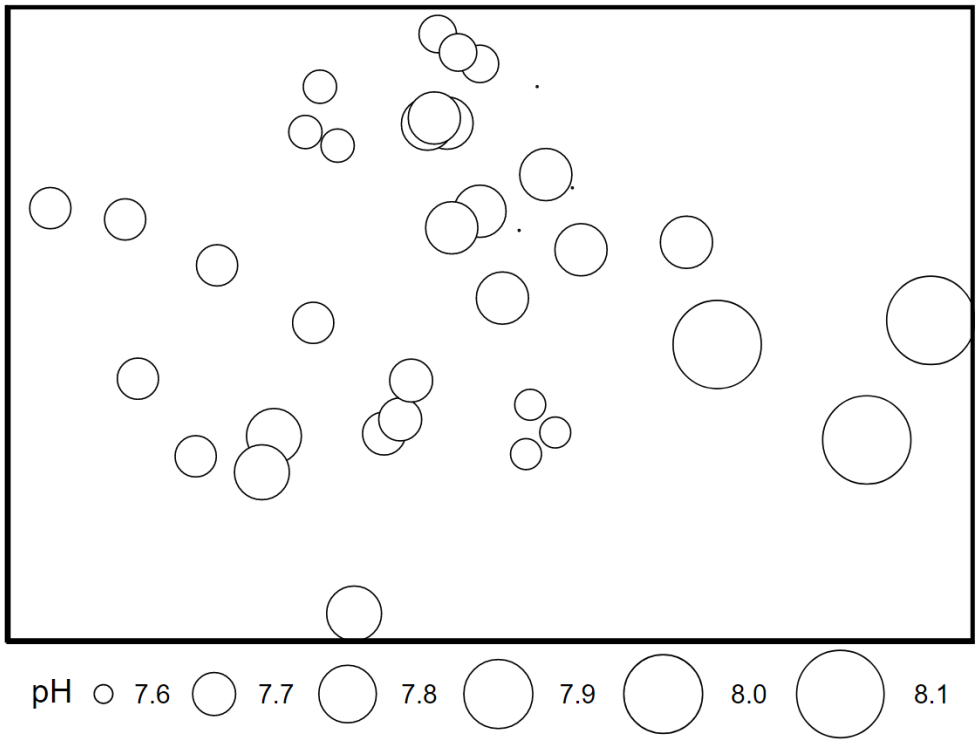

Fig. 4.20: MDS ordination of fourth-root transformed nematode percentage abundances, with circles proportional in size to sediment pH

MDS plots based on salinity, organic carbon, sediment granulometry, and pH (Figures 4.17 – 4.19) were poorly indicative of nematode community dissimilarities across the sites. Figure 4.17 overlaid with salinity values appears to broadly separate communities into those of low (< 30 S, left region) and high (> 30 S, right region) salinity. No clear pattern was, however, detectable from top to bottom. Also, with the exclusion of the reference Breydon Water site as well as RA, less contaminated areas of the Fal appear to be slightly more enriched with organic carbon than the grossly-contaminated group (Figure 4.18). No apparent distinctions were observed for median grain size and percentage fines. And within the less-contaminated site group, pH appeared to increase diagonally, but provided no clear distinction in comparison with the grossly-contaminated sites.

Overall, whilst most univariate diversity indices were confounded with "nuisance" physicochemical characteristics, with only VarTD and SPN showing significant correlations with metals, multivariate analysis was able to clearly distinguish the study sites based on their levels of metal contamination. Cu, rather than Zn, appears to be more strongly influencing nematode community structure across the sites. And amongst all the chemical measures of metal concentrations assessed, PW Cu appeared to be best indicative of nematode community dissimilarity across the study sites.

4.3.5 Relationship between nematode community dissimilarity and trophic composition

MDS ordination of community dissimilarities overlaid with respect to the proportion of Wieser's (1953) trophic groups 1A, 1B, and 2A nematodes reveal no clear pattern across the study sites (Figures 4.21 – 4.23). However, an interesting trend based on sediment metal contamination is revealed when predatory (Group 2B) worms are considered (Figure 4.24). This group is nearly absent in grossly contaminated sediments of the Restronguet Creek (RA – RC) and Hayle (HB). However, below a certain threshold concentration, their relative abundance appears to increase with increasing contamination from Breydon Water to Pill Creek, inclusive of the River Hayle (HA). Considering that those are some of the most contaminated sediments in the world, it could be inferred that Group 2B worms are stressed by extreme sediment metal pollution.

4.3.6 Species responsible for nematode community dissimilarities across the sites

SIMPER analysis was used to identify species contributing up to 70% dissimilarities between the grossly-contaminated (Restronguet Creek and Hayle) and less-contaminated sites, given significant difference identified by the ANOSIM procedure (Table 4.5).

Restronguet Creek and Hayle nematode communities were distinguished by higher abundances of deposit and epistrate feeders such as *Daptonema setosum*, *Ptycholaimellus ponticus*, *Tripyloides marinus*, and *Daptonema hirsutum* (in decreasing order of contribution). The species list (Table A4.2) confirms that these species were either entirely absent or depleted in areas of low contamination. Both *Tripyloides* species were significantly discriminating in the SIMPER analysis, with *T. marinus* favouring more contaminated sites as opposed to *T. gracilis*. Similarly, within the genus *Daptonema*, *D. normandicum* tended to favour the grossly contaminated sites compared to *D. oxycerca*. Indeed, monhysterids of genera *Theristus* and *Daptonema* were generally more abundant in contaminated areas.

Another set of species discriminating between the grossly-contaminated and less contaminated sites are the chromadorids and larger bodied predators from the genus *Sphaerolaimus*. *Praeacanthonchus punctatus* and other chromadorids, *Chromadoropsis vivipara* and *Metachromadoroides remanei*, formerly in the genus *Metachromadora*, were highlighted in the SIMPER analysis. These species were generally absent or in relatively low abundance in the Hayle and Restronguet (Table A4.2).

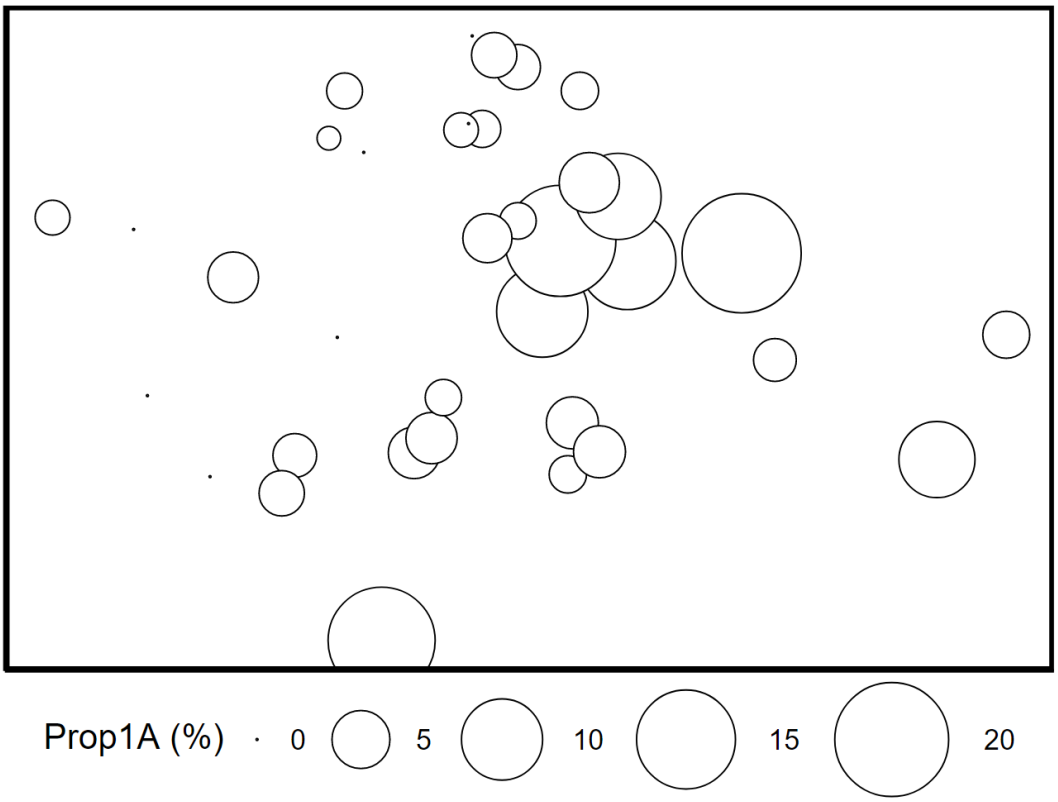

Fig. 4.21: MDS ordination of fourth-root transformed nematode percentage abundances, with circles proportional in size to the % abundance of individuals in Trophic Group 1A

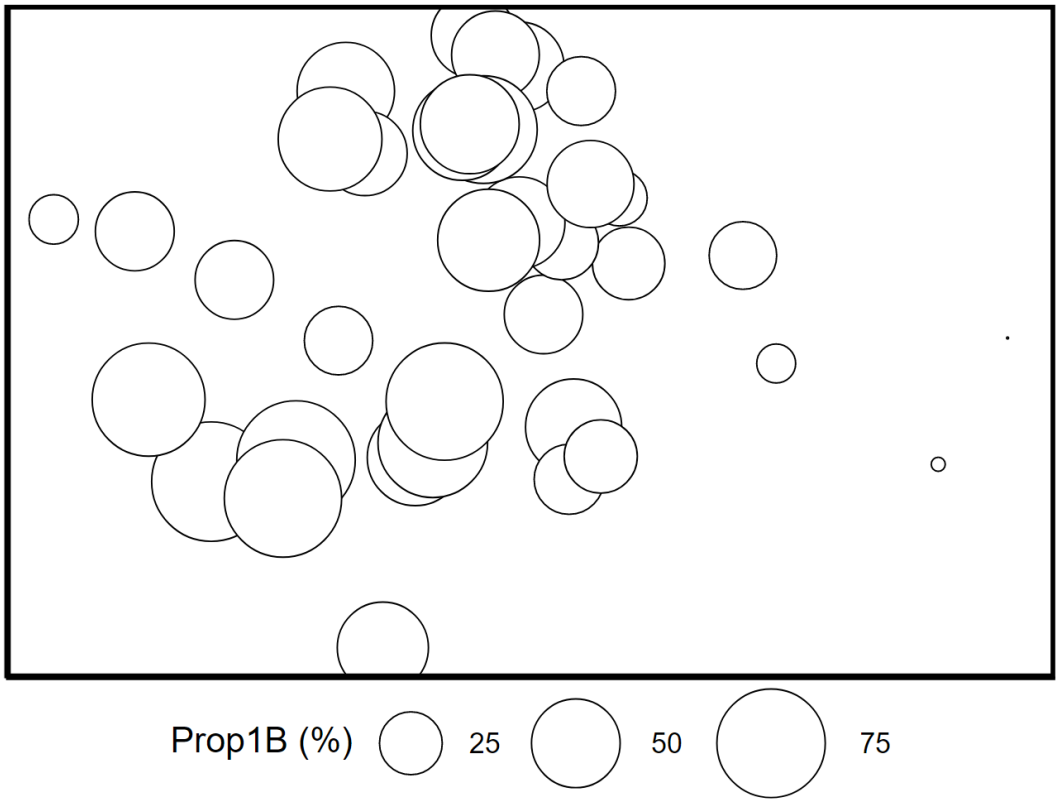

Fig. 4.22: MDS ordination of fourth-root transformed nematode percentage abundances, with circles proportional in size to the % abundance of individuals in Trophic Group 1B

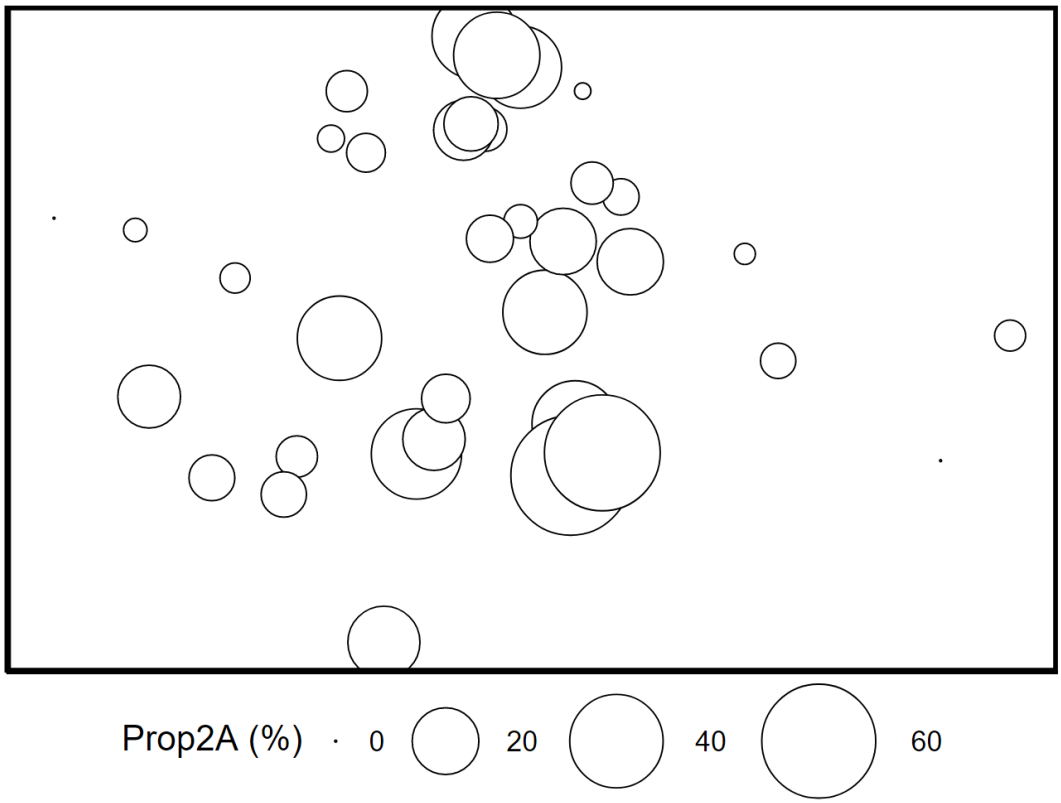

Fig. 4.23: MDS ordination of fourth-root transformed nematode percentage abundances, with circles proportional in size to the % abundance of individuals in Trophic Group 2A

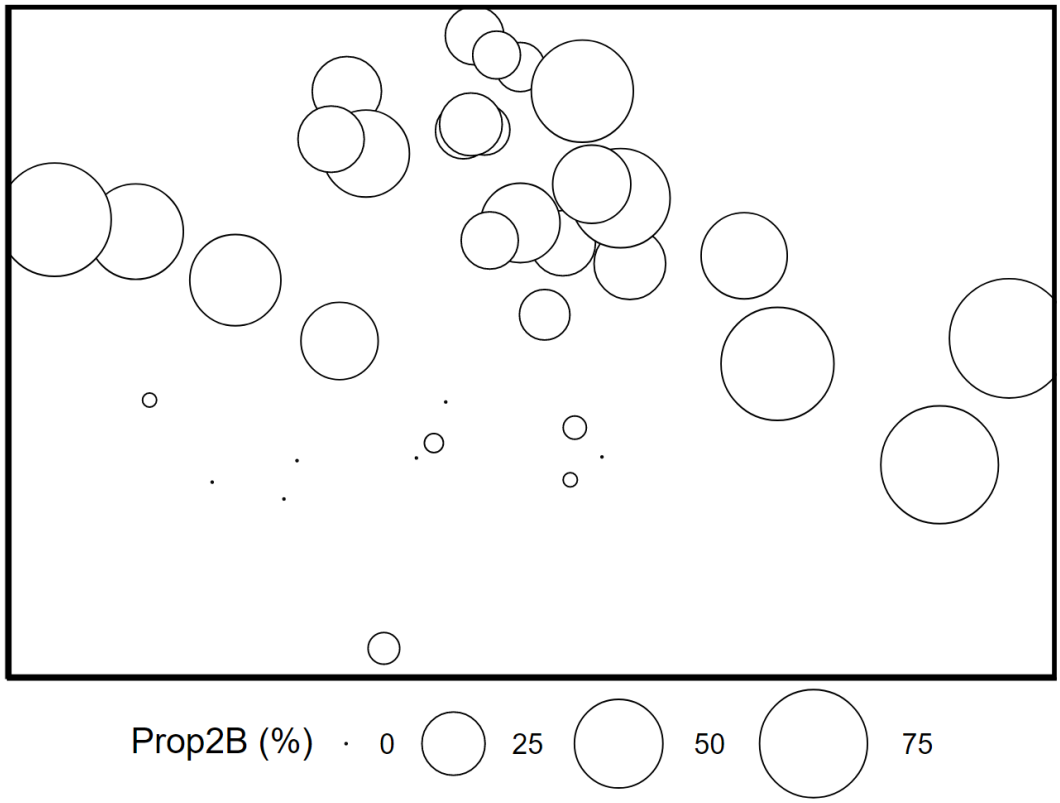

Fig. 4.24: MDS ordination of fourth-root transformed nematode percentage abundances, with circles proportional in size to the % abundance of individuals in Trophic Group 2B

Table 4.4: Summary of SIMPER analysis for discriminating species. Species contributing up to 70% of dissimilarities between grossly-contaminated (RA, RB, RC, HA, and HB) and less-contaminated (all others) sites are ranked in order of their percentage contribution. Relational operators represent species abundance with respect to the grossly-contaminated sites, i.e. greater or less abundances in contaminated sites than cleaner sites. Actual species abundances are provided in A4.2

Rank	Grossly-contaminated vs less-contaminated sites		
	Species		Cumulative contribution (%)
1	*Daptonema setosum*	>	4.2
2	*Chromadoropsis vivipara*	<	8.2
3	*Axonolaimus paraspinosus*	<	11.8
4	*Ptycholaimellus ponticus*	>	15.2
5	*Metachromadoroides remanei*	<	18.5
6	*Praeacanthonchus punctatus*	<	21.6
7	*Tripyloides marinus*	>	24.5
8	*Daptonema oxycerca*	<	27.1
9	*Viscosia viscosa*	<	29.7
10	*Tripyloides gracilis*	<	32.3
11	*Sphaerolaimus hirsutus*	<	34.9
12	*Daptonema hirsutum*	>	37.4
13	*Hypodontolaimus balticus*	>	39.9
14	*Nudora bipapillata*	<	42.3
15	*Sphaerolaimus gracilis*	<	44.6
16	*Sabatieria pulchra*	<	46.9
17	*Oncholaimus oxyuris*	>	49.1
18	*Anoplostoma viviparum*	<	51.2
19	*Chromadora macrolaima*	<	53.3
20	*Daptonema normandicum*	>	55.3
21	*Microlaimus marinus*	>	57.3
22	*Calyptronema maxweberi*	>	59.3
23	*Theristus acer*	>	61.3
24	*Terschellingia longicaudata*	<	63.2
25	*Sphaerolaimus balticus*	<	65.1
26	*Atrochromadora microlaima*	<	67
27	*Desmolaimus zeelandicus*	<	68.9
28	*Terschellingia communis*	<	70.7

The nematode *Oncholaimus oxyuris* was included as a discriminatory species between the grossly contaminated and less contaminated sites. This species was highly abundant in sandy sediments of River Hayle (HA), rare in the Hayle Copperhousepool (HB, only two individuals), but absent in every other site, including the Restronguet creek. Indeed, River Hayle was dominated by few species, with similarly high abundance of *Halichoanolaimus*

robustus, which was also absent from all other sites (Table A4.2). However, the presence of *T. marinus* and an unidentified species, possibly of the genus *Calyptronema*, in HA helped to link these sandy sediments with HB and Restronguet Creek communities (Table A4.2), and to discriminate it from the less-contaminated sites.

Overall, the pattern across the sites appears to be (i) a high abundance of several predatory nematodes in fine sediments of lower contamination versus fine, grossly-contaminated sediments (Copperhouse Pool and Restronguet Creek), (ii) the dominance of few species in the sandy, but grossly-contaminated, sediment of River Hayle, and (iii) the shared presence of even fewer species, especially *T. marinus*, to distinguish the grossly-contaminated (River Hayle, Copperhouse Pool, and the Restronguet Creek) from cleaner sites.

4.4 Discussion

Benthic community composition has for long been used to distinguish clean from grossly polluted marine sites (Tietjen, 1980; Bryan & Gibbs, 1983; Langston *et al.*, 2006). As pollution tends to affect the growth, reproduction, and/or survival of sensitive species, these areas are often characterised by dominant, species-poor communities in comparison with well-colonised sites of low contamination (Grant, 2010; Rainbow, 2020).

A well-acknowledged limitation, however, of benthic community studies in ecology is their tendency to reflect environmental characteristics other than pollution (Grant, 2010; Semprucci *et al.*, 2019). Although the development of multivariate methods have resulted in the improved detection of ecological effects (Gray *et al.*, 1990; Clarke 1993), the influence of these "nuisance variables" means that most successful studies have been carefully designed with controls to account for varying site characteristics (Somerfield *et al.*, 1994b; Olsgard & Gray, 1995; Warwick & Clarke, 1998; Ogilvie & Grant, 2008). For example, in assessing the impact of metal contamination on meiofaunal community composition in the Fal estuarine system, Somerfield *et al.* (1994b) sampled locations with fine mud and at similar tidal height. Their analyses using MDS clearly distinguished nematode communities in the most contaminated reaches of the Restronguet Creek from several less-contaminated creeks in the estuary. Similarly, Millward's (1995) study of nematode community composition in the same system sampled sites of comparable sediment grain size in addition to matching salinity controls. Using both PCA and MDS, he was able to distinguish nematode communities in the Restronguet Creek from those of the less-contaminated Helford and Percuil Rivers. He however noted the strong influence of salinity on within-

group variation, with sites ordinated along a salinity gradient in the Restronguet and control groups. In contrast, clustering of microbial communities from the Fal and Hayle estuaries appeared to vary randomly, despite a three orders of magnitude difference in thymidine and leucine tolerance across the contamination gradient (Ogilvie & Grant, 2008). This was attributed to differences in environmental conditions at the sites.

Whilst desirable, the availability and designation of true control sites in ecological monitoring can be challenging (Grant, 2010). Moreover, as metal bioavailability in estuaries can differ temporally and spatially either due to natural fluctuations in physicochemical conditions (Rainbow, 2020; Chapter 2) or anthropogenic discharges (Somerfield *et al.*, 1994a), conditions favouring the use of whole creeks as sampling units may not always be achievable. It is for this reason that techniques such as pollution-induced community tolerance have been used to quantify ecological impacts (Millward & Grant, 2000; Ogilvie & Grant, 2008; Chapter 3). The heritable development of tolerance to a contaminant surely indicates a selection pressure due to that specific contaminant or, as in co-tolerance, another contaminant with a similar mode of action (Blanck, 2002; Grant, 2002; Pook *et al.*, 2009).

The current study extended the use of meiobenthic community composition as an indicator of pollution to highly heterogeneous sediments, assessing whether nematode communities were sensitive to a strong contamination gradient or responding to "nuisance" environmental variables. The study sites in Breydon Water, Norfolk, East England, and the Fal and Hayle estuaries, Cornwall, Southwest England, vary widely in sediment granulometry, salinity, organic carbon, and geological catchment, amongst others, but show a strong gradient in Cu and Zn sediment concentrations spanning nearly three orders of magnitude (Chapter 2).

Overall, findings reveal that whilst univariate indices more strongly reflect differences in salinity, redox, pH, and grain size, multivariate analysis of nematode abundance clearly distinguished sites based on their level metal contamination, despite the wide-ranging environmental conditions. Only two of eleven univariate indices, number of species (SPN) and variation in taxonomic distinctness (VarTD), were significantly correlated with metal concentrations. In contrast, the MDS ordination of relative species abundances separated sites into two groups consisting of (i) grossly-contaminated areas of the Restronguet Creek and Hayle as well as (ii) reference and less-contaminated locations in the rest of the Fal (Figure 4.05a), with ordination within groups also reflecting the gradient of metal contamination. BIOENV analysis confirmed that Bray-Curtis community dissimilarities

across the sites were significantly correlated with variations in PW Cu concentrations, and other environmental variables only marginally improved or even diminished the correlation upon inclusion in the model (Table 4.4). Furthermore, constrained clustering using MRT showed that differences in metal concentrations, mainly PW Cu and Sed Cu/Zn, was responsible for nearly all of the variation in nematode community composition, predicting site groupings and nematode abundances across the study sites (Figure 4.07). Superimposing MDS plots with bubbles proportional to environmental variables showed that community structures between and within the groups were strongly associated with Cu contamination (Figures 4.09a and 4.010a), further reflecting increasing distance from the Carnon River within the Fal estuary catchment (Figure 4.05a). The influence of salinity, organic carbon enrichment, and pH on multivariate ordination was less apparent (Figures 4.17, 4.18 & 4.20). And sediment granulometry did not appear to affect nematode community dissimilarities (Figures 4.16a and b). Indeed, nematode community structure across the sites was sensitive to metal contamination despite other widely varying physicochemical characteristics.

Results from this study are consistent with established findings in the Fal and Hayle (see reviews by Grant, 2010; Rainbow, 2020). The Restronguet Creek, in particular, has been the subject of numerous studies on pollution assessment, both in terms of chemical contamination and in the characterisation of benthic communities (e.g. Bryan & Gibbs, 1983; Bryan & Langston, 1992; Grant 1989, Somerfield *et al.* 1994b; Millward, 1995; Milward & Grant, 2000; Warwick, 2001; Shipp, 2006; Leornard *et al.*, 2006; Ogilvie & Grant, 2008; Chapter 3). These studies report a reduction in benthos abundance, species richness, and diversity; a shift in benthic community composition; and an increase in tolerance of both individual populations and communities of species within the Restronguet Creek versus less-contaminated tributaries of the Fal. The impact of pollution on the Fal community has been summarised as the development of tolerance among inhabiting populations and a replacement of sensitive species by more tolerant ones (Millward & Grant, 2000), which is common in chronically-contaminated marine sites (Grant, 2010). In the current study, the number of species (positively) and variation in taxonomic distinctness (negatively) were significantly correlated with metal concentrations, suggesting that the loss of species in increasing contamination across the sites coincided with the addition of new species-poor taxa. Nematode abundance[34] was not determined. However, the current study documents a

[34] Abundance here refers to the number of individuals per core (Somerfield *et al.*, 1994b)

shift in community composition that extends through the contamination gradient until Percuil River, where nematode communities do not appear to differ from those at the Helford River and another less-contaminated site, Breydon Water, in the East of England (Figure 4.05a). The separation of nematode communities into those from grossly-contaminated versus cleaner sites as well as their within-group ordination with respect to metal contamination contributes to the body of proof on the impacts of metal pollution due to mining activities in the Fal and Hayle estuaries.

What species are responsible for the observed nematode community (dis)similarities in the Fal and Hayle estuaries? Previous studies on nematode communities within the Fal indicated the presence of certain species common to both cleaner and grossly-contaminated sites as well as species unique to the different groups, given the variation in other site characteristics. Using SIMPER analysis, Somerfield *et al.* (1994b) noted the particular presence of *Desmodora communis* and *Tripyloides gracilis* in relatively high numbers within the Restronguet Creek. The (near) absence of several species such as *Metachromadora* (now *Chromadoropsis*) *vivipara*, *Calomicrolaimus* (now *Microlaimus*) *honestus*, *Daptonema normandicum*, *Tershellingia longicaudata*, and *Tershellingia communis* from the Restronguet were also key distinctions from less contaminated creeks assessed. Millward and Grant (1995) reported the presence of *Axonolaimus spinosus*, *Daptonema setosa* [*sic*], *Eleutherolaimus sp*., *Theristus acer*, and *Tripyloides marinus* with increased tolerance in the Restronguet Creek, suggesting a genetic adaptation to pollution therein. In the full study, Millward (1995) reported *Ptycholaimellus ponticus*, *Dichromadora geophila*, *Axonolaimus paraspinosus*, *Chromadora macrolaima*, and *Sabatiera punctata* as species common across the study sites. He corroborated the dominance of *Tripyloides*, *T. acer*, and *Sabatiera pulchra* in the Restronguet. He further noted the absence several species including *Daptonema oxycerca*, *Calyptronema maxweberi*, *Viscosia viscosa*, *T. longicaudata*, *M.* (now *C.*) *vivipara* as well as *Metachromadora* (now *Metachromadoroides*) *remanei*. And upon exposing nematodes from the Lynher estuary to Fal sediments, Austen and Somerfield (1997) found that *C. macrolaima*, *P. ponticus*, *D. normandicum*, *T. gracilis*, and *D. procerum* were significantly more abundant in control and less contaminated creeks.

Species listings in the current study is consistent with the above description (Table A4.2), only differing slightly from Austen and Somerfield's bioassay. Predatory/omnivorous (2B) species, *C. vivipara*, *M. remanei*, *Praeacanthonchus punctatus*, and others from the genus *Sphaerolaimus*, were notably absent from Restronguet Creek. This diminished abundance of

Group 2B nematodes in metal-enriched sediments has been previously documented (Millward, 1995; Warwick & Clarke, 1998). *Daptonema hirsutum*, *Atrochromadora microlaima*[35], *P. ponticus*, *S. pulchra*, and *A. paraspinosus* were identified at most or all of the sites. *A. spinosus* was limited to the less saline site at the Upper Restronguet Creek (RA). Nematodes of the genus *Terschellingia* were generally limited to the cleaner sites. However, other than *D. oxycerca*, species of the genera *Theristus* and *Daptonema* were more abundant in grossly-contaminated sites, with *D. setosum* discriminating the most versus less contaminated sites (SIMPER analysis, Table 4.5).

The current study recorded the two common species of the genus *Tripyloides* – *T. gracilis* and *T. marinus* – separately observed in previous studies (Somerfield *et al.*, 1994b; Millward, 1995). Both species were identified across the study sites. Although, whilst *T.gracilis* was more abundant in less contaminated sites, *T. marinus* dominated in the Hayle and Restronguet Creek as observed by Millward (1995). River Hayle (HA) was mainly dominated by *Oncholaimus oxyuris* and *Halichoanolaimus robustus*. However, this site was linked with other grossly-contaminated areas especially by a shared abundance of *T. marinus*, which has been identified as a key contributor to overall community tolerance in these sites (Millward, 1995, 1996).

What chemical measures are best predictive of the shift in community composition? A central focus of this thesis, as explained in Chapter 1, is the relationship between ecological effects in marine sites and chemical measurements of metal concentration and availability, in order to determine what measures of contamination are the best predictors of effects and to identify threshold concentrations at which these effects begin to occur. Given this objective, the evaluation of ecological effects here are only useful to such extent that they can be correlated with metal concentrations, ultimately supporting the development of appropriate sediment regulatory criteria and the management of marine pollution. In Chapter 3, ecological effects were quantified using pollution-induced community tolerance – a subject already addressed in detail therein and further highlighted in the earlier part of this discussion. And the current study has reconfirmed the shift in nematode community composition as a response to the metal contamination gradient in the Fal and Hayle estuaries, despite varying environmental characteristics. Whether this change in community structure

[35] *Atrochromadora microlaima* is nearly identical to *Chromadora macrolaima*, making it difficult to distinguish specimens of both species. In the current study, the former is identified as common across sites (c.f. Millward, 1995).

constitutes a deleterious effect remains a subject of debate (see Grant, 2010); however, it is generally considered to be of ecotoxicological significance (Chapman, 2007; Grant, 2010; Birk *et al.*, 2012; Schratzberger, 2012; Rainbow, 2020). The following paragraphs therefore proceed bearing in mind this nuance.

First, which metals are leading to effects in the Fal and Hayle? Mining of ores in Cornwall, England has led to contamination with several metals including As, Cu, Fe, Pb, Sn, and Zn, but Cu and Zn are present at elevated concentrations in bioavailable forms (Bryan & Gibbs, 1983; Rainbow, 2020; Chapter 2). Although there is often a correlation between Cu and Zn levels in the Fal and Hayle (Chapter 2; Greenwood, 2001), the combination of BIOENV analysis, MRT, and bubble plots of MDS ordinations in the current study showed that nematode community structure is more strongly associated with Cu, especially PW Cu, contamination (Table 4.3; Figures 4.07; 4.09 – 4.20). This observation is consistent with established evidence within the Fal. Grant *et al.* (1989) observed that whilst populations of the polychaete, *Hediste* (formerly *Nereis*) *diversicolor*, in Restronguet Creek are tolerant to both Cu and Zn, tolerance to Zn is limited to the most contaminated reaches of the creek. This higher tolerance to Cu, versus Zn, has been noted in the seaweed, *Fucus vesiculosus* (Bryan & Gibbs, 1983), microbes (Ogilvie & Grant, 2008), as well as in individual species (Millward, 1995) and communities (Ogilvie, 2004) of nematodes. Although the contributions of synergistic toxicity (i.e., both Cu and Zn) and co-tolerance cannot be completely overruled, the preponderance of evidence suggests that Cu may be responsible for toxicity across these sites. The reduced effect attributable to Zn may be due to the homeostatic regulation of the metal or, simply, the higher threshold concentrations required for toxicity (Bryan & Hummerstone, 1971, 1973; Bryan & Gibbs, 1983).

The best measure of Cu concentration predicting community dissimilarity in the current study is unclear. DGT-labile, EqP, and PW/OC Cu concentrations were less successful than the traditional total measures in characterising site dissimilarities. Amongst these, PW Cu had the highest correlation for a single variable in the BIOENV analysis (Table 4.3) and explained the much of the variance across the MRT (Figure 4.07). MDS ordination by PW Cu also provided the clearest distinction between grossly-contaminated and the less contaminated sites (Figure 4.06a). However, Sed Cu (and correlated variables) explained the single most variance in nematode dissimilarities in the MRT analysis (Figure 4.07) as well as the structuring of communities within individual groups in the superimposed bubble plots (Figure 4.10a), in line with Somerfield *et al.* (1994b). The correlations of interstitial and

sediment Cu concentrations is complicated by Sites HA and RA, where metal partitioning to the dissolved phase appears to be facilitated, respectively, by the coarser grain size and lower salinity (Bryan & Gibbs, 1983; Grant, 2010). Given that non-selective deposit feeders (1B) – which primarily ingest sediment particles – form the most abundant trophic groups at most of the sites, and that this is followed closely by epistrate-feeding (2A) or predatory (2B) species (Table 4.2), metal uptake by the nematode community is likely from a combination of both dissolved (e.g. Howell, 1983) and also sediment-bound forms.

In view of the foregoing, threshold concentrations in the current study reflect the higher metal concentrations between Percuil and Helford Rivers, given their multivariate ordination with nematode communities from Breydon Water. Considering total sediment concentration, the threshold would be 215 µg Cu/g, consistent with previous findings in the Fal estuary (Somerfield *et al.*, 1994b; Millward & Grant, 2000; Shipp & Grant, 2006). This threshold is, however, significantly greater than most proposed SQG trigger values, e.g. 34 µg Cu/g by Long *et al*. (1995), 18.7 µg Cu/g by MacDonald *et al.* (1996), and 65 µg Cu/g by Simpson *et al.* (2013). For total porewater concentration, threshold for the current study would be 3.5 µg Cu/L, similar to the 3 µg Cu/L final chronic value proposed by Simpson *et al.* (2013) and 3.76 µg Cu/L nominal WFD (2015) standard at low DOC (≤ 1 mg/L). The predictive capability of EqP Cu is limited – negative at Sites CO, SJ, and HR, which are all lower than the value at BW. Relationship between EqP Cu and community dissimilarity was also negligible, with this measure actually reducing overall correlation upon inclusion in the BIOENV model. Based on Site PR, threshold concentration for EqP Cu is 9.82 µmol Cu/g OC (623 µg/g OC), significantly less than the 130 µmol Cu/g OC (8255 µg Cu/g OC) threshold by USEPA (2005). Simpson *et al.* (2013), instead, propose OC-normalised thresholds based on the <63 µm fraction of total metal concentrations: 11000 µg Cu/g OC (for acute) and 3500 µg Cu/g OC (for chronic toxicity). This measure of contamination is of similar predictive capacity to the EqP variant at negligible AVS concentrations in oxic surface sediments (Strom *et al*., 2011). The equivalent for the current study is 4636 µg Cu/g OC. The PW Cu/OC threshold (based on Site HR) is 0.60 µg Cu/ mg OC.

Are univariate indices still useful in ecological monitoring, considering the general lack of correlation with chemical pollution in this study? Univariate indices can provide a useful, albeit low-resolution indicator of chemical pollution in marine sites. Given their careful selection of sampling sites, both previous studies of nematode communities within the Fal recorded a reduction in species richness and diversity between the Restronguet Creek and

Percuil River (Somerfield *et al.*, 1994b; Millward, 1995). Austen and Somerfield (1997) exposing nematodes from the Lynher estuary to sediment samples from the Fal also found significant differences in overall abundance, number of species, Shannon-Wiener diversity, and Pielou's evenness between creeks, with a decreasing trend in increasing metal contamination. Also notable is John Gray's study of oil pollution, which recorded a zone of reduced diversity in the immediate vicinity of the Ekofisk platform (Gray *et al.*, 1990).

In the current study, although univariate indices differed significantly between sites, only species number (SPN) and the variation in taxonomic distinctness (VarTD) correlated significantly with metal contamination. That previous observations with tailored sampling protocols were not fully corroborated by the current study further highlights the challenge of environmental heterogeneity. The results support Leonard *et al.*'s (2006) findings that standard univariate indices are more reflective of habitat characteristics in heterogeneous environments than the actual gradient of pollution, as opposed to more robust measures (such as VarTD, Tax dist, and Tax div used in the current study) which are relatively independent of sampling effort and habitat type. Several confounding biotic and abiotic factors, in this context, have been identified in the literature (Somerfield *et al.*, 1994b; Millward, 1995; Semprucci *et al.*, 2019), including water depth, salinity, grainsize, redox, dissolved oxygen, and nutrient concentration. The current study supports the case for grainsize and sulphide concentrations, as a proxy for redox conditions. Notwithstanding, the occurrence of dominant species and a reduction in diversity at a given site are often useful markers for stress in marine ecosystems (Johnston & Roberts, 2009; Grant, 2010). Temporal changes in univariate diversity scores can, therefore, be instructive in ecological monitoring, as has been recently proposed (Semprucci *et al.*, 2015).

Chapter 5.

Toxicity of sedimentary Cu (sulphides) to the deposit-feeding mudsnail, *Peringia ulvae*: revisiting the EqP model

5.1 Introduction

The Equilibrium Partitioning Model (EqP) is widely accepted as giving a set of criteria which can be used to dismiss the risk of metal toxicity in aquatic sediments (Burton, 2010; Burgess *et al*., 2013; Simpson & Batley, 2016; Chapman, 2018). As a result, the model remains a key feature in the most advanced sediment quality guidelines (SQGs) currently available (e.g. Burgess *et al*., 2013). Core assumptions of the model are summarised as follows (Ankley *et al*., 1996; Di Toro *et al*., 2005; Burgess *et al*., 2013):

I. The partitioning of metals between porewater (the dissolved phase) and the sediment phase(s) is at equilibrium, such that metal activity at any one phase is equal.
II. An organism receives equivalent exposures from each of the metal phases in the equilibrated system. Specifically, the magnitude of metal exposure to an organism is the same whether from water-only phases (e.g. porewater via integument or respiration), from sediment via ingestion, or from a combination of the exposure routes. Metal activity based on a single phase (usually the dissolved phase, given widespread variations in sediment physico-chemical characteristics) can, therefore, be used to predict biological effects.
III. In anoxic sediments, insoluble Acid Volatile Sulphides (AVS) constitute the dominant binding phase and control metal partitioning to porewater. Divalent metals (measured as Simultaneously Extracted Metals [SEM]) bind with AVS in a 1:1 molar ratio, becoming available in the porewater only when in excess. Therefore, in excess AVS (i.e. when [AVS > SEM] or [SEM – AVS] < 0), porewater metal activity would be negligible and the sediment would not be toxic. This allows the expression of potential porewater toxicity in terms of equivalent sediment concentrations.
IV. In the absence or exhaustion of AVS, other sediment binding phases, including organic carbon (OC), Fe, and Mn, can influence metal partitioning to the porewater. The influence of OC can be accounted for by normalising excess SEM using the fraction of OC ($f$oc, i.e. [SEM – AVS]/$f$oc). Where OC is the dominant phase, this latter equation can be used to predict sediment toxicity.

Although the EqP is widely adopted, most studies establishing the model were conducted using spiked sediments with high metal concentrations and relatively short equilibration times (Lee *et al*., 2000a,b; Simpson & Batley, 2007). Conditions in such poorly-equilibrated, spiked sediments bias metal partitioning to the porewater (Lee *et al*., 2000a; Simpson *et al.*, 2004; Simpson & Batley, 2007), resulting in unrealistically high exposure concentrations in comparison with field or well-equilibrated sediments of similar contamination. This potentially overestimates the influence of porewater concentrations on metal toxicity for certain organisms. More recent studies conducted using deposit-feeding macroinvertebrates demonstrate the bioavailability of sedimentary metals as a result of dietary uptake despite negligible porewater concentrations and in excess AVS (Lee *et al*., 2000a; De Jonge *et al*., 2009), raising concerns about the validity of the EqP model. However, only a few studies have linked this dietary uptake to metal toxicity in invertebrates (e.g. Campana *et al*., 2012).

Using feeding depression as an endpoint, this study aims to assess the potential for dietary toxicity, assess the validity of the EqP model in predicting (non-)toxicity, and determine the best predictor(s) of toxicity to the deposit-feeding mudsnail, *Peringia* (formerly *Hydrobia*) *ulvae*. The suitability of *P. ulvae* as a test organism has been established in the literature (Shipp & Grant, 2006; Krell *et al*., 2011; Araujo *et al*.,2012; Campana *et al*., 2013). In this species, feeding rate is correlated with metal contamination, and the short-term feeding rate is predictive of long-term growth in field sediments (Shipp & Grant, 2006). Therefore, feeding rate constitutes an ecologically-relevant endpoint in this species.

5.2 Methodology

5.2.1 Experimental design

This study was designed to (i) test the influence of dietary versus dissolved routes for toxicity, (ii) assess the validity of the EqP (SEM – AVS) model in predicting non-toxicity, and (iii) determine which measure(s) of metal concentration best predict(s) toxicity of Cu to the deposit-feeding mudsnail, *P. ulvae*. To accomplish objectives (i) and (iii), mudsnails were exposed to oxic (AVS < 0.5 µmol/g) sediments spiked at environmentally-relevant concentrations and aged to achieve porewater concentrations comparable to those at field sites. For objectives (ii) and (iii), snails were exposed to anoxic sediments with similar AVS concentrations (starting AVS ~ 25 µmol/g), spiked at such levels that molar AVS more than doubled SEM Cu in the most contaminated treatment (i.e. AVS >> SEM Cu). Both oxic and anoxic sediments were spiked at similar Cu concentrations and equally aged. By comparing

feeding rates of snails exposed to the spiked treatments and to controls (i.e. uncontaminated oxic and anoxic sediments), it was possible to assess sediment toxicity and model dose-response relationships.

5.2.2 Endpoints

P. ulvae feeding rate, measured using egestion rate as a surrogate, was used as an endpoint in this study. Feeding was assessed in two ways. Firstly, by in-exposure feeding rate, which represents feeding of snails during exposure to the test sediments. Shipp and Grant (2006) showed that this endpoint is sensitive and linked to growth rate at the population level, thus ecologically relevant. Feeding was also assessed using post-exposure feeding rate (Krell *et al.*, 2011), representing the ingestion of fresh, uncontaminated, oxic sediments after exposure and gut clearance. This latter endpoint was used to determine whether any feeding depression was due to the toxicity of ingested test sediments or to avoidance of same (e.g. Arujo *et al.*, 2012). It was hypothesised that the persistence of toxic stress after exposure is an indicator of toxicity rather than simply indicating avoidance.

5.2.3 Collection and preparation of test sediments

In January 2019, brown, oxic (top 1 cm, AVS < 0.5 µmol/g) as well as dark, anoxic (5 – 10 cm depth; AVS ~ 49 µmol/g)[36] sediment was collected from Breydon Water, an uncontaminated site (BW_2, Figure 5.01a)[37]. Collection procedures and sediment physicochemical characteristics here are similar to those reported in the Winter 2019 survey (Chapter 2). Sediment samples were stored in plastic bags (~ 20 L). The anoxic samples were double-bagged, with a layer of anoxic sediment in-between both bags. To further limit oxidation of anoxic samples, the bags were stored in plastic containers sealed with anoxic sediment at the top and around the lid. Both oxic and anoxic sediments were transported to the laboratory within 1 hr and refrigerated at 4 ^{o}C until use.

Oxic sediment was sieved to less than 500 µm, on the day of collection, in order to remove coarse particles and resident macrofauna. This sediment had high enough water content to

[36] Quantification limit of the AVS method = 0.5 µmol/g (Chapter 2). 49 µmol/g represents concentration measured in July 2019 (Chapter 2). Actual AVS concentration of anoxic test sediments is reported in Section 5.3.3.

[37] BW_2 is used to distinguish this site from Breydon Water (BW), a different sampling point in the same location. Sediment physicochemical characteristics at both sites are similar (Udochi, *personal obs.*).

permit sieving. Anoxic sediment was sieved, within three days of collection, after the addition of artificial seawater (ASW, 30 S, Tropic Marin® PRO-REEF), which was deoxygenated by bubbling with N_2 gas for three hours before use. The sieved sediment was allowed to settle for at least 5 hrs at 4 ^oC prior to spiking, and overlying water was discarded.

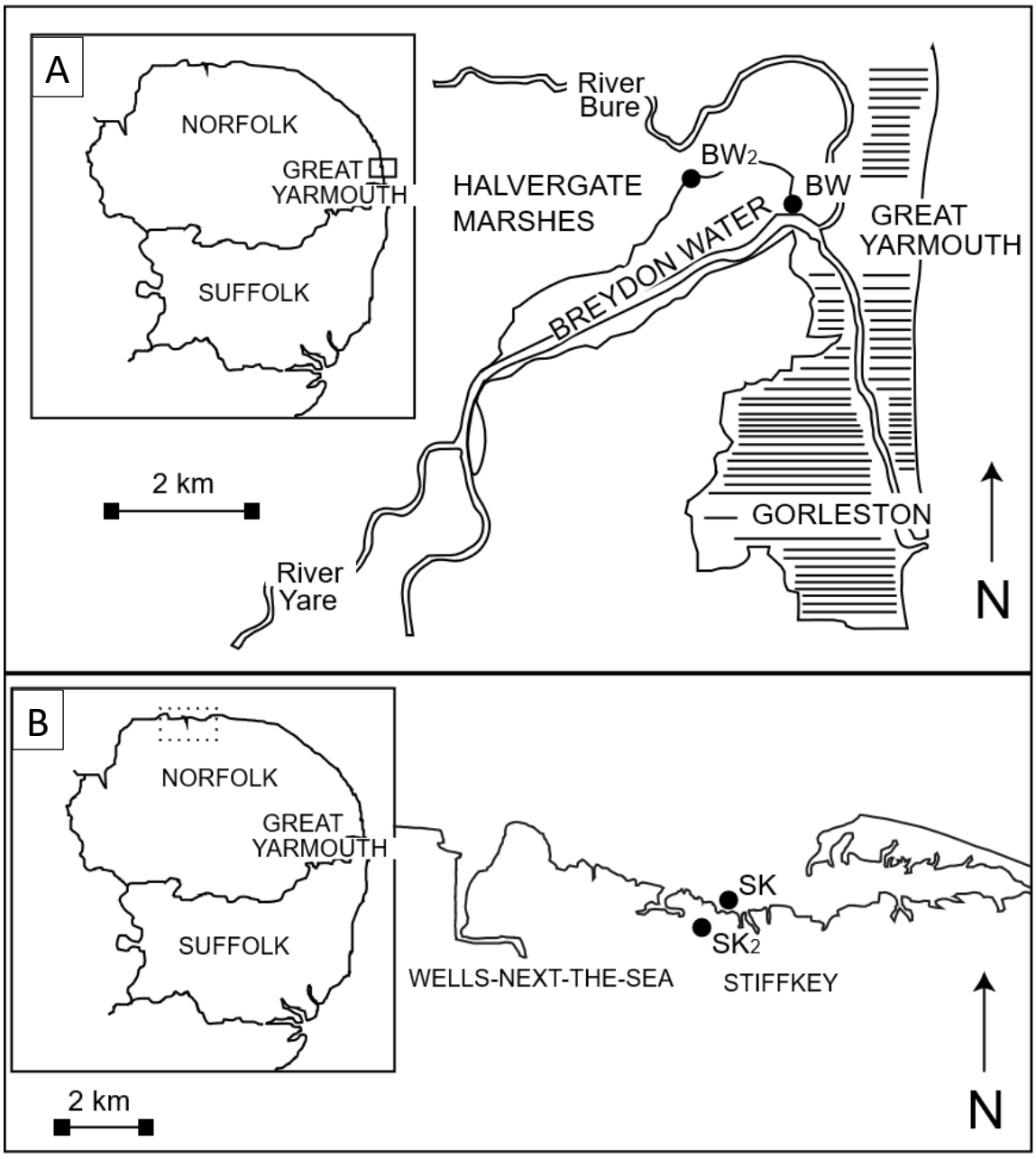

Fig. 5.01: Sampling locations in Norfolk, England. British Grid Reference: BW_2 = TF 501085; BW = Breydon Water site in Chapter 2; SK (April 2019, Lower marsh) = TF 969446; SK_2 (September 2018, Upper marsh) = TF 965442

Sediments were spiked in plastic containers by adding appropriate amounts of a 20 g Cu/L stock solution to sediment-ASW mixtures (4:1 dry weight:weight Simpson *et al.*, 2004). The stock solution was prepared in ultrapure water (UPW) using anhydrous $CuSO_4$ (BDH Poole, England). Spiking was done to achieve 2, 4, 6, 8, and 10 µmol Cu/g (127 – 635 µg/g; final salinity 30 – 30.6 S) nominal concentrations in treatments. Control sediments were similarly treated, albeit with clean ASW only. After agitation for 2 and 5 hrs at laboratory temperature, pH of the sediment slurry was neutralised to 7.0 by dropwise addition of 1 M NaOH. Oxic and anoxic sediments were then transferred to a temperature-controlled room to equilibrate at 4 ^{o}C for 117 and 111 days, respectively. The sediments were vigorously agitated, once a day, in the first week, with overlying water discarded on the last day of equilibration.

After equilibration, sediment pH was neutralised to 7.0, where required. The sediments were allowed for 48 hrs in the environmental chamber to adjust to test conditions before use. Sediments were then homogenised using a plastic spatula immediately prior to toxicity testing. Samples were collected for physicochemical analysis before the feeding assay.

5.2.4 Collection and maintenance of test organisms

In September 2018 and April 2019, *P. ulvae* was obtained at low tide from pools in the Stiffkey saltmarsh, North Norfolk coast (SK, Figure 5.01b) – the same site used by Shipp and Grant (2006). Metal concentrations here are low and similar to those at Breydon Water (Shipp, 2006), precluding either preadaptation or the development of metal tolerance in test organisms. Snails were collected by sieving surface (0 – 1 cm) sediment, *in situ*, using a 500 µm sieve. Organisms retained on the surface of the sieve were then transported to the laboratory in plastic aquariums, each containing a minimal volume of local seawater (salinity = 30.5 S; pH = 7.07) and a layer of sieved sediment. Sieved sediment was also collected in plastic bags, on the same day, from both SK and BW_2 sites. This latter set of sieved sediment was used in the preliminary experiments (see Section 5.2.5) and/or for post-exposure feeding quantification (see Section 5.2.7).

Upon arrival at the laboratory[38], aquariums were filled to volume[39] using ASW and maintained aerated at 20 ^{o}C in an environmental chamber under a 12:12 hr light:dark cycle.

[38] Samples from Stiffkey and Breydon Water reached the laboratory within 1 and 5 hrs, respectively.

[39] Total volume of aquariums in 2018 and 2019 is 10 L and 20 L, respectively. Both aquariums were filled to about three-quarter of total volume.

Evaporated overlying water was replenished, daily, with ultrapure water to a marked point in order to maintain similar salinity. The snails were allowed to acclimatise in the laboratory for at least one week before the main toxicity tests, and overlying water was renewed once every week. Sieved sediments for post-exposure feeding were refrigerated under a layer of ASW, until use, to prevent drying. Sediments for use in the preliminary experiments were refrigerated in plastic bags. All tests were completed within 17 days of mudsnail collection.

5.2.5 Preliminary experiments

An initial feeding assay was completed using freshly-spiked sediments and snails sampled in September 2018 (results not reported) in order to confirm endpoint sensitivity. This test was conducted in 1 L plastic containers (base dimension = 10 x 10 cm) with overlying water as described by Shipp and Grant (2006). However, most snails were found either afloat or on the wall of the test containers by the end of the 24-hr test period. Because this behaviour limits exposure of snails to the test sediments and further risks a potential gut clearance in climbing individuals, it was decided to complete subsequent tests without overlying water. Instead, the walls of test containers were smeared with a ~5 mm thick layer of test sediment in order to maximise exposure. This is the case for preliminary experiments reported here as well as the main assay described in Section 5.2.6.

In order to determine optimal conditions for the main assay, preliminary experiments were conducted to assess the influence of (i) snail size, (ii) AVS concentration, (iii) sediment origin, (iv) time-of-day, and (v) day/night regime on *P. ulvae* feeding rate. These experiments, except the first AVS experiment (see paragraph below), were conducted using snails collected in April 2019. Furthermore, unless stated otherwise, all preliminary experiments were completed using fresh[40], sieved sediments from BW_2 and assay procedures as described in Section 5.2.6.

To assess the influence of size, in-exposure feeding rate was determined using snails with varying shell heights (n = 49; shell height = 2.72 - 6.30 mm) after 24 hrs in fresh sediment.

The influence of AVS was determined in two sets of experiments. Firstly, five groups of snails (n = 18, each) where exposed for 24 hrs to uncontaminated BW_2 sediments with a range of AVS concentrations (<0.5 – 32 µmol/g). Variation in AVS concentration was

[40] "Fresh sediment" is used to refer to sediment that was not aged, which is different from "control sediments" from the same site that were aged as described in Section 5.2.2.

achieved by mixing anoxic (AVS 4, AVS = 32 µmol/g) and oxic (Control, AVS <0.5 µmol/g) sediment at 1/4 (AVS 1), 2/4 (AVS 2), and 3/4 (AVS 3) wet weight proportions. Experimental setups here were gently aerated, leading to considerable oxidation of AVS. A second experiment was conducted for 24 hrs without aeration. In this latter experiment, five groups of snails (n = 21, each) were exposed to freshly-spiked anoxic sediments (AVS ~ 49 µmol/g; nominal Cu = 1, 2, 3, 4, and 5 µmol/g, i.e. 63.5 – 317.5 µg/g). The sixth and seventh group (n = 21, each) were exposed to control oxic and anoxic sediments. In-exposure and post-exposure feeding rates were determined in both experiments.

The influence of time-of-day, day/night regime, and sediment origin on feeding rate was determined in a three-level, partial-factorial experiment (Table 5.1). The test on sediment origin was important to determine which sediment, SK or BW_2, to use in post-exposure feeding rate determination. In groups of snails (n = 24 – 30, per group) fed with both sets of sediment for 24 hrs, feeding rate was determined following exposure in darkness versus light as well as morning (10 – 11:40 am) versus afternoon (3 – 4 pm) versus evening (> 8 pm).

Table 5.1: Partial-factorial design table for determining the influence of time-of-day, day/night regime, and sediment origin on *P. ulvae* feeding rate

Day/Night regime	**Time of day**		
	Morning	**Afternoon**	**Evening**
Light	Stiffkey Breydon Water	Stiffkey Breydon Water	–
Dark	Breydon Water	–	Stiffkey

5.2.6 P. ulvae feeding assay

24-hr feeding assay was completed by modifying documented methods (Shipp & Grant, 2006; Krell *et al.*, 2011) in light of the preliminary experiments. Assays were conducted in clear, plastic containers (14 x 8 x 5cm, l x b x sh) filled with homogenised test sediment to a depth of ~1.5 cm. The tests were conducted without overlying water. To maximise sediment exposure in the event of climbing, the walls of test containers were smeared with a ~5 mm thick layer of test sediment. Each test container was stocked with 10 snails, with triplicate exposures per treatment and control group. Snails used were active and of shell height 3.4 – 4.0 mm. Tests were conducted in environmental chambers at 20 ^{o}C and in 24 hr

darkness. Lastly, assays with anoxic sediments were completed with both oxic and anoxic controls in order to account for the influence of AVS concentration. To minimise oxidation of anoxic sediments, experimental setups were not directly aerated. Air pumps were, instead, placed in the environmental chamber to ensure oxygen circulation, and the lids of test containers were perforated to enable gas exchange. The experimental setups were gently homogenised 12 hrs into the assay to maintain an anoxic surface.

In-exposure feeding rate was assessed immediately after exposure to test sediments. Here, snails were allowed[41] to defaecate for 2 hrs in individual, 3-cm petri-dishes with clean ASW. Faecal pellets voided were counted under a binocular microscope. Egestion using this procedure has been shown to reflect feeding rate of snails in the past hour (Barnes, 2001). A defaecation period of 2 hrs was chosen because, corroborating Krell *et al.* (2011), several snails continued to void pellets after the 1-hr period proposed by Barnes (2001).

Following the initial defaecation, mudsnails were transferred in groups of 10 to similar petri-dishes containing fresh, sieved BW_2 sediment in clean ASW to feed for 1 hr. The snails were then allowed to defaecate, as earlier described. The number of faecal pellets voided in this second period of defaecation was used to quantify post-exposure feeding rate (Krell *et al.*, 2011). There was a total of 5 hrs between removal of snail from test sediment and completion of post-exposure defaecation.

5.2.7 Physicochemical characterisation of sediments

Physicochemical characterisation of samples followed the detailed methodology described in Chapter 2 for the 2019 summer survey. Sediment organic carbon was assessed by Loss on Ignition after heating for 24 hrs at 400 ^{o}C. Total sediment Cu (SED Cu), AVS, porewater Cu (PW Cu), and dilute acid-extractable Cu (SEM Cu) for the oxic sediment assay were measured before the assay. Metal concentrations in these oxic setups were expected to remain stable throughout the 24-hr test period (Costello *et al.*, 2016). Due to the anticipated

[41] Snails were picked-up using plastic forceps and rinsed gently in clean ASW to remove potential food particles before the egestion step. This recovery was completed as quickly and carefully as possible to minimise further oxidation or perturbation of the surface sediment, which could affect metal concentrations. Snails not readily found on the surface were treated as missing individuals (<5 in combined treatment groups of 30) to enable timely processing of samples for physicochemical analyses. All of the missing mudsnails later discovered were alive. Therefore, missing individuals in this study were not considered dead.

oxidation of AVS in the anoxic sediment assay, AVS, PW Cu, and SEM Cu concentrations were determined in samples collected before and after the toxicity test. For the latter group, sediment was scraped from the top ~5 mm layer to reflect the burrowing and foraging behaviour of *P. ulvae* (Huxham *et al.*, 1995)[42]. This sampling did not, however, yield sufficient material for porewater extraction, which was consequently determined in composite samples from the three replicates.

5.2.8 Data analysis

Data analysis in this study was completed using R (R Core Team, 2020). Errors in mean values are reported as standard errors to reflect closeness to the true population mean. For [SEM Cu – AVS] concentration, combined standard errors were estimated from summed individual variances (Gaussian error propagation, see Farrance & Frenkel, 2012).

Egestion rates are based on counts, therefore were analysed using generalised linear models (GLM) with Poisson errors and a log link (Shipp & Grant, 2006). Treatments, here, were inputted as multiple factors. All counts, including zeros, were modelled as no mortality was recorded[43]. Parametric confidence intervals for individual treatments were extracted from the GLM using the R package "ciTools", which computes non-negative, asymmetric intervals transformed to the scale of the response level (Haman & Avery, 2019). In the GLM, overall significance of differences between groups was determined using analysis of deviance, whereas comparison of individual groups with the control was completed using *a priori* linear contrasts (Shipp & Grant, 2006). These comparisons were done using the R package "MultComp" (Hothorn *et al.*, 2020).

In order to determine the best predictor of toxicity and derive effect levels, three- and four-parameter log-logistic models with Poisson errors were attempted for individual assays as well as the combined response in the oxic and anoxic sediment assays, using the R package "drc" (Ritz *et al*., 2015). The models were completed, separately, using SEM Cu, PW Cu, and Sed Cu as predictor variables. For the anoxic sediment assay, models were fitted using metal concentrations measured before and after the 24-hr toxicity test as well as the time-

[42] In some cases, *P. ulvae* can burrow up to 2 cm deep (Hale *et al*., 2015)

[43] A proportion of live snails – especially in the most contaminated treatments – voided no faecal pellets. As this is a possible influence of toxicant on feeding rate, all zero counts were included in the analysis.

averaged concentrations. Model fit was assessed using log-likelihood values and calculated Akaike Information Criterion (AIC)[44]. Negative "dose" values precluded the modelling of SEM – AVS concentrations.

5.3 Results

5.3.1 Confounding factors influencing ingestion of uncontaminated sediments

Preliminary experiments were used to identify the potentially confounding effects of snail size, AVS concentration, sediment origin, time-of-day, and day/night regime on *P.ulvae* feeding rate when fed with uncontaminated, control sediments.

The influence of snail size is shown in Figure 5.02. In snails with shell height up to 4.4 mm, for which there was sufficient data, a significant, positive correlation was observed between feeding rate and snail size ($r = 0.40$, $t = 2.88$, $p < 0.01$). However, within the size range 3.4 – 4.4 mm, this correlation was non-significant ($r = 0.22$, $t = 1.35$, $p = 0.19$). Consequently, only snails with shell height 3.4 - 4.4 mm were used in this study[45].

In-exposure feeding rates reduced significantly with increase in AVS concentration after the AVS 1 treatment (AVS ~ 8 µmol/g; $p < 0.05$; Figure 5.03a), despite aeration of experimental setups. In the highest AVS treatment (AVS 4 = 32 µmol/g), average feeding rate had decreased to 58% of values in control, non-sulphidic exposures (i.e. a 42% depression). Exposed snails were, however, seen to recover post-exposure, with similar feeding rates and a notable stimulation of feeding relative to the control (Figure 5.03b). This stimulation became more apparent in snails exposed to spiked, non-aerated sediments at a higher AVS concentration (Experiment 2; base AVS ~ 49 µmol/g). Exposed snails, here, did not feed during exposure; however, they recovered post-exposure with a two-fold increase in average feeding rate relative to the control (Figure 5.04). Overall, increasing AVS reduced feeding during exposure, consequently stimulating the ingestion of clean sediments post-exposure. As a result, control, anoxic sediment with similar AVS concentration as treatments were included in the main anoxic assay. The setups were not aerated to limit loss of AVS.

[44] AIC = (2* number of parameters) – (2 * Log Likelihood) (Akaike, 1978). The "drc" package yields positive Log Likelihood (LL) values for Poisson regressions. However, conclusions on model fit from "drc" LL values are similar to those obtained from the traditional generalised linear modelling.

[45] All the mudsnails used in the main assays were within the height range 3.4 – 4.0 mm.

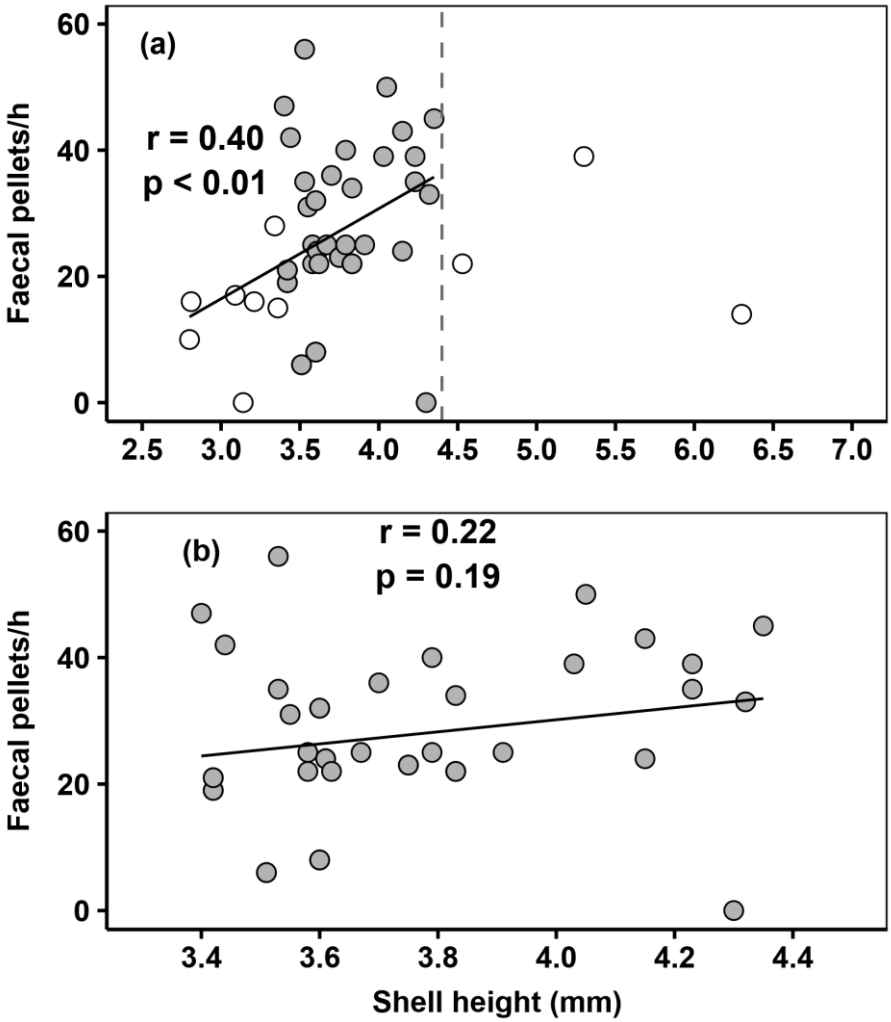

Fig. 5.02: Correlation between feeding rate, as measured by egestion rate, of *P. ulvae* and snail size, as measured by height of shell. All snails fed with clean, oxic sediment (Panel a; n = 49). Dashed line represents limit where Pearson correlation is significant. Filled circles represent size range where Pearson correlation is non-significant (Panels a & b; n = 39)

The highest feeding rates were observed in snails fed with sediment from BW_2, rather than SK where they originated (Figure 5.05, highest mean [95% CL] rates = 42.5 [40.0 – 45.2] versus 37.2 [35.1 – 39.5] /h). Within these two groups, feeding rate appeared to increase with time: snails fed better in the evening versus afternoon versus morning (non-significant for SK, but significant for BW_2, $p < 0.05$). Similarly, higher feeding rates were observed when snails were fed in darkness versus light, and this difference was more prominent when using BW_2 sediment. These results reveal a strong preference of snails for feeding on BW_2 sediment and in dark conditions. As a result, the main feeding assays – both exposure and feeding quantification – were conducted in darkness to increase test sensitivity, and BW_2 sediment was used in assessing post-exposure feeding rates. Direct comparison between in-

exposure and post-exposure rates is discouraged as (i) there was a 5-hr time difference between the end of toxicity testing and the end of post-exposure assessment (thus, overlapping into a different time-of-day), and (ii) sediment used for in-exposure assessment was different from that used post-exposure (aged versus fresh, submerged BW_2 sediment).

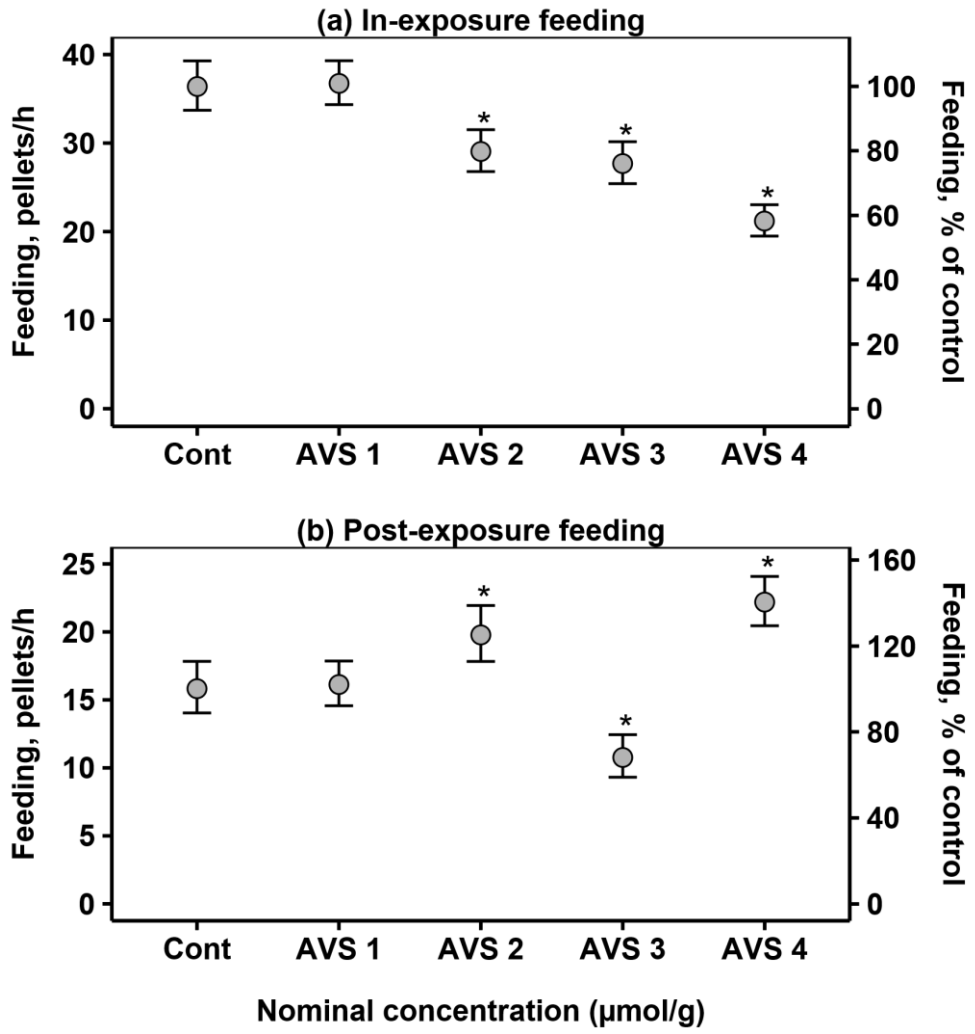

Fig. 5.03: In-exposure (Panel a) and post-exposure (Panel b) feeding rate, as measured by egestion rate (mean ± 95% CI), of *P. ulvae* exposed to clean sediments with a range of AVS concentrations. AVS 4 = anoxic sediment of 32 µmol/g sulphide. Cont = control, oxic sediment with sulphide < 0.5 µmol/g. AVS 1, AVS 2, and AVS 3 represent mixtures of AVS 4 and Control sediments at 1/4, 2/4, and 3/4 wet weight proportions, respectively. Asterisks (*) represent significant difference ($p < 0.05$) from control exposure

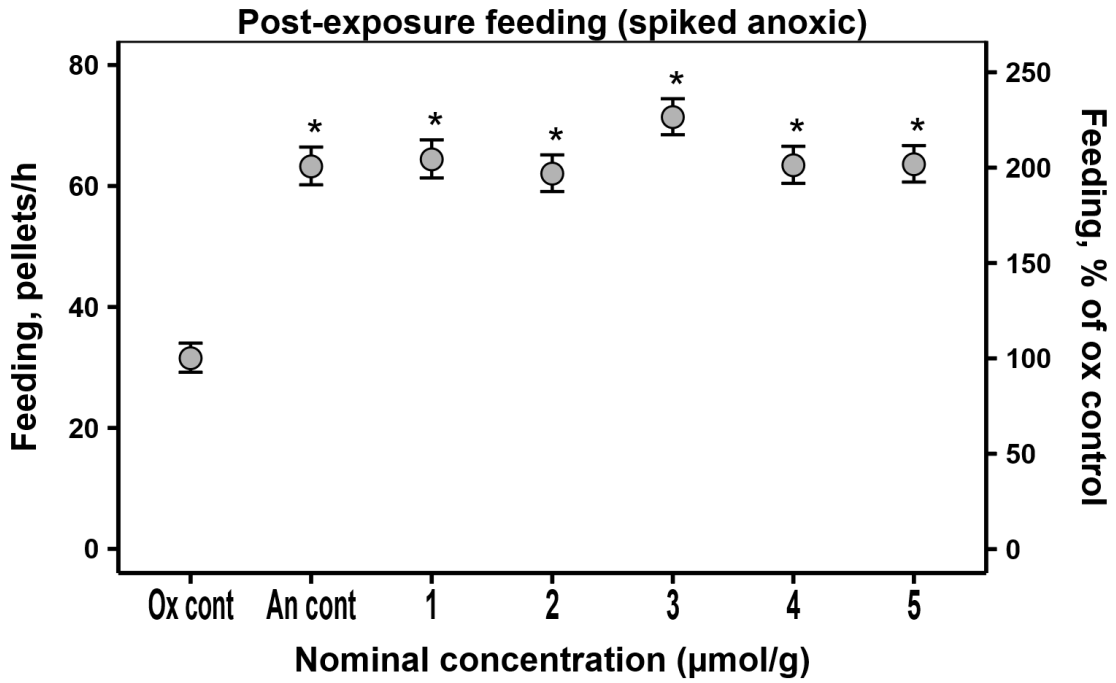

Fig. 5.04: Post-exposure feeding rate, as measured by egestion rate (mean ± 95% CI), of *P. ulvae* initially exposed to oxic and anoxic (base AVS ~ 49 µmol/g) sediments spiked to a range of Cu concentrations. Snails exposed to anoxic sediments did not feed during exposure. Ox cont = oxic control. An cont = anoxic control (AVS ~ 49 µmol/g). Asterisks (*) represent significant difference ($p < 0.05$) from oxic control

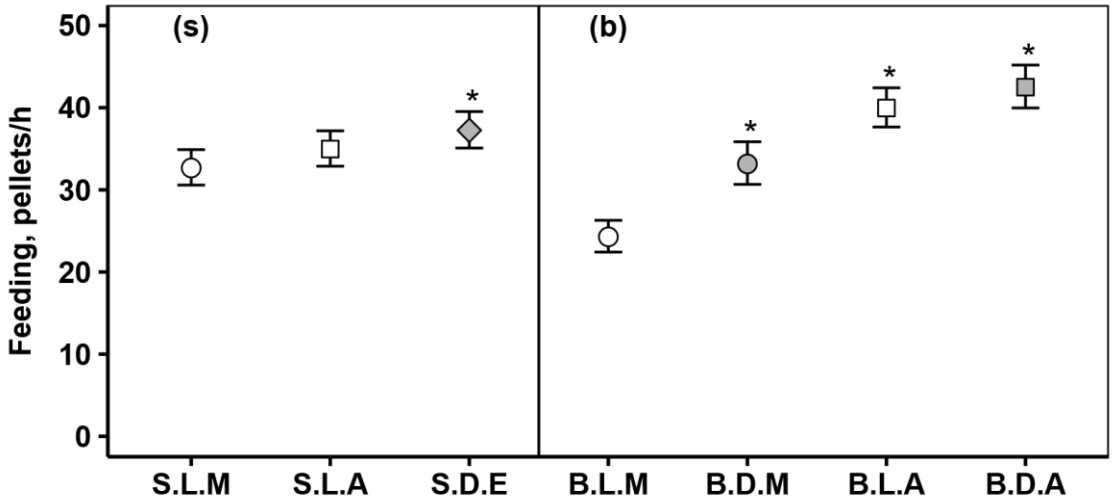

Fig. 5.05: Feeding rate, as measured by egestion rate (mean ± 95% CI), of *P. ulvae* fed with clean, oxic sediment from Stiffkey (Panel s) and Breydon Water (Panel b) at different light/dark conditions and time of day. Filled vs open points: snails fed in darkness (D) vs light (L), respectively. Circle, square, and rhombus points: snails fed in the morning (M), afternoon (A), and evening (E), respectively. Asterisks (*) represent significant difference ($p < 0.05$) from S.L.M or B.L.M

5.3.2 Physicochemical properties of oxic test sediments

Physicochemical properties of oxic test sediments are shown in Figure 5.06 and Appendix A5.1a. As expected, AVS was non-detectable. Total concentrations of Cu increased proportionally with nominal spike concentration (0.6 – 10.9 µmol/g, 37 – 695 µg/g), most of which was extractable as SEM Cu (mean ± SE 0.5 ± 0.2 – 7.7 ± 0.1 µmol/g; ~32 – 489 µg/g) thus potentially bioavailable. The percentage of total Cu extractable seemed to increase with Cu concentration in the spike[46].

Porewater concentrations recorded were minimal (mean ± SE 1.9 ± 0.7 – 40.6 ± 1.3 µg/L), indicating that most of the spiked metal was bound to sediment particles. Unlike SEM Cu, concentrations, there was no significant difference in mean PW Cu between the control sediment and the 2 µmol Cu/g nominal treatment ($t = 0.31$, $p = 0.79$). PW Cu rose steadily in the treatments from the 4 µmol/g spike upwards, covarying with SEM Cu concentrations. However, PW Cu concentration in the highest treatment was within the 48-hr water-only feeding EC_{20} derived for *P. ulvae* – twice the duration of exposure in the current study (Table 5.2; Krell *et al.*, 2011)[47]. The porewater concentrations recorded were also comparable to those in field sediments of similar particulate metal concentrations (Chapter 2, Winter Survey). This low PW Cu (i) suggests that spiked metals were fully equilibrated during the sediment ageing process and (ii) precludes porewater toxicity in the oxic feeding assays. Therefore, toxicity in the oxic setups was attributed entirely to sediment-bound Cu exposure.

5.3.3 Physicochemical properties of anoxic test sediments

Physicochemical properties of anoxic sediments measured before and after the 24-hr feeding assay are shown in Figure 5.07 and Appendix A5.1b. Total sediment Cu concentration measured before the experiment was similar to the range in oxic sediments (0.7 – 10.3 µmol/g, 43 – 657 µg/g), suggesting a uniformity in the spiking process.

[46] SEM Cu as a percentage of Sed Cu for oxic test sediments: 76.7, 43.0, 54.3, 57.5, 70.6, and 70.7% for sediments spiked at 0, 2, 4, 6, 8, and 10 µmol/g, respectively.

[47] Krell *et al.* (2011) measured post-exposure feeding end-points (EC_{20} and EC_{50}) after exposing snails for 48 hrs in test solutions. However, snails remained in test solution during their 2-hr post-exposure feeding quantification, precluding the possibility of physiological recovery. Their effect thresholds, therefore, approximate expectations from in-exposure feeding.

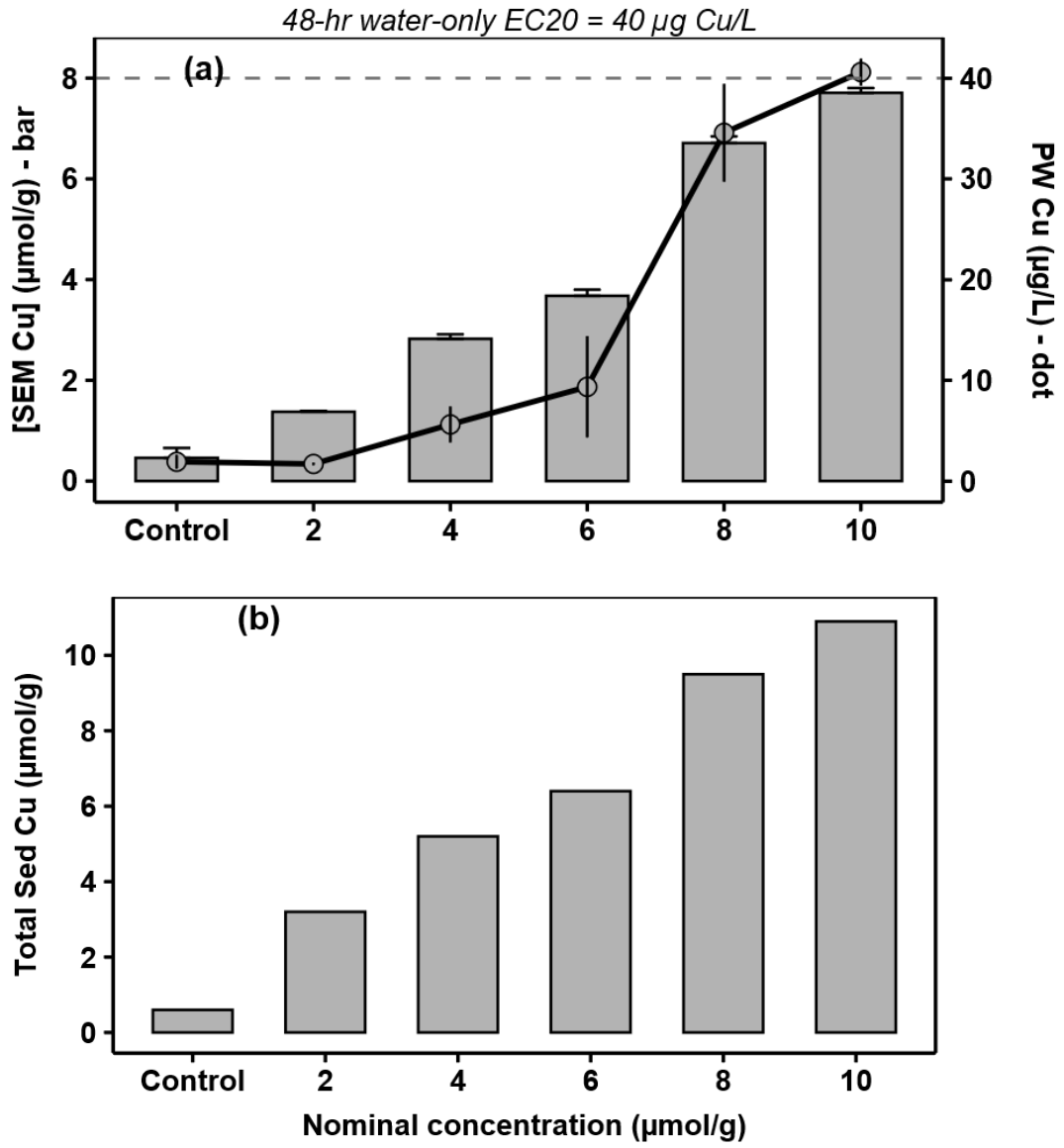

Fig. 5.06: Extractable (SEM Cu) and porewater (PW Cu) Cu concentrations in oxic sediments before 24-hr feeding assay with *P. ulvae* (Panel a; mean ± SE; n = 2 or 3). Exact number of replicates provided in Table A5.1a. Dashed line represents the 48-hr water-only EC_{20} (Krell *et al*., 2011), below which dissolved Cu is not expected to contribute to toxicity. Note that this is for double the 24-hr exposure period in the current study. Total Cu (Sed Cu) measurement was not replicated (Panel b)

Table 5.2: Effect concentrations derived for feeding depression in *P. ulvae* exposed to Cu-spiked seawater for 48 hours (Krell *et al*., 2011)

Effect level	Cu Concentration (µg/L)
EC_{20} (95% CL)	40 (17 – 63)
EC_{50} (95% CL)	207 (146 – 269)

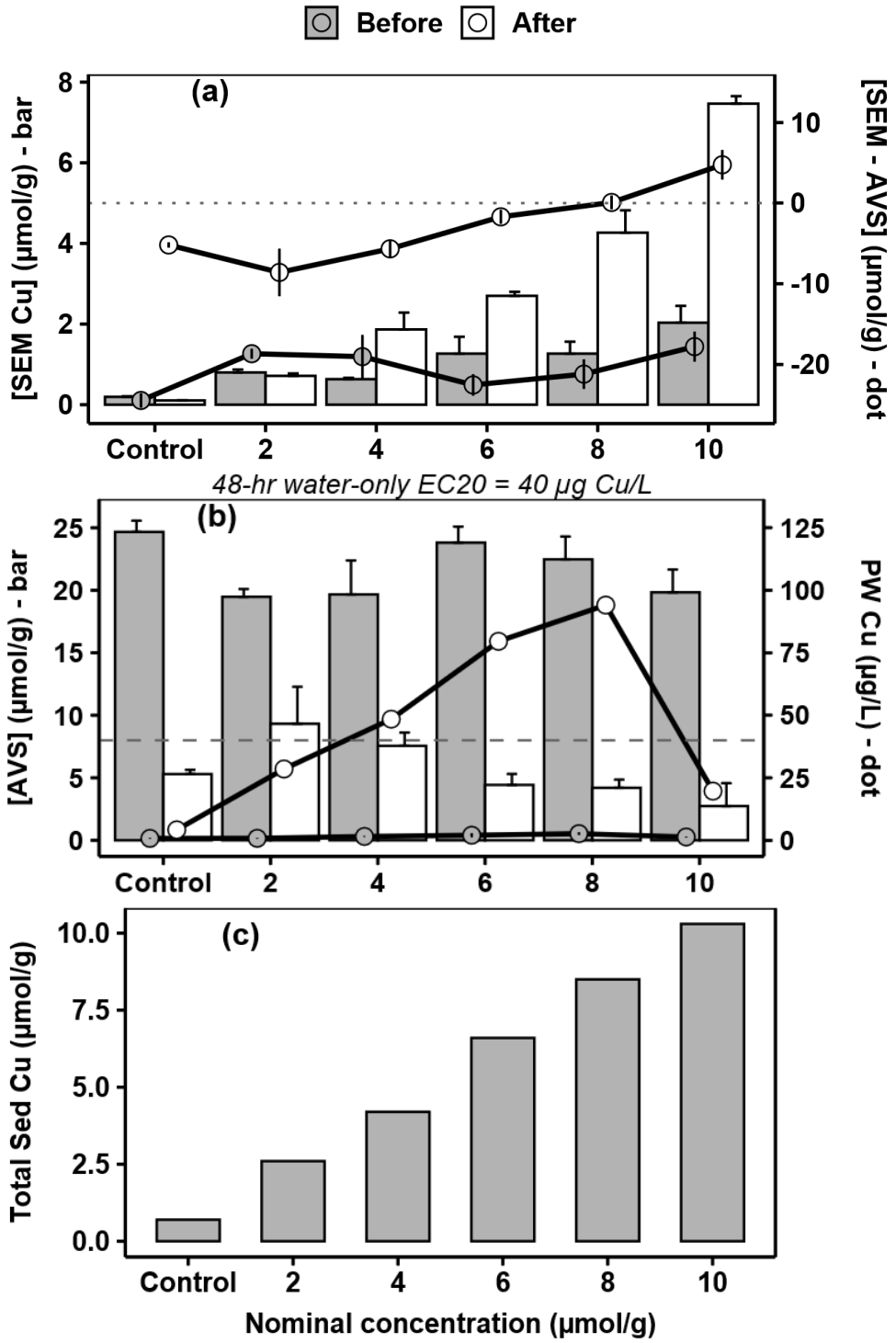

Fig. 5.07: Extractable (SEM Cu), AVS, and porewater (PW Cu) Cu concentrations in anoxic sediments before (filled symbols) and after (open symbols) 24-hr feeding assay with *P. ulvae* (mean ± SE; n = 2 or 3). Exact number of replicates provided in Table A5.1b. PW after test not replicated. Total sediment Cu (Sed Cu) measured once. Dotted line (Panel a) represents [SEM – AVS] = 0, below which Cu is not expected to be toxic, according to the EqP model (Di Toro *et al*., 2005). Dashed line (Panel b) represents the 48-hr water-only EC_{20} (Krell *et al*., 2011), below which PW Cu is not expected to contribute to toxicity. Note that this is for double the 24-hr exposure period in the current study

AVS concentration in the anoxic control sediment before the assay was 24.7 ± 0.9 (mean ± SE), representing the base concentration across the anoxic sediments. In the spiked treatments, detectable AVS concentrations dropped slightly to around 20 µmol/g, which is nearly twice the total Cu concentration in the most contaminated sediment. This high AVS concentration before the experiment corresponded with diminished Cu in porewater (0.8 ± 0.1 – 2.7 ± 0.6 µg/L) and SEM (0.2 ± <0.1 – 2.0 ± 0.7 µmol/g, ~13 – 44 µg/g) as well as negative SEM Cu – AVS (– 24.5 ± 0.9 to –17.8 ± 1.9 µmol/g, mean ± SE) concentrations. SEM Cu was relatively low (14.9 – 30.7% of total Cu)[48], showing that although nearly all of the spiked Cu was bound in the sediment, only a small fraction of this was extractable by 1M HCl treatment. In summary, AVS >> SEM Cu, SEM Cu << Sed Cu, and PW Cu << 48-hr EC_{20} before the experiment. Porewater concentrations recorded were, again, comparable to the range observed in Fal estuary (Chapter 2, Summer 2019 anoxic sediment Survey).

AVS concentration dropped considerably due to oxidation during the 24-hr toxicity test (decreased by 52.1 – 86.2% of starting levels)[49]. This depletion of AVS corresponded with a uniform increase in PW Cu (4.2 – 94 µg/L), SEM Cu (0.1 ± <0.1 – 7.5 ± 0.2 µmol/g, ~6 – 476 µg/g), and SEM – AVS (–8.6 ± 3.0 to 4.8 ± 1.8 µmol/g) concentrations. The percentage of total sediment concentrations extractable as SEM Cu also increased (15 – 72%)[50], achieving a proportion at 10 µmol/g which was comparable to the oxic sediments. PW Cu was also relatively low in the 10 µmol/g treatment (19.7 µg/L), which in addition to the control and 2 µmol/g setups remained lower than the 48-hr water-only EC_{20}. In the rest of the treatments (at 4, 6, and 8 µmol/g), PW Cu exceeded the EC_{20} but all remained considerably below the 48-hr water-only EC_{50} (207 µg/L). Therefore, toxicity as a result of dissolved Cu is not expected in these setups. Considering the EqP model, SEM – AVS remained negative up to 6 µmol/g, close to zero at 8 µmol/g, but positive at 10 µmol/g nominal Cu. The results suggest significant oxidation of AVS in the 10 µmol/g treatment during 24-hr exposure period. It can be summarised that (i) AVS-after ≥ SEM Cu-after until 8 µmol/g nominal concentration and (ii) SEM Cu-after >> SEM Cu-before.

[48] Starting SEM Cu as a percentage of Sed Cu in anoxic sediments: 27.8, 30.7, 15.1, 19.2, 14.9, and 19.7% for sediments spiked at Control, 2, 4, 6, 8, and 10 µmol/g, respectively.

[49] Final AVS as a percentage of starting concentrations: 21.5, 47.9, 38.4, 18.6, 18.7, 13.8% for sediments spiked at Control, 2, 4, 6, 8, and 10 µmol/g respectively.

[50] Percentage of Total sediment concentration extractable as SEM Cu in anoxic sediments after toxicity tests: 15.1, 27.5, 44.4, 40.9, 50.1, and 72.5% for sediments spiked at Control, 2, 4, 6, 8, and 10 µmol/g respectively.

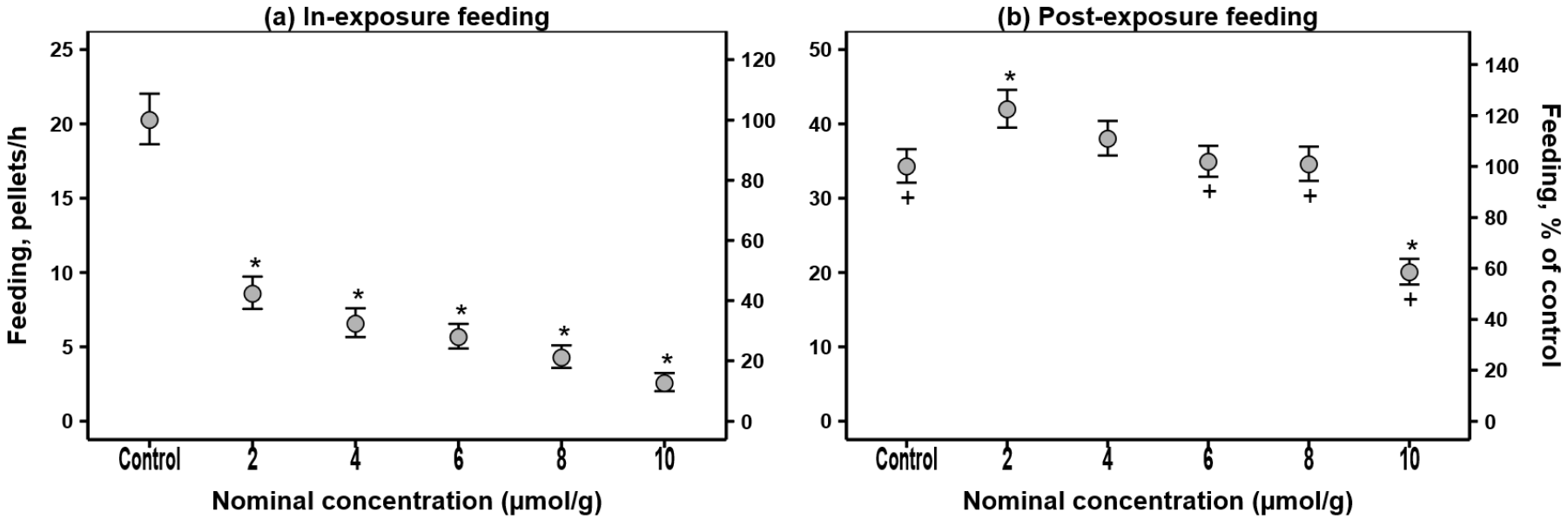

Fig. 5.08: In-exposure (Panel a) and post-exposure (Panel b) feeding rate, as measured by egestion rate (mean ± 95% CI), of *P. ulvae* exposed to spiked oxic sediments for 24 hrs. Asterisks (*) represent significant difference ($p < 0.05$) from control. Crosses (+) represent significant difference ($p < 0.05$) from the 2 µmol/g treatment

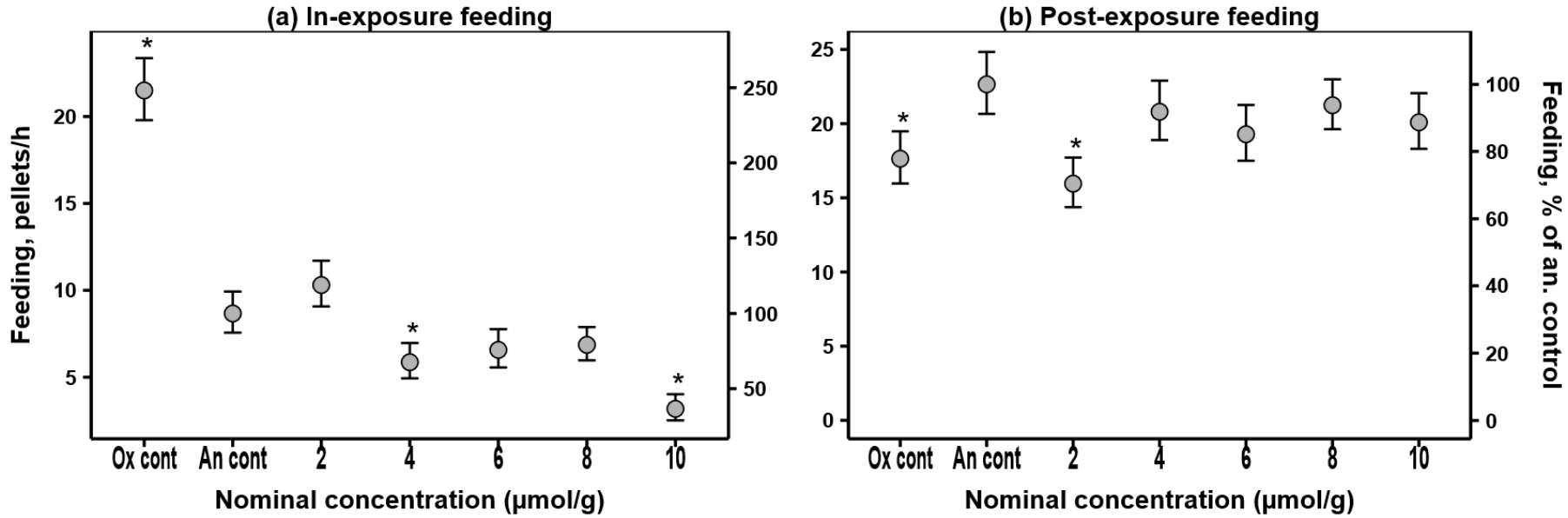

Fig. 5.09: In-exposure (Panel a) and post-exposure (Panel b) feeding rate, as measured by egestion rate (mean ± 95% CI), of *P. ulvae* exposed to spiked anoxic sediments with similar AVS concentrations for 24 hrs. Ox cont = Control oxic sediment. An cont = Control anoxic sediment. Feeding expressed as a percentage of anoxic control mean values. Asterisks (*) represent significant difference ($p < 0.05$) from anoxic control. Notice that the biggest effect is due to anoxia, comparing oxic and anoxic controls.

5.3.4 Toxicity of oxic sediments to P. ulvae

Figure 5.08 shows results of the 24-hr feeding assay on *P. ulvae*. Despite porewater concentrations less than the 48-hr EC_{50}, there was a significant depression ($p < 0.001$) in in-exposure feeding rate in all treatments compared to the control exposure (Figure 5.08a). This feeding depression was most prominent for the 2 µmol/g treatment versus control (>50% decrease), notwithstanding the similarity in PW Cu, suggesting that the effect was due primarily to particulate metals. Feeding rates continued to reduce with increase in nominal Cu concentration. The lowest rate (2.0 – 3.2 /h, 95% LCL – UCL) was observed in the 10 µmol/g set, which was significantly different from all other treatments ($p < 0.01$).

Toxicity of Cu in test sediments continued even after exposure of snails to clean sediments, albeit in a less prominent fashion (Figure 5.08b). The clearest post-exposure feeding depression versus the control was observed in the 10 µmol/g treatment ($p < 0.001$). For the 2 µmol/g treatment, there was a significant stimulation of feeding in comparison with the control ($p < 0.001$), similar to observations in the preliminary AVS test where post-exposure feeding rate increased in starved snails (Figure 5.04). However, a downward trend in feeding was observed thenceforth, with significantly reduced feeding rate in the 6 – 10 µmol/g treatments ($p < 0.001$) when compared to the 2 µmol/g treatment (Figure 5.08b). An implicit post-exposure feeding threshold of 4 µmol/g suggests that this is a less-sensitive endpoint than in-exposure feeding. Importantly, the depression of feeding post-exposure is strongly indicative of the toxicity of ingested test sediments, rather than mere avoidance.

5.3.5 Toxicity of anoxic sediments to P. ulvae

The trend in in-exposure feeding rates for the anoxic setups was similar to that in oxic sediments (Figure 5.09a). Although the most prominent depression in feeding was primarily due to the effect of anoxia (oxic versus anoxic control was a 59.7% decrease; $p < 0.001$), mudsnail feeding rates reduced with increasing metal contamination.

Comparing spiked versus control anoxic sediments, feeding depression was visible at 4 – 10 µmol/g, albeit only significant in the 4 µmol/g ($p < 0.01$) and 10 µmol/g ($p < 0.001$) treatments. Depression versus control was less significant in the intervening treatments (6 µmol/g: $p = 0.058$; 8 µmol/g: $p = 0.088$). At 2 µmol/g, feeding rate was similar to the control group ($p = 0.28$) – a higher nominal threshold concentration than in the oxic sediment assay. Feeding rate was also similar between 4 – 8 µmol/g treatments. The snails were largely

recovered upon post-exposure feeding (Figure 5.09b), and feeding depression, relative to the control, was significant only at 2 µmol/g. Overall, the results suggest reduced test sensitivity due to the influence of anoxia, but demonstrate Cu toxicity in the anoxic sediment assay.

5.3.6 Feeding depression: best predictor, SEM – AVS model, and (non-)toxicity of copper sulphides

Dose-response model fits based on in-exposure feeding rates are shown in Figures 5.10 – 5.12 for SEM Cu, PW Cu, and Sed Cu, respectively, and Appendices 5.2 and 5.3 for combined SEM and PW models. The relationship between SEM-AVS concentration and feeding rate is shown in scatter plots in Figure 5.13. Derived effect concentrations as well as log-likelihood and AIC values for fitted models are provided in Table 5.3. Due to their relatively poor dose-response relationships, models based on anoxic-only assays as well as post-exposure feeding rates did not converge. However, it is noteworthy that models based on the combined oxic and anoxic assays converged, with feeding in the spiked sediments related to sediment concentrations after the experiments regardless of starting AVS concentrations. The implications of this observation is also highlighted in this section.

As expected, better fits were achieved for particulate metals (SEM and Sed Cu) than porewater, despite the covariance in concentrations (Figures 5.10 – 5.12, A5.2, A5.3). Considering oxic-only models (Figures 5.10a, 5.11a, and 5.12a; Table 5.3), the best fit was reached using Sed Cu (AIC = – 8754) followed by SEM Cu (AIC = – 8746) and then PW Cu (AIC = – 8590). This was the case for comparisons involving respective combined models – i.e. models combining responses from both oxic and anoxic assays (Figures 5.10 – 5.12). Further indication of poorer dose-response relationships with PW Cu was seen in the slope. Slope of the fits was relatively low for models based on PW Cu, with curves flattening out upon the inclusion of anoxic treatments in the combined model (A5.3). For most treatments, PW Cu remained within the 48-hr EC_{20} (Figure 5.11), which is a conservative threshold given the longer exposure duration. PW Cu in the 6 – 10 µmol/g exceeded this threshold at the end of the experiment, albeit remained within the EC_{50} (Table 5.2). The strong relationship of feeding rate with particulate, rather than dissolved, metal concentrations is further evidence in support of dietary toxicity for *P. ulvae*.

That model convergence was achieved using the combined responses from the oxic and anoxic assays suggests a conformity in expected feeding rates (Figures 5.10, 5.12, A5.2, A5.3). Examining responses to spiked sediments, feeding rate in the oxic and anoxic

treatments were strongly predicted by SEM and Sed Cu concentrations irrespective of starting AVS concentrations. When combined models based on SEM Cu are compared (Figure 5.10 – 5.11; A5.2; Table 5.3), the best fit is observed for concentrations measured (in the anoxic setups) after the experiment, followed closely by the time-averaged concentrations. A similarly good fit is obtained using Sed Cu, where concentrations in both oxic and anoxic setups were expected to remain stable throughout the experiment. The results are equivocal. It could be that Cu toxicity observed in the anoxic sediments was more likely reflective of the relatively oxidised conditions at the end of the experiment, suggesting that Cu bound to sulphide was non-toxic. However, this interpretation fails to account for the relatively reduced exposure time to oxidised Cu in the anoxic sediment treatments, which remained anoxic for much of the exposure period. A second interpretation is that both sulphidic and non-sulphidic forms of Cu were of similar potency. This latter hypothesis seems particularly plausible, considering that Sed Cu was the best predictor of effects and measurable SEM Cu only approaches this value upon oxidation (i.e., concentrations measured at the end of the experiment; Figure 5.07). Indeed, the convergence in feeding rates from oxic and anoxic spiked sediments is possible evidence for the dietary toxicity of Cu sulphides to *P. ulvae*.

The SEM-AVS EqP derivation proved unsuitable for predicting the absence of toxicity when applied using time-averaged concentrations or those measured before the experiment (Figure 5.13). Feeding depression occurred despite all anoxic setups maintaining higher AVS than SEM concentrations. However, a similar convergence in feeding rates in oxic and anoxic treatments was observed using concentrations measured after the assay. Here, the SEM-AVS value seemed to capture the transition to toxicity from the 8 µmol/g treatment, albeit that it failed to predict the significant feeding depression at 4 µmol/g despite a negative SEM-AVS value similar to the control. Comparison of fit with other measures of metal contamination was impracticable, as negative "dose" values precluded modelling of the EqP measure. However, given the poor relationship observed between feeding rate and PW Cu, any predictive capability of SEM-AVS here is not likely related to dissolved concentrations, as designed.

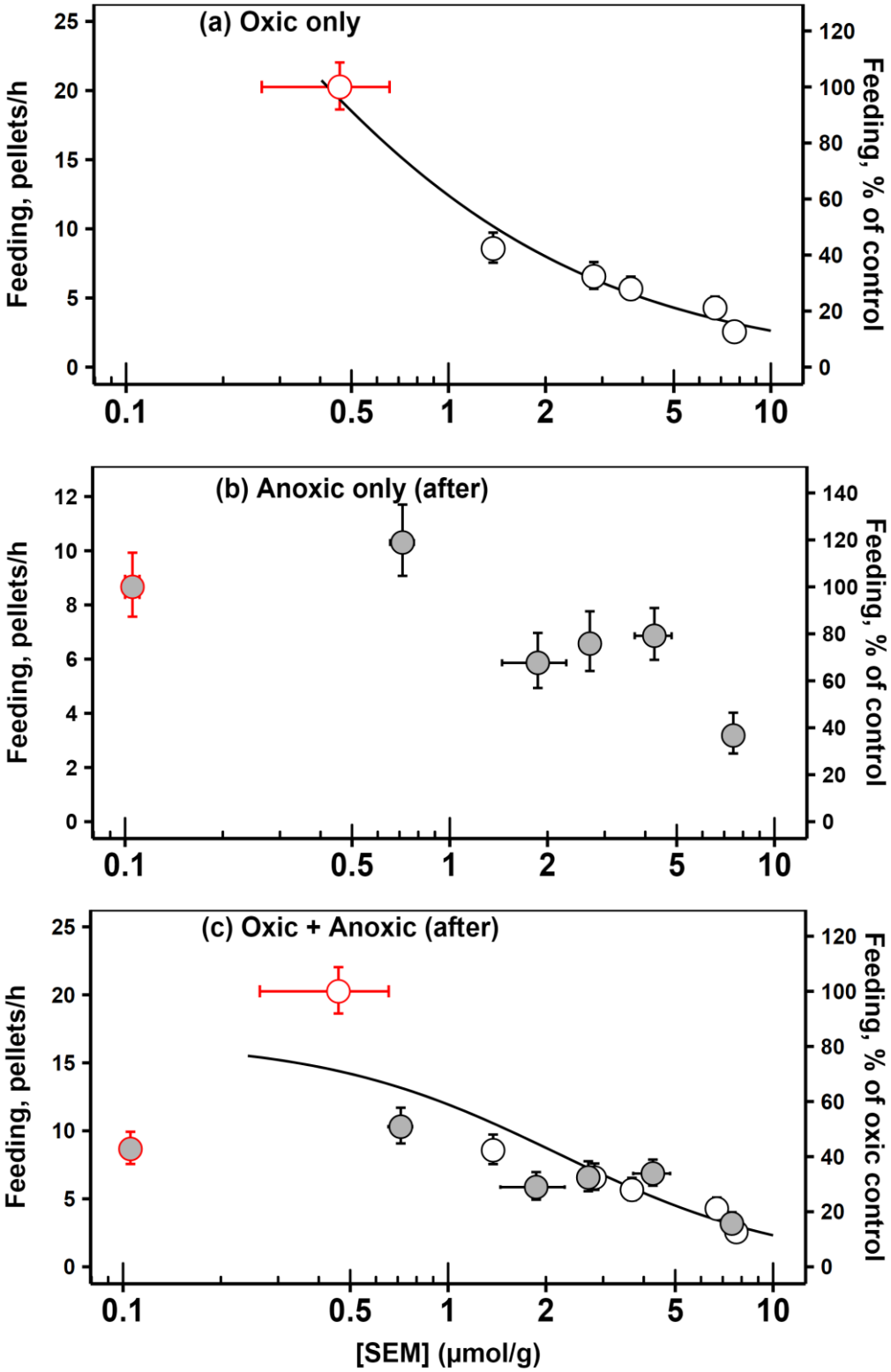

Fig. 5.10: In-exposure feeding rate, as measured by egestion rate (mean ± 95% CI), of *P. ulvae* exposed to spiked oxic (open symbols) and anoxic (filled symbols) sediments for 24 hrs in relation to SEM Cu concentration (mean ± SE) after the experiment. Model with only anoxic values did not converge. Red symbols represent control exposures. EC 10, 20, & 50 provided in Table 5.3. Difference in feeding between the oxic and anoxic controls is due to the significant effect of anoxia (see Fig. 5.09)

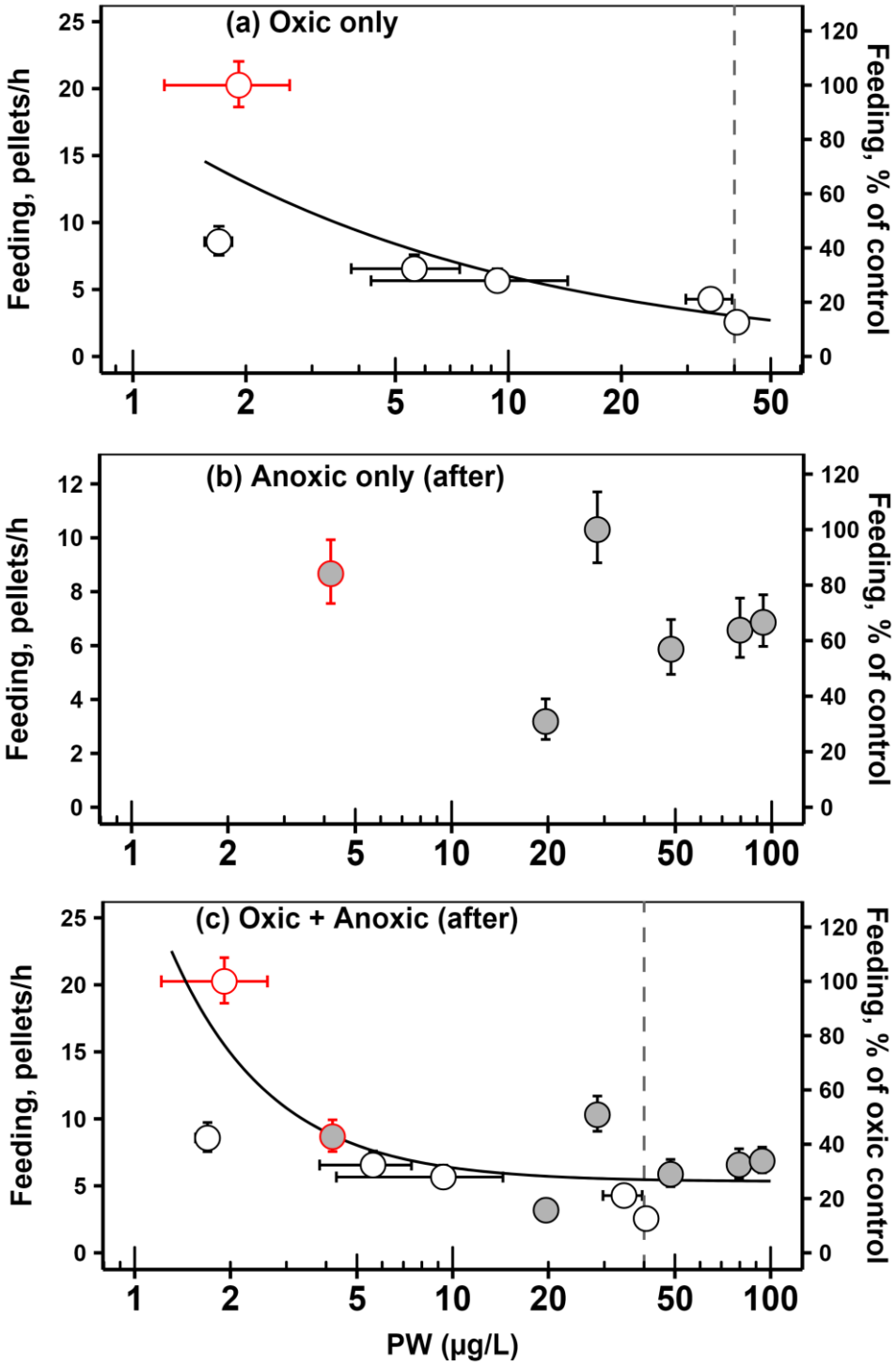

Fig. 5.11: In-exposure feeding rate, as measured by egestion rate (mean ± 95% CI), of *P. ulvae* exposed to spiked oxic (open symbols) and anoxic (filled symbols) sediments for 24 hrs in relation to porewater Cu concentration (mean ± SE) after the experiment. Model with only anoxic values did not converge. Red symbols represent control exposures. EC 10, 20, & 50 provided in Table 5.3. Dashed line represents the 48-hr water-only EC_{20} (Krell *et al.*, 2011), below which dissolved Cu is not expected to contribute to toxicity for a 48-hr exposure period. Difference both controls is due to the effect of anoxia (see Fig. 5.09)

Table 5.3. Model fit and effect concentrations for in-exposure feeding rate of *P. ulvae* exposed to Cu-spiked oxic and anoxic sediments for 24 hours

Measure	Sediment Group	Log Likelihood	AIC	Effect concentrations		
				EC_{10} (95% CL)	EC_{20} (95% CL)	EC_{50} (95% CL)
Porewater concentration (µg/L)	Oxic only	4298	-8589	<LE	<LE	<LE
	Oxic + anoxic (before)	9378	-18750	<LE	<LE	<LE
	Oxic + anoxic (mean) [LL.4]	9562	-19115	<LE	<LE	<LE
	Oxic + anoxic (after) [LL.4]	9573	-19137	<LE	<LE	<LE
[SEM] concentration (µmol/g)	Oxic only	4376	-8746	<LE	<LE	<LE
	Oxic + anoxic (before)	9545	-19084	<LE	0.19 (0.06 – 0.32)	0.97 (0.54 – 1.41)
	Oxic + anoxic (mean)	9619	-19232	0.25 (0.15 – 0.36)	0.51 (0.34 – 0.68)	1.73 (1.38 – 2.08)
	Oxic + anoxic (after)	9630	-19254	0.35 (0.22 – 0.47)	0.68 (0.49 – 0.88)	2.18 (1.81 – 2.56)
Total sediment concentration (µmol/g)	Oxic only	4380	-8754	<LE	<LE	1.7 (0.4 – 2.9)
	Oxic + anoxic	9687	-19368	<LE	<LE	<LE

All groups fitted with three-parameter Log-logistic models with Poisson distribution, except otherwise indicated.
Combined plots for SEM and Porewater concentrations are provided in Appendices 5.2 and 5.3, respectively.
[LL.4] = Four-parameter model.
[SEM] = Extractable Cu concentration in sediment
AIC = Akaike Information Criterion = (2* number of parameters) – (2 * Log Likelihood)
<LE: Estimate less than the lowest exposure concentration

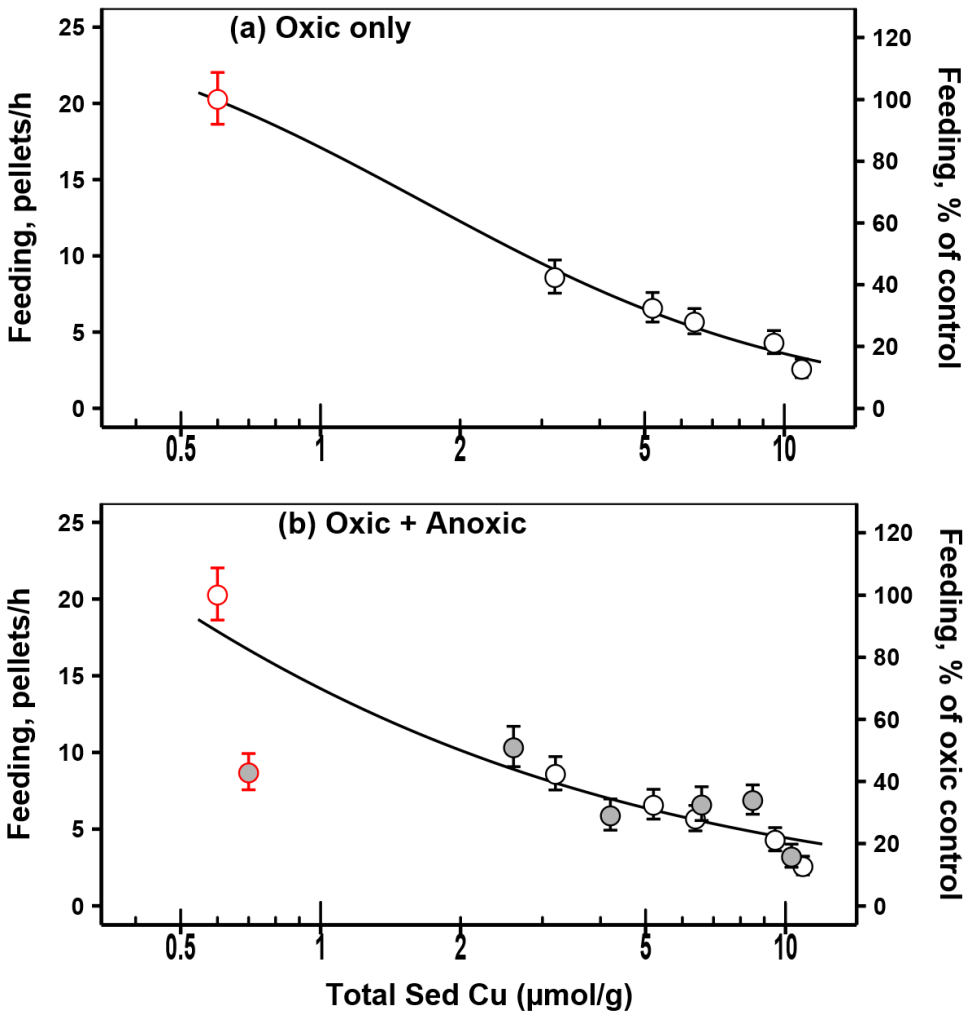

Fig. 5.12: In-exposure feeding rate, as measured by egestion rate (mean ± 95% CI), of *P. ulvae* exposed to spiked oxic (open symbols) and anoxic (filled symbols) sediments for 24 hours in relation to total sediment Cu concentration (mean ± SE). Red symbols represent control exposures. EC 10, 20, & 50 provided in Table 5.3. The difference in feeding rates between the oxic and anoxic controls is due to the significant effect of anoxia (see Fig. 5.09)

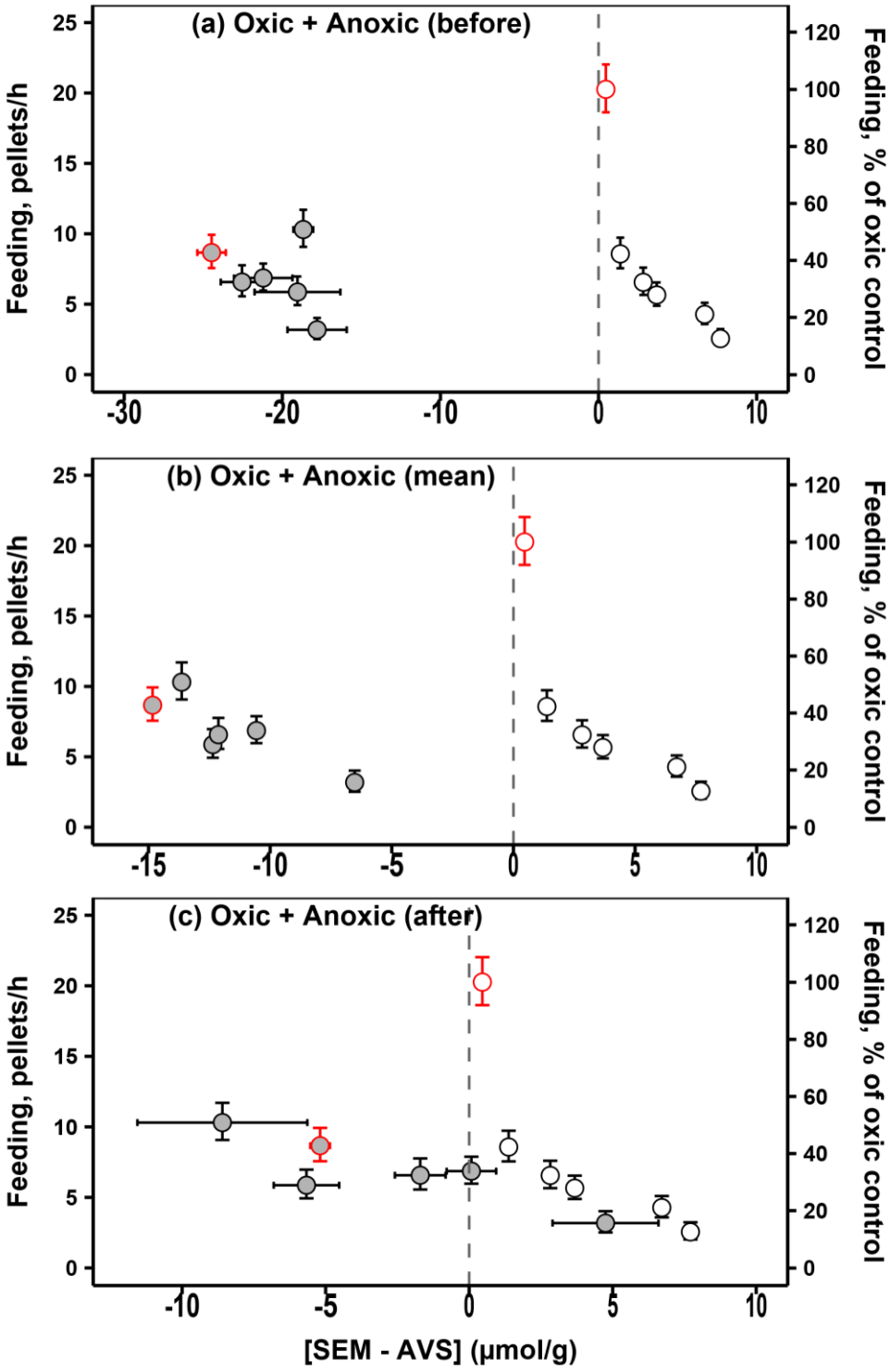

Fig. 5.13: In-exposure feeding rate, as measured by egestion rate (mean ± 95% CI), of *P. ulvae* exposed to spiked oxic (open symbols) and anoxic (filled symbols) sediments for 24 hrs in relation to [SEM Cu – AVS] concentration (mean ± SE). Red symbols represent control exposures. Anoxic mean values represent time-averaged [SEM Cu – AVS] concentrations. Dashed line represents [SEM – AVS] = 0, below which Cu is not expected to be toxic, according to the EqP model (Di Toro *et al*., 2005). EC 10, 20, & 50 provided in Table 5.3

5.4 Discussion

5.4.1 Assay and endpoint sensitivity

Feeding rates of *P. ulvae* can be affected by a range of factors, including sediment grain size, sediment organic carbon content, day/night regime, salinity, temperature, and snail density (Levinton, 1979; Barnes, 1986, 2001, 2006; Blanchard *et al*., 2000; Shipp & Grant, 2006; Krell *et al*., 2011), all of which can potentially affect test sensitivity. In the current study, exposing equal numbers of snails to similar sediments at constant temperature helped to limit confounding effects of most of these factors. Where the literature was conflicting, preliminary experiments helped to determine optimal test conditions. The current study corroborates Krell and co-workers' observation of snail preference for feeding in darkness (c.f. Orvain & Sauriau, 2002; Barnes, 2003; Pascal *et al*., 2008). This feeding preference appears to be linked to snail activity, as snails have been found to be more active at night than in daylight (Barnes, 1986; c.f. Orvain & Sauriau, 2002). The current study maximised sediment exposure by removing overlying water, thus limiting the climbing and floatation behaviour usually associated with submerged snails (Barnes, 1981). The current study also showed the positive association of feeding rate with snail size. Lastly, the current study showed the strongly negative influence of anoxia, an important factor to be considered in AVS-manipulating toxicity tests involving deposit feeders.

In-exposure feeding proved to be significantly more sensitive than post-exposure feeding, with an EC_{50} of 1.7 µmol/g versus an estimated 10.9 µmol/g total Cu using oxic sediment exposures. An EC_{50} of 1.7 µmol/g (108 µg/g) agrees with Shipp and Grant's (2006) observation of feeding depression at Percuil River, the least contaminated site within the Fal estuary with similar total concentration (108 – 150 µg Cu/g in the current study; Chapter 2). The lack of effect levels for SEM Cu is possibly linked to the high feeding depression observed at the lowest test concentration (> 50% decrease at 2 µmol Cu/g). As a result, effect concentrations reported in this study should be interpreted with caution.

Previous studies attribute the loss in post-exposure sensitivity to physiological recovery upon removal of the toxic stressor (McWilliam & Baird, 2002; Krell *et al*., 2011). This recovery can be minimised by conducting the initial gut clearance phase in experimental overlying water (Krell *et al*., 2011). Recovery may, therefore, have been accelerated in this study by exposure of snails to clean ASW, which was necessary for the unhindered quantification of in-exposure feeding rates. However, post-exposure feeding might remain a

useful endpoint for *in-situ* monitoring in wide-ranging site conditions (McWilliam & Baird, 2002; Baird *et al*., 2007; Krell *et al*., 2011). An additional importance of post-exposure feeding in the current study was in distinguishing feeding avoidance – as seen in the AVS-only manipulations – from actual toxicity of ingested metal-spiked sediments, which was observed to persist post-exposure.

Beyond the reduced sensitivity, it is important to note another drawback of post-exposure feeding quantification in *P. ulvae*. It was observed in the current study that although egestion of faecal pellets was discontinued within 2 hrs of transfer into ASW upon post-exposure feeding, retransfer of same snails into fresh ASW stimulated a new egestion cycle. Indeed, re-exposure of supposedly gut-cleared individuals to clean ASW continued to stimulate egestion 48 hrs after feeding with sediment. This phenomenon was not observed during in-exposure feeding quantification. It is unlikely to be an effect of coprophagy, which is rare in *P. ulvae* (Levinton, 1979; Lopez-Figueroa & Niell, 1987; Barnes, 2001) and was not observed in this study. Possibly, in-exposure starvation (e.g. in the AVS preliminary experiment) or the conditions of post-exposure feeding (i.e. aged vs clean, submerged sediments) stimulated feeding rates in this study. Also plausible is that snails fed on microorganisms associated with faecal pellets (Levinton & Bianchi, 1981; Lopez & Levinton, 1987; Lopez-Figueroa & Niell, 1987; Pascal *et al*., 2008); although, pellets are not expected to disintegrate in the 2-hr defaecation period (Levinton, 1979). It is further likely that the presumed short gut-retention time in *P. ulvae* is innacurate, hence the wide variation reported in the literature (30 – 40 min by Lopez & Kofoed, 1980; 1 hr by Barnes, 2001; 3 hrs by Pascual & Drake, 2008; 2 hrs by Krell *et al*., 2011). Nevertheless, quantification of post-exposure feeding based on a fraction of egested sediment may bias conclusions.

5.4.2 Dietary toxicity of Cu to P. ulvae

Dietary uptake is an important route of metal exposure for many aquatic organisms, including benthic invertebrates (Lee *et al*., 2000a; Wang, 2013b). For *P. ulvae*, dietary accumulation of Cd and CdS-nanoparticles has previously been documented (Sokolowski *et al*., 2004; Khan *et al*., 2013); however, the link to toxicity had not been shown. DeForest and Meyer (2015) in their recent review linking dietary uptake to Cu toxicity in aquatic organisms observed that water-only toxicity often exceeds (a combined water and) dietary toxicity, concluding that water-only effect thresholds are protective against diet-borne toxicity at field sites. However, (i) most of the reviewed studies involved pelagic species,

and (ii) the high ratio of dissolved to dietary metal exposure concentrations used may not reflect actual field conditions.

In the current study, the dietary toxicity of Cu to the deposit-feeding mudsnail, *P. ulvae*, was demonstrated by exposing individuals to aged sediments at environmentally-realistic concentrations. A significant depression of feeding was observed in spiked, oxic sediments after 24 hrs of exposure, despite dissolved Cu concentrations remaining within the 48-hr water-only EC_{20} in all treatments. Even at the lowest oxic sediment treatment, with similar dissolved Cu as the control group, mudsnail feeding rate was reduced by more than 50%. Feeding depression in exposed snails continued post-exposure, suggesting that the toxic response must have been elicited by the ingestion of contaminated sediments rather than mere avoidance. The results show that dietary metal uptake through sediment ingestion is primarily responsible for metal toxicity in *P. ulvae* and can occur at concentrations below water-only thresholds.

Modelling dose-response relationships from oxic only as well as the combined oxic and anoxic sediment setups contributed further proof of dietary toxicity in the test species. Feeding rates were best predicted by sedimentary concentrations (Sed Cu and SEM Cu), with flattened curves for the relationships with pore water concentrations. Furthermore, regardless of AVS concentration, there was a convergence of feeding rates in the combined models based on sedimentary concentrations, suggesting that both oxidised Cu and Cu incorporated into sulphides in the anoxic sediments were toxic to *P. ulvae.* These results are in remarkable contradiction to expectations of the EqP model, where metal toxicity is assumed to be related only to dissolved exposures and metal sulphides considered non-toxic (Ankley *et al*., 1996; Di Toro *et al*., 2005; see Section 5.4.4). The current study corroborates previous findings of dietary uptake contributing to overall metal toxicity in some deposit-feeding invertebrates (Strom *et al*., 2011; Campana *et al*., 2012). Both Strom *et al*. (2011) and Campana *et al*. (2012) observed that Cu toxicity to the epibenthic amphipod, *Melita plumulosa*, is best predicted by the organic carbon-normalised total sediment concentration. However, in the current study, test and control sediments were of similar organic carbon content, precluding any confounding effects.

Dietary metal toxicity to *P. ulvae* may explain field observations, for example in Restronguet Creek, England (Sed Cu > 30 µmol/g or 1900 µg/g; PW Cu = 16 – 134 µg/L). In this creek,

dissolved Cu concentrations are below water-only thresholds[51], yet the sediments remain acutely toxic to *P. ulvae* (Shipp & Grant, 2006) and natural populations are absent, despite being present elsewhere within the Fal system (Bryan & Gibbs, 1983; Shipp, 2006). The occurrence of significant dietary toxicity in sensitive deposit-feeding species may require an update of existing SQGs. In this regard, work using the biodynamic model (Luoma & Rainbow, 2005) can the inclusion of dietary metal assimilation in regulatory guidelines. The model has proved useful (e.g. Simpson, 2005; Croteau & Luoma, 2009) in predicting species-specific concentration thresholds for dietborne metal toxicity.

5.4.3 Oxidation of AVS in anoxic sediments during toxicity testing: implications

AVS concentrations dropped from ~32 µmol/g at the start of equilibration to 24.7 µmol/g in the anoxic control sediment after equilibration, indicating slight oxidation during the equilibration process. However, measurable AVS concentrations after equilibration were slightly lower in the spiked sediments (19.5 – 23.8 µmol/g). In addition, PW Cu and SEM Cu remained low, despite being treated at similar concentrations with the oxic sediments. These observations are consistent with the incorporation of Cu from the spike into sulphides. Unlike other divalent metals, Cu and Ni sulphides are poorly soluble in 1 M HCl (Cooper & Morse, 1998; Simpson, 2001). Therefore, only AVS in excess of SEM Cu is usually detectable. The detectable AVS concentration, when present in excess, would depend on the oxidation state (e.g. CuS or Cu_2S) of the metal sulphides formed (Simpson *et al*., 2000), which is indicative of the amount of sulphide used up per unit metal[52].

For the abovementioned reason, extractability of SEM Cu (14 – 30% of Sed Cu) from spiked anoxic sediments in the current study was lower than in the oxic sediments. More Cu was, however, extractable than previously documented in model CuS, prepared by spiking Na_2S with Cu salt, using the same methodology (0.8 ± 0.2%, Simpson, 2001). The higher extractability of Cu in this study might be linked to the presence of Fe(III) phases, possibly as a result of minimal oxidation during the equilibration process. Fe(III) can chemically oxidise Cu sulphides during 1 M HCl extraction, liberating more Cu than would otherwise be expected (Simpson *et al*., 1998).

[51] 96-h LC50 (95% CL) = 549 (438–716) µg/L (Krell *et al.*, 2011); 1890 (790 – 3930) µg/L (Shipp, 2006, using Percuil River populations).

[52] More sulphide, per unit SEM Cu, is used up in the formation of CuS (metal:sulphide 1:1) than Cu_2S (metal:sulphide 2:1) (Simpson *et al.*, 2000).

AVS concentrations decreased significantly during the 24-hr assay period, but remained at least as high as SEM Cu in treatments spiked with less than 8 µmol Cu/g. Accordingly, PW Cu and SEM Cu concentrations were expected to remain low in these setups. Both concentrations were, however, observed to increase consistently, suggesting the existence of oxidised phases within the anoxic sediments. This oxidation of AVS and associated rises in SEM and dissolved metals has been reported in previous toxicity tests involving anoxic sediments (e.g. Di Toro *et al*., 1990; Lee *et al*., 2000a; Simpson *et al*., 2012a). Alongside direct oxygen penetration, significant bioturbation, either as a result of burrowing or foraging can lead to the existence of oxidised microhabitats within seemingly anoxic sediment (Fenchel, 1996; Bertics & Ziebis, 2010), releasing metals previously bound in AVS. Where dissolved concentrations are important for toxicity, bioturbation can lead to gross under-protection of species under the current EqP guidelines (e.g. Remaili *et al*., 2016, 2018). I argue that the unstable nature of AVS in surface sediments or burrows greatly limits its use in setting regulatory limits for metals.

Average PW Cu, except in the 6 µmol/g and 8 µmol/g treatment, remained lower than the 48-hr water-only EC_{20}, and final concentrations in all setups remained lower than the corresponding EC_{50} to *P. ulvae* (Krell *et al*., 2011). This relatively low PW Cu reduces the risk of porewater toxicity in this study. In the 10 µmol/g treatment, final AVS was less than SEM Cu. The high recovery of SEM Cu (70% of Sed Cu), despite measurable AVS, further supports the existence of oxidised microhabitats. Lower PW Cu in the 10 µmol/g than the 8 µmol/g treatment may be explained by the precipitation of dissolved metals in oxidised Fe(III) phases (Vidal-Dura *et al*., 2018). Overall, time-averaged concentrations of SEM and AVS (Figure 5.13b) in this study suggest that all treatments remained considerably anoxic, at least, mid-way through the experiment. However, the exposure of snails to oxidised sediments cannot be ruled out.

5.4.4 Has the EqP model (SEM-AVS) outlived its usefulness?

Prediction of metal (non-)toxicity in the EqP model is dependent on porewater concentrations, which are believed to be in equilibrium with particulate exposures (United States Environmental Protection Agency [USEPA], 2005; Di Toro *et al*., 2005; Burgess *et al*., 2013). According to Di Toro and colleagues (2005):

> …it is assumed that there is no additional exposure due to transformations of the metal in the gut of sediment-ingesting organisms, or via exposure to contaminated food… If sediment processing in the gut changes the chemical form of the metal, then EqP no longer applies…

However, the current study has shown that in the deposit-feeding mudsnail, *P. ulvae*, metal toxicity is primarily through sediment ingestion (Section 5.4.2). I have reported significant feeding depression (> 50% versus control) in sediments with dissolved Cu lower than conservative water-only thresholds, including at the lowest exposure concentration with similar dissolved Cu to the control group. Feeding depression in this species has been linked to a depression in long-term growth rates in the field (Shipp & Grant, 2006), therefore this constitutes an important ecological effect. The results have also been helpful in explaining mudsnail mortality and absence in a contaminated creek (Section 5.4.2), despite porewater concentrations less than half the acute water-only thresholds.

In anoxic sediments, the EqP predicts the absence of toxicity in excess AVS, and Cu bound in sulphides is not expected to elicit toxicity (Ankley *et al*., 1996; Burgess *et al*., 2013). Modifications based on OC content (Di Toro *et al*., 2005) do not apply to the current study as all test and control sediments had similar TOC content (Table A5.1 a & b). As in previous experiments (e.g. Di Toro *et al*., 1990; Simpson *et al*., 2012a), I observed significant oxidation of AVS in the anoxic setups, with concentrations depleted below SEM Cu in the two highest treatments. Applying time-averaged SEM and AVS concentrations (e.g. as done by Di Toro *et al*., 1990), the EqP fails to predict (non-)toxicity in all the treatments. When final concentrations are used (Figure 5.13), the EqP also fails to predict (non-)toxicity, especially in the 4 µmol/g treatment, where there is a significant depression in feeding rate despite similar SEM – AVS concentration with the control group. I note the existence of oxidised microhabitats within the treatments, as observed in field sediments (Section 5.4.3). However, porewater concentrations in most treatments remained within conservative thresholds and poorly predicted feeding depression in comparison with sedimentary metals (Figure 5.11). Indeed, the model fits for the combined oxic and anoxic sediment exposures show a convergence in feeding rates regardless of AVS concentration, suggesting that both sedimentary Cu and Cu sulphides are toxic to the deposit-feeding *P. ulvae*.

As enumerated above, my observations contradict tenets of the EqP model. Similar departures from porewater-based predictions have previously been reported for deposit

feeders. Notably, Lee *et al*. (2000a) observed significant bioaccumulation of metals by a range of benthic invertebrates, despite exposure in excess AVS. They argued that sediment ingestion was primarily responsible for metal exposure in the organisms. Gerald Ankley (1996) in his review also noted the "…linear accumulation of metals with increasing sediment metal concentrations irrespective of the metal/AVS ratio". Furthermore, De Jonge *et al*. (2009) confirmed the accumulation of metals by *Tubifex tubifex* and *Chironomus gr. thummi* in excess AVS and low porewater concentrations. Within oxidised sediments, Campana *et al.* (2012) showed significant depression in reproduction of the deposit-feeding amphipod, *Melita plumulosa*, at porewater concentrations less than water-only thresholds. The exact mechanism for the bioavailability of sedimentary metal sulphides remains unclear and has been reviewed extensively by Griscom and Fisher (2004). They confirm that the gut fluid of marine molluscs can effectively desorb metals bound in AVS and Fe-oxide, suggesting the digestive assimilation of metals in this taxon. I note that bioaccumulation is not a toxic endpoint, hence not predictable by the EqP (Di Toro *et al*., 2005; USEPA, 2005). However, my results, using *P. ulvae*, can serve as a critical link between the bioavailability of metals in sulphidic sediments and their toxicity to sediment ingesters.

Is it, therefore, time to re-evaluate the EqP model? Alternatively, has the model outlived its usefulness? These are key questions to be answered by the regulatory community in line with specific environmental protection goals (e.g. Brown *et al*., 2017 for Europe). My results add to the increasing body of evidence on the need to incorporate dietary toxicity in the development of aquatic guidelines (Wang, 2013b). The exposure of invertebrates to oxic microhabitats within seemingly anoxic sediments is now well-documented (Remaili *et al*., 2016), further complicating application of the EqP model in field sediments. Even where dissolved metals are critical for toxicity, we know that the existence of other phases, especially iron (oxy)hydroxides, may limit the predictive capability of the EqP (Di Toro *et al*., 2005). Indeed, the development of more sophisticated passive-samplers (Chapters 1 & 3; Peijnenburg *et al*., 2014) and chelation techniques (Chapter 2; Bowles *et al*., 2006) – both of which allow for metal speciation – may favour the direct assessment of porewater over complex models. Considering the multiplicity of metal exposure routes, my results support the conclusion (Simpson & Batley, 2007) that a "one-size-fits-all" approach to sediment regulation is inappropriate.

Chapter 6.

Metal remobilisation in redox fluctuations from sediments of the Fal and Hayle estuaries

6.1 Introduction

Estuaries are highly dynamic systems. Within the intertidal zone, continual disturbances such as bioturbation and tidal flooding may lead to the resuspension of anoxic, sub-surface sediments and the burial of oxidised, surface sediments (Aller, 1994; Cantwell *et al*., 2002; Vidal-Dura *et al.*, 2018). These disturbances are exacerbated by the presence of burrowing organisms, which tend to create oxidised conditions within their burrows in otherwise anoxic sediments (Forster, 1996; Gallon *et al.*, 2008). The overall result is the cyclic reduction of oxidised or sub-oxic sediments and the oxidation of anoxic sediments (Aller, 1994) – redox fluctuations which may have implications for the fate of potentially-toxic metals and, thus, metal exposure to benthic fauna (Simpson *et al.*, 2012a; Remaili *et al.*, 2016, 2018).

The reduction of oxidised sediments is driven by microbial respiration, with microbes using oxygen as an electron acceptor in oxic conditions and then using a range of other electron acceptors when free oxygen is depleted. Metals in oxic sediments are primarily bound in organic carbon and in Fe(III) and/or Mn(IV) phases – mainly as (oxy)hydroxides (Di Toro *et al.*, 2005). Within anoxic environments, Fe and Mn (oxy)hydroxides can act as electron acceptors in the oxidation of reduced species or the metabolism of organic carbon by anaerobes (Forstner, 1995; Lovley *et al*., 2004; Raiswell & Canfield, 2012). The dissimilatory reduction of Fe(III) and Mn(IV) is expected to remobilise Fe(II), Mn(II), as well as potentially-toxic metals hitherto bound. Although still debated in the literature and subject to sediment physicochemical characteristics (Bethke *et al.*, 2011), the dissimilatory reduction of electron acceptors is widely accepted to proceed in order of decreasing energy generation: $O_2 > NO_3^- \geq$ Mn(IV) > Fe(III) > SO_4^{2-} (Froelich *et al.*, 1979; Thamdrup & Canfield, 2000). Sustained reduction of oxidised sediments is, therefore, expected to result in the formation of insoluble sulphides (in sulphate-rich sediments, Jorgensen *et al.*, 2019), which immobilise dissolved metals to the solid phase.

The chemistry of anoxic sediment oxidation is well described in the literature. Metals in anoxic sediment layers are bound in highly reduced complexes, especially those which have

been categorised as acid volatile sulphides (AVS). These consist principally of FeS in Fe-rich sediments (Simpson *et al.*, 2000; Di Toro *et al.*, 2005). The displacement of Fe(II) in AVS by divalent metals forms the basis for the equilibrium-partitioning model, already discussed in detail in preceding chapters of this thesis (see Chapters 1 and 5). In extremely reduced conditions, mineral phases such as pyrite (FeS_2) may account for much of metal complexation (Rollinson *et al.*, 2007; Jorgensen *et al.*, 2019). As AVS is readily oxidised, the oxidation of sulphide-rich sediments is expected to remobilise bound metals into the dissolved phase (Saulnier & Mucci, 2000; Simpson *et al.*, 2000; Vidal-Dura *et al*., 2018). Removal of metals from AVS is expected to proceed in order of decreasing metal sulphide solubility: Mn > Fe > Ni > Zn > Cd > Pb > Cu > Ag (Ankley *et al.*, 1996; Rickard & Luther, 2006). This metal remobilisation from anoxic sediments is expected to continue with increase in redox potential, until a redox maximum that that favours the formation, and subsequent precipitation, of Fe(III) and Mn(IV) phases. At this maximum, metals are expected to co-precipitate with or be adsorbed onto Fe and Mn (oxy)hydroxides (Raiswell & Canfield, 2012; Vidal-Dura *et al*., 2018). Sediments differ in their ability to sequester metals from solution, with several factors, including pH and particle size, playing important roles in this process (Saulnier & Mucci, 2000; Vidal-Dura *et al*., 2018).

Studies abound in the literature on the dissimilatory reduction of electron acceptors in marine sediments, seeking to understand key geochemical processes (see review by Raiswell & Canfield, 2012). There are also several studies on metal remobilisation from resuspended anoxic sediments, especially in the prospective risk assessment of dredging works (notably Saulnier & Mucci, 2000). However, only a few studies in the literature have combined both of these processes – particularly in the context of metal exposure to benthic invertebrates. Even fewer investigations have been undertaken on grossly-contaminated field sediments. In this study, the potential remobilisation of Cu and Zn from sediments in the Fal and Hayle estuaries as a consequence of redox fluctuations is investigated by simulating resuspension events under both oxidised and reduced conditions. Key geochemical processes are highlighted and metal remobilisation is discussed in the context of benthic ecotoxicology.

6.2 Methodology

6.2.1 Experimental design

The current study was designed to assess the remobilisation of Cu and Zn, as well as the redox-sensitive metals, Fe and Mn, as a result of redox fluctuations in sediments of the Fal

and Hayle estuaries, Cornwall, England. This was done by suspending a defined mass of sediment in artificial seawater under continual agitation to ensure proper mixing (Gerringa, 1990, 1991). In order to separate metal desorption from exchangeable phases (e.g. Gao *et al.*, 2003) from their remobilisation due to redox changes, both surface and deeper sediments were incubated in oxidised (to air saturation) and reduced (limited oxygen) conditions. Metal concentrations, pH, dissolved oxygen concentration (DO), temperature, and redox potential (ORP) were measured at fixed time intervals in the sediment slurries. It was hypothesised that any additional release of metals in redox transitions – for example in the oxidation versus reduction of anoxic sediments – was due to redox changes in the sediments. Metal remobilisation from eleven sites across the contamination gradient in the Fal and Hayle estuaries was compared with that from the uncontaminated Breydon Water site. All study sites here are the same ones studied in Chapter 2 of this thesis.

6.2.2 Materials and fieldwork

Unlike in the preceding chapters of this thesis, all laboratory wares used in this study were washed in phosphate-free detergent (Decon 90 ®) prior to acid-washing. Acid-washing of wares in 10% v/v HNO_3 and subsequent rinsing in ultrapure water (UPW) was completed as described in Chapter 2.

Fieldwork for this study coincided with the Summer 2019 survey already described in detail in Chapter 2, therefore metal concentrations and sediment physicochemical properties are expected[53] to be similar as detailed therein (summarised in Appendices 6.01 and 6.02 for ease of reference). Briefly, surface (0 - 2 cm) and bottom (5 – 10 cm) sediments were sampled from eleven sites across the contamination gradient in the Fal and Hayle estuaries as well as from the uncontaminated Breydon Water site in Norfolk. Because sediments were sampled by depth and in summer, surface sediments at certain sites were not (fully) oxic, having dark colouration that is typical of reduced Fe sediment phases (Hutchings *et al.*, 2019). Consequently, the term "oxic" in this study refers to surface sediments and not necessarily their redox status. Conversely, deeper sediments sampled were dark and visibly reduced, therefore the term "anoxic" can be interpreted in terms of the sediment redox status. Sediments were transported to the laboratory within two days of sampling.

[53] Sediment physicochemical properties were assessed following fieldwork, as described in Chapter 2, and may have changed slightly in the storage period prior to the start of the current study.

6.2.3 Preparation of sediment samples and artificial seawater

The incubation of oxic and anoxic sediments was completed at different times – treated here as different experiments[54]. Incubation experiments were started within two months of sediment sampling. In the intervening period, sediments were preserved by refrigerating in darkness at 4 ^{o}C. Anoxic sediment samples were double-bagged with a layer of anoxic sediment in-between to limit oxidation. For both experiments, final sediment samples used were collected from the middle of the storage bags, homogenised, press-sieved[55] to <2mm to remove any gravel, and weighed into acid-washed 250 mL Nalgene HDPE bottles. Anoxic sediments were processed in a glove bag (Sigma-Aldrich AtmosBag) filled with N_2 gas.

For each of the twelve study sites in both experiments, 10 g of sediment (dry weight equivalent) was weighed in triplicates and in two batches – to be incubated concurrently in oxidised (henceforth, oxic) and reduced (henceforth, anoxic) conditions. For the twelve sites, this yielded a total of 72 individual samples per experiment, taking about 6 -7 hrs to weigh. In the intervening period between weighing and commencement of the experiment, sediment samples for the oxic experiment were covered with lids in the HDPE bottles and refrigerated at 4 ^{o}C. Sediment samples here were deliberately not stored in an anoxic atmosphere to prevent dissimilatory reduction of oxidised phases during the storage period. The storage conditions, however, meant that certain samples may have been further oxidised prior to the actual incubation. By contrast, sediment samples for the anoxic experiment were covered with lids and additionally double-bagged in N_2 gas atmosphere, using 20 L plastic bags, prior to refrigeration. It is therefore likely that sediments here may have been further reduced prior to the actual incubation. These storage conditions were necessary in order not to compromise the experimental design by oxidising anoxic sediments and/or reducing oxic sediments. The results should, therefore, be interpreted bearing in mind this nuance.

Artificial seawater (ASW) for the incubation experiments was prepared according to Kester *et al.* (1967) to more accurately reflect natural seawater composition. The ASW was diluted

[54] The two experiments were the incubation of "oxic" and anoxic sediments. Within each experiment, sediment samples were incubated in both oxidised and reduced conditions.

[55] Press-sieving was done using a stainless steel sieve, applying pressure through an acid-washed plastic bag.

to 30 S, using UPW, to match the average salinity across the study sites[56] and, subsequently, refrigerated at 4 ^{o}C in the dark until use. Prior to sediment incubation, prepared ASW was allowed to adjust, for 24 hrs, to laboratory temperature: 22 ± 1 ^{o}C for both oxic and anoxic sediment incubations. An aliquot of seawater, separated for sediment incubations in anoxic condition, was bubbled with N_2 gas for 3 hrs to deplete dissolved oxygen. The pH[57] was then adjusted to 7.5 by dropwise addition of 1 M HCl.

6.2.4 Sediment incubation and slurry sampling

To begin incubation experiments, 200 mL of ASW was added to weighed sediment samples in the HDPE bottles to give a solid:solution ratio of 1/20 g/mL – similar to 1/17 g/mL (Gerringa, 1991) and 1/25 g/mL (Saulnier & Mucci, 2000) used in previous studies. The sediment-seawater mixture was agitated, by hand, to form a slurry. Replicates for each study site, for incubation in both oxic and anoxic conditions, were started at the same time in the order in which they were weighed. Sediment incubations in anoxic condition were carried out in a glove bag filled with N_2 gas. The setups were covered with plastic lids and maintained in suspension on a mechanical shaker at 120 rpm. For incubations in oxic condition, the lid of the HDPE bottles was replaced with an acid-washed foam bung to allow gas exchange with the atmosphere but exclude dust (Vidal-Dura *et al.*, 2018).

Sediment slurries were sampled at defined time intervals to assess physicochemical characteristics: 0, 2, 5, 9, and 12 days (288 hrs) for oxic sediment incubations and 0, 0.5, 5, 50 and 250 hrs for anoxic sediment incubations[58]. To achieve this, individual replicates were agitated vertically, by hand, for a few seconds, and 30 mL of slurry was drawn using a plastic syringe. Given the prior agitation, it was assumed that samples were representative of the sediment slurry and had the same solid:solution ratio (Saulnier & Mucci, 2000).

---

[56] This represents salinity measured from surface sediments in Autumn 2017. The salinity of surface sediments in Summer 2019 (25.2 – 43.2) was possibly exaggerated as a result of evaporation due to high temperatures at low tide when the sediments were sampled. Porewater from anoxic sediments was insufficient to measure salinity.

[57] Porewater pH across the study sites in Summer 2019 was 7.00 – 7.42, except in Breydon Water (8.04; see Table 2.01 for details).

[58] Sampling at Timepoint 0 was done in the first minute of ASW addition following agitation by hand. Anoxic sediment incubations were sampled in logarithmic timescales to exhaustively assess metal release, as in previous studies (e.g. Vidal-Dura *et al.*, 2018).

6.2.5 Assessment of the physicochemical characteristics of sediment slurries

Sampled slurries were filtered to <0.45 µm (Fisherbrand PES syringe filters) directly into centrifuge tubes for metal analysis. Slurry pH, temperature, and ORP were determined in unfiltered replicate samples. DO was measured in composite samples, combining all triplicates to generate sufficient volume. At the end of the experiments, salinity of sediment slurries was determined as a proxy for evaporation in the oxidised incubations. It was assumed that, given the conditions of incubation, evaporation would be negligible in the slurries incubated in anoxic condition, hence salinity would remain (fairly) constant therein. Therefore, the relative increase in salinity of the setups incubated in oxic conditions was attributed to moisture loss due to evaporation. An assessment of evaporation was important to isolate metals purely due to the concentration of analytes during the experiment.

Measurement of metal (Cu, Zn, Fe, and Mn) concentrations in filtered samples was done by Inductively Coupled Plasma – Optical Emission Spectrometry (ICP-OES) analysis, after separation from the seawater matrix using chelating resin (as detailed in Chapter 2). Methods for the measurement of salinity, pH and ORP using calibrated electrodes are as detailed in Chapter 2. ORP is reported as standard hydrogen potential (Eh), converted using manufacturer-supplied half-cell potential and temperature coefficient. The temperature was measured using combined temperature and pH electrodes fitted to the Mettler Toledo (SevenEasy S20) pH meter. DO was measured using the HANNA HI 9146 microprocessor DO meter, with gentle stirring. The device was calibrated according to the manufacturer's instructions and adjusted for altitude and sample salinity.

Total dissolved Fe and Fe(II) concentrations were additionally measured using the Ferrozine (Fz) method, in the presence and absence, respectively, of hydroxylamine hydrochloride as reducing agent (Stookey, 1970). 1 mL of slurry samples were originally added to 4 mL of 1 g/L Fz solution prepared in 50 mM HEPES buffer matrix (Thamdrup *et al.*, 1994; final Fz concentration of 1.56 mM). However, this method was not sensitive enough to detect Fe concentrations in preliminary trials conducted on the reduction of oxic sediments. Reduction of the final Fz concentration to 0.1 mM (30 µL of 10 mM Fz in 3 mL sample) was necessary to measure down to 0.5 µM Fe (27.9 µg/L) in samples (see calibration plots in Figure A6.03). However, the maximum detectable concentration of the modified method was 30 µM Fe (1674µg Fe/L), which was a significant limitation of the Fz method in this study.

Calibration standards for the Fz method were prepared from ammonium Fe(II) sulphate hexahydrate in a matrix of 4 g/L hydroxylamine hydrochloride and 50 mM HEPES buffer. Recovery of the method was assessed by measuring triplicate samples of a known (21.58 µM or 1204 µg/L; determined by ICP-OES) Fe solution prepared from a single-element calibration standard (PlasmaCAL). Recovery of this solution was 103.6 ± 2.6%, confirming that the Fz method was in agreement with ICP-OES analysis for solutions in a clear matrix.

6.3 Results

For clarity, results of the two incubation experiments have been separated in this section.

*6.3.1 Results of the **anoxic sediment** incubations*

6.3.1.1 Accuracy of the Ferrozine method in anoxic sediment slurries

Although recovery of the Fz method was within 5% of ICP-OES concentration for an Fe solution prepared in UPW matrix, concentrations measured in the sediment slurries were overestimated by up to 50% (Figure 6.01). There was, however, a strong relationship between Fe concentrations measured by both methods, up to the maximum quantifiable limit of the Fz method (30 µM; 1674 µg/L). As expected, this relationship was stronger for total Fe concentrations than for Fe(II), given that the ICP-OES (chelation) procedure measures total metal concentrations in the samples.

For a typical anoxic sediment (from St Just, SJ, but applicable across the study sites), remobilisation of Fe(II) and total Fe (measured by both methods) with incubation time is shown in Figure 6.02. Nearly all of the Fe released in the setups was present in the reduced form (Fe^{2+}, rather than Fe^{3+}). There was also a consistent trend across all three measures of Fe. Consequently, the discussion in the following sections shall be limited to total Fe concentrations measured using ICP-OES. The results should be interpreted with caution, bearing in mind this nuance. Plots involving total Fz Fe and Fe^{2+} are provided as appendices.

6.3.1.2 Physicochemical properties of anoxic sediment slurries

The typical trend in DO, Eh, and pH of anoxic sediment slurries incubated in both oxic and anoxic conditions is shown in Figure 6.03. As expected, incubation of sediment in oxic conditions led to an increase in DO, resulting in a simultaneous rise in Eh. The marked increase in both DO and Eh measured at timepoint 5 hrs suggests that much of the reduced species in the slurries were consumed within the first 5 hrs of exposure to atmospheric

oxygen. For SJ sediments, shown in Figure 6.03, DO and Eh at the start of incubation were 0.44 mg/L and 157 mV, respectively, rising to 4.39 mg/L and 526 mV after 250 hrs of incubation in oxic conditions. In contrast, incubation in anoxic conditions led to a decrease in both DO (0.44 – 0.12 mg/L) and Eh (157 – 127 mV). The decline in both DO and Eh values was noticeable within 30 mins of incubation, confirming that oxygen was, indeed, limited in the anoxic experimental setups.

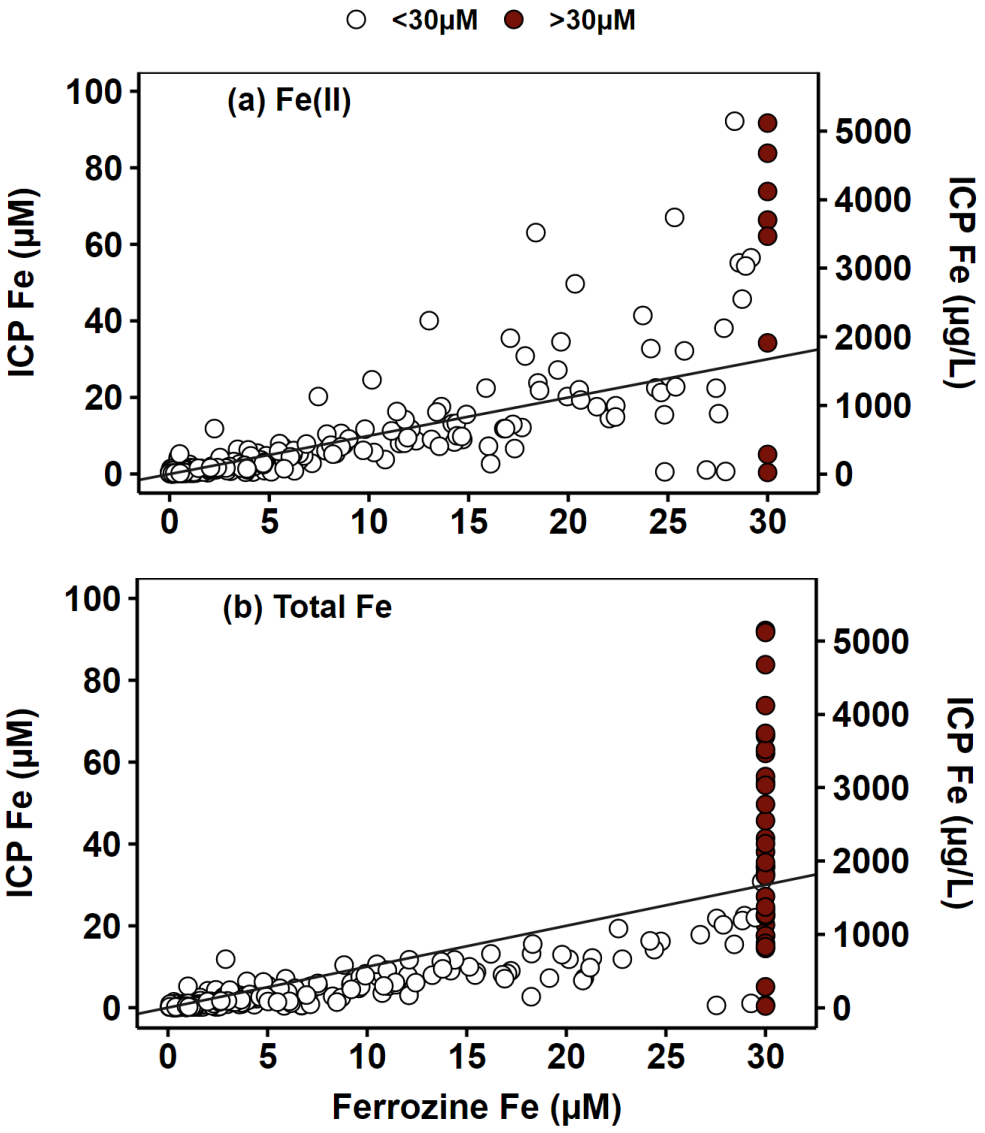

Fig. 6.01: Relationship of total Fe measured by ICP-OES with Ferrozine-labile Fe(II) (panel a) and Ferrozine-labile total Fe (panel b) in ***anoxic sediment*** incubations (all mean values). Filled dots represent Ferrozine measurements ≥ 30 µM (1674 µg/L), which is the method maximum. ***Diagonal line represents a 1:1 relationship***, where Ferrozine Fe = ICP Fe

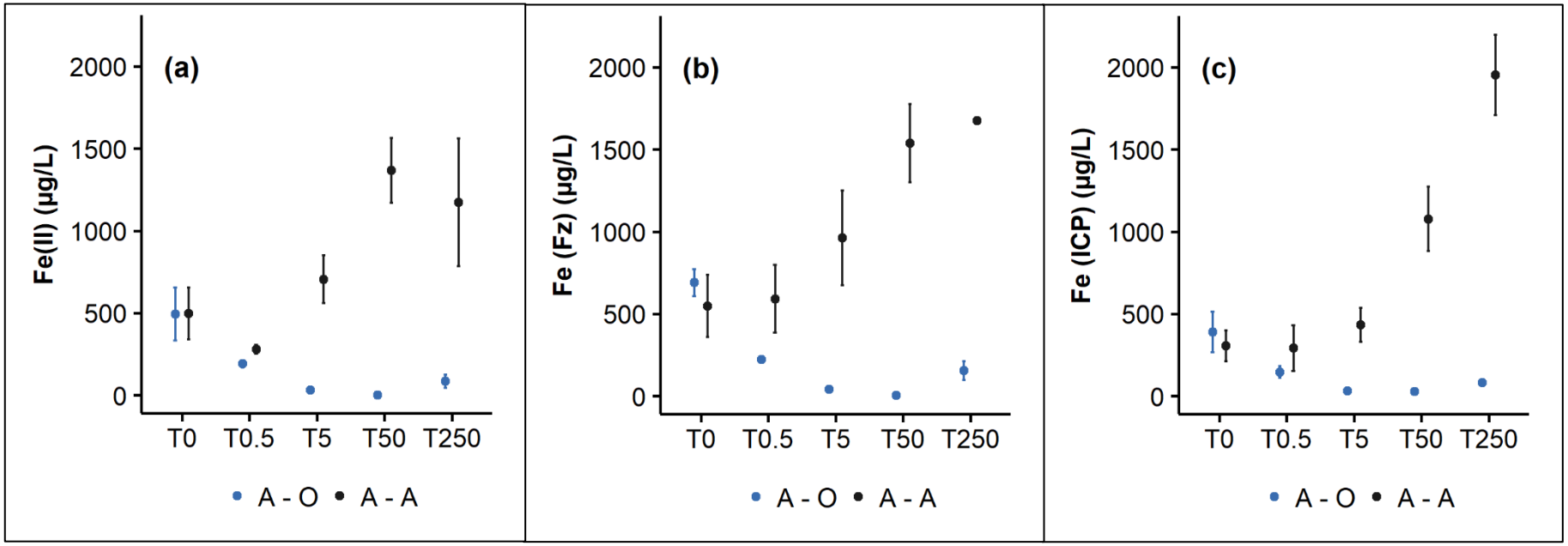

Fig. 6.02: Typical trend in Fe concentrations (mean ± SD) measured during ***anoxic sediment*** incubations: Ferrozine-labile Fe(II) (panel a) and total Fe (panel b) as well as total Fe measured by ICP-OES (panel c). Concentrations represent measurements for St Just sediment. Maximum Ferrozine range = 1674 µg/L. A – O (blue): Anoxic sediments incubated in oxidised conditions. A – A (black): Anoxic sediments incubated in anoxic conditions. T0, 0.5, 5, 50, and 250 represent sampling at timepoints 0, 0.5, 5, 50, and 250 hrs of incubation

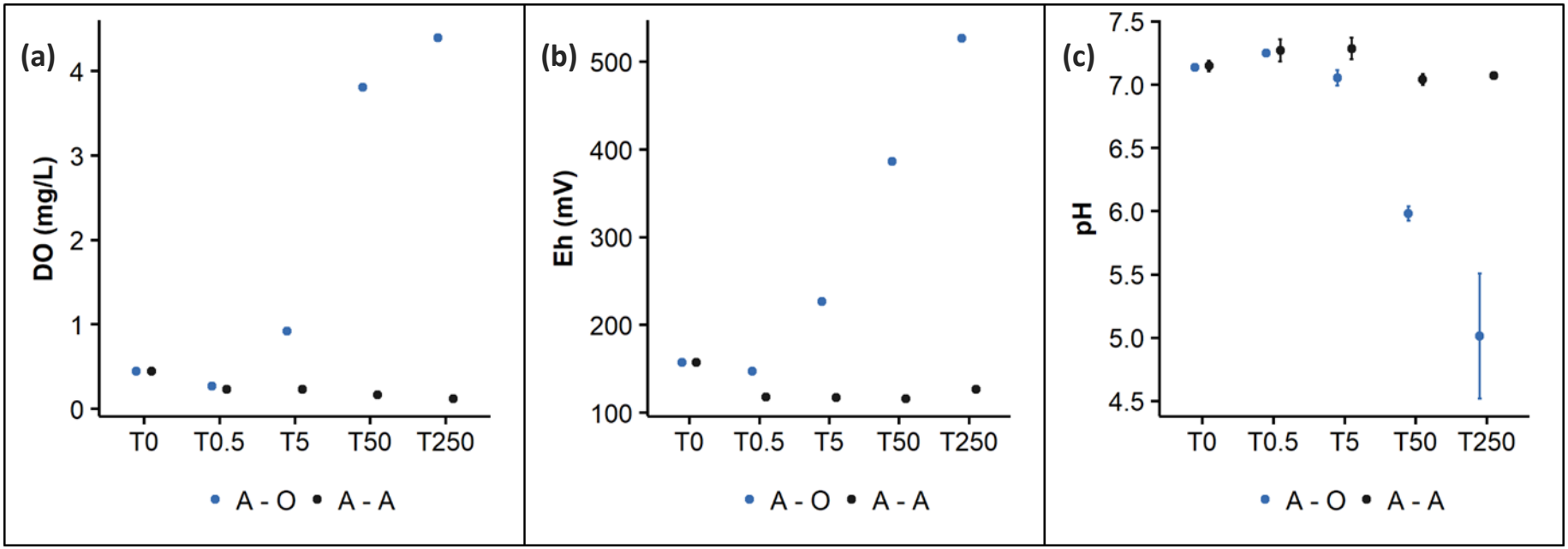

Fig. 6.03: Typical trend in dissolved oxygen concentration (panel a), redox potential (panel b) and pH (panel c) (all mean ± SD) measured during ***anoxic sediment*** incubations. Values represent measurements for St Just sediment. Trend in pH here is typical for all sites, except in Hayle (HA and HB). A – O (blue): Anoxic sediments incubated in oxidised conditions. A – A (black): Anoxic sediments incubated in anoxic conditions. T0, 0.5, 5, 50, and 250 represent sampling at timepoints 0, 0.5, 5, 50, and 250 hrs of incubation

Study sites were divided in two groups based on the trend in pH with incubation time. For all sites, except at Hayle (HA and HB), pH remained fairly stable in slurries incubated in anoxic conditions (Figure 6.03c). But the oxidation of anoxic sediments led to a sharp decline in pH (7.1 – 5.0) after 5 hrs of incubation, suggesting that this decline is linked to the removal of reduced species in the slurries. By contrast, the oxidation of anoxic Hayle sediments led to a consistent increase in pH (up to 0.3 units; Figure 6.04). The trend of pH in anoxic conditions was similar to those in the Fal and BW, varying by ~ 0.15 units after 250 hrs.

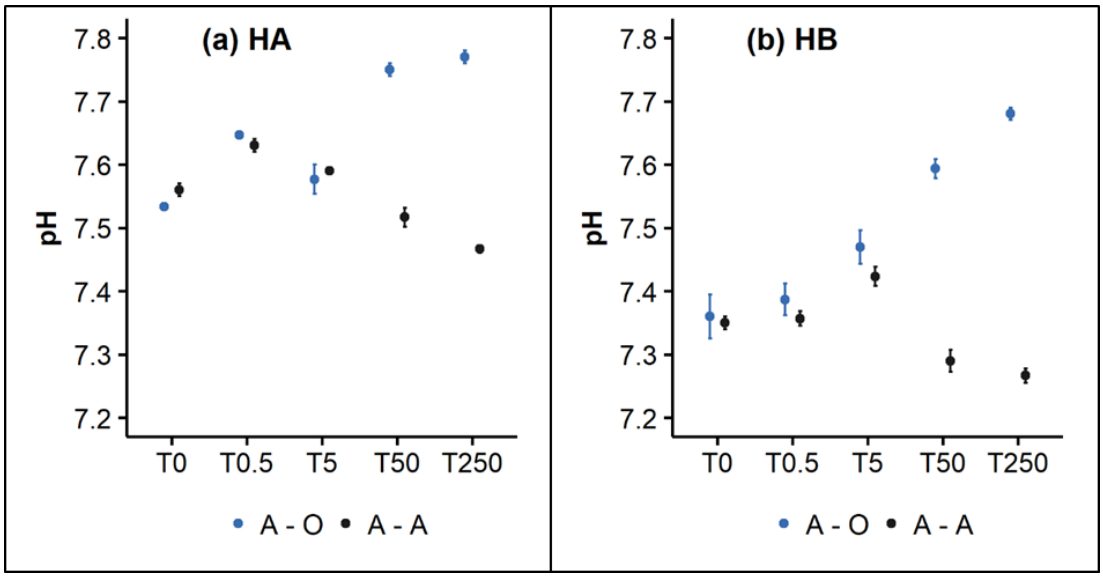

Fig. 6.04: Trend in pH (mean ± SD) of HA (panel a) and HB (panel b) sediment slurries in the ***anoxic sediment*** incubations. A – O (blue): Anoxic sediments incubated in oxidised conditions. A – A (black): Anoxic sediments incubated in anoxic conditions. T0, 0.5, 5, 50, and 250 represent sampling at timepoints 0, 0.5, 5, 50, and 250 hrs of incubation

Combined sites plots of DO, Eh, and pH in anoxic sediment incubations confirm the general pattern described in the preceding paragraph (Figures 6.05 – 6.09). For incubations in oxic conditions, the highest DO concentration after 250 hrs of incubation was measured in HA (5.2 mg/L) and the lowest, at Cowlands (CO, 3.6 mg/L). There was, however, a slight increase in DO (~ 1.5 mg/L) for HA and Helford River (HR) sediments maintained in anoxic conditions, possibly due to some leakage of oxygen into the system.

The increase in Eh with time was well correlated with DO (Figures 6.06 & 6.07). For sediments incubated in oxic conditions, the highest increase in Eh was observed in

Restronguet C (RC, 439 mV relative to starting Eh) and the lowest, in HA and HR (118 mV and 140 mV, respectively, relative to starting Eh). Despite incubation in anoxic conditions, Eh, like DO, increased by up to 100 mV in certain sites, especially in HA and HR. There was a wide range in actual redox potentials at the commencement of incubation (109 – 349 mV; Figure A6.04), which was negatively correlated with Fe^{2+} ($r = -0.62$, $p = 0.03$) and sediment AVS (albeit, correlation not significant: $p = 0.54$) concentrations (Figures A6.05a & b). However, regardless of the starting potential, peak Eh for all sites, except Hayle, clustered around 500 mV after 250 hrs of oxidation. This suggests that the maximum possible redox potential in fine sediments of the Fal and Breydon Water estuaries is about 500 mV. For HA and HB sediments, regardless of starting redox potential, the maximum possible redox potential in Hayle sediments appear to be about 400 mV. This confirms that the Hayle sediments are geochemically distinct from those in the rest of the study sites.

Combined site plots of pH in anoxic sediment incubations are provided in Figures 6.08 and 6.09, also confirming the trend highlighted earlier. The pH at the start of incubation ranged between 7.5 (in both Hayle sites) and 6.90 at CO. Slurry pH remained fairly constant for incubations in anoxic conditions, slightly dropping to 6.4 and 6.3, respectively, for CO and BW. Conversely, pH in of sediments incubated in oxic conditions dropped drastically with time and redox potential for all sites except in Hayle (Figures 6.08 & 6.09). Terminal pH ranged between 4.5 and 5.0 for most Fal sites and BW, except in the upper Restronguet Creek (RA = 5.7, RB = 5.5). These sites had relatively high AVS (13.4 – 61.5 µmol/g) and low carbonate[59] (CaO = 0.35 – 1.39%, except BW = 8.0%) concentrations in the sediments (Table A6.2). For HA and HB, with relatively low AVS (6.4 & 10 µmol/g, respectively) and high carbonate (CaO = 5.65 & 6.79%, respectively) in sediment, the terminal pH was ~7.8.

The salinity of sediment slurries after 250 hrs confirm considerable evaporation from setups incubated in oxic conditions (Figure 6.10). Differences in salinity between oxidised and reduced anoxic sediments ranged between 4.5% in HA and 13.5% in BW. Therefore, both the sediment:solution ratio and metal levels in these setups may have increased simply due to evaporation over time. The subsequent sections should be interpreted bearing this nuance in mind.

[59] See Figure 6.39 and Equation 9 for relationship between CaO and carbonate

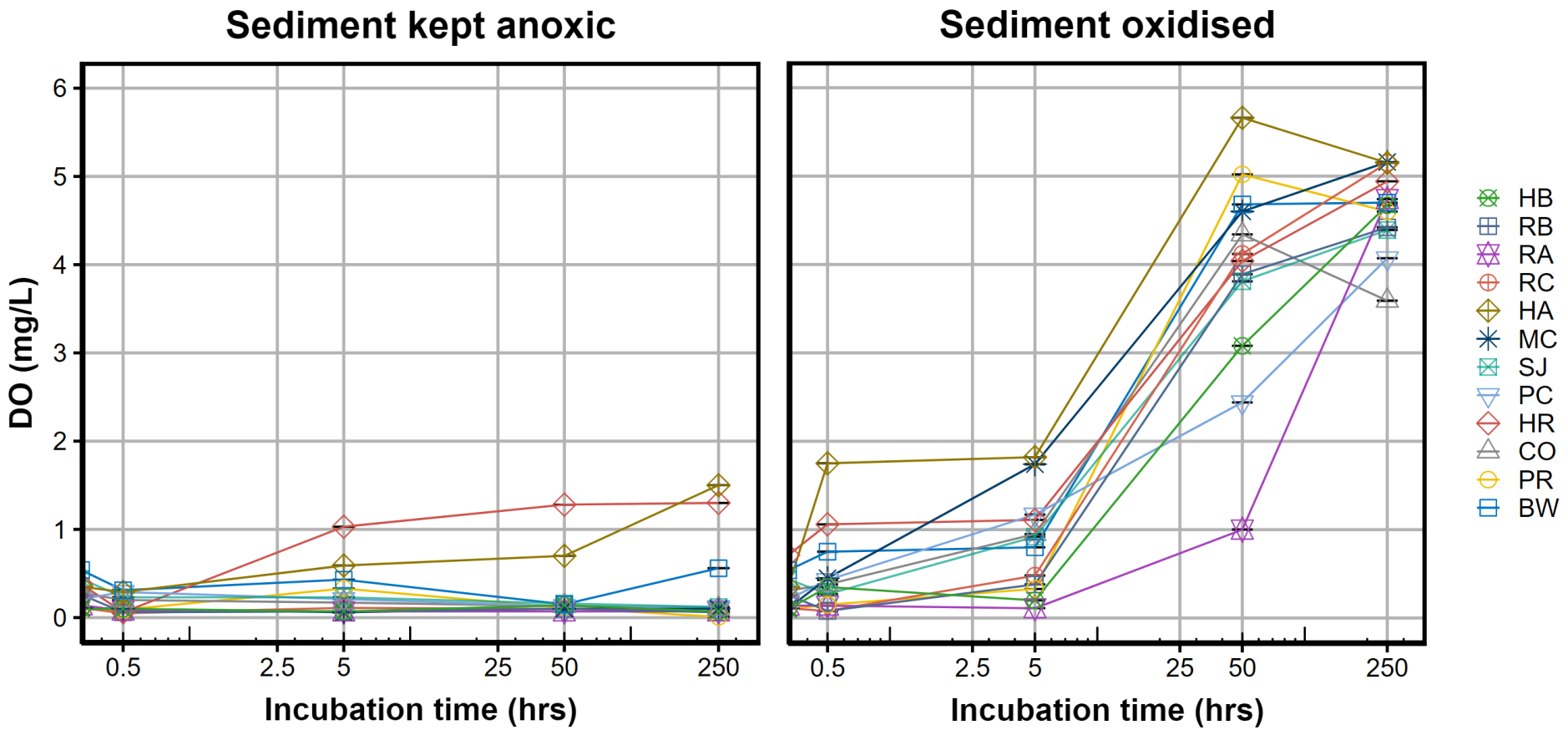

Fig. 6.05: Variation of dissolved oxygen (mean ± SD) with time in ***anoxic sediment*** incubations across the study sites. Left hand panel = sediments incubated in anoxic conditions. Right hand panel = sediments incubated in oxic conditions

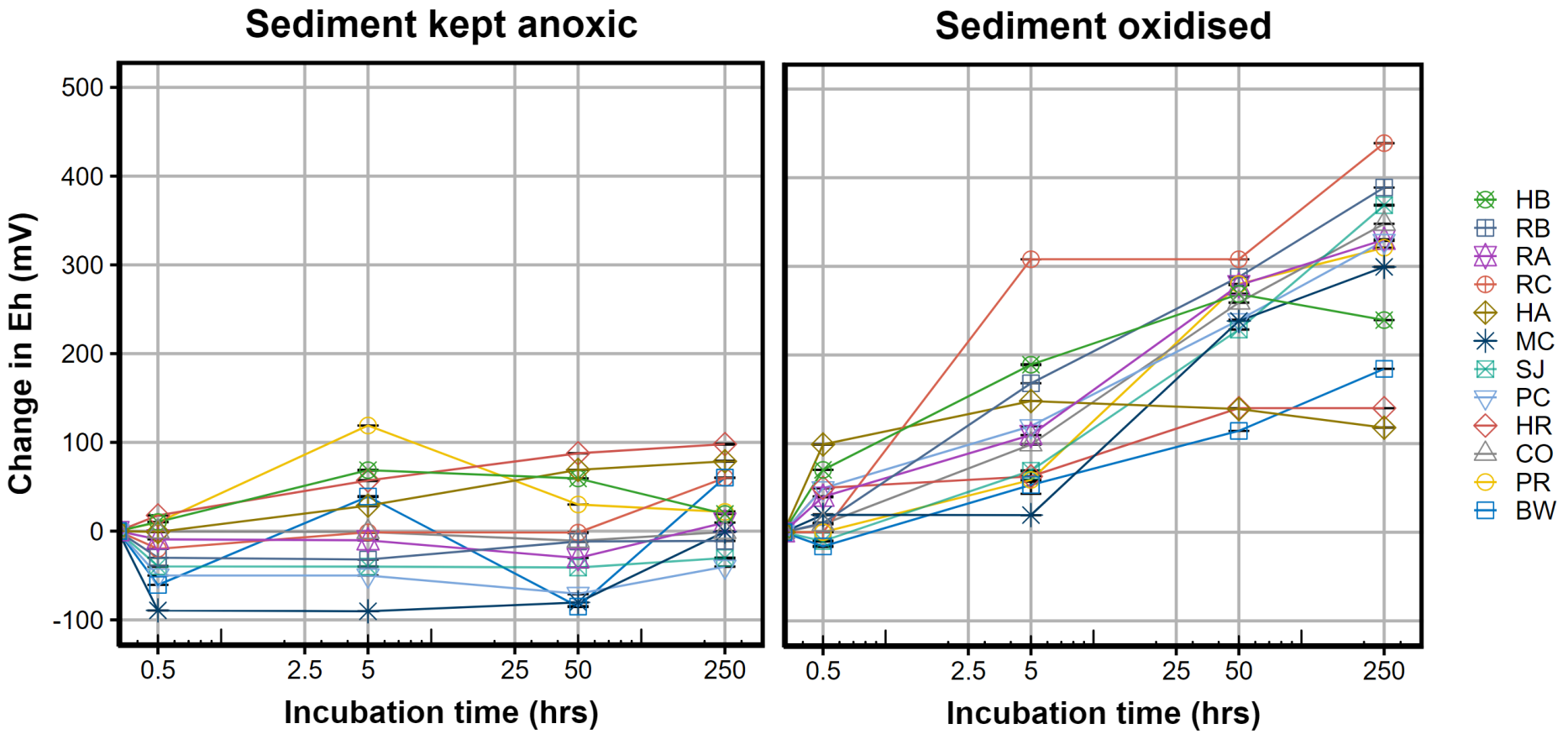

Fig. 6.06: Change in redox potential (Eh) (mean ± SD), relative to starting potential, with time in ***anoxic sediment*** incubations across the study sites. Left hand panel = sediments incubated in anoxic conditions. Right hand panel = sediments incubated in oxic conditions. Actual values in Appendix 6.03

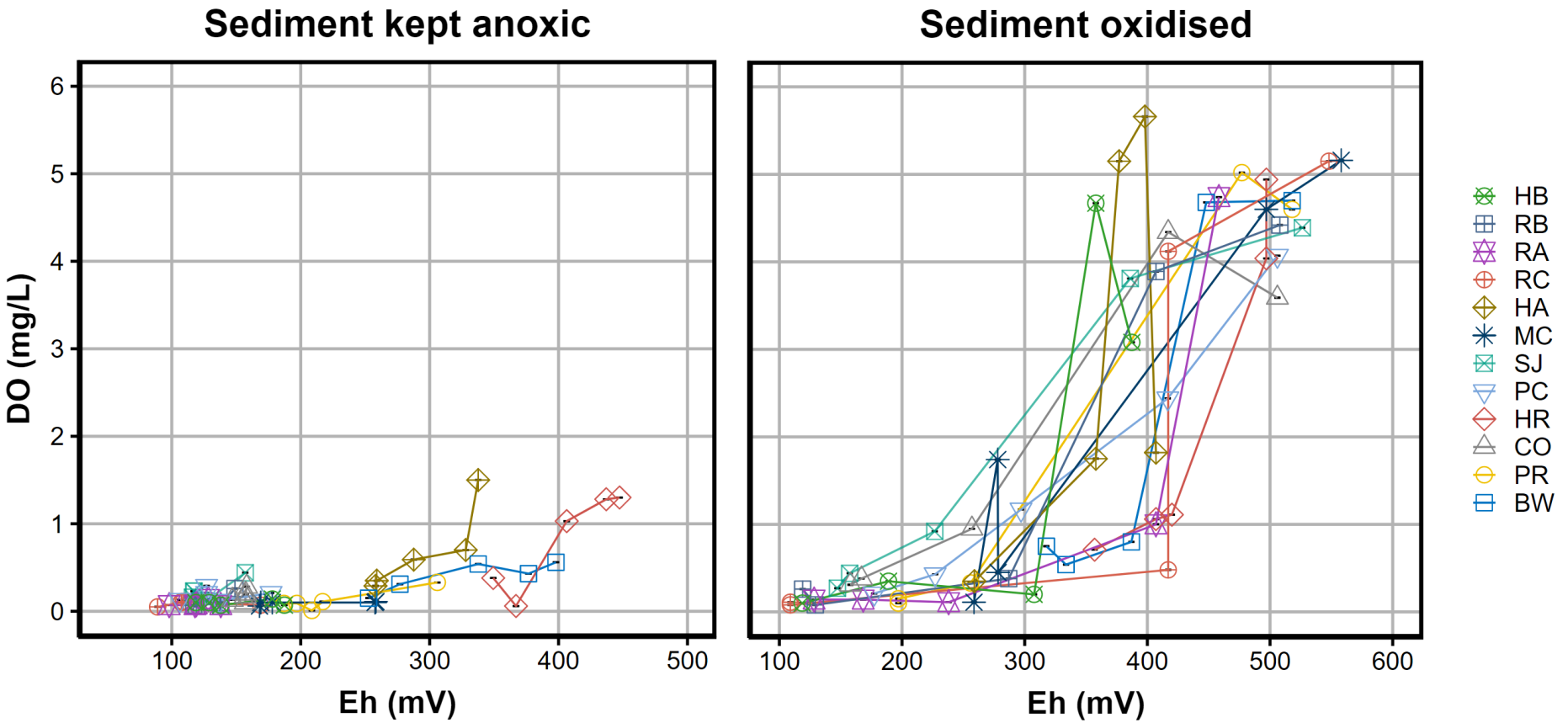

Fig. 6.07: Variation of dissolved oxygen (mean ± SD) with increase in redox potential in ***anoxic sediment*** incubations across the study sites. Left hand panel = sediments incubated in anoxic conditions. Right hand panel = sediments incubated in oxic conditions

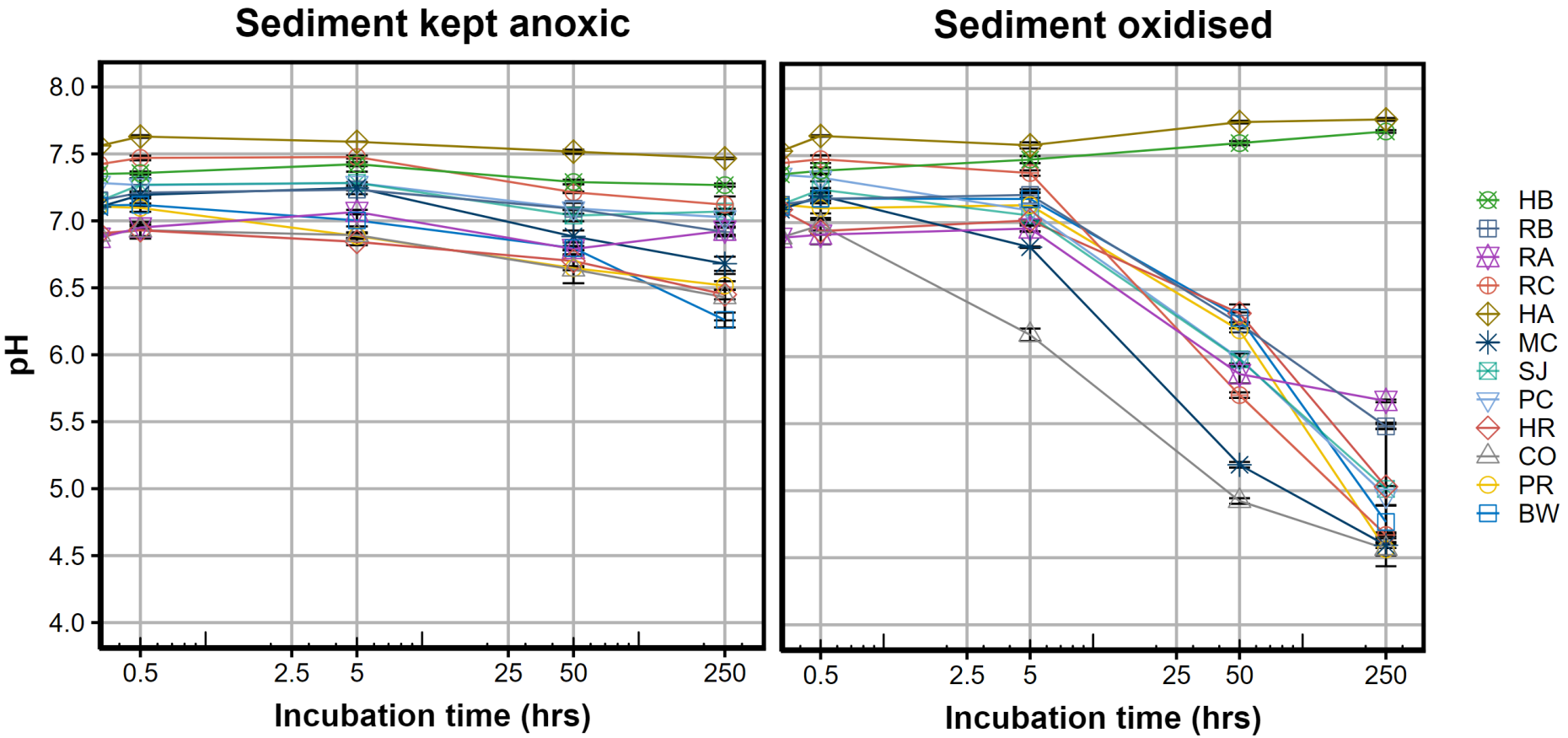

Fig. 6.08: Variation of pH (mean ± SD) with time in ***anoxic sediment*** incubations across the study sites. Left hand panel = sediments incubated in anoxic conditions. Right hand panel = sediments incubated in oxic conditions

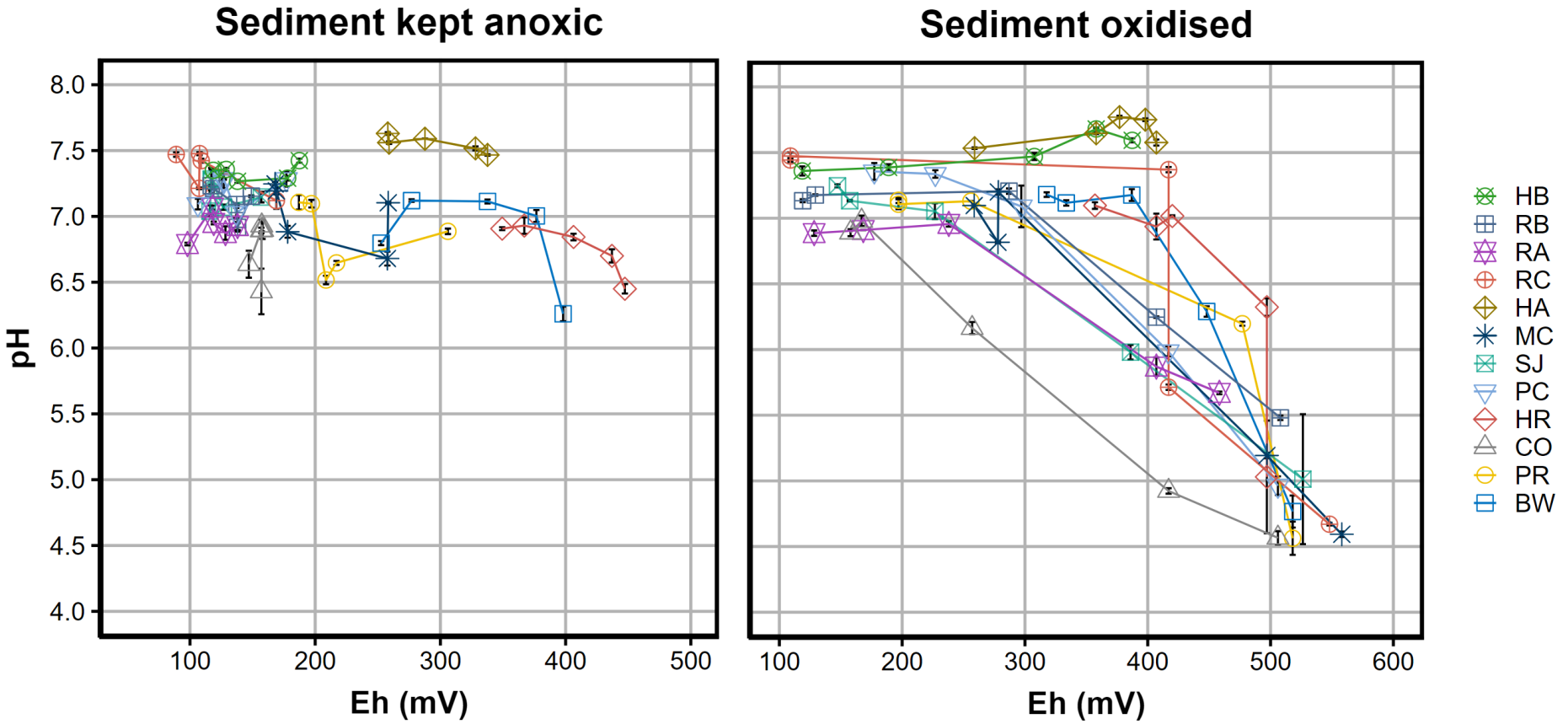

Fig. 6.09: Variation of pH (mean ± SD) with increase in redox potential in ***anoxic sediment*** incubations across the study sites. Left hand panel = sediments incubated in anoxic conditions. Right hand panel = sediments incubated in oxic conditions

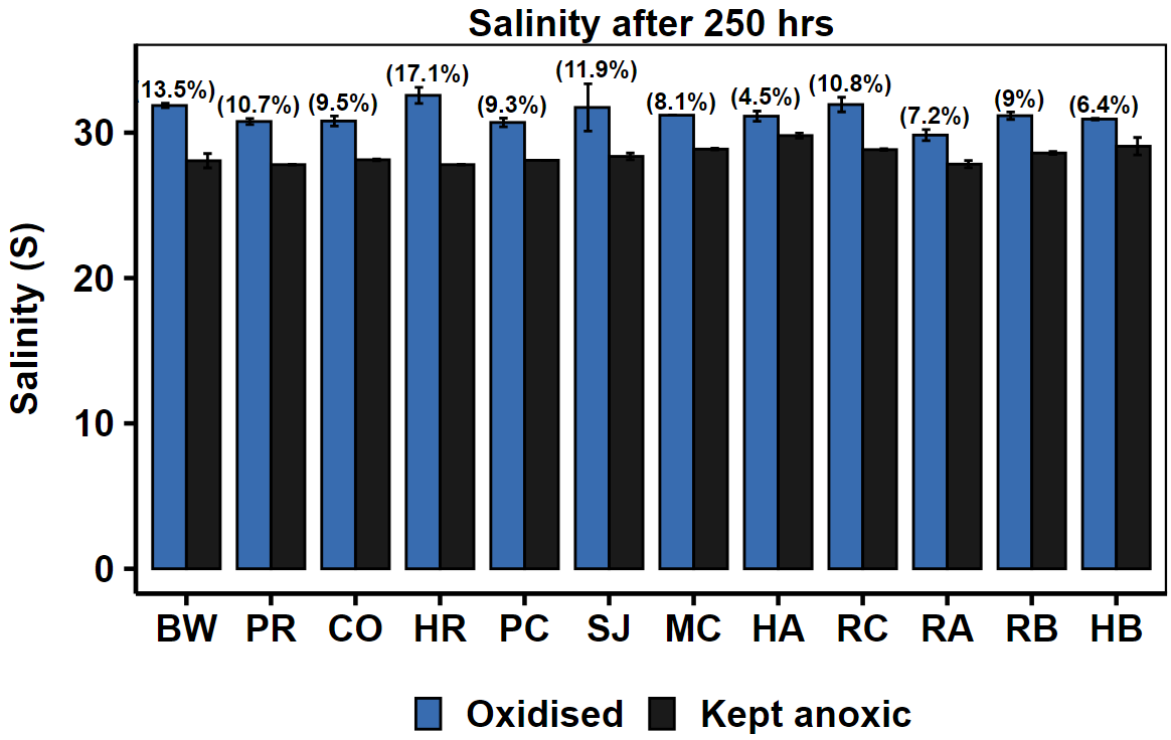

Fig. 6.10: Salinity (mean ± SD) of ***anoxic sediment*** slurries, as a proxy for evaporation, after 250 hrs of incubation in oxidised (blue bars) and reduced (black bars) conditions. Numbers in parentheses represent percentage difference between salinity of oxidised and reduced setups

6.3.1.3 Remobilisation of metals in anoxic sediment incubation

The concentrations of Cu and Zn (0 – 3 µg/L) as well as Mn (1 – 12 µg/L) across the sites were negligible at the start of the experiment (Timepoint 0 hrs, T0), albeit within the range measured in sediment porewater prior to incubation. Considering that porewater was diluted more than ten-fold in the slurries (sediment:solution ratio = 1/20 mL), this observation suggests minimal contribution of desorbed metals in the agitation prior to incubation. For Fe, concentrations at T0 (15 – 1034 µg/L) were about twice those in porewater, suggesting substantial desorption from sediment. Plotting the concentration of Fe in slurries at T0 with AVS in sediment (Figure A6.06a) revealed a strong positive relationship up to an AVS concentration of ~ 45 µmol/g, above which soluble Fe began to decline. This decline is possibly due to the equilibration of sulphide with the dissolved phase, limiting further desorption of Fe from sediment and/or sequestering already-desorbed Fe. This behaviour of Fe suggests that, although bubbled with N_2 gas, the seawater medium used was not fully

anoxic. There was no relationship between initial Mn concentrations and AVS in the sediments (A6.06b).

The remobilisation of metals (Cu, Zn, Fe and Mn) with incubation time for the typical Fal site and for the Hayle sites is depicted in Figures 6.11 and 6.12. Across all sites, incubation in anoxic conditions led to the further release of Fe, which in some sites reached a maximum, above which dissolved concentrations began to decline, possibly as a result of the formation of sulphides. Cu, Zn, and Mn releases in anoxic conditions were negligible. In Hayle, the release of Mn after 250 hrs of incubation appears to be associated with the near complete sequestration of Fe from solution.

In contrast, the oxidation of anoxic sediments across the sites led to the rapid removal of Fe from solution, possibly precipitating as Fe (oxy)hydroxides. In sediments of the Fal and BW, this oxidation was associated with the release of Mn, Zn, and Cu, in sequence. Peak concentrations of Cu and Zn were, overall, many times higher than the Water Framework Directive (2015) [WFD] standards for England and Wales (25.1 µg Cu/L[60] and 7.9 µg Zn/L), below which surface water bodies are legally designated as being of "good" chemical status. In Restronguet Creek, concentrations reached 18886 µg/L (378 µg/g sediment dry weight equivalent, dw) for Cu in RC and 11377 µg/L (228 µg/g dw) for Zn in RB (Table 6.01). In both Hayle sites, Mn was not released in the oxidation of anoxic sediment. Zn concentrations here (151 µg/L = 3.01 µg/g dw at HA and 436 µg/L = 8.71 µg/g dw at HB) were, at least, ten times less than in the rest of the sites, regardless of total sediment concentration. Cu concentrations (31 µg/L = 0.62 µg/g dw at HA and 57 µg/L = 1.15 µg/g dw at HB) were, at least, ten times less than in contaminated creeks of the Fal estuary (Table 6.01). The ordering of peak metal concentrations across the sites (e.g RC >> RB for Cu and SJ > RA for Zn) suggests that AVS concentration, in addition to sediment metal concentration, was an important factor in determining the scale of Cu and Zn remobilisation.

Combined site plots of metal release confirm the general pattern earlier described, showing the correlation between remobilisation and incubation time (Figures A6.07 – A6.10), redox potential (Figures 6.13 – 6.16), and pH (Figures 6.17 – 6.20). Plots with Fz Fe concentrations are provided in Figures A6.11 – A6.16. The remobilisation of Mn and Zn in oxic conditions was marked after 5 hrs of incubation, with concentrations dropping in some sites by T250,

[60] Corrected for average DOC across the sites in 2017 and 2019 (17.0 mg/L).

possibly as a result of precipitation with Fe and/or Mn (oxy)hydroxides. However, the release of Cu was visible in some sites from T5 but only remarkable after 50 hrs of incubation.

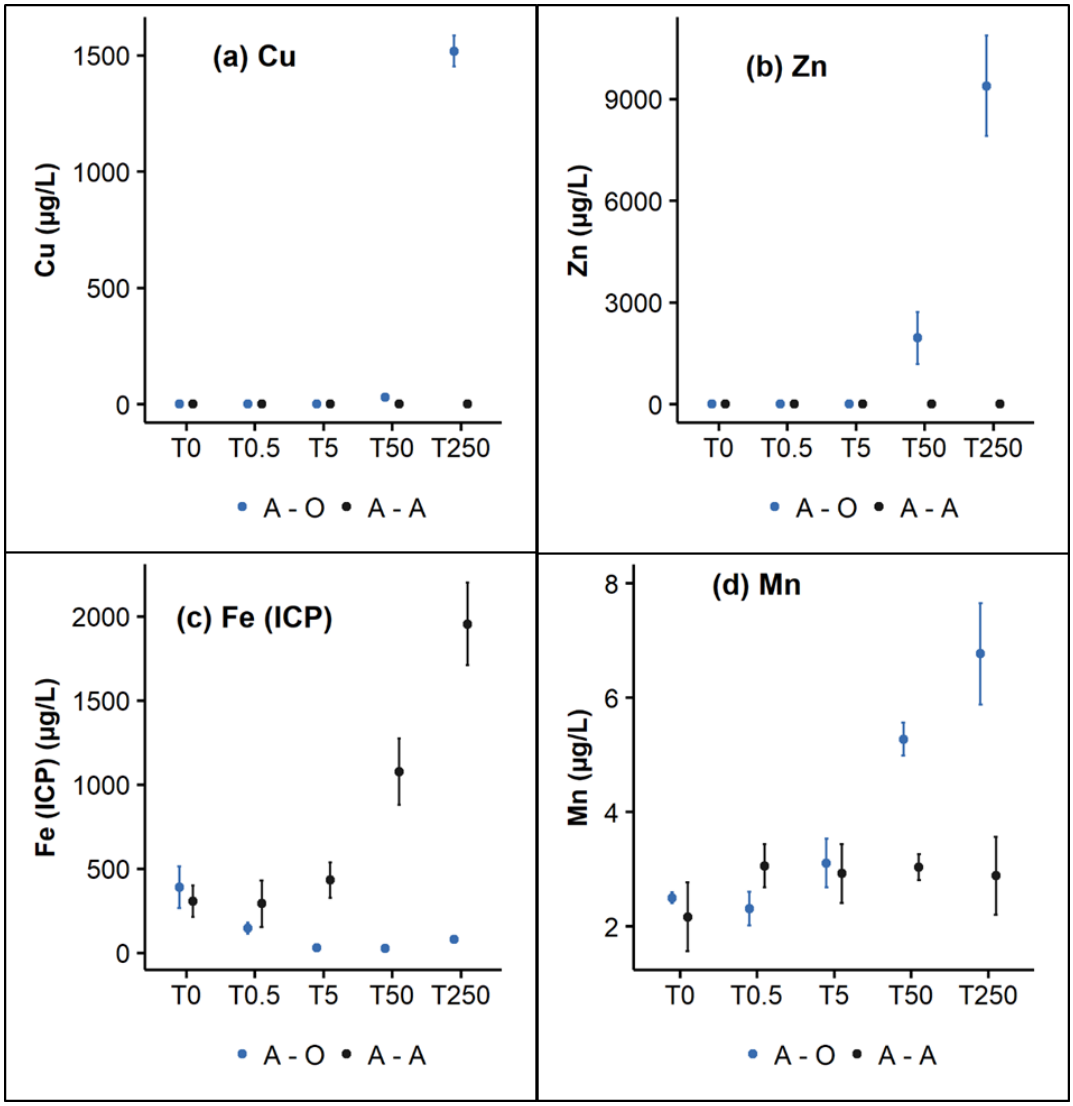

Fig. 6.11: Typical trend in metal remobilisation during ***anoxic sediment*** incubations: Cu (panel a), Zn (panel b), Total Fe (ICP) (panel c), and Mn (panel d) (all mean ± SD). Values represent measurements for St Just (SJ) sediment, but are typical for all sites, except Hayle (HA & HB). A – O (blue): Anoxic sediments incubated in oxidised conditions. A – A (black): Anoxic sediments incubated in anoxic conditions. T0, 0.5, 5, 50, and 250 represent sampling at timepoints 0, 0.5, 5, 50, and 250 hrs of incubation

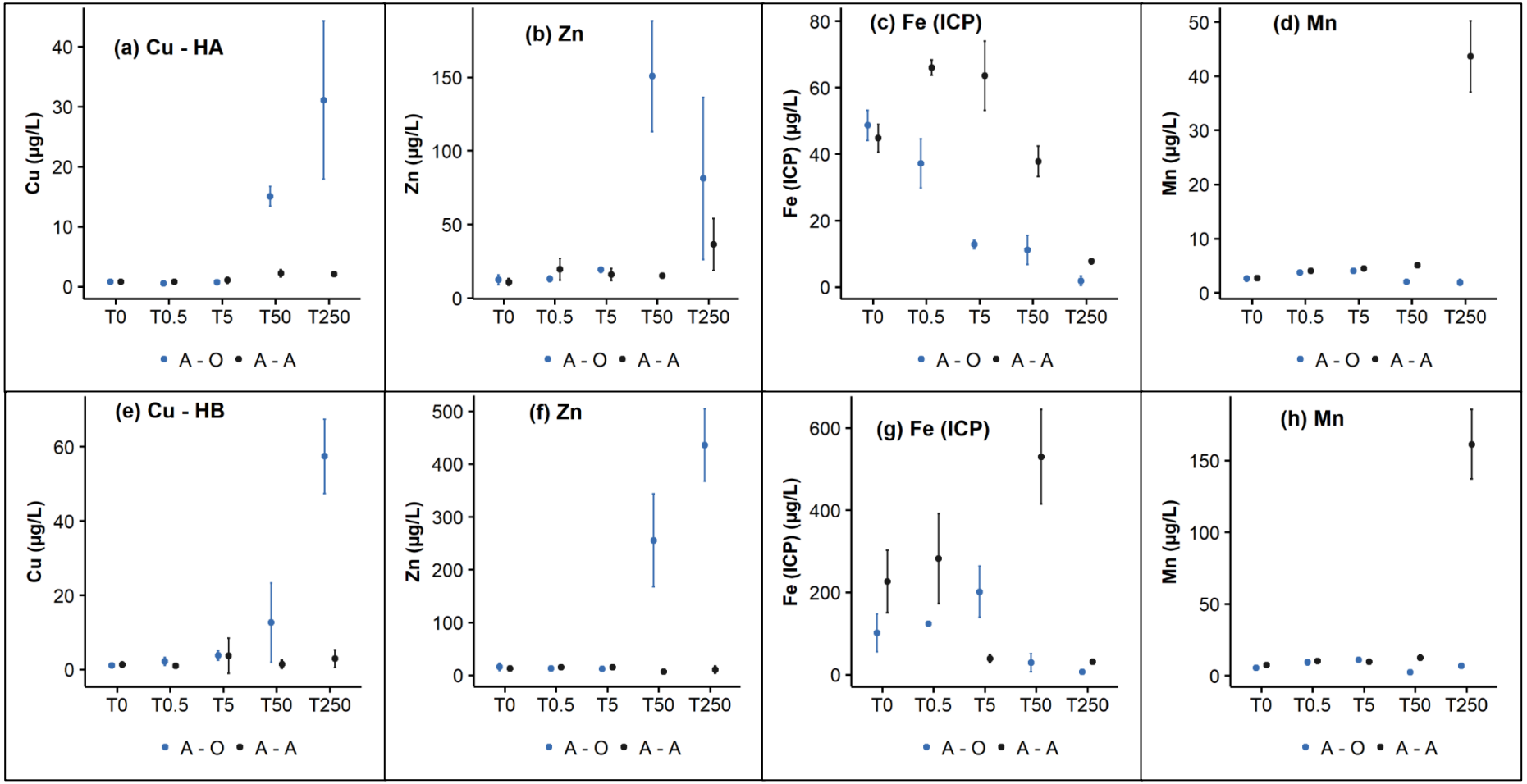

Fig. 6.12: Typical trend in Cu, Zn, Total Fe (ICP), and Mn (all mean ± SD) remobilisation during ***anoxic Hayle sediment*** (HA = a – d, top row; HB = e – h, bottom row) incubations. A – O (blue): Anoxic sediments incubated in oxidised conditions. A – A (black): Anoxic sediments incubated in anoxic conditions. T0, 0.5, 5, 50, and 250 represent sampling at timepoints 0, 0.5, 5, 50, and 250 hrs of incubation

Table 6.01: Peak metal remobilisation (mean values) during the ***oxidation of anoxic sediments*** across the study sites. 10 g (dry weight equivalent) of sediments for all sites, except HR (12 g), incubated in 200 mL of seawater. Concentrations provided as direct measurements in sediment slurries (µg/L) and as metals released per unit mass of sediment (µg/g dry weight equivalent). Note that Mn concentrations represent approximately 2% of actual values. Values have *not* been corrected for concentration as a result of evaporation during incubation (4.5 – 13.5 %, see Figure 6.03)

Site	**Cu**		**Zn**		**Fe**		**Mn**	
	µg/L	**µg/g**	**µg/L**	**µg/g**	**µg/L**	**µg/g**	**µg/L**	**µg/g**
BW	51	1.03	1806	36.11	89	1.78	15	0.29
PR	120	2.39	3090	61.79	812	16.24	14	0.29
CO	145	2.89	2851	57.02	1034	20.68	50	1.01
HR	48	0.79	2233	36.65	41	0.68	12	0.20
PC	851	17.02	7442	148.83	263	5.26	5	0.11
SJ	1517	30.34	9387	187.74	389	7.78	7	0.14
MC	2327	46.54	9663	193.26	319	6.37	70	1.39
HA	31	0.62	151	3.01	49	0.97	4	0.08
RC	18886	377.72	*8520	*170.40	**1125	**22.49	NA	NA
RA	1962	39.25	8627	172.54	**1674	**33.48	NA	NA
RB	4384	87.68	11377	227.53	**1529	**30.59	NA	NA
HB	57	1.15	436	8.71	201	4.02	11	0.22

NA = Not available as a result of missing data

*Peak release recorded after 50 hours, possibly as a result of precipitation of metals with Fe(oxy)hydroxides at the 250-hour timepoint

**Fe (total) measured by Ferrozine. Note that this method overestimates Fe in the slurries by up to 50% (see Figure 6.01)

The plots of metal concentrations with redox potential further explain their remobilisation with time of incubation in oxic conditions, providing broadly-applicable thresholds. Cu appeared to remain bound in sediment until a threshold Eh of 400mV across the sites. Zn appeared to be released into solution between 220 – 300 mV, albeit at 410 mV for HR. Mn appeared to be remobilised from the anoxic sediments at the onset of incubation in oxic conditions, with variable "threshold" Eh which depended on the starting Eh across the study sites. The precipitation of Mn was at 400 mV in RA, RC, and CO sediments, but 300 mV in HB. Similarly, the remobilisation and precipitation of Fe varied across the study sites, being released between 100 and 200 mV and precipitated between 150 and 300 mV (see incubations in anoxic conditions). In CO, with the second lowest pH (4.56), Fe remained in solution until 500 mV. Overall, threshold Eh for Cu and Zn remobilisation appeared to be uniform across the sites, whilst Mn and Fe showed relatively high site-specificity in remobilisation or precipitation in the experimental setups.

The correlation between pH and Eh in this experiment complicates the interpretation of redox thresholds for metal remobilisation in the Fal and in BW. Metals appeared to be released at defined pH ranges across the study sites. Cu was remobilised between pH 5.7 and 6.3. Zn was remobilised between pH 6.8 and 7.4. Mn appears to have been remobilised at pH 6.3, although this was not clear as incubations in anoxic conditions showed metal release between pH 6.7 and 7.4, which was better explained by time of incubation. In the same vein, the remobilisation of Fe did not seem to be affected by pH of the sediment slurry. In setups incubated in anoxic conditions, Fe concentrations increased with a decrease in pH, whereas they increased for incubations in oxic conditions. Overall, both Eh and pH changes with time of incubation appeared to affect the remobilisation of Cu and Zn, but Fe and Mn appeared to be more responsive to Eh changes in the sediment slurries.

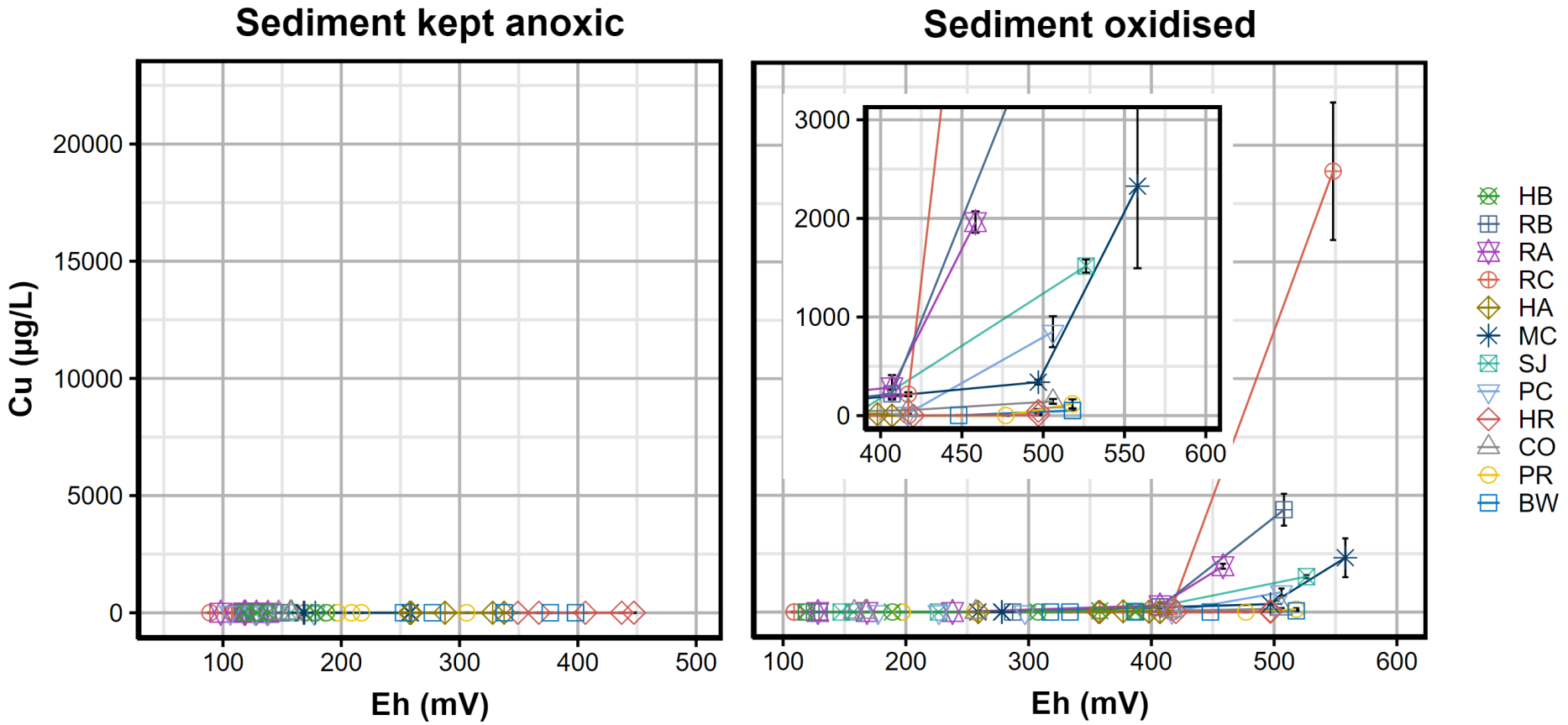

Fig. 6.13: Remobilisation of Cu (mean ± SD) with increase in redox potential in ***anoxic sediment*** incubations across the study sites. Left hand panel = sediments incubated in anoxic conditions. Right hand panel = sediments incubated in oxic conditions. Inset plot in right hand panel magnifies Cu remobilisation at concentrations lower than 3000 µg/L

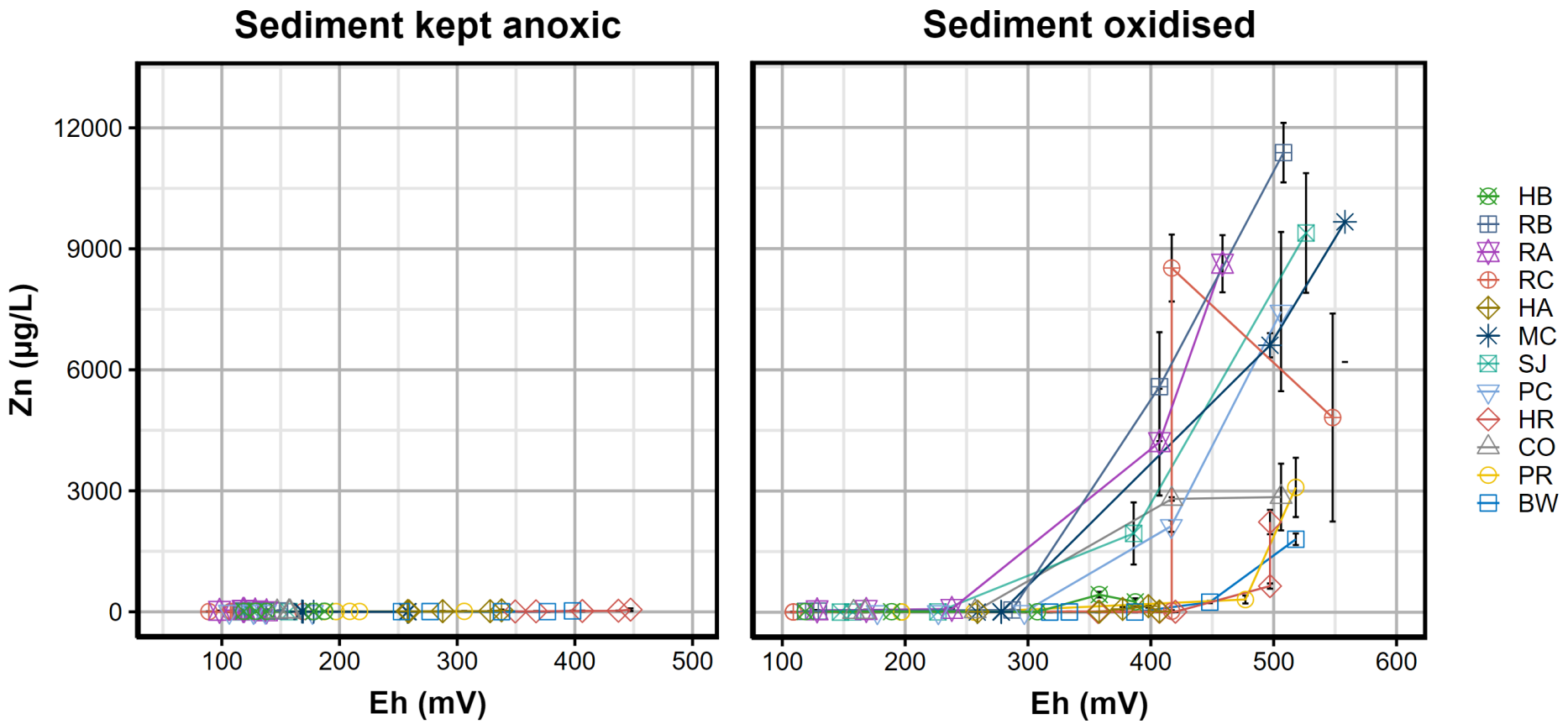

Fig. 6.14: Remobilisation of Zn (mean ± SD) with increase in redox potential in ***anoxic sediment*** incubations across the study sites. Left hand panel = sediments incubated in anoxic conditions. Right hand panel = sediments incubated in oxic conditions

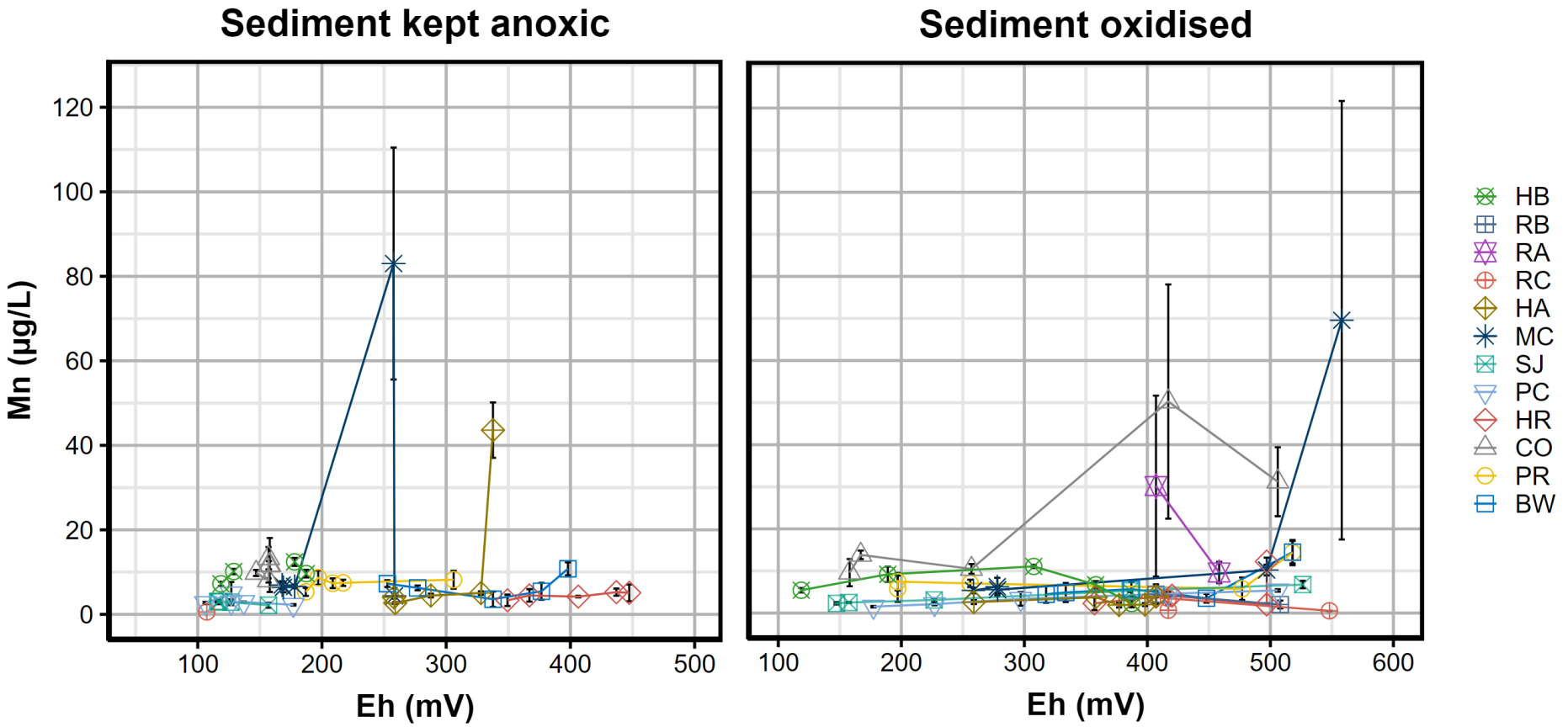

Fig. 6.15: Remobilisation of Mn (mean ± SD) with increase in redox potential in ***anoxic sediment*** incubations across the study sites. Note that Mn concentrations represent approximately 2% of actual values (see Chapter 2). Left hand panel = sediments incubated in anoxic conditions. Right hand panel = sediments incubated in oxic conditions. Missing data for RA, RB, and RC (except oxidised incubation for all three sites at T50 and T250, for RC oxidised at T5, and for RC reduced at T50)

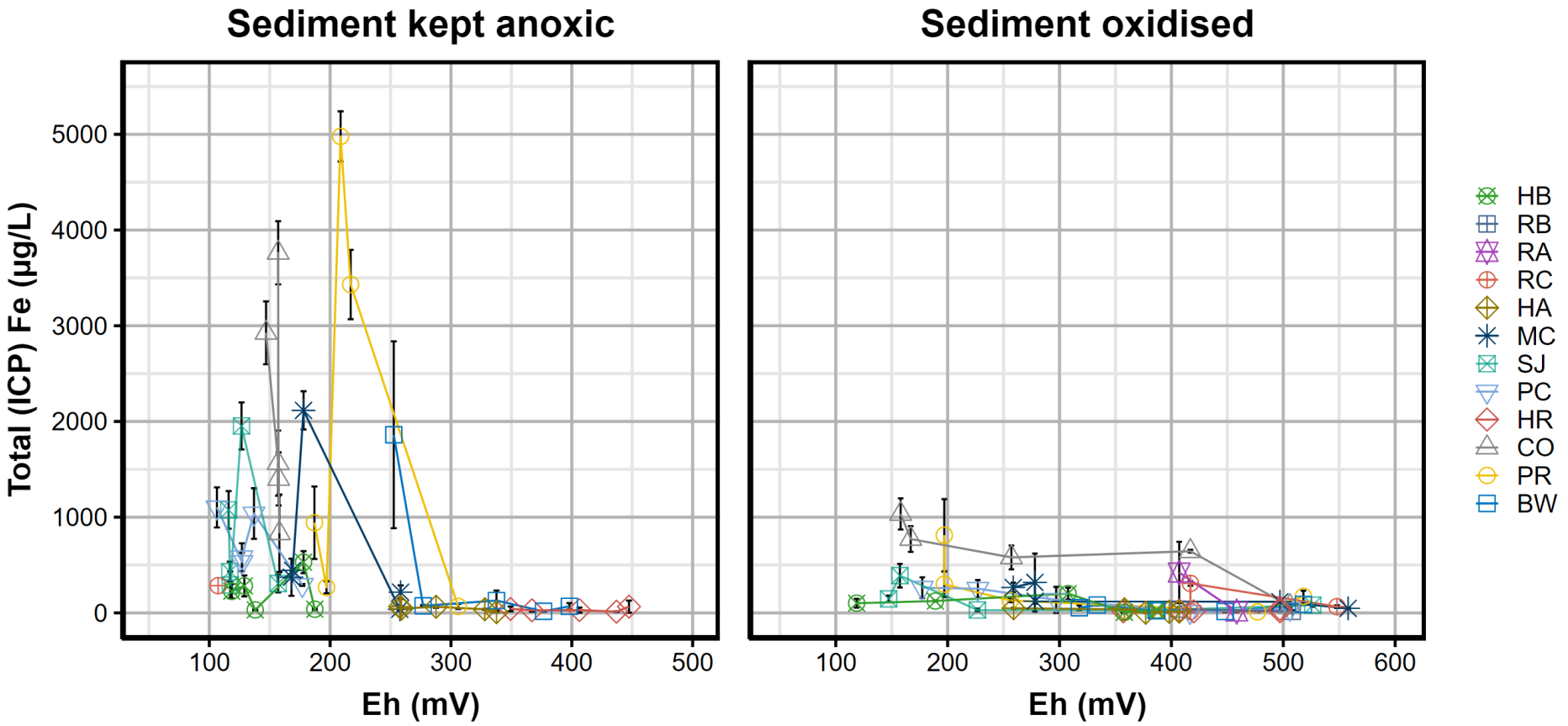

Fig. 6.16: Remobilisation of Fe (total Fe measured by ICP-OES) (mean ± SD) with increase in redox potential in ***anoxic sediment*** incubations across the study sites. Left hand panel = sediments incubated in anoxic conditions. Right hand panel = sediments incubated in oxic conditions. Missing data for RA, RB, and RC (except oxidised incubation for all three sites at T50 and T250, for RC oxidised at T5, and for RC reduced at T50)

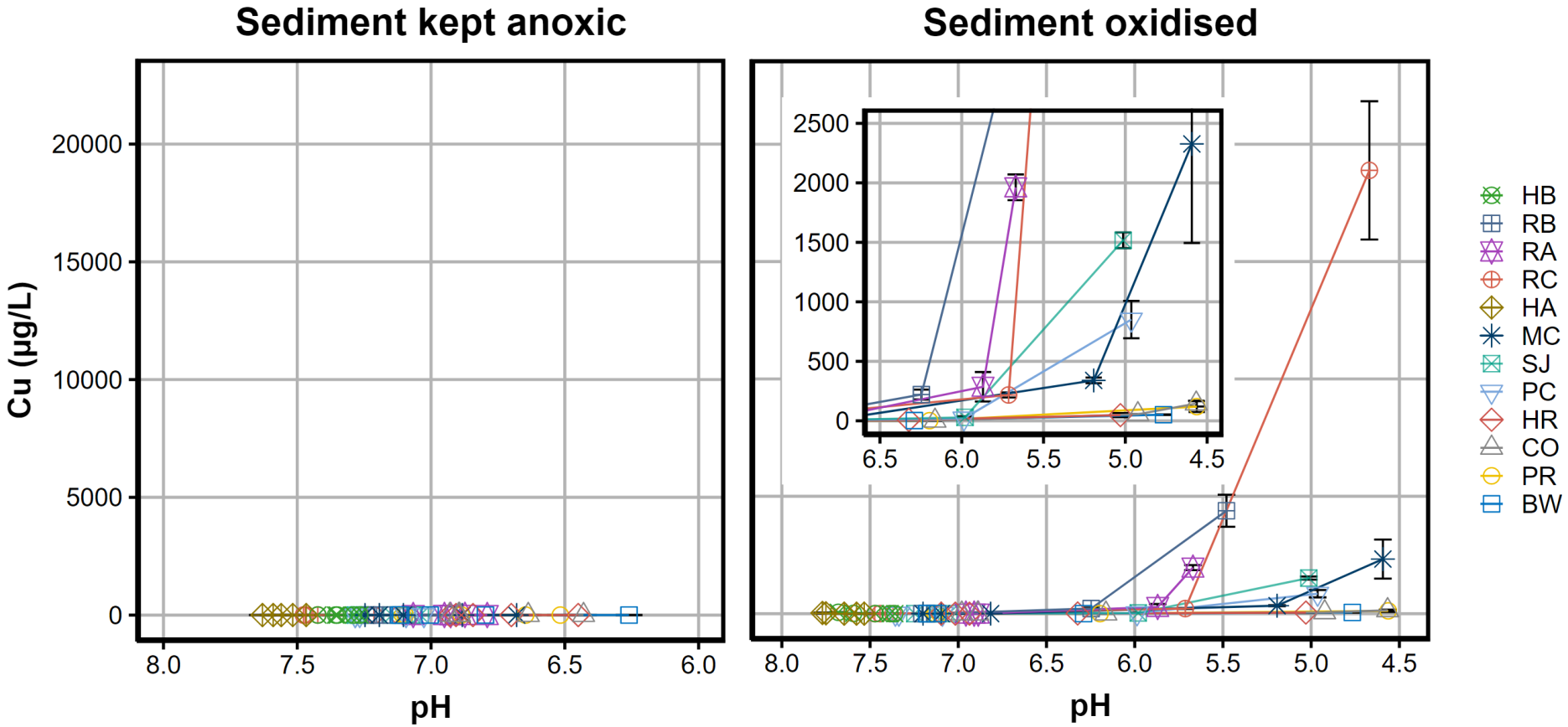

Fig. 6.17: Remobilisation of Cu (mean ± SD) with decrease in pH in ***anoxic sediment*** incubations across the study sites. Note the reverse pH scale. Left hand panel = sediments incubated in anoxic conditions. Right hand panel = sediments incubated in oxic conditions. Inset plot in right hand panel magnifies Cu remobilisation at concentrations lower than 2500 µg/L

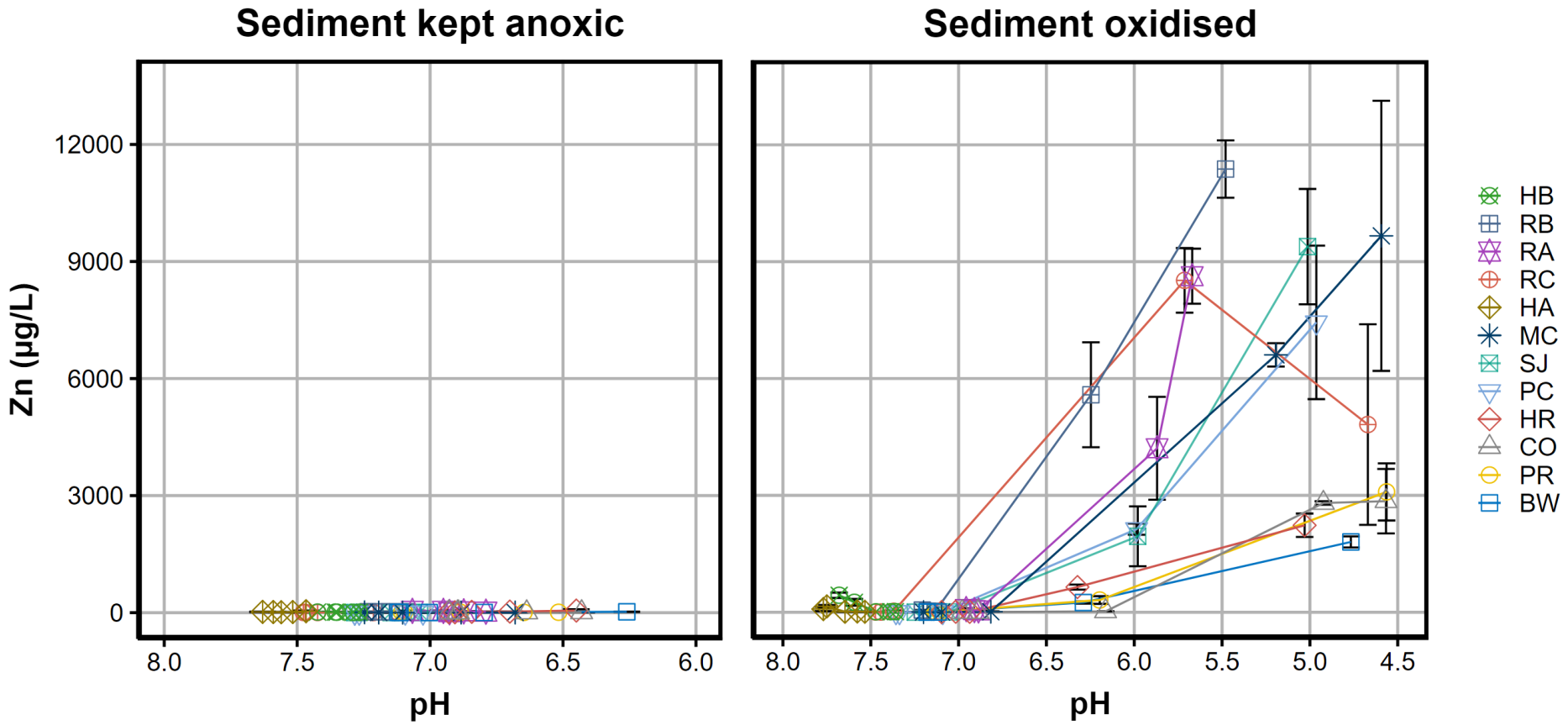

Fig. 6.18: Remobilisation of Zn (mean ± SD) with decrease in pH in ***anoxic sediment*** incubations across the study sites. Note the reverse pH scale. Left hand panel = sediments incubated in anoxic conditions. Right hand panel = sediments incubated in oxic conditions

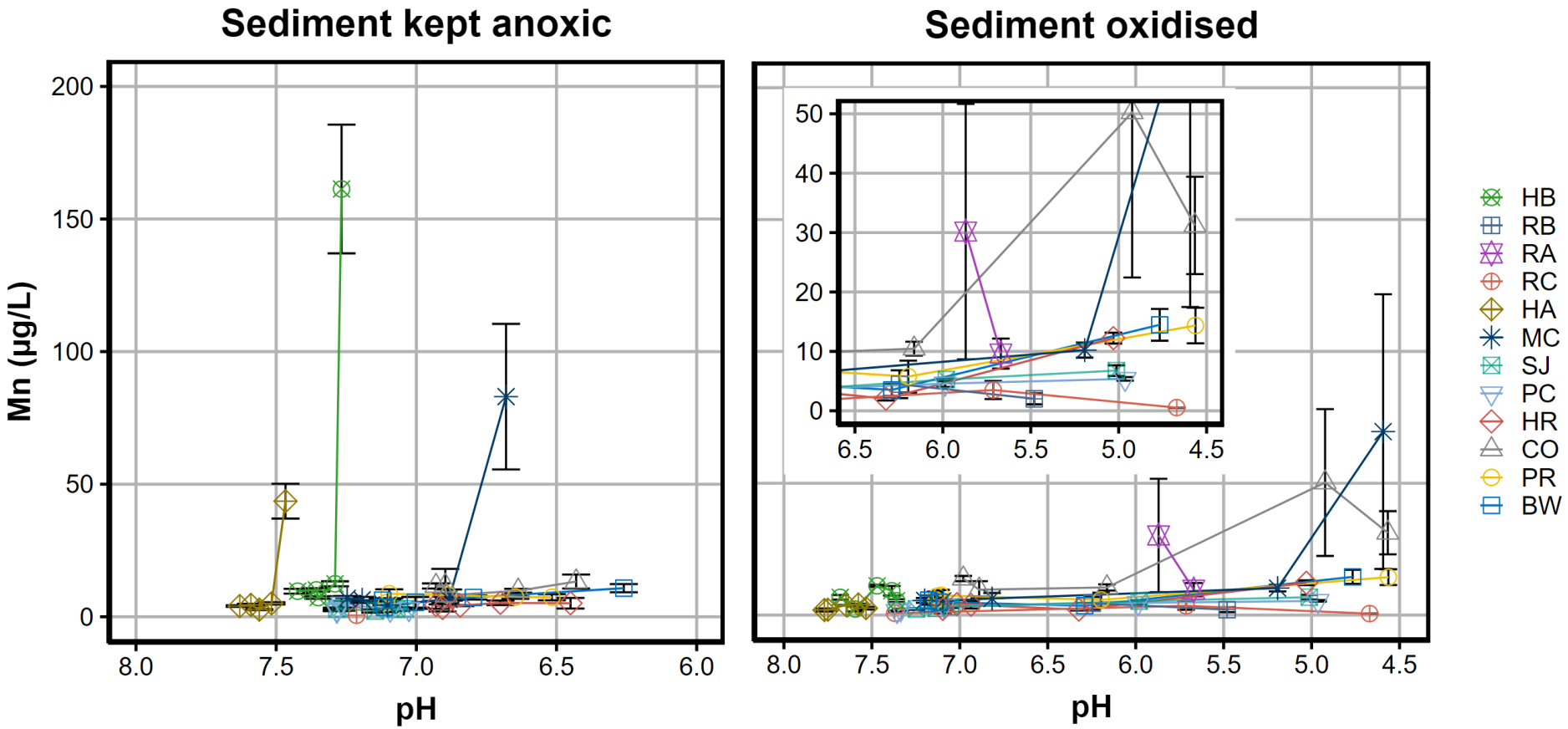

Fig. 6.19: Remobilisation of Mn (mean ± SD) with decrease in pH in ***anoxic sediment*** incubations across the study sites. Note the reverse pH scale. Mn concentrations represent approximately 2% of actual values (see Chapter 2). Left hand panel = sediments incubated in anoxic conditions. Right hand panel = sediments incubated in oxic conditions. Missing data for RA, RB, and RC (except oxidised incubation at T50 and T250). Inset plot in right hand panel magnifies Cu remobilisation at concentrations lower than 50 µg/L

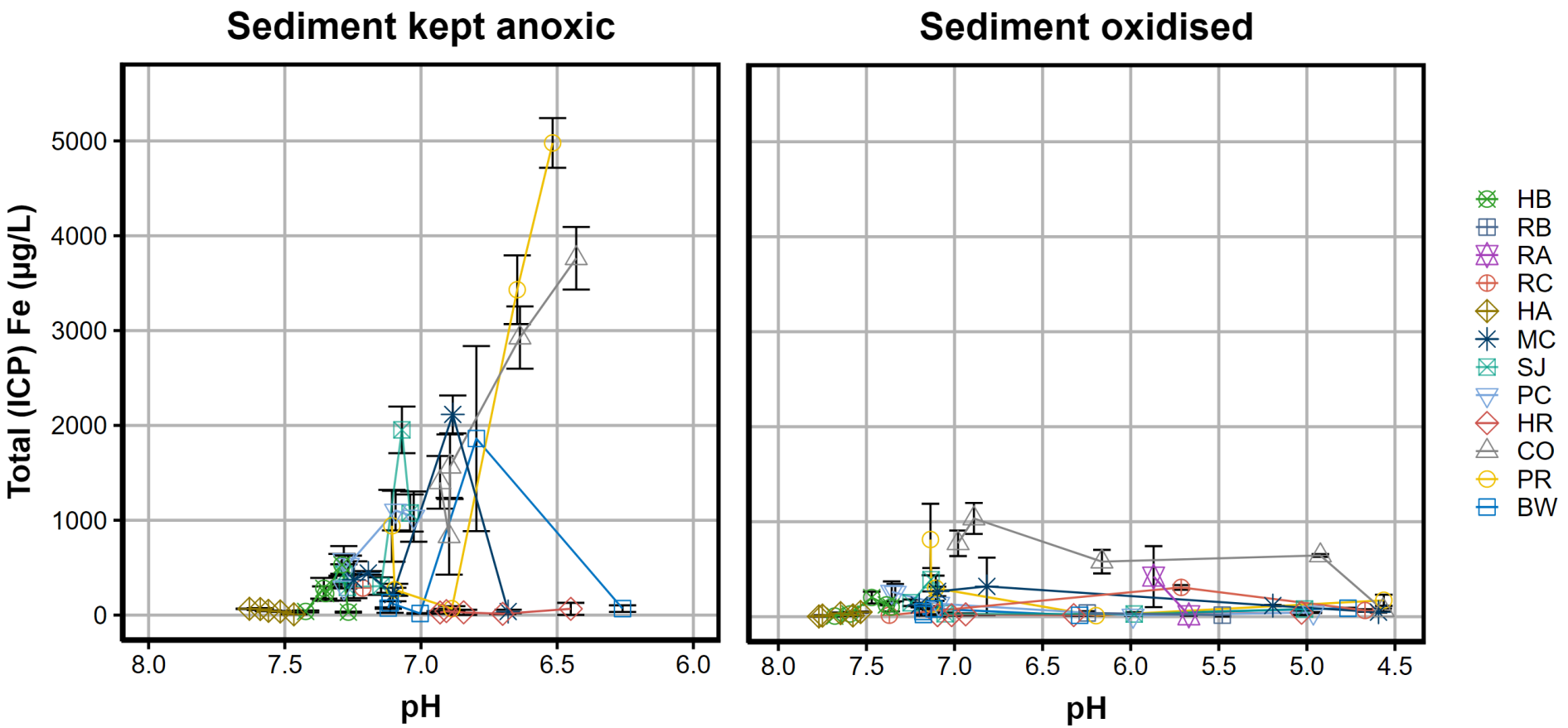

Fig. 6.20: Remobilisation of Fe (mean ± SD; total Fe measured by ICP-OES) with decrease in pH in ***anoxic sediment*** incubations across the study sites. Note the reverse pH scale. Left hand panel = sediments incubated in anoxic conditions. Right hand panel = sediments incubated in oxic conditions. Missing data for RA, RB, and RC (except oxidised incubation at T50 and T250)

*6.3.2 Results of the **oxic sediment** incubations*

6.3.2.1 Accuracy of the Ferrozine method in oxic sediment slurries

There was a poor relationship between Fz and ICP-OES Fe concentrations in the oxic sediment slurries (Figure 6.21). The exact reason for this is unclear. For the typical oxic sediment, the trend in Fe remobilisation as Fe(II), total Fz Fe, and total ICP-OES Fe is shown in Figure 6.22. The clearest disparities appear to be in slurries incubated in anoxic conditions, especially measurements made after two days of incubation (Day 2, D2). Most sediment slurries appeared to be reduced after two days of incubation, with colouration starting to darken. The Fz method detected the release of Fe (mainly as Fe^{2+}), occurring above the maximum quantifiable limit until subsequent precipitation from solution after D9. However, this Fe remobilisation was not detected in ICP-OES measurements, before D5, suggesting that the Fz method may have been biased by analytes other than Fe[61]. Correlating Fz Fe(II) and Fe (ICP-OES) concentrations with redox potential measured in both oxidised and reduced slurries confirmed that Fe (ICP-OES) ($r_s = -0.71$, $p < 0.001$), rather than Fz Fe(II) (no correlation), was reliable (Figures 6.23a & b)[62]. Consequently, only Fe (ICP-OES) is discussed in the subsequent sections. Plots based on Fz Fe concentrations are reported as appendices.

6.3.2.2 Physicochemical properties of oxic sediment slurries

The typical trends in DO, Eh, and pH in oxic sediment slurries incubated in both oxic and anoxic conditions are shown in Figures 6.24 and 6.25 for Fal/BW and Hayle sites, respectively. As expected, the incubation of oxic sediments across the sites in oxic conditions led to a marked increase in DO and Eh. However, despite incubation in anoxic conditions, DO and Eh also increased in certain sites in the Fal and in both Hayle sites. For the two sites in Hayle, DO and Eh were similar in slurries incubated in both oxic and anoxic conditions up until the final day of incubation. However, pH of these slurries behaved differently, increasing by up to 0.3 units in oxic conditions before plateauing, and decreasing by up to 0.2 units in anoxic conditions. Sediments from the Fal and BW were divided in two groups

[61] For example, it has been demonstrated that Cu(I) and Co(II) ions can be measured quantitatively using the Ferrozine method (Kundra *et al.*, 1974; Anusiem & Ojo, 1978), both of which may represent a significant interference in the measurement of Fe.

[62] Recall that in the anoxic sediment experiments (Figure A6.05a), ORP was well correlated with dissolved Fe concentrations in the setups.

based on the behaviour of pH. Sediments from Restronguet Creek (RC & RB) and BW behaved in a similar fashion to the Hayle sediments, with pH rising in oxic conditions but dropping in anoxic conditions. For sediments from SJ, PR, and MC with relatively high sediment AVS concentrations, pH of slurries dropped with incubation in oxic conditions, similar to the oxidation of anoxic sediments (see Section 6.3.1.2). In slurries of sediments from CO and PC, also with relatively high sediment AVS, pH dropped with incubation time until D5, before rising with further oxidation to D12 (individual plots not shown).

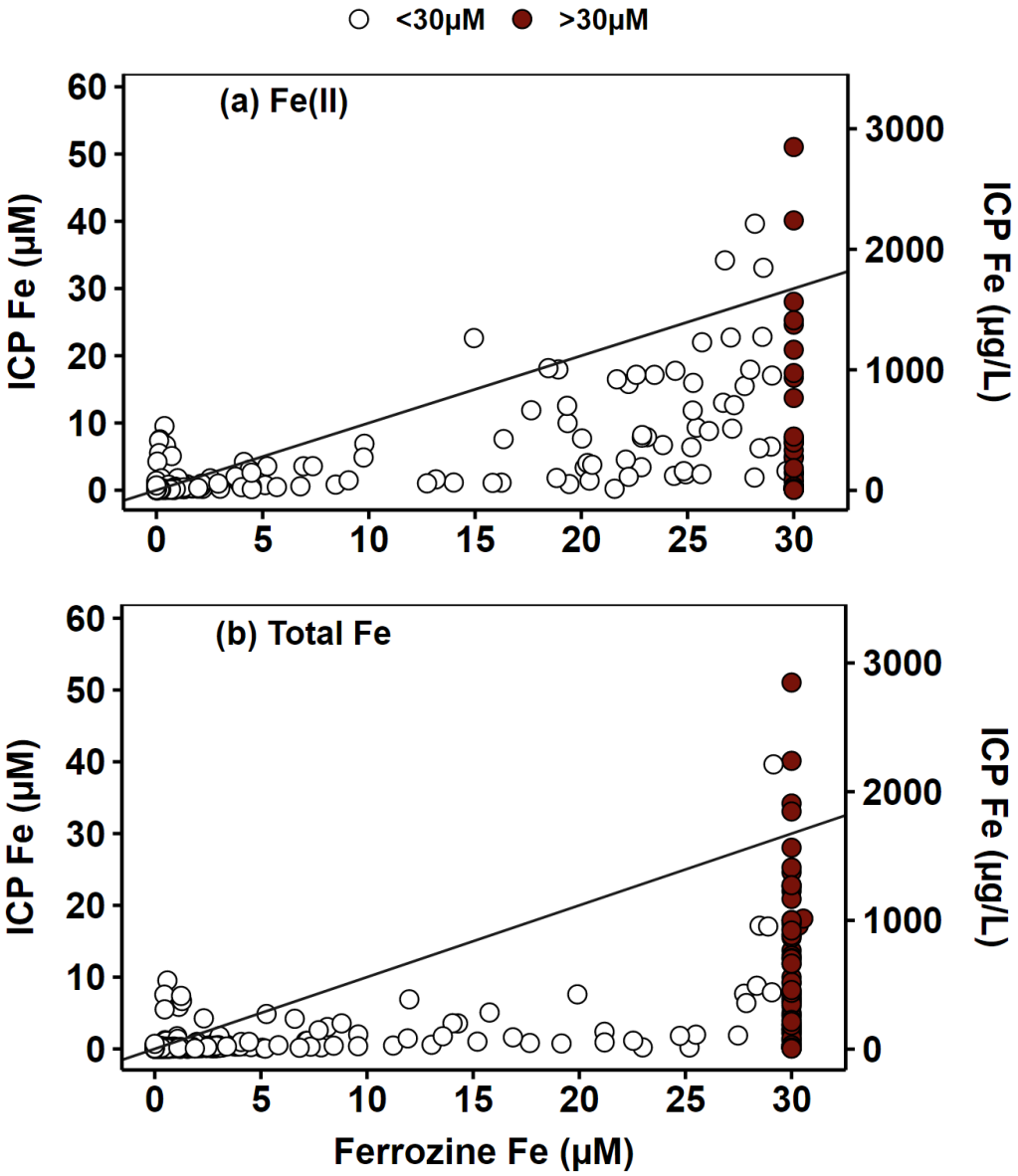

Fig. 6.21: Relationship of total Fe measured by ICP-OES with Ferrozine-labile Fe(II) (panel a) and Ferrozine-labile total Fe (panel b) in ***oxic sediment*** incubations (all mean values). Filled dots represent Ferrozine measurements ≥ 30 µM (1674 µg/L), which is the method maximum. ***Diagonal line represents a 1:1 relationship***, where Ferrozine Fe = ICP Fe

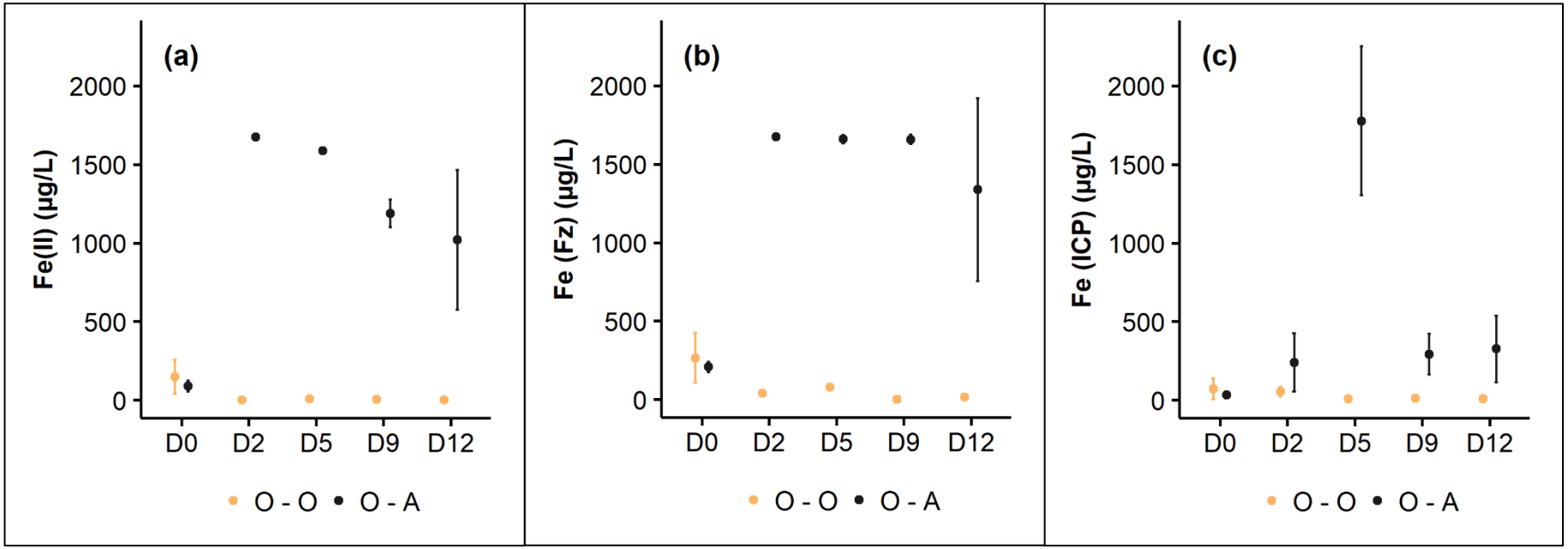

Fig. 6.22: Typical trend in Fe (mean ± SD) concentrations measured during ***oxic sediment*** incubations: Ferrozine-labile Fe(II) (panel a) and total Fe (panel b) as well as total Fe measured by ICP-OES (panel c). Concentrations represent measurements for St Just sediment. Maximum Ferrozine range = 1674 µg/L. O – O (yellow): Oxic sediments incubated in oxidised conditions. O – A (black): Oxic sediments incubated in anoxic conditions. D0, D2, D5, D9, and D12 represent sampling at timepoints 0, 2, 5, 9, and 12 days (288 hrs) of incubation

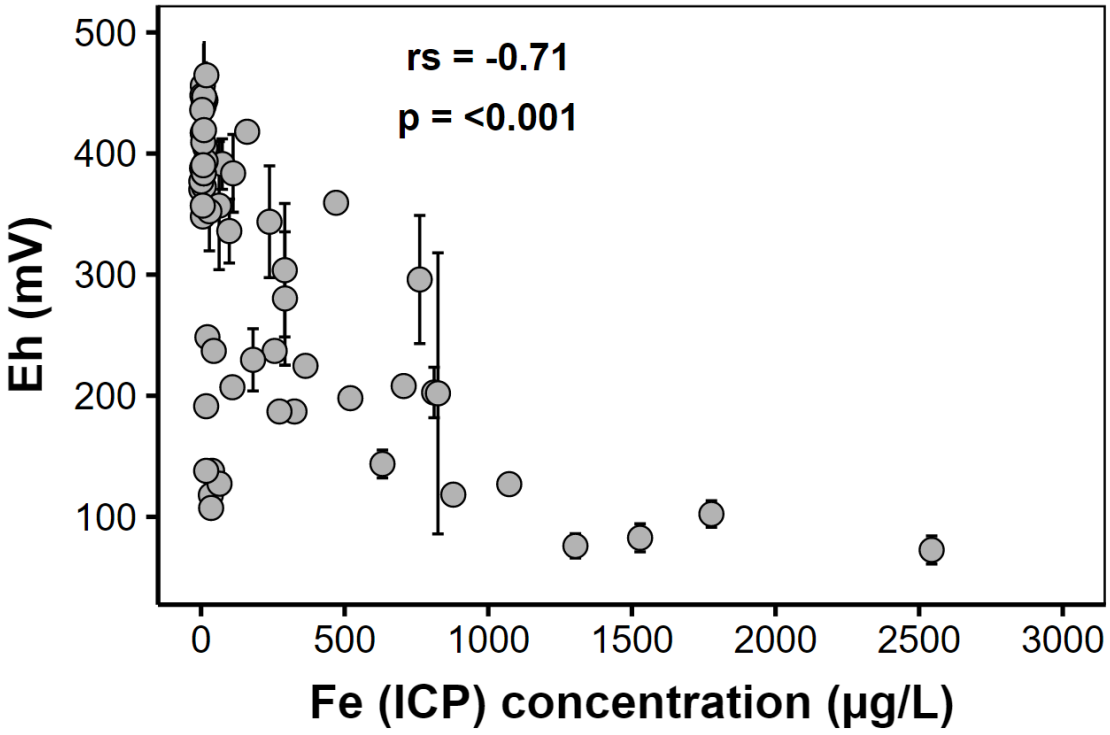

Fig. 6.23a: Relationship between Fe (ICP-OES) concentrations and redox potential (mean ± SD) measured in oxic sediment incubations

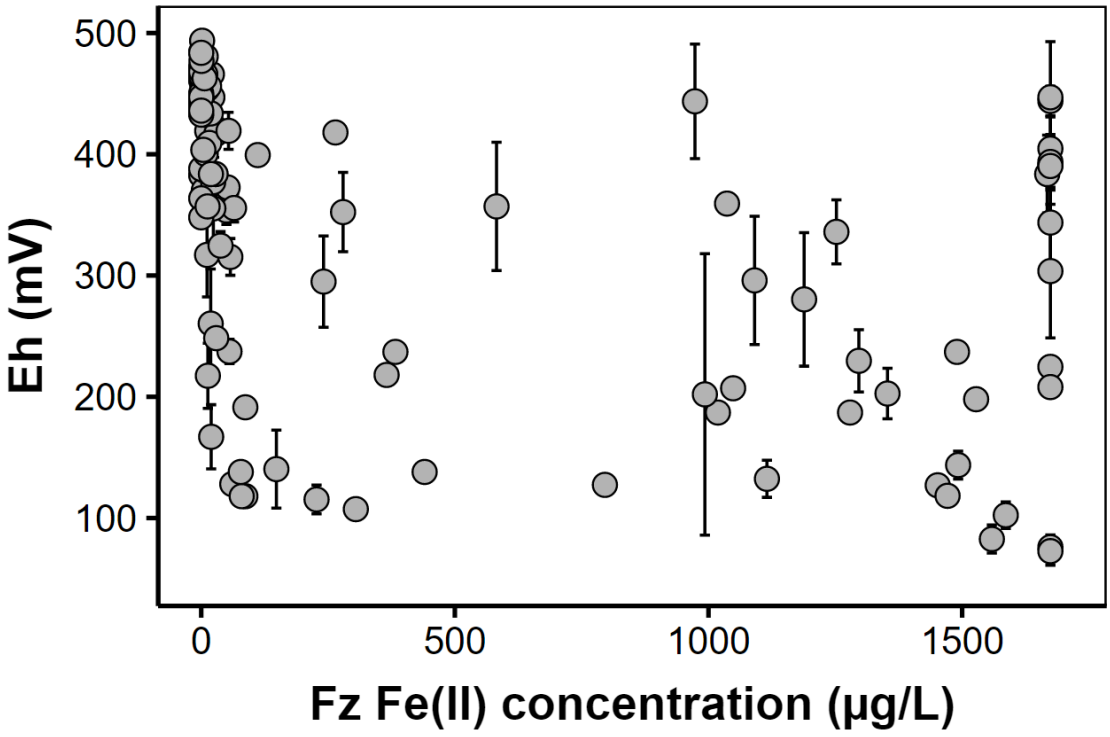

Fig. 6.23b: Relationship between Ferrozine Fe(II) concentrations and redox potential (mean ± SD) measured in oxic sediment incubations

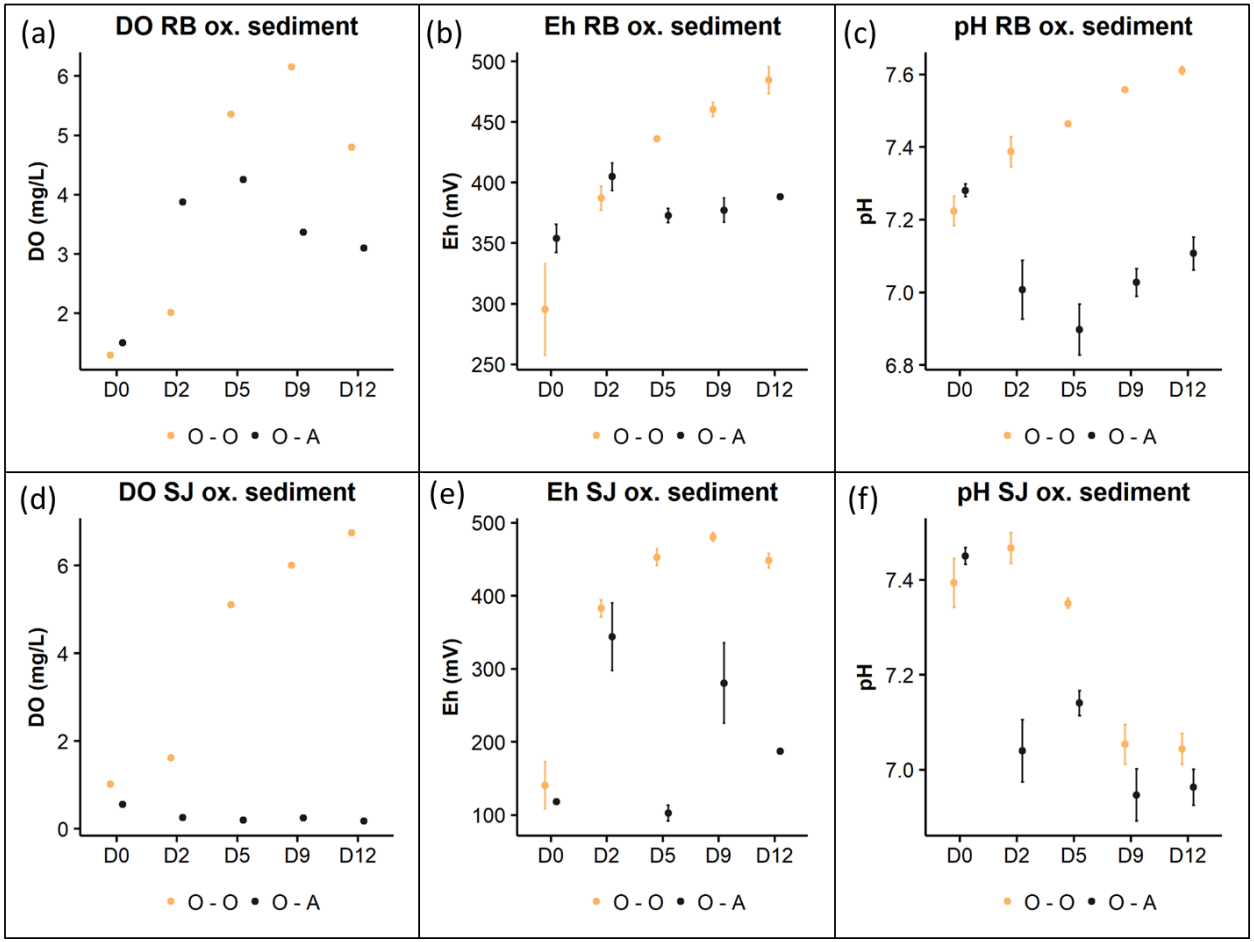

Fig. 6.24: Dissolved oxygen concentration (DO), redox potential (Eh), and pH (all mean ± SD) measured during ***oxic sediment*** incubations. O – O (yellow): Oxic sediments incubated in oxidised conditions. O – A (black): Oxic sediments incubated in anoxic conditions. D0, D2, D5, D9, and D12 represent sampling at timepoints 0, 2, 5, 9, and 12 days (288 hrs) of incubation. *Two typical groups of sites marked by the increase (panels a – c: RC, RB, HB, HA, BW) and decrease (panels e – f: SJ, PR, RA MC) of pH in oxidised conditions. pH for PC and CO decrease and then increase with time*

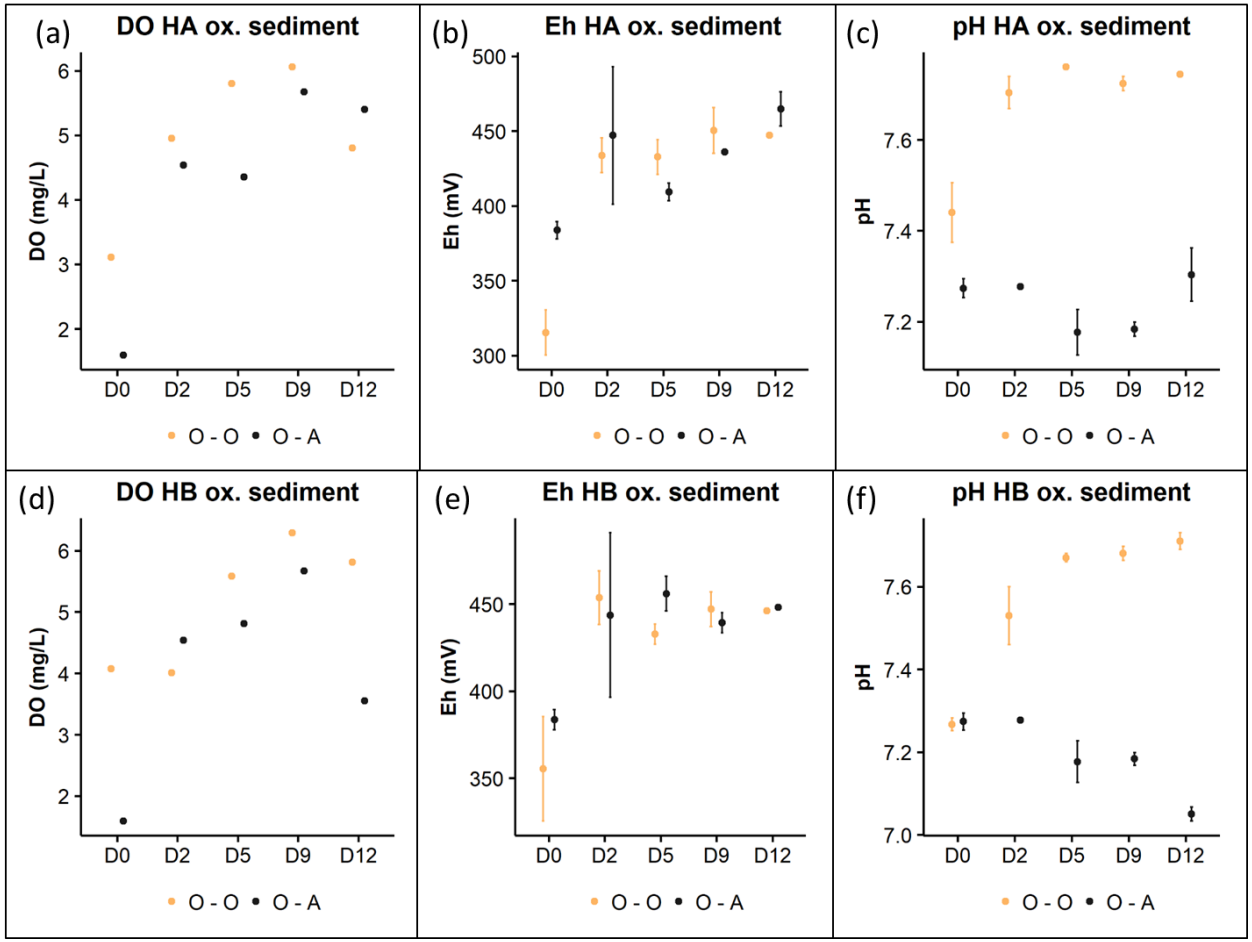

Fig. 6.25: Dissolved oxygen concentration (DO), redox potential (Eh), and pH (all mean ± SD) measured during incubation of ***oxic*** HA (panels a – c) and HB (panels e – f) sediments. O – O (yellow): Oxic sediments incubated in oxidised conditions. O – A (black): Oxic sediments incubated in anoxic conditions. D0, D2, D5, D9, and D12 represent sampling at timepoints 0, 2, 5, 9, and 12 days (288 hrs) of incubation. *Similarity in DO and Eh in both conditions*

Combined sites plots of DO, Eh, and pH in oxic sediment incubations also confirm the general patterns earlier described (Figures 6.25 – 6.28). DO concentrations rose in some sediments incubated in anoxic conditions, with the highest concentrations observed in the Hayle sites on D9 (~ 6 mg/L). For sediments incubated in oxic conditions, DO increased with incubation time, peaking at similar concentrations across the sites – 6 mg/L in some and 6.5 – 6.8 mg/L in others. Similarly, despite the range in starting Eh, terminal Eh across all sites, including in Hayle, converged around 450 – 480 mV. Eh increased in most sites (by up to 270 mV) relative to D0 (Figure A6.15), before dropping to around starting levels. The lowest Eh across the sites were recorded in Days 2 or 5.

The pH in reduced slurries, overall, dropped by 0.5 units, from a starting range of 7.2 – 7.6. In the oxidised slurries, the behaviour of pH was variable, as earlier noted. Terminal pH ranged from 6.8 at RA to ~7.7 in the Hayle sites. Although slurry pH across the sites was lower in sediments incubated in anoxic rather than oxic conditions, pH appeared to decrease with increasing Eh within each group of incubations (Figure 6.29). Overall, the results confirm that sediments in most sites were not fully oxic prior to incubation, with the oxic incubations here depicting the oxidation of anoxic sediments earlier described. Only a few sites, especially RB in the Fal, were truly oxic.

Similar to that in anoxic sediments, the salinity of oxic sediments incubated in oxic conditions were considerably higher than those in anoxic conditions, confirming evaporation in the former group (Figure 6.30). Differences in salinity between oxidised and reduced oxic sediments ranged between 4.9% for HA and 10.5% for RB, within the range observed in the anoxic sediments. Starting salinities (assumed from salinity of slurries in the reduced setups) were higher in the oxic sediment incubations than in the anoxic sediments. This difference in starting salinities is likely due to crystallised salt particles present in the oxic sediments, further confirming that salinity was exaggerated by high temperatures during sampling at low tide. Because both the sediment:solution ratio and metal levels may have increased in the setups incubated in oxic conditions simply due to evaporation over time, subsequent sections should be interpreted with caution.

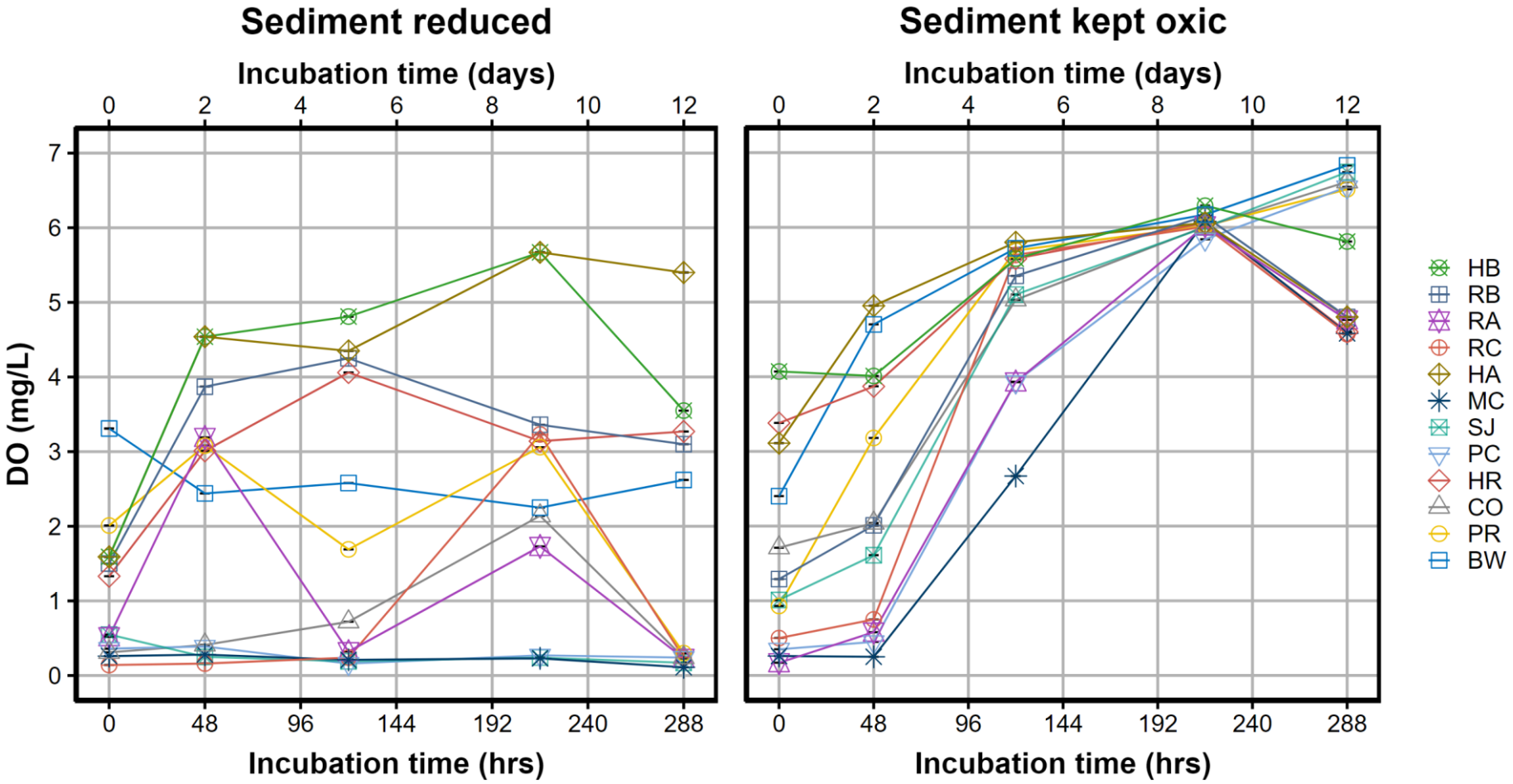

Fig. 6.26: Variation of dissolved oxygen (mean ± SD) with time in ***oxic sediment*** incubations across the treatments. Left hand panel = sediments incubated in anoxic conditions. Right hand panel = sediments incubated in oxic conditions

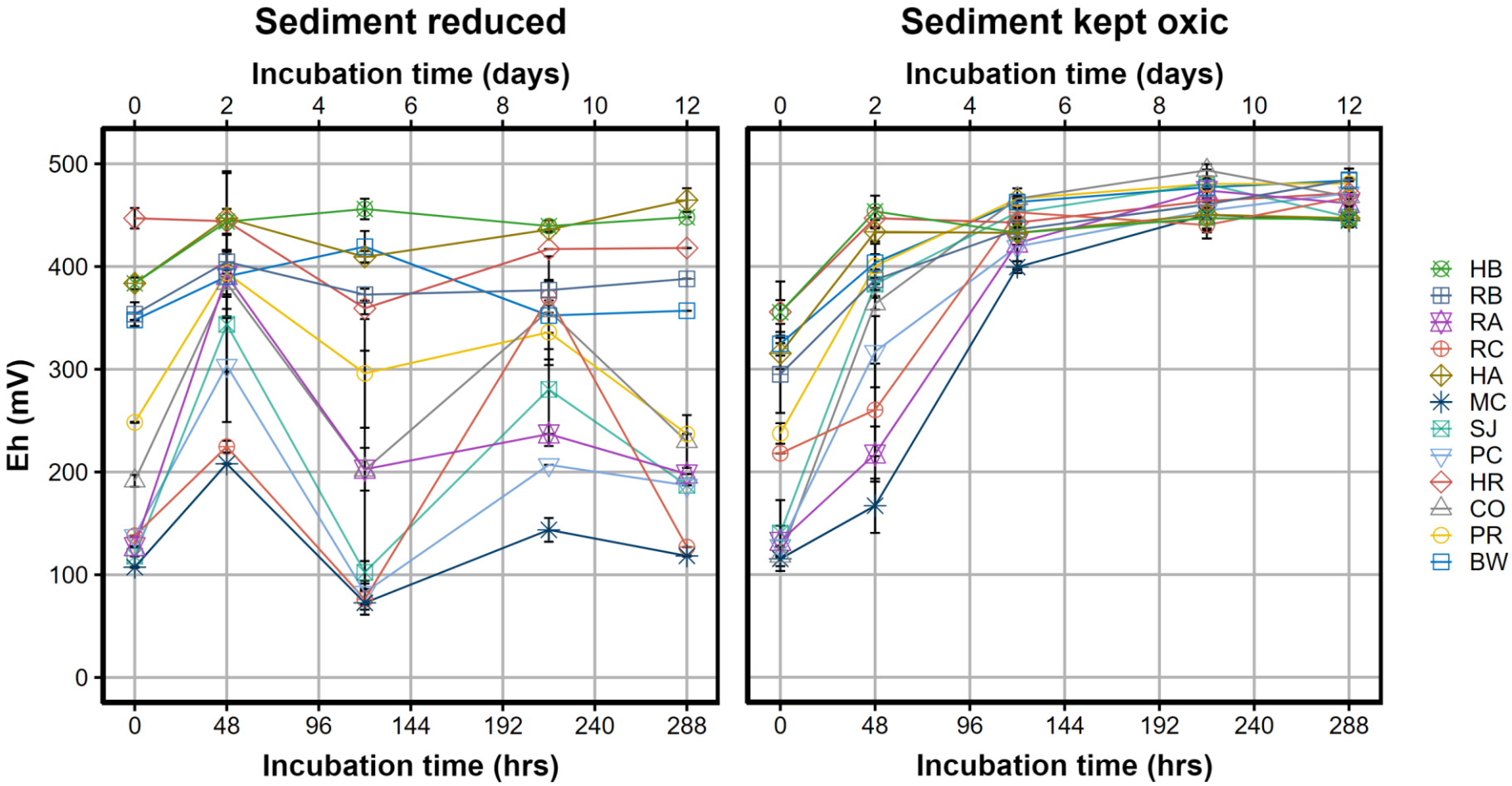

Fig. 6.27: Variation of redox potential (mean ± SD) with time in ***oxic sediment*** incubations across the study sites. Left hand panel = sediments incubated in anoxic conditions. Right hand panel = sediments incubated in oxic conditions. See Appendix A.6.14 for summary of change in redox potential

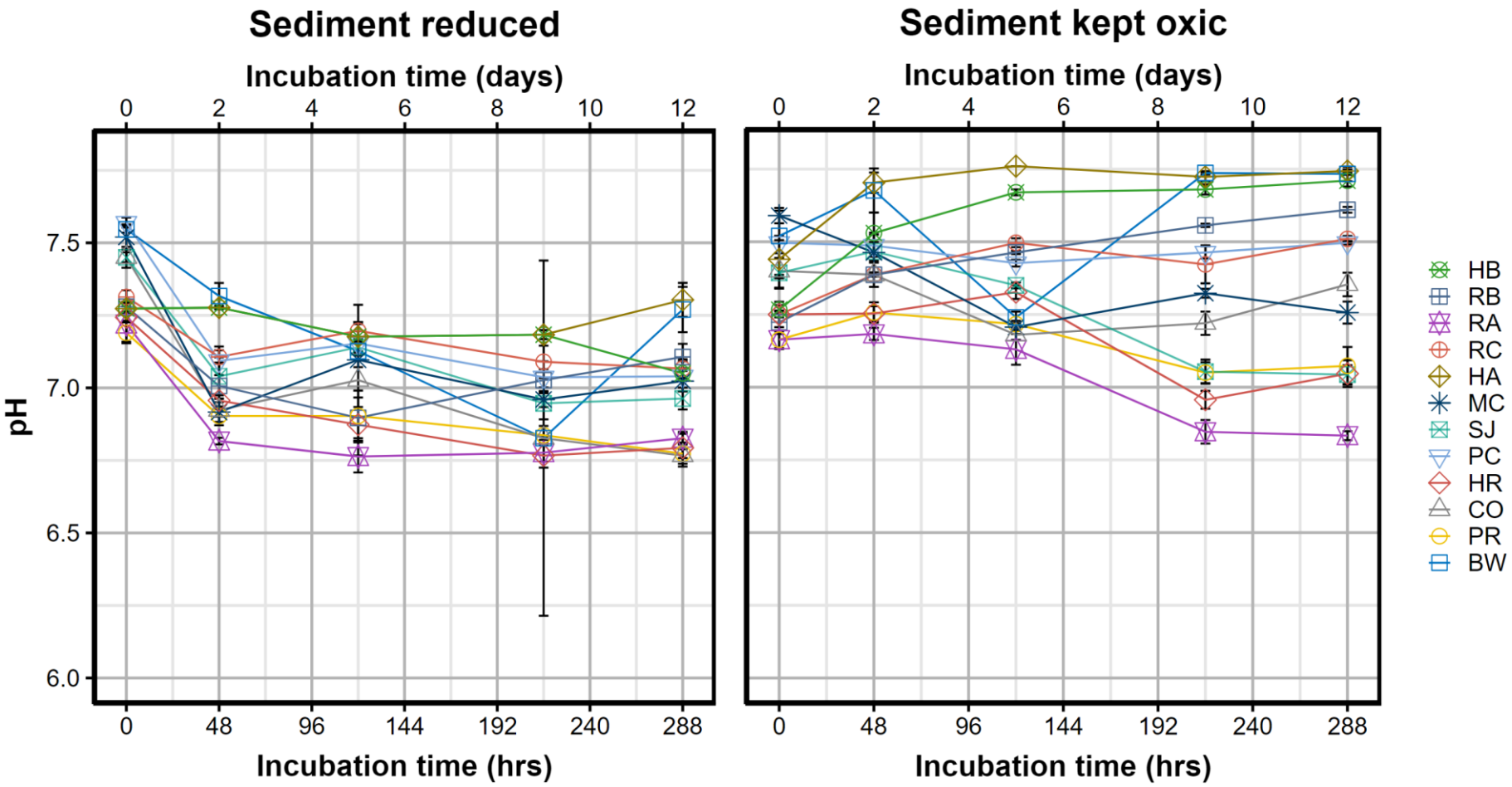

Fig. 6.28: Variation of pH (mean ± SD) with time in ***oxic sediment*** incubations across the study sites. Left hand panel = sediments incubated in anoxic conditions. Right hand panel = sediments incubated in oxic conditions

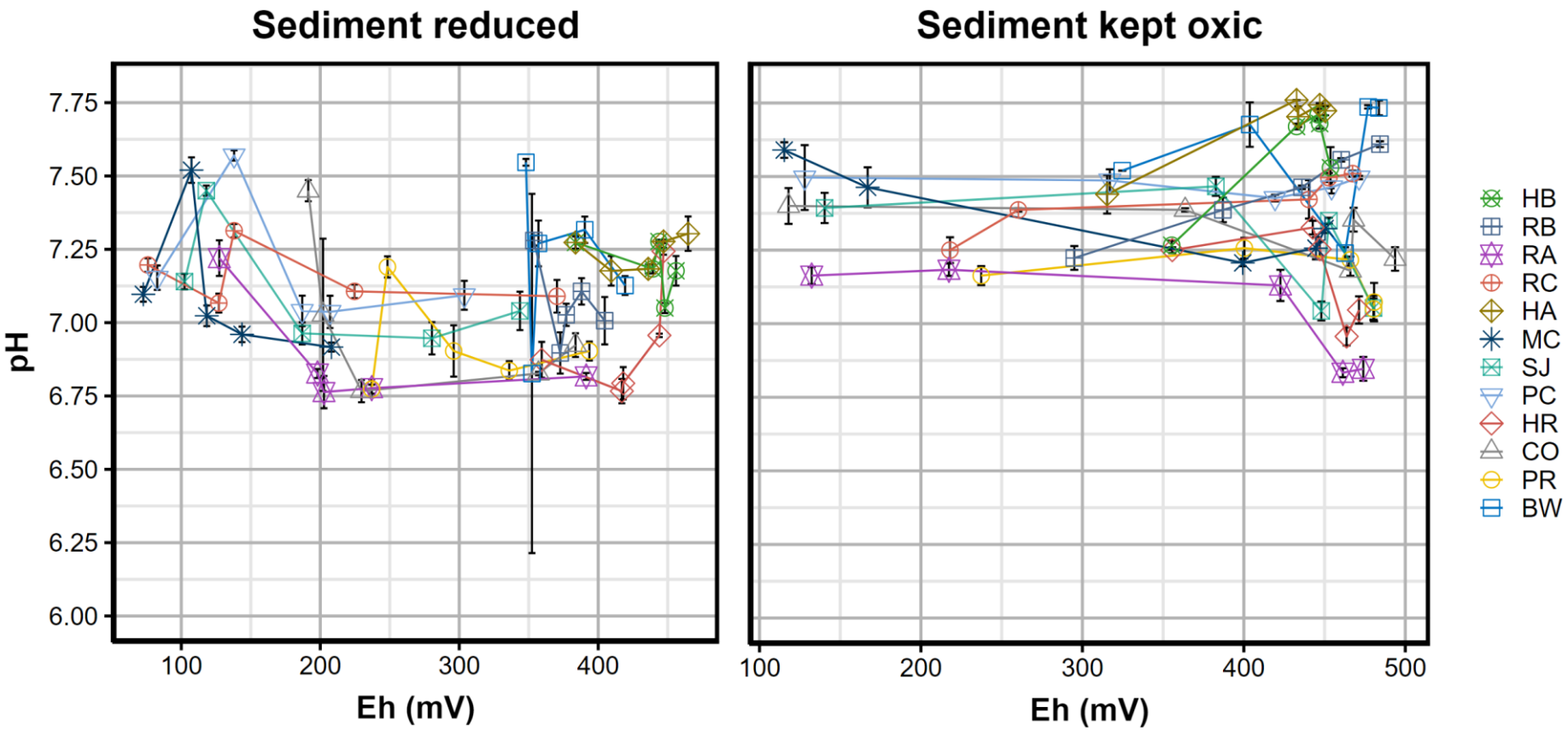

Fig. 6.29: Variation of pH (mean ± SD) with redox potential in ***oxic sediment*** incubations across the study sites. Left hand panel = sediments incubated in anoxic conditions. Right hand panel = sediments incubated in oxic conditions

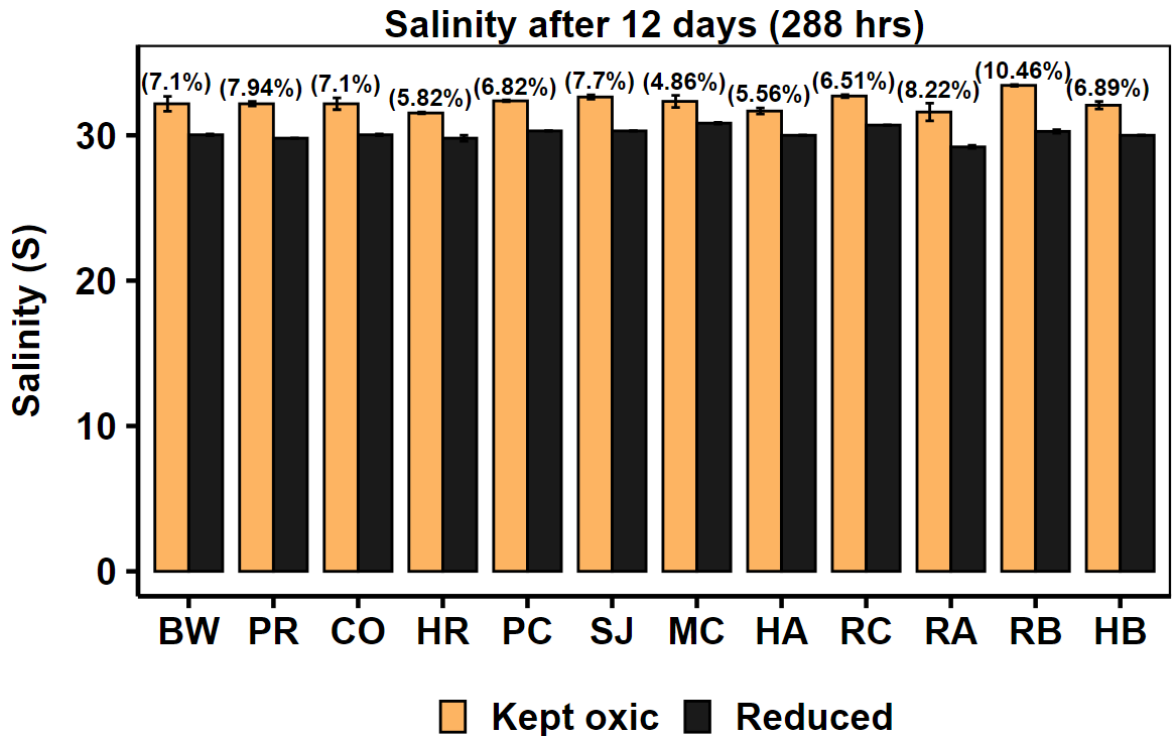

Fig. 6.30: Salinity (mean ± SD) of ***oxic sediment*** slurries, as a proxy for evaporation, after 12 days (288 hrs) of incubation in oxidised (yellow bar) and reduced (black bar) conditions. Numbers in parentheses represent percentage difference between salinity of oxidised and reduced setups

6.3.2.3 Remobilisation of metals in oxic sediment incubation

The trend in metal (Cu, Zn, Fe and Mn) remobilisation with time in the oxic sediment incubations was similar across the treatments, despite differences in the trend in pH. For the typical sediment, metal remobilisation is shown in Figure 6.31. And for RB, with an actual oxic sediment, trend in metal remobilisation is shown in Figure 6.32. Overall, reduction of the typical Fal sediment led to the remobilisation of Fe and Mn, but not Cu and Zn. However, oxidation of these sediments led to a precipitation of Fe and Mn, possibly as Fe and/or Mn oxy(hydroxides), and the release of Cu and Zn before subsequent precipitation by D5. For RB, oxic sediment reduction appeared to remobilise Mn, Cu, and Zn from sediments, whilst sediment oxidation led to the removal of all metals from solution. Where oxic sediment incubations led to the remobilisation of Cu and Zn, the concentrations were low relative to those from anoxic sediment incubations (up to two orders of magnitude less).

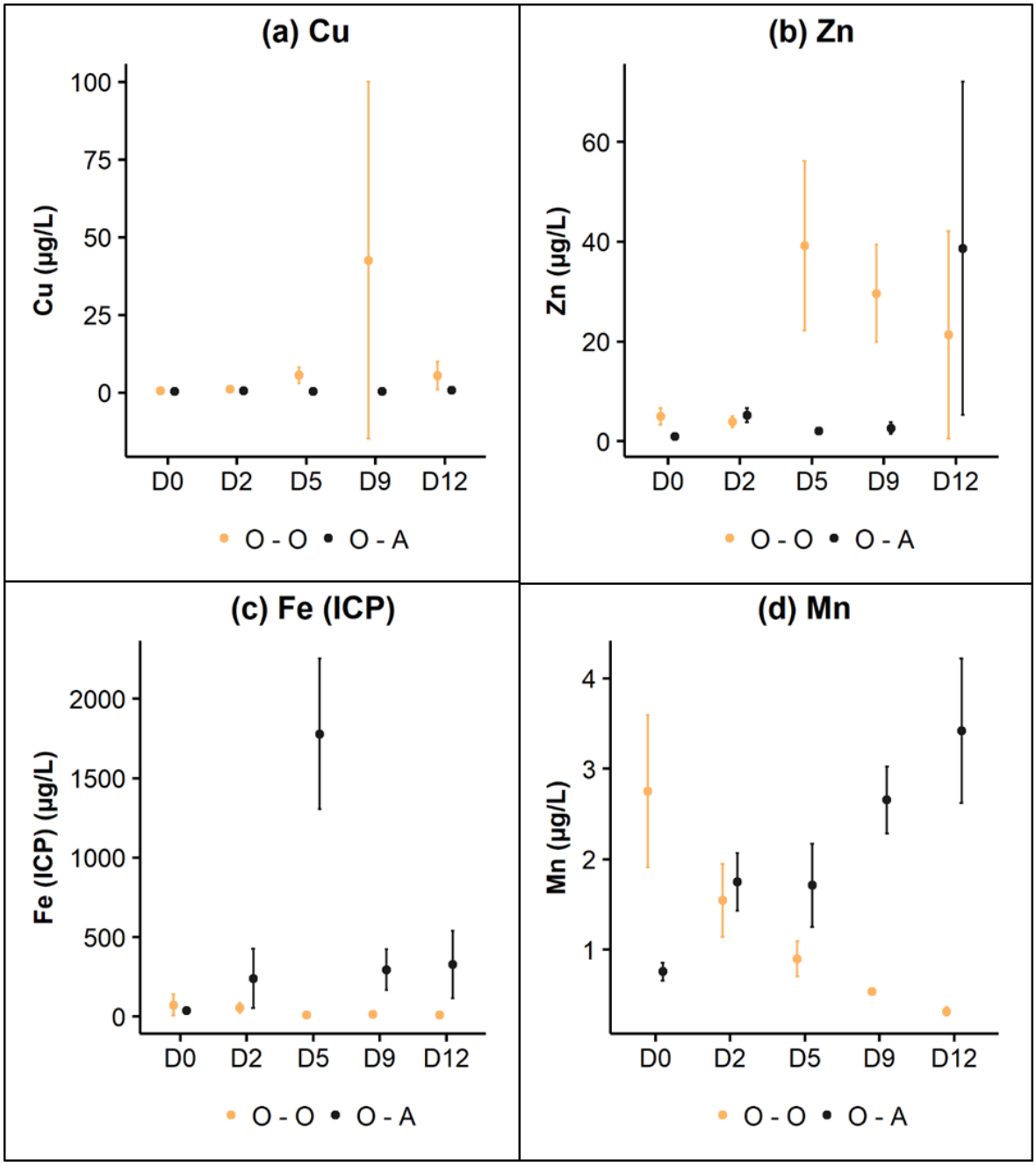

Fig. 6.31: Typical trend in metal remobilisation during ***oxic sediment*** incubations: Cu (panel a), Zn (panel b), Fe (total ICP) (panel c), and Mn (panel d) (all mean ± SD). Values represent measurements for St Just (SJ) sediment. O – O (yellow): Oxic sediments incubated in oxidised conditions. O – A (black): Oxic sediments incubated in anoxic conditions. D0, D2, D5, D9, and D12 represent sampling at timepoints 0, 2, 5, 9, and 12 days (288 hrs) of incubation

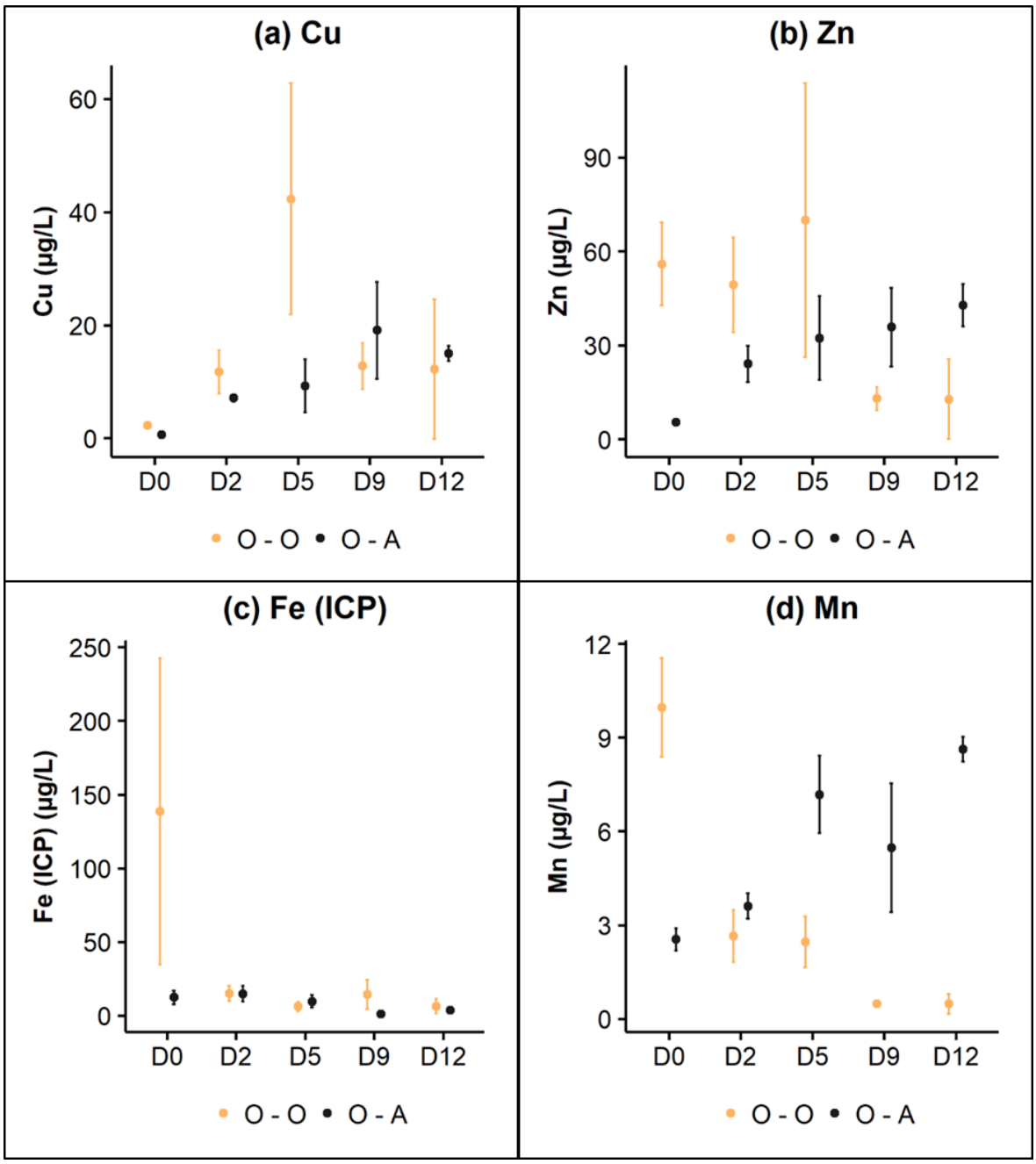

Fig. 6.32: Trend in metal remobilisation during incubation of ***oxic sediment from RB***: Cu (panel a), Zn (panel b), Fe (total ICP) (panel c), and Mn (panel d) (all mean ± SD). Values represent measurements for St Just (SJ) sediment. O – O (yellow): Oxic sediments incubated in oxidised conditions. O – A (black): Oxic sediments incubated in anoxic conditions. D0, D2, D5, D9, and D12 represent sampling at timepoints 0, 2, 5, 9, and 12 days (288 hrs) of incubation

Peak metal concentrations remobilised through the reduction of oxic sediments across the treatments are provided in Table 6.02. For Cu, concentrations across the sites were less than the DOC-corrected WFD standards (25.1 µg Cu/L), except for River Hayle (HA) sediments (38.2 µg /L; 0.76 µg /g dw). However, Zn concentrations (3.7 – 167.8 µg /L; 0.07 – 3.36 µg /g dw) were higher than the WFD standard (7.9 µg Zn/L) in all sites, except BW, CO, and MC. Unlike in the anoxic sediment incubations, peak metal concentrations were higher in Hayle than in Restronguet Creek. The ordering of peak Cu and Zn concentrations across the study sites suggests that starting redox potential, possibly reflective of the availability of metals bound in Fe and Mn (oxy)hydroxides, were, in addition to sediment metal concentrations, important in determining the scale of metal remobilisation.

Combined sites plots of metal concentrations with incubation time and redox show that remobilised metals were generally higher in sediments incubated in oxic conditions than those reduced in anoxic incubations (Figures 6.33 – 6.38; A6.16 – A6.20), confirming the general pattern described earlier. The release of Cu upon oxidation of sediment peaked at around 400 mV across the sites, before being precipitated from solution with further oxidation (Figure 6.34). Similarly, Zn concentrations peaked at 420 – 450 mV. But Fe and Mn continued to be removed from solution with oxidation, precipitating above 350 mV and 420 mV, respectively. Changes in pH did not appear to affect metal remobilisation from the oxic sediments, with pH remaining higher than 6.7 in all setups.

6.4 Discussion

Tidal flooding, epibenthic bioturbation, and benthic faunal burrowing are some of the recurring redox-altering processes in intertidal estuarine sediments (Aller, 1994; Vidal-Dura *et al*., 2018), capable of remobilising metals from redox sensitive phases such as Fe and Mn (oxy)hydroxides in oxic, surface sediments or AVS in anoxic, deeper sediments. The study of sediment physicochemical characteristics in the Fal and Hayle estuaries reported in Chapter 2 of this thesis revealed strong associations between Cu and Zn in surface sediments with Fe concentrations (Figure 2.09), confirming previous findings (Bryan & Gibbs, 1983; Johnson, 1986) that the former metals are adsorbed and/or co-precipitated with Fe-(oxy)hydroxides. In the deeper (5 – 10 cm) sediments, evidence for the incorporation of

metals into sulphide phases included the relatively low porewater metal (Figure 2.12) and acid-extractable Cu (Figure 2.10) concentrations observed, as expected in anoxic marine sediments (Ankley *et al.* 1996). Considering that these estuaries are highly contaminated, the remobilisation of potentially-toxic metals by redox fluctuations may be a significant source of metal for uptake by the inhabiting fauna. In the current study, the incubation of surface ("oxic") and deeper (anoxic) sediments in redox-altering experiments have revealed that medium to long-term redox changes (above 5 hrs) in the Fal and Hayle estuaries can remobilise Cu and Zn at elevated concentrations.

Table 6.02: Peak metal remobilisation (mean values) during the ***reduction of oxic sediments*** across the study sites. For all sites, 10 g (dry weight equivalent) of sediments incubated in 200 mL of seawater. Concentrations provided as direct measurements in sediment slurries (µg/L) and as metals released per unit mass of sediment (µg/g dry weight equivalent). Note that Mn concentrations represent approximately 2% of actual values. Values have *not* been corrected for concentration as a result of evaporation during incubation (4.9 – 10.5 %, see Figure 6.21)

Site	Cu		Zn		Fe		Mn	
	µg/L	µg/g	µg/L	µg/g	µg/L	µg/g	µg/L	µg/g
BW	0.6	0.01	6.9	0.14	29	0.58	19.6	0.39
PR	1.3	0.03	9	0.18	761.3	15.23	14	0.28
CO	0.5	0.01	5.3	0.11	824.8	16.50	11	0.22
HR	10.2	0.20	39.8	0.80	470.2	9.40	9.4	0.19
PC	1.7	0.03	7.9	0.16	1528.5	30.57	3.2	0.06
SJ	0.7	0.01	38.6	0.77	1776.9	35.54	3.4	0.07
MC	0.7	0.01	3.7	0.07	2543.6	50.87	4.6	0.09
HA	38.2	0.76	167.8	3.36	18.5	0.37	19.3	0.39
RC	9	0.18	20.4	0.41	1303.4	26.07	8	0.16
RA	2.9	0.06	64.3	1.29	811.4	16.23	24.3	0.49
RB	19	0.38	42.8	0.86	14.8	0.30	8.6	0.17
HB	6.1	0.12	77.2	1.54	9.3	0.19	23.5	0.47

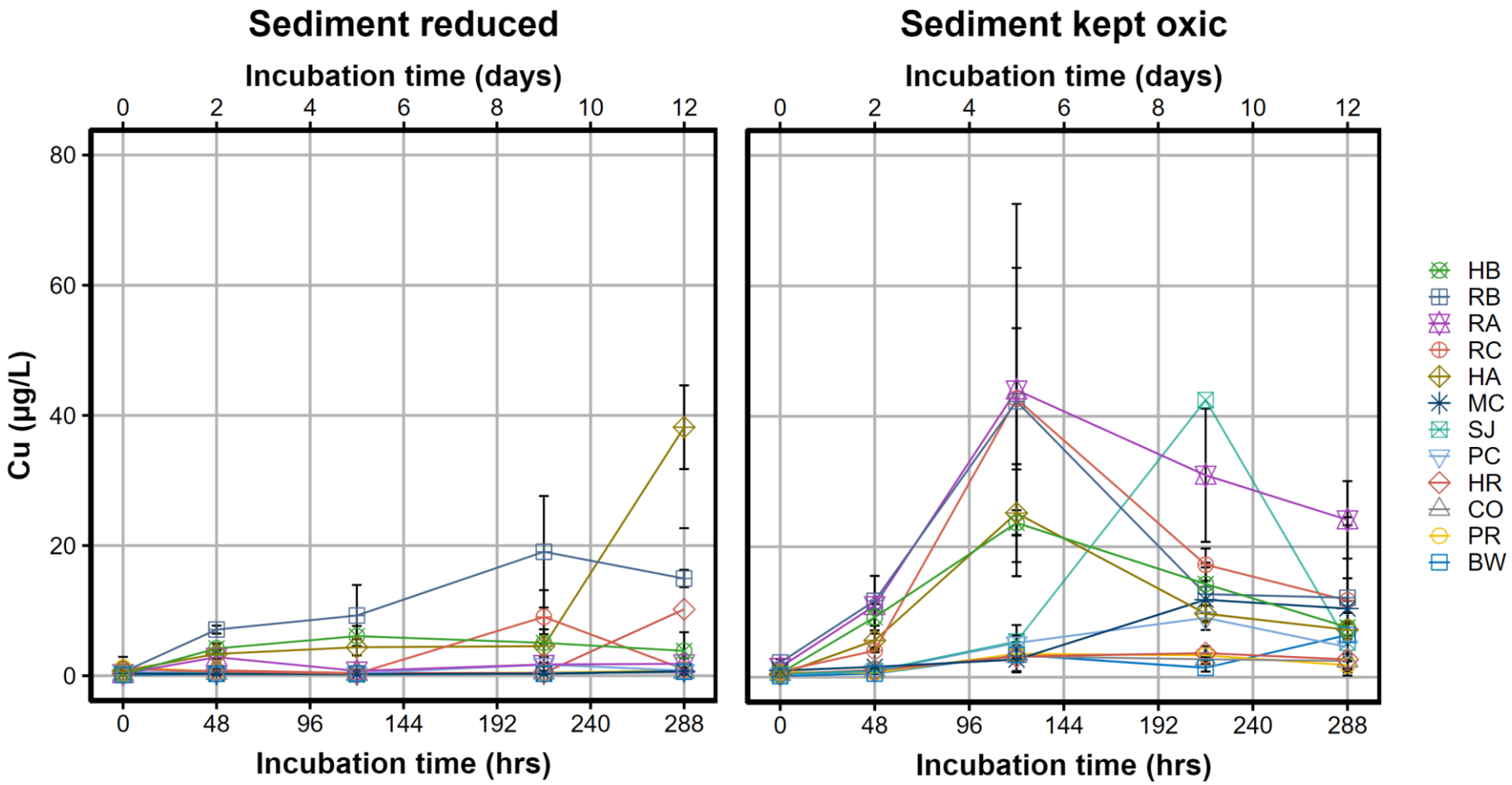

Fig. 6.33: Remobilisation of Cu (mean ± SD) with time in ***oxic sediment*** incubations across the study sites. Left hand panel = sediments incubated in anoxic conditions. Right hand panel = sediments incubated in oxic conditions

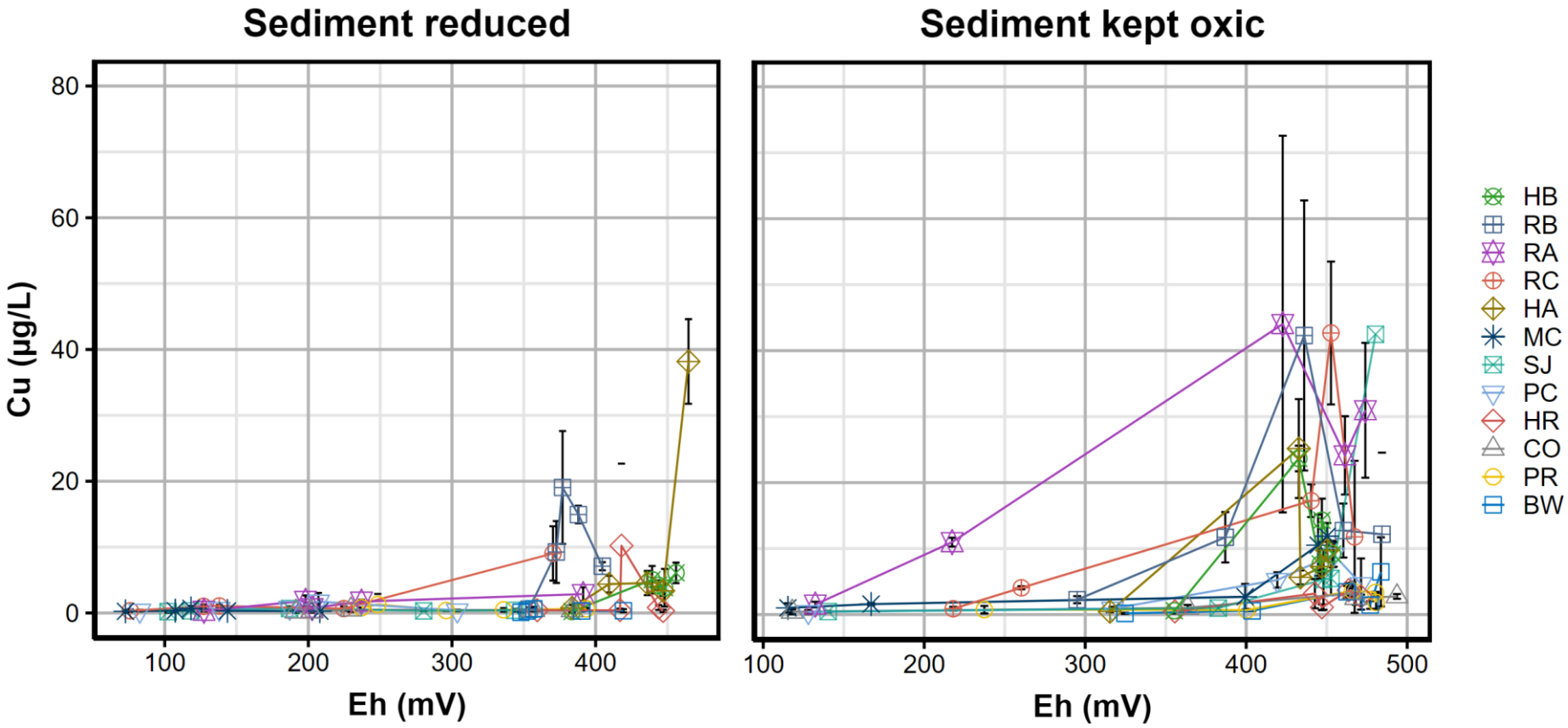

Fig. 6.34: Remobilisation of Cu (mean ± SD) with redox potential in ***oxic sediment*** incubations across the study sites. Left hand panel = sediments incubated in anoxic conditions. Right hand panel = sediments incubated in oxic conditions

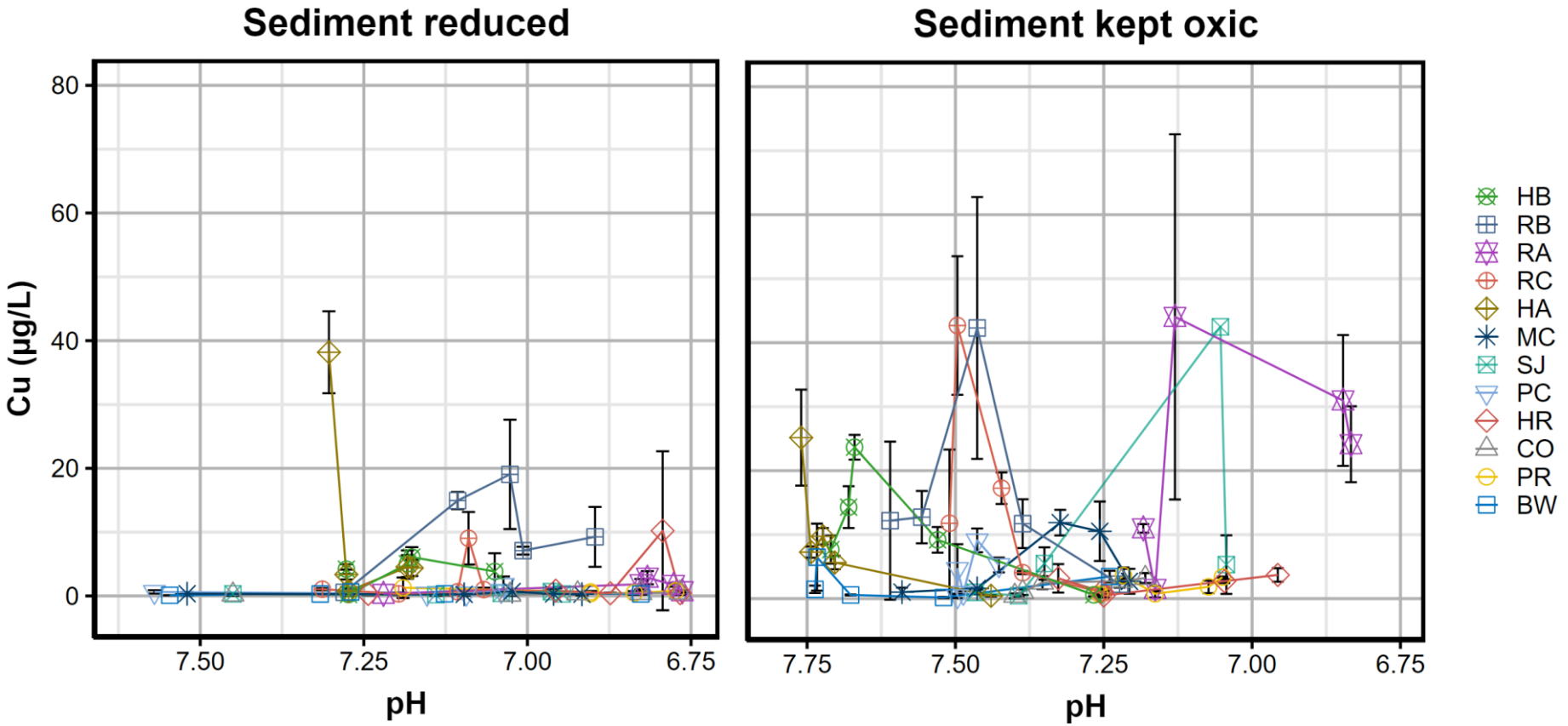

Fig. 6.35: Remobilisation of Cu (mean ± SD) with decreasing pH in ***oxic sediment*** incubations across the study sites. Note the reverse pH scale. Left hand panel = sediments incubated in anoxic conditions. Right hand panel = sediments incubated in oxic conditions

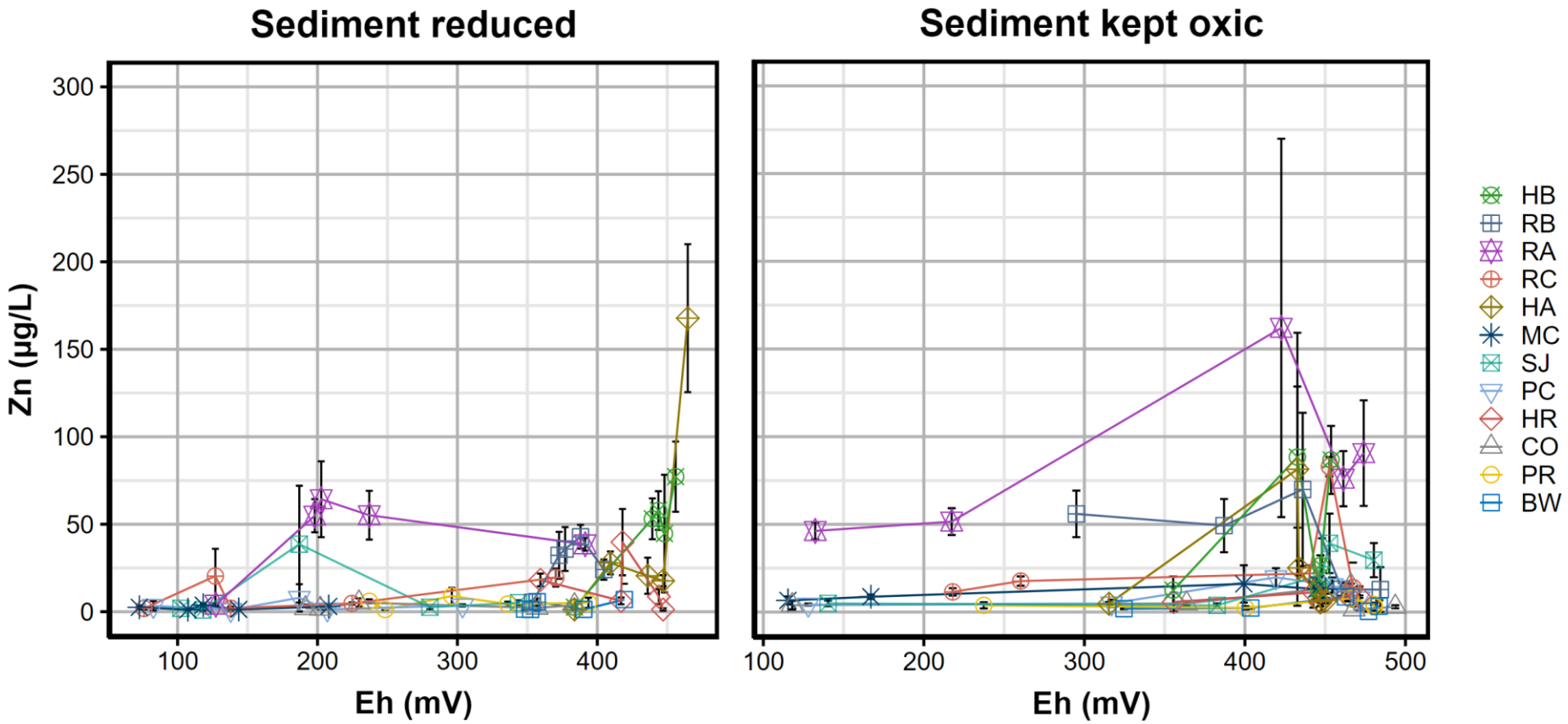

Fig. 6.36: Remobilisation of Zn (mean ± SD) with redox potential in ***oxic sediment*** incubations across the study sites. Left hand panel = sediments incubated in anoxic conditions. Right hand panel = sediments incubated in oxic conditions

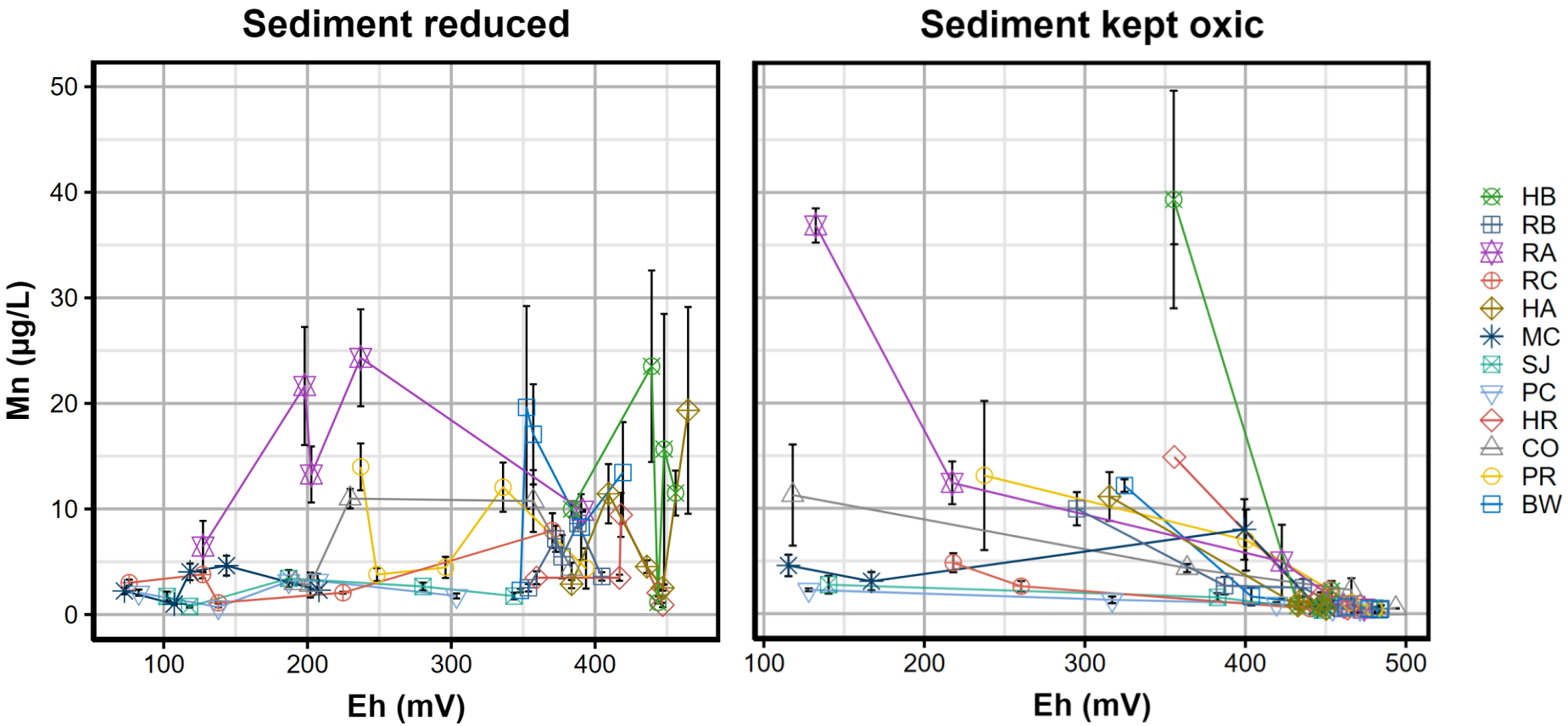

Fig. 6.37: Remobilisation of Mn (mean ± SD) with redox potential in ***oxic sediment*** incubations across the study sites. Left hand panel = sediments incubated in anoxic conditions. Right hand panel = sediments incubated in oxic conditions. Note that Mn concentrations represent approximately 2% of actual concentrations (see Chapter 2)

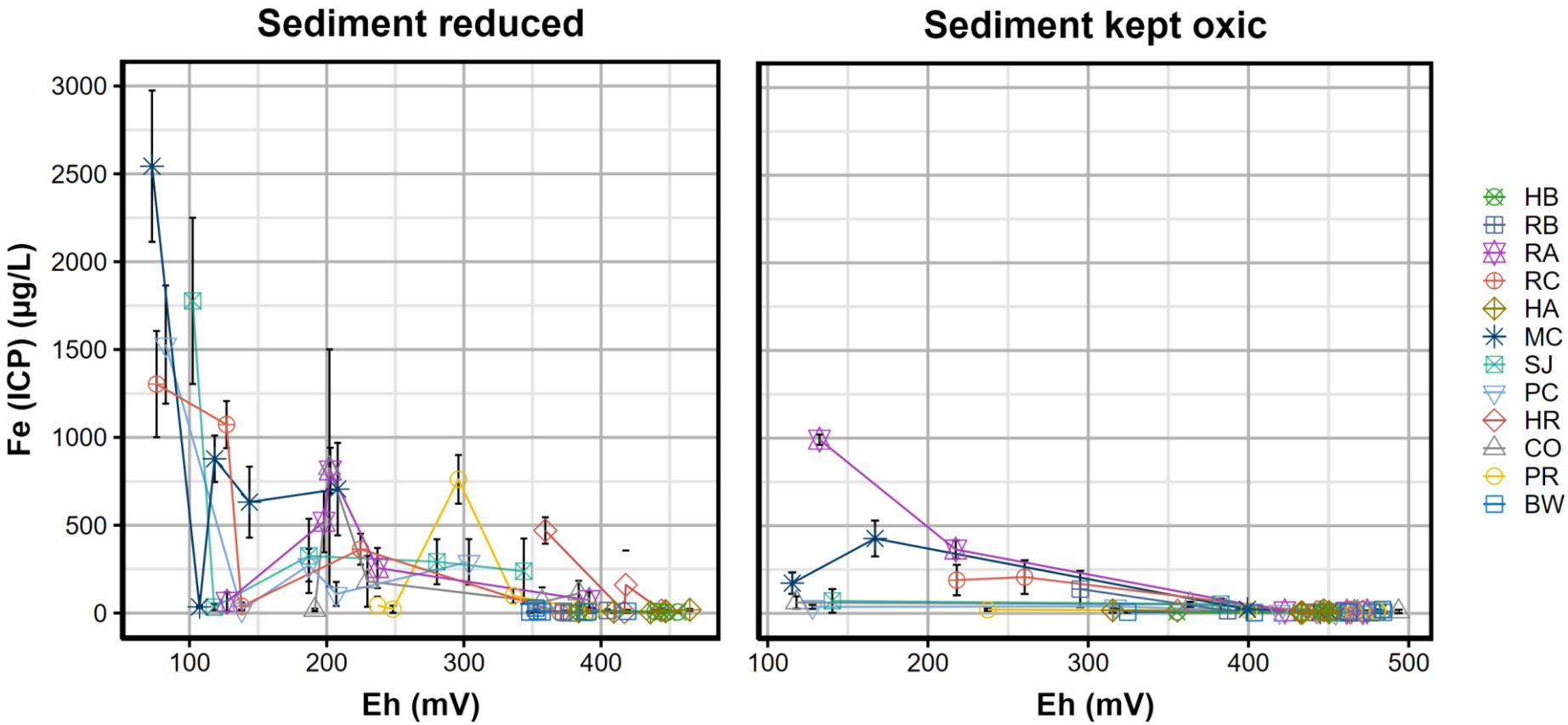

Fig. 6.38: Remobilisation of Fe (total measured by ICP-OES) (mean ± SD) with redox potential in ***oxic sediment*** incubations across the study sites. Left hand panel = sediments incubated in anoxic conditions. Right hand panel = sediments incubated in oxic condition

The oxidation of anoxic sediments in this study, evidenced by an increase in dissolved oxygen concentration (DO) and redox potential (Eh) with time, led to largescale remobilisations of Cu and Zn. Metal concentrations in the slurries increased steadily after 5 hrs of incubation, reaching peak concentrations of 31 – 18886 µg Cu/L (0.62 – 377.72 µg Cu/g) and 151 – 11377 µg Zn/L (3.01 – 277.53 µg Zn/g). The metals were remobilised in sequence: Mn, Zn, and then Cu. The scale of Cu and Zn remobilisation was, in addition to sediment metal concentrations, dependent on sediment AVS concentrations, which also influenced the pH of sediment slurries. For example, despite the lower total Cu concentrations in RC (total Cu = 3013 µg/g; AVS = 56.5 µmol/g), peak Cu concentration in the oxidised slurry was approximately ten times higher than in the treatment from the Upper Restronguet Creek (RA; total Cu = 3166 µg/g; AVS = 26.4 µmol/g) with only a two-fold increase in AVS concentration. Peak concentrations observed were many times higher than WFD thresholds for "good" chemical quality, an indication of "safe" limits for organisms inhabiting transitional waters. Sediment oxidation was also marked by the release of Mn and removal of Fe from solution. In slurries maintained in anoxic conditions, Cu and Zn release was negligible, with maximum average concentrations of 6.6 µg Cu/L and 53.3 µg Zn/L, whilst Fe was remobilised and subsequently precipitated with further reduction.

These observations are consistent with the release of metals bound in sulphide phases (Simpson, 2000), with Fe rapidly precipitated as Fe (oxy)hdryoxides (Benjamin, 1983; Vidal-Dura *et al*., 2018). As earlier highlighted, metal sulphides are unstable sediment phases, releasing bound metals upon oxidation (Simpson *et al.*, 2000, 2012a; Vidal-Dura *et al*., 2018). The sequence of metal release is also consistent with the solubility of metal sulphides, as expected: in order of decreasing metal sulphide solubility: Mn > Fe > Ni > Zn > Cd > Pb > Cu > Ag (Ankley *et al.*, 1996; Rickard & Luther, 2006). The transient release of Fe in reduced conditions is consistent with the reduction of any existing Fe oxide phases (Equation 1; Hutchings *et al*., 2019) and/or the formation of (Equations 2 – 3; Raiswell & Canfield, 2012) and subsequent incorporation of metals into AVS (Equation 4; Simpson *et al.*, 2000). By the end of incubation in anoxic conditions, all Fe had been incorporated into sulphides.

$HS^- + 2Fe(OH)3 + 5H+ \rightarrow 2Fe^{2+} + S^0 + 6H_2O$ (Equation 1)

$2CH_2O + SO_4^{2-} \rightarrow H_2S + 2HCO_3^-$ (Equation 2)

$2FeOOH + 3H_2S \rightarrow 2FeS + S^0 + 4H_2O$ (Equation 3)

$M^{2+} + FeS\ (s) \rightleftharpoons MS\ (s) + Fe^{2+}$ (Equation 4)

Similar observations have been reported in the literature. Amongst others, Vidal-Dura *et al.* (2018) observed the rapid decline of Fe and limited release of Mn in the oxidation of sub-surface sediments from the Humber Estuary. In saline segments of the estuary, they observed peak Cu and Zn within the first few minutes of incubation (~ 7 µg Cu/g and 20 µg Zn/g), which were subsequently precipitated upon further oxidation. Resuspension of anoxic Saguenay Fjord sediments was also associated with the release of As and Mn, but rapid precipitation of Fe (Saulnier & Mucci, 2000). Caetano *et al.* (2003) noted significant remobilisation of Fe and Cu from Tagus Estuary sediments, which were subsequently scavenged from solution. Hwang *et al.* (2011) observed the continual remobilisation of Zn from Nakdong River sediments within 24 hrs. In anoxic, grossly-contaminated sediments (34808 µg Cu/g) from Victoria Harbour, Wong and Yang (1997) observed substantial release of Cu, but precipitation of Fe upon resuspension at pH 8.0. And Shipley *et al.* (2011) observed largescale remobilisation of metals from Trepangier Bayou sediments.

As highlighted earlier, the scale of metal remobilisation in this study was influenced by both metal and AVS concentrations in the sediments, with the highest values, overall, observed in sediments from the most anoxic site in the Restronguet Creek (RC). Peak metal concentrations from anoxic sediments observed in the current study are higher those reported in several studies conducted at circumneutral pH, including in the resuspension of surface sediments herein, but are within range for studies carried out at low pH values. Therefore, the low pH in sediment slurries must have facilitated the dissolution of metals in sediment phases. The large reduction in pH (down to 4.5) observed in this study is expected, and has been observed in similar resuspensions of highly anoxic sediments (e.g. Dubrovsky *et al.*, 1985; Calmano *et al.*, 1993; Degtiareva & Elektorowicz, 2001; Lors *et al.*, 2004; Shipley *et al.*, 2011). In these studies, the drop in pH has been attributed to the oxidation of AVS and

pyrite, if present (Equations 5 – 7; Simpson, 2000; Shipley *et al.*, 2011), releasing protons in sufficient quantities to disrupt the buffering system in seawater. For example, in anoxic sediments from Trepangier Bayou (AVS = 125 µmol/g), resuspension in 1/25 g/mL solid:solution ratios led to pH decreases down to 4, with resulting remobilisation of Zn at around 2500 mg/L in a six-day incubation (Shipley *et al.*, 2011). Although less likely due to the scale of the experiment, a second possible reason for the reduction in pH in the current study may be the possible dissolution of atmospheric $CO_{2\ (g)}$ during the incubation process. The potential decrease in seawater pH following the dissolution of $CO_{2\ (g)}$ has been well described in the literature (Equation 7, Feely *et al.*, 2009). In this process, the formation of carbonic acid can disrupt carbonate/bicarbonate buffering in natural seawater, leading to subsequent release of protons and a drop in pH.

$HS^- + 4H_2O \rightleftharpoons SO_4^{2-} + 9H^+ + 8e-$ (Equation 5)

$2FeS_{(s)} + 9/2O_2 + 5H_2O \rightarrow 2Fe(OH)_{3(s)} + 2SO_4^{2-} + 4H^+$ (Equation 6)

$FeS_{2(s)} + 15/4O_2 + 5/2H_2O \rightarrow 2FeOOH_{(s)} + 2SO_4^{2-} + 4H^+$ (Equation 7)

$CO_{2(aq)} + H_2O \rightleftharpoons H_2CO^3 \rightleftharpoons H^+ + HCO_3^- \rightleftharpoons 2H^+ + CO_3^{2-}$ (Equation 8)

Unlike in the Fal and BW sediments, the oxidation of Hayle sediments led to a rise in pH, with the pH remaining fairly stable upon reduction. This observation suggests that the Hayle sediments have a high buffering capacity, which in addition to low sulphide concentrations, might be responsible for the increase in pH. The high buffering capacity in Hayle sediments is possibly due to the presence of relatively high carbonates (Feely *et al.*, 2009). Carbonates (as inorganic carbon) were not assessed in this study; however, they are well correlated with CaO concentrations across the study sites (Figure 6.39; data derived from Greenwood, 2001; Equation 9). Across the Fal, CaO concentrations (0.40 – 3.48%) were substantially less than in both Hayle sediments (5.65% in HA and 6.79% in HB)[63] (Table A6.02). The relatively

[63] CaO concentrations were also relatively high in Breydon Water (8.06%, Table A6.02), but without the buffering observed in the Hayle. The exact reason for this is unclear, but may be related to the high sulphide concentrations in the site, as earlier highlighted.

low sulphide concentrations in Hayle are possibly due to its more coarse grainsize, limiting the formation of reactive Fe(III) phases – i.e. amorphous Fe oxide (Thomson-Becker & Luoma, 1985), from which AVS is formed upon further reduction (Equation 10; Raiswell & Canfield, 2012). In surface sediments of both Hayle sites, 1M HCl extractable Fe concentrations (as a measure of reactive Fe phases, Kostka *et al.*, 2002) are consistently lower than or similar to those in less contaminated sediments of the Fal and BW, despite much higher Total Fe concentration (Tables A2.05 – A2.15). This suggests that much of the sedimentary Fe in Hayle, relative to the rest of the sites, is present in crystalline, unreactive forms. Indeed, Hayle sediments were geochemically distinct from the rest of the sites. The coarse grainsize in Hayle is also expected to enhance oxygen penetration, which would limit the formation of sulphides in the deeper sediments.

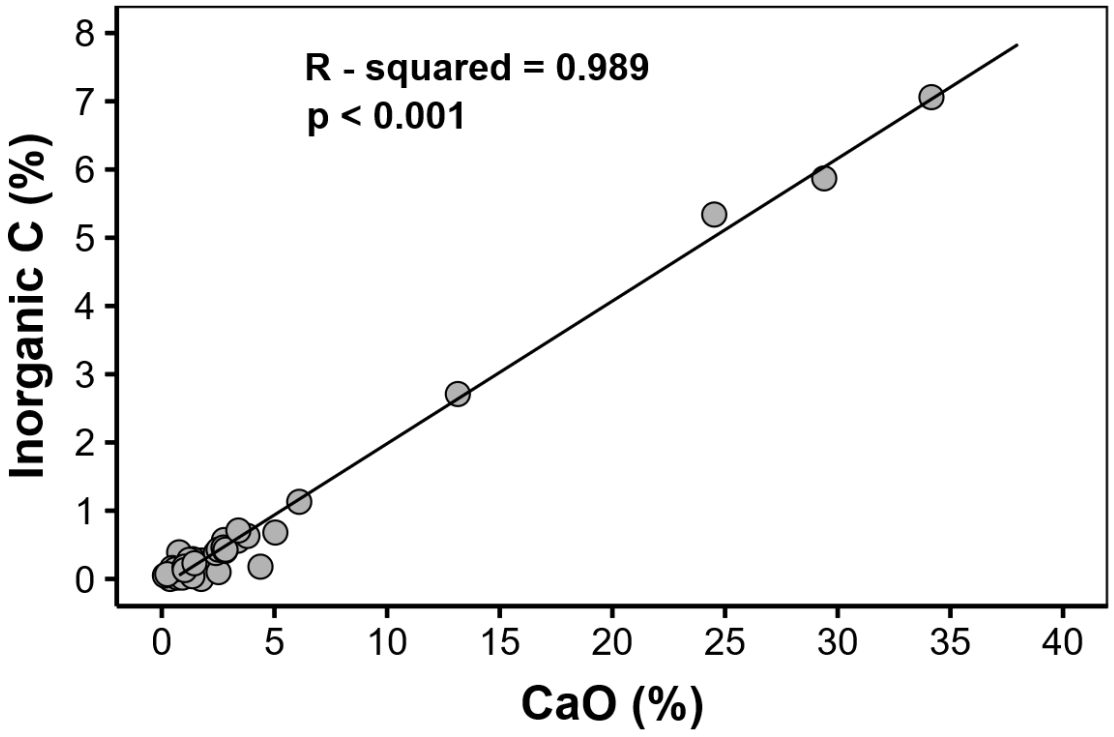

Fig. 6.39: Predicting sediment inorganic carbon composition (as the difference between percentage total carbon and organic carbon) from the percentage calcium oxide content. All mean values from three replicates. Data derived from Greenwood (2001) for oxic sediments sampled from 14 sites in Cornwall, England in May 1998, July 1999, and February 2000

$CaCO_{3(s)} \rightarrow CaO_{(s)} + CO_{2(g)}$ (Equation 9)

$2FeOOH + 3H_2S \rightarrow 2FeS + S^0 + 4H_2O$ (Equation 10)

Considering the low pH values observed upon anoxic sediment oxidation in the current study, such largescale remobilisation Cu and Zn may not be realistic in actual resuspension events in estuarine systems, where buffering up to pH 7 is expected given higher seawater/sediment ratios (Vidal-Dura *et al.*, 2018). Moreover, resuspension events lasting 5 – 50 hrs, under which more prominent metal remobilisation was observed in the current study, are infrequent in natural systems, occurring at large timescales (Vidal-Dura *et al*., 2018). However, in microhabitats within surface or deeper sediments, e.g. in oxidised burrows, with lower seawater/sediment ratio, or as a result of human activity, e.g. dredging, deep-sea mining, bait digging, or installing moorings, the local remobilisation of Cu and Zn from sediment phases may contribute to metal toxicity in marine sediments. In the Hayle, where sediments were well buffered (~7.8), peak release of Cu (31 and 57 µg/L in HA and HB, respectively) and Zn (151 and 436 µg/L in HA and HB, respectively) in the current study may be achievable in natural systems. These concentrations are still considerably higher than the WFD thresholds and may represent possible concentrations in equally contaminated portions of the Fal. Linking metal remobilisation as a result of bioturbation with toxicity to benthic fauna has been recently demonstrated in several studies, notably in the studies by Remaili *et al*. (2018) and Simpson *et al.* (2012a) described earlier. The potential remobilisation of metals from anoxic sediments is therefore an important consideration in toxicity assessments.

Unlike the oxidation of anoxic sediments, the reduction of oxic sediments in this study led to minimal remobilisation of metals into solution, with peak concentrations of Cu (0.5 – 38.2 µg/L = 0.01 – 0.76 µg/g) and Zn (3.7 – 167.8 µg/L = 0.07 – 3.36 µg/g) observed after 5 days of incubation. As observed in the current study, the reduction of Fe (oxy)hydroxide phases is expected to release bound metals, including Fe, either by chemical (Equation 1) or dissimilatory mechanisms (Equation 11) (Hutchings *et al.*, 2019; Raiswell & Canfield, 2012). However, the low porewater Cu and Zn concentrations and presence of AVS in

surface sediments sampled demonstrates that Fe(III) phases may have been minimal in these sediments (Raiswell & Canfield, 2012). Only few sediments were truly oxic – mainly at RB. There, peak concentration of Zn (42.8 µg/L; 0.86 µg/g), but not Cu (19 µg/L; 0.38 µg/g), was higher than the WFD threshold, and both metals were rapidly sequestered back to the sediment phases with further oxidation. Indeed, more metals were released from the incubation of these surface sediments in oxic conditions (Figures 6.33 – 6.36), under largely similar circumstances to those described earlier for the oxidation of anoxic sediments, before being precipitated back into the solid phase. As pH changes in these setups were much less pronounced than in the anoxic sediments (minimum pH = 6.77), the relatively low remobilisation of metals is expected and corroborates findings from previous resuspension studies described earlier (notably, Vidal-Dura *et al.*, 2018). In the current study, peak concentrations were highest in sediments from HA (38.2 µg Cu/L = 0.76 µg Cu/g and 167.8 µg Zn/L = 3.36 µg Zn/g), and only peak Cu concentration from this site was above WFD thresholds, suggesting that metal remobilisation at potentially toxic concentrations at this site is plausible. During the colder seasons (e.g autumn and winter, see Chapter 2), when redox potential in surface sediments across the study sites is expected to be relatively high, the sediments are expected to be fully oxic and largescale remobilisation of metals cannot be not ruled out.

$$4Fe(OH)_3 + 7H^+ + CH_2O \rightarrow HCO_3^- + 4Fe^{2+} + 10H_2O \qquad \text{(Equation 11)}$$

Overall, the current study has shown that redox changes occurring in estuarine sediments may remobilise metals bound in seemingly non-labile sediment phases at concentrations that may be potentially toxic to benthic fauna. As demonstrated by Remaili and colleagues (2018), and similar studies (e.g. Simpson *et al.*, 2012a), this potential is plausible in marine sediments and should not be overlooked in the risk assessment of metal contaminated sites.

Chapter 7.

Conclusions, recommendations, and future work

7.1 Conclusions

The main aim of this thesis was to assess dose-response relationships of metals in marine sediments – specifically to investigate what chemical measures are the best predictors of ecological effects and the threshold concentrations at which these effects begin to occur. **A key gap in knowledge is how measures of metal concentration in the *field* relate to *ecological* endpoints (Chapter 1). Until now, sediment regulatory benchmarks and the identification of bioavailable fractions of metals have been based largely on tests using poorly-equilibrated, highly-spiked sediments and of surrogate endpoints, such as bioaccumulation.** Whilst these studies were helpful in identifying potential tools or chemical measures for predicting sediment metal toxicity, the experimental conditions and/or endpoints used may depart significantly from realities in field-contaminated sites, resulting in over- or under-protective threshold values. For example, in evaluating the dataset used in the development of the Sediment Biotic Ligand Model (sBLM, Di Toro *et al*., 2007; see Figure 7.01), which is the most advanced form of the widely-accepted equilibrium partitioning model (EqP), Simpson and Batley (2007) remarked:

> In region A, porewater metal concentrations are in the region of environmental realism. In region B, porewater metal concentrations range from high to very high and are at the limit of environmental realism. In region C, porewater metal concentrations are extremely high and are well beyond the limits of environmental realism…

In view of this, an important aspect of this thesis was the use of actual ecological effects in field-contaminated marine sediments. The Fal and Hayle estuaries in Cornwall, Southwest England, were ideal candidates in this regard, as they have a long history of contamination by mine drainage. The sediments across the estuaries exhibit a gradient of metal contamination. They include some of the most contaminated sites in the United Kingdom and have negligible concentrations of other potentially-toxic contaminants (Rainbow, 2020).

Sediment metal concentrations at both estuaries have remained stable for several decades of measurement (Bryan & Gibbs, 1983; Bryan & Langston, 1992; Rainbow, 2020), ensuring that the resident benthic fauna remained exposed to metal contamination and that only metal-tolerant species and individuals can thrive (Grant, 2002, 2010).

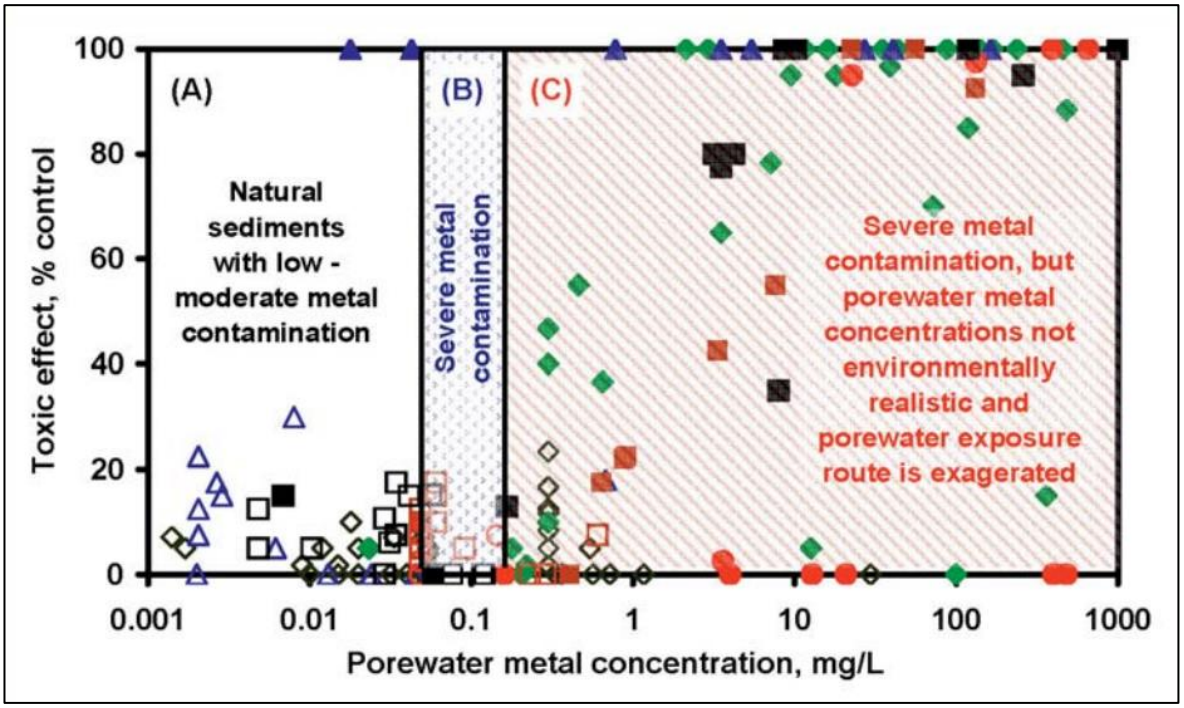

Fig. 7.01: Dose-response data used for the EqP and sBLM model development. Symbols represent sediments in which AVS > SEM (open symbols) and AVS < SEM (filled symbols) for the metals Cd (diamond), Cu (triangle), Ni (circle), Pb (red square) and Zn (black square). (Republished with permission of John Wiley & Sons - Books, from Simpson & Batley, 2007)

I began, in **Chapter 2**, by assessing the physicochemical characteristics of sediments and porewater at eleven sites along the contamination gradient in the Fal and Hayle estuaries. The assessment was undertaken over a two-year period in three different sampling seasons – autumn, winter and summer. This work was important to ascertain the current state of metal contamination across the estuaries and, by implication, metal exposure to the benthic fauna. The results from Cornwall were compared with those from an unimpacted site, Breydon Water (BW), in Norfolk, England.

Overall, the work confirmed a stable gradient of sediment metal concentration across both estuaries, with the lowest concentrations measured in Percuil River (PR) and the highest concentrations in the Upper Restronguet Creek. Total sediment metal concentrations determined across the sites were similar to those previously reported (Bryan & Gibbs, 1983; Somerfield 1994a, 1994b; Greenwood, 2001; Rainbow, 2020). **In the Hayle estuary, sediment metal concentrations were of a similar magnitude to those found in Restronguet Creek.** And in Summer 2019, grain size-normalised concentrations in Copperhouse Pool (HB) exceeded the maximum in the Restronguet Creek. Whilst total metal concentrations in Breydon Water sediments were lower than those in average shale, which has been used as an indicator of pre-industrial, uncontaminated conditions for marine muds, concentrations in the Upper Restronguet Creek (RA and RB) as well as in Hayle were more than two orders of magnitude greater. Concentrations at Percuil River (PR), the least contaminated tributary, were ten times higher than in average shale, and there was a nearly three orders of magnitude difference in total metal concentrations between BW and the most contaminated sites (HB and RB).

Although total sediment metal concentrations were stable across the contamination gradient **in the Fal and Hayle, Chapter 2 also revealed the occurrence of temporal changes in metal bioavailability within relatively short timescales** (e.g. between January and July, 2019). In some sites, more than ten-fold variations were observed in porewater metal and AVS concentrations, amongst others, between the three sampling periods. The variation in acid-extractable Cu concentration in the surface sediments was up to two-fold, as Cu was incorporated into insoluble sulphides. **The highest porewater concentrations were recorded in River Hayle (HA), where metals appeared to be most bioavailable due to the coarse grainsize and relatively low organic carbon content in the sediment. An important message is the potential for short-term variation in metal exposure to the resident benthic fauna, possibly explaining some of the variations observed in studies of ecological effects in the Fal**. For example, the ordering of pollution-induced tolerance of nematode communities (PICT) to Cu across the study sites, as a measure of ecological effects, varied markedly between Autumn 2017 and Winter 2019 (results reported in Chapter 3), reflecting porewater Cu concentrations measured at the time of sampling.

In **Chapter 3**, the capability of DGT as a tool to predict the ecological effects of Cu in the contamination gradient across the twelve study sites was compared with more traditional measures of metal contamination: total porewater (PW) Cu, acid-extractable (AEM) Cu, total sediment (Sed) Cu, the EqP organic carbon-normalised derivation [SEM Cu – AVS]/fOC, and the organic carbon-normalised porewater concentrations (PW Cu/OC), the last of which was inspired by observations of limited dissolved Cu bioavailability and toxicity in high DOC environments (Water Framework Directive [WFD], 2015; Paller *et al*., 2019; Strivens *et al*., 2019). DGT has been suggested to be a useful tool for the assessment of metal bioavailability, based mainly on its selective uptake of potentially-labile metal fractions in water and sediment deployments (Zhang & Davison, 2015). Given strong correlations between DGT metal uptake and faunal uptake and toxicity, several authors (e.g. Strivens *et al.*, 2019; Marras *et al.*, 2020) have suggested the setting of SQGs based on DGT-labile concentrations. As discussed earlier, the EqP (SEM – AVS) is also widely accepted as a model to identify aquatic sediments where the risk of metal toxicity is low. With the normalisation by the fraction of sediment organic carbon, the model is expected to predict metal toxicity to benthic fauna (Di Toro *et al.*, 2005) and has been incorporated into some of the most advanced SQGs currently available (e.g. Burgess *et al.*, 2013; Simpson *et al*., 2013). Ecological effects of Cu across the study sites were assessed using nematode PICT. This is one of very few studies to assess DGT against actual ecological effects in field-contaminated sites.

Amongst the measures of metal contamination assessed, **only DGT-labile (C_{DGT} Cu) and PW Cu concentrations were predictive of ecological effects, measured as nematode PICT, across the study sites**. **C_{DGT} Cu was the best predictor of effects; however, C_{DGT} Cu measured in the sediment layer offered little advantage over traditional porewater measurement** (r C_{DGT}-SED = 0.68 versus r PW = 0.66). **The Derived NOAELs were 31.5 µg/L PW, 3.62 µg/L C_{DGT}-OLW, and 9.19 µg/L C_{DGT}-SED**, based on concentrations up until the Hayle Copperhouse Pool, where nematode PICT was not significantly different from the reference Breydon Water site. These thresholds are higher than those previously proposed in SQGs, but closer to both dissolved (WFD, 2015) and DGT (Strivens *et al.*, 2019) thresholds corrected for dissolved organic carbon (DOC) concentration. The results reaffirm

the influence of high DOC on dissolved Cu bioavailability. **I therefore recommend the incorporation of DOC measurements into dissolved-phase SQGs for Cu**.

An assessment was also made of the strengths and weaknesses of DGT as a tool in marine sediment monitoring for setting SQG thresholds. Although DGT was predictive of ecological effects in the study, several limitations, including the low dynamic range, the influence of non-relevant site-specific factors, such as rate of resupply, in measurable concentrations, and the time constraint in intertidal deployment, preclude any such use. Moreover, the technique is labour and capital intensive, relative to direct porewater measurements. **I therefore do not recommend DGT for use in marine sediment monitoring or in setting universal regulatory values**.

Chapter 4 was a study of the nematode community structure along the metal contamination gradient in the Fal and Hayle estuaries, using both univariate diversity indices and multivariate (MDS, BIOENV, and MRT) methods. Benthic community composition has for long been used to distinguish clean from grossly-polluted marine sites, although the confounding effects of other environmental characteristics on community composition may limit the sensitivity of this approach. As a result, previous studies of the Fal system (e.g. Somerfield *et al*., 1994a, 1994b; Millward, 1995) have been limited to comparing nematode community between creeks and included extensive controls for grainsize, tidal height, and/or salinity influences. **The current study extended the use of meiobenthic community composition as an indicator of pollution in heterogeneous intertidal sediments**, further including Breydon Water, two Hayle sites, and additional sites within the Fal. The variation in nematode community composition was then related to variations of the different measures of metal contamination to derive relevant threshold concentrations.

The results revealed that, unlike univariate diversity measures, multivariate analysis of nematode communities in the Fal and Hayle estuaries is responsive to metal contamination and robust to the variation in other site characteristics. This suggests that the "nuisance" effect of site physicochemical variations become pronounced in low-resolution, larger-scale studies comparing whole creeks or estuaries, such as in the previous studies: replication in the current study was done within sites, with metal concentrations measured at comparatively higher resolution to represent the particular sampling location.

Sites were separated into groups consisting of grossly-contaminated areas of the Restronguet Creek and Hayle as well as reference and less-contaminated locations in the rest of the Fal. **Nematode community structure across the estuaries was more strongly associated with Cu contamination, rather than Zn, corroborating previous findings** (e.g. Bryan & Gibbs, 1983). **Total porewater Cu concentration was the best predictor of community composition and provided the clearest distinction between the grossly contaminated sites and other sites of less contamination**. However, **the ordination of sites based on total sediment Cu within individual groups indicates that both sedimentary and dissolved Cu are contributing to the variation in nematode community composition in the Fal and Hayle estuaries**.

In the multivariate analysis, nematode communities from Sites PR and the Helford River (HR) were ordinated close to the reference BW site, but away from other more-contaminated sites along the gradient. NOAELs for the shift in community composition were therefore derived from metal concentrations at Sites PR or HR, whichever was higher. The **threshold for total porewater and sediment Cu concentrations are 3.5 µg/L and 215 µg/g, respectively**. The porewater threshold is similar to SQG Cu thresholds for low-DOC waters and ten times higher than that derived for nematode PICT (from Site HB), suggesting that **nematode community composition is more sensitive than community tolerance as an indicator of metal pollution.** Furthermore, **DGT-labile concentrations were poor predictors of nematode community structure, and PW/OC and EqP Cu were less predictive than total Cu concentrations in the porewater and sediment**.

In **Chapter 5**, I assessed the potential for dietary toxicity as well as the validity of the EqP model in predicting (non-) toxicity of Cu to a deposit-feeding snail, *Peringia ulvae*. **A significant limitation of the EqP in marine sediments is that it ignores dietary uptake of metals by deposit feeders**. The model assumes that organisms receive equivalent exposure of metals from the dissolved phase as from any other uptake route, including the ingestion of sediments, such that if metal activity in the dissolved phase is negligible, as when metals are incorporated in sulphides, then sediment toxicity is not expected (Di Toro *et al.*, 2005). Dietary metal uptake in sulphidic sediments and at negligible porewater concentrations have been shown in several deposit-feeding invertebrates (e.g. Lee *et al.*,

2000a; De Jonge *et al.,* 2009). **In oxic sediments, few studies have linked this uptake to metal toxicity at dissolved concentrations below water-only thresholds** (Strom *et al*., 2011 and Campana *et al*., 2012). **However, no study has demonstrated the toxicity of metal sulphides to deposit feeders.** EqP proponents argue that bioaccumulation is immaterial and water-only thresholds are protective of dietary toxicity (Di Toro *et al.*, 2005; DeForest & Meyer, 2015).

Contrary to expectations from the EqP model, I demonstrate that (i) sediment-bound metals – and not dissolved concentrations – are primarily responsible for Cu toxicity in *P. ulvae*, and that (ii) Cu sulphides, in the presence of excess AVS, may also be toxic to this species. This was done using feeding depression as an endpoint in snails exposed to spiked oxic and anoxic sediments for a 24-hr period. Feeding depression in this species is an important ecological effect and has been linked to long-term growth rates in field sediments (Shipp & Grant, 2006). I observed significant feeding depression in oxic sediment treatments despite porewater concentrations below the 48-hr water-only EC_{20} – a very conservative threshold. In the least contaminated oxic sediment treatment, with similar porewater concentrations to the control sediment, I observed > 50% depression in feeding, relative to the control. **The results were consistent when using anoxic sediments with excess molar AVS concentrations**, and porewater Cu concentrations herein remained less than the 48-hr water-only EC_{50} even after oxidation at the end of the experiment.

Modelling dose-response relationships from oxic sediment exposures as well as combining both oxic and anoxic sediment exposures contributed further proof of dietary toxicity to *P. ulvae*. **Only sedimentary metals (total Cu and SEM concentrations, in decreasing order of importance) were predictive of toxicity** in the test species. Both total porewater concentrations and the EqP (as SEM – AVS) were poorly predictive of Cu toxicity. **Modelled EC_{50} for total Cu concentration was 1.7 µmol/g (108 µg/g)**, similar to concentrations at Percuil River (PR). In the combined dose-response fits based on sedimentary metals, there was a convergence in snail feeding rates: **toxic response in spiked oxic and anoxic treatments were strongly predicted by total Cu and SEM concentrations irrespective of starting AVS concentrations, thus providing evidence for a possible toxicity of Cu sulphides** to *P. ulvae*. The results provide a critical link between

previous observations of the bioavailability of metals in sulphidic sediments and their toxicity to sediment ingesters.

The use of field-contaminated sediments was not practical in Chapter 5. However, sediments were spiked at environmentally-realistic concentrations and aged, in line with best practice (see Lee *et al.*, 2000; Simpson *et al.*, 2004; Hutchins *et al.*, 2008), to achieve porewater-sediment metal partitioning similar to those observed in the Fal. The results are, therefore, relevant to field scenarios. For example, dietary metal toxicity to *P. ulvae* may explain the absence of natural populations in Restronguet Creek, despite it occurring elsewhere within the Fal. Although porewater concentrations therein are below acute water-only thresholds, Restronguet Creek sediments are highly contaminated and acutely toxic to *P. ulvae* (Shipp & Grant, 2006). **Overall, results from this chapter reveal a significant flaw in the applicability of the EqP model to deposit-feeding invertebrates**.

The predictive capability of the different chemical measures of metal contamination assessed against various endpoints in this thesis are summarised in Table 7.1. **The results demonstrate that nematode PICT is strongly correlated with dissolved metals, that the shift in nematode community composition reflects variations in both dissolved and sediment-bound metals, and that feeding-depression to the deposit-feeding *P.ulvae* is strongly predicted by sediment-bound metals**. Where dissolved metals were important predictors, **DGT, as a tool, offered little above the traditional measurement of total porewater concentration in the sediment**. And where sediment-bound metals were important, the **total sediment Cu concentration proved more useful than originally hypothesised** at the start of the thesis. In both instances, **the EqP approach to predicting metal toxicity did not perform as well as expected, given its prominence in the literature**. **The combination of metal exposure routes observed in this thesis, even within the same taxon (as in nematode communities), represents the realities typical of marine sediments and highlights the difficulty in setting SQGs based on single measures**. My recommendations for the regulation of metals in contaminated marine sediments are provided in Section 7.2.

Table 7.1: Predictive capability of the chemical measures of metal contamination assessed against various endpoints in this thesis. Tick marks represent significant predictors and crosses represent poor predictors. The best predictor(s) are represented with double ticks

Metal measure	**Nematode PICT**	**[a]Nematode community composition**	***P. ulvae* feeding depression**
Sed Cu	✕	✓✓	✓✓
SEM/AEM Cu	✕	✓	✓
PW Cu	✓	✓✓	✕
C_{DGT}-Cu OLW	✓✓	✕	**NA**
C_{DGT}-Cu SWI	✕	✕	**NA**
C_{DGT}-Cu SED	✓	✕	**NA**
EqP: [SEM Cu – AVS]	✕	**NA**	✕
EqP: [SEM Cu – AVS]/fOC	✕	✓	**NA**
PW Cu/OC	✕	✓	**NA**

PICT = Pollution induced community tolerance

[a]Combining both BIOENV, MRT, and visual MDS ordination in bubble plots

NA = Not Assessed

Sed Cu = Total Sediment Cu concentration; SEM/AEM Cu = Simultaneously/Extractable Cu concentration; PW Cu = Total Porewater Cu concentration; C_{DGT}-Cu OLW, SWI and SED = DGT-labile Cu concentrations in the overlying water, sediment-water interface, and sediment layer; EqP: [SEM Cu – AVS] = EqP excess SEM concentration; EqP: [SEM Cu – AVS]/fOC = EqP organic carbon-normalised excess SEM concentration; PW Cu/OC = Total porewater concentration normalised by dissolved organic carbon concentration.

Earlier work in Chapter 2 revealed strong associations between Cu and Zn in surface sediments and Fe concentrations, confirming their adsorption/co-precipitation with Fe-(oxy)hydroxides, as previously reported (Bryan & Gibbs, 1983; Johnson, 1986). In the deeper (5 – 10 cm) sediments, the incorporation of Cu into sulphides was also confirmed. Given their redox sensitivities, fluctuations in redox potential, such as during resuspension events or through bioturbation, may remobilise Cu and Zn from Fe (oxy)hydroxides or sulphide phases, releasing these metals in potentially toxic concentrations (Simpson *et al.*, 1998, 2012a; Vidal-Dura *et al*., 2018). The second aim of this thesis was to assess this

potential for Cu and Zn remobilisation in response to redox fluctuations in the Fal and Hayle estuaries. This was investigated in **Chapter 6** by simulating resuspension events in both oxidised and anoxic conditions.

The results revealed that medium to long-term redox changes in intertidal sediments of the Fal and Hayle estuaries can remobilise Cu and Zn at potentially toxic concentrations. Resuspension of anoxic sediments in oxidised conditions remobilised metals from 5 hrs of incubation, although more prominently after 50 hrs. **For 10 g (dry weight equivalent) of anoxic sediment incubated for 250 hrs in 200 mL seawater, peak metal release ranged between 39 – 378 µg Cu/g and 170 – 228 µg Zn/g sediment (dry weight equivalent) in Restronguet Creek, and down to 0.6 µg Cu/g and 3 µg Zn/g in River Hayle (HA) sediments.** These dissolved concentrations were greater than the Water Framework Directive (2015) [WFD] guidance for "good" chemical quality, with concentrations from Restronguet Creek sediments up to two orders of magnitude greater. Threshold redox for metal release across the treatments varied with metal and sulphide concentrations – approximately 400 mV for Cu and 220 – 410 mV for Zn.

Peak metal remobilisation from the reduction of oxic Restronguet Creek sediments ranged between 0.06 – 0.38 µg Cu/g and 0.41 – 1.29 µg Zn/g sediment (dry weight equivalent). In River Hayle sediments, peak Cu and Zn concentrations were 0.76 µg Cu/g and 3.36 µg Zn/g sediment (dry weight equivalent). Across the treatments, peak concentrations were measured after 5 days (120 hrs) of the 12-day (288 hrs) incubation period. Peak Cu concentrations in the slurries here were less than the WFD guidance, except for HA sediments. However, except for BW, CO, and MC, peak Zn concentrations were higher than the WFD guidance in all treatments – up to twenty-fold in HA sediments.

In the anoxic sediment incubations, where metal remobilisation was more prominent, **pH was found to be strongly correlated with metal remobilisation**, with pH dropping down to 5 in most setups. Cu was released at pH below 6.5, and Zn, below 7.5. **The large drops in pH mean that remobilisation of metals, especially Cu, at the observed scale is unlikely to occur during largescale resuspension events in field sites, where buffering up to pH 7 is expected given higher seawater/sediment ratios**. However, **in microhabitats within surface or deeper sediments, with lower seawater/sediment ratio,**

or as a result of human activity, e.g. dredging, deep-sea mining, bait digging, or installing moorings, the local remobilisation of Cu and Zn from sediment phases may contribute to metal toxicity in marine sediments. To the author's knowledge, metal remobilisation from field sediments with such elevated concentrations of toxic metals have been reported only few times in the published literature.

7.2 Recommendations for the regulation of metals in marine sediments

7.2.1 On the use of the EqP model in predicting metal bioavailability

There is now sufficient proof to discontinue the use of the EqP model (and its variants) in regulating metal toxicity in marine sediments. This thesis has shown that, under environmentally-relevant conditions, the model predicts neither dissolved nor dietary toxicity to the benthic invertebrates examined. Recent studies have shown that the model can be misleading in the presence of oxidised microhabitats in burrows within anoxic deeper sediments (Remaili *et al.*, 2016) or of bioturbation in anoxic surface sediments (Remaili *et al.*, 2018). The EqP proponents (e.g. Di Toro *et al.*, 2005) also acknowledge its weakness in predicting dissolved metal concentrations even after organic carbon normalisation, due to the existence of other important sediment phases. Although measuring actual (steady state) porewater metal concentrations in marine sediments is confounded by sampling protocols and redox changes (Simpson & Batley, 2003), so too is the determination of AVS concentration – the latter of which is a more painful process (see Allen *et al*., 1993 and Simpson, 2001 for protocols). As shown in this thesis and other studies (e.g. Simpson & Batley, 2003), careful sampling and filtration of porewater, especially under an inert atmosphere, can yield ecotoxicologically-relevant concentrations. The use of DET, peepers, and, upon further development, DGT (see Chapter 1) can also help measure dissolved metals at even more relevant concentrations. I recommend that where dissolved metals are deemed important, the direct assessment of porewater should be favoured instead of modelling sediment phases. In the case of Cu, normalisations for dissolved organic carbon concentration may be required.

7.2.2 On the use of DGT in setting regulatory thresholds

This subject has been discussed in detail in the earlier part of this Chapter. Using the standard methodology, the dynamic range of DGT-labile concentrations in field-contaminated marine sediments is very low, with only a ten-fold difference in concentration between a grossly-polluted site (Upper Restronguet Creek, one of the most metal contaminated sites in the world) and an uncontaminated reference site (Breydon Water, see Chapter 3). This low range, in addition to potential errors in measurement and to the influence of less-relevant, site-specific factors in determining DGT-labile concentrations or fluxes, makes it impractical to set universal thresholds based on DGT values. Moreover, this thesis and some previous studies (e.g. Simpson *et al*., 2012b) have revealed that DGT offers few benefits, if any, over the measurement of total dissolved metal concentrations in porewater or overlying water. For these reasons, I do not recommend DGT for setting SQG thresholds.

7.2.2 On setting relevant thresholds given the multiplicity of uptake routes

The multiplicity of metal uptake routes significantly challenges the setting of single-value thresholds. For example, in the most recent revision to the Australian and New Zealand Guidelines for Fresh and Marine Water Quality, Simpson *et al.* (2013, p. 110), using results from species sensitivity distributions (SSDs), concluded that:

> The provision of SQGs that better predict the effects of metals in sediments of varying properties and thus provide adequate protection against toxicity now appears quite achievable… Adequate protection for all benthic organisms is expected to be achieved for an OC-normalised copper concentration of the <63 µm sediment fraction particulate copper concentration of 3.5 mg Cu/g OC and when dissolved copper in the sediment pore waters or overlying waters is below 3 µg Cu/L…

Whilst the above thresholds were protective in the instance of dissolved Cu toxicity in this thesis (see Section 7.1), dietary sediment toxicity to *P. ulvae* was observed below those values (Chapter 5). Total <63 µm oxic sediment EC_{50} for in-exposure feeding depression was 1.7 µmol Cu/g – an equivalent of 2.9 mg Cu/g OC for the oxic test sediments with organic carbon content of 3.72% (LOI = 7.0%, see Figure 2.04). Also, feeding depression in excess of 50% relative to the control was observed in the least contaminated treatment,

despite having similar porewater concentrations (1.7 µg Cu/L in the 2 µmol Cu/g spiked sediment). The implication of this result is that, depending on sediment-water partitioning of metals at a particular site, dissolved metal concentrations non-toxic to the most sensitive species may exist within potentially toxic solid-phase fractions. Moreover, setting a SQG below 1.7 µg Cu/L is impractical, as this concentration is lower than those at several uncontaminated sites (e.g. Breydon Water, see Chapter 2). Indeed, contrary to Simpson and coworkers' (2013) conclusion, this thesis demonstrates that the protection of *all* benthic organisms may not be feasible with single-value thresholds.

What, then, is the way forward? In Chapter 5, I highlighted the potential use of the biodynamic model (Luoma & Rainbow, 2005) in incorporating dietary toxicity into contaminant regulation. Although this model has been applied successfully in estimating potentially-toxic dietary concentrations (e.g. Croteau & Luoma, 2005), the approach is highly organism-specific and, depending on metal partitioning, may result in potentially-toxic dissolved metal concentrations. Simpson (2005) earlier suggested having a range of SQGs for different sediment types. However, this approach does not address the challenge of dietary toxicity occurring at very low dissolved concentrations. Until future studies show otherwise, regulators must realise that no individual SQG is protective of *all* organisms and must set specific environmental protection goals to reflect this reality. For chemicals, this subject has been discussed in detail by Brown and colleagues (2017). They argue that most existing goals are highly generic, failing to define what constitutes "adverse" impacts or the specific "ecological entities (e.g. single-species, populations, functional groups, communities, habitats, ecosystems)" to be protected. This non-specificity, they argue, limits the definition of safe concentrations for chemicals, which should be targeted at different locations and ecological scenarios. I propose that this functional approach of Brown *et al.* be combined with benthic community assessments (at a relevant spatial scale, e.g. site-specific or nationwide) to discern which entities can and should be protected. Targeted thresholds can then be defined in line with already-existing practices, e.g. using SSDs.

7.3 Recommendations for future studies

In defining dose-response relationships in marine sediments, this thesis assessed a range of chemical measurements of metal concentration against actual ecological effects that reflect the key metal exposure routes. Resuspension experiments were also conducted to assess the potential for metal remobilisation from contaminated sediments in response to redox fluctuations. Overall, the results have been helpful in explaining dose-response relationships in field-contaminated sites and recommendations have been made for the development of more reliable SQGs. Several possible areas of research have, however, been highlighted that warrant further investigation:

1. This thesis has shown the importance of dietary Cu toxicity to the estuarine mudsnail, *P. ulvae*. However, further evaluations of other potentially-toxic metals as well as sensitive species are important in defining "safe" limits.
2. Few studies have demonstrated the influence of DOC concentration on dissolved Cu bioavailability and toxicity to marine invertebrates. These studies were conducted using synthetic organic compounds, especially humic acids. Further controlled studies in actual marine sites may be required to derive normalisation protocols for inclusion in SQGs. It is also important to investigate this effect for other metals.
3. In Chapter 3, Nematode PICT was observed to be sensitive to short-term changes in metal bioavailability in the Fal and Hayle estuaries. The potential for using temporal changes in metal bioavailability at single sites, or a small group of sites, in the comparative assessment of chemical measures of metal contamination is, therefore, great. Given the disadvantages associated with using spiked sediments, these temporal *in situ* variations could be used as an indication of dose in microcosms or field mesocosms (see Austen *et al.*, 1994 and Austen & Somerfield, 1997 for examples using nematodes). The approach would be useful in locations without a natural metal contamination gradient as in the Fal and Hayle estuaries.
4. The remobilisation study in Chapter 6 showed a significant drop in pH values that was likely responsible for much of the metal remobilisation. This situation may not be relevant in large-scale resuspension events, given the expected buffering at higher seawater/sediment ratios. It may therefore be important to reassess Cu and Zn

remobilisation in the Fal and Hayle in response to changes in redox potential whilst maintaining constant pH by buffering sediment slurries. Using pH microelectrodes and metal ion sensitive electrodes in transparent test chambers, it might also be possible to investigate pH changes and associated metal remobilisation in real-time bioturbation, e.g. burrowing by lugworms (*Arenicola marina*).

References

Ackermann, F. (1980). A procedure for correcting the grain size effect in heavy metal analyses of estuarine and coastal sediments. *Environmental Technology Letters*, *1*(11), 518–527. https://doi.org/10.1080/09593338009384008

Adams, W. J., Blust, R., Borgmann, U., Brix, K. V, DeForest, D. K., Green, A. S., Meyer, J. S., McGeer, J. C., Paquin, P. R., Rainbow, P. S., & Wood, C. M. (2011). Utility of tissue residues for predicting effects of metals on aquatic organisms. *Integrated Environmental Assessment and Management*, *7*(1), 75–98. https://doi.org/10.1002/ieam.108

Adams, W., Kimerle, R., & Mosher, R. (1985). Aquatic safety assessment of chemicals sorbed to sediments. In: *Aquatic Toxicology and Hazard: Seventh Symposium*, R. Cardwell, R. Purdy, & R. B. Comotto, Eds. West Conshohocken, PA: ASTM International. pp. 429 - 453. http://doi.org.10.1520/STP36282S

Aiken, G. R., Hsu-Kim, H., & Ryan, J. N. (2011). Influence of dissolved organic matter on the environmental fate of metals, nanoparticles, and colloids. *Environmental Science & Technology*, *45*(8), 3196–3201. https://doi.org/10.1021/es103992s

Akaike, H. (1978). A Bayesian analysis of the minimum AIC procedure. *Annals of the Institute of Statistical Mathematics*, *30*(1), 9–14. https://doi.org/10.1007/BF02480194

Allen, H. E., Fu, G., & Deng, B. (1993). Analysis of acid-volatile sulfide (AVS) and simultaneously extracted metals (SEM) for the estimation of potential toxicity in aquatic sediments. *Environmental Toxicology and Chemistry*, *12*(8), 1441–1453. https://doi.org/10.1002/etc.5620120812

Allen, H. E., Hall, R. H., & Brisbin, T. D. (1980). Metal speciation. Effects on aquatic toxicity. *Environmental Science & Technology*, *14*(4), 441–443. https://doi.org/10.1021/es60164a002

Aller, R. C. (1994). Bioturbation and remineralization of sedimentary organic matter: effects of redox oscillation. *Chemical Geology*, *114*(3–4), 331–345. https://doi.org/10.1016/0009-2541(94)90062-0

Amato, E. D., Marasinghe Wadige, C. P. M., Taylor, A. M., Maher, W. A., Simpson, S. L., & Jolley, D. F. (2018). Field and laboratory evaluation of DGT for predicting metal bioaccumulation and toxicity in the freshwater bivalve Hyridella australis exposed to contaminated sediments. *Environmental Pollution*, *243*, 862–871. https://doi.org/10.1016/j.envpol.2018.09.004

Amato, E. D., Simpson, S. L., Belzunce-Segarra, M. J., Jarolimek, C. V., & Jolley, D. F. (2015). Metal Fluxes from Porewaters and Labile Sediment Phases for Predicting Metal Exposure and Bioaccumulation in Benthic Invertebrates. *Environmental Science & Technology*, *49*(24), 14204–14212. https://doi.org/10.1021/acs.est.5b03655

Amato, E. D., Simpson, S. L., Jarolimek, C. V., & Jolley, D. F. (2014). Diffusive Gradients in Thin Films Technique Provide Robust Prediction of Metal Bioavailability and Toxicity in Estuarine Sediments. *Environmental Science & Technology*, *48*(8), 4485–4494. https://doi.org/10.1021/es404850f

Amato, E. D., Simpson, S. L., Remaili, T. M., Spadaro, D. A., Jarolimek, C. V., & Jolley, D. F. (2016). Assessing the Effects of Bioturbation on Metal Bioavailability in Contaminated Sediments by Diffusive Gradients in Thin Films (DGT). *Environmental Science & Technology*, *50*(6), 3055–3064. https://doi.org/10.1021/acs.est.5b04995

Amiard, J.-C., Geffard, A., Amiard-Triquet, C., & Crouzet, C. (2007). Relationship between the lability of sediment-bound metals (Cd, Cu, Zn) and their bioaccumulation in benthic invertebrates. *Estuarine, Coastal and Shelf Science*, *72*(3), 511–521. https://doi.org/10.1016/j.ecss.2006.11.017

Anderson, D., & Morel, F. (1978). Copper sensitivity of *Gonyaulax tamarensis*. *Limnol Oceanogr*. http://www.aslo.org/lo/pdf/vol_23/issue_2/0283.pdf

Anderson, M. A., Morel, F. M. M., & Guillard, R. R. L. (1978). Growth limitation of a coastal diatom by low zinc ion activity. *Nature*, *276*(5683), 70–71. https://doi.org/10.1038/276070a0

Ankley, G. T., Di Toro, D. M., Hansen, D. J., & Berry, W. J. (1996). Technical basis and proposal for deriving sediment quality criteria for metals. *Environmental Toxicology*

and Chemistry, *15*(12), 2056–2066. https://doi.org/10.1002/etc.5620151202

Anusiem, A. C. I., & Ojo, G. B. (1978). Limitations on the Spectrophotometric Determination of Copper(I) with Ferrozine [3]. *Analytical Chemistry*. American Chemical Society. https://doi.org/10.1021/ac50025a040

Araujo, C. V. M., Blasco, J., & Moreno-Garrido, I. (2012). Measuring the avoidance behaviour shown by the snail Hydrobia ulvae exposed to sediment with a known contamination gradient. *Ecotoxicology*, *21*(3), 750–758. https://doi.org/10.1007/s10646-011-0835-6

Austen, M. C., McEvoy, A. J., & Warwick, R. M. (1994). The specificity of meiobenthic community responses to different pollutants: results from microcosm experiments. *Marine Pollution Bulletin*, *28*(9), 557-563. https://doi.org/10.1016/0025-326X(94)90075-2

Austen, M. C., & Somerfield, P. J. (1997). A community level sediment bioassay applied to an estuarine heavy metal gradient. *Marine Environmental Research, 43*(4), 315-328. https://doi.org/10.1016/S0141-1136(96)00094-3

Bacon, J. R., & Davidson, C. M. (2008). Is there a future for sequential chemical extraction? *The Analyst*, *133*(1), 25–46. https://doi.org/10.1039/B711896A

Baird, D. J., Brown, S. S., Lagadic, L., Liess, M., Maltby, L., Moreira-Santos, M., … Scott, G. I. (2007). In Situ–Based Effects Measures: Determining the Ecological Relevance of Measured Responses. *Integrated Environmental Assessment and Management*, *3*(2), 259. https://doi.org/10.1897/IEAM_2006-031.1

Barnes, R S K. (1986). *Daily Activity Rhythms in the Intertidal Gastropod Hydrobiu ulnae (Pennant). Estuarine, Coastal and Shelf Science* (Vol. 22).

Barnes, R. S K. (2003). Feeding rates of continually submerged Hydrobia ulvae vary during the daylight hours. *Journal of the Marine Biological Association of the United Kingdom*, *83*(6), 1273–1275. https://doi.org/10.1017/S0025315403008646

Barnes, R. S.K. (2006). Variation in feeding rate of the intertidal mudsnail Hydrobia ulvae

in relation to the tidal cycle. *Marine Ecology*, *27*, 154–159. https://doi.org/10.1111/j.1439-0485.2006.00082.x

Barnes, Richard Stephen Kent. (2001). Interference competition in the intertidal mud snail Hydrobia ulvae: egestion rates revisited. *Journal of the Marine Biological Association of the UK*, *81*(2001), 491–495. https://doi.org/10.1017/S0025315401004131

Barton, D. B. (1968). *Essays in Cornish mining history: volume 1* (Vol. 1). Truro, England: D. Bradford Barton Ltd.

Barton, D. B. (1971). *Essays in Cornish Mining History - volume two* (Vol. 2). Truro, England: D Bradford Barton Ltd.

Batley, G., Apte, S., & Stauber, J. (2004). Speciation and bioavailability of trace metals in water: progress since 1982. *Australian Journal of Chemistry*. http://www.publish.csiro.au/ch/CH04095

Beltrame, M. O., De Marco, S. G., & Marcovecchio, J. E. (2010). Influences of Sex, Habitat, and Seasonality on Heavy-Metal Concentrations in the Burrowing Crab (*Neohelice granulata*) From a Coastal Lagoon in Argentina. *Archives of Environmental Contamination and Toxicology*, *58*(3), 746–756. https://doi.org/10.1007/s00244-009-9405-9

Belzunce-Segarra, M. J., Simpson, S. L., Amato, E. D., Spadaro, D. A., Hamilton, I. L., Jarolimek, C. V., & Jolley, D. F. (2015). The mismatch between bioaccumulation in field and laboratory environments: Interpreting the differences for metals in benthic bivalves. *Environmental Pollution*, *204*, 48–57. https://doi.org/10.1016/j.envpol.2015.03.048

Benjamin, M. M. (1983). Adsorption and Surface Precipitation of Metals on Amorphous Iron Oxyhydroxide. *Environmental Science and Technology*, *17*(11), 686–692. https://doi.org/10.1021/es00117a012

Benner, R., & Strom, M. (1993). A critical evaluation of the analytical blank associated with DOC measurements by high-temperature catalytic oxidation. *Mar. Chem.*, *41*(1–3), 153–160. Retrieved from

http://www.academia.edu/download/41657656/A_Critical_Evaluation_of_the_Analytical_20160127-20386-1p8vex2.pdf

Bergamaschi, B. A., Tsamakis, E., Keil, R. G., Eglinton, T. I., Montluçon, D. B., & Hedges, J. I. (1997). The effect of grain size and surface area on organic matter, lignin and carbohydrate concentration, and molecular compositions in Peru Margin sediments. *Geochimica et Cosmochimica Acta*, *61*(6), 1247–1260. https://doi.org/10.1016/S0016-7037(96)00394-8

Berkovits, L. A., & Lukashin, V. N. (1984). Three Marine Sediment Reference Samples: SDO-1, SDO-2 and SDO-3. *Geostandards and Geoanalytical Research*, *8*(1), 51–56. https://doi.org/10.1111/j.1751-908X.1984.tb00412.x

Berry, W. J., Cantwell, M. G., Edwards, P. A., Serbst, J. R., & Hansen, D. J. (1999). Predicting toxicity of sediments spiked with silver. *Environmental Toxicology and Chemistry*, *18*(1), 40–48. https://doi.org/10.1897/1551-5028(1999)018<0040:PTOSSW>2.3.CO;2

Bertics, V. J., & Ziebis, W. (2010). Bioturbation and the role of microniches for sulfate reduction in coastal marine sediments. *Environmental Microbiology*, *12*(11), 3022–3034. https://doi.org/10.1111/j.1462-2920.2010.02279.x

Bervoets, L., Voets, J., Covaci, A., Chu, S., Qadah, D., Smolders, R., Schepens, P., & Blust, R. (2005). Use of transplanted zebra mussels (*Dreissena polymorpha*) to assess the bioavailability of microcontaminants in flemish surface waters. *Environmental Science and Technology*, *39*(6), 1492–1505. https://doi.org/10.1021/es049048t

Bezerra, T.N.; Decraemer, W.; Eisendle-Flöckner, U.; Hodda, M.; Holovachov, O.; Leduc, D.; Miljutin, D.; Mokievsky, V.; Peña Santiago, R.; Sharma, J.; Smol, N.; Tchesunov, A.; Venekey, V.; Zhao, Z.; Vanreusel, A. (2020). *Nemys: World Database of Nematodes*. Accessed at http://nemys.ugent.be on 2020-08-23. doi:10.14284/366

Biddanda, B. A., & Cotner, J. B. (2002). Love handles in aquatic ecosystems: The role of dissolved organic carbon drawdown, resuspended sediments, and terrigenous inputs in the carbon balance of Lake Michigan. *Ecosystems*, *5*(5), 431–445.

https://doi.org/10.1007/s10021-002-0163-z

BioRad. (n.d). *Chelex® 100 and Chelex 20 Chelating Ion Exchange Resin: Instruction Manual.* Retrieved from http://www.bio-rad.com/webroot/web/pdf/lsr/literature/LIT200.pdf

Birch, G. F. (2003). A test of normalization methods for marine sediment, including a new post-extraction normalization (PEN) technique. *Hydrobiologia*, *492*(1–3), 5–13. https://doi.org/10.1023/A:1024844629087

Birch, G. F. (2018). A review of chemical-based sediment quality assessment methodologies for the marine environment. *Marine Pollution Bulletin*, *133*(November 2017), 218–232. https://doi.org/10.1016/j.marpolbul.2018.05.039

Birk, S., Bonne, W., Borja, A., Brucet, S., Courrat, A., Poikane, S., … Hering, D. (2012). Three hundred ways to assess Europe's surface waters: An almost complete overview of biological methods to implement the Water Framework Directive. *Ecological Indicators*, *18*, 31–41. https://doi.org/10.1016/j.ecolind.2011.10.009

Blanchard, G. F., Guarini, J. M., Provot, L., Richard, P., & Sauriau, P. G. (2000). Measurement of ingestion rate of Hydrobia ulvae (Pennant) on intertidal epipelic microalgae: The effect of mud snail density. *Journal of Experimental Marine Biology and Ecology*, *255*(2), 247–260. https://doi.org/10.1016/S0022-0981(00)00292-6

Blanck, H. (2002). A Critical Review of Procedures and Approaches Used for Assessing Pollution-Induced Community Tolerance (PICT) in Biotic Communities. *Human and Ecological Risk Assessment: An International Journal*, *8*(5), 1003–1034. https://doi.org/10.1080/1080-700291905792

Bleninger, T., Niepelt, A., & Jirka, G. H. (2010). Desalination plant discharge calculator. *Desalination and Water Treatment*, *13*, 156–173. https://doi.org/doi: 10.5004

Blowes, D.W., Ptacek, C.J., Jambor, J.L., & Weisener, C.G. (2003). The Geochemistry of Acid Mine Drainage. *Treatise on Geochemistry*, *9*, 149-204. https://doi.org/10.1016/B0-08-043751-6/09137-4

Borcard, D., Gillet, F., & Legendre, P. (2018). *Numerical ecology with R, 2nd edition*. Springer. https://doi.org/10.1007/978-3-319-71404-2

Borgå, K. (2013). Ecotoxicology: bioaccumulation. *Reference Module in Earth Systems and Environmental Sciences*. https://doi.org/10.1016/B978-0-12-409548-9.00765-X

Borgmann, U, Néron, R., & Norwood, W. (2001). Quantification of bioavailable nickel in sediments and toxic thresholds to Hyalella azteca. *Environmental Pollution*, *111*(2), 189–198. https://doi.org/10.1016/S0269-7491(00)00076-2

Borgmann, U. (2000). Methods for assessing the toxicological significance of metals in aquatic ecosystems: bio-accumulation-toxicity relationships, water concentrations and sediment spiking approaches. *Aquatic Ecosystem Health & Management*, *3*(3), 277–289. https://doi.org/10.1080/14634980008657027

Borgmann, Uwe. (2003). Derivation of cause-effect based sediment quality guidelines. *Canadian Journal of Fisheries and Aquatic Sciences*, *60*(3), 352–360. https://doi.org/10.1139/f03-026

Borja, A., & Dauer, D. M. (2008). Assessing the environmental quality status in estuarine and coastal systems: Comparing methodologies and indices. *Ecological Indicators*, *8*(4), 331–337. https://doi.org/10.1016/j.ecolind.2007.05.004

Borja, Angel, Elliott, M., Uyarra, M. C., Carstensen, J., & Mea, M. (2017). Editorial: Bridging the Gap between Policy and Science in Assessing the Health Status of Marine Ecosystems. *Frontiers in Marine Science*, *4*, 1–3. https://doi.org/10.3389/fmars.2017.00032

Bowles, K. C., Apte, S. C., Batley, G. E., Hales, L. T., & Rogers, N. J. (2006). A rapid Chelex column method for the determination of metal speciation in natural waters. *Analytica Chimica Acta*, *558*(1–2), 237–245. https://doi.org/10.1016/j.aca.2005.10.071

Brookes, R., Davies, A., Ketwaroo, G., & Madden, P. A. (2005). Diffusion coefficients in ionic liquids: Relationship to the viscosity. *Journal of Physical Chemistry B*, *109*(14), 6485–6490. https://doi.org/10.1021/jp046355c

Brown, A. R., Whale, G., Jackson, M., Marshall, S., Hamer, M., Solga, A., … Maltby, L. (2017). Toward the definition of specific protection goals for the environmental risk assessment of chemicals: A perspective on environmental regulation in Europe. *Integrated Environmental Assessment and Management, 13*(1), 17–37. https://doi.org/10.1002/ieam.1797

Brown, P. L., & Markich, S. J. (2000). Evaluation of the free ion activity model of metal-organism interaction: extension of the conceptual model. *Aquatic Toxicology, 51*(2), 177–194. https://doi.org/10.1016/S0166-445X(00)00115-6

Bruker. (2020). *GEO-QUANT – Trace analysis solution, XRF - XRF Solutions | Bruker*. Retrieved June 19, 2020, from https://www.bruker.com/products/x-ray-diffraction-and-elemental-analysis/x-ray-fluorescence/xrf-solutions/geo-quant.html

Bryan, G. W., & Gibbs, P. E. (1983). Heavy metals in the Fal estuary, Cornwall: A study of long term contamination by mining waste and its effects on estuarine organisms. *Occasional Publication of the Marine Biological Association, 2*. Retrieved from http://plymsea.ac.uk/275/

Bryan, G. W., & Hummerstone, L. G. (1971). Adaptation of the polychaete *Nereis diversicolor* to estuarine sediments containing high concentrations of heavy metals. I. General observations and adaptation to copper. *Journal of the Marine Biological Association of the United Kingdom, 51*(4), 845-863. https://doi.org/10.1017/S0025315400018014

Bryan, G. W., & Langston, W. J. (1992). Bioavailability, accumulation and effects of heavy metals in sediments with special reference to United Kingdom estuaries: a review. *Environmental Pollution, 76*(2), 89–131. https://doi.org/10.1016/0269-7491(92)90099-V

Burdige, D. J. (2007). Preservation of organic matter in marine sediments: Controls, mechanisms, and an imbalance in sediment organic carbon budgets? *Chemical Reviews, 107*(2), 467–485. https://doi.org/10.1021/cr050347q

Burgess, R. M., Berry, W. J., Mount, D. R., & Di Toro, D. M. (2013). Mechanistic

sediment quality guidelines based on contaminant bioavailability: Equilibrium partitioning sediment benchmarks. *Environmental Toxicology and Chemistry*, *32*(1), 102–114. https://doi.org/10.1002/etc.2025

Burton, G. A. (2002). Sediment quality criteria in use around the world. *Limnology*, *3*(2), 65–75. https://doi.org/10.1007/s102010200008

Burton, G. A. (2010). Metal Bioavailability and Toxicity in Sediments. *Critical Reviews in Environmental Science and Technology*, *40*(9–10), 852–907. https://doi.org/10.1080/10643380802501567

Burton, G. A. (2013). Assessing sediment toxicity: Past, present, and future. *Environmental Toxicology and Chemistry*, *32*(7), 1438–1440. https://doi.org/10.1002/etc.2250

Caetano, M., Madureira, M. J., & Vale, C. (2003, February). Metal remobilisation during resuspension of anoxic contaminated sediment: Short-term laboratory study. *Water, Air, and Soil Pollution*. Springer. https://doi.org/10.1023/A:1022877120813

Calmano, W., Hong, J., & Forstner, U. (1993). Binding and mobilization of sediments affected by pH and redox potential. *Wal. Sci. Tech*, *28*(8), 223–235.

Campana, O., Rodríguez, A., & Blasco, J. (2013). Evaluating the suitability of Hydrobia ulvae as a test species for sediment metal toxicity testing applying a tissue residue approach to metal mixtures in laboratory and field exposures. *Chemosphere*, *91*(8), 1136–1145. https://doi.org/10.1016/J.CHEMOSPHERE.2013.01.018

Campana, O., Simpson, S. L., Spadaro, D. A., & Blasco, J. (2012). Sub-Lethal Effects of Copper to Benthic Invertebrates Explained by Sediment Properties and Dietary Exposure. *Environmental Science & Technology*, *46*(12), 6835–6842. https://doi.org/10.1021/es2045844

Campana, O., Taylor, A. M., Blasco, J., Maher, W. A., & Simpson, S. L. (2015). Importance of subcellular metal partitioning and kinetics to predicting sublethal effects of copper in two deposit-feeding organisms. *Environmental Science and Technology*, *49*(3), 1806–1814. https://doi.org/10.1021/es505005y

Campbell, P. G., Chapman, P. M., & Hale, B. A. (2006). Risk assessment of metals in the environment. In: R. M. Harrison, & R. E. Hester Eds. *Chemicals in the Environment: assessing and managing risk*. Cambridge, UK: Royal Society of Chemistry.

Cantwell, M. G., Burgess, R. M., & Kester, D. R. (2002). Release and phase partitioning of metals from anoxic estuarine sediments during periods of simulated resuspension. *Environmental Science and Technology*, *36*(24), 5328–5334. https://doi.org/10.1021/es0115058

Carmen Casado-Martinez, M., Smith, B. D., Luoma, S. N., & Rainbow, P. S. (2010). Metal toxicity in a sediment-dwelling polychaete: Threshold body concentrations or overwhelming accumulation rates? *Environmental Pollution*, *158*(10), 3071–3076. https://doi.org/10.1016/j.envpol.2010.06.026

Chaichana, S., Jickells, T., & Johnson, M. (2019). Interannual variability in the summer dissolved organic matter inventory of the North Sea: implications for the continental shelf pump. *Biogeosciences*, *16*(5), 1073–1096. https://doi.org/10.5194/bg-16-1073-2019

Chao, T. T., & Zhou, L. (1983). Extraction techniques for selective dissolution of amorphous iron oxides from soils and sediments. *Soil Science Society of America Journal, 47*(2), 225-232. https://doi.org/10.2136/sssaj1983.03615995004700020010x

Chapman, P. M. (2007). Determining when contamination is pollution - Weight of evidence determinations for sediments and effluents. *Environment International, 33*(4), 492–501. https://doi.org/10.1016/j.envint.2006.09.001

Chapman, P. M. (2018). Environmental quality benchmarks—the good, the bad, and the ugly. *Environmental Science and Pollution Research*, *25*(4), 3043–3046. https://doi.org/10.1007/s11356-016-7924-2

Chapman, P. M., & Wang, F. (2001). Assessing sediment contamination in estuaries. *Environmental Toxicology and Chemistry*, *20*(1), 3–22. https://doi.org/10.1002/etc.5620200102

Chapman, P. M., Wang, F., Janssen, C., Persoone, G., & Allen, H. E. (1998).

Ecotoxicology of metals in aquatic sediments: binding and release, bioavailability, risk assessment, and remediation. *Canadian Journal of Fisheries and Aquatic Sciences*, *55*(10), 2221–2243. https://doi.org/10.1139/f98-145

Chapman, Peter M, Wang, F., Germano, J. D., & Batley, G. (2002). Pore water testing and analysis: the good, the bad, and the ugly. In *Marine Pollution Bulletin* (Vol. 44, Issue 5). https://doi.org/10.1016/S0025-326X(01)00243-0

Chapman, Peter M, Wang, F., Janssen, C., Persoone, G., & Allen, H. E. (1998). Ecotoxicology of metals in aquatic sediments: binding and release, bioavailability, risk assessment, and remediation. *Canadian Journal of Fisheries and Aquatic Sciences*, *55*(10), 2221–2243. https://doi.org/10.1139/f98-145

Chapman, Peter M. (1985). Effects of gut sediment contents on measurements of metal levels in benthic invertebrates—a Cautionary Note. *Bulletin of Environmental Contamination and Toxicology*, *35*(1), 345–347. https://doi.org/10.1007/BF01636520

Chapman, Peter M. (2018). Environmental quality benchmarks—the good, the bad, and the ugly. *Environmental Science and Pollution Research*, *25*(4), 3043–3046. https://doi.org/10.1007/s11356-016-7924-2

Chapman, Peter M., & Wang, F. (2001). Assessing sediment contamination in estuaries. *Environmental Toxicology and Chemistry*, *20*(1), 3–22. https://doi.org/10.1002/etc.5620200102

Chen, Z, & Mayer, L. (1999). Sedimentary metal bioavailability determined by the digestive constraints of marine deposit feeders:gut retention time and dissolved amino acids. *Marine Ecology Progress Series*, *176*, 139–151. https://doi.org/10.3354/meps176139

Cindrić, A. M., Marcinek, S., Garnier, C., Salaün, P., Cukrov, N., Oursel, B., … Omanović, D. (2020). Evaluation of diffusive gradients in thin films (DGT) technique for speciation of trace metals in estuarine waters - A multimethodological approach. *Science of the Total Environment*, *721*, 137784. https://doi.org/10.1016/j.scitotenv.2020.137784

Clarke, K. R. (1993). Non-parametric multivariate analyses of changes in community structure. *Australian Journal of Ecology, 18*(1), 117–143. https://doi.org/10.1111/j.1442-9993.1993.tb00438.x

Clarke, K. R., & Ainsworth, M. (1993). *A method of linking multivariate community structure to environmental variables. MARINE ECOLOGY PROGRESS SERIES Mar. Ecol. Prog. Ser* (Vol. 92). Retrieved from https://www.int-res.com/articles/meps/92/m092p205.pdf

Clarke, K. R., Chapman, M. G., Somerfield, P. J., & Needham, H. R. (2006). Dispersion-based weighting of species counts in assemblage analyses. *Marine Ecology Progress Series, 320*, 11-27. https://doi.org/10.3354/meps320011

Clarke, K.R., Gorley, R.N., Somerfield, P.J., Warwick, R.M. (2014). *Change in marine communities: an approach to statistical analysis and interpretation, 3rd edition*. PRIMER-E: Plymouth, UK.

Clarke, K. R., Somerfield, P. J., & Gorley, R. N. (2008). Testing of null hypotheses in exploratory community analyses: similarity profiles and biota-environment linkage. *Journal of experimental marine biology and ecology, 366*(1-2), 56-69. https://doi.org/10.1016/j.jembe.2008.07.009

Clarke, K., & Warwick, R. (2001). A further biodiversity index applicable to species lists: variation in taxonomic distinctness. *Marine Ecology Progress Series*, *216*, 265–278. https://doi.org/10.3354/meps216265

Clarke, K. R., & Warwick, R. M. (1998). Quantifying structural redundancy in ecological communities. *Oecologia*, *113*(2), 278-289. https://doi.org/10.1007/s004420050379

Cline, J. D. (1969). Spectrophotometric determination of hydrogen sulfide in natural waters 1. *Limnology and Oceanography*, *14*(3), 454-458.

Cooper, D. C., & Morse, J. W. (1998). Extractability of metal sulfide minerals in acidic solutions: Application to environmental studies of trace metal contamination within anoxic sediments. *Environmental Science and Technology*, *32*(8), 1076–1078. https://doi.org/10.1021/es970415t

Costello, D. M., Burton, G. A., Hammerschmidt, C. R., & Taulbee, W. K. (2012). Evaluating the Performance of Diffusive Gradients in Thin Films for Predicting Ni Sediment Toxicity. *Environmental Science & Technology*, 120827132457006. https://doi.org/10.1021/es302390m

Costello, D. M., Hammerschmidt, C. R., & Burton, G. A. (2016). Nickel Partitioning and Toxicity in Sediment during Aging: Variation in Toxicity Related to Stability of Metal Partitioning. *Environmental Science & Technology*, *50*(20), 11337–11345. https://doi.org/10.1021/acs.est.6b04033

Coull, B., & Chandler, G. (1992). Pollution and meiofauna: field, laboratory, and mesocosm studies. *Oceanography and Marine Biology: An Annual Review*, *30*, 191–271. Retrieved from http://www.vliz.be/en/imis?refid=212222

Croteau, M. N., & Luoma, S. N. (2009). Predicting dietborne metal toxicity from metal influxes. *Environmental Science and Technology*, *43*(13), 4915–4921. https://doi.org/10.1021/es9007454

Danovaro, R., & Gambi, C. (2002). Biodiversity and trophic structure of nematode assemblages in seagrass systems: Evidence for a coupling with changes in food availability. *Marine Biology*, *141*(4), 667–677. https://doi.org/10.1007/s00227-002-0857-y

Davison, W, & Zhang, H. (1994). In situ speciation measurements of trace components in natural waters using thin-fil gels. *Nature*, *367*(6463), 546–548. https://doi.org/10.1038/367546a0

Davison, W. (2016). Appendix: Table for calculating diffusion coefficients of commonly measured analytes in the APA gel and water at any temperature between 0°C and 35°C. In: Davison, W. (Ed). *Diffusive gradients in thin-films for environmental measurements*. Cambridge, UK: Cambridge University Press

Davison, W., & Zhang, H. (2016a). Diffusion Layer Properties. In: Davison, W. (Ed). *Diffusive gradients in thin-films for environmental measurements* (pp. 32 – 65). Cambridge, UK: Cambridge University Press

Davison, W., & Zhang, H. (2016b). Principles of Measurements in Simple Solutions. In: Davison, W. (Ed). *Diffusive gradients in thin-films for environmental measurements* (pp. 10 – 31). Cambridge, UK: Cambridge University Press

Davison, W., & Zhang, H. (2016c). Introduction to DGT. In: Davison, W. (Ed). *Diffusive gradients in thin-films for environmental measurements* (pp. 1 – 9). Cambridge, UK: Cambridge University Press

Davison, W., Grime, G. W., Morgan, J. A. W., & Clarke, K. (1991). Distribution of dissolved iron in sediment pore waters at submillimetre resolution. *Nature*, *352*(6333), 323–325. https://doi.org/10.1038/352323a0

Davison, William, & Zhang, H. (2012). Progress in understanding the use of diffusive gradients in thin films (DGT) - back to basics. *Environmental Chemistry*, *9*(1), 1. https://doi.org/10.1071/EN11084

Davison, William, Zhang, H., Schintu, M., Marras, B., Durante, L., Meloni, P., … Buffle, J. (2012). Progress in understanding the use of diffusive gradients in thin films (DGT) ? back to basics. *Environmental Chemistry*, *9*(1), 1. https://doi.org/10.1071/EN11084

De Jonge, M., Dreesen, F., De Paepe, J., Blust, R., & Bervoets, L. (2009). Do acid volatile sulfides (AVS) influence the accumulation of sediment-bound metals to benthic invertebrates under natural field conditions? *Environmental Science and Technology*, *43*(12), 4510–4516. https://doi.org/10.1021/es8034945

de Klein, J. J. M., Overbeek, C. C., Juncher Jørgensen, C., & Veraart, A. J. (2017). Effect of Temperature on Oxygen Profiles and Denitrification Rates in Freshwater Sediments. *Wetlands*, *37*(5), 975–983. https://doi.org/10.1007/s13157-017-0933-1

de Mendiburu, F. (2020). Package 'agricolae'. Statistical Procedures for Agricultural Research, version, 1.3-2. Available April 29, 2020 at https://cran.r-project.org/web/packages/agricolae/agricolae.pdf

De'ath, G. (2002). Multivariate regression trees: a new technique for modeling species–environment relationships. *Ecology*, *83*(4), 1105-1117. https://doi.org/10.1890/0012-

9658(2002)083[1105:MRTANT]2.0.CO;2

De'ath, G. (2014). Package 'mvpart'. Multivariate partitioning, version, 1.6-2. Available April 29, 2021 at https://mran.microsoft.com/snapshot/2014-10-31/web/packages/mvpart/mvpart.pdf

DeForest, D. K., & Meyer, J. S. (2015). Critical review: Toxicity of dietborne metals to aquatic organisms. *Critical Reviews in Environmental Science and Technology*, *45*(11), 1176–1241. https://doi.org/10.1080/10643389.2014.955626

Degtlareva, A., & Elektorowicz, M. (2001). A computer simulation of water quality change due to dredging of heavy metals contaminated sediments in the Old Harbour of Montreal. *Water Quality Research Journal of Canada*, *36*(1), 1–19. https://doi.org/10.2166/wqrj.2001.001

Degryse, F., & Smolders, E. (2016). DGT and Bioavailability. In: Davison, W. (Ed). *Diffusive gradients in thin-films for environmental measurements*. Cambridge, UK: Cambridge University Press

Di Toro, D. M., Allen, H. E., Bergman, H. L., Meyer, J. S., Paquin, P. R., & Santore, R. C. (2001). Biotic ligand model of the acute toxicity of metals. 1. Technical Basis. *Environmental Toxicology and Chemistry*, *20*(10), 2383–2396. https://doi.org/10.1002/etc.5620201034

Di Toro, D. M., Mahony, J. D., Hansen, D. J., Scott, K. J., Carlson, A. R., & Ankley, G. T. (1992). Acid volatile sulfide predicts the acute toxicity of cadmium and nickel in sediments. *Environmental Science & Technology*, *26*(1), 96–101. https://doi.org/10.1021/es00025a009

Di Toro, D. M., Mahony, J. D., Hansen, D. J., Scott, K. J., Hicks, M. B., Mayr, S. M., & Redmond, M. S. (1990). Toxicity of cadmium in sediments: The role of acid volatile sulfide. *Environmental Toxicology and Chemistry*, *9*(12), 1487–1502. https://doi.org/10.1002/etc.5620091208

Di Toro, D. M., McGrath, J. A., Hansen, D. J., Berry, W. J., Paquin, P. R., Mathew, R., Wu, K. B., & Santore, R. C. (2005). Predicting sediment metal toxicity using a

sediment biotic ligand model: methodology and initial application. *Environmental Toxicology and Chemistry*, *24*(10), 2410. https://doi.org/10.1897/04-413R.1

Di Toro, D. M., Zarba, C. S., Hansen, D. J., Berry, W. J., Swartz, R. C., Cowan, C. E., Pavlou, S. P., Allen, H. E., Thomas, N. A., & Paquin, P. R. (1991). Technical basis for establishing sediment quality criteria for nonionic organic chemicals using equilibrium partitioning. *Environmental Toxicology and Chemistry*, *10*(12), 1541–1583. https://doi.org/10.1002/etc.5620101203

Dines, H. G. (1969). *The Metalliferous Mining Region of South-West England. Volumes I and II . 2nd impression with amendments*. London: Her Majesty's Stationery Office.

Doig, L., & Liber, K. (2000). Dialysis minipeeper for measuring pore-water metal concentrations in laboratory sediment toxicity and bioavailability tests. *Environmental Toxicology and Chemistry*, *19*(12), 2882–2889. https://doi.org/10.1002/etc.5620191205

Dubrovsky, N. M., Cherry, J. A., Reardon, E. J., & Vivyurka, A. J. (1985). Geochemical evolution of inactive pyritic tailings in the Elliot Lake uranium district. *Canadian Geotechnical Journal*, *22*(1), 110–128. https://doi.org/10.1139/t85-011

Dunn, R. J.K., Teasdale, P. R., Warnken, J., Jordan, M. A., & Arthur, J. M. (2007). Evaluation of the in situ, time-integrated DGT technique by monitoring changes in heavy metal concentrations in estuarine waters. *Environmental Pollution*, *148*(1), 213–220. https://doi.org/10.1016/j.envpol.2006.10.027

Dunn, Ryan J.K., Teasdale, P. R., Warnken, J., & Schleich, R. R. (2003). Evaluation of the diffusive gradient in a thin film technique for monitoring trace metal concentrations in estuarine waters. *Environmental Science and Technology*, *37*(12), 2794–2800. https://doi.org/10.1021/es026425y

Eismann, C. E., Menegário, A. A., Gemeiner, H., & Williams, P. N. (2020). Predicting Trace Metal Exposure in Aquatic Ecosystems: Evaluating DGT as a Biomonitoring Tool. *Exposure and Health*. Springer. https://doi.org/10.1007/s12403-018-0280-3

Elder, J. (1988). *Metal biogeochemistry in surface-water systems; a review of principles*

and concepts. https://pubs.er.usgs.gov/publication/cir1013%3B

Farrance, I., & Frenkel, R. (2012). Uncertainty of measurement: A review of the rules for calculating Uncertainty components through functional relationships. *Clinical Biochemist Reviews*. The Australian Association of Clinical Biochemists.

Feely, R. A., Orr, J., Fabry, V. J., Kleypas, J. A., Sabine, C. L., & Langdon, C. (2009). Present and future changes in seawater chemistry due to ocean acidification. In *Geophysical Monograph Series* (Vol. 183, pp. 175–188). American Geophysical Union. https://doi.org/10.1029/2005GM000337

Fenchel, T. (1996). Worm burrows and oxic microniches in marine sediments. 1. Spatial and temporal scales. *Marine Biology*, *127*(2), 289–295. https://doi.org/10.1007/BF00942114

Field, M. P., Lavigne, M., Murphy, K. R., Ruiz, G. M., & Sherrell, R. M. (2007). Direct determination of P, V, Mn, As, Mo, Ba and U in seawater by SF-ICP-MS. *Journal of Analytical Atomic Spectrometry*, *22*(9), 1145–1151. https://doi.org/10.1039/b617597j

Figura, P., & McDuffie, B. (1980). Determination of Labilities of Soluble Trace Metal Species in Aqueous Environmental Samples by Anodic Stripping Voltammetry and Chelex Column and Batch Methods. *Analytical Chemistry*, *52*(9), 1433–1439. https://doi.org/10.1021/ac50059a015

Folk, R.L.& Ward, W.C. (1957). A Study in the Significance of Grain-Size Parameters. *Journal of Sedimentary Petrology, 27,* 3-26. https://doi.org/10.1306/74D70646-2B21-11D7-8648000102C1865D

Fox, J., Weisbert, S., Price, B., Bates, D., Baud-Bovy, G.,… Graves, S. (2020). Package 'car'. Companion to Applied Regression, version, 3.0-10. Available April 29, 2021 at https://cran.r-project.org/web/packages/car/car.pdf

Forster, S. (1996). Spatial and Temporal Distribution of Oxidation Events Occurring Below the Sediment-Water Interface. *Marine Ecology*, *17*(1–3), 309–319. https://doi.org/10.1111/j.1439-0485.1996.tb00510.x

Forstner, U. (1995). Non-linear release of metals from aquatic sediments. In *Biogeodynamics of pollutants in soils and sediments* (pp. 247-307), Eds: W, Salomons & W. M. Stigliani. Berlin, Heidelberg: Springer.

Fortin, C., & Campbell, P. G. C. (2000). Silver uptake by the green alga *Chlamydomonas reinhardtii* in relation to chemical speciation: Influence of chloride. *Environmental Toxicology and Chemistry*, *19*(11), 2769–2778. https://doi.org/10.1002/etc.5620191123

Froelich, P. N., Klinkhammer, G. P., Bender, M. L., Luedtke, N. A., Heath, G. R., Cullen, D., … Maynard, V. (1979). Early oxidation of organic matter in pelagic sediments of the eastern equatorial Atlantic: suboxic diagenesis. *Geochimica et Cosmochimica Acta*, *43*(7), 1075–1090. https://doi.org/10.1016/0016-7037(79)90095-4

Furrer, G., & Wehrli, B. (1993). Biogeochemical processes at the sediment-water interface: measurements and modeling. *Applied Geochemistry*, *8*(2), 117–119. https://doi.org/10.1016/S0883-2927(09)80021-8

Gallon, C., Hare, L., & Tessier, A. (2008). Surviving in anoxic surroundings: how burrowing aquatic insects create an oxic microhabitat. *Journal of the North American Benthological Society*, *27*(3), 570–580. https://doi.org/10.1899/07-132.1

Gao, C., & Liu, X. (2018). Spatio-temporal distribution of meiofaunal assemblages and its relationship with environmental factors in a semi-enclosed bay. *Marine Pollution Bulletin, 131*. https://doi.org/10.1016/j.marpolbul.2018.03.047

Gao, Y., Kan, A. T., & Tomson, M. B. (2003). Critical Evaluation of Desorption Phenomena of Heavy Metals from Natural Sediments. *Environmental Science and Technology*, *37*(24), 5566–5573. https://doi.org/10.1021/es034392w

Gao, Y., Leermakers, M., Gabelle, C., Divis, P., Billon, G., Ouddane, B., … Baeyens, W. (2006). High-resolution profiles of trace metals in the pore waters of riverine sediment assessed by DET and DGT. *Science of the Total Environment*, *362*(1–3), 266–277. https://doi.org/10.1016/j.scitotenv.2005.11.023

Gerringa, L. J. A. (1990). Aerobic degradation of organic matter and the mobility of Cu,

Cd, Ni, Pb, Zn, Fe and Mn in marine sediment slurries. *Marine Chemistry*, *29*(C), 355–374. https://doi.org/10.1016/0304-4203(90)90023-6

Gerringa, L. J. A. (1991). Mobility of Cu, Cd, Ni, Pb, Zn, Fe and Mn in marine sediment slurries under anaerobic conditions and at 20% air saturation. *Netherlands Journal of Sea Research*, *27*(2), 145–156. https://doi.org/10.1016/0077-7579(91)90007-N

Gillan, D. C., Baeyens, W., Bechara, R., Billon, G., Denis, K., Grosjean, P., Leermakers, M., Lesven, L., Pede, A., Sabbe, K., & Gao, Y. (2012). Links between bacterial communities in marine sediments and trace metal geochemistry as measured by in situ DET/DGT approaches. *Marine Pollution Bulletin*, *64*(2), 353–362. https://doi.org/10.1016/j.marpolbul.2011.11.001

Gillis, P. L., Chow-Fraser, P., Ranville, J. F., Ross, P. E., & Wood, C. M. (2005). Daphnia need to be gut-cleared too: the effect of exposure to and ingestion of metal-contaminated sediment on the gut-clearance patterns of *D. magna*. *Aquatic Toxicology*, *71*(2), 143–154. https://doi.org/10.1016/j.aquatox.2004.10.016

Gladney, E. S., & Roelandts, I. (1990). 1988 Compilation of Elemental Concentration Data for USGS Geochemical Exploration Reference Materials GXR-1 to GXR-6. *Geostandards and Geoanalytical Research*, *14*(1), 21–118. https://doi.org/10.1111/j.1751-908X.1990.tb00065.x

Grant, A. (2002). Pollution-tolerant species and communities: Intriguing toys or invaluable monitoring tools? *Human and Ecological Risk Assessment*. Taylor and Francis Inc. https://doi.org/10.1080/1080-700291905765

Grant, A. (2010). Detecting ecological effects of pollutants in the aquatic environment. In: Batty, L. C., & Hallberg, K. B. (Eds). *Ecology of industrial pollution (pp. 147 - 161)*. Cambridge, UK: Cambridge University Press

Grant, A., & Middleton, R. (1990). An assessment of metal contamination of sediments in the humber estuary, U.K. *Estuarine, Coastal and Shelf Science*, *31*(1), 71–85. https://doi.org/10.1016/0272-7714(90)90029-Q

Grant, A., & Middleton, R. (1998). Contaminants in sediments: Using robust regression for grain-size normalization. *Estuaries, 21*(2), 197–203. https://doi.org/10.2307/1352468

Grant, A., Hateley, J. G., & Jones, N. V. (1989). Mapping the ecological impact of heavy metals on the estuarine polychaete Nereis diversicolor using inherited metal tolerance. *Marine Pollution Bulletin*, *20*(5), 235–238. https://doi.org/10.1016/0025-326X(89)90438-4

Greenwood, N. (2001). *Metal speciation and toxicity in sediments from the Fal and Hayle estuaries, Cornwall, UK*. PhD thesis. University of East Anglia, Norwich, UK.

Greenwood, R., Mills, G., & Vrana, B. (Eds.). (2007). *Passive sampling techniques in environmental monitoring*, Vol. 48 (1st ed.). Amsterdam, Netherlands: Elsevier.

Griscom, S. B., & Fisher, N. S. (2004). Bioavailability of sediment-bound metals to marine bivalve molluscs: An overview. *Estuaries, 27*(5), 826–838. https://doi.org/10.1007/BF02912044

Hale, R., Boardman, R., Mavrogordato, M. N., Sinclair, I., Tolhurst, T. J., & Solan, M. (2015). High-resolution computed tomography reconstructions of invertebrate burrow systems. *Scientific data, 2*(1), 1-5. https://doi.org/10.1038/sdata.2015.52

Haman, J., & Avery, M. (2019). Package 'ciTools': Confidence or Prediction Intervals, Quantiles, and Probabilities for Statistical Models. https://cran.r-project.org/web/packages/ciTools/ciTools.pdf

Hansen, D. J., Berry, W. J., Mahony, J. D., Boothman, W. S., Toro, D. M. Di, Robson, D. L., Ankley, G. T., Ma, D., Yan, Q., & Pescha, C. E. (1996). Predicting the toxicity of metal-contaminated field sediments using interstitial concentration of metals and acid-volatile sulfide normalizations. *Environmental Toxicology and Chemistry, 15*(12), 2080–2094. https://doi.org/10.1897/1551-5028(1996)015<2080:pttomc>2.3.co;2

Harper, M. P., Davison, W., & Tych, W. (1997). Temporal, spatial, and resolution constraints for in situ sampling devices using diffusional equilibration: Dialysis and DET. *Environmental Science and Technology*, *31*(11), 3110–3119.

https://doi.org/10.1021/es9700515

Harper, M. P., Davison, W., Zhang, H., & Tych, W. (1998). Kinetics of metal exchange between solids and solutions in sediments and soils interpreted from DGT measured fluxes. *Geochimica et Cosmochimica Acta*, *62*(16), 2757–2770. https://doi.org/10.1016/S0016-7037(98)00186-0

Heip, C., Vincx, M., & Vrank. (1985). The ecology of marine nematodes. *Oceanogr. Mar. Biol. Ann. Rev.*, *23*(February), 399–489.

Heiri, O., Lotter, A. F., & Lemcke, G. (2001). Loss on ignition as a method for estimating organic and carbonate content in sediments: reproducibility and comparability of results. *Journal of Paleolimnology*, *25*(1), 101–110. https://doi.org/10.1023/A:1008119611481

Herrin, R. T., Andren, A. W., & Armstrong, D. E. (2001). Determination of silver speciation in natural waters. 1. Laboratory tests of Chelex-100 chelating resin as a competing ligand. *Environmental Science and Technology*, *35*(10), 1953–1958. https://doi.org/10.1021/es001509x

Hesslein, R. H. (1976). An in situ sampler for close interval pore water studies. *Limnology and Oceanography*, *21*(6), 912–914. https://doi.org/10.4319/lo.1976.21.6.0912

Hill, N. A., Johnston, E. L., King, C. K., & Simpson, S. L. (2011). Physico-chemical changes in metal-spiked sediments deployed in the field: Implications for the interpretation of in situ studies. *Chemosphere*, *83*(4), 400-408. https://doi.org/10.1016/j.chemosphere.2010.12.089

Hosmer, D. W., Lemeshow, S., & May, S. (2008). *Applied survival analysis*, 2nd ed. Cambridge, NJ, USA: John Wiley & Sons, Inc.

Hothorn, T., Bretz, F., & Westfall, P. (2020). Package 'multcomp': Simultaneous Inference in General Parametric Models. https://cran.r-project.org/web/packages/multcomp/multcomp.pdf

Howell, R. (1983). Heavy metals in marine nematodes: uptake, tissue distribution and loss

of copper and zinc. *Marine Pollution Bulletin, 14*(7), 263-268. https://doi.org/10.1016/0025-326X(83)90170-4

Hutchings, A. M., Antler, G., Wilkening, J. V., Basu, A., Bradbury, H. J., Clegg, J. A., … Turchyn, A. V. (2019). Creek Dynamics Determine Pond Subsurface Geochemical Heterogeneity in East Anglian (UK) Salt Marshes. *Frontiers in Earth Science, 7*. https://doi.org/10.3389/feart.2019.00041

Hutchins, C. M., Teasdale, P. R., Lee, S. Y., & Simpson, S. L. (2008). Cu and Zn concentration gradients created by dilution of pH neutral metal-spiked marine sediment: a comparison of sediment geochemistry with direct methods of metal addition. *Environmental science & technology*, *42*(8), 2912-2918. https://doi.org/ 10.1021/es702673w

Huxham, M., Raffaelli, D., & Pike, A. W. (1995). The effect of larval trematodes on the growth and burrowing behaviour of *Hydrobia ulvae* (gastropoda:prosobranchiata) in the Ythan estuary, north-east Scotland. *Journal of Experimental Marine Biology and Ecology*, *185*(1), 1–17. https://doi.org/10.1016/0022-0981(94)00119-X

Hwang, K. Y., Kim, H. S., & Hwang, I. (2011). Effect of Resuspension on the Release of Heavy Metals and Water Chemistry in Anoxic and Oxic Sediments. *Clean - Soil, Air, Water*, *39*(10), 908–915. https://doi.org/10.1002/clen.201000417

International Seabed Authority [ISA]. (2011). *Marine benthic nematode molecular protocol handbook (Nematode Barcoding), ISA technical study No. 7.* Kingston, Jamaica: International Seabed Authority. https://isa.org.jm/files/files/documents/tstudy7.pdf

Jackson, S. L., Spence, J., Janssen, D. J., Ross, A. R. S., & Cullen, J. T. (2018). Determination of Mn, Fe, Ni, Cu, Zn, Cd and Pb in seawater using offline extraction and triple quadrupole ICP-MS/MS. *Journal of Analytical Atomic Spectrometry*, *33*(2), 304–313. https://doi.org/10.1039/c7ja00237h

Jager, T. (2012). Bad habits die hard: The NOEC's persistence reflects poorly on ecotoxicology. *Environmental Toxicology and Chemistry*, *31*(2), 228–229.

https://doi.org/10.1002/etc.746

Johnson, A. C., & Sumpter, J. P. (2016). Are we going about chemical risk assessment for the aquatic environment the wrong way? *Environmental Toxicology and Chemistry*, *35*(7), 1609–1616. https://doi.org/10.1002/etc.3441

Johnson, C. A. (1986). The regulation of trace element concentrations in river and estuarine waters contaminated with acid mine drainage: The adsorption of Cu and Zn on amorphous Fe oxyhydroxides. *Geochimica et Cosmochimica Acta*, *50*(11), 2433–2438. https://doi.org/10.1016/0016-7037(86)90026-8

Johnston, E. L., & Roberts, D. A. (2009). Contaminants reduce the richness and evenness of marine communities: A review and meta-analysis. *Environmental Pollution*. Elsevier. https://doi.org/10.1016/j.envpol.2009.02.017

Jolley, D. F., Mason, S., Gao, Y., & Zhang, H. (2016). Practicalities of Working with DGT. In: Davison, W. (Ed). *Diffusive gradients in thin-films for environmental measurements*. Cambridge, UK: Cambridge University Press.

Jorgensen, B. B., Findlay, A. J., & Pellerin, A. (2019). The biogeochemical sulfur cycle of marine sediments. *Frontiers in Microbiology*, *10*(APR), 849. https://doi.org/10.3389/fmicb.2019.00849

Kadiene, E. U., Ouddane, B., Hwang, J. S., & Souissi, S. (2019). Bioaccumulation of metals in calanoid copepods by oral intake. *Scientific Reports*, *9*(1), 1–9. https://doi.org/10.1038/s41598-019-45987-2

Kaiser, K., & Guggenberger, G. (2007). Sorptive stabilization of organic matter by microporous goethite: Sorption into small pores vs. surface complexation. *European Journal of Soil Science*, *58*(1), 45–59. https://doi.org/10.1111/j.1365-2389.2006.00799.x

Kassambara, A., Kosinski, M., & Biecek, P. (2020). Package ‘survminer’: Drawing Survival Curves using 'ggplot2. https://cran.r-project.org/web/packages/survminer/survminer.pdf

Kemp, P. F., & Swartz, R. C. (1988). Acute toxicity of interstitial and particle-bound cadmium to a marine infaunal amphipod. *Marine Environmental Research*, *26*(2), 135–153. https://doi.org/10.1016/0141-1136(88)90023-2

Kenny, A. J., & Sotheran, I. (2013). Characterising the Physical Properties of Seabed Habitats. In: Eleftheriou, A. (Ed). *Methods for the study of marine benthos, 4th ed.* Chichester, UK: John Wiley & Sons

Kent W. Warnken, *, Hao Zhang, and, & Davison, W. (2006). Accuracy of the Diffusive Gradients in Thin-Films Technique: Diffusive Boundary Layer and Effective Sampling Area Considerations. https://doi.org/10.1021/AC060139D

Kester, D. R., Duedall, I. W., Connors, D. N., & Pytkowicz, R. M. (1967). Preparation of artificial seawater. *Limnology and Oceanography*, *12*(1), 176–179. https://doi.org/https://doi.org/10.4319/lo.1967.12.1.0176

Khan, F. R., Schmuecking, K., Krishnadasan, S. H., Berhanu, D., Smith, B. D., deMello, J. C., … Valsami-Jones, E. (2013). Dietary bioavailability of cadmium presented to the gastropod *Peringia ulvae* as quantum dots and in ionic form. *Environmental Toxicology and Chemistry*, *32*(11), n/a-n/a. https://doi.org/10.1002/etc.2348

Kingston, H. M., Barnes, I. L., Brady, T. J., Rains, T. C., & Champ, M. A. (1978). Separation of Eight Transition Elements from Alkali and Alkaline Earth Elements in Estuarine and Seawater with Chelating Resin and Their Determination by Graphite Furnace Atomic Absorption Spectrometry. *Analytical Chemistry*, *50*(14), 2064–2070. https://doi.org/10.1021/ac50036a031

Kostka, J. E., Gribsholt, B., Petrie, E., Dalton, D., Skelton, H., & Kristensen, E. (2002). The Rates and Pathways of Carbon Oxidation in Bioturbated Saltmarsh Sediments, *47*(1), 230–240.

Krell, B., Moreira-Santos, M., & Ribeiro, R. (2011). An estuarine mudsnail in situ toxicity assay based on postexposure feeding. *Environmental Toxicology and Chemistry*, *30*(8), 1935–1942. https://doi.org/10.1002/etc.585

Kubo, A., & Kanda, J. (2017). Seasonal variations and sources of sedimentary organic

carbon in Tokyo Bay. *Marine Pollution Bulletin*, *114*(2), 637–643. https://doi.org/10.1016/j.marpolbul.2016.10.030

Kundra, S. K., Katyal, M., & Singh, R. P. (1974). Spectrophotometric Determination of Copper(I) and Cobalt(II) with Ferrozine. *Analytical Chemistry*, *46*(11), 1605–1606. https://doi.org/10.1021/ac60347a022

Landis, W. G., & Chapman, P. M. (2011). Well past time to stop using NOELs and LOELs. *Integrated Environmental Assessment and Management*, *7*(4), vi–viii. https://doi.org/10.1002/ieam.249

Landner, L., & Reuther, R. (2004). *Metals in society and in the environment: A critical review of current knowledge on fluxes, speciation, bioavailability and risk for adverse effects of copper, chromium, nickel and zinc*. New York: Kluwer Academic Publishers.

Langston, W. J., Chesman, B. S., Burt, G. R., Taylor, M., Covey, R., Cunningham, N., … Hawkins, S. J. (2006). Characterisation of the European Marine Sites in South West England: The Fal and Helford candidate Special Area of Conservation (cSAC). *Hydrobiologia*, *555*, 321–333. https://doi.org/10.1007/s10750-005-1128-y

Lee, B.G., Griscom, S. B., Lee, J.-S., Choi, H. J., Koh, C.-H., Luoma, S. N., & Fisher, N. S. (2000a). Influences of Dietary Uptake and Reactive Sulfides on Metal Bioavailability from Aquatic Sediments. *Science*, *287*(5451). Retrieved from http://science.sciencemag.org/content/287/5451/282

Lee, B. G., Lee, J. S., Luoma, S. N., Choi, H. J., & Koh, C. H. (2000b). Influence of acid volatile sulfide and metal concentrations on metal bioavailability to marine invertebrates in contaminated sediments. *Environmental Science and Technology*, *34*(21), 4517–4523. https://doi.org/10.1021/es001033h

Leermakers, M., Gao, Y., Gabelle, C., Lojen, S., Ouddane, B., Wartel, M., & Baeyens, W. (2005). Determination of high resolution pore water profiles of trace metals in sediments of the Rupel River (Belgium) using DET (diffusive equilibrium in thin films) and DGT (diffusive gradients in thin films) techniques. *Water, Air, and Soil*

Pollution, *166*(1–4), 265–286. https://doi.org/10.1007/s11270-005-6671-7

Legendre, P., & Legendre, R. (2012). *Numerical ecology, 3rd English edition*. Elsevier: Oxford, UK.

Lehto, N. J. (2016). Principles and Application in Soils and Sediments. In: Davison, W. (Ed). *Diffusive gradients in thin-films for environmental measurements*. Cambridge, UK: Cambridge University Press

Leonard, D. R. P., Clarke, K. R., Somerfield, P. J., & Warwick, R. M. (2006). The application of an indicator based on taxonomic distinctness for UK marine biodiversity assessments. *Journal of Environmental Management, 78*(1), 52-62. https://doi.org/10.1016/j.jenvman.2005.04.008

Levinton, J. S. (1979). Deposit-Feeders, Their Resources, and the Study of Resource Limitation. In *Ecological Processes in Coastal and Marine Systems* (pp. 117–141). Springer US. https://doi.org/10.1007/978-1-4615-9146-7_7

Levinton, J., & Bianchi, T. (1981). Nutrition and food limitation of deposit feeders 1. the role of microbes in the growth of mud snails Hydrobiidae. *Journal of Marine Research*, *39*(3), 531–546.

Liber, K., Doig, L. E., & White-Sobey, S. L. (2011). Toxicity of uranium, molybdenum, nickel, and arsenic to *Hyalella azteca* and *Chironomus dilutus* in water-only and spiked-sediment toxicity tests. *Ecotoxicology and Environmental Safety*, *74*(5), 1171–1179. https://doi.org/10.1016/j.ecoenv.2011.02.014

Long, E. R., MacDonald, D. D., Smith, S. L., & Calder, F. D. (1995). Incidence of adverse biological effects within ranges of chemical concentrations in marine and estuarine sediments. *Environmental management*, *19*(1), 81-97. https://doi.org/10.1007/BF02472006

Lopez, G. R., & Kofoed, L. H. (1980). Epipsammic browsing and deposit feeding in mud snails hydrobiidae. *Journal of Marine Research*, *38*(4), 585–600.

Lopez, G. R., & Levinton, J. S. (1987). Ecology of deposit-feeding animals in marine

sediments. *Quarterly Review of Biology*, *62*(3), 235–260. https://doi.org/10.1086/415511

López-Figueroa, F., & Niell, F. X. (1987). Feeding behaviour of *Hydrobia ulvae* (Pennant) in microcosms. *Journal of Experimental Marine Biology and Ecology*, *114*(2–3), 153–167. https://doi.org/10.1016/0022-0981(88)90135-9

Lors, C., Tiffreau, C., & Laboudigue, A. (2004). Effects of bacterial activities on the release of heavy metals from contaminated dredged sediments. *Chemosphere*, *56*(6), 619–630. https://doi.org/10.1016/j.chemosphere.2004.04.009

Lovley, D. R., Holmes, D. E., & Nevin, K. P. (2004). Dissimilatory Fe(III) and Mn(IV) reduction. *Advances in Microbial Physiology*. Academic Press. https://doi.org/10.1016/S0065-2911(04)49005-5

Luoma, S. N. (1983). Bioavailability of trace metals to aquatic organisms - A review. *Science of the Total Environment, 28* (1–3), 1–22. https://doi.org/10.1016/S0048-9697(83)80004-7

Luoma, S. N. (1985). Biological availability of sediment-bound trace metals. *La Baie de Seine. Colloque National Du CNRS, 24-26*. http://archimer.ifremer.fr/doc/00000/1302/

Luoma, S. N. (1989). Can we determine the biological availability of sediment-bound trace elements? *Hydrobiologia, 176–177*(1), 379–396. https://doi.org/10.1007/BF00026572

Luoma, S. N., & Bryan, G. W. (1981). A statistical assessment of the form of trace metals in oxidized estuarine sediments employing chemical extractants. *Science of The Total Environment*, *17*(2), 165–196. https://doi.org/10.1016/0048-9697(81)90182-0

Luoma, S. N., & Rainbow, P. S. (2005). Why is metal bioaccumulation so variable? Biodynamics as a unifying concept. *Environmental Science and Technology*, *39*(7), 1921–1931. https://doi.org/10.1021/es048947e

Luoma, S. N., & Rainbow, P. S. (2008). *Metal contamination in aquatic environments: science and lateral management*. Cambridge, UK: Cambridge University Press.

Macdonald, D. D., Carr, R. S., Calder, F. D., Long, E. R., & Ingersoll, C. G. (1996). Development and evaluation of sediment quality guidelines for Florida coastal waters. *Ecotoxicology*, *5*(4), 253-278. https://doi.org/ 10.1007/BF00118995

Marras, B., Montero, N., Marrucci, A., Bettoschi, A., Atzori, M., & Schintu, M. (2020). Operational DGT threshold values for metals in seawater from protected coastal areas in Sardinia (Western Mediterranean). *Marine Pollution Bulletin*, *150*, 110692. https://doi.org/10.1016/j.marpolbul.2019.110692

Martin, J. ., Nirel, P., & Thomas, A. (1987). Sequential extraction techniques: Promises and problems. *Marine Chemistry*, *22*(2–4), 313–341. https://doi.org/10.1016/0304-4203(87)90017-X

Mclachlan, A., & Defeo, O. (2018). *The ecology of sandy shores, 3rd ed*. London, UK: Academic Press.

McLusky, D. S., Bryant, V., & Campbell, R. (1986). The effects of temperature and salinity on the toxicity of heavy metals to marine and estuarine invertebrates. In: Barnes, M. (Ed). *Oceanography and Marine Biology: An Annual Review (pp. 481 - 520).* Aberdeen, UK: Aberdeen University Press

McWilliam, R. A., & Baird, D. J. (2002). Postexposure feeding depression: A new toxicity endpoint for use in laboratory studies with *Daphnia magna* . *Environmental Toxicology and Chemistry*, *21*(6), 1198–1205. https://doi.org/10.1002/etc.5620210612

Middleton, R., & Grant, A. (1990). Heavy metals in the Humber estuary: Scrobicularia clay as a pre-industrial datum. *Proceedings of the Yorkshire Geological Society*, *48*(1), 75–80. https://doi.org/10.1144/pygs.48.1.75

Miller, J. N., & Miller, J. C. (2010). Statistics and chemometrics for analytical chemistry, 6th Ed. London: Pearson.

Millward, R. N., & Grant, A. (2000). Pollution-induced tolerance to copper of nematode communities in the severely contaminated restronguet creek and adjacent estuaries, Cornwall, United Kingdom. *Environmental Toxicology and Chemistry*, *19*(2), 454–461. https://doi.org/10.1002/etc.5620190227

Millward, R. N., & Grant, A. (1995). Assessing the impact of copper on nematode communities from a chronically metal-enriched estuary using pollution-induced community tolerance. *Marine Pollution Bulletin, 30(11),* 701-706. https://doi.org/10.1016/0025-326X(95)00053-P

Millward, R.N. (1995). *The effects of chronic and acute metal-enrichment on the nematode community structure, composition and function in Restronguet Creek, S W England*. PhD thesis. University of East Anglia, Norwich, UK.

Millward, R. N. (1996). Intracellular inclusions in the nematode Tripyloides marinus from metal-enriched and cleaner estuaries in Cornwall, south-west England. Journal of the *Marine Biological Association of the United Kingdom, 76*(4), 885-895. https://doi.org/10.1017/S0025315400040868

Millward, Rod N., & Klerks, P. L. (2002). Contaminant-adaptation and community tolerance in ecological risk assessment: Introduction. *Human and Ecological Risk Assessment*. Taylor and Francis Inc. https://doi.org/10.1080/1080-700291905747

Moens, T., Van Gansbeke, D., & Vincx, M. (1999). Linking estuarine nematodes to their suspected food. A case study from the Westerschelde Estuary (south-west Netherlands). *Journal of the Marine Biological Association of the United Kingdom*, *79*(6), 1017–1027. https://doi.org/10.1017/S0025315499001253

Monserrat, J. M., Martínez, P. E., Geracitano, L. A., Lund Amado, L., Martinez Gaspar Martins, C., Lopes Leães Pinho, G., Soares Chaves, I., Ferreira-Cravo, M., Ventura-Lima, J., & Bianchini, A. (2007). Pollution biomarkers in estuarine animals: Critical review and new perspectives. *Comparative Biochemistry and Physiology Part C: Toxicology & Pharmacology*, *146*(1), 221–234. https://doi.org/10.1016/j.cbpc.2006.08.012

Naylor, C., Davison, W., Motelica-Heino, M., Van Den Berg, G. A., & Van Der Heijdt, L. M. (2004). Simultaneous release of sulfide with Fe, Mn, Ni and Zn in marine harbour sediment measured using a combined metal/sulfide DGT probe. *Science of the Total Environment*, *328*(1–3), 275–286. https://doi.org/10.1016/j.scitotenv.2004.02.008

Nicolai, M., Rosin, C., Tousset, N., & Nicolai, Y. (1999). Trace metals analysis in estuarine and seawater by ICP-MS using on line preconcentration and matrix elimination with chelating resin. *Talanta*, *50*(2), 433–444. https://doi.org/10.1016/S0039-9140(99)00130-7

Nirel, P. M. V., & Morel, F. M. M. (1990). Pitfalls of sequential extractions. *Water Research*, *24*(8), 1055–1056. https://doi.org/10.1016/0043-1354(90)90129-T

Ogilvie, L. A. (2004). *Quantifying the effects of metals on estuarine sediment microbial communities*. PhD thesis. University of East Anglia, Norwich, UK.

Ogilvie, L. A., & Grant, A. (2008). Linking pollution induced community tolerance (PICT) and microbial community structure in chronically metal polluted estuarine sediments. *Marine Environmental Research*, *65*(2), 187–198. https://doi.org/10.1016/j.marenvres.2007.10.002

Oksanen, J., Blanchet, F. G., Friendly, M., Kindt, R., Legendre, P., McGlinn, D., ... & Wagner, H. (2020). Package 'vegan'. Community ecology package, version, 2.5-7. Available Aug. 16, 2021 at https://cran.r-project.org/web/packages/vegan/vegan.pdf

Olsgard, F., & Gray, J. (1995). A comprehensive analysis of the effects of offshore oil and gas exploration and production on the benthic communities of the Norwegian continental shelf. *Marine Ecology Progress Series*, *122*(1–3), 277–306. https://doi.org/10.3354/meps122277

Orvain, F., & Sauriau, P. G. (2002). Environmental and behavioural factors affecting activity in the intertidal gastropod *Hydrobia ulvae*. *Journal of Experimental Marine Biology and Ecology*, *272*(2), 191–216. https://doi.org/10.1016/S0022-0981(02)00130-2

Pai, S. C., Whung, P. Y., & Lai, R. L. (1988). Pre-concentration efficiency of chelex-100 resin for heavy metals in seawater. Part 1. Effects of pH and Salts on the Distribution Ratios of Heavy Metals. *Analytica Chimica Acta*, *211*, 257–270. https://doi.org/10.1016/S0003-2670(00)83686-7

Paller, M. H., Harmon, S. M., Knox, A. S., Kuhne, W. W., & Halverson, N. V. (2019).

Assessing effects of dissolved organic carbon and water hardness on metal toxicity to *Ceriodaphnia dubia* using diffusive gradients in thin films (DGT). *Science of the Total Environment, 697*, 134107. https://doi.org/10.1016/j.scitotenv.2019.134107

Pascal, P. Y., Dupuy, C., Richard, P., Haubois, A. G., & Niquil, N. (2008). Influence of environment factors on bacterial ingestion rate of the deposit-feeder *Hydrobia ulvae* and comparison with meiofauna. *Journal of Sea Research*, *60*(3), 151–156. https://doi.org/10.1016/j.seares.2008.05.003

Pascual, E., & Drake, P. (2008). Physiological and behavioral responses of the mud snails *Hydrobia glyca* and *Hydrobia ulvae* to extreme water temperatures and salinities: Implications for their spatial distribution within a system of temperate lagoons. *Physiological and Biochemical Zoology*, *81*(5), 594–604. https://doi.org/10.1086/588173

Peijnenburg, W. J., Teasdale, P. R., Reible, D., Mondon, J., Bennett, W. W., & Campbell, P. G. (2014). Passive sampling methods for contaminated sediments: State of the science for metals. *Integrated Environmental Assessment and Management*, *10*(2), 179–196. https://doi.org/10.1002/ieam.1502

Peng, S., Wang, W., Li, X., & Yen, Y. (2004). Metal partitioning in river sediments measured by sequential extraction and biomimetic approaches. *Chemosphere*, *57*(8), 839–851. https://doi.org/10.1016/j.chemosphere.2004.07.015

Platt, H., & Warwick, R. (1983). *Freeliving marine nematodes: Part I. British enoplids. Synopses of the British Fauna No. 28*. Cambridge, UK: Cambridge University Press.

Platt, H., & Warwick, R. (1988). *Freeliving marine nematodes: Part II. British Chromadorids. Synopses of the British Fauna No. 38*. Leiden, Netherlands: Brill.

Pradit, S., Gao, Y., Faiboon, A., De Galan, S., Baeyens, W., & Leermakers, M. (2013). Application of DET (diffusive equilibrium in thin films) and DGT (diffusive gradients in thin films) techniques in the study of the mobility of sediment-bound metals in the outer section of Songkhla Lake, Southern Thailand. *Environmental Monitoring and Assessment*, *185*(5), 4207–4220. https://doi.org/10.1007/s10661-012-2862-z

Puy, J., Uribe, R., Mongin, S., Galceran, J., Cecília, J., Levy, J., Zhang, H., & Davison, W. (2012). Lability Criteria in Diffusive Gradients in Thin Films. *The Journal of Physical Chemistry A*, *116*(25), 6564–6573. https://doi.org/10.1021/jp212629z

Quattrini, F., Galceran, J., David, C. A., Puy, J., Alberti, G., & Rey-Castro, C. (2017). Dynamics of trace metal sorption by an ion-exchange chelating resin described by a mixed intraparticle/film diffusion transport model. The Cd/Chelex case. *Chemical Engineering Journal*, *317*, 810–820. https://doi.org/10.1016/j.cej.2017.02.115

R Core Team (2020). R: A language and environment for statistical computing. R Foundation for Statistical Computing, Vienna, Austria. http://www.R-project.org/

Rainbow, P. S. (2002). Trace metal concentrations in aquatic invertebrates: why and so what? *Environmental Pollution*, *120*(3), 497–507. https://doi.org/10.1016/S0269-7491(02)00238-5

Rainbow, P. S. (2007). Trace metal bioaccumulation: Models, metabolic availability and toxicity. In *Environment International* (Vol. 33, Issue 4, pp. 576–582). Elsevier Ltd. https://doi.org/10.1016/j.envint.2006.05.007

Rainbow, P. S. (2020). Mining-contaminated estuaries of Cornwall - Field research laboratories for trace metal ecotoxicology. *Journal of the Marine Biological Association of the United Kingdom*, *100* (2), 195–210. Cambridge University Press. https://doi.org/10.1017/S002531541900122X

Rainbow, P.S., Kriefman, S., Smith, B. D., & Luoma, S. N. (2011). Have the bioavailabilities of trace metals to a suite of biomonitors changed over three decades in SW England estuaries historically affected by mining? *Science of The Total Environment*, *409*(8), 1589–1602. https://doi.org/10.1016/j.scitotenv.2011.01.012

Raiswell, R., & Canfield, D. E. (2012). The Iron Biogeochemical Cycle Past and Present. *Geochemical Perspectives*, *1*(1), 1–220. https://doi.org/10.7185/geochempersp.1.1

Remaili, T. M., Simpson, S. L., Amato, E. D., Spadaro, D. A., Jarolimek, C. V., & Jolley, D. F. (2016). The impact of sediment bioturbation by secondary organisms on metal bioavailability, bioaccumulation and toxicity to target organisms in benthic bioassays:

Implications for sediment quality assessment. *Environmental Pollution*, *208*, 590–599. https://doi.org/10.1016/j.envpol.2015.10.033

Remaili, T. M., Yin, N., Bennett, W. W., Simpson, S. L., Jolley, D. F., & Welsh, D. T. (2018). Contrasting effects of bioturbation on metal toxicity of contaminated sediments results in misleading interpretation of the AVS-SEM metal-sulfide paradigm. *Environmental Science: Processes and Impacts*, *20*(9), 1285–1296. https://doi.org/10.1039/c8em00266e

Richards, C. M., Moal, O., & Pallud, C. (2018). Changes in water quality following opening and closure of a bar-built estuary (Pescadero, California). *Marine Chemistry*, *198*, 10–27. https://doi.org/10.1016/j.marchem.2017.11.004

Rickard, D., & Luther, G. W. (2006). Metal sulfude complexes and clusters. *Reviews in Mineralogy and Geochemistry*, *61*(1), 421–504.

Ritz, C., Baty, F., Streibig, J. C., & Gerhard, D. (2015). Dose-response analysis using R. *PloS one*, *10*(12), 1 - 13. https://doi.org/10.1371/journal.pone.0146021

Rollinson, G. K., Pirrie, D., Power, M. R., Cundy, A., & Camm, G. S. (2007). Geochemical and mineralogical record of historical mining, Hayle Estuary, Cornwall, UK. *Geoscience in South-West England*, *11*(4), 326–337.

Salomons, W., de Rooij, N. M., Kerdijk, H., & Bril, J. (1987). Sediments as a source for contaminants? *Hydrobiologia*, *149*(1), 13–30. https://doi.org/10.1007/BF00048643

Santner, J., & Williams, P. N. (2016). Measurement at High Spatial Resolution. In: Davison, W. (Ed). *Diffusive gradients in thin-films for environmental measurements* (pp. 174 – 215). Cambridge, UK: Cambridge University Press

Santner, J., Kreuzeder, A., Schnepf, A., & Wenzel, W. W. (2015). Numerical Evaluation of Lateral Diffusion Inside Diffusive Gradients in Thin Films Samplers. *Environmental Science & Technology*, *49*(10), 6109–6116. https://doi.org/10.1021/acs.est.5b00134

Saulnier, I., & Mucci, A. (2000). Trace metal remobilization following the resuspension of estuarine sediments: Saguenay Fjord, Canada. *Applied Geochemistry*, *15*(2), 191–210.

https://doi.org/10.1016/S0883-2927(99)00034-7

Scally, S., Davison, W., & Zhang, H. (2006). Diffusion coefficients of metals and metal complexes in hydrogels used in diffusive gradients in thin films. *Analytica Chimica Acta*, *558*(1), 222–229. https://doi.org/10.1016/j.aca.2005.11.020

Schratzberger, M., & Warwick, R. M. (1999). Differential effects of various types of disturbances on the structure of nematode assemblages: an experimental approach. *Marine Ecology Progress Series*, *181*, 227–236. Retrieved from http://www.int-res.com/articles/meps/181/m181p227.pdf

Schratzberger, M., Gee, J. M., Rees, H. L., Boyd, S. E., & Wall, C. M. (2000). The structure and taxonomic composition of sublittoral meiofauna assemblages as an indicator of the status of marine environments. *Journal of the Marine Biological Association of the United Kingdom*, *80*(6), 969–980. https://doi.org/10.1017/S0025315400003039

Schratzberger, M., Warr, K., & Rogers, S. I. (2006). Patterns of nematode populations in the southwestern North Sea and their link to other components of the benthic fauna. *Journal of Sea Research*, *55*(2), 113–127. https://doi.org/10.1016/j.seares.2005.07.002

Schratzberger, Michaela. (2012). On the relevance of meiobenthic research for policy-makers. *Marine Pollution Bulletin*, *64*(12), 2639–2644. https://doi.org/10.1016/j.marpolbul.2012.08.028

Selwood, E., Durrance, E., & Bristow, C. (1998). *The geology of Cornwall: and the Isles of Scilly*. (E. Selwood, E. Durrance, & C. Bristow, Eds.). Exeter, UK: University of Exeter Press.

Semprucci, F., Cesaroni, L., Guidi, L., & Balsamo, M. (2018). Do the morphological and functional traits of free-living marine nematodes mirror taxonomical diversity? *Marine Environmental Research*, *135*, 114–122. https://doi.org/10.1016/j.marenvres.2018.02.001

Semprucci, F., Sbrocca, C., Rocchi, M., & Balsamo, M. (2015). Temporal changes of the

meiofaunal assemblage as a tool for the assessment of the ecological quality status. *Journal of the Marine Biological Association of the United Kingdom*, *95*(2), 247–254. https://doi.org/10.1017/S0025315414001271

Semprucci, Federica, Facca, C., Ferrigno, F., Balsamo, M., Sfriso, A., & Sandulli, R. (2019). Biotic and abiotic factors affecting seasonal and spatial distribution of meiofauna and macrophytobenthos in transitional coastal waters. *Estuarine, Coastal and Shelf Science*, *219*, 328–340. https://doi.org/10.1016/j.ecss.2019.02.008

Shipley, H. J., Gao, Y., Kan, A. T., & Tomson, M. B. (2011). Mobilization of Trace Metals and Inorganic Compounds during Resuspension of Anoxic Sediments from Trepangier Bayou, Louisiana. *Journal of Environment Quality*, *40*(2), 484. https://doi.org/10.2134/jeq2009.0124

Shipp, E. (2006). *The impact of heavy metal contamination on invertebrates in the Fal and Hayle estuaries, Cornwall, UK*. PhD thesis. University of East Anglia, Norwich, UK.

Shipp, E., & Grant, A. (2006). *Hydrobia ulvae* feeding rates: A novel way to assess sediment toxicity. *Environmental Toxicology and Chemistry, 25*(12), 3246–3252. https://doi.org/10.1897/06-057R.1

Simpson, J. H., & Carr, H. Y. (1958). Diffusion and nuclear spin relaxation in water. *Physical Review*, *111*(5), 1201. https://doi.org/10.1103/PhysRev.111.1201

Simpson, S. L. (2016). Appendix C: Acid volatile sulfide (AVS) analysis. In: S.L., Simpson, & G.E. Batley (Eds.), *Sediment quality assessment: a practical guide*, 2nd ed. Victoria, Australia: CSIRO Publishing.

Simpson, S. L., Rosner, J., & Ellis, J. (2000). Competitive displacement reactions of cadmium, copper, and zinc added to a polluted, sulfidic estuarine sediment. *Environ. Toxicol. Chem.*, *19*(8), 1992–1999.

Simpson, S. L., & Batley, G. E. (2003). Disturbances to metal partitioning during toxicity testing of iron (II)-rich estuarine pore waters and whole sediments. *Environmental Toxicology and Chemistry: An International Journal, 22*(2), 424-432. https://doi.org/10.1002/etc.5620220225

Simpson, S.L. (2016). Appendix C: Acid volatile sulfide (AVS) analysis. In: S.L., Simpson, & G.E., Batley (Eds.). *Sediment quality assessment: a practical guide*, 2nd ed. Victoria, Australia: CSIRO Publishing.

Simpson, S.L., & Batley, G.E. (Eds.). (2016). *Sediment quality assessment: a practical guide*, 2nd ed. Victoria, Australia: CSIRO Publishing.

Simpson, S.L., Batley, G. E., & Chariton, A. A. (2013). *Revision of the ANZECC/ARMCANZ Sediment Quality Guidelines*. CSIRO. https://doi.org/10.4225/08/5894C6184320C

Simpson, S.L., Batley, G. E., & Maher, W. A. (2016). Chemistry of sediment contaminants. In: S.L., Simpson, & G.E., Batley (Eds.). *Sediment quality assessment: a practical guide*, 2nd ed. Victoria, Australia: CSIRO Publishing.

Simpson, Stuart L, & Batley, G. E. (2007). Predicting metal toxicity in sediments: A critique of current approaches. *Integrated Environmental Assessment and Management*, *3*(1), 18–31. https://doi.org/10.1002/ieam.5630030103

Simpson, Stuart L. (2001). A rapid screening method for acid-volatile sulfide in sediments. *Environmental Toxicology and Chemistry*, *20*(12), 2657–2661. https://doi.org/10.1002/etc.5620201201

Simpson, Stuart L. (2005). Exposure-effect model for calculating copper effect concentrations in sediments with varying copper binding properties: A synthesis. *Environmental Science and Technology*, *39*(18), 7089–7096. https://doi.org/10.1021/es050765c

Simpson, Stuart L., Angel, B. M., & Jolley, D. F. (2004). Metal equilibration in laboratory-contaminated (spiked) sediments used for the development of whole-sediment toxicity tests. *Chemosphere*, *54*(5), 597–609. https://doi.org/10.1016/j.chemosphere.2003.08.007

Simpson, Stuart L., Apte, S. C., & Batley, G. E. (1998). Effect of short-term resuspension events on trace metal speciation in polluted anoxic sediments. *Environmental Science and Technology*, *32*(5), 620–625. https://doi.org/10.1021/es970568g

Simpson, Stuart L., Batley, G. E., Hamilton, I. L., & Spadaro, D. A. (2011). Guidelines for copper in sediments with varying properties. *Chemosphere*, *85*(9), 1487–1495. https://doi.org/10.1016/j.chemosphere.2011.08.044

Simpson, Stuart L., Rochford, L., & Birch, G. F. (2002). Geochemical influences on metal partitioning in contaminated estuarine sediments. *Marine and Freshwater Research*, *53*(1), 9–17. https://doi.org/10.1071/MF01058

Simpson, Stuart L., Ward, D., Strom, D., & Jolley, D. F. (2012a). Oxidation of acid-volatile sulfide in surface sediments increases the release and toxicity of copper to the benthic amphipod *Melita plumulosa*. *Chemosphere*, *88*(8), 953–961. https://doi.org/10.1016/j.chemosphere.2012.03.026

Simpson, Stuart L., Yverneau, H., Cremazy, A., Jarolimek, C. V., Price, H. L., & Jolley, D. F. (2012b). DGT-induced copper flux predicts bioaccumulation and toxicity to bivalves in sediments with varying properties. *Environmental Science and Technology*, *46*(16), 9038–9046. https://doi.org/10.1021/es301225d

Slaveykova, V. I., & Wilkinson, K. J. (2005). Predicting the bioavailability of metals and metal complexes: critical review of the Biotic Ligand Model. *Environmental Chemistry*, *2*(1), 9. https://doi.org/10.1071/EN04076

Smith, R. G. (1974). Improved Ion-Exchange Technique for the Concentration of Manganese from Sea Water. *Analytical Chemistry*, *46*(4), 607–608. https://doi.org/10.1021/ac60340a031

Sokolowski, A., Richard, P., Fichet, D., & Radenac, G. (2005). Cd transfer in the deposit-feeder Prosobranch *Hydrobia ulvae* (Pennant) from benthic diatoms: The kinetics of rapid Cd assimilation and efflux. *Journal of Experimental Marine Biology and Ecology*, *317*(2), 159–174. https://doi.org/10.1016/j.jembe.2004.11.020

Somerfield, P. J., Gee, J. M., & Warwick, R. M. (1994a). Benthic community structure in relation to an instantaneous discharge of waste water from a tin mine. *Marine Pollution Bulletin, 28*(6), 363-369. https://doi.org/10.1016/0025-326X(94)90273-9

Somerfield, P. J., Gee, J. M., & Warwick, R. M. (1994b). Soft sediment meiofaunal

community structure in relation to a long-term heavy metal gradient in the Fa1 estuary system. *Marine Ecology Progress Series, 105*, 79–88. Retrieved from http://researchrepository.murdoch.edu.au/id/eprint/23355/1/soft_sediment_meiofaunal_community_structure.pdf

Sondergaard, J., Asmund, G., & Larsen, M. M. (2015). Trace elements determination in seawater by ICP-MS with on-line pre-concentration on a Chelex-100 column using a "standard" instrument setup. *MethodsX*, *2*, 323–330. https://doi.org/10.1016/j.mex.2015.06.003

Song, Z., Dong, L., Shan, B., & Tang, W. (2018). Assessment of potential bioavailability of heavy metals in the sediments of land-freshwater interfaces by diffusive gradients in thin films. *Chemosphere*, *191*, 218–225. https://doi.org/10.1016/j.chemosphere.2017.10.048

Stookey, L. L. (1970). Ferrozine-A New Spectrophotometric Reagent for Iron. *Analytical Chemistry*, *42*(7), 779–781. https://doi.org/10.1021/ac60289a016

Stratasys. (2013). Guide to basic post process applications: objet line of 3D printers. Available at https://www.stratasys.com/

Stratasys. (2015). VeroGray: PolyJet technology material specifications. Retrieved from https://www.stratasysdirect.com/materials/-/media/files/direct/material-datasheets/polyjet/polyjet_verogray_material_specifications.pdf?la=en&hash=26EDEA9EEA127AA779F4ED10711E02A25309512E

Strivens, J., Hayman, N., Johnston, R., & Rosen, G. (2019). Effects of Dissolved Organic Carbon on Copper Toxicity to Embryos of *Mytilus galloprovincialis* as Measured by Diffusive Gradient in Thin Films. *Environmental Toxicology and Chemistry*, *38*(5), 1029–1034. https://doi.org/10.1002/etc.4404

Strom, D., Simpson, S. L., Batley, G. E., & Jolley, D. F. (2011). The influence of sediment particle size and organic carbon on toxicity of copper to benthic invertebrates in oxic/suboxic surface sediments. *Environmental Toxicology and Chemistry*, *30*(7), 1599–1610. https://doi.org/10.1002/etc.531

Swartz, R. C., Ditsworth, G. R., Schults, D. W., & Lamberson, J. O. (1985). Sediment toxicity to a marine infaunal amphipod: Cadmium and its interaction with sewage sludge. *Marine Environmental Research, 18*(2), 133–153. https://doi.org/10.1016/0141-1136(86)90004-8

Tan, Q.-G., Ke, C., & Wang, W.-X. (2013). Rapid assessments of metal bioavailability in marine sediments using coelomic fluid of sipunculan worms. *Environmental Science & Technology*, 130614114324009. https://doi.org/10.1021/es401112d

Tankere-Muller, S., Zhang, H., Davison, W., Finke, N., Larsen, O., Stahl, H., & Glud, R. N. (2007). Fine scale remobilisation of Fe, Mn, Co, Ni, Cu and Cd in contaminated marine sediment. *Marine Chemistry*, *106*(1), 192–207. https://doi.org/10.1016/j.marchem.2006.04.005

Teasdale, P. (1995). Pore water sampling with sediment peepers. *TrAC Trends in Analytical Chemistry*, *14*(6), 250–256. https://doi.org/10.1016/0165-9936(95)91617-2

Tercier-Waeber, M.-L., & Taillefert, M. (2008). Remote in situ voltammetric techniques to characterize the biogeochemical cycling of trace metals in aquatic systems. *J. Environ. Monit.*, *10*(1), 30–54. https://doi.org/10.1039/B714439N

Tessier, A., & Campbell, P. (1987). Partitioning of trace metals in sediments: relationships with bioavailability. *Hydrobiologia*. https://doi.org/10.1007/BF00048645

Tessier, A., Campbell, P. G. C., Auclair, J. C., & Bisson, M. (1984). Relationships between the Partitioning of Trace Metals in Sediments and Their Accumulation in the Tissues of the Freshwater Mollusc *Elliptio complanata* in a Mining Area. *Canadian Journal of Fisheries and Aquatic Sciences*, *41*(10), 1463–1472. https://doi.org/10.1139/f84-180

Tessier, A., Campbell, P., & Bisson, M. (1979). Sequential extraction procedure for the speciation of particulate trace metals. *Analytical Chemistry, 51*(7), 844–851. https://doi.org/10.1021/ac50043a017

Thamdrup, B., & Canfield, D. E. (2000). Benthic Respiration in Aquatic Sediments. In Sala O.E., Jackson R.B., Mooney H.A., & Howarth R.W. (Eds.), *Methods in*

Ecosystem Science (pp. 86–103). Springer New York. https://doi.org/10.1007/978-1-4612-1224-9_7

Thamdrup, B., Fossing, H., & Jørgensen, B. B. (1994). Manganese, iron and sulfur cycling in a coastal marine sediment, Aarhus bay, Denmark. *Geochimica et Cosmochimica Acta*, *58*(23), 5115–5129. https://doi.org/10.1016/0016-7037(94)90298-4

Therneau, T. M. (2020). Package 'survival': Survival Analysis. https://cran.r-project.org/web/packages/survival/survival.pdf

Thomson-Becker, E. A., & Luoma, S. N. (1985). Temporal fluctuations in grain size, organic materials and iron concentrations in intertidal surface sediment of San Francisco Bay. *Hydrobiologia*, *129*(1), 91-107. https://doi.org/10.1007/BF00048689

Tietjen, J. H. (1980). Population structure and species composition of the free-living nematodes inhabiting sands of the New York Bight Apex. *Estuarine and Coastal Marine Science*, *10*(1), 61–73. https://doi.org/10.1016/S0302-3524(80)80049-1

Tlili, A., Berard, A., Blanck, H., Bouchez, A., Cássio, F., Eriksson, K. M., … Behra, R. (2016). Pollution-induced community tolerance (PICT): towards an ecologically relevant risk assessment of chemicals in aquatic systems. *Freshwater Biology*, *61*(12), 2141–2151. https://doi.org/10.1111/fwb.12558

Tupas, L. M., Popp, B. N., & Karl, D. M. (1994). Dissolved organic carbon in oligotrophic waters: experiments on sample preservation, storage and analysis. *Marine Chemistry*, *45*(3), 207–216. https://doi.org/10.1016/0304-4203(94)90004-3

Turekian, K. K., & Wedepohl, K. H. (1961). Distribution of the elements in some major units of the earth's crust. *Geological Society of America Bulletin*, *72*(2), 175-192. https://doi.org/10.1130/0016-7606(1961)72[175:DOTEIS]2.0.CO;2

United States Environmental Protection Agency [USEPA]. (2005). *Procedures for the Derivation of Equilibrium Partitioning Sediment Benchmarks (ESBs) for the Protection of Benthic Organisms: Metal Mixtures (Cadmium, Copper, Lead, Nickel,*

Silver and Zinc), EPA-600-R-02-011. Washington, DC: Office of Research and Development.

Vaananen, K., Leppänen, M. T., Chen, X. P., & Akkanen, J. (2018). Metal bioavailability in ecological risk assessment of freshwater ecosystems: From science to environmental management. In *Ecotoxicology and Environmental Safety* (Vol. 147, pp. 430–446). Academic Press. https://doi.org/10.1016/j.ecoenv.2017.08.064

Vafeiadou, A.-M., Materatski, P., Adão, H., De Troch, M., & Moens, T. (2014). Resource utilization and trophic position of nematodes and harpacticoid copepods in and adjacent to *Zostera noltii* beds. *Biogeosciences*, *11*, 4001–4014. https://doi.org/10.5194/bg-11-4001-2014

Vangheluwe, M. L. U., Verdonck, F. A. M., Besser, J. M., Brumbaugh, W. G., Ingersoll, C. G., Schlekat, C. E., & Garman, E. R. (2013). Improving sediment-quality guidelines for nickel: Development and application of predictive bioavailability models to assess chronic toxicity of nickel in freshwater sediments. *Environmental Toxicology and Chemistry*, *32*(11), 2507–2519. https://doi.org/10.1002/etc.2373

Verardo, D. J., Froelich, P. N., & McIntyre, A. (1990). Determination of organic carbon and nitrogen in marine sediments using the Carlo Erba NA-1500 analyzer. *Deep Sea Research Part A. Oceanographic Research Papers*, *37*(1), 157–165. https://doi.org/10.1016/0198-0149(90)90034-S

Vershinn, A., & Rozanov, A. (1982). Eh measurement with a platinum electrode and evaluation of redox conditions in marine media. *Geochem. Int.*, *19*(1), 121–128.

Vidal-Dura, A., Burke, I. T., Stewart, D. I., & Mortimer, R. J. G. (2018). Reoxidation of estuarine sediments during simulated resuspension events: Effects on nutrient and trace metal mobilisation. *Estuarine, Coastal and Shelf Science*, *207*(April), 40–55. https://doi.org/10.1016/j.ecss.2018.03.024

Wang, W.-X. (2013b). Dietary toxicity of metals in aquatic animals: Recent studies and perspectives, *58*(2). https://doi.org/10.1007/s11434-012-5413-7

Wang, W.-X. (2013a). Prediction of metal toxicity in aquatic organisms. *Chinese Science*

Bulletin, *58*(2), 194–202. https://doi.org/10.1007/s11434-012-5403-9

Wang, W.-X., & Fisher, N. S. (1999). Delineating metal accumulation pathways for marine invertebrates. *Science of The Total Environment*, *237*, 459–472. https://doi.org/10.1016/S0048-9697(99)00158-8

Warwick, R. M. (2001). Evidence for the effects of metal contamination on the intertidal macrobenthic assemblages of the Fal estuary. *Marine Pollution Bulletin*, *42*(2), 145–148. https://doi.org/10.1016/S0025-326X(00)00120-X

Warwick, R. M., & Clarke, K. R. (1998). Taxonomic distinctness and environmental assessment. *Journal of Applied Ecology*, *35*(4), 532–543. https://doi.org/10.1046/j.1365-2664.1998.3540532.x

Warwick, R., Platt, H., & Somerfield, P. (1998). *Freeliving marine nematodes: part III. Monhysterids. Synopses of the British Fauna no. 53*. Shrewsbury, UK: Field Studies.

Water Framework Directive. (2015). *The Water Framework Directive (Standards and Classification) Directions (England and Wales) 2015*. https://www.legislation.gov.uk/uksi/2015/1623/resources

Whalley, C., & Grant, A. (1994). Assessment of the phase selectivity of the European Community Bureau of Reference (BCR) sequential extraction procedure for metals in sediment. *Analytica Chimica Acta*, *291*(3), 287–295. https://doi.org/10.1016/0003-2670(94)80024-3

Whitaker, D., & Christman, M. (2015). Package 'clustsig'. Significant Cluster Analysis, version, 1.1. Available Aug. 16, 2021 at https://cran.r-project.org/web/packages/clustsig/clustsig.pdf

Wieser, W. (1953). Die Beziehung zwischen Mundholengestalt, Ernahrungswiese und Vorkommen bei freilebenden marinen Nematoden. *Archiv for Zoologi*, *26*, 439–484.

Wong, J. W. C., & Yang, C. L. (1997). The effect of pH and redox potential on the release of nutrients and heavy metals from a contaminated marine sediment. *Toxicological and Environmental Chemistry*, *62*(1–4), 1–10.

https://doi.org/10.1080/02772249709358493

Wood, T. M., Baptista, A. H., Kuwabara, J. S., & Flegal, A. R. (1995). Diagnostic modeling of trace metal partitioning in south San Francisco Bay. *Limnol. Oceanogr*, *40*(2), 345–358.

Wu, Z., He, M., & Lin, C. (2011). In situ measurements of concentrations of Cd, Co, Fe and Mn in estuarine porewater using DGT. *Environmental Pollution*, *159*(5), 1123–1128. https://doi.org/10.1016/j.envpol.2011.02.015

Wuttig, K., Townsend, A. T., van der Merwe, P., Gault-Ringold, M., Holmes, T., Schallenberg, C., … Bowie, A. R. (2019). Critical evaluation of a seaFAST system for the analysis of trace metals in marine samples. *Talanta*, *197*, 653–668. https://doi.org/10.1016/j.talanta.2019.01.047

Yan, Q. L., & Wang, W. X. (2002). Metal exposure and bioavailability to a marine deposit-feeding sipuncula, *Sipunculus nudus*. *Environmental Science and Technology*, *36*(1), 40–47. https://doi.org/10.1021/es015604x

Yoder, M., Wm King, I., De Ley, I. T., Mann, J., Mundo-Ocampo, M., Poiras, L., … Blaxter, M. (2006). DESS: a versatile solution for preserving morphology and extractable DNA of nematodes. *Nematology*, *8*(3), 367–376. https://doi.org/10.1163/156854106778493448

Yuan-Hui, L., & Gregory, S. (1974). Diffusion of ions in sea water and in deep-sea sediments. *Geochimica et Cosmochimica Acta*, *38*(5), 703–714. https://doi.org/10.1016/0016-7037(74)90145-8

Zhang, C., Yu, Z., Zeng, G., Jiang, M., Yang, Z., Cui, F., Zhu, M., Shen, L., & Hu, L. (2014). Effects of sediment geochemical properties on heavy metal bioavailability. *Environment International*, *73*, 270–281. https://doi.org/10.1016/j.envint.2014.08.010

Zhang, H., & Davison, W. (1999). Diffusional characteristics of hydrogels used in DGT and DET techniques. *Analytica Chimica Acta*, *398*(2), 329–340. https://doi.org/10.1016/S0003-2670(99)00458-4

Zhang, H., & Davison, W. (2000). Direct in situ measurements of labile inorganic and organically bound metal species in synthetic solutions and natural waters using diffusive gradients in thin films. *Analytical Chemistry*, *72*(18), 4447–4457. https://doi.org/10.1021/ac0004097

Zhang, H., & Davison, W. (2015). Use of diffusive gradients in thin-films for studies of chemical speciation and bioavailability. *Environmental Chemistry*, *12*(2), 85–101. https://doi.org/10.1071/EN14105

Zhang, H., Davison, W., Miller, S., & Tych, W. (1995). In situ high resolution measurements of fluxes of Ni, Cu, Fe, and Mn and concentrations of Zn and Cd in porewaters by DGT. *Geochimica et Cosmochimica Acta*, *59*(20), 4181–4192. https://doi.org/10.1016/0016-7037(95)00293-9

Zhang, H., Davison, W., Mortimer, R. J. G., Krom, M. D., Hayes, P. J., & Davies, I. M. (2002). Localised remobilization of metals in a marine sediment. *Science of The Total Environment*, *296*(1), 175–187. https://doi.org/10.1016/S0048-9697(02)00078-5

Zhang, K., Li, A., Zhang, J., Lu, J., & Wang, H. (2020). Seasonal variations in the surficial sediment grain size in the East China Sea continental shelf and their implications for terrigenous sediment transport. *Journal of Oceanography*, *76*(1), 1–14. https://doi.org/10.1007/s10872-019-00523-8

Zhang, Y., Yang, J., Simpson, S. L., Wang, Y., & Zhu, L. (2019). Application of diffusive gradients in thin films (DGT) and simultaneously extracted metals (SEM) for evaluating bioavailability of metal contaminants in the sediments of Taihu Lake, China. *Ecotoxicology and Environmental Safety*, *184*, 109627. https://doi.org/10.1016/j.ecoenv.2019.109627

Zhao, C.-M., Campbell, P. G. C., & Wilkinson, K. J. (2016). When are metal complexes bioavailable? *Environmental Chemistry*, *13*(3), 425–433. https://doi.org/10.1071/EN15205

Appendices to Chapter 2.

A2.01: Percentage Total Organic Carbon (TOC) and Loss on Ignition (LOI; at 400 ^{o}C) across the study sites. Errors represent standard deviation (n = 3)

Site	2017 Autumn		2019 Winter		2019 Summer	
	TOC (%)	LOI (%)	TOC (%)	LOI (%)	LOI Oxic (%)	LOI Anoxic (%)
BW	1.83 ± 0.06	3.63	1.17 ± 0.03	2.48	5.80	4.47
PR	10.04 ± 0.12	19.35	4.91 ± 0.04	9.19	10.80	11.97
CO	5.15 ± 0.02	9.23	4.71 ± 0.03	8.49	13.04	11.47
HR	4.65 ± 0.01	9.10	5 ± 0.03	9.73	9.57	7.25
PC	4.28 ± 0.03	8.17	3.86 ± 0.03	6.22	7.66	10.97
SJ	4.5 ± 0.02	8.15	4.34 ± 0.01	8.04	7.28	9.39
MC	6.46 ± 0.02	12.57	4.06 ± 0.01	7.44	12.26	6.46
HA	1.42 ± 0.06	3.82	2.19 ± 0.01	4.55	4.87	3.73
RC	3.38 ± 0.02	7.56	4.03 ± 0.04	7.07	8.95	7.69
RA	6.53 ± 0.09	12.55	5.16 ± 0.03	9.44	10.15	11.19
RB	2.99 ± 0.02	6.76	3.3 ± 0.01	6.89	6.80	9.03
HB	1.64 ± 0.06	2.90	4.9 ± 0.16	7.28	11.30	6.92

A2.02: Precision and accuracy of Total Organic Carbon (TOC) and Loss on Ignition (LOI; at 400 ^{o}C) analyses

Sample	Certified value (%)	N	Mean (%)	SD (%)	Precision (%)	Accuracy (%)	Analysis
1941-B	2.99 ± 0.24	9	3.11	0.11	3.6	104	TOC
BW-Sep	NA	3	3.63	0.22	6.1	NA	LOI
GH	NA	6	4.32	0.28	6.5	NA	TOC
PACS-1	NA	6	3.51	0.07	1.9	NA	TOC

BW-Sep = Breydon Water sediment sampled in September 2017
GH = Goole Harbour sediment (QUASIMEME laboratory performance studies)
N = Number of replicates
NA = Not applicable

A2.03: Dissolved Organic Carbon (DOC) concentrations across the study sites

Site	2017 Autumn		2019 Winter
	0.2 µm	0.45 µm	0.45 µm
BW	NA	10.5	34.9
PR	18.6	11.0	26.8
CO	12.7	12.2	32.6
HR	4.6	4.9	8.4
PC	9.1	9.2	17.9
SJ	8.2	8.9	9.2
MC	13.4	13.3	20.9
HA	38.4	30.9	47.0
RC	8.5	8.5	27.2
RA	4.3	7.4	21.3
RB	10.3	9.3	14.5
HB	5.4	5.9	14.1

NA = Not available

A2.04: Precision and accuracy of Dissolved Organic Carbon analysis

Sample	Certified value (mg/L)	N	Mean (mg/L)	SD (mg/L)	Precision (%)	Recovery (%)	Analysis
25 UPW	NA	3	24.6	0.1	0.6	98.2	2019-W
25 saline	NA	3	24.5	0.2	0.9	98.2	2019-W
30 UPW	NA	10	30.0	0.1	0.4	100.1	2017-A
Cran – 05*	3.48 ± 0.53	2	3.85	0.73	18.9	110.6	2017-A

25 UPW = 25 mg C/L in ultrapure water matrix
25 saline = 25 mg C/L in 30 S seawater matrix
30 UPW = 30 mg C/L in ultrapure water matrix
Cran – 05 = Cranberry-05 lake water reference
N = Number of replicates
NA = Not applicable
Limit of detection 0.12 mg/L (calculated according to Miller & Miller, 2010)
* Error represents uncertainty value supplied by manufacturer

A2.05: Total sediment metal concentrations (trace elements, µg/g) across the study sites in Autumn 2017. Concentrations of As, Cu, Ni, Pb and Zn are normalised for grain size fraction <63 µm

Site	Sc	V	Cr	Ni	Cu	Zn	As	Rb	Sr	Y	Zr	Nb	Mo	Ba	La	Ce	Pb	Th	U
Shale	NA	130	90	68	45	95	13	140	300	26	160	11	NA	580	92	59	20	NA	NA
BW	13	115	85	33	8	103	26	78	188	22	259	15	4	316	21	89	49	10	1
PR	10	114	90	46	118	232	47	126	125	23	202	17	5	434	54	51	96	15	1
CO	10	101	76	49	183	355	82	172	107	26	222	21	4	397	37	76	93	14	2
HR	12	108	112	55	215	491	49	190	127	28	251	22	4	326	45	79	85	23	4
PC	10	97	80	42	645	668	190	217	129	27	226	25	5	375	52	51	144	20	3
SJ	10	103	86	44	554	621	99	168	116	24	170	20	5	448	42	58	250	21	2
MC	10	111	92	53	792	801	266	169	105	34	212	22	5	301	67	81	184	20	3
HA	5	66	46	56	862	1261	558	209	245	26	141	31	5	142	46	126	211	48	5
RC	10	116	75	45	2413	2367	1356	211	121	31	158	29	6	287	50	69	653	41	3
RA	8	103	75	44	2978	2467	2228	205	97	34	161	27	6	249	66	73	309	41	7
RB	9	113	70	44	3183	3015	1834	206	101	32	146	30	5	250	56	66	292	40	3
HB	14	119	99	214	2565	3753	1603	118	212	31	222	25	4	259	32	81	410	14	2

NA = Not available. Shale = Average shale values as reported by Turekian and Wedepohl (1961)

A2.06: Total sediment metal concentrations (major element oxides, weight %) across the study sites in Autumn 2017

Site	SiO_2	TiO_2	Al_2O_3	MnO	MgO	Fe_2O_3	CaO	P_2O_5	K_2O	Na_2O
Shale	58.52	0.77	15.12	0.11	2.49	6.75	3.09	0.16	3.2	1.29
BW	58.43	0.68	10.55	0.06	1.91	4.5	7.18	0.21	2.14	1.74
PR	48.92	0.77	14.46	0.12	1.33	5.9	0.71	0.34	2.56	1.86
CO	56.37	0.72	17.7	0.04	1.18	5.39	0.58	0.25	2.76	1.36
HR	55.69	0.82	15.3	0.05	1.78	5.66	1.64	0.28	2.79	1.59
PC	52.11	0.71	18.35	0.04	1.56	5.81	1.32	0.26	2.78	2.11
SJ	52.69	0.68	16.73	0.04	1.57	5.87	0.75	0.23	2.63	2.97
MC	52.36	0.75	15.09	0.07	1.68	6.13	0.89	0.34	2.54	2.14
HA	61.67	0.48	10.77	0.11	1.22	7.31	5.11	0.28	2.23	0.73
RC	51.5	0.59	16.56	0.08	1.62	9.48	1.64	0.34	2.42	1.53
RA	50.28	0.56	15.29	0.09	1.38	10.06	0.8	0.46	2.33	0.76
RB	52.22	0.56	16.08	0.09	1.59	10.45	1.42	0.32	2.27	1.31
HB	57.13	0.79	13.25	0.16	2.71	9.98	4.39	0.21	1.98	2.08

Shale = Average shale values as reported by Turekian and Wedepohl (1961)

A2.07: Total sediment metal concentrations (trace elements, µg/g) across the study sites in Winter 2019. Concentrations of As, Cu, Ni, Pb and Zn are normalised for grain size fraction <63 µm

Site	Sc	V	Cr	Ni	Cu	Zn	As	Rb	Sr	Y	Zr	Nb	Mo	Ba	La	Ce	Pb	Th	U
Shale	NA	130	90	68	45	95	13	140	300	26	160	11	NA	580	92	59	20	NA	NA
BW	11	90	69	34	18	91	31	66	200	21	255	13	<10	299	20	88	41	<10	<10
PR	10	108	90	39	108	194	40	129	111	28	320	18	<10	418	42	73	68	13	<10
CO	13	104	83	36	135	249	68	167	115	28	266	21	<10	394	47	71	72	16	<10
HR	13	107	110	53	206	440	54	202	105	28	240	21	<10	332	49	73	80	23	<10
PC	12	108	87	41	579	596	186	198	118	30	286	23	<10	434	44	73	133	20	<10
SJ	12	114	91	40	544	549	102	186	130	25	182	21	<10	488	38	68	208	21	<10
MC	10	98	90	49	533	562	196	149	84	34	279	21	<10	293	61	72	152	17	<10
HA	10	66	52	52	961	1118	572	217	236	27	145	29	<10	158	49	114	193	48	<10
RC	11	110	72	44	2243	1999	1226	226	122	30	153	26	<10	273	40	73	680	38	<10
RA	<10	97	69	41	2594	2137	1858	227	94	32	177	26	<10	239	54	79	275	37	<10
RB	<10	109	72	40	2936	2553	1696	208	100	31	154	28	<10	233	40	73	260	37	<10
HB	12	98	88	68	1056	1703	629	166	274	22	157	22	<10	271	35	82	230	21	<10

NA = Not available. Shale = Average shale values as reported by Turekian and Wedepohl (1961)

A2.08: Total sediment metal concentrations (major element oxides, weight %) across the study sites in Winter 2019

Site	SiO_2	TiO_2	Al_2O_3	MnO	MgO	Fe_2O_3	CaO	P_2O_5	K_2O	Na_2O
Shale	58.52	0.77	15.12	0.11	2.49	6.75	3.09	0.16	3.2	1.29
BW	62.0	0.57	8.54	0.07	1.50	3.96	7.56	0.16	1.90	1.32
PR	58.7	0.85	14.4	0.07	1.15	5.23	0.59	0.23	2.59	1.72
CO	56.0	0.81	17.3	0.07	1.07	5.29	0.77	0.26	2.80	1.62
HR	54.6	0.82	15.6	0.06	1.77	6.13	0.88	0.30	2.91	1.61
PC	54.7	0.82	18.0	0.05	1.42	6.18	0.94	0.23	2.87	1.60
SJ	49.7	0.73	18.0	0.05	1.57	6.31	1.07	0.26	2.86	2.56
MC	62.1	0.86	13.0	0.07	1.38	5.31	0.76	0.20	2.43	1.42
HA	58.8	0.51	11.3	0.13	1.27	7.59	4.78	0.27	2.33	0.80
RC	50.2	0.57	16.5	0.09	1.59	8.95	1.58	0.32	2.68	1.99
RA	52.9	0.57	15.2	0.09	1.29	10.1	0.70	0.38	2.61	0.73
RB	50.4	0.57	16.0	0.09	1.55	10.4	1.21	0.32	2.30	1.57
HB	52.9	0.66	11.5	0.11	1.72	7.27	5.62	0.27	2.39	1.41

Shale = Average shale values as reported by Turekian and Wedepohl (1961)

A2.09: Total sediment metal concentrations (trace elements, µg/g) across the study sites in Summer 2019. Concentrations of As, Cu, Ni, Pb and Zn are normalised for grain size fraction <63 µm

	Site	Sc	V	Cr	Ni	Cu	Zn	As	Rb	Sr	Y	Zr	Nb	Mo	Ba	La	Ce	Pb	Th	U
	Shale	NA	130	90	68	45	95	13	140	300	26	160	11	NA	580	92	59	20	NA	NA
Oxic	BW	14	117	86	36	21	104	27	80	202	22	225	16	<10	311	32	95	53	12	<10
	PR	11	114	93	44	150	254	51	143	115	28	279	18	<10	411	42	78	91	15	<10
	CO	11	103	80	41	202	336	101	178	125	28	237	21	<10	373	45	76	103	18	<10
	HR	12	105	112	53	179	422	52	187	137	25	213	19	<10	292	41	72	81	20	<10
	PC	10	96	78	38	610	622	181	222	115	30	301	28	<10	393	39	72	129	21	<10
	SJ	<10	92	79	38	435	566	76	147	116	23	185	19	<10	709	31	67	311	19	<10
	MC	11	104	87	48	777	718	239	164	98	30	215	21	<10	283	62	68	169	20	<10
	HA	<10	63	48	55	932	1121	577	206	278	26	134	29	<10	144	46	120	204	48	<10
	RC	10	103	74	38	1897	1736	954	198	105	30	185	26	<10	253	48	73	229	29	<10
	RA	10	91	77	52	3260	2570	2229	193	109	30	157	26	<10	249	37	83	282	36	<10
	RB	<10	105	67	39	3158	2708	1676	206	91	32	162	30	<10	226	48	76	255	37	<10
	HB	10	102	80	205	3565	5924	2069	149	255	21	155	23	<10	270	41	83	684	26	<10
Anoxic	BW	12	115	91	38	37	150	33	75	192	22	230	15	<10	316	27	99	81	12	<10
	PR	12	119	92	45	166	277	44	142	106	27	268	19	<10	420	50	75	98	16	<10
	CO	14	110	85	46	150	294	67	170	107	28	230	20	<10	430	50	72	97	17	<10
	HR	<10	92	99	102	319	810	79	197	85	22	182	19	<10	262	33	63	194	20	<10
	PC	10	108	81	63	1037	1205	276	199	114	28	215	23	<10	396	48	74	287	22	<10
	SJ	<10	109	81	50	665	827	112	163	97	22	152	18	<10	453	34	68	335	20	<10
	MC	<10	100	81	82	1243	1315	344	154	76	28	166	19	<10	307	51	63	283	19	<10
	HA	<10	63	47	57	1001	1295	490	208	260	24	129	29	<10	142	47	113	243	48	<10
	RC	<10	110	73	45	3013	3019	1134	219	87	30	163	28	<10	253	44	74	340	37	<10
	RA	<10	96	69	51	3166	2810	1698	223	92	32	168	26	<10	226	52	74	325	38	<10
	RB	<10	119	72	50	3717	3739	1549	209	95	32	146	29	<10	252	45	76	354	40	<10
	HB	13	100	87	95	1393	2473	631	154	316	22	155	22	<10	261	32	89	310	24	<10

NA = Not available. Shale = Average shale values as reported by Turekian and Wedepohl (1961)

A2.10: Total sediment metal concentrations (major element oxides, weight %) across the study sites in Summer 2019

	Site	SiO_2	TiO_2	Al_2O_3	MnO	MgO	Fe_2O_3	CaO	P_2O_5	K_2O	Na_2O
	Shale	58.52	0.77	15.12	0.11	2.49	6.75	3.09	0.16	3.2	1.29
Oxic	BW	54.1	0.66	10.7	0.08	1.98	4.89	7.85	0.20	2.20	1.53
	PR	55.4	0.84	15.2	0.04	1.36	5.81	0.61	0.28	2.77	1.99
	CO	50.7	0.74	17.2	0.04	1.18	5.03	1.12	0.32	2.73	1.80
	HR	54.1	0.75	14.5	0.06	1.89	5.78	2.19	0.26	2.77	2.01
	PC	55.1	0.79	17.4	0.05	1.40	5.78	1.09	0.22	2.81	1.42
	SJ	55.0	0.66	16.7	0.04	1.38	6.04	0.40	0.17	2.60	1.85
	MC	51.0	0.73	14.1	0.06	1.78	5.80	0.94	0.29	2.49	3.16
	HA	56.9	0.46	10.6	0.11	1.31	7.49	5.98	0.28	2.22	1.16
	RC	51.7	0.62	15.2	0.07	1.60	8.51	1.44	0.29	2.41	1.92
	RA	47.9	0.6	14.3	0.10	1.47	9.85	3.48	2.37	2.27	1.47
	RB	53.0	0.56	15.3	0.09	1.51	10.4	1.26	0.29	2.23	1.48
	HB	49.1	0.64	10.9	0.12	1.75	7.78	5.22	0.28	2.24	1.86
Anoxic	BW	55.9	0.64	10.0	0.06	1.68	4.71	8.06	0.15	2.07	1.31
	PR	53.8	0.85	15.7	0.04	1.34	5.31	0.48	0.17	2.82	2.21
	CO	53.3	0.83	17.8	0.04	1.14	5.30	0.35	0.27	2.94	1.88
	HR	62.6	0.65	13.6	0.09	1.70	5.21	0.79	0.18	2.84	1.56
	PC	50.5	0.71	17.6	0.05	1.40	6.11	0.86	0.20	2.75	1.75
	SJ	58.1	0.71	14.8	0.04	1.27	5.53	1.39	0.15	2.41	1.63
	MC	60.9	0.64	14.2	0.07	1.49	5.92	0.56	0.14	2.50	1.62
	HA	59.8	0.44	10.5	0.11	1.22	7.44	5.65	0.25	2.18	0.87
	RC	52.3	0.58	16.5	0.08	1.51	9.05	0.88	0.24	2.44	1.60
	RA	51.4	0.55	14.8	0.08	1.38	9.34	0.71	0.37	2.62	1.63
	RB	49.1	0.57	16.6	0.08	1.61	10.4	1.07	0.31	2.40	1.84
	HB	52.8	0.65	11.3	0.10	1.77	7.21	6.79	0.31	2.30	1.37

Shale = Average shale values as reported by Turekian and Wedepohl (1961)

A2.11: Maximum concentration, limit of detection, accuracy and precision of minor elements determined in XRF pellets. All concentrations expressed in µg/g, except otherwise stated

		Sc	**V**	**Cr**	**Ni**	**Cu**	**Zn**	**As**	**Rb**	**Sr**	**Y**	**Zr**	**Nb**	**Mo**	**Ba**	**La**	**Ce**	**Pb**	**Th**	**U**
Max		100	500	3000	2500	1000	3000	350	3500	1500	150	1000	1000	150	2500	350	2500	2500	1000	600
LOD		1.5	1.6	2.8	1.6	2.1	1.6	2.3	0.8	0.8	0.9	1.4	0.9	0.7	4.9	4.5	4.6	1.4	1.2	1.1
GXR-1	Cert	1.58	80	12	41	1110	760	427	14	275	32	38	0.8	18	750	7.5	17	730	2.44	34.9
(N = 4)	Mean	NA	107	NA	32	1216	814	520	NA	286	26	NA	NA	19	846	23	31	815	1072	32
	%RSD	NA	2.1	NA	1.8	0.7	0.5	0.3	NA	1.4	1.8	NA	NA	4.1	0.9	37.1	16.3	0.5	0.9	1.7
	% Acc	NA	133.9	NA	78.8	109.5	107.2	121.7	NA	104.0	82.1	NA	NA	105.7	112.8	311.8	181.1	111.6	43934.0	90.4
GXR-4	Cert	7.7	87	64	42	6520	73	98	160	221	14	186	10	310	1640	64.5	102	52	22.5	6.2
(N = 4)	Mean	NA	85	60	24	6349	63	105	142	216	14	206	13	272	1662	63	94	65	39	5
	%RSD	NA	1.2	1.7	0.2	0.4	5.4	3.1	0.9	0.5	4.2	0.5	0.2	0.4	0.5	4.2	7.0	2.0	3.2	0.3
	% Acc	NA	98.1	93.1	57.2	97.4	86.4	107.0	88.5	97.6	96.5	110.7	130.1	87.9	101.4	97.4	92.2	124.1	174.6	80.8
MESS-2	Cert	NA	252	106	49.3	39.3	172	20.7	NA	125	NA	NA	NA	2.85	NA	NA	NA	21.9	NA	NA
(N = 2)	Mean	16	250	99	47	44	145	22	143	132	26	142	17	5	1037	45	81	25	14	4
	%RSD	4.6	0.0	0.7	1.5	0.0	1.0	6.4	0.0	0.5	2.8	0.5	0.0	15.7	1.4	3.1	7.0	11.3	10.1	20.2
	% Acc	NA	99.2	92.9	94.3	112.0	84.3	106.3	NA	105.2	NA	NA	NA	157.9	NA	NA	NA	114.2	NA	NA

A2.11 continued:

		Sc	V	Cr	Ni	Cu	Zn	As	Rb	Sr	Y	Zr	Nb	Mo	Ba	La	Ce	Pb	Th	U
NIST 2702 (N = 1)	Cert	25.9	357.6	352	75.4	117.7	485.3	45.3	128	120	NA	NA	63	10.8	397	73.5	123	132.8	20.51	10.4
	% Acc	83.0	109.9	95.1	88.2	94.8	90.5	101.6	93.7	92.3	NA	NA	103.9	113.7	94.0	125.3	87.1	99.4	109.8	68.9
PACS-1 (N = 4)	Cert	NA	127	113	44.1	452	824	211	NA	277	NA	NA	NA	12.3	NA	NA	NA	404	NA	NA
	Mean	14	135	103	41	416	763	187	44	255	17	128	12	14	663	15	45	372	14	1
	%RSD	9.8	1.0	0.8	3.5	2.7	4.8	5.9	2.4	2.0	4.0	2.1	6.8	3.8	1.5	27.2	8.8	4.5	7.8	NA
	% Acc	NA	106.6	91.5	92.8	92.0	92.6	88.9	NA	92.1	NA	NA	NA	110.2	NA	NA	NA	92.1	NA	NA
SDO-1	Cert	13.2	160	66.4	99.5	60.2	64.1	68.5	126	75.1	40.6	165	NA	134	397	38.5	79.3	27.9	10.5	48.8
	Mean	13	172	58	88	61	56	62	131	72	39	163	15	129	398	47	74	35	13	44
	%RSD	7.1	0.5	0.9	1.3	1.6	1.8	3.5	0.6	0.0	1.2	0.5	3.8	0.0	1.3	7.2	1.8	8.3	12.5	1.3
	% Acc	95.5	107.6	88.0	88.8	101.3	87.4	90.8	103.8	95.9	95.6	98.9	NA	96.3	100.2	121.6	93.6	125.4	127.6	89.3
STSD-2 (N = 5)	Cert	16	101	116	53	47	246	42	104	400	37	185	20	13	540	59	93	66	17	19
	Mean	16	105	109	58	47	240	41	101	419	37	186	21	13	534	60	97	74	21	17
	%RSD	7.3	2.1	0.4	1.4	2.4	0.6	2.2	0.4	0.4	1.5	0.5	0.0	3.4	1.0	5.0	4.2	3.7	3.9	2.7
	% Acc	97.5	104.0	94.1	109.8	100.0	97.4	96.7	96.9	104.8	100.0	100.0	105.0	101.5	98.9	102.4	104.5	111.5	124.7	88.4

Max = Maximum concentration of calibration range; LOD = Limit of Detection; Cert = Certified concentration; Mean = Mean of measured concentration; N = Number of replicates; RSD = Precision (Relative Standard Deviation); Acc = Accuracy (percentage recovery)
NA = Not Available
Note that recommended values (Gladney & Roelandts, 1990) are used in lieu of certified concentrations for GXR-1 and GXR-4 reference materials

A2.12: Maximum concentration, limit of detection, accuracy and precision of minor elements determined in XRF fused beads. All concentrations expressed in percentage, except otherwise stated

		SiO_2	TiO_2	Al_2O_3	MnO	MgO	Fe_2O_3	CaO	P_2O_5	K_2O	Na_2O
Max		NA	2.6	NA	0.5	NA	20	NA	NA	NA	NA
LOD		NA	0	NA	0	NA	0	NA	NA	NA	NA
PACS-1	Cert	55.7	0.703	12.23	NA	2.41	6.96	2.92	0.233	1.5	4.4
(N = 2)	Mean	55.57	0.73	12.16	0.06	2.31	7.01	2.79	0.23	1.46	4.31
	% RSD	2.9	1.2	1.3	1.2	1.2	0.9	1.2	1.2	0.2	1.0
	% Acc	99.8	103.3	99.4	NA	95.8	100.8	95.7	99.5	97.5	98.0
GXR-1	Cert	48.57	0.06	6.64	0.11	0.36	32.9	1.34	0.15	0.06	0.07
(N = 2)	Mean	48.35	0.05	6.23	0.13	0.34	37.41	1.25	0.15	0.05	NA
	% RSD	2.2	0.3	0.2	5.3	2.4	2.2	0.3	0.3	0.3	NA
	% Acc	99.6	83.5	93.8	113.9	93.3	113.7	93.5	100.2	83.5	NA
GXR-4	Cert	66.19	0.48	13.6	0.02	2.75	4.42	1.41	0.27	4.83	0.76
(N = 2)	Mean	64.00	0.47	13.91	0.02	2.82	4.40	1.28	0.29	4.83	NA
	% RSD	4.7	3.3	3.4	0.3	2.8	0.6	1.4	5.1	0.7	NA
	% Acc	96.7	98.1	102.2	100.2	102.4	99.6	90.9	107.6	100.1	NA
SDO-1	Cert	49.28	0.71	12.27	0.04	1.54	9.34	1.05	0.11	3.35	0.38
(N = 2)	Mean	48.86	0.70	12.16	0.04	1.48	9.53	1.02	0.12	3.34	0.43
	% RSD	0.8	0.8	1.3	0.0	2.2	1.4	1.1	4.9	0.6	8.2
	% Acc	99.1	99.1	99.1	100.0	96.3	102.1	96.8	106.1	99.6	112.3

Max = Maximum concentration of calibration range; LOD = Limit of Detection; Cert = Certified concentration; Mean = Mean of measured concentration; N = Number of replicates; RSD = Precision (Relative Standard Deviation); Acc = Accuracy (percentage recovery)
NA = Not Available
Note that recommended values (Gladney & Roelandts, 1990) are used in lieu of certified concentrations for GXR-1 and GXR-4 reference materials

A2.13: Acid-extractable metal (AEM) concentrations across the study sites in Autumn 2017. Concentrations of metals binding to AVS are expressed as SEM (µmol/g) and for others as AEM. Errors represent the standard deviation (n = 3**)**

Site	Cd	Cu	Ni	Pb	Zn	As	Fe	Mn
	Concentration in µmol/g					Concentration in µg/g		
BW	ND	0.14 ± 0.002	0.06 ± 0	0.15 ± 0	0.59 ± 0.02	ND	6094.1 ± 420.5	334.6 ± 8.3
PR	ND	1.01 ± 0.08	0.08 ± 0.01	0.2 ± 0.01	1.56 ± 0.17	ND	12415.3 ± 1867.6	676.9 ± 49
CO	0.001 ± 0.001	1.24 ± 0.02	0.06 ± 0	0.23 ± 0	2.50 ± 0.20	ND	5670.8 ± 586.5	116.9 ± 8.4
HR	0.004 ± 0.001	1.60 ± 0.10	0.08 ± 0.01	0.23 ± 0.01	3.05 ± 0.22	ND	6111.1 ± 693.6	47.7 ± 8.9
PC	0.004 ± 0.001	3.81 ± 0.21	0.06 ± 0.01	0.41 ± 0.03	5.44 ± 0.36	37.9 ± 1.7	8501.9 ± 424.7	41.2 ± 2.2
SJ	0.003 ± 0.001	3.98 ± 0.36	0.06 ± 0	0.92 ± 0.03	6.13 ± 0.19	24.7 ± 2	6971.7 ± 82.5	29.5 ± 0.2
MC	0.008 ± 0.001	5.32 ± 0.14	0.14 ± 0.01	0.57 ± 0.1	6.94 ± 0.18	77.4 ± 10.7	11831.2 ± 333.7	217.8 ± 6.4
HA	0.003 ± 0.001	5.18 ± 0.05	0.12 ± 0.01	0.26 ± 0	8.13 ± 0.04	117.1 ± 7.1	5518.3 ± 93.9	170.8 ± 6.5
RC	0.021 ± 0.002	22.70 ± 0.72	0.14 ± 0.01	2.35 ± 0.31	23.37 ± 0.46	630.2 ± 3.1	20030.3 ± 448.4	122.8 ± 1.6
RA	0.033 ± 0.002	27.72 ± 2.67	0.15 ± 0.01	0.87 ± 0.07	21.73 ± 1.96	1026.4 ± 162.4	22247.7 ± 3142.6	253.9 ± 24.3
RB	0.026 ± 0.007	26.98 ± 1.28	0.15 ± 0.01	0.89 ± 0.04	25.87 ± 0.85	748.3 ± 57.7	18562.9 ± 1247	95.4 ± 6.8
HB	0.009 ± 0.001	4.69 ± 0.22	0.15 ± 0.01	0.42 ± 0.08	11.76 ± 1.15	159.6 ± 13.5	7206.2 ± 530.8	134.7 ± 10.4

ND = Not detectable

A2.14: Acid-extractable metal (AEM) concentrations across the study sites in Winter 2019. Concentrations of metals binding to AVS are expressed as SEM (µmol/g) and for others as AEM. Errors represent the standard deviation (n = 3)

Site	Cu	Ni	Pb	Zn	Fe	Mn
	Concentration in µmol/g				Concentration in µg/g	
BW	0.07 ± 0.01	0.07 ± 0.064	0.1 ± 0.005	0.31 ± 0.03	3998.4 ± 414.6	328.9 ± 19.3
PR	0.61 ± 0.12	0.05 ± 0.031	0.15 ± 0.027	0.86 ± 0.21	4344.4 ± 798.7	163.3 ± 17.8
CO	1.01 ± 0.17	0.04 ± 0.002	0.2 ± 0.007	1.76 ± 0.5	5144.3 ± 289.7	333.8 ± 59.6
HR	1.49 ± 0.06	0.05 ± 0.003	0.21 ± 0.003	2.22 ± 0.11	5305.5 ± 139.2	78.6 ± 3
PC	2.86 ± 0.24	0.03 ± 0.002	0.39 ± 0.022	4.01 ± 0.2	5691.7 ± 265.7	56.6 ± 5.1
SJ	2.22 ± 0.24	0.03 ± 0.004	0.61 ± 0.039	3.63 ± 0.43	4875.3 ± 345.2	27.7 ± 1.3
MC	2.28 ± 0.12	0.06 ± 0.003	0.32 ± 0.019	3.24 ± 0.17	5415.7 ± 196	78.1 ± 2.4
HA	5.82 ± 0.2	0.12 ± 0.007	0.23 ± 0.005	7.08 ± 0.18	4761.6 ± 191.2	195.8 ± 4
RC	14.6 ± 0.67	0.24 ± 0.241	1.63 ± 0.101	15.27 ± 0.58	13369.3 ± 109.8	148 ± 11.9
RA	14.48 ± 0.59	0.09 ± 0.008	0.48 ± 0.014	12.99 ± 0.44	11220.9 ± 83.1	107.9 ± 17.4
RB	19.03 ± 0.58	0.09 ± 0.006	0.62 ± 0.016	17.61 ± 0.46	11495.7 ± 390.6	86.8 ± 3.4
HB	5.2 ± 0.22	0.14 ± 0.029	0.41 ± 0.011	10.52 ± 0.54	6821.7 ± 296.6	196.4 ± 4.7

A2.15: Acid-extractable metal (AEM) concentrations across the study sites in Summer 2019. Concentrations of metals binding to AVS are expressed as SEM (µmol/g) and for others as AEM. Errors represent the standard deviation (n = 3)

Site		Cu	Zn	Fe	Mn
		Concentration in µmol/g		Concentration in µg/g	
BW	Oxic	0.37 ± 0.06	0.7 ± 0.12	6734.5 ± 497.2	303 ± 31.8
PR		1.56 ± 0.05	2.47 ± 0.19	23469.3 ± 629.7	193.6 ± 9.3
CO		0.67 ± 0.24	1.09 ± 0.22	4514.4 ± 781	51.8 ± 7
HR		0.89 ± 0.1	1.54 ± 0.11	4303.7 ± 548.1	32.6 ± 2.4
PC		1.5 ± 0.13	3.5 ± 0.7	4999.7 ± 97.6	23.1 ± 1.2
SJ		2.14 ± 0.43	2.92 ± 0.43	4106.7 ± 341.8	15.6 ± 1.3
MC		0.97 ± 0.02	3.44 ± 0.12	6561.7 ± 250.4	24 ± 0.7
HA		3.34 ± 0.26	5.78 ± 0.1	3380.4 ± 119.9	91.2 ± 9.3
RC		7.86 ± 0.92	13.83 ± 1.62	9415.7 ± 1157.3	30.7 ± 2.9
RA		13.61 ± 1.19	15.5 ± 1.11	11620.9 ± 869.1	147.9 ± 8.2
RB		19.71 ± 1.34	22.36 ± 2.56	10417.7 ± 1035.1	68.1 ± 4
HB		4.57 ± 0.23	12.84 ± 1.18	6683.1 ± 672.1	193.5 ± 4.8
BW	Anoxic	0.1 ± 0.02	0.51 ± 0.43	5289.1 ± 156.6	194 ± 5.6
PR		0.21 ± 0.04	0.63 ± 0.26	3282.2 ± 930.4	15.9 ± 4.3
CO		0.15 ± 0.02	1.11 ± 0.27	5777.1 ± 1056.2	35 ± 6.6
HR		0.68 ± 0.24	1.62 ± 1	2026.5 ± 1126.9	13.5 ± 8.3
PC		0.34 ± 0.08	3 ± 0.12	5727.3 ± 331.8	14.3 ± 0.9
SJ		0.21 ± 0.01	3 ± 0.65	3931.4 ± 759.9	11.3 ± 2.3
MC		0.11 ± 0.08	5.12 ± 1.01	4853.7 ± 372.6	25.7 ± 2.1
HA		2.12 ± 0.14	5.91 ± 0.04	3518.3 ± 66.2	47.8 ± 1.3
RC		0.17 ± 0.04	14.85 ± 3.15	13833.9 ± 3393.5	23.9 ± 5.3
RA		3.58 ± 0.65	14.51 ± 1.34	13521.3 ± 935.8	56.7 ± 4.3
RB		6.22 ± 1.37	17.75 ± 2.44	10013.8 ± 1722.9	28.2 ± 3.6
HB		1.79 ± 0.25	10.34 ± 0.69	5437 ± 407.1	84.7 ± 7.3

A2.16: Limit of detection, accuracy and precision for the determination of acid-extractable metal concentrations across the surveys. All concentrations are in µg/L

Sample		**As**	**Cd**	**Cu**	**Fe**	**Mn**	**Ni**	**Pb**	**Zn**	**Survey**
LOD		16.4	0.5	0.1	0.3	0.1	0.9	2.5	0.1	
TM 27.3 (N = 3)	Cert	2.15	1.05	6.16	10.9	2.44	2.27	2.32	16.2	Autumn 2017
	% Acc	NA	113.5	97.1	NA	NA	164.8	96.7	109.3	
	%RSD	NA	4.8	1.1	NA	NA	4.0	13.6	3.8	
TMDA 64.2 (N = 3)	Cert	162.0	266.0	275.0	306.0	263.0	295.0	289.0	310.0	
	% Acc	101.5	NA	103.1	100.3	103.2	NA	103.3	103.3	
	%RSD	3.5	NA	0.9	1.5	0.6	NA	0.5	0.2	
TM 27.3 (N = 6)	% Acc	NA	100.1	133.1	NA	NA	152.1	90.4	134.6	Winter 2019
	%RSD	NA	5.2	4.5	3.7	2.4	27.0	4.8	2.7	
TMDA 64.2 (N = 2)	% Acc	NA	95.7	100.1	107.2	105.6	98.0	88.7	93.9	
	%RSD	NA	0.0	0.6	8.5	3.8	0.0	4.9	3.3	
CLMS2A (N = 6)	%RSD	NA	1.0	1.0	1.0	5.0	1.0	1.0	1.0	
TM 27.3 (N = 1)	% Acc	NA	NA	83.9	NA	NA	NA	NA	87.9	Summer 2019
TMDA 64.2 (N = 1)	% Acc	NA	NA	110.3	114.2	114.1	NA	NA	114.8	
CLMS2A (N = 3)	% RSD	NA	NA	0.8	2.3	1.3	NA	NA	1.4	

LOD = Limit of Detection (derived from 2017 ICP-OES analysis, but typical across the surveys); Cert = Certified concentration; N = Number of replicates; RSD = Precision (Relative Standard Deviation); Acc = Accuracy (percentage recovery); NA = Not Available

A2.17: Concentration of Acid Volatile Sulphide (AVS) across the study sites. All concentrations in µmol/g

Site	A-2017	W-2019	S-2019-Ox	S-2019-Anox
BW	< 0.5	< 0.5	2.7 ± 0.4	48.9 ± 8.9
PR	< 0.5	< 0.5	1.5 ± 0.6	23.6 ± 3.7
CO	1.5 ± 0.2	< 0.5	17.2 ± 3.6	44 ± 6.6
HR	1.7 ± 0.5	0.6 ± 0.1	5.3 ± 0.5	13.4 ± 0.4
PC	1.2 ± 0.8	2.8 ± 0.7	21.3 ± 1.7	61.5 ± 6.7
SJ	4.3 ± 2.7	1.4 ± 0.4	23.8 ± 1	30 ± 4.9
MC	4.2 ± 1.3	2.6 ± 0.4	19.6 ± 0.5	23.6 ± 6.3
HA	< 0.5	< 0.5	< 0.5	6.4 ± 0.7
RC	0.5 ± 0.2	< 0.5	3.6 ± 1.6	56.5 ± 6.5
RA	< 0.5	< 0.5	0.9 ± 0.4	26.4 ± 2.3
RB	< 0.5	< 0.5	< 0.5	26.1 ± 11
HB	< 0.5	1.1 ± 0.3	4.5 ± 1.1	10 ± 1.4

Method limit of quantification = 0.5 µmol/g; A-2017 = Autumn 2017; W-2019 = Winter 2019; S-2019-Ox and -Anox = Summer 2019 Oxic and Anoxic sediment

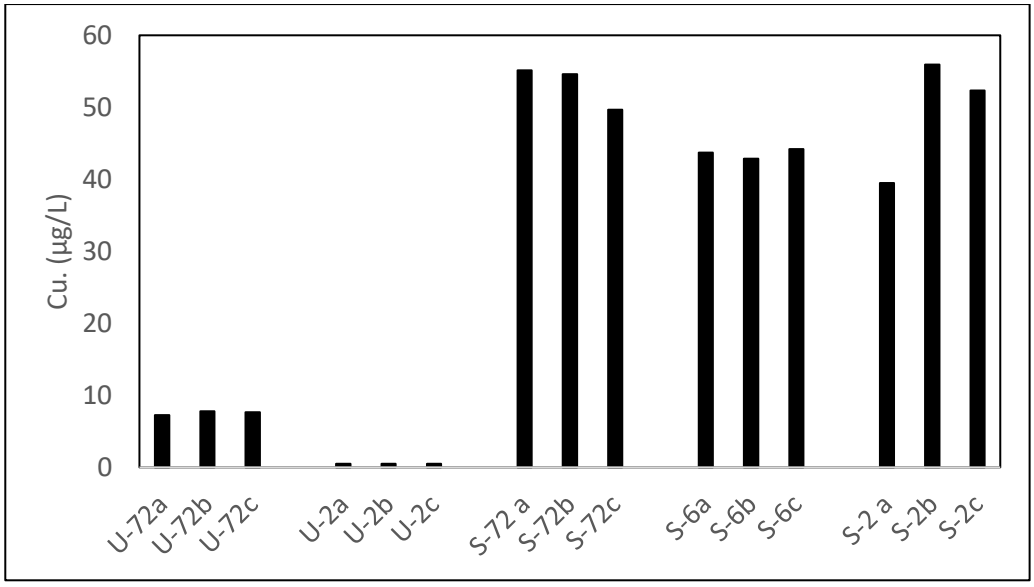

A2.18: Recovery of Cu from unspiked (prefix "U") and 50 µg/L spiked (prefix "S") seawater samples equilibrated with Chelex resins for 2 ("2"), 6 ("6"), and 72 ("72") hours. Resins from the 2-hour samples were extracted for 72 hours with 2 M Nitric Acid, in comparison with 12 hours for the other samples. Letters "a", "b", and "c" represent replicates of the same sample

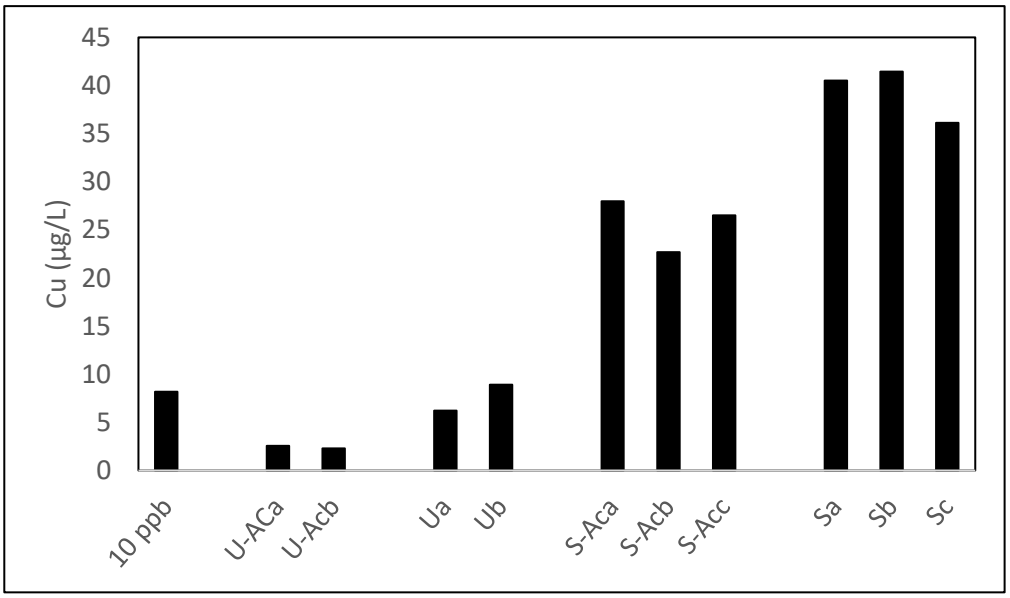

A2.19: Recovery of Cu from unspiked (prefix "U") and 50 µg/L spiked (prefix "S") seawater samples, with ("Ac") and without ammonium acetate pre-extraction. Letters "a", "b", and "c" represent replicates of the same sample. "10 ppb" represents recovery from a 10 µg/kg CLMS2A standard

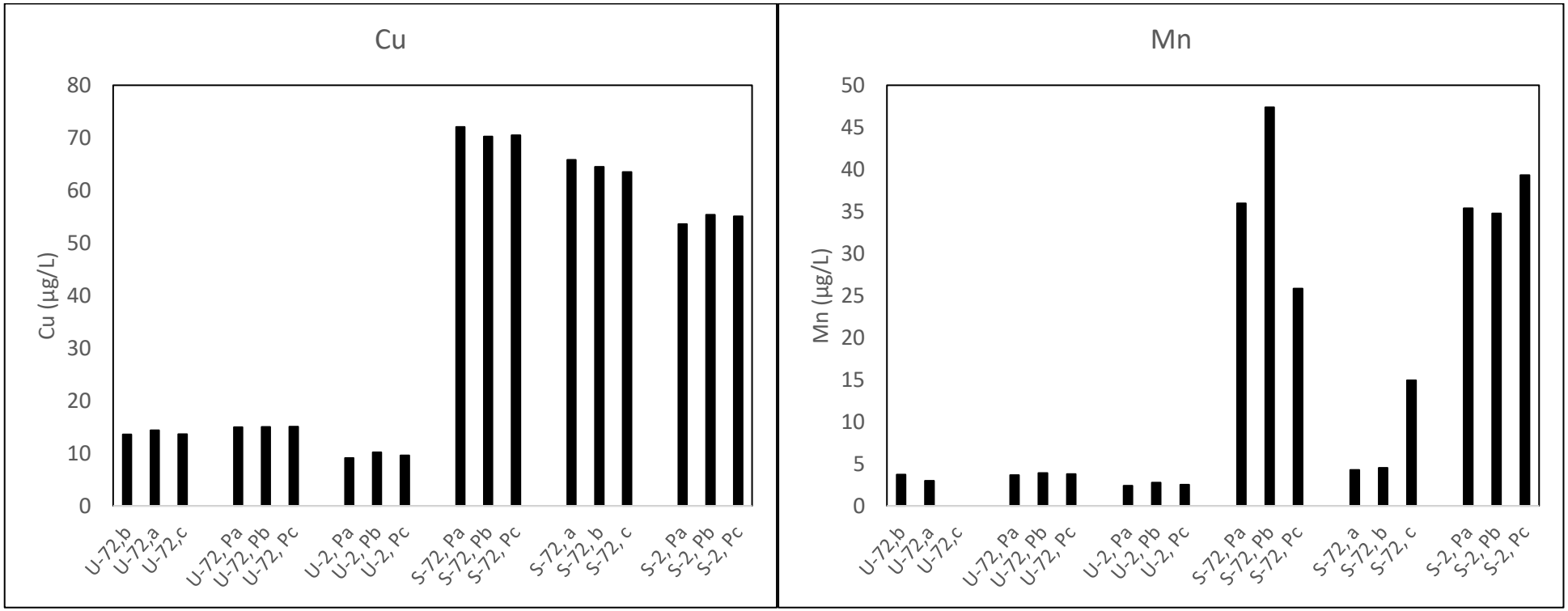

A2.20: Recovery of Cu and Mn from unspiked (prefix "U") and 50 µg/L spiked (prefix "S") seawater samples equilibrated for 2 ("2") and 72 ("72") hours with ("P") or without Hydrogen Peroxide and high temperature digestion. Resins from all samples were extracted for 12 hours. Letters "a", "b", and "c" represent replicates of the same sample

A2.21: Limit of detection, accuracy, and precision for the determination of porewater metal concentrations in Autumn 2017 and Winter 2019 using chelated calibration standards. All concentrations in µg/L

Sample		**Cu**	**Zn**	**Fe**
LOD		0.5	0.7	1.4
Geotraces GS (N = 2)	Conc	27.1	48.9	55.2
	% Rec	103.7	97.7	97.7
	% RSD	1.2	1.3	5.8
BW RM (N = 3)	% RSD	1.4	3.9	5.3
CLMS2A (N = 3)	% RSD	3.3	1.9	1.5

LOD = Limit of Detection; Conc = Spike concentration; N = Number of replicates; RSD = Precision (Relative Standard Deviation); Rec = Percentage spike recovery
Geotraces GS = saline Geotraces spike; BW RM = Spiked seawater from Breydon Water

A2.22: Limit of detection, accuracy, and precision for the determination of porewater metal concentrations across the surveys using non-saline calibration standards. All concentrations in µg/L. Note the poor recovery of Mn from seawater

Sample		**Cu**	**Zn**	**Fe**	**Mn**
LOD		0.3	0.7	2.9	0.1
TM 27.3 (N = 4)	Cert	6.16	16.2	10.9	2.44
	% Acc	90.2	111.3	80.5	84.6
	% RSD	3.5	2.1	8.9	1.6
TMDA 64.2 (N = 4)	Cert	275	310	306	263
	% Acc	95.5	104.4	93.5	105.6
	% RSD	1.0	0.5	0.7	0.8
North Sea (N = 7) seawater	Conc	100	100	100	100
	% Rec	79.4	79.5	83.3	2.5
	% RSD	3.8	9.3	3.7	10.2

LOD = Limit of Detection; Conc = Spike concentration; N = Number of replicates; RSD = Precision (Relative Standard Deviation); Rec = Percentage spike recovery; Cert = Certified concentration; Acc = Accuracy (percentage recovery)
North Sea = Spiked seawater collected from the North Sea

A2.23: Porewater metal concentrations in Autumn 2017. All concentrations in µg/L. Errors represent standard deviation (n = 2). Note that Mn concentrations represent around 2% of actual values (See A2.22)

Site	Method	Cu	Zn	Fe	Mn
UK WFD		25.1	7.9	1000	-
BW	Non-saline calibration standard	1.8	20.0	32.5	405.7
PR		3.2	72.0	106.3	501.8
CO		1.9 ± 0.2	111.8 ± 4.4	56.3 ± 3.1	206 ± 2.9
HR		3.5 ± 0.2	62.1 ± 1.5	98.3 ± 9.1	4.6 ± 0.2
PC		2.6	134.3	249.5	15.1
SJ		1.6 ± 0	81.4 ± 2.7	908.8 ± 36.8	14.8 ± 0.2
MC		3.4	57.2	1407.6	207.0
HA		223.9 ± 13.1	270 ± 19.8	68.9 ± 38.2	319 ± 21.2
RC		23.6	98.9	142.3	44.9
RA		130.3 ± 5.5	211.2 ± 10.4	64.9 ± 1.1	81.4 ± 12.6
RB		62 ± 1.3	191.4 ± 5.1	123.3 ± 58.3	36.6 ± 4.8
HB		31.5 ± 1	913.6 ± 80.4	40.3 ± 5.3	84.4 ± 7
BW	Saline calibration standard	4.2	26.2	93.8	NA
PR		3.2	50.0	188.8	NA
CO		0.8	96.8	64.4	NA
HR		1.9	52.2	94.7	NA
PC		1.0	40.0	375.6	NA
SJ		0.9	84.6	1148.3	NA
MC		2.7	33.3	1364.7	NA
HA		230.8	252.6	76.4	NA
RC		31.3	94.6	150.0	NA
RA		227.4	232.3	213.8	NA
RB		97.8	253.9	962.2	NA
HB		34.2	687.2	12.6	NA

Sites without standard deviations analysed as composite, due to insufficient samples.
NA = Not analysed. Calibration of Mn was not practical using saline standards
Samples with non-saline calibration = fraction < 0.2 µm
Samples with saline calibration = fraction <0.45 µm
UK WFD = Water Framework Directive (2015) standards for England and Wales. Cu limit derived using average DOC (<0.45 µm) across the sites in 2017 and 2019 (17.0 mg/L)

A2.24: Porewater metal concentrations in Winter 2019. All concentrations in µg/L. Errors represent standard deviation (n = 2). Note that Mn concentrations represent around 2% of actual values (See A2.22)

Site	Method	Cu	Zn	Fe	Mn
UK WFD		25.1	7.9	1000	-
BW	Non-saline calibration standard	2.2 ± 0.1	5.8 ± 1.9	10.9 ± 1.4	124.9 ± 17.1
PR		7.6 ± 3.4	15.8 ± 7.5	52.6 ± 21.4	245.7 ± 108.5
CO		11 ± 3.9	14.9 ± 5.6	116.5 ± 57.5	603.4 ± 39
HR		8.2 ± 0.5	44.3 ± 3.8	18.4 ± 5.5	47.7 ± 10
PC		17.7 ± 2.7	24.6 ± 5	46.7 ± 12.2	86.9 ± 10.3
SJ		3 ± 0.4	4.8 ± 0.8	30.2 ± 6.6	43.9 ± 9.4
MC		19.8 ± 9.8	36.7 ± 9.1	315.4 ± 75	159.9 ± 24.4
HA		112.7 ± 22.3	219.1 ± 45.9	71.4 ± 19.5	281.6 ± 78.2
RC		60.5 ± 7.4	88.3 ± 10.2	54.6 ± 4.3	138 ± 18.5
RA		18.3 ± 1.5	17.6 ± 3.8	5932.6 ± 471	43.8 ± 8.2
RB		128.6 ± 6.5	213.7 ± 15.8	28 ± 3.4	65.4 ± 8.2
HB		50.5 ± 15.6	88.5 ± 27.3	39.5 ± 15.3	96.2 ± 11.5
BW	Saline calibration standard	2.6	4.1	51.6	NA
PR		12.9	24.1	71.5	NA
CO		10.3	11.1	87.1	NA
HR		10.6	47.8	13.5	NA
PC		10.1	10.1	18.6	NA
SJ		3.8	6.0	26.1	NA
MC		20.3	39.9	368.5	NA
HA		182.4	313.5	87.9	NA
RC		82.8	132.7	60.0	NA
RA		170.1	216.9	319.3	NA
RB		189.9	297.4	32.8	NA
HB		72.6	118.4	58.4	NA

Sites without standard deviations analysed as composite, due to insufficient samples.
NA = Not analysed. Calibration of Mn was not practical using saline standards
All samples are sieved to <0.45 µm
Note the difference in concentrations for Site RA
UK WFD = Water Framework Directive (2015) standards for England and Wales. Cu limit derived using average DOC (<0.45 µm) across the sites in 2017 and 2019 (17.0 mg/L)

A2.25: Porewater metal concentrations in Summer 2019 measured using non-saline calibration standards. All concentrations in µg/L. Errors represent standard deviation (n = 2* or 3**). Note that Mn concentrations represent around 2% of actual values (See A2.22)

Site		Cu	Zn	Fe	Mn
UK WFD		25.1	7.9	1000	-
BW	Oxic	1.4	5.2	25.9	256.4
PR		1.6	16.8	3878.4	728.1
CO		3.5	9.5	1749.4	508.8
HR		3.6	14.9	125.6	248.1
PC		7.4	59.0	22352.5	571.8
SJ		7.6	8.0	12744.3	134.3
MC		2.9	8.6	7893.4	170.7
HA		12.5	34.6	3660.0	1489.8
RC		3.6	33.0	20022.1	468.0
RA		34.8	37.0	8152.9	1111.8
RB		17.5	138.3	714.9	469.8
HB		15.8	61.8	165.9	5079.2
PR*	Anoxic	2.4 ± 1.4	6.2 ± 0.9	64.7 ± 1.8	19.3 ± 1.9
CO		16.3	3.0	226.5	48.0
HR		2.9	13.7	502.9	14.3
PC		4.9	8.1	119.6	4.9
SJ*		3.5 ± 0.8	30.1 ± 5.1	44.9 ± 0.6	3.7 ± 0.3
RC**		2.5 ± 0.4	23.5 ± 2.6	337.4 ± 37.5	3.8 ± 0.4
RA**		5.3 ± 0.4	46 ± 1.8	314.3 ± 1.9	31.2 ± 1.5
RB		2.8	21.5	98.9	4.3
HB**		3.1 ± 0.2	14.5 ± 0.8	329 ± 24	22.9 ± 1.7

Insufficient anoxic sample for BW, MC, and HA analysis. Sites without standard deviations analysed as composite, due to insufficient samples.

All samples are sieved to <0.45 µm

UK WFD = Water Framework Directive (2015) standards for England and Wales. Cu limit derived using average DOC (<0.45 µm) across the sites in 2017 and 2019 (17.0 mg/L)

Appendices to Chapter 3.

A3.01: Properties of the VeroGray plastic-like material used in 3-D printing

Mechanical properties	Test method	Metric	English
Colour	Visual	Light gray	Light gray
Tensile strength	ASTM D638	58 Mpa	8350 psi
Elongation at break	ASTM D638	10 - 25%	10 - 25%
Modulus of elasticity	ASTM D638	2500 Mpa	362500 psi
Flexural strength	ASTM D790	93 Mpa	13500 psi
Flexural modulus	ASTM D790	2700 Mpa	392500 psi
Izod Notched Impact	ASTM D256	25 J/m	0.47 Ft lb/inch
Shore hardness (D)	-	85 D	85 D
HDT at 264 PSI	ASTM D638	48 ºC	118 ºF
HDT at 66 PSI	ASTM D638	48 ºC	118 ºF

HDT = Heat Deflection Temperature
Source: Stratasys (2015)

A3.02: Physicochemical characteristics of Breydon Water sediment in September 2017 and October 2017

Characteristic	September 2017	October 2017
Porewater Cu (µg/L)	1.8	NA
AVS (µmol/g)	<0.5	NA
SEM Cu (µmol/g)	0.14	0.10
Total Cu (µg/g)	8	8
<63 µm (%)	84.3	76.4
Eh (mV)	56	244
DOC <0.45 µm (mg/L)	10.5	19.6
TOC (%, ± SD)	1.83 ± 0.06	1.12 ± 0.08
LOI (%)	3.6	4.1

NA = Not available

A3.03: Key physicochemical characteristics of surface (top 2 cm) sediments sampled in Autumn 2017. Mean values reported. See Chapter 2 for more details.

Site	Total Cu (µg/g)	Total Zn (µg/g)	Fe_2O_3 (%)	SEM Cu (µmol/g)	SEM Zn (µmol/g)	AEM Cu (µg/g)	AEM Zn (µg/g)	<63 µm (%)	AVS (µmol/g)	PW Cu (µg/L)	PW Zn (µg/L)	TOC (%)	DOC (mg/L)	EqP Cu (µmol/g OC)	PW/OC Cu (µg/mg OC)	Sal (S)
BW	8	103	4.5	0.14	0.59	8.7	38.4	84.3	< 0.5	1.8	20.0	1.83	10.5	7.60	0.14	36.6
PR	118	232	5.9	1.01	1.56	64.0	102.1	72.9	< 0.5	3.2	72.0	10.04	11.0	9.82	0.26	19.8
CO	183	355	5.39	1.24	2.50	78.8	163.8	73.4	1.5	1.9	111.8	5.15	12.2	-5.01	0.14	35
HR	215	491	5.66	1.60	3.05	101.5	199.5	84.8	1.7	3.5	62.1	4.65	4.9	-3.10	0.60	21
PC	645	668	5.81	3.81	5.44	242.0	355.9	77.9	1.2	2.6	134.3	4.28	9.2	60.38	0.25	35.9
SJ	554	621	5.87	3.98	6.13	253.0	400.9	80.8	4.3	1.6	81.4	4.5	8.9	-6.12	0.16	39.5
MC	792	801	6.13	5.32	6.94	337.9	454.2	74.7	4.2	3.4	57.2	6.46	13.3	16.60	0.24	31.2
HA	862	1261	7.31	5.18	8.13	328.7	531.6	57.0	< 0.5	223.9	270	1.42	30.9	336.53	6.92	21.3
RC	2413	2367	9.48	22.70	23.37	1441.4	1528.4	84.9	0.5	23.6	98.9	3.38	8.5	626.56	2.49	32
RA	2978	2467	10.06	27.72	21.73	1760.3	1420.9	77.4	< 0.5	130.3	211.2	6.53	7.4	399.34	15.60	6.6
RB	3183	3015	10.45	26.98	25.87	1713.2	1691.9	82.8	< 0.5	62	191.4	2.99	9.3	910.57	6.00	31.3
HB	2565	3753	9.98	4.69	11.76	297.6	769.2	69.5	< 0.5	31.5	913.6	1.64	5.9	173.38	4.57	26.8

BW = BW September; AEM = Average SEM concentration in µg/g (i.e. acid-extractable metals); <63 µm (%) = Percentage fine composition of the fraction <2mm; Sal = Salinity

A3.04: Limit of detection, accuracy and precision for the analysis of metal concentrations in deployed DGT probes. All concentrations in µg/L

Sample		**Cu**	**Zn**	**Fe**	**Mn**
LOD		0.1	0.1	0.5	0.1
TM 27.3 (N = 4)	Cert	6.16	16.2	10.9	2.44
	% Acc	104.3	117.3	111.9	101.1
	% RSD	5.0	3.2	4.9	0.9
TMDA 64.2 (N = 3)	Cert	-	-	306	263
	% Acc	-	-	100.4	98.7
	% RSD	-	-	2.0	1.6
CLMS2A (N = 6)	Conc	5.0	5.0	5.0	5.0
	% RSD	2.1	3.1	7.4	0.7

LOD = Limit of Detection; Conc = Spike concentration; N = Number of replicates; RSD = Precision (Relative Standard Deviation); Cert = Certified concentration; Acc = Accuracy (percentage recovery)

A3.05: DGT-labile metal concentrations (C_{DGT}, in µg/L) and fluxes (J_{DGT}, in µg/m^2/h) at the overlying water layer (OLW) across the study sites

Site	C_{DGT}-Cu		C_{DGT}-Zn		C_{DGT}-Fe		C_{DGT}-Mn		J_{DGT}-Cu		J_{DGT}-Zn		J_{DGT}-Fe		J_{DGT}-Mn	
	Mean	SE	Mean	SE	Mean	SE	Mean	SE	Mean	SE	Mean	SE	Mean	SE	Mean	SE
BW	*0.93	0.23	13.34	2.79	886.22	444.04	143.36	64.07	1.53	0.38	21.39	4.48	1428.47	715.73	221.29	98.89
PR	1.60	0.11	19.70	1.10	88.87	7.74	41.91	10.05	2.82	0.20	33.94	1.89	153.90	13.41	69.50	16.67
CO	0.92	0.16	16.73	2.27	32.07	6.36	29.71	8.67	1.61	0.28	28.60	3.88	55.09	10.93	48.88	14.26
HR	2.48	0.96	26.59	4.44	70.06	29.62	10.14	1.04	4.07	1.57	42.60	7.11	112.82	47.69	15.63	1.60
PC	1.61	0.12	13.73	0.85	69.80	20.22	11.56	0.14	2.90	0.21	24.14	1.50	123.42	35.75	19.58	0.23
SJ	2.74	0.88	25.02	4.36	64.77	13.04	4.79	0.55	4.74	1.52	42.26	7.36	109.98	22.14	7.79	0.89
MC	3.62	1.04	26.01	1.72	67.33	2.67	17.37	1.79	6.10	1.76	42.73	2.82	111.16	4.40	27.47	2.83
HA	17.79	7.37	149.10	47.16	24.04	7.67	55.80	41.35	28.60	11.86	233.96	74.00	37.91	12.10	84.27	62.45
RC	3.58	0.33	19.02	0.57	42.92	15.35	6.28	0.42	6.59	0.60	34.14	1.01	77.44	27.70	10.86	0.73
RA	4.25	0.36	33.18	4.91	55.58	3.18	18.57	3.51	7.29	0.62	55.49	8.21	93.42	5.34	29.89	5.65
RB	7.13	1.22	40.04	1.05	46.79	9.55	13.21	1.60	11.97	2.05	65.55	1.72	77.00	15.71	20.82	2.52
HB	3.26	0.41	37.28	3.22	19.65	2.63	23.70	0.58	5.29	0.67	59.04	5.09	31.26	4.19	36.12	0.89

SE = Standard Error, n = 3, except PR, MC, and RB for which n = 2
*Less than method detection limit (see Section 3.3.1)

A3.06: DGT-labile metal concentrations (C_{DGT}, in µg/L) and fluxes (J_{DGT}, in µg/m^2/h) at the sediment-water interface (SWI) across the study sites

Site	C_{DGT}-Cu		C_{DGT}-Zn		C_{DGT}-Fe		C_{DGT}-Mn		J_{DGT}-Cu		J_{DGT}-Zn		J_{DGT}-Fe		J_{DGT}-Mn	
	Mean	**SE**	**Mean**	**SE**	**Mean**	**SE**	**Mean**	**SE**	**Mean**	**SE**	**Mean**	**SE**	**Mean**	**SE**	**Mean**	**SE**
BW	*0.75	0.10	11.91	1.08	603.25	356.25	109.98	39.45	1.24	0.16	19.11	1.74	972.35	574.23	169.76	60.90
PR	2.33	0.64	20.90	0.95	678.16	136.88	295.45	147.48	4.12	1.14	36.01	1.65	1174.46	237.05	490.01	244.59
CO	1.51	0.80	42.38	10.99	1588.07	437.18	267.48	85.32	2.64	1.41	72.43	18.77	2727.96	750.99	440.04	140.36
HR	2.91	1.06	32.79	6.16	125.00	41.95	33.73	8.89	4.78	1.75	52.54	9.86	201.29	67.55	52.02	13.71
PC	1.78	0.36	14.27	1.89	2743.24	263.40	36.24	2.18	3.21	0.65	25.11	3.33	4850.49	465.73	61.37	3.70
SJ	5.37	1.71	55.89	7.21	3232.47	144.31	42.17	8.51	9.29	2.97	94.42	12.17	5488.87	245.05	68.58	13.84
MC	6.88	2.64	65.40	4.25	1262.08	434.09	308.80	103.01	11.58	4.44	107.43	6.98	2083.61	716.65	488.24	162.87
HA	17.66	1.32	113.20	0.10	18.73	1.53	64.86	14.13	28.40	2.13	177.62	0.16	29.53	2.41	97.96	21.34
RC	11.77	1.25	84.70	7.58	873.40	101.80	63.24	11.30	21.65	2.30	152.05	13.61	1575.94	183.69	109.28	19.53
RA	7.84	1.54	66.90	13.15	327.19	107.16	115.91	17.15	13.43	2.64	111.87	21.99	549.90	180.10	186.55	27.60
RB	15.64	4.35	161.01	2.79	2646.02	766.42	178.90	52.68	26.24	7.30	263.61	4.57	4354.24	1261.21	281.94	83.02
HB	3.60	0.80	80.27	14.37	1490.19	803.33	249.96	35.93	5.84	1.29	127.10	22.76	2371.56	1278.47	380.96	54.76

SE = Standard Error, n = 3, except PR, MC, and RB for which n = 2

*Less than method detection limit (see Section 3.3.1)

A3.07: DGT-labile metal concentrations (C_{DGT}, in µg/L) and fluxes (J_{DGT}, in µg/m^2/h) in the sediment column (SED) across the study sites

Site	C_{DGT}-Cu		C_{DGT}-Zn		C_{DGT}-Fe		C_{DGT}-Mn		J_{DGT}-Cu		J_{DGT}-Zn		J_{DGT}-Fe		J_{DGT}-Mn	
	Mean	SE	Mean	SE	Mean	SE	Mean	SE	Mean	SE	Mean	SE	Mean	SE	Mean	SE
BW	1.21	0.35	16.21	1.60	1190.96	1091.71	120.65	101.11	1.99	0.58	26.00	2.57	1919.67	1759.69	186.24	156.07
PR	2.26	0.61	24.31	2.21	3545.67	492.24	437.37	143.00	3.98	1.09	41.89	3.80	6140.47	852.48	725.40	237.16
CO	1.45	0.71	47.71	13.78	6210.90	749.90	190.11	109.34	2.54	1.24	81.54	23.56	10668.97	1288.16	312.75	179.87
HR	4.09	1.66	38.75	6.69	2894.91	765.65	71.66	10.06	6.71	2.72	62.09	10.72	4661.85	1232.97	110.51	15.52
PC	2.12	0.33	13.06	1.89	884.39	69.67	38.51	3.25	3.83	0.59	22.97	3.33	1563.75	123.18	65.22	5.51
SJ	9.19	4.43	34.36	3.74	7059.18	1489.91	42.35	2.54	15.91	7.68	58.04	6.31	11986.80	2529.93	68.88	4.14
MC	7.22	3.64	45.10	4.53	2915.39	1058.77	277.72	159.38	12.16	6.13	74.08	7.44	4813.13	1747.96	439.10	251.99
HA	28.66	11.25	122.68	32.51	39.45	19.70	229.54	167.85	46.08	18.08	192.51	51.01	62.22	31.06	346.68	253.50
RC	4.80	1.03	45.46	6.74	5454.33	152.87	106.13	20.24	8.83	1.90	81.61	12.10	9841.59	275.83	183.39	34.97
RA	10.54	4.90	79.76	11.39	3109.30	634.81	307.05	89.74	18.06	8.40	133.37	19.05	5225.66	1066.90	494.20	144.44
RB	9.55	4.13	119.92	2.42	9561.41	3106.04	153.90	4.60	16.03	6.94	196.34	3.96	15734.07	5111.23	242.53	7.25
HB	2.91	0.69	60.61	6.39	3639.79	1382.70	459.89	66.89	4.72	1.12	95.97	10.12	5792.55	2200.49	700.91	101.95

SE = Standard Error, n = 3, except PR, MC, and RB for which n = 2

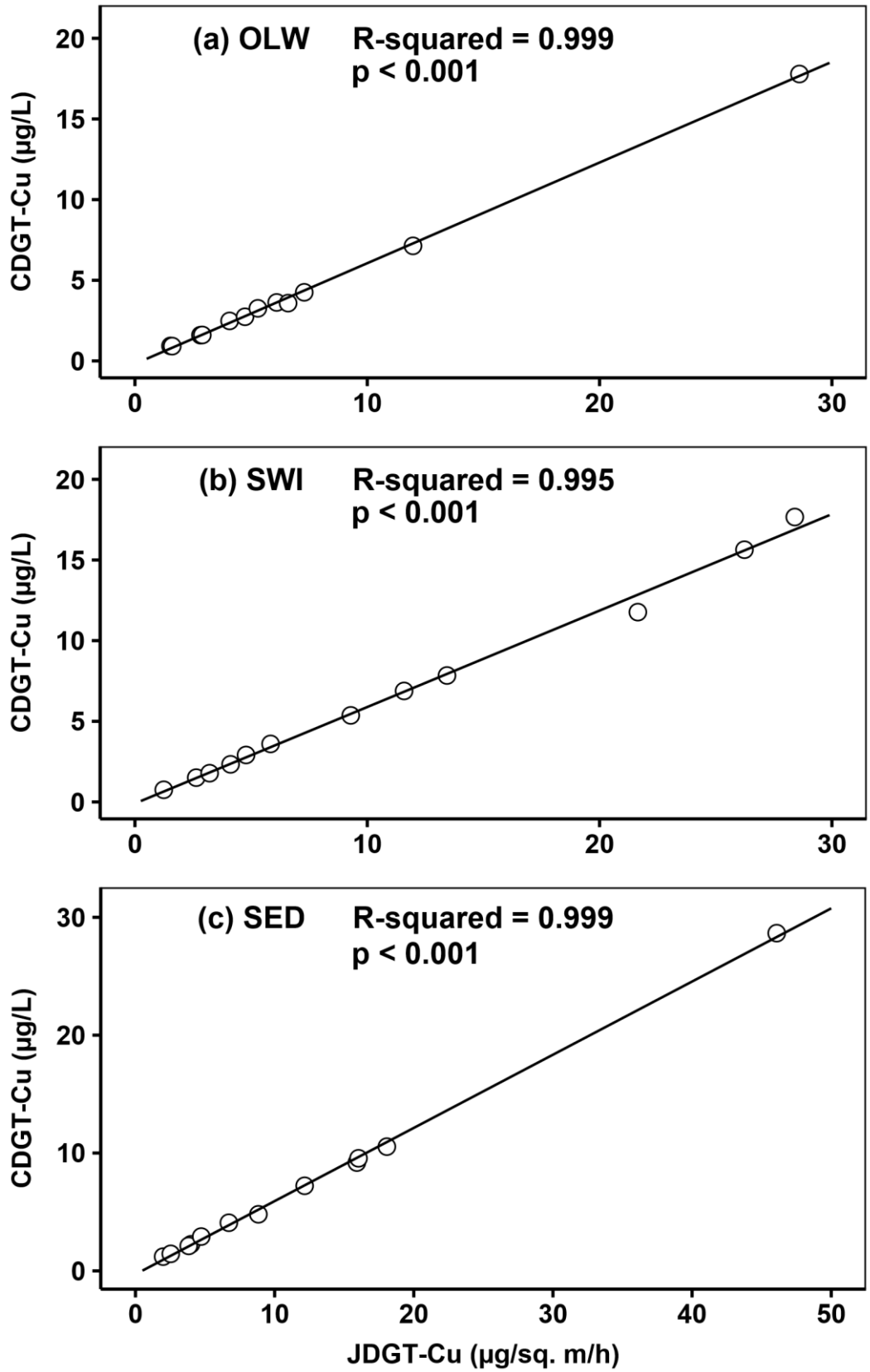

A3.08: Relationship between DGT Cu concentrations (C_{DGT}-Cu) and fluxes (J_{DGT}-Cu) at the overlying water (OLW), sediment-water interface (SWI), and sediment column (SED)

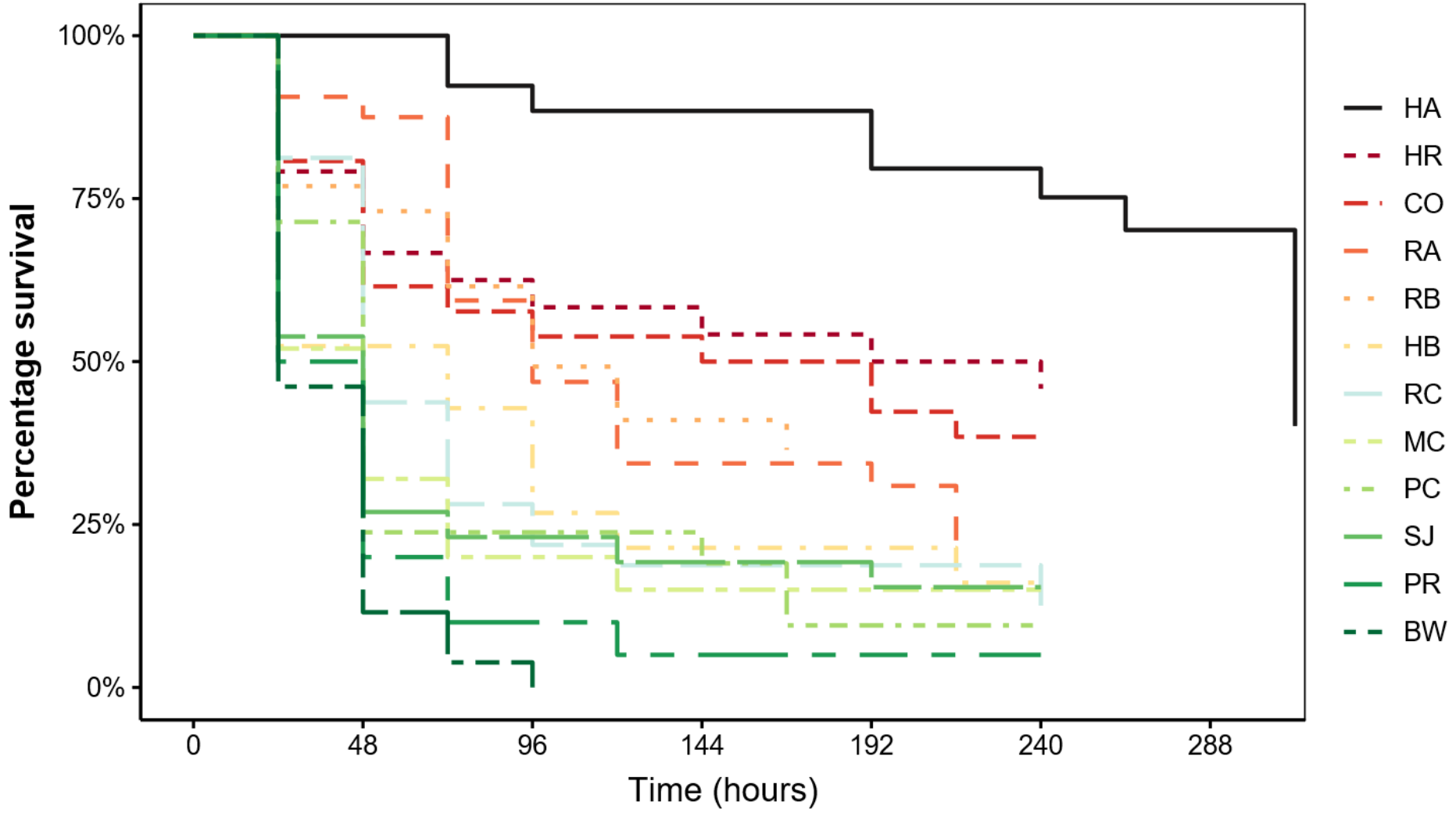

A3.09: Kaplan-Meier curves showing nematode survival in 200 µg Cu/L (nominal concentration) across the study sites

A3.10: Survival times, duration of exposure as well as percentage control and test mortality at the termination of nematode PICT toxicity test

Site	Control mortality (%)	Test mortality (%)	Duration of exposure (hrs)	Survival time (hrs)		
				LT_{50}	95% LCL	95% UCL
BW	0	100	240	24	24	48
BW – Wk 5	4	92	240	48	24	48
PR	15	95	240	36	24	48
CO	15	62	240	168	48	*240
HR	0	54	240	216	48	*240
PC	14	90	240	48	24	48
SJ	19	85	240	48	24	48
MC	12	84	240	48	24	72
HA	5	50	312	312	264	*312
HA – Wk 5	0	12	240	-	-	-
RC	15	77	240	48	48	72
RA	19	78	216	96	72	192
RB	15	62	168	96	72	*168
HB	8	81	240	72	24	96

LT_{50} = Median survival time; LCL and UCL are the lower and upper confidence limits, respectively; *UCL = UCL marked by maximum duration of exposure (Millward & Grant, 2000); "Wk 5" = second exposure in Week 5 of nematode storage

Appendices to Chapter 4.

A4.1: R codes inputted for the Multivariate Regression Tree (MRT) procedure

```
install.packages("devtools")
library(devtools)
install_github("cran/mvpart", force = TRUE)
install_github("cran/MVPARTwrap", force = TRUE)
env.rep.mvpart <- phy.chem.rep[,c(17,18,24,31)]  #environmental variables
str(env.rep.mvpart)
env.rep.mvpart$PWCu <- round(env.rep.mvpart$PWCu, digits = 1)
env.rep.mvpart$Cu63 <- round(env.rep.mvpart$Cu63, digits = 0)
env.rep.mvpart$pH <- round(env.rep.mvpart$pH, digits = 1)
env.rep.mvpart$DOC <- round(env.rep.mvpart$DOC, digits = 1)
str(env.rep.mvpart)
rep.mvpart.bray <-
  mvpart(
    gdist(p.trans.rep, method = "bray", full = T, sq = F) ~ .,
    env.rep.mvpart,
    margin = 0.08,
    cp = 0,
    xv = "pick",
    xval = 36,
    xvmult = 100,
    plot.add = T,
    text.add = T
  )
summary(rep.mvpart.bray)
```

A4.2a: Nematode species, trophic groups, and raw (i.e. unstandardised and untransformed) abundances in the first replicate (Replicate A) samples across the study sites. Site totals are provided at the bottom

S/N	Species	Trophic group	BW A	PR A	CO A	HR A	PC A	SJ A	MC A	HA A	RC A	RA A	RB A	HB A
1	*Acantholaimus polydentatus*	1A	0	0	0	0	0	0	0	0	0	0	0	0
2	*Anomonema sp.*	1A	0	0	0	0	0	0	0	0	0	1	0	0
3	*Anoplostoma viviparum*	1B	12	0	2	2	0	8	0	0	0	0	0	0
4	*Ascolaimus elongatus*	1B	2	0	0	0	0	0	0	0	0	0	0	0
5	*Atrochromadora microlaima*	2A	0	0	0	17	0	0	0	0	0	0	0	0
6	*Axonolaimus paraspinosus*	1B	37	12	3	7	0	15	16	1	0	10	0	0
7	*Axonolaimus spinosus*	1B	0	0	0	0	0	0	0	0	0	14	0	0
8	*Calyptronema maxweberi*	2B	0	19	0	0	0	0	0	12	0	0	0	0
9	*Chromadora macrolaima*	2A	1	0	0	12	0	0	0	0	0	0	0	0
10	*Chromadora nudicapitata*	2A	1	0	0	0	0	0	0	0	0	0	0	0
11	*Chromadorella filiformis*	2A	0	0	0	0	0	0	0	0	0	0	0	0
12	*Chromadorita tenuis*	2A	0	0	0	1	0	0	0	0	0	0	0	0
13	*Chromadoropsis vivipara*	2B	0	0	16	0	102	19	9	0	0	0	0	0
14	*Chromaspirina inglisi*	2B	0	0	0	1	0	0	0	0	0	0	0	0
15	*Daptonema biggi*	1B	0	0	0	0	0	0	0	0	0	0	0	0
16	*Daptonema hirsutum*	1B	17	0	1	2	0	4	0	2	16	1	9	2
17	*Daptonema normandicum*	1B	0	0	0	0	0	4	0	0	0	0	15	0
18	*Daptonema oxycerca*	1B	26	6	0	4	0	0	0	0	0	0	1	0
19	*Daptonema procerum*	1B	1	0	0	0	0	0	0	0	0	0	0	1
20	*Daptonema setosum*	1B	0	0	0	0	0	0	1	0	0	61	7	91
21	*Deontolaimus sp.*	2A	0	0	0	0	0	0	0	0	0	0	0	0
22	*Desmodora communis*	2A	0	0	1	0	0	0	0	2	0	0	2	0
23	*Desmolaimus zeelandicus*	1B	0	0	0	0	1	0	14	0	1	0	0	0
24	*Dichromadora geophila*	2A	0	0	0	0	0	0	0	0	0	1	0	0

A4.2a cont'd: Nematode species, trophic groups, and raw (i.e. unstandardised and untransformed) abundances in the first replicate (Replicate A) samples across the study sites. Site totals are provided at the bottom

S/N	Species	Trophic group	BW A	PR A	CO A	HR A	PC A	SJ A	MC A	HA A	RC A	RA A	RB A	HB A
25	*Dichromadora hyaliocheile*	2A	2	0	0	0	0	2	0	0	0	0	3	0
26	*Dichromadora sp.*	2A	0	0	0	0	0	0	0	0	0	0	0	0
27	*Diplolaimella sp.*	1B	0	0	0	0	0	0	0	0	0	0	0	0
28	*Dorylaimopsis punctata*	2A	0	0	0	0	0	0	0	0	0	0	0	0
29	*Eleutherolaimus stenosoma*	1B	0	0	0	0	0	0	0	0	0	0	0	0
30	*Halalaimus gracilis*	1A	3	2	0	0	0	0	0	0	0	0	0	0
31	*Halalaimus longicaudatus*	1A	0	0	0	0	0	0	0	0	0	0	0	0
32	*Halalaimus sp.*	1A	0	0	0	0	0	0	0	0	0	1	0	0
33	*Halichoanolaimus robustus*	2B	0	0	0	0	0	0	0	2	0	0	0	0
34	*Hypodontolaimus colesi*	2A	0	0	0	0	0	0	0	0	0	0	0	0
35	*Hypodontolaimus balticus*	2A	1	0	0	6	0	1	2	1	0	2	4	5
36	*Innocuonema tentabunda*	2A	0	0	0	0	0	1	0	0	3	0	7	0
37	*Leptolaimus limicolus*	1A	0	0	0	0	0	0	0	0	0	0	4	0
38	*Paralinhomoeus conicaudatus*	1B	0	0	0	1	0	0	0	0	0	0	0	0
39	*Linhomoeus hirsutus*	1B	0	0	0	0	0	0	0	0	0	0	0	0
40	*Linhomoeus sp.*	1B	0	0	2	0	0	0	0	0	0	0	0	0
41	*Paralinhomoeus tenuicaudatus*	1B	0	0	0	3	0	0	0	0	0	0	0	0
42	*Metachromadoroides remanei*	2B	6	2	10	10	0	6	0	0	0	0	0	0
43	*Microlaimus honestus*	2A	0	0	0	0	0	0	0	0	0	0	2	0
44	*Microlaimus marinus*	2A	0	5	0	0	0	0	0	0	2	1	2	0
45	*Microlaimus sp.*	2A	0	0	0	0	0	0	0	0	0	0	0	0
46	*Microlaimus tenispiculum*	2A	0	0	0	0	0	0	0	0	0	0	0	0
47	*Monoposthia costata*	2B	2	0	0	0	0	1	6	0	0	0	0	0
48	*Nemanema cylindraticaudatum*	1A	0	0	0	0	0	0	0	0	0	0	0	0

A4.2a cont'd: Nematode species, trophic groups, and raw (i.e. unstandardised and untransformed) abundances in the first replicate (Replicate A) samples across the study sites. Site totals are provided at the bottom

S/N	Species	Trophic group	BW A	PR A	CO A	HR A	PC A	SJ A	MC A	HA A	RC A	RA A	RB A	HB A
49	*Nudora bipapillata*	2B	2	0	32	0	0	0	16	0	0	0	0	0
50	*Odontophora setosa*	1B	0	0	3	0	0	2	1	0	0	0	0	0
51	*Oncholaimus brachycercus*	2B	0	0	0	0	0	0	0	0	0	0	0	0
52	*Oncholaimus oxyuris*	2B	0	0	0	0	0	0	0	28	0	0	0	0
53	*Onyx sagittarius*	2B	0	0	0	0	0	0	0	0	0	0	0	0
54	*Oxystomina asetosa*	1A	0	0	0	0	0	0	0	0	0	0	0	0
55	*Oxystomina elongata*	1A	0	0	0	0	0	2	7	0	0	0	0	0
56	*Paracanthonchus caecus*	2A	0	0	0	0	0	0	0	0	0	0	0	0
57	*Paracanthonchus heterodontus*	2A	0	0	0	0	0	0	0	0	0	0	0	0
58	*Paracomesoma dubium*	2B	0	0	0	0	0	8	0	0	0	0	0	0
59	*Paracyatholaimus pentodon*	2A	0	0	0	3	0	0	0	0	0	0	0	0
61	*Pomponema sedecima*	2B	0	0	0	0	0	0	0	0	0	0	0	0
62	*Praeacanthonchus punctatus*	1B	3	0	13	26	0	5	0	18	21	0	0	2
63	*Ptycholaimellus ponticus*	2A	8	2	0	0	0	1	0	0	29	4	18	5
64	*Sabatieria pulchra*	1B	1	0	0	8	1	1	0	0	4	0	1	0
65	*Sabatieria punctata*	1B	12	0	0	0	0	1	0	0	13	0	4	0
66	*Sphaerolaimus balticus*	2B	0	3	4	2	0	1	0	0	0	0	0	0
67	*Sphaerolaimus gracilis*	2B	6	3	2	2	0	2	0	0	0	0	0	0
68	*Sphaerolaimus hirsutus*	2B	7	2	2	5	0	4	2	0	0	0	0	0
69	*Spilophorella paradoxa*	2A	0	1	0	0	0	0	0	0	0	0	0	0
70	*Spirinia parasitifera*	2A	0	0	0	0	0	0	0	0	0	0	0	0
71	*Terschellingia communis*	1A	0	0	0	0	3	0	3	0	2	0	0	0
72	*Terschellingia gourbaultae*	1A	0	0	0	0	7	0	12	1	1	0	0	0

A4.2a cont'd: Nematode species, trophic groups, and raw (i.e. unstandardised and untransformed) abundances in the first replicate (Replicate A) samples across the study sites. Site totals are provided at the bottom

S/N	Species	Trophic group	BW A	PR A	CO A	HR A	PC A	SJ A	MC A	HA A	RC A	RA A	RB A	HB A
73	*Terschellingia longicaudata*	1A	0	0	0	0	0	0	3	1	1	0	0	0
74	*Thalassoalaimus tardus*	1A	0	0	1	0	0	0	0	0	0	0	0	0
75	*Theristus acer*	1B	0	0	0	0	0	2	0	0	2	0	3	1
76	*Theristus flevensis*	1B	0	0	0	0	0	9	0	0	0	3	4	2
77	*Tripyloides gracilis*	1B	0	25	2	0	0	1	0	1	0	1	10	0
78	*Tripyloides marinus*	1B	1	23	4	0	0	4	1	9	2	7	6	0
79	*Unidentified sp. - Likely from Genus Calyptronema*	1A	0	0	0	0	0	0	0	1	0	1	0	0
80	*Unidentified sp. - Likely new sp. from Genus Trichethmolaimus or Symplocostoma*	1A	0	0	1	0	0	0	0	0	0	0	0	0
81	*Viscosia abyssorum*	2B	1	0	0	0	0	0	0	0	0	0	0	0
82	*Viscosia viscosa*	2B	0	4	1	5	0	1	21	0	3	0	0	0
	Total number of individuals identified		**152**	**109**	**100**	**117**	**114**	**105**	**114**	**79**	**100**	**108**	**102**	**109**

A4.2b: Nematode species, trophic groups, and raw (i.e. unstandardised and untransformed) abundances in the second replicate (Replicate B) samples across the study sites. Site totals are provided at the bottom

S/N	Species	Trophic group	BW B	PR B	CO B	HR B	PC B	SJ B	MC B	HA B	RC B	RA B	RB B	HB B
1	*Acantholaimus polydentatus*	1A	0	0	1	0	0	0	0	0	0	0	0	0
2	*Anomonema sp.*	1A	0	0	0	0	0	0	0	0	0	0	0	0
3	*Anoplostoma viviparum*	1B	15	0	0	1	0	11	0	0	0	0	0	0
4	*Ascolaimus elongatus*	1B	0	0	0	0	0	0	0	0	0	0	0	0
5	*Atrochromadora microlaima*	2A	1	1	3	16	2	0	0	1	0	0	1	0
6	*Axonolaimus paraspinosus*	1B	22	8	12	5	0	12	14	0	0	2	1	0
7	*Axonolaimus spinosus*	1B	0	0	0	0	0	0	0	0	0	6	3	0
8	*Calyptronema maxweberi*	2B	1	27	0	0	0	1	0	8	0	0	0	0
9	*Chromadora macrolaima*	2A	7	0	0	11	0	1	6	0	0	0	0	2
10	*Chromadora nudicapitata*	2A	0	0	0	0	0	0	0	0	0	0	0	0
11	*Chromadorella filiformis*	2A	0	0	0	0	0	0	0	0	0	0	0	0
12	*Chromadorita tenuis*	2A	0	1	0	0	0	0	0	0	0	0	0	0
13	*Chromadoropsis vivipara*	2B	0	0	3	0	112	12	1	0	0	0	0	0
14	*Chromaspirina inglisi*	2B	0	0	0	0	0	0	0	0	0	0	0	0
15	*Daptonema biggi*	1B	0	0	0	0	0	1	0	0	0	0	0	0
16	*Daptonema hirsutum*	1B	10	7	1	0	0	5	1	1	8	0	6	0
17	*Daptonema normandicum*	1B	0	0	0	0	0	0	1	1	1	0	36	0
18	*Daptonema oxycerca*	1B	18	6	0	3	0	7	0	0	0	0	0	2
19	*Daptonema procerum*	1B	1	0	0	0	0	1	0	1	0	0	0	0
20	*Daptonema setosum*	1B	0	1	0	0	0	0	0	1	1	71	3	72
21	*Deontolaimus sp.*	2A	0	0	0	0	0	0	0	1	0	0	0	0
22	*Desmodora communis*	2A	0	0	1	0	0	0	0	0	0	0	1	0
23	*Desmolaimus zeelandicus*	1B	1	0	2	0	0	1	10	0	1	0	0	0
24	*Dichromadora geophila*	2A	0	0	0	0	0	0	0	0	0	1	0	0

A4.2b cont'd: Nematode species, trophic groups, and raw (i.e. unstandardised and untransformed) abundances in the second replicate (Replicate B) samples across the study sites. Site totals are provided at the bottom

S/N	Species	Trophic group	BW B	PR B	CO B	HR B	PC B	SJ B	MC B	HA B	RC B	RA B	RB B	HB B
25	*Dichromadora hyaliocheile*	2A	0	0	0	0	0	3	4	0	0	0	0	1
26	*Dichromadora sp.*	2A	0	0	0	0	0	0	0	0	0	0	0	0
27	*Diplolaimella sp.*	1B	0	0	0	0	0	1	0	0	0	0	0	0
28	*Dorylaimopsis punctata*	2A	0	0	0	0	0	1	0	0	0	0	0	0
29	*Eleutherolaimus stenosoma*	1B	0	0	0	0	1	0	0	0	0	0	0	0
30	*Halalaimus gracilis*	1A	2	0	0	0	0	0	1	0	0	0	0	0
31	*Halalaimus longicaudatus*	1A	0	0	1	0	0	0	0	0	0	0	0	0
32	*Halalaimus sp.*	1A	0	0	0	0	0	0	0	0	0	0	0	0
33	*Halichoanolaimus robustus*	2B	0	0	0	0	0	0	0	4	0	0	0	0
34	*Hypodontolaimus colesi*	2A	0	0	0	0	1	0	0	0	0	0	0	0
35	*Hypodontolaimus balticus*	2A	3	0	2	2	0	1	12	0	0	1	1	12
36	*Innocuonema tentabunda*	2A	1	0	0	0	0	0	0	0	4	0	4	0
37	*Leptolaimus limicolus*	1A	0	0	2	0	0	0	0	0	0	0	1	0
38	*Paralinhomoeus conicaudatus*	1B	0	0	1	0	0	0	0	0	0	0	0	0
39	*Linhomoeus hirsutus*	1B	0	0	0	0	0	0	0	0	0	0	0	0
40	*Linhomoeus sp.*	1B	0	0	1	0	0	0	0	0	0	0	0	0
41	*Paralinhomoeus tenuicaudatus*	1B	0	0	1	0	0	0	0	0	0	0	0	0
42	*Metachromadoroides remanei*	2B	12	5	6	4	0	9	0	0	0	0	0	0
43	*Microlaimus honestus*	2A	0	0	0	0	0	1	0	0	0	0	0	0
44	*Microlaimus marinus*	2A	0	3	10	0	0	2	2	0	2	1	2	0
45	*Microlaimus sp.*	2A	1	0	1	1	0	0	0	0	0	0	0	0
46	*Microlaimus tenispiculum*	2A	0	0	0	0	0	1	0	0	0	0	0	0
47	*Monoposthia costata*	2B	1	0	0	0	1	0	4	0	0	0	0	0
48	*Nemanema cylindraticaudatum*	1A	0	0	1	1	0	0	0	0	0	0	0	0

A4.2b cont'd: Nematode species, trophic groups, and raw (i.e. unstandardised and untransformed) abundances in the second replicate (Replicate B) samples across the study sites. Site totals are provided at the bottom

S/N	Species	Trophic group	BW B	PR B	CO B	HR B	PC B	SJ B	MC B	HA B	RC B	RA B	RB B	HB B
49	*Nudora bipapillata*	2B	1	0	9	0	0	0	10	0	0	0	0	0
50	*Odontophora setosa*	1B	0	0	4	0	0	0	2	0	0	0	0	0
51	*Oncholaimus brachycercus*	2B	0	1	0	0	0	0	0	0	0	0	0	0
52	*Oncholaimus oxyuris*	2B	0	0	0	0	0	0	0	41	0	0	0	1
53	*Onyx sagittarius*	2B	0	0	0	0	1	0	0	0	0	0	0	0
54	*Oxystomina asetosa*	1A	0	0	0	0	0	0	1	0	0	0	0	0
55	*Oxystomina elongata*	1A	0	0	2	1	0	0	0	0	0	0	0	0
56	*Paracanthonchus caecus*	2A	0	0	0	0	1	0	0	0	0	0	0	0
57	*Paracanthonchus heterodontus*	2A	0	0	0	0	1	0	0	0	0	0	0	0
58	*Paracomesoma dubium*	2B	0	0	0	0	0	0	0	0	0	0	0	0
59	*Paracyatholaimus pentodon*	2A	0	0	0	0	0	0	0	0	0	0	0	0
61	*Pomponema sedecima*	2B	0	1	0	0	0	0	0	0	0	0	0	0
62	*Praeacanthonchus punctatus*	1B	1	0	1	39	0	3	5	12	0	0	0	9
63	*Ptycholaimellus ponticus*	2A	6	2	6	1	0	1	9	0	60	6	9	3
64	*Sabatieria pulchra*	1B	0	0	5	4	0	1	1	0	12	0	0	0
65	*Sabatieria punctata*	1B	5	0	1	0	0	0	1	0	3	0	0	0
66	*Sphaerolaimus balticus*	2B	1	4	1	3	0	0	0	0	0	0	0	0
67	*Sphaerolaimus gracilis*	2B	2	2	1	3	0	1	0	0	0	0	0	0
68	*Sphaerolaimus hirsutus*	2B	5	1	0	3	0	0	0	0	0	0	0	0
69	*Spilophorella paradoxa*	2A	0	0	0	0	0	0	0	0	0	0	0	0
70	*Spirinia parasitifera*	2A	0	0	0	0	0	0	0	0	0	0	0	0
71	*Terschellingia communis*	1A	0	0	5	0	3	3	0	0	1	0	0	0
72	*Terschellingia gourbaultae*	1A	0	0	0	0	0	0	7	0	0	0	1	0

A4.2b cont'd: Nematode species, trophic groups, and raw (i.e. unstandardised and untransformed) abundances in the second replicate (Replicate B) samples across the study sites. Site totals are provided at the bottom

S/N	Species	Trophic group	BW B	PR B	CO B	HR B	PC B	SJ B	MC B	HA B	RC B	RA B	RB B	HB B
73	*Terschellingia longicaudata*	1A	0	0	10	1	1	1	4	0	1	0	1	0
74	*Thalassoalaimus tardus*	1A	0	0	0	0	0	0	0	0	0	0	0	0
75	*Theristus acer*	1B	0	0	0	0	0	0	0	0	4	0	9	0
76	*Theristus flevensis*	1B	0	0	0	0	0	21	0	0	0	1	0	0
77	*Tripyloides gracilis*	1B	1	20	6	0	0	5	1	1	1	1	11	0
78	*Tripyloides marinus*	1B	0	7	5	0	0	6	4	19	0	7	10	0
79	*Unidentified sp. - Likely from Genus Calyptronema*	1A	0	0	0	0	0	0	0	0	0	3	1	0
80	*Unidentified sp. - Likely new sp. from Genus Trichethmolaimus or Symplocostoma*	1A	0	0	0	0	0	0	0	0	0	0	0	0
81	*Viscosia abyssorum*	2B	0	0	1	0	0	0	0	0	0	0	0	0
82	*Viscosia viscosa*	2B	0	11	10	2	0	0	1	0	1	0	2	0
	Total number of individuals identified		**118**	**108**	**116**	**101**	**124**	**113**	**102**	**91**	**100**	**100**	**103**	**102**

A4.2c: Nematode species, trophic groups, and raw (i.e. unstandardised and untransformed) abundances in the third replicate (Replicate C) samples across the study sites. Site totals are provided at the bottom

S/N	Species	Trophic group	BWC	PRC	COC	HRC	PCC	SJC	MCC	HAC	RCC	RAC	RBC	HBC
1	*Acantholaimus polydentatus*	1A	0	0	0	0	0	0	0	0	0	0	0	0
2	*Anomonema sp.*	1A	0	0	0	0	0	0	0	0	0	0	0	0
3	*Anoplostoma viviparum*	1B	15	0	1	1	0	5	0	0	0	0	0	0
4	*Ascolaimus elongatus*	1B	0	0	0	0	0	2	0	0	0	0	0	0
5	*Atrochromadora microlaima*	2A	1	0	0	6	0	0	3	0	0	0	0	1
6	*Axonolaimus paraspinosus*	1B	16	9	4	11	1	13	9	0	2	0	8	0
7	*Axonolaimus spinosus*	1B	0	0	0	0	0	0	0	0	0	6	2	0
8	*Calyptronema maxweberi*	2B	0	9	0	0	0	0	0	8	0	0	0	0
9	*Chromadora macrolaima*	2A	2	0	0	20	1	0	1	0	0	0	0	5
10	*Chromadora nudicapitata*	2A	0	0	0	0	0	0	0	0	0	0	0	0
11	*Chromadorella filiformis*	2A	0	0	0	0	0	1	0	0	0	0	0	0
12	*Chromadorita tenuis*	2A	0	0	0	0	0	0	0	0	1	0	0	0
13	*Chromadoropsis vivipara*	2B	0	0	7	0	92	31	9	0	0	1	0	0
14	*Chromaspirina inglisi*	2B	0	0	0	0	0	0	0	0	0	0	0	0
15	*Daptonema biggi*	1B	0	0	0	0	0	0	0	0	0	0	0	0
16	*Daptonema hirsutum*	1B	10	6	0	5	0	3	2	1	12	0	7	0
17	*Daptonema normandicum*	1B	0	0	3	0	0	0	0	0	2	0	27	0
18	*Daptonema oxycerca*	1B	20	8	1	2	1	1	0	0	0	0	0	1
19	*Daptonema procerum*	1B	7	0	1	0	0	0	0	0	0	0	0	0
20	*Daptonema setosum*	1B	0	8	0	0	0	0	0	0	0	0	6	16
21	*Deontolaimus sp.*	2A	0	0	0	0	0	0	0	0	0	0	0	0
22	*Desmodora communis*	2A	0	0	0	0	0	0	0	0	0	3	0	0
23	*Desmolaimus zeelandicus*	1B	0	2	1	0	0	0	20	0	1	0	0	1
24	*Dichromadora geophila*	2A	0	0	2	0	0	0	0	0	0	0	0	0

A4.2c cont'd: Nematode species, trophic groups, and raw (i.e. unstandardised and untransformed) abundances in the third replicate (Replicate C) samples across the study sites. Site totals are provided at the bottom

S/N	Species	Trophic group	BW C	PR C	CO C	HR C	PC C	SJ C	MC C	HA C	RC C	RA C	RB C	HB C
25	*Dichromadora hyaliocheile*	2A	0	0	0	0	0	6	2	0	0	0	1	1
26	*Dichromadora sp.*	2A	0	0	0	3	0	0	0	0	0	0	0	0
27	*Diplolaimella sp.*	1B	0	0	0	0	0	1	0	0	0	0	0	0
28	*Dorylaimopsis punctata*	2A	0	0	0	0	0	0	0	0	0	0	0	0
29	*Eleutherolaimus stenosoma*	1B	0	0	0	0	0	0	0	0	0	0	0	0
30	*Halalaimus gracilis*	1A	0	1	0	0	0	0	0	0	0	0	0	0
31	*Halalaimus longicaudatus*	1A	0	0	0	0	0	0	0	0	0	0	0	0
32	*Halalaimus sp.*	1A	0	0	0	0	0	0	0	0	0	0	0	0
33	*Halichoanolaimus robustus*	2B	0	0	0	0	0	0	0	7	0	0	0	0
34	*Hypodontolaimus colesi*	2A	0	0	0	0	0	0	0	0	0	0	0	0
35	*Hypodontolaimus balticus*	2A	1	0	3	5	0	0	15	0	0	1	0	19
36	*Innocuonema tentabunda*	2A	0	1	0	0	2	1	0	0	3	0	3	0
37	*Leptolaimus limicolus*	1A	0	0	0	0	0	0	0	0	0	0	1	0
38	*Paralinhomoeus conicaudatus*	1B	0	0	0	0	0	0	0	0	0	0	0	0
39	*Linhomoeus hirsutus*	1B	0	1	0	0	0	0	0	0	0	0	0	0
40	*Linhomoeus sp.*	1B	0	0	0	0	0	0	0	0	0	0	0	0
41	*Paralinhomoeus tenuicaudatus*	1B	0	1	0	0	0	1	0	0	0	0	0	0
42	*Metachromadoroides remanei*	2B	6	6	38	3	0	5	0	0	0	0	0	0
43	*Microlaimus honestus*	2A	0	0	0	0	0	0	0	0	0	0	0	0
44	*Microlaimus marinus*	2A	0	0	1	0	0	1	0	0	2	0	4	0
45	*Microlaimus sp.*	2A	0	0	0	0	0	0	0	0	0	0	0	0
46	*Microlaimus tenispiculum*	2A	0	0	0	0	0	0	0	0	0	0	0	0
47	*Monoposthia costata*	2B	0	0	1	0	0	0	4	0	0	0	0	0
48	*Nemanema cylindraticaudatum*	1A	0	0	0	0	0	0	0	0	0	0	0	0

A4.2c cont'd: Nematode species, trophic groups, and raw (i.e. unstandardised and untransformed) abundances in the third replicate (Replicate C) samples across the study sites. Site totals are provided at the bottom

S/N	Species	Trophic group	BWC	PRC	COC	HRC	PCC	SJC	MCC	HAC	RCC	RAC	RBC	HBC
49	*Nudora bipapillata*	2B	2	0	19	0	1	5	19	0	0	0	0	0
50	*Odontophora setosa*	1B	0	0	1	0	0	1	0	0	0	0	0	0
51	*Oncholaimus brachycercus*	2B	0	0	0	0	0	0	0	0	0	0	0	0
52	*Oncholaimus oxyuris*	2B	0	0	0	0	0	0	0	33	0	0	0	1
53	*Onyx sagittarius*	2B	0	0	0	0	0	0	0	0	0	0	0	0
54	*Oxystomina asetosa*	1A	0	0	0	0	0	0	1	0	0	0	0	0
55	*Oxystomina elongata*	1A	0	0	1	1	0	0	1	0	0	0	0	0
56	*Paracanthonchus caecus*	2A	0	3	0	0	0	0	0	0	0	0	0	0
57	*Paracanthonchus heterodontus*	2A	0	0	0	0	3	0	0	0	0	0	0	0
58	*Paracomesoma dubium*	2B	0	0	0	0	0	4	0	0	0	0	0	0
59	*Paracyatholaimus pentodon*	2A	0	0	0	0	0	0	0	0	0	0	0	0
61	*Pomponema sedecima*	2B	0	0	0	0	0	0	0	0	0	0	0	0
62	*Praeacanthonchus punctatus*	1B	1	0	5	24	7	2	4	5	0	0	15	4
63	*Ptycholaimellus ponticus*	2A	13	0	0	0	0	0	1	0	56	0	3	9
64	*Sabatieria pulchra*	1B	1	0	2	6	1	0	0	0	8	0	1	7
65	*Sabatieria punctata*	1B	9	0	0	0	0	0	0	0	5	0	1	0
66	*Sphaerolaimus balticus*	2B	4	5	1	0	0	0	0	0	0	0	0	0
67	*Sphaerolaimus gracilis*	2B	11	1	0	3	0	1	0	0	0	0	0	0
68	*Sphaerolaimus hirsutus*	2B	8	0	1	5	0	4	1	0	0	0	0	0
69	*Spilophorella paradoxa*	2A	0	0	0	0	0	0	0	0	0	0	0	1
70	*Spirinia parasitifera*	2A	0	0	0	0	0	1	0	0	0	0	0	0
71	*Terschellingia communis*	1A	0	0	1	0	1	2	3	0	2	0	1	0
72	*Terschellingia gourbaultae*	1A	0	0	0	0	1	0	6	0	1	0	0	0

A4.2c cont'd: Nematode species, trophic groups, and raw (i.e. unstandardised and untransformed) abundances in the first replicate (Replicate A) samples across the study sites. Site totals are provided at the bottom

S/N	Species	Trophic group	BWC	PRC	COC	HRC	PCC	SJC	MCC	HAC	RCC	RAC	RBC	HBC
73	*Terschellingia longicaudata*	1A	0	0	10	0	1	4	4	0	1	0	0	0
74	*Thalassoalaimus tardus*	1A	0	0	0	2	0	0	0	0	0	0	0	0
75	*Theristus acer*	1B	0	0	0	0	1	0	0	0	3	0	12	0
76	*Theristus flevensis*	1B	0	0	0	0	0	18	0	0	0	0	0	1
77	*Tripyloides gracilis*	1B	2	39	1	0	0	8	2	0	0	1	6	0
78	*Tripyloides marinus*	1B	0	18	1	0	0	7	0	3	1	2	8	3
79	*Unidentified sp. - Likely from Genus Calyptronema*	1A	0	0	0	0	0	1	1	1	0	3	0	0
80	*Unidentified sp. - Likely new sp. from Genus Trichethmolaimus or Symplocostoma*	1A	0	0	0	0	0	0	0	0	0	0	0	0
81	*Viscosia abyssorum*	2B	1	0	0	0	0	0	0	0	0	0	0	0
82	*Viscosia viscosa*	2B	0	16	0	3	0	0	3	0	0	0	0	41
	Total number of individuals identified		**130**	**134**	**106**	**100**	**113**	**129**	**111**	**58**	**100**	**17**	**106**	**111**

A4.3: Eigenvalues and total variance (up to 100%) explained by the components extracted from the correlation-based Principal Component Analysis of mean univariate diversity indices and environmental variables

Total Variance Explained

	Initial Eigenvalues		
Component	Total	% of Variance	Cumulative %
1	12.772	38.702	38.702
2	6.810	20.637	59.339
3	4.449	13.481	72.820
4	3.148	9.538	82.358
5	2.037	6.174	88.532
6	1.293	3.917	92.449
7	0.973	2.948	95.397
8	0.706	2.140	97.537
9	0.357	1.080	98.617
10	0.322	0.976	99.594
11	0.134	0.406	100.000

A4.4: Component matrix for the correlation-based Principal Component Analysis of mean univariate diversity indices and environmental variables

Component Matrix[a]

	Component					
Variables	1	2	3	4	5	7
PWCu	0.953	0.106	-0.003	-0.185	-0.036	0.155
PWCu.OC	0.937	0.042	0.195	-0.207	-0.093	0.100
SedCu.OC	0.888	-0.133	0.234	0.327	0.151	-0.039
SedZn	0.882	-0.111	0.364	0.236	0.034	-0.121
DGTCuA	0.876	0.261	-0.148	0.135	0.142	0.225
SedCu	0.827	-0.108	0.280	0.425	-0.099	-0.149
DGTCuS	0.825	0.344	0.083	0.338	0.051	0.191
DGTZnB	0.811	0.504	0.030	0.072	0.082	-0.118
PWZn	0.810	-0.285	-0.009	-0.023	0.081	-0.487
DGTZnA	0.797	0.330	-0.385	-0.062	0.189	0.011
DGTZnS	0.796	0.420	0.188	0.293	0.209	-0.132
AEMCu	0.784	0.005	0.329	0.447	-0.185	0.069
DGTCuB	0.738	0.404	-0.174	0.292	-0.003	0.243
Var.TD	0.719	-0.241	0.094	-0.461	0.181	-0.316
EqP	0.699	-0.240	0.128	-0.255	-0.083	0.334
SPN	-0.680	0.590	0.102	0.239	0.238	-0.139
ORP	0.528	0.412	-0.509	-0.170	-0.474	0.049
Tax.div	-0.296	0.942	-0.014	-0.065	0.042	-0.040
Pielou.eve	-0.286	0.941	0.098	-0.051	0.051	-0.007
Simpson.div	-0.331	0.927	0.095	-0.041	0.108	-0.016
Shannon.div	-0.488	0.839	0.122	0.066	0.146	-0.055
Tax.dist	-0.103	0.831	-0.289	-0.004	-0.377	0.207
pH	-0.088	-0.740	-0.163	0.233	-0.152	0.365
Prop2B	-0.203	-0.433	-0.819	0.270	0.064	-0.022
DOC	0.166	0.275	-0.815	0.071	0.232	0.242
percFines	-0.482	-0.018	0.780	0.096	-0.072	0.331
Prop2A	0.139	0.075	0.768	0.115	0.119	0.183
MedianPS	0.582	0.186	-0.717	0.031	0.080	-0.220
Sulphide	-0.456	-0.007	0.030	0.826	0.014	-0.103
Prop1A	-0.135	0.194	-0.105	0.680	-0.343	-0.060
Prop1B	0.189	0.446	0.526	-0.563	-0.084	-0.083
TOC	-0.263	0.089	0.123	0.278	-0.793	-0.339
Salinity	-0.523	-0.168	0.054	0.378	0.696	0.018

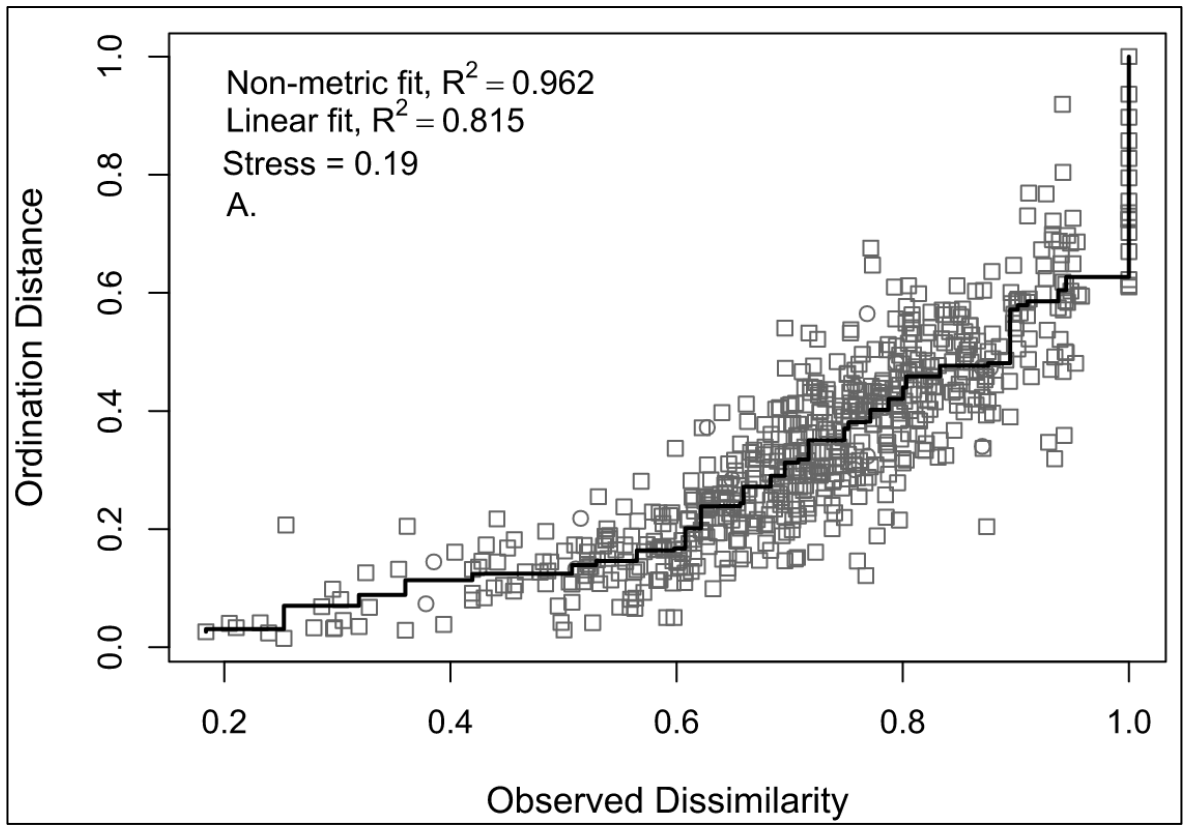

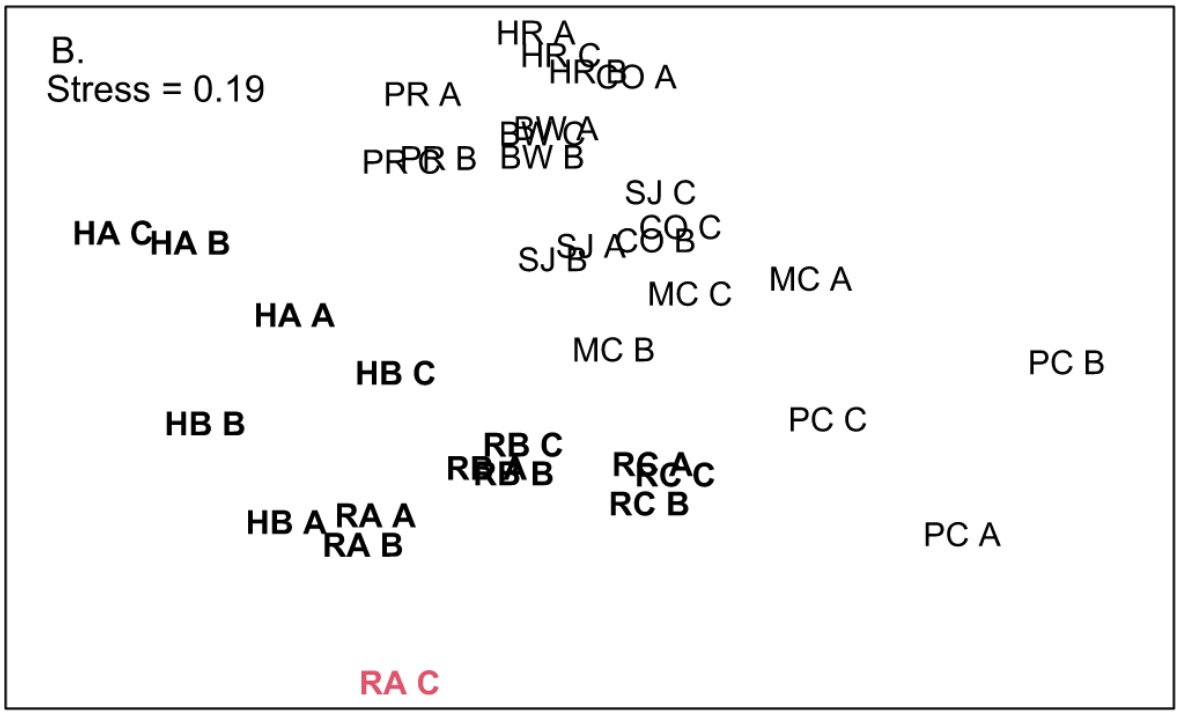

A4.5: Shepard diagram (A) and MDS plot (B) of fourth-root transformed species percentage abundances across the study sites, generated with dispersion weighting applied before data transformation (Clarke *et al.*, 2014) to account for the relatively low sample size in RA-C (red font), which is the replicate of Restronguet Creek A with only 17 individuals in the bulk sample. Bold font: grossly contaminated sites. Normal font: less contaminated sites

Appendices to Chapter 5.

A5.1a. Physicochemical properties of oxic test sediments. Standard errors (n = 3; n = 2*; n = 1**) provided, where available

Sample (Nominal)	Sed Cu (µmol/g)	LOI (%)	< 63 µm (%)	AVS (µmol/g)	SEM Cu (µmol/g)	PW Cu (µg/L)
Control	0.6	7.0 ± 0.1	79	< 0.5	0.5 ± 0.2	1.9 ± 0.7
2	3.2				1.4 ± <0.1	1.7 ± 0.1
4	5.2				2.8 ± 0.1	5.6 ± 1.8*
6	6.4				3.7 ± 0.1	9.3 ± 5.0*
8	9.5				6.7 ± 0.1*	34.6 ± 4.9
10	10.9				7.7 ± 0.1*	40.6 ± 1.3*

A5.1b. Physicochemical properties of anoxic sediments before (t = 0 h) and after (t = 24 h) toxicity tests. Standard errors (n = 3; n = 2*; n = 1**) provided, where available

Sample (Nominal)	Sed Cu (µmol/g)	LOI (%)	< 63 µm (%)	AVS (µmol/g)		SEM Cu (µmol/g)		PW Cu (µg/L)	
				t = 0 h	t = 24 h	t = 0 h	t = 24 h	t = 0 h	t = 24 h
Control	0.7	7.2 ± 0.1	77	24.7 ± 0.9	5.3 ± 0.3	0.2 ± <0.1	0.1 ± <0.1	0.8 ± 0.1*	4.2**
2	2.6			19.5 ± 0.6*	9.3 ± 3.0	0.8 ± 0.1	0.7 ± 0.1	0.8 ± 0.2*	28.5**
4	4.2			19.7 ± 2.7*	7.6 ± 1.1	0.6 ± 0.1	1.9 ± 0.4	1.5 ± <0.1*	48.5**
6	6.6			23.8 ± 1.3	4.4 ± 0.9	1.3 ± <0.7	2.7 ± 0.1	2.0 ± 0.9*	79.6**
8	8.5			22.5 ± 1.8	4.2 ± 0.7	1.3 ± 0.5	4.3 ± 0.6	2.7 ± 0.6*	94.1**
10	10.3			19.8 ± 1.8*	2.7 ± 1.8	2.0 ± 0.7	7.5 ± 0.2	1.3 ± <0.1*	19.7**

Sed Cu = Total sediment Cu (grain-size normalised); SEM Cu = 1M HCl extractable Cu; PW Cu = Total Porewater

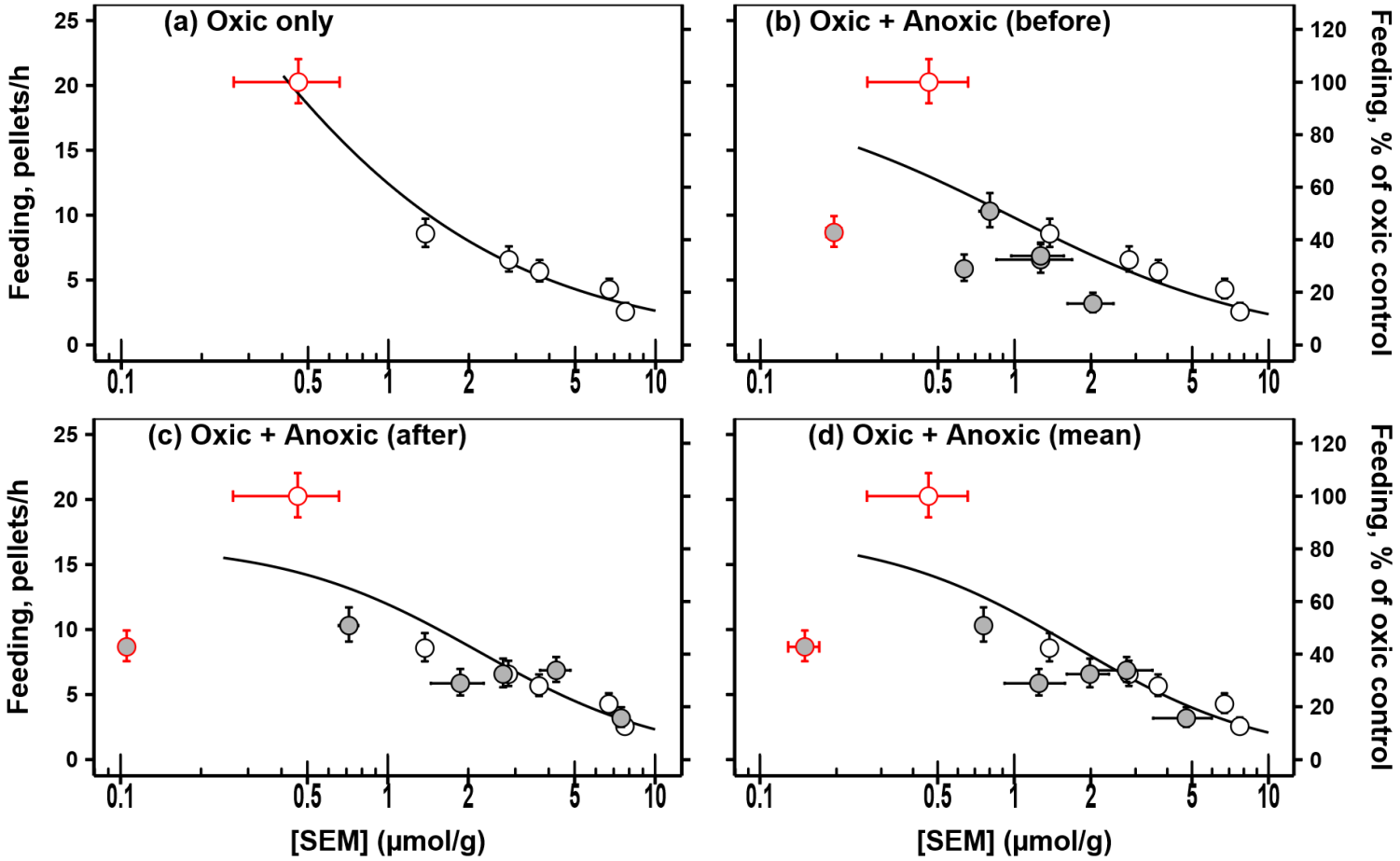

A5.2: In-exposure feeding rate, as measured by egestion rate (mean ± 95% CI), of *P. ulvae* exposed to spiked oxic (open symbols) and anoxic (filled symbols) sediments for 24 hrs in relation to SEM Cu concentration (mean ± SE). Red symbols represent control exposures. Anoxic mean values represent time-averaged SEM concentrations. EC 10, 20, & 50 provided in Table 5.3. The difference in feeding rates between the oxic and anoxic controls is due to the significant effect of anoxia (see Fig. 5.09)

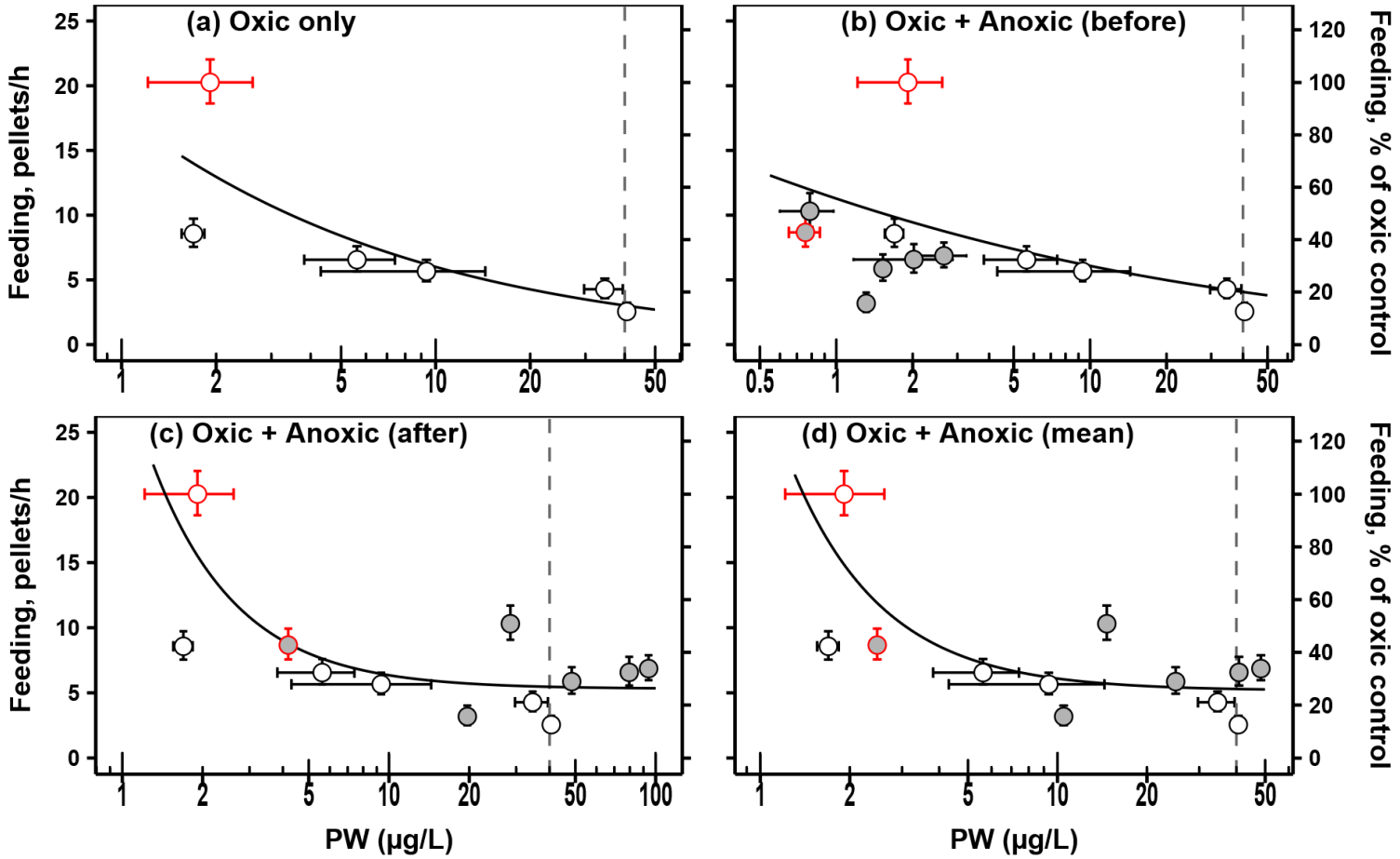

A5.3: In-exposure feeding rate, as measured by egestion rate (mean ± 95% CI), of *P. ulvae* exposed to spiked oxic (open symbols) and anoxic (filled symbols) sediments for 24 hrs in relation to porewater Cu concentration (mean ± SE). Red symbols represent control exposures. Anoxic mean values represent time-averaged porewater concentrations. EC 10, 20, & 50 provided in Table 5.3. Dashed line represents the 48-hr water-only EC_{20} (Krell *et al*., 2011), below which dissolved Cu is not expected to contribute to toxicity for a 48-hr exposure period

Appendices to Chapter 6.

A6.01: Key physicochemical characteristics of ***oxic (top 2 cm) sediments*** sampled in Summer 2019. Mean values reported. See Chapter 2 for further details

Site	Total Cu (µg/g)	Total Zn (µg/g)	Fe_2O_3 (%)	MnO (%)	CaO (%)	AEM Cu (µg/g)	AEM Zn (µg/g)	AEM Fe (µg/g)	AEM Mn (µg/g)	PW Cu (µg/L)	PW Zn (µg/L)	PW Fe (µg/L)	PW Mn (µg/L)	<63 µm (%)	AVS (µmol/g)	LOI (%)	TOC (%)
BW	21	104	4.89	0.08	7.85	23.2	45.7	6734.5	303.0	1.4	5.2	25.9	1.83	71.1	2.7	5.80	3.07
PR	150	254	5.81	0.04	0.61	99.2	161.3	23469.3	193.6	1.6	16.8	3878.4	10.04	69.6	1.5	10.80	5.77
CO	202	336	5.03	0.04	1.12	42.5	71.5	4514.4	51.8	3.5	9.5	1749.4	5.15	61.4	17.2	13.04	6.98
HR	179	422	5.78	0.06	2.19	56.7	100.9	4303.7	32.6	3.6	14.9	125.6	4.65	81.8	5.3	9.57	5.11
PC	610	622	5.78	0.05	1.09	95.3	229.1	4999.7	23.1	7.4	59.0	22352.5	4.28	55.1	21.3	7.66	4.08
SJ	435	566	6.04	0.04	0.40	136.2	191.2	4106.7	15.6	7.6	8.0	12744.3	4.5	72.6	23.8	7.28	3.87
MC	777	718	5.80	0.06	0.94	61.3	225.2	6561.7	24.0	2.9	8.6	7893.4	6.46	71.9	19.6	12.26	6.56
HA	932	1121	7.49	0.11	5.98	212.4	378.2	3380.4	91.2	12.5	34.6	3660.0	1.42	53.3	< 0.5	4.87	2.57
RC	1897	1736	8.51	0.07	1.44	498.8	904.5	9415.7	30.7	3.6	33.0	20022.1	3.38	74.8	3.6	8.95	4.78
RA	3260	2570	9.85	0.10	3.48	864.0	1013.5	11620.9	147.9	34.8	37.0	8152.9	6.53	67.6	0.9	10.15	5.42
RB	3158	2708	10.4	0.09	1.26	1251.6	1462.4	10417.7	68.1	17.5	138.3	714.9	2.99	76.4	< 0.5	6.80	3.61
HB	3565	5924	7.78	0.12	5.22	290.2	839.8	6683.1	193.5	15.8	61.8	165.9	1.64	29.1	4.5	11.30	6.04

AEM = Acid-extractable metals (or SEM expressed in µg/g); PW = Total porewater concentration; <63 µm (%) = Percentage fine composition of the fraction <2mm; AVS = Acid Volatile Sulphide concentration; LOI = Percentage loss on ignition at 400 ^{o}C for 24 hr; TOC = Total organic carbon content estimated from LOI using the equation in Figure 2.04. Note that PW Mn = approximately 2% of actual values (see A2.22)

A6.02: Key physicochemical characteristics of ***anoxic (5 – 10 cm) sediments*** sampled in Summer 2019. Mean values reported. See Chapter 2 for further details

Site	Total Cu (µg/g)	Total Zn (µg/g)	Fe_2O_3 (%)	MnO (%)	CaO (%)	AEM Cu (µg/g)	AEM Zn (µg/g)	AEM Fe (µg/g)	AEM Mn (µg/g)	PW Cu (µg/L)	PW Zn (µg/L)	PW Fe (µg/L)	PW Mn (µg/L)	<63 µm (%)	AVS (µmol/g)	LOI (%)	TOC (%)
BW	37	150	4.71	0.06	8.06	6.6	33.1	5289.1	194.0	-	-	-	-	78.1	48.9	4.47	2.35
PR	166	277	5.31	0.04	0.48	13.6	41.2	3282.2	15.9	2.4	6.2	64.7	19.3	66.4	23.6	11.97	6.40
CO	150	294	5.30	0.04	0.35	9.3	72.9	5777.1	35.0	16.3	3.0	226.5	48.0	65.5	44.0	11.47	6.13
HR	319	810	5.21	0.09	0.79	43.1	105.6	2026.5	13.5	2.9	13.7	502.9	14.3	75.9	13.4	7.25	3.85
PC	1037	1205	6.11	0.05	0.86	21.7	196.4	5727.3	14.3	4.9	8.1	119.6	4.9	56.6	61.5	10.97	5.87
SJ	665	827	5.53	0.04	1.39	13.6	196.3	3931.4	11.3	3.5	30.1	44.9	3.7	72.1	30.0	9.39	5.01
MC	1243	1315	5.92	0.07	0.56	7.1	334.6	4853.7	25.7	-	-	-	-	67.6	23.6	6.46	3.43
HA	1001	1295	7.44	0.11	5.65	134.3	386.2	3518.3	47.8	-	-	-	-	50.7	6.4	3.73	1.95
RC	3013	3019	9.05	0.08	0.88	11.0	971.4	13833.9	23.9	2.5	23.5	337.4	3.8	75.2	56.5	7.69	4.09
RA	3166	2810	9.34	0.08	0.71	227.1	948.8	13521.3	56.7	5.3	46	314.3	31.2	64.3	26.4	11.19	5.98
RB	3717	3739	10.4	0.08	1.07	395.2	1160.9	10013.8	28.2	2.8	21.5	98.9	4.3	73.8	26.1	9.03	4.81
HB	1393	2473	7.21	0.10	6.79	113.4	675.9	5437.0	84.7	3.1	14.5	329	22.9	51.6	10.0	6.92	3.67

AEM = Acid-extractable metals (or SEM expressed in µg/g); PW = Total porewater concentration; <63 µm (%) = Percentage fine composition of the fraction <2mm; AVS = Acid Volatile Sulphide concentration; LOI = Percentage loss on ignition at 400 ^{o}C for 24 hr; TOC = Total organic carbon content estimated from LOI using the equation in Figure 2.04. Note that PW Mn = approximately 2% of actual values (see A2.22)

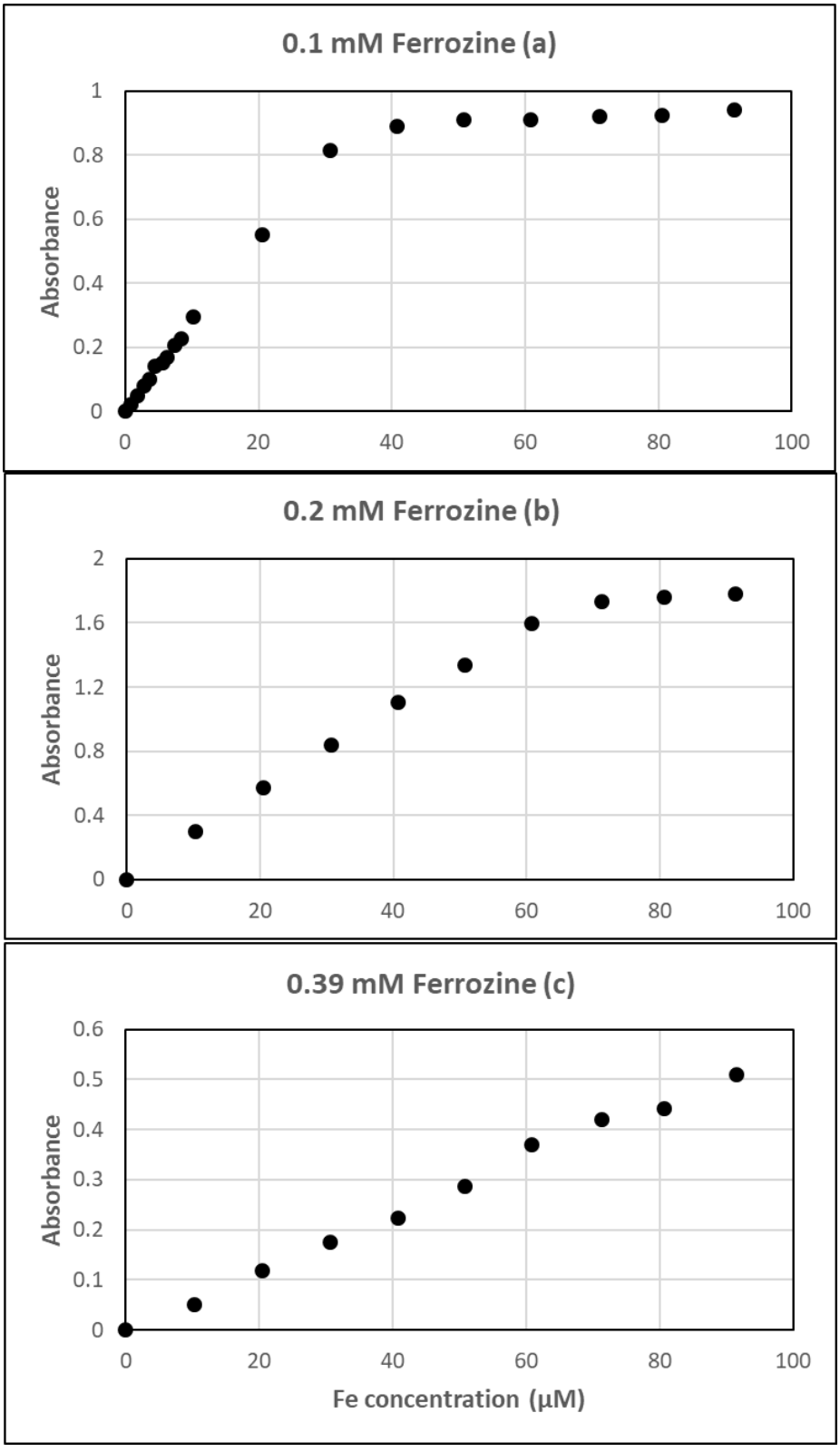

A6.03: Calibration of the Ferrozine method using final Ferrozine concentrations of 0.1 mM (panel a), 0.2 mM (panel b), and 0.39 mM (panel c). Maximum linear range for calibrations with 0.1 mM Ferrozine is 30 µM Fe

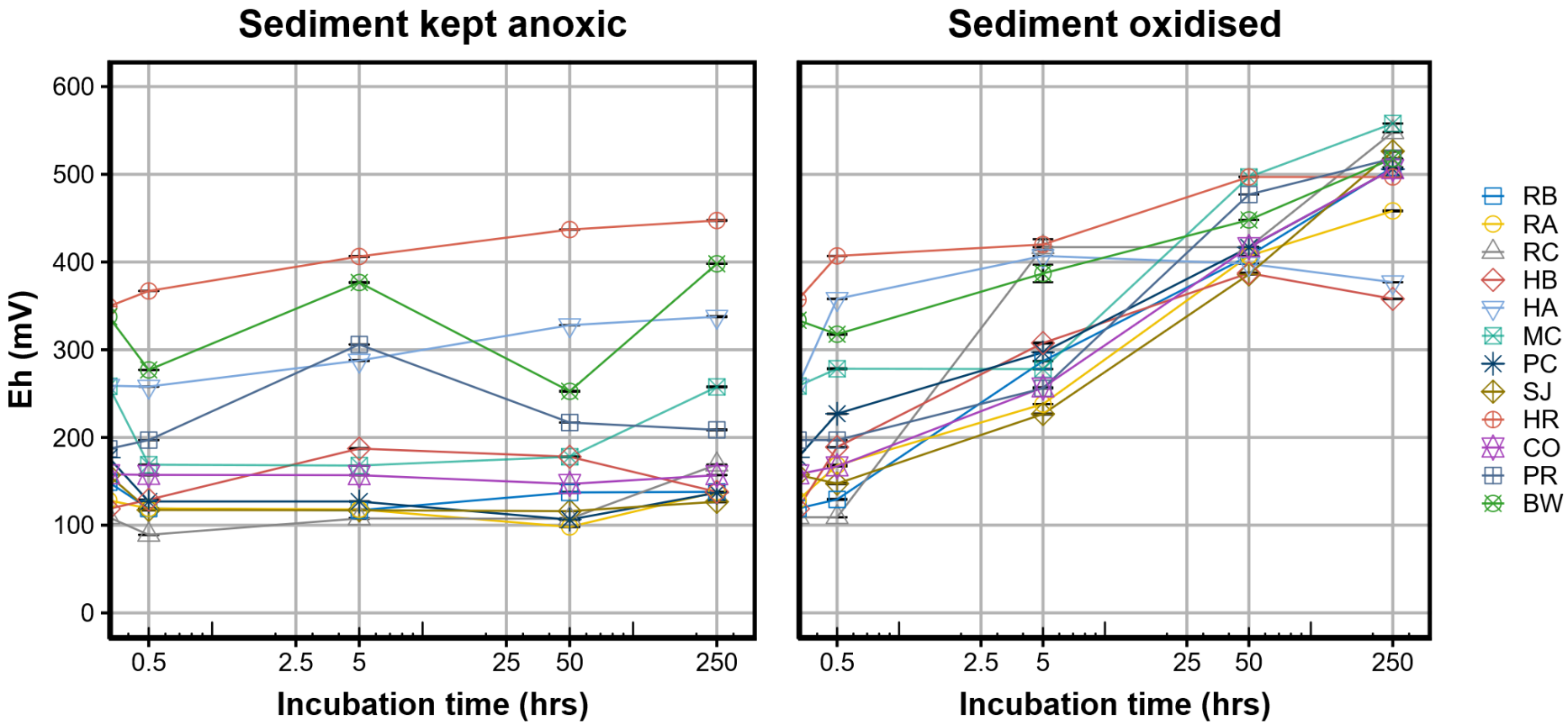

A6.04: Variation of redox potential (Eh) (mean ± SD) with time in ***anoxic sediment*** incubations across the study sites. Left hand panel = sediments incubated in anoxic conditions. Right hand panel = sediments incubated in oxic conditions

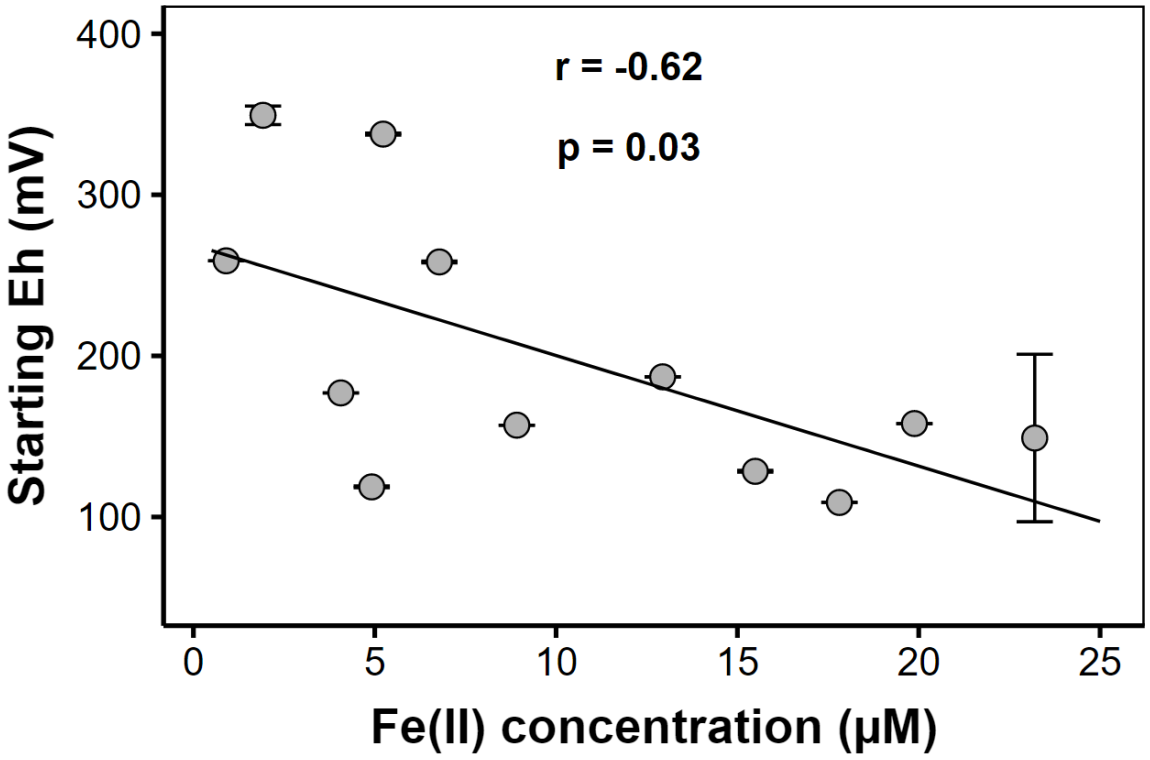

A6.05a: Relationship between starting redox potential (Eh, mean ± SD) in anoxic sediment incubations and starting Fe(II) concentration

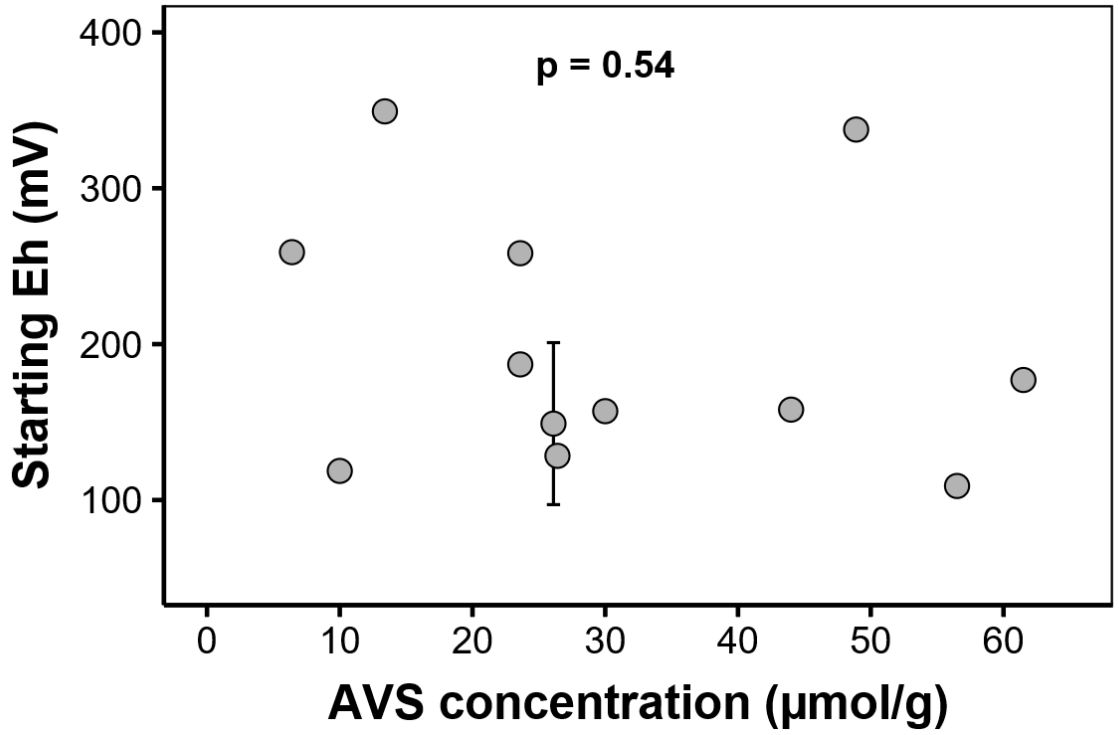

A6.05b: Relationship between starting redox potential (Eh, mean ± SD) in anoxic sediment incubations and sediment AVS concentration prior to incubation. Correlation, however, not significant p = 0.54

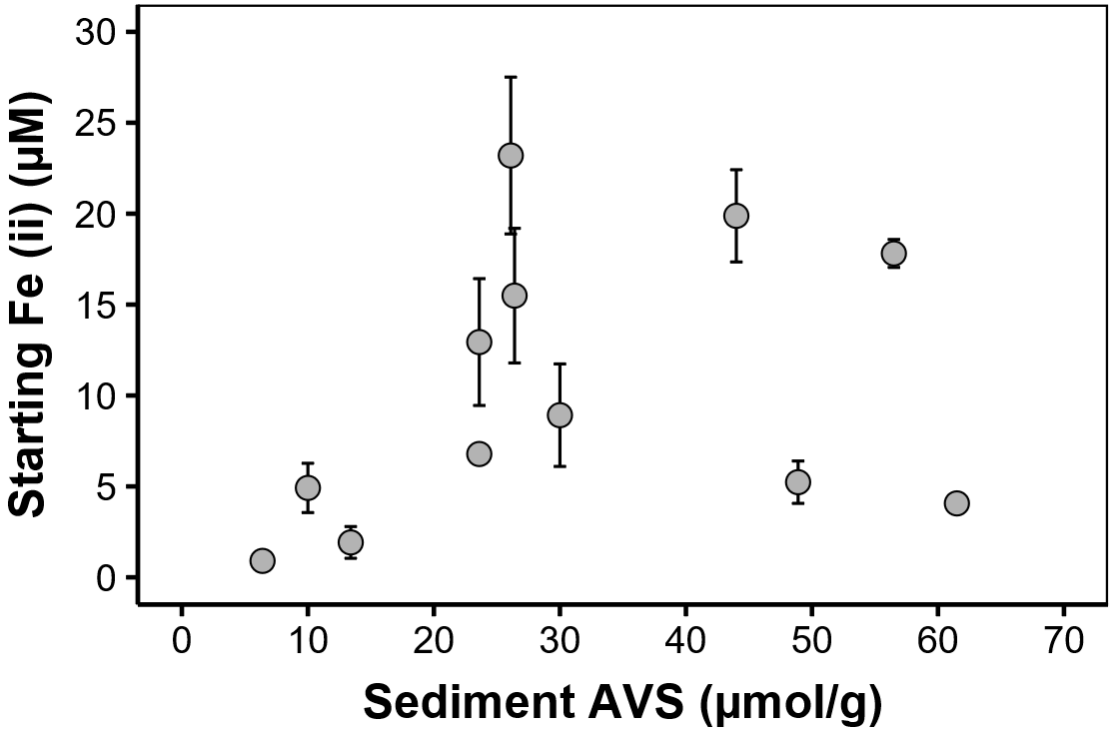

A6.06a: Relationship between starting Fe(II) concentration (mean ± SD) in anoxic sediment incubations and sediment AVS concentration prior to incubation

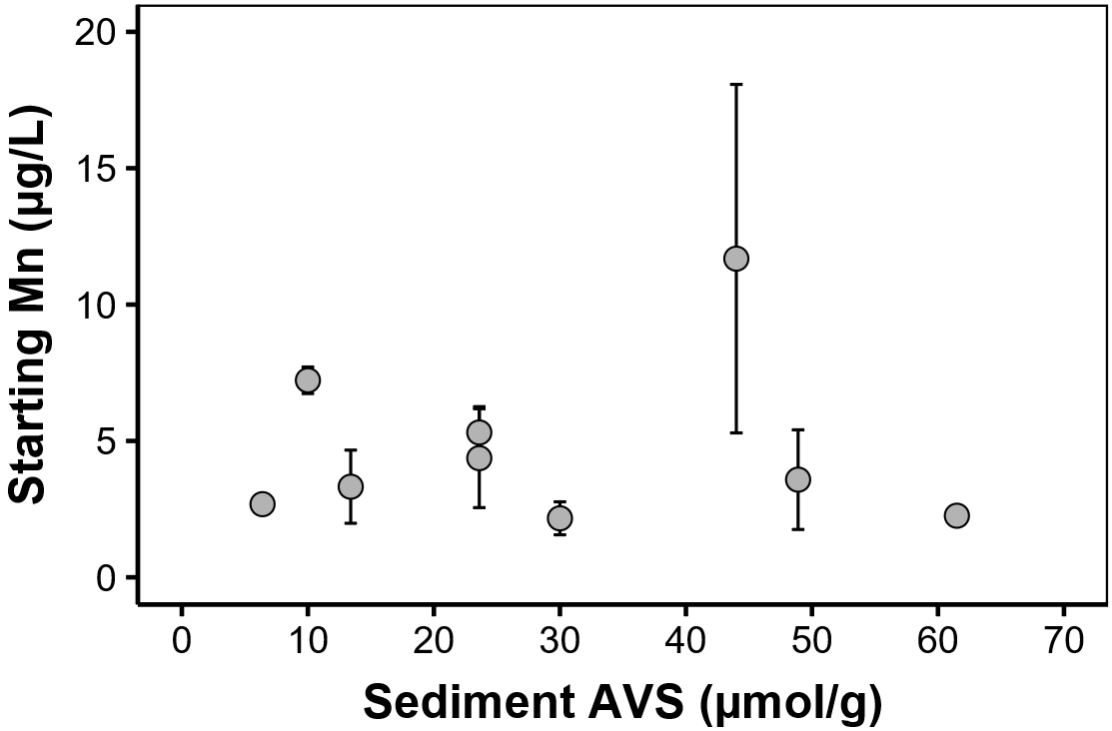

A6.06b: Relationship between starting Mn concentration (mean ± SD) in anoxic sediment incubations and sediment AVS concentration prior to incubation. Missing data for Sites RA,RB, and RC. Note that Mn concentrations represent approximately 2% of actual values (see Chapter 2)

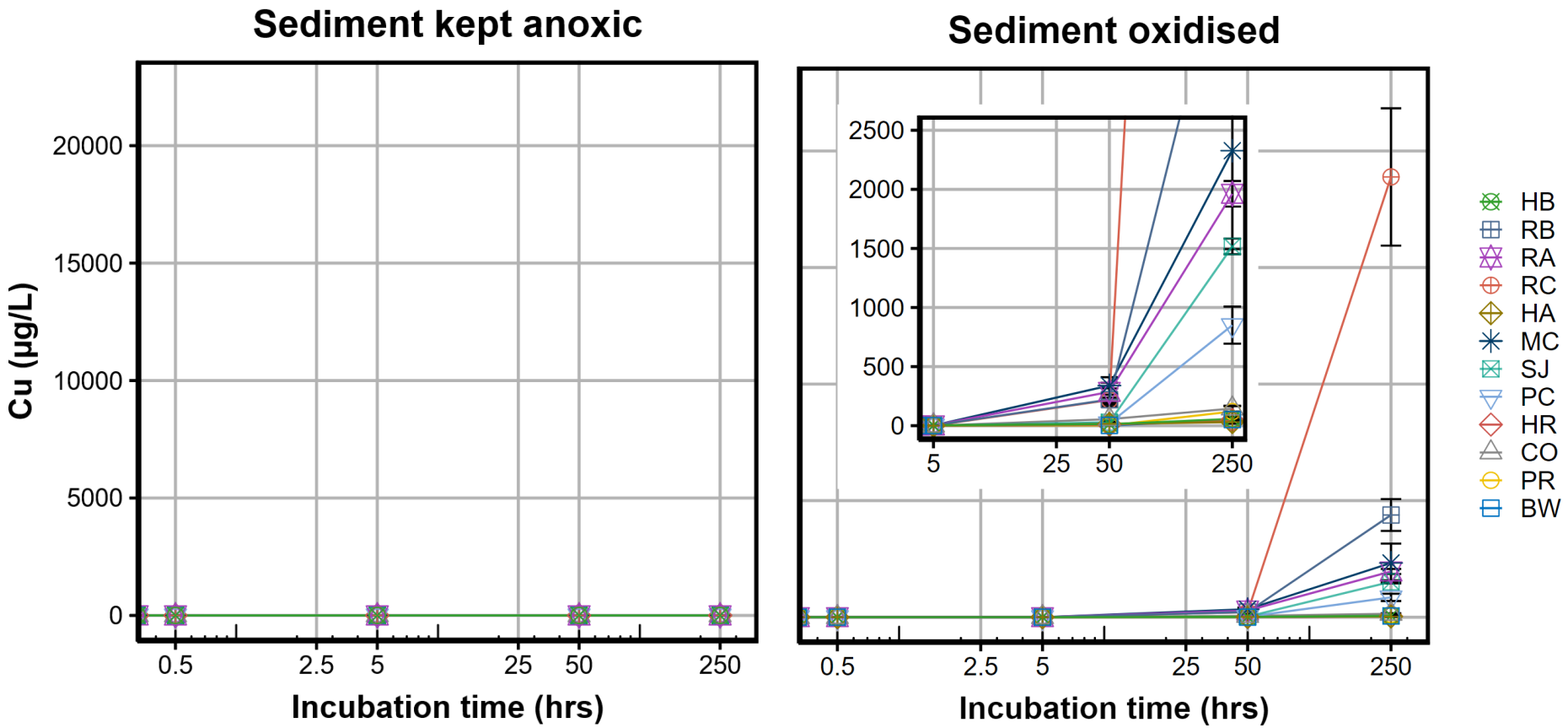

A6.07: Remobilisation of Cu (mean ± SD) with time in ***anoxic sediment*** incubations across the study sites. Left hand panel = sediments incubated in anoxic conditions. Right hand panel = sediments incubated in oxic conditions

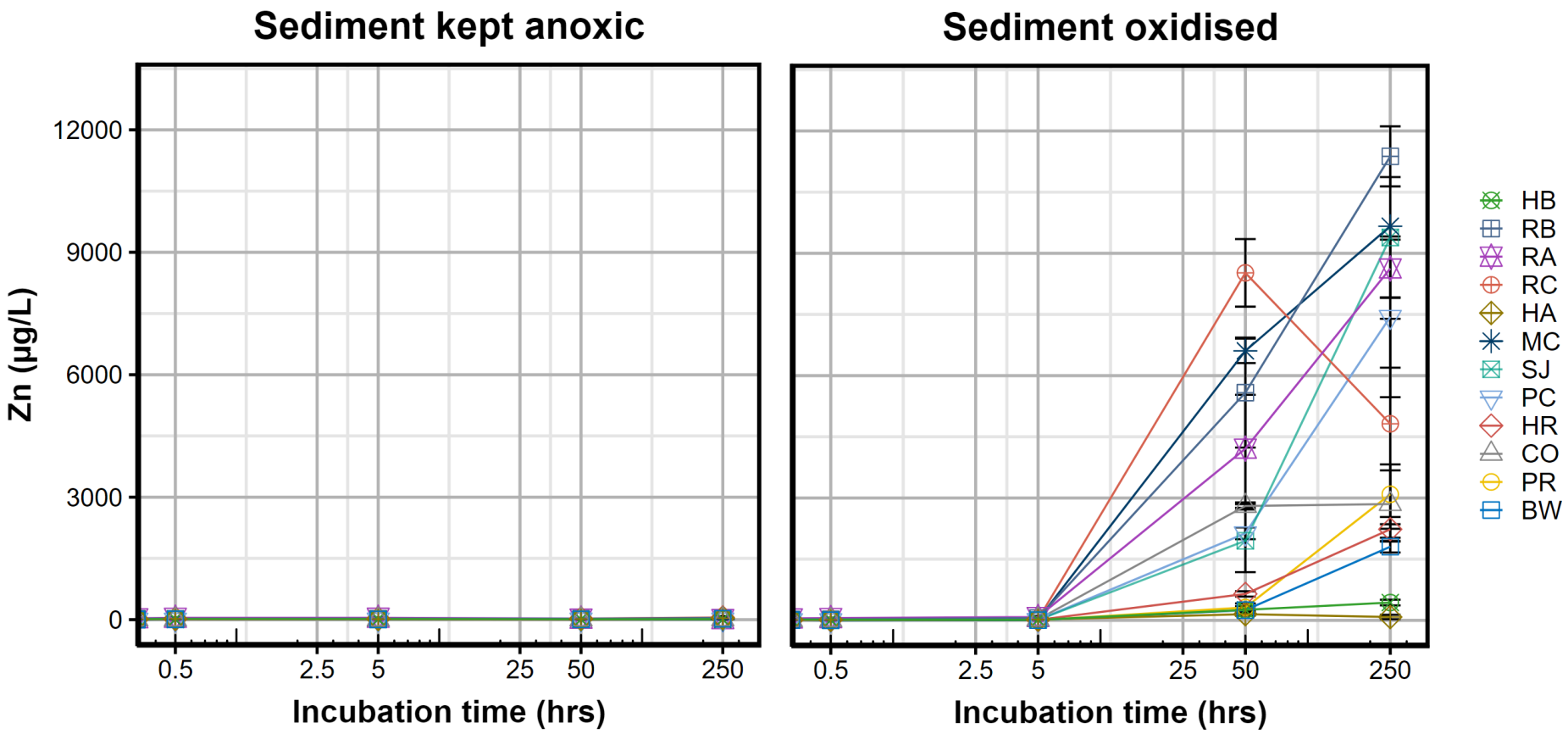

A6.08: Remobilisation of Zn (mean ± SD) with time in ***anoxic sediment*** incubations across the study sites. Left hand panel = sediments incubated in anoxic conditions. Right hand panel = sediments incubated in oxic conditions

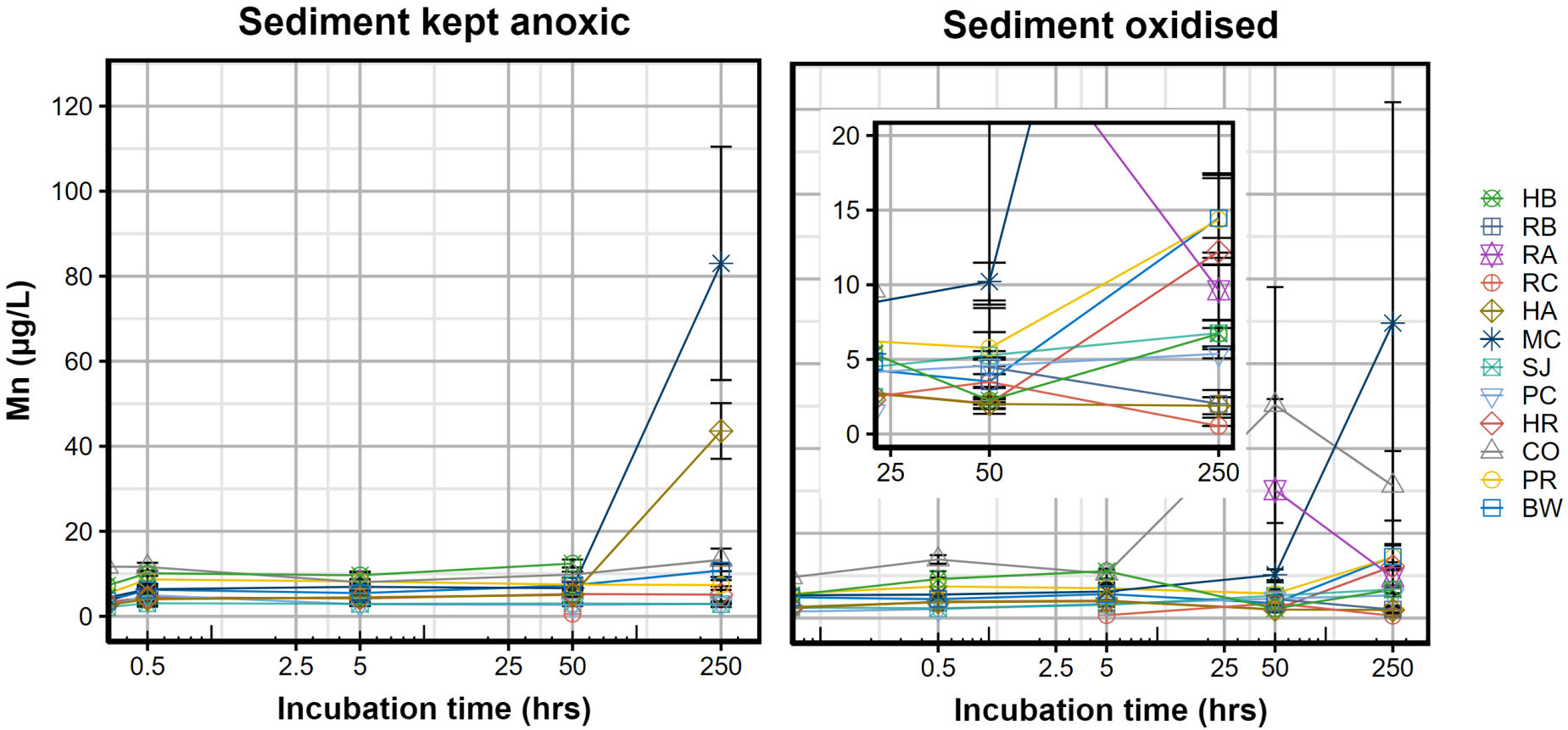

A6.09: Remobilisation of Mn (mean ± SD) with time in ***anoxic sediment*** incubations across the study sites. Note that Mn concentrations represent approximately 2% of actual values (see Chapter 2). Left hand panel = sediments incubated in anoxic conditions. Right hand panel = sediments incubated in oxic conditions. Missing data for Sites RA, RB, and RC (except oxidised incubation for all three sites at T50 and T250, for RC oxidised at T5, and for RC reduced at T50)

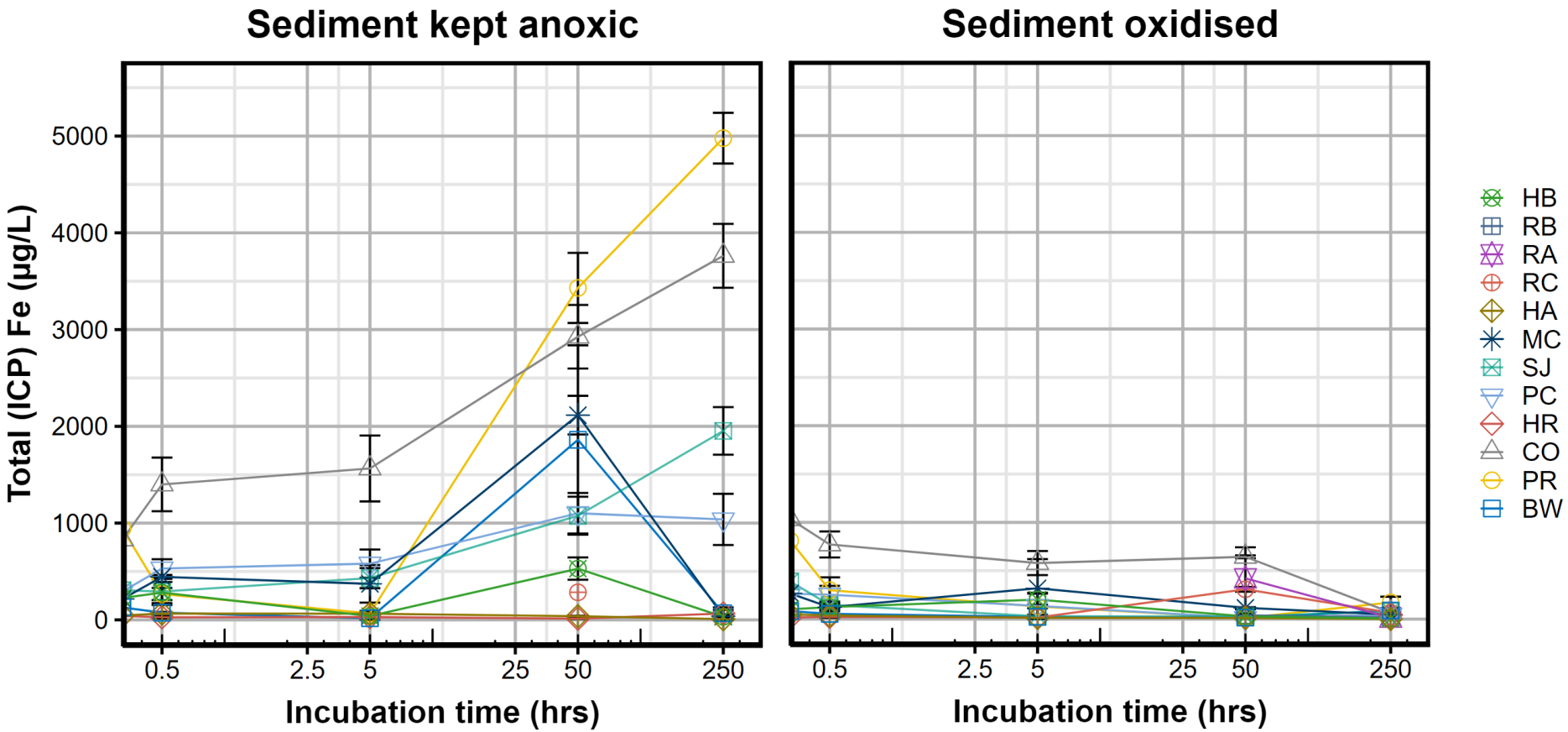

A6.10: Remobilisation of Fe (total Fe measured by ICP-OES) (mean ± SD) with time in ***anoxic sediment*** incubations across the study sites. Left hand panel = sediments incubated in anoxic conditions. Right hand panel = sediments incubated in oxic conditions. Missing data for Sites RA, RB, and RC (except oxidised incubation for all three sites at T50 and T250, for RC oxidised at T5, and for RC reduced at T50)

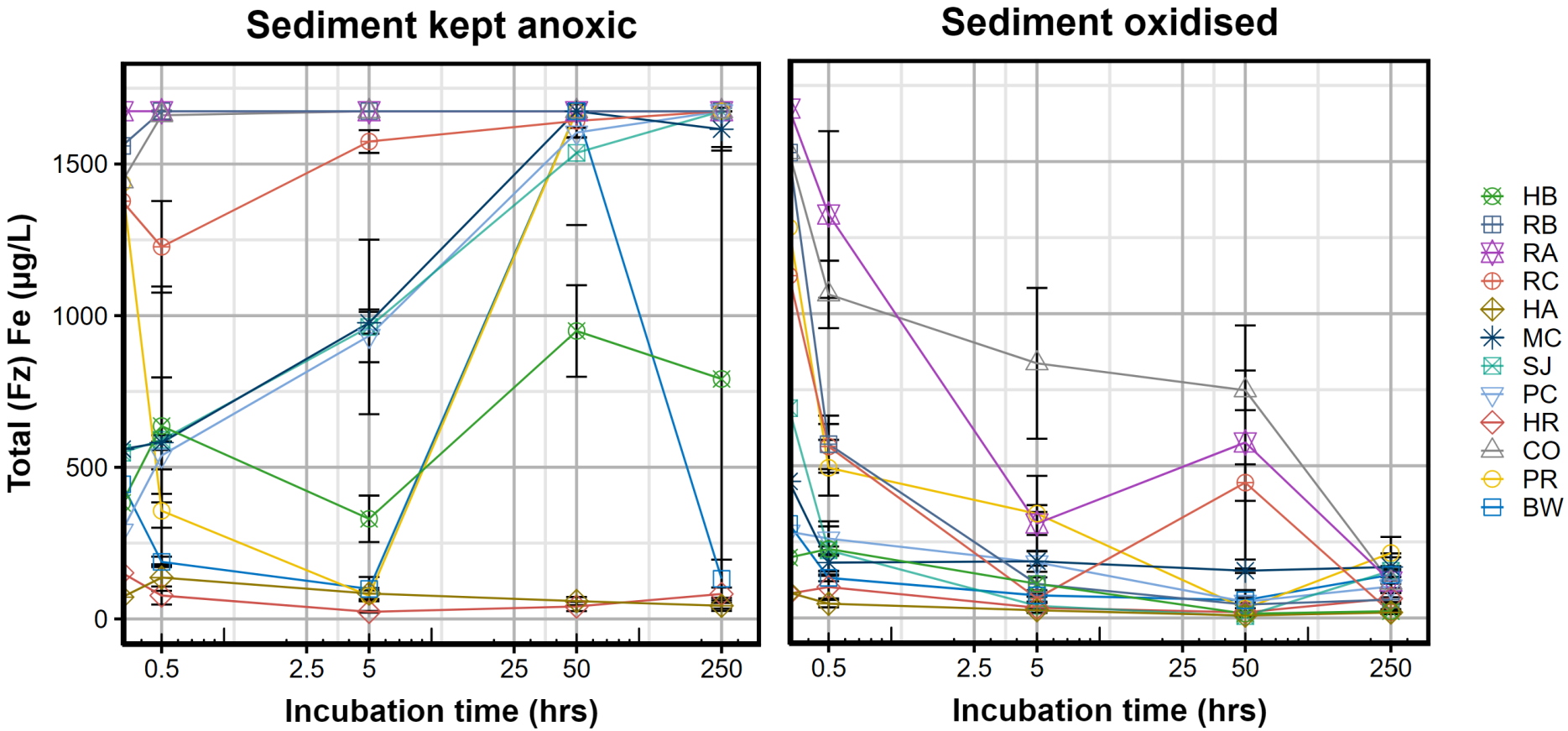

A6.11: Remobilisation of Fe (total Fe measured by Ferrozine) (mean ± SD) with time in ***anoxic sediment*** incubations across the study sites. Maximum Ferrozine range = 1674 µg/L. Left hand panel = sediments incubated in anoxic conditions. Right hand panel = sediments incubated in oxic conditions

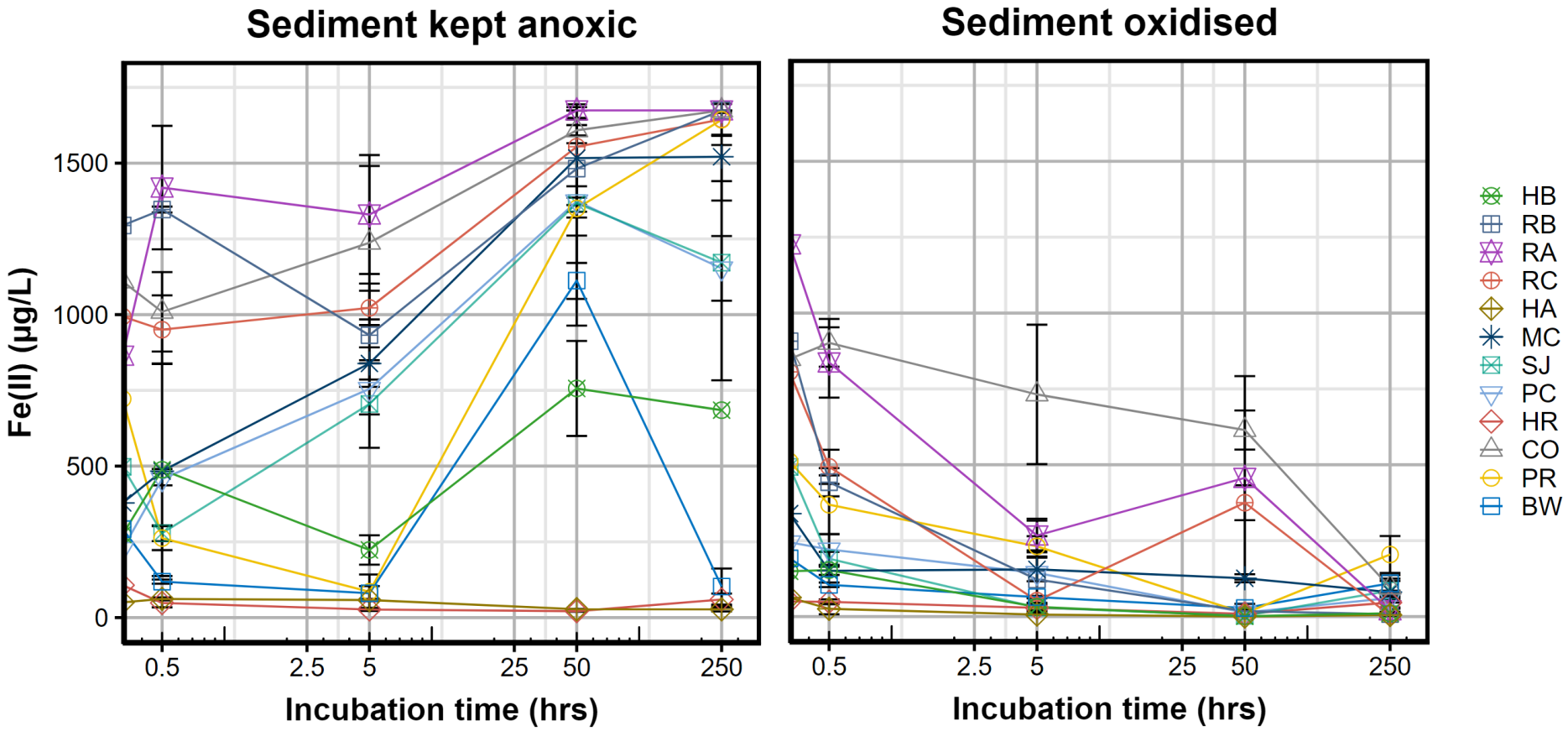

A6.12: Remobilisation of Fe (Fe^{2+} measured by Ferrozine) (mean ± SD) with time in ***anoxic sediment*** incubations across the study sites. Maximum Ferrozine range = 1674 µg/L. Left hand panel = sediments incubated in anoxic conditions. Right hand panel = sediments incubated in oxic conditions

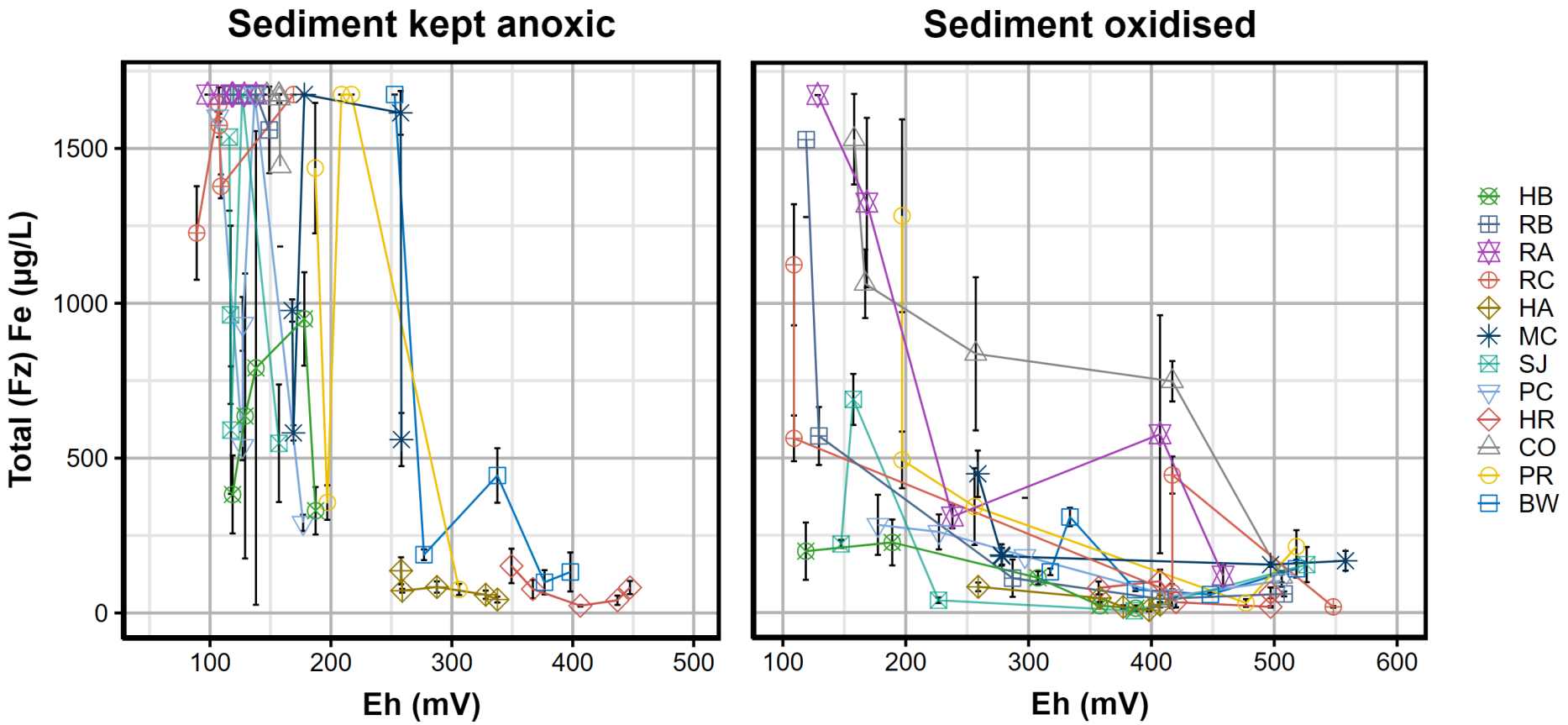

A6.13: Remobilisation of Fe (total Fe measured by Ferrozine) (mean ± SD) with redox potential in ***anoxic sediment*** incubations across the study sites. Maximum Ferrozine range = 1674 µg/L. Left hand panel = sediments incubated in anoxic conditions. Right hand panel = sediments incubated in oxic conditions

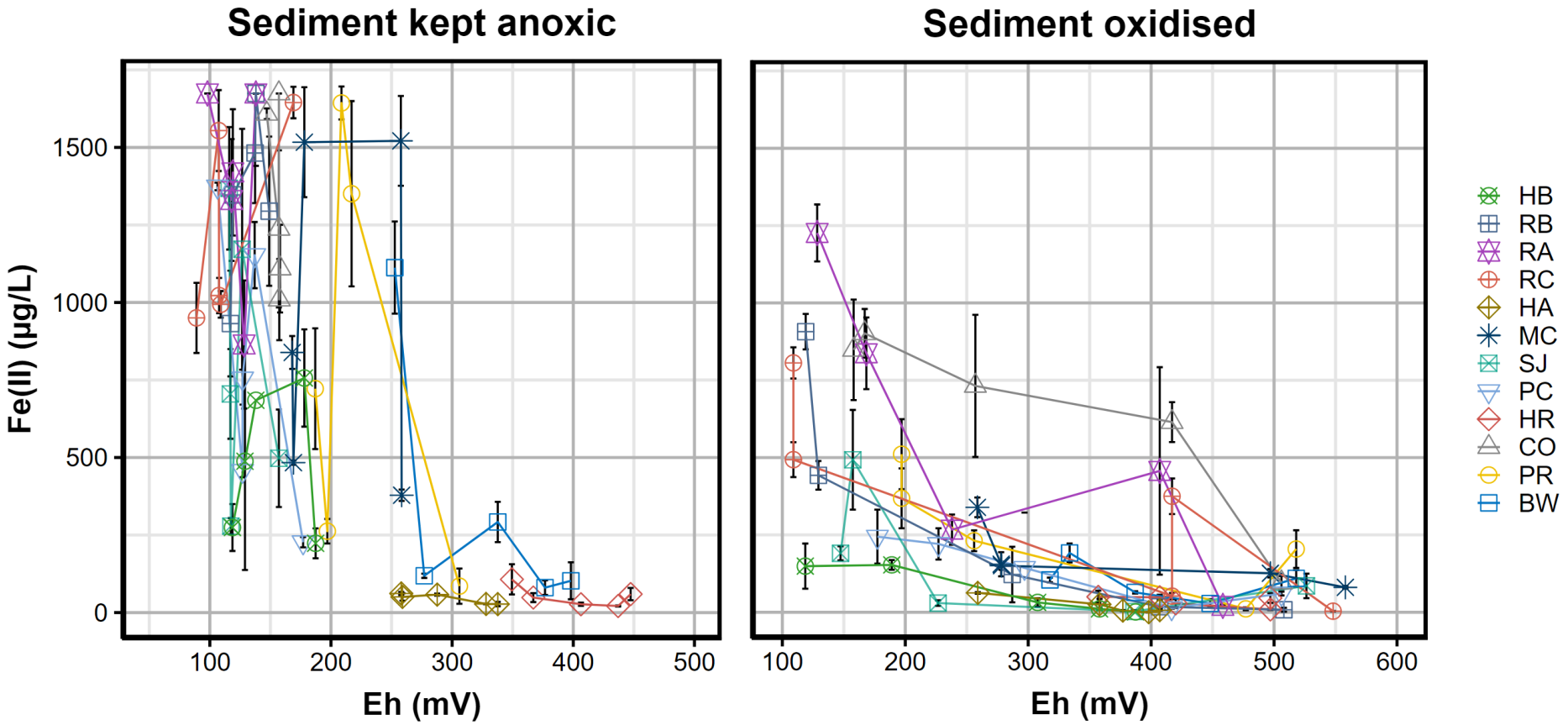

A6.14: Remobilisation of Fe (Fe^{2+} measured by Ferrozine) (mean ± SD) with redox potential in ***anoxic sediment*** incubations across the study sites. Maximum Ferrozine range = 1674 µg/L. Left hand panel = sediments incubated in anoxic conditions. Right hand panel = sediments incubated in oxic conditions

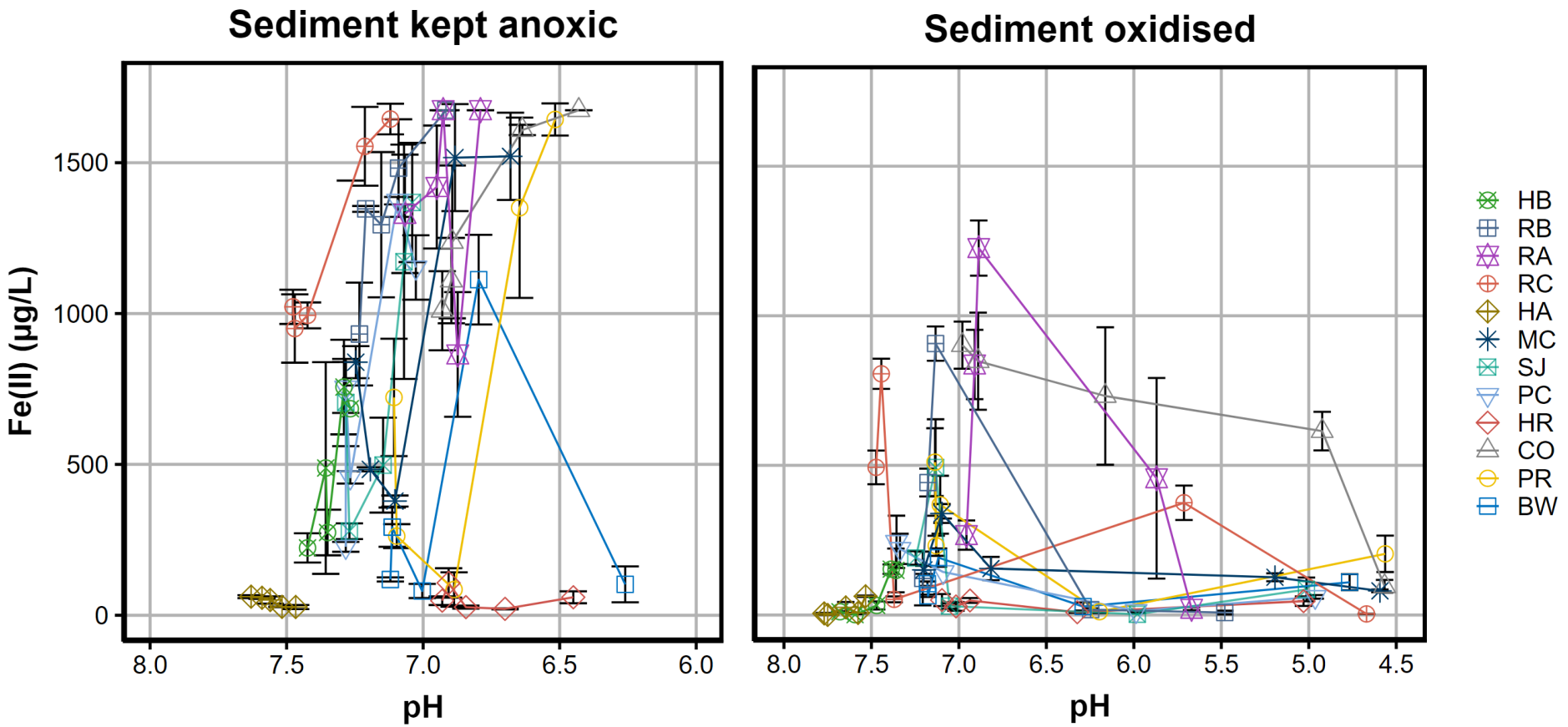

A6.15: Remobilisation of Fe ii (measured by Ferrozine) (mean ± SD) with decrease in pH in ***anoxic sediment*** incubations across the study sites. Maximum Ferrozine range = 1674 µg/L. Note the reverse pH scale. Left hand panel = sediments incubated in anoxic conditions. Right hand panel = sediments incubated in oxic conditions

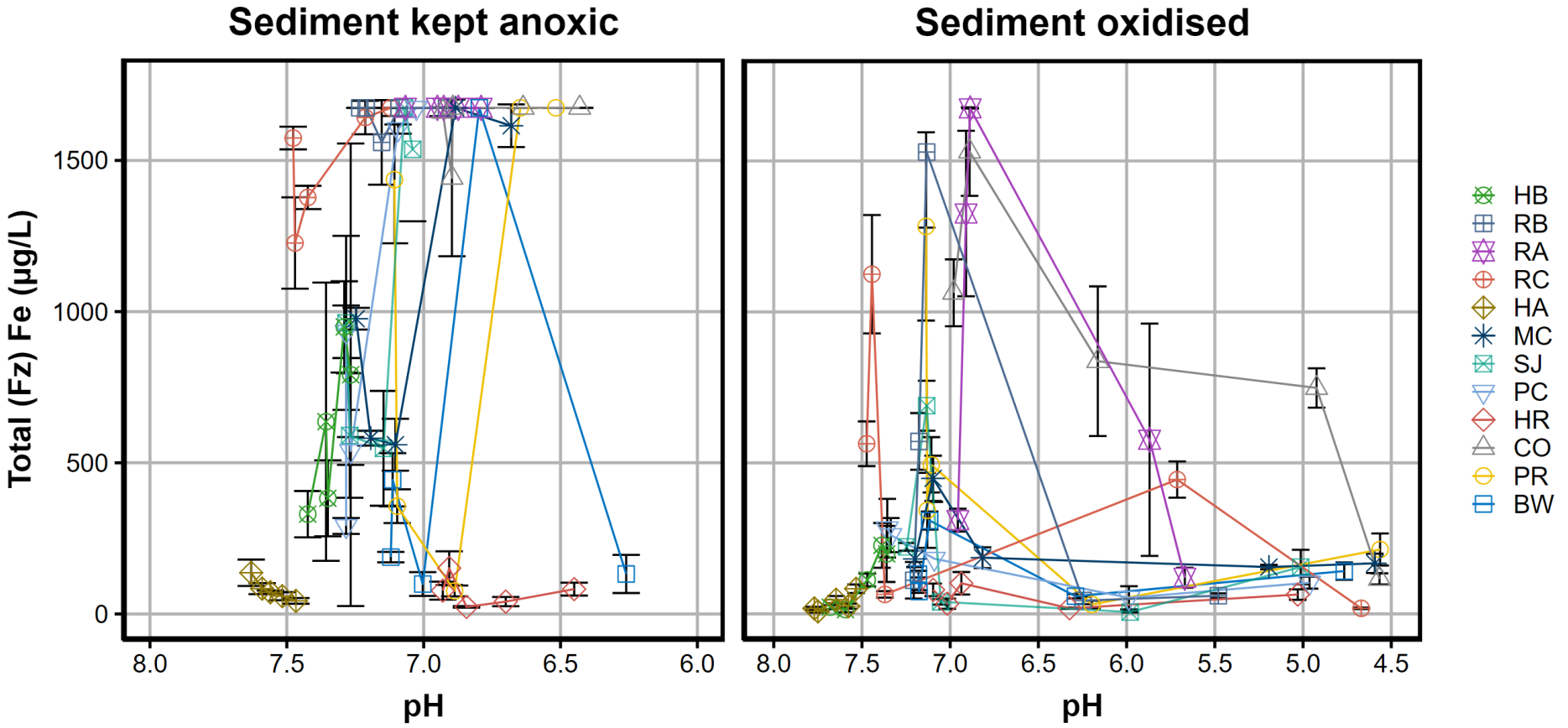

A6.16: Remobilisation of Fe (measured by Ferrozine) (mean ± SD) with decrease in pH in ***anoxic sediment*** incubations across the study sites. Maximum Ferrozine range = 1674 µg/L. Note the reverse pH scale. Left hand panel = sediments incubated in anoxic conditions. Right hand panel = sediments incubated in oxic conditions

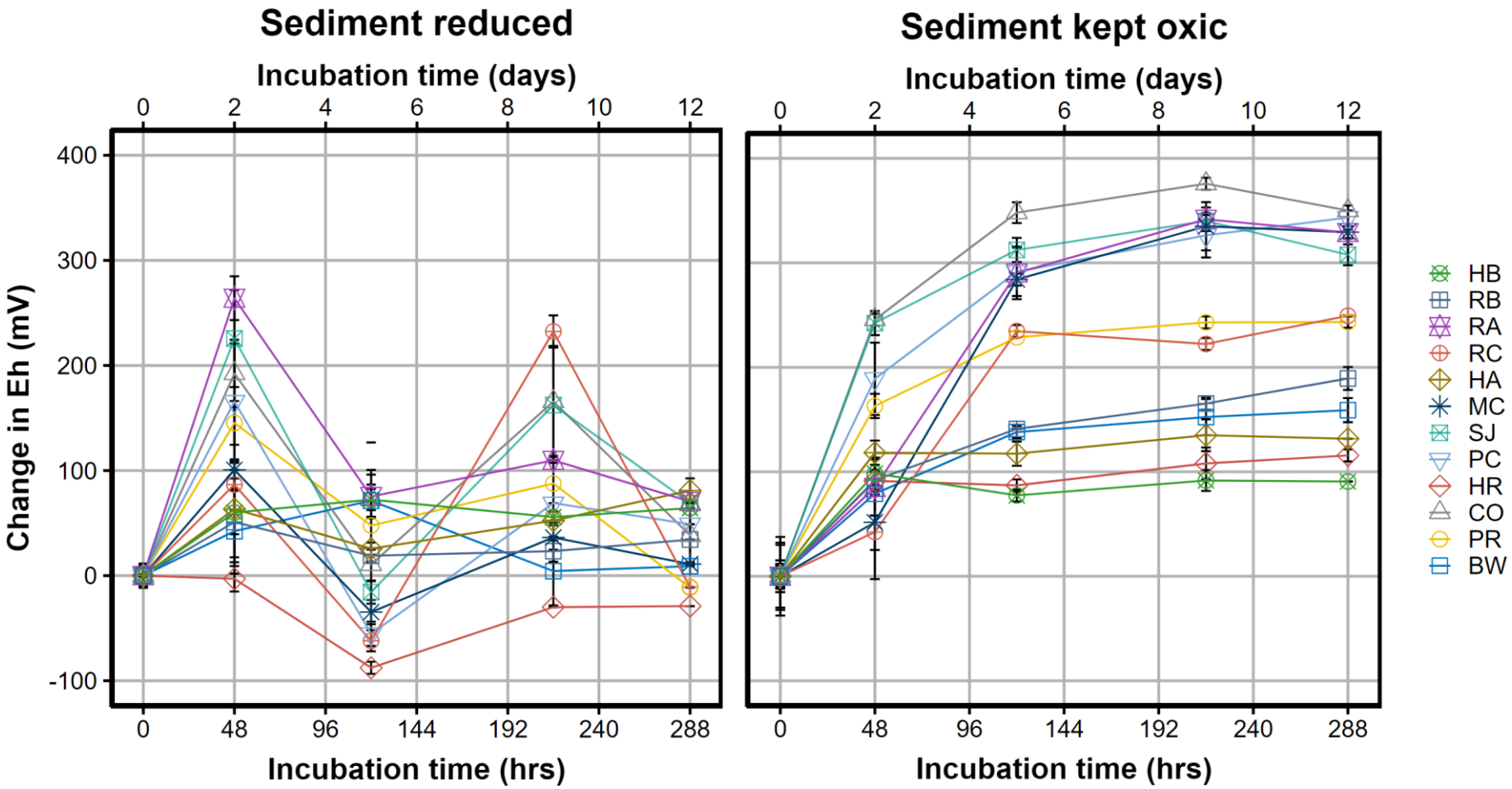

A6.17: Change in redox potential, relative to starting potential, (mean ± SD) with time in ***oxic sediment*** incubations across the study sites. Left hand panel = sediments incubated in anoxic conditions. Right hand panel = sediments incubated in oxic conditions

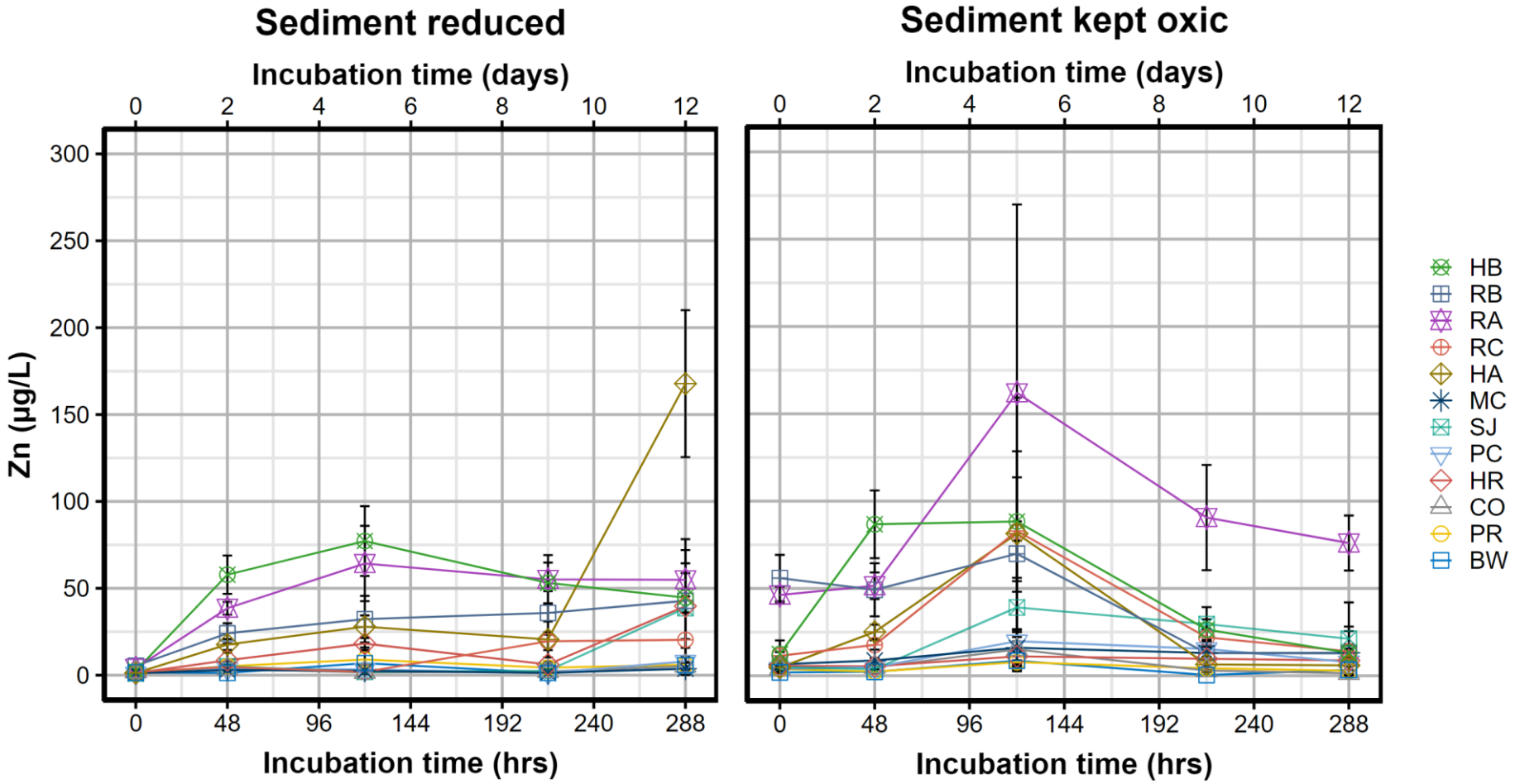

A6.18: Remobilisation of Zn (mean ± SD) with time in ***oxic sediment*** incubations across the study sites. Left hand panel = sediments incubated in anoxic conditions. Right hand panel = sediments incubated in oxic conditions

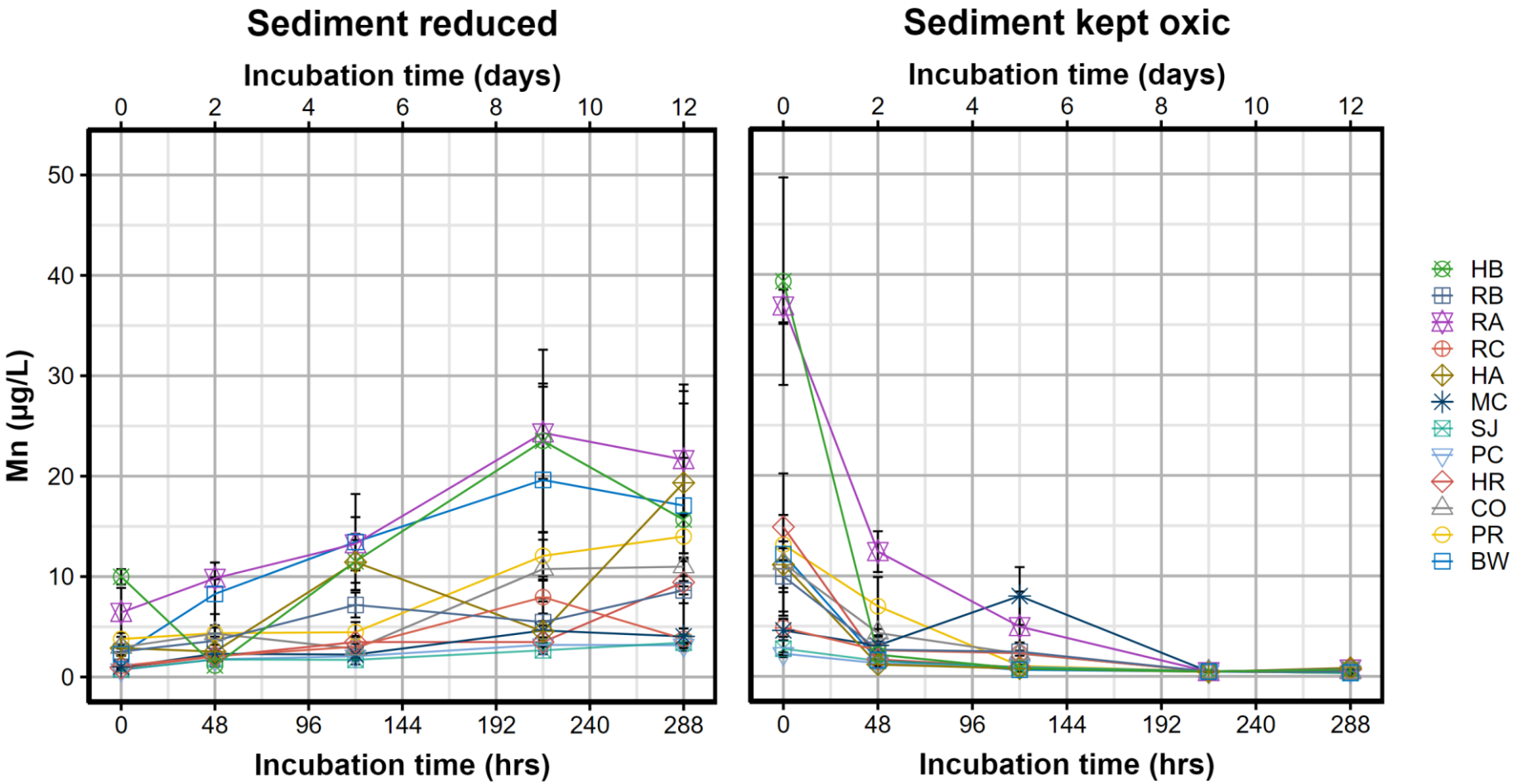

A6.19: Remobilisation of Mn (mean ± SD) with time in ***oxic sediment*** incubations across the study sites. Left hand panel = sediments incubated in anoxic conditions. Right hand panel = sediments incubated in oxic conditions. Note that Mn concentrations represent approximately 2% of actual concentrations (see Chapter 2)

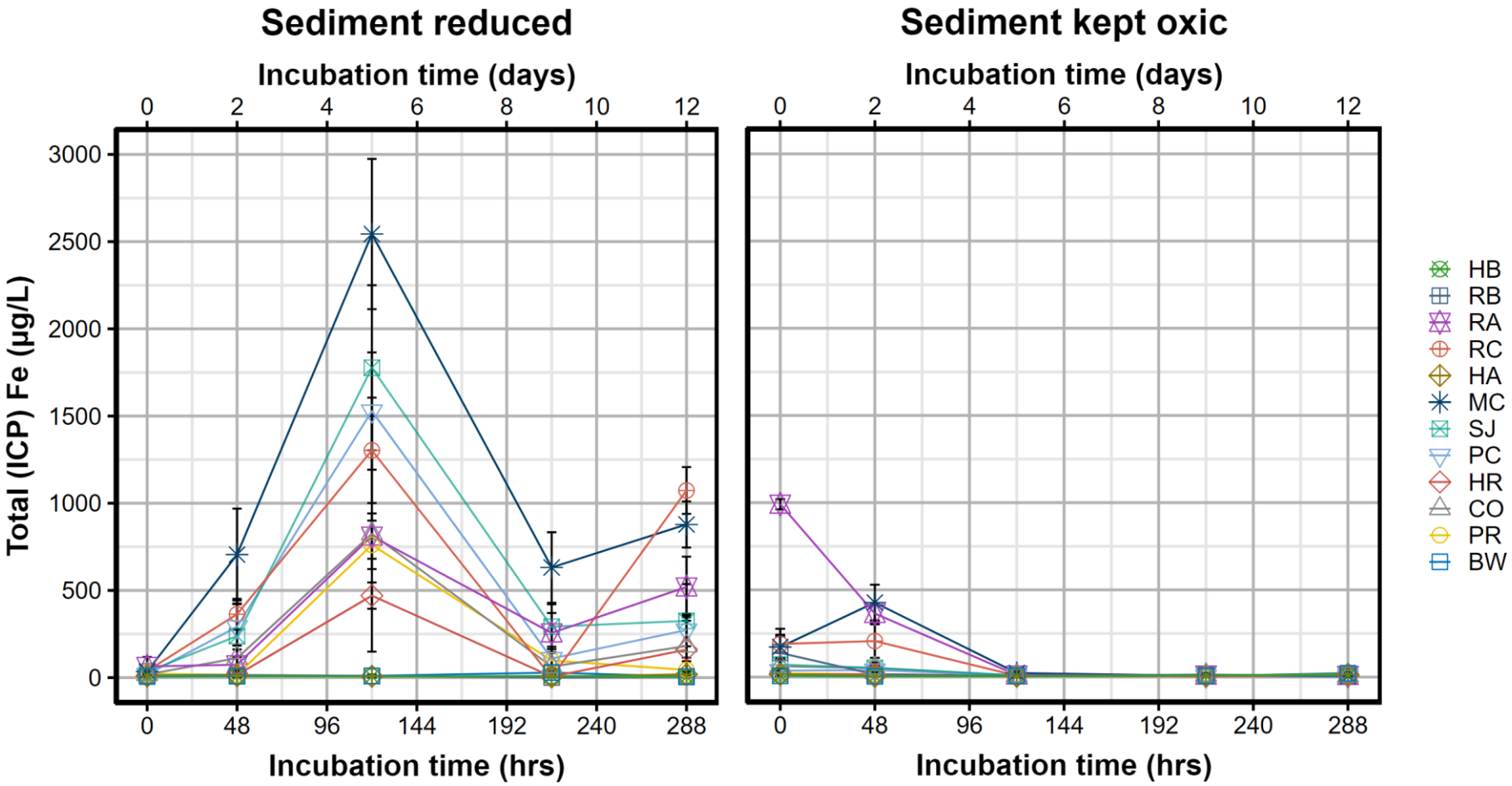

A6.20: Remobilisation of Fe (total measured by ICP-OES) (mean ± SD) with time in ***oxic sediment*** incubations across the study sites. Left hand panel = sediments incubated in anoxic conditions. Right hand panel = sediments incubated in oxic conditions

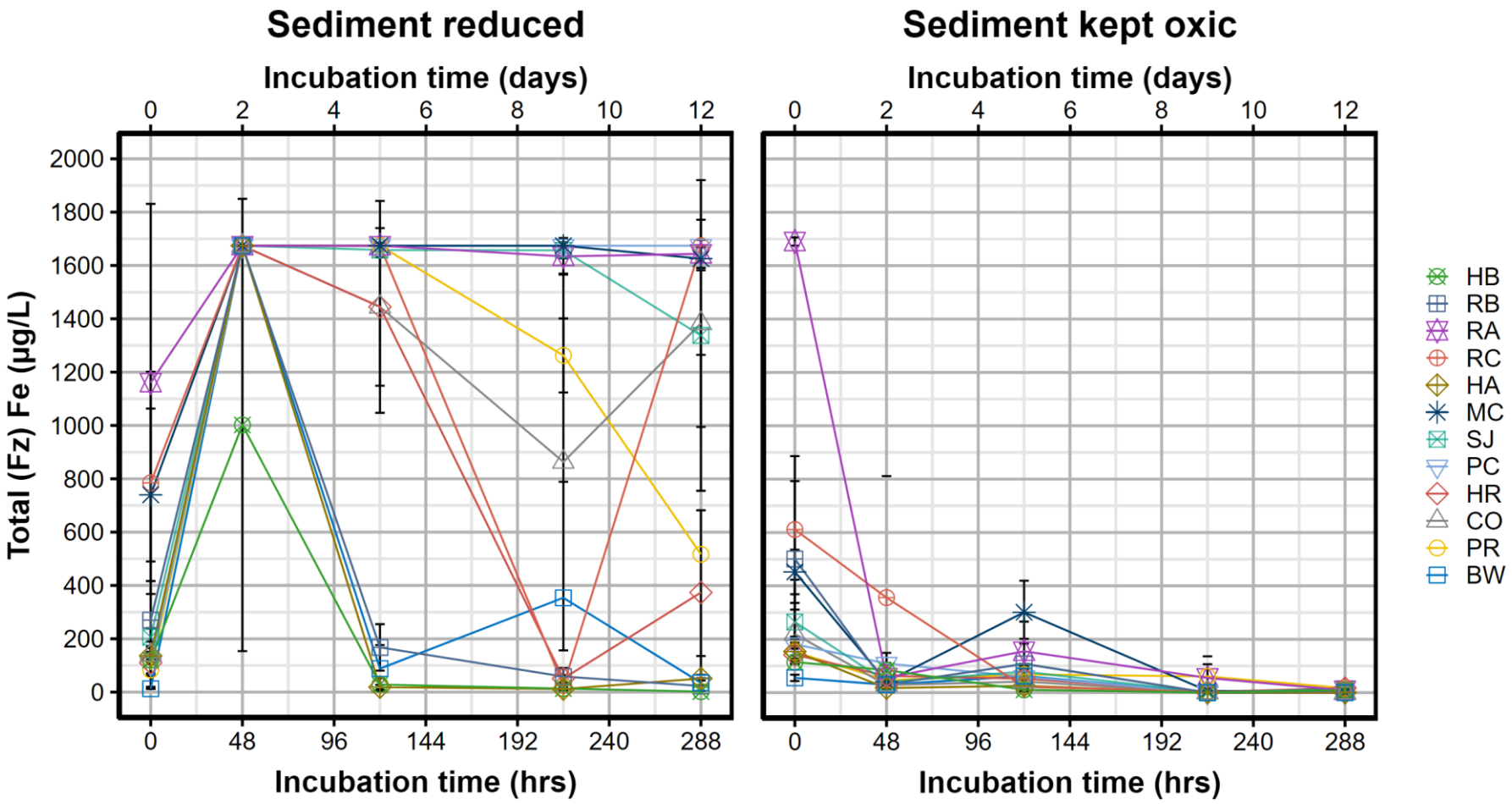

A6.21: Remobilisation of total Fe (measured by Ferrozine) (mean ± SD) with time in ***oxic sediment*** incubations across the study sites. Maximum Ferrozine range = 1674 µg/L. Left hand panel = sediments incubated in anoxic conditions. Right hand panel = sediments incubated in oxic conditions

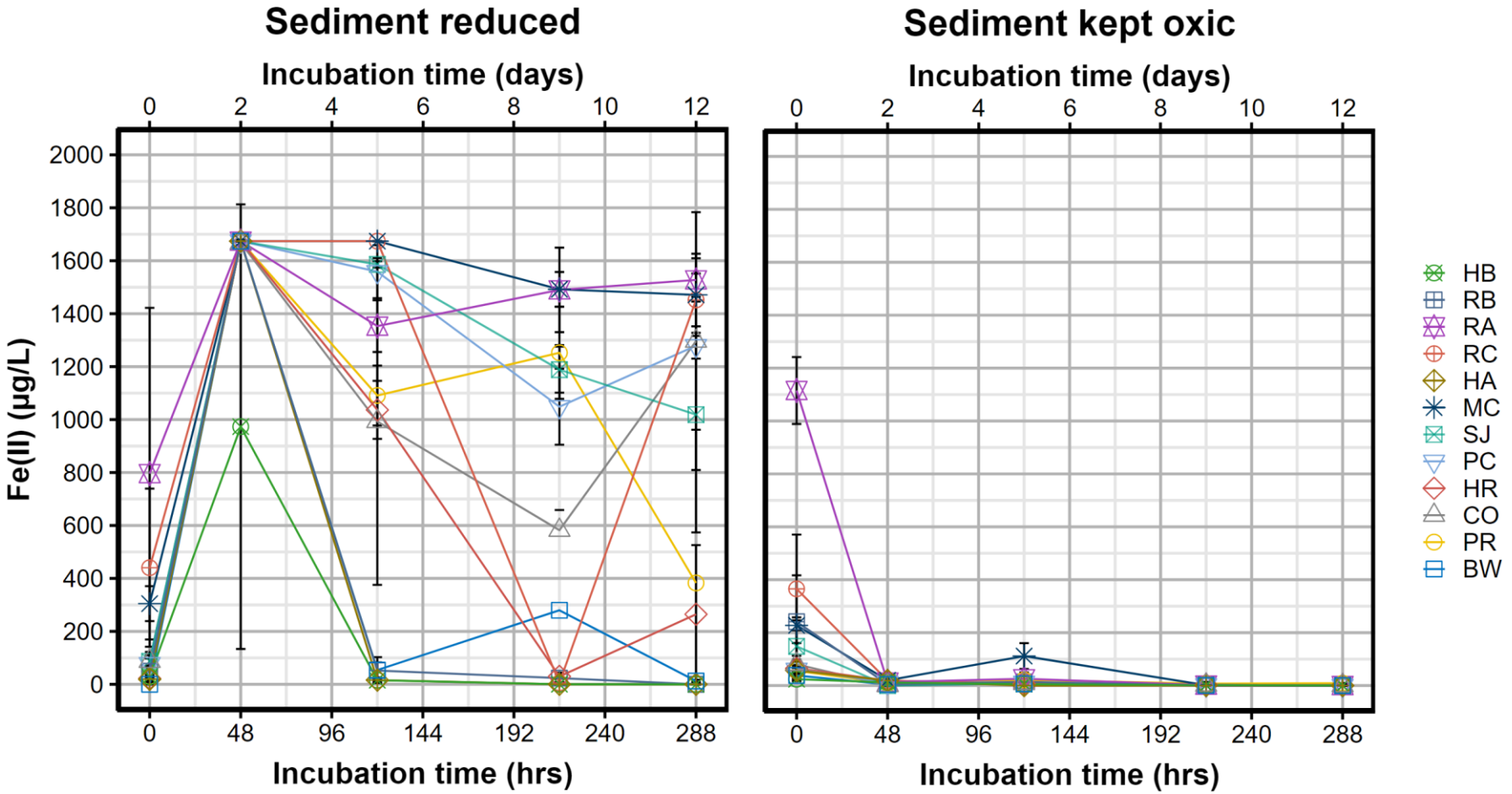

A6.22: Remobilisation of Fe(II) (measured by Ferrozine) (mean ± SD) with time in ***oxic sediment*** incubations across the study sites. Maximum Ferrozine range = 1674 µg/L. Left hand panel = sediments incubated in anoxic conditions. Right hand panel = sediments incubated in oxic conditions

Page intentionally left blank